WBS: 1.2.1.5
SCPB: N/A
QA: L

DOE/RW/00134--T31

Civilian Radioactive Waste Management System
Management and Operating Contractor

Engineered Barrier System Performance Requirements Systems Study Report

BB0000000-01717-5705-00001 REV 02

January 14, 1997

Prepared for:

U.S. Department of Energy
Yucca Mountain Site Characterization Project
P.O. Box 98608
Las Vegas, Nevada 89193-8608

Prepared by:

TRW Environmental Safety Systems, Inc.
101 Convention Center Drive
Suite P-110
Las Vegas, Nevada 89109-2006

Under Contract Number
DE-AC01-91RW00134

INTENTIONALLY LEFT BLANK

WBS: 1.2.1.5
SCPB: N/A
QA: L

Civilian Radioactive Waste Management System
Management and Operating Contractor

Engineered Barrier System Performance Requirements Systems Study Report

BB0000000-01717-5705-00001 Rev. 02

January 14, 1997

Prepared by:

Mark A. Balady
Study Manager,
Systems Analysis and
Modeling

Signature

1/14/97
Date

QA Concurrence:

O. J. Gilstrap
QA Manager, Nevada

Signature

1/14/97
Date

Approved by:

Richard D. Memory
Department Manager,
Systems Analysis and
Modeling

Signature

1/14/97
Date

Richard C. Wagner
Office Manager,
Systems Engineering

Signature

1/14/97
Date

INTENTIONALLY LEFT BLANK

ACKNOWLEDGMENT

This report was prepared from work done by the Civilian Radioactive Waste Management System (CRWMS) Management and Operating Contractor (M&O) under Contract Number DE-AC01-91RW00134 for the U.S. Department of Energy (DOE) Civilian Radioactive Waste Management System. This report satisfies the deliverable requirement TR150075.

The following individuals are gratefully acknowledged for their support and participation in this study:

Joel Atkins	Daniel Hong	Paul Pierce	Vinod Vallikat
Robert Bahney	Joon Lee	Bruce Robinson	Hongyan Wang
Thomas Buscheck	Jerry McNeish	Eric Ryder	
Gilles Bussod	Annmarie Meike	Thomas Scotese	
Zekai Ceylan	Richard Nolting	Anthony Smith	
Jim Conca	Mark Peters	David Stahl	
William Glassley		Ines Triay	

INTENTIONALLY LEFT BLANK

EXECUTIVE SUMMARY

This study evaluates the current design concept for the Engineered Barrier System (EBS), in concert with the current understanding of the geologic setting to assess whether enhancements to the required performance of the EBS are necessary. The reference design concept for the EBS is described in the *Mined Geologic Disposal System Advanced Conceptual Design Report* (ACD Report) (Civilian Radioactive Waste Management System (CRWMS) Management and Operating Contractor (M&O) (CRWMS M&O 1996b)). The performance assessment calculations are performed by coupling the EBS with the geologic setting based on the models (some of which were updated for this study) and assumptions used for the 1995 Total System Performance Assessment (TSPA) (CRWMS M&O 1995d). The need for enhancements is determined by comparing the performance assessment results against the EBS related performance requirements.

At present, there is no regulation that provides a long-term performance standard for radiological releases from the potential repository since 40 CFR 191, Environmental Radiation Protection Standards for Management and Disposal of Spent Nuclear Fuel, High-Level and Transuranic Radioactive Wastes, was remanded by the courts and repromulgated by the Environmental Protection Agency (EPA) to be inapplicable to disposal sites for high-level waste that are licensed in accordance with the Nuclear Waste Policy Act of 1982. The potential Yucca Mountain repository would be licensed per this Act, so 40 CFR 191 does not apply to Yucca Mountain. The EPA is currently considering the recommendations of the National Academy of Sciences, among others, in developing a long term performance standard for Yucca Mountain. In the absence of such a standard, an "Interim Postclosure Standard" has been established by the DOE (Yucca Mountain Site Characterization Office (YMSCO) 1996, Attachment 1). This standard requires that the probability of exceeding a dose rate of 15 mrem/yr not exceed 50 percent over 10,000 years when calculated for the average individual in a critical group in the Amargosa Valley area (about 30 km from Yucca Mountain). In addition, doses are required to be evaluated out to the time of peak dose to gain insight regarding longer-term repository performance and to assess whether engineering measures, with the potential for causing significant reductions in peak dose over very long time frames, can be implemented at reasonable cost.

Subsystem quantitative performance requirements related to the EBS include the requirement to allow no more than 1 percent of the waste packages (WPs) to fail before 1000 years after permanent closure of the repository, as well as a requirement to control the release rate of radionuclides from the EBS (CRWMS M&O 1996a).

The EBS performance enhancements considered included additional engineered components as well as evaluating additional performance available from existing design features but for which no performance credit is currently being taken. These features are summarized in Table ES-1.

Table ES-1
Performance Enhancement Options

Design/Performance Feature	Description
Performance Credit for Cladding	Include the effects of the spent nuclear fuel (SNF) cladding as a barrier contributing to waste isolation in performance assessment calculations
Credit for Cathodic Protection of Waste Package	Include the cathodic protection effects in the performance assessment calculations of the corrosion allowance material outer barrier of the waste package on the corrosion resistant material inner barrier of the waste package
Single-Layer Backfill	Quartz sand/crushed tuff uniformly covering the emplaced waste packages
Chemically Conditioned single layer backfill	Treat backfill with chemical additives in order to condition water infiltrating the emplacement drifts to reduce its corrosion properties
Multi-Layer Backfill (e.g., Richards Barrier)	Emplace two layers of material (e.g. sloped layer of gravel below a layer of sand or silt) to divert aqueous water from the waste package
Drip Shield	Emplace a metallic barrier above the waste package to divert aqueous water from the waste package surface
Chemically Conditioned Invert	Include mineral additive in the invert in order to sequester, or at least retard, radionuclide transport
Enhanced Thermal Protection through Line Loading of Waste Packages	Closely space the waste packages within the emplacement drifts in order to decrease the relative humidity and increase the temperature at the waste package surface.

CURRENT PERFORMANCE EXPECTATIONS

Calculations similar to those conducted for the 1995 TSPA give results for the repository as currently envisioned (see the ACD Report); that is, without backfill, drip shields, or any other additional EBS barrier beyond the waste package that is below the 10,000 year 15 mrem/year limit by more than four orders of magnitude. These results also show, excluding the potential effects of rockfall, a 70 percent probability that peak dose rates at 30 km from the repository, even after 10,000 years, do not exceed 10^{-4} mrem/year. Further, these results give a 99 percent probability of not exceeding 0.04 mrem/year. In addition, estimates of waste package performance indicate no breaches of waste packages within 1,000 years after permanent closure of the repository.

The effect of rockfall on the performance of the waste packages, and thus the performance of the repository, is estimated to result in a two-fold degradation in peak dose performance. This estimate was established by assuming that 1 percent of the waste packages would be breached by rockfall at the beginning of the postclosure period. This is considered a conservative assumption since it is likely that waste package degradation due to rockfall could occur much later.

The calculations that consider a time frame of one million years after permanent closure result in a 50 percent probability that dose rates at 30 km from the repository will not exceed 10 mrem/year for the current EBS concept, and a 99 percent probability that dose rates will not exceed 150 mrem/year.

As in the shorter-term analysis, rockfall on the waste packages is estimated to result in a two-fold degradation in calculated peak dose rates.

Potential improvements in the performance over the one million year time frame are described below.

POTENTIAL PERFORMANCE ENHANCEMENTS

The design/performance features described in Table ES-1 were evaluated individually and, in some cases, in combination with one another to assess their potential for enhancing performance over the one million year time frame. The results of these evaluations are summarized below.

- Indications are that the benefits of spent nuclear fuel (SNF) cladding on total system performance could result in an order of magnitude decrease in peak dose rates at the accessible environment (AE) (CRWMS M&O 1996d).

- Credit for cathodic protection results in predictions of a 50 percent probability of not exceeding 0.6 mrem/year, a 90 percent probability of not exceeding 2 mrem/year, and a 99 percent probability of not exceeding 5 mrem/year peak dose rate.

- Emplacing quartz sand backfill over the waste packages at the end of the preclosure period results in a 50 percent probability of not exceeding 0.6 mrem/year peak dose rate at 30 km from the repository. The same analysis indicates a 99 percent probability of not exceeding 11 mrem/year without violating any current thermal goals.

- Quartz sand backfill, chemically treated with magnetite and lime, was found to be ineffectual over long time periods in reducing the corrosion properties of the water entering the emplacement drifts.

- Use of a capillary barrier, such as a Richards Barrier, or a drip shield, if it functioned constantly, could result in significant reductions in the peak dose. However, to noticeably affect total system performance over 1,000,000 years requires that these barriers perform their EBS function for approximately 700,000 years. In addition to this extremely long time frame, emplacement concerns and costs associated with the Richards Barrier, and issues with the drip shield/waste package interface make these two concepts unattractive as EBS performance barriers.

- Use of an emplacement drift invert chemically treated with a phosphate containing sedimentary apatite ore has been found, in bounding calculations, to severely retard the transport of ^{237}Np to the accessible environment. The calculations predict about half the improvement in repository performance as is realized with the use of emplacement drift backfill. However, the bounding calculations assumed a sufficient amount of apatite under a waste package to retard all the ^{237}Np, as well as any of the other actinides that may sorb to apatite, in a waste package. The actual amount of apatite needed and whether this amount is compatible with the need of the drift invert to structurally support the waste package and rail carriage has not been determined.

- Tightly packing (line loading) the waste packages and backfilling after 100 years results in a 50 percent probability of not exceeding 0.1 mrem/year at 30 km from the repository. However, there is still significant uncertainty in whether the SNF cladding or drift wall temperature thermal goals would be violated in this scenario.

Table ES-2 summarizes these performance results in the context of the "Interim Postclosure Standard" and two potential alternative standards. The Richards Barrier, drip shield, and chemically treated backfill alternatives were not included in the table since they are not considered feasible, for the reasons provided above, for enhancing EBS performance. The lineloading concept was also not included due to the significant yet unresolved thermal uncertainties associated with it.

Table ES-2
Quantitative Assessment of Compliance With Alternative Post Closure Performance Standards
(mrem/year)

Standard peak dose/ percentile/ release point	Time Frame	EBS Performance Options				
		ACD[1] Reference	Cathodic Protection[1]	Cladding[1,2]	Backfill	Chemically Treated Invert[1]
Interim Postclosure Standard 15 mrem/50%/ 30km	10,000 years	$<<10^{-4}$	$<<10^{-4}$	$<<10^{-4}$	$<<10^{-4}$	$<<10^{-4}$
	1,000,000 years	10	0.6	0.3	0.6	2
Hypothetical Alternative Postclosure Standard 15 mrem/50%/ 5km	10,000 years	0.02	$<<10^{-4}$	$4X10^{-3}$	N/A[3] (<0.02)	N/A[3] (<0.02)
	1,000,000 years	270[4]	N/A[3] (<270)	6	18[4]	N/A[3] (<270)
Hypothetical Alternative Postclosure Standard 15 mrem/90%/ 30km	10,000 years	0.003	$<<10^{-4}$	$3X10^{-3}$	N/A[3] (<0.003)	N/A[3] (<0.003)
	1,000,000 years	45[4]	2	0.8	3	N/A[3] (<45)

[1] Does not reflect conservative estimate of 2-fold degradation in performance due to emplacement drift rockfall
[2] Data from "Thermal Loading System Study for FY 1996" (CRWMS M&O 1996d)
[3] N/A= Quantitative assessment not available
[4] Shaded boxes indicate violation of requirement

ADDITIONAL COSTS

The additional repository costs (relative to those costs found in the ACD Report [CRWMS M&O 1996b]) associated with backfilling of emplacement drifts include both the cost of constructing larger (5.5 meter, rather than 5.0 meter diameter) emplacement drifts as well as the cost of emplacing the backfill over the waste packages. The additional repository costs amount to approximately $461M, which is about 25 percent of the current estimates for repository construction costs (about $1.8 billion). Of this $461M, $116M is due to construction of the larger emplacement drifts and the remainder ($345M) results from emplacing the backfill.

The additional repository costs associated with a chemically conditioned invert, using a layer of phosphate containing sedimentary apatite ore, range from $20M for a 0.2m thick layer to about $330M for a 1.2m thick layer.

The costs associated with confirming the potentially available margin from cathodic protection or cladding performance have not been estimated.

CONCLUSIONS

The calculations considered in this study (based on the ACD EBS design) indicate significant margin to the "Interim Postclosure Standard" limits out to 10,000 years. Performance is also calculated to be acceptable out through one million years, although the performance margin is significantly reduced in comparison to the 10,000 year performance if no additional barriers or performance credits are applied. These calculations give a 50 percent probability of reaching 10 mrem/yr over a 1,000,000 year period, less than the 10,000 year limit of 15 mrem/year.

There are a number of uncertainties pertinent to the required and/or potential contribution of the EBS to long term performance, including: the long term performance standard; uncertainties in our understanding of significant site parameters (e.g., water flux at the repository horizon, and the timing and impacts of postclosure emplacement drift rockfall); confidence in the performance obtainable with the enhancements (e.g., thermohydrologic properties of backfill materials, long term settlement of backfill and its impact on the performance of the backfill, the ability of the backfill material to evaporate water, the offset in backfill performance due to microbial-influenced corrosion (MIC), and in the case of the chemically treated invert, the amount of phosphate needed under a waste package); and the general validity of the process models and abstractions used in the unqualified performance assessment codes. These uncertainties must be considered in developing a recommendation regarding EBS performance requirements.

Currently, the project-level technical baseline does not require emplacement drift backfill. The current findings of this study indicate that no technical basis can be established for imposing a requirement for the use of backfill, chemically conditioned inverts, drip shields, or other EBS performance enhancements. However, it should be noted that a recent interpretation (CRWMS M&O 1996p) of the ^{36}Cl bomb-pulse findings in the Exploratory Studies Facility leading to higher fluxes (approximately 7 mm/yr) at the repository horizon was not considered in this FY 1996 study. At this time it is not known if this information would have changed either the previous findings or the

following recommendations to carry the option for backfill; further analysis is required and recommended to assess the impact of such interpretations.

As a result of considering the uncertainties associated with performance, the small margins available with current concepts against the potential long-term (one million year) standard, the potential for significant total system performance improvements with EBS performance enhancements, and the costs associated with those improvements, the following recommendations are made:

A. A design requirement should be levied on the underground repository layout to provide a sufficient envelope such that a reasonable backfill emplacement system could be designed and backfit at a later date. As a contingency, this requirement should be demonstrated at the time of the Viability Assessment through an appropriate design study based primarily on analysis of emplacement drift design coupled with minimal backfill system concept development.

B. As part of the overall license strategy, a regulatory compliance strategy should be adopted for this issue at the time of the Viability Assessment. This strategy should take advantage of the repository's predicted performance being compliant with established limits, acknowledge the small calculated margin to the limits, acknowledge the uncertainties in the performance models, and identify contingency activities that need to be carried out to better quantify the performance benefits of the EBS enhancements (e.g., activities related to MIC, thermohydrologic value of backfill, and feasibility of chemically conditioned invert). The strategy should also take advantage of a long-term performance confirmation program for monitoring the need for an additional EBS performance barrier and the ability to backfit the repository with backfill (for example) if additional performance margin is required. This issue could be monitored and tracked as a potential license condition to be resolved during the performance confirmation period after repository operations have commenced.

CONTENTS

CONTENTS (Continued)

CONTENTS (Continued)

CONTENTS (Continued)

TABLES

TABLES (Continued)

FIGURES

FIGURES (Continued)

FIGURES (Continued)

Page

FIGURES (Continued)

FIGURES (Continued)

FIGURES (Continued)

Page

FIGURES (Continued)

INTENTIONALLY LEFT BLANK

1. INTRODUCTION

1.1 STUDY OBJECTIVE

This document reports the work conducted in the Engineered Barrier System Performance Requirements System Study over the period from October 1, 1995 through September 30, 1996. This study is a continuation of the fourth-quarter FY 1995 Backfill System Study (CRWMS M&O 1995g) and builds on the framework of that effort. The objective of this report is to provide a technical basis and a recommendation on whether additional barriers in the EBS beyond the waste package, such as backfill or other concepts, should be incorporated into the system design, and if so, to recommend proposed changes to the Repository Design Requirements Document (RDRD, DOE 1994b) as well as the Engineered Barrier Design Requirements Document (EBDRD, DOE 1994c).

1.2 STUDY SCOPE

The study establishes postclosure performance functions that can be provided by the EBS. Various specific concepts are developed that satisfy one or more of the functions described. Although the focus of this study concerns concepts that are physically external to the waste package, any developments that consider modifications to the internals of the waste package, and that are relevant to this study, will be pondered with regard to implications on EBS requirements.

Not all of the concepts described in this study are evaluated to the same level of detail. Rather, a limited number of generic concepts (no more than four) are chosen for detailed analysis and are selected such that they encompass and represent the significant postclosure performance functions that can be provided by the EBS. The concepts addressed in this study are not limited to those usually thought of as the classical backfill; a layer, or layers, of crushed tuff, gravel, and/or sand placed over individual waste packages. Rather, concepts are defined and pursued, if appropriate, that are composed of man-made materials and structures placed around the individual waste packages and that satisfy one or more of the EBS functions.

The various EBS concepts examined in detail in this study are evaluated first in terms of their impact on total system performance. If a concept appears feasible and is estimated to have promising impacts on total system performance, then cost estimates are conducted. The uncertainties and risks associated with some of the concepts are also delineated.

Assessments of performance are measured against the waste package containment requirement (CRWMS M&O 1996a, Key Assumption 038) as well as an assumed performance standard identified as the "Interim Postclosure Standard" (YMSCO, 1996, Attachment 1).

The study was managed by the Systems Analysis and Modeling Department and interfaced with the following organizations within the M&O:

- Waste Package Design
- Waste Package Materials
- Scientific Programs
- Subsurface Design
- Performance Assessment
- Repository/ACD Project Engineering
- Systems Engineering
- National Laboratories to include:
  - Lawrence Livermore National Laboratory
  - Los Alamos National Laboratory
  - Sandia National Laboratories

1.3 BACKGROUND

The ability to meet the overall performance requirements for the proposed MGDS at Yucca Mountain, Nevada, requires the two major subsystems (engineered barrier and natural barrier) to positively contribute to containment and radionuclide migration retardation. In addition to the postclosure performance, the proposed repository must meet certain preclosure requirements of safety, retrievability, and operability, and also must take into consideration cost and schedule. The EBS ultimately selected for such a repository will affect both the preclosure and postclosure performance of the repository. A waste package conceptual design (CRWMS M&O 1996b) has already been developed and described. However, to date, no significant effort has been conducted in the attempt to establish the viability of additional barriers in the EBS beyond the waste package for the proposed repository described in the ACD. Whether the EBS as currently conceived requires additional barriers to satisfy an assumed performance standard is essential information for the Viability Assessment design, and so too are the cost estimates of such barrier(s) if they are deemed necessary.

An initial effort on the benefits emplacement drift backfill may provide to the proposed repository was initiated in August of 1995 and completed in September of 1995 (CRWMS M&O 1995g). This current study is a continuation and expansion of that work. The two-month FY 1995 effort concluded that if the required total-system performance time frame is 10,000 years, the ACD repository should satisfy any likely standards. The study also indicated the substantial reduction in peak dose rate realized when employing a Richards Barrier (a two-layered backfill) for as long as necessary, but also indicated some issues associated with the concept. Further, the FY 1995 study indicated that a single-layer backfill may provide a substantial reduction in peak dose rates due to reduction of relative humidity (RH) on the waste package surface at early times, and may be beneficial in reducing waste package failures due to rockfall. However, at the time of the study, the near-field thermohydrological effects of backfill were still being evaluated, as was any assessment of the effects emplacement drift rockfall might have on waste package performance. Finally, the study addressed the possibility that chemically conditioning the backfill may be of benefit to long-term repository performance, if materials can be identified that appropriately alter the chemistry around the waste packages for an extensive period.

This current study addresses the issues raised in the previous two-month FY 1995 effort, and also identifies and addresses additional issues associated not only with backfill but other engineered barrier concepts as well.

1.4 REPORT ORGANIZATION

This document provides a report of the Engineered Barrier System Performance Requirements System Study. The report is organized as follows:

- The Executive Summary provides a top-level description of the study and the results
- Section 1, INTRODUCTION, provides the study objective, scope, background, and organization of the report.
- Section 2, REQUIREMENTS AND STANDARDS, documents the requirements and standards to include quality assurance, any requirements used, and the inputs and assumptions considered.
- Section 3, ANALYSIS OF REPOSITORY WITHOUT EBS ENHANCEMENTS, discusses both TSPA-1995 (CRWMS M&O 1995d) and improved estimations of the postclosure performance of a repository that, with regard to the EBS, consists of the waste package and drift spacing concept as described in the ACD Report (CRWMS M&O 1996b), and a waste package and drift spacing concept different from that described in the ACD. This section also includes an estimation of the effects of rockfall on waste package performance as well as a discussion of the implications of recent ^{36}Cl findings in the Exploratory Studies Facility (ESF).
- Section 4, POTENTIAL EBS FUNCTIONS AND ASSOCIATED CONCEPTS, identifies potential postclosure EBS performance functions as well as the concepts associated with those functions.
- Section 5, EBS CONCEPTS EVALUATION, conducts a preliminary performance assessment of the majority of the potential EBS functions identified in Section 4 to determine whether limited-lifetime functions have a significant impact on long-term repository performance. The associated concepts of those functions that appear promising are then evaluated in more detail in this section in terms of their impact on total system performance. If that proves promising, their costs are estimated and the uncertainties associated with the concepts are identified.
- Section 6, STUDY RESULTS, CONCLUSIONS, AND RECOMMENDATIONS, provides the study results, conclusions, uncertainties, and recommendations.
- Section 7, REFERENCES, provides the references.
- Section 8, ACRONYMS, contains the acronym list.

INTENTIONALLY LEFT BLANK

2. REQUIREMENTS AND STANDARDS

2.1 QUALITY ASSURANCE

The development of this technical document shall be accomplished in accordance with the CRWMS quality assurance (QA) . Although a classification of permanent items in accordance with Quality Administrative Procedure (QAP)-2-3, *Classification of Permanent Items*, has yet to be conducted, the QAP-2-0, *Conduct of Activities*, activity evaluation of *Perform System Studies* (CRWMS M&O 1995f) determined that the work performed to conduct a system study is quality affecting because the items impacted by this activity are included on the *Q-List* (DOE 1994) by direct inclusion. There are no applicable determination of importance evaluations in accordance with NLP-2-0, *Determination of Importance Evaluations*. This study may provide recommendations for requirements to be included in the RDRD (DOE 1994b) and the EBDRD (DOE 1994c). The appropriate QAP procedures, QAP-3-5, *Development of Technical Documents*, in particular, will be used in the preparation, review, approval, and, if necessary, the revision of the report. Accordingly, a Technical Document Preparation Plan for this document was developed, issued, and utilized to guide its preparation (CRWMS M&O 1996k).

The work documented in this technical report represents scoping analyses with the intention of facilitating the design process by providing requirements for design. Much of the data and many of the models and codes used to support the development of these requirements are not qualified. However, it was not the purpose of this study to document the safety of the repository design compared to a performance standard, but rather to assess the need to mandate additional barriers to radionuclide transport. Any requirements recommended by this study related to enhancing or preserving repository performance relative to a safety standard, will be designated as *To Be Verified* (TBV). For these requirements, it is recommended that an aggressive program be undertaken to qualify the data, models, and software necessary to allow verification of the requirements. For those requirements that are not related to enhancing or preserving repository performance relative to safety, no such verification is required because they do not impact repository performance. Therefore, it is not necessary to contain within this report the listings of all input and output files for the computer analyses conducted in support of this study. As a result, this document contains the appropriate level of documentation related to the use of computer software, per QAP-3-5.

2.2 REQUIREMENTS

The requirements relevant to this study were obtained from the RDRD (DOE 1994b), the EBDRD (DOE 1994c), and the Controlled Design Assumptions Document (CDA Document) (CRWMS M&O 1996a). The specific requirements related to backfill are:

CDA Key Assumption 046

> Current design assumes no backfill in emplacement drifts. Options for backfill will be considered based on ongoing and future backfill studies.

RDRD 3.2.1.1.A

During the early or developmental stages of construction, a program for in situ testing of such features as borehole and shaft seals, backfill, and thermal interaction effects of the waste packages, backfill, rock, and groundwater shall be conducted.

[10 CFR 60.142(a)]

RDRD 3.2.1.5

When the NRC amends the repository license to authorize permanent closure, the underground facility will be backfilled (if required and authorized) and sealed; the surface facilities will be decontaminated and dismantled or converted to other uses.

The final state of the GROA shall conform to plans approved as part of the license for permanent closure and decontamination and dismantlement of surface facilities.

[10 CFR 60.52(c)(2)]

RDRD 3.7.6.F

A backfill test section shall be constructed to test the effectiveness of backfill placement and compaction procedures against design requirements before permanent backfill placement is begun.

[10 CFR 60.52(c)(2)]

EBDRD 3.2.1.5

When permanent closure is authorized, the underground facility will be backfilled (if required and authorized) and sealed; the surface facilities will be decontaminated and dismantled or converted to other uses; and an institutional barrier system will be established to preclude human activities for thousands of years that could compromise waste isolation.

The final state of the Engineered Barrier Segment shall conform to plans approved as part of the license for permanent closure.

[10 CFR 60.52(c)(2)]

While the requirements listed above address the need to accommodate backfill if employed, none of these requirements necessitates the use of backfill.

Requirements that address postclosure Engineered Barrier Segment performance are defined as follows:

EBDRD 3.7.B

The Engineered Barrier Segment shall be designed to ensure that releases of radioactive materials from the Engineered Barrier Segment, and then through the geologic setting to the accessible environment following permanent closure, conform to applicable environmental

standards for radioactivity established by the EPA with respect to both anticipated and unanticipated processes and events.

[10 CFR 60.112]

EBDRD 3.7.C

The Engineered Barrier Segment shall be designed so that assuming anticipated processes and events: (A) containment of HLW will be substantially complete during the period when radiation and thermal conditions in the Engineered Barrier Segment are dominated by fission product decay; and (B) any release of radionuclides from the Engineered Barrier Segment shall be a gradual process which results in small fractional releases to the geologic setting over long times.

[Derived][10 CFR 60.113(a)(1)(I)]

EBDRD 3.7.D

In satisfying the preceding requirement, the Engineered Barrier Segment shall be designed, assuming anticipated processes and events, so that containment of radioactive material within the waste packages will be substantially complete for a period to be determined by the NRC, but not less than 300 years nor more than 1,000 years after permanent closure of the geologic repository.

[10 CFR 60.113(a)(1)(ii)(A)]

The above requirement has been superseded by the following CDA assumption:

CDA EBDRD 3.7.D

The EBS shall be designed, assuming anticipated processes and events, so that containment of radioactive material within the waste packages will be substantially complete for 1000 years (with less than 1% of the waste packages failing within 1000 years after permanent closure of the geologic repository) and with a mean waste package lifetime well in excess of 1000 years.

[10 CFR 60.113(a)(1)(ii)(A)]

CDA Key Assumption 038

The fraction of waste packages breached at 1000 years shall be less than 1%...

EBDRD 3.7.E

The Engineered Barrier Segment shall be designed, assuming anticipated processes and events, so that the release rate of any radionuclide from the Engineered Barrier Segment following the containment period shall not exceed one part in 100,000 per year of the inventory of that radionuclide calculated to be present at 1,000 years following permanent closure, or such other fraction of the inventory as may be approved or specified by the Commission; provided, that this requirement does not apply to any radionuclide which is released at a rate less than 0.1%

of the calculated total release rate limit. The calculated total release rate limit shall be taken to be one part in 100,000 per year of the inventory of radioactive waste, originally emplaced in the underground facility, that remains after 1,000 years of radioactive decay.

[10 CFR 60.113(a)(1)(ii)(B)]

RDRD 3.7.1

Groundwater Travel Time. The geologic repository shall be located so that pre-waste-emplacement groundwater travel time along the fastest path of likely radionuclide travel from the disturbed zone to the accessible environment shall be at least 1,000 years or such other travel time as may be approved or specified by the Commission.

[10 CFR 60.113(a)(2)]

RDRD 3.7.5.E.3

The orientation, geometry, layout, and depth of the underground facility, and the design of any engineered barriers that are part of the underground facility shall contribute to the containment and isolation of radionuclides.

[10 CFR 60.133(a)(1)]

RDRD 3.7.5.I

Control of water and gas. The design of the underground facility shall provide for control of water or gas intrusion.

[10 CFR 60.133(d)]

EBDRD 3.7.A

The Engineered Barrier Segment shall be designed to assist the geologic setting in meeting the performance objectives for the period following permanent closure.

[10 CFR 60.133(h)]

Requirements that are not postclosure-performance related, but are related to the Engineered Barrier Segment follow:

RDRD 3.7.5.D

Retrieval of waste. The underground facility shall be designed to permit retrieval of waste in accordance with the performance objectives of 10 CFR 60.111.

[10 CFR 60.133(c)]

RDRD 3.7.5.H

Flexibility. The underground facility shall be designed with sufficient flexibility to allow adjustments where necessary to accommodate specific site conditions identified through in situ monitoring, testing, or excavation.

[10 CFR 60.133(b)]

RDRD 3.2.2.5.A

> All systems for processing, transporting, handling, storing, retrieving, emplacing, and isolating radioactive waste shall be designed to ensure that a nuclear criticality accident is not possible unless at least two unlikely, independent, and concurrent or sequential changes have occurred in the conditions essential to nuclear criticality safety. Each system shall be designed for criticality safety under normal and accident conditions. The calculated effective multiplication factor (k[eff]) must be sufficiently below unity to show at least a 5% margin, after allowance for the bias in the method of calculation and the uncertainty in the experiments used to validate the method of calculation.
>
> [10 CFR 60.131(b)(7)]

The specific, quantitative subsystem performance requirements mentioned above include:

- A requirement to allow no more than 1 percent of the waste packages to fail before 1000 years after permanent closure of the repository (substantially complete containment) (CDA EBDRD 3.7.D).

- A requirement to control the release rate of radionuclides from the EBS (EBDRD 3.7.E).

The first requirement, for substantially complete containment, is directly addressed in this study. The second requirement is indirectly addressed as follows, and as such was not explicitly modeled for the study. Previous analyses (CRWMS M&O 1995d) identified eleven radionuclides calculated to have a maximum release rate exceeding 0.1% of the U. S. Nuclear Regulatory Commission (NRC) total release rate limit. Only one of these radionuclides is calculated to be a driver in terms of total peak dose rates at the accessible environment over a ten thousand year time frame, and only two of the eleven radionuclides are considered drivers over the one million year time frame. The focus of this study was not to address a subsystem requirement, such as the EBS release rate requirement that could over-constrain the EBS by forcing the reduction of the release rates of radionuclides that are calculated to have no effect on the doses seen at the accessible environment. Rather, the focus of this study is to address the characteristics of the EBS that may contribute in ensuring the future health and safety of the general public by evaluating peak dose release rates only at the accessible environment.

This study specifically and quantitatively addresses the substantially complete containment requirement of 10 CFR 60, Disposal of High-Level Radioactive Wastes in Geologic Repositories, Section 113(a)(1)(ii)(A), as well as an assumed performance standard described in the following section. The remainder of the Engineered Barrier Segment postclosure subsystem requirements delineated above were not specifically evaluated within this study and were considered outside the scope.

2.3 INPUTS AND ASSUMPTIONS

This section identifies the reference case, the major input conditions for the study, the computer codes employed, and the assumptions used. In many cases specific input parameters and/or assumptions for a given analytic model or for a particular option are discussed in the relevant section of the report. Unless otherwise indicated, the unqualified inputs are employed in this report. The computer codes used in the work conducted in support of this study are listed below by section number so that the origination of the analyses can be known.

Sections 3.1 and 3.2

ANSYS Version 5.1 (Computer Software Configuration Item (CSCI) #30003 V5.1 HP)—The code was run on a Hewlett Packard 9000 series 735 workstation. The software has been qualified and this is described in the *Software Qualification Report for ANSYS 5.1HP (CSCI# 30003 V5.1HP)*, DI Number: 30003-2006 REV 01, CRWMS M&O. The Life Cycle Plan and the QAP-SI series procedures for the code are described in *Life Cycle Plan for ANSYS Version 5.1HP (CSCI# 30003 V5.1HP*, DI Number: 30003-2007 REV 01, CRWMS M&O]. The code was run over the range that it has been validated for and is appropriate for the application.

FEHM (Finite Element Heat and Mass), May 7, 1996—Developed by Los Alamos National Laboratory and runs on an HP9000 workstation. This code has not been validated nor is it configuration controlled. The code was used over the range for which it was designed and is appropriate for the application.

NUFT, Version 4-16-96b, 1996—Developed by Lawrence Livermore National Laboratory and runs on an IBM RISC6000 Powerserver Model 375. This code has not been verified nor is it configuration controlled. The code was used over the range for which it was designed and is appropriate for the applications.

RIP—Repository Integrating Program, Version 4.04, November 1995 —This code runs on a PC. It has not been validated although Golder, the developer, has it under configuration control. The code was used over the range for which it was designed and it is appropriate for the application.

WAPDEG, version 1.0, developed by INTERA—This code runs on an HP9000 workstation. The code has not been validated nor is it configuration controlled. The code was used over the range for which it was designed and is appropriate for the applications.

Section 3.3

ANSYS Version 5.1 (CSCI# 30003 V5.1 HP)—The code was run on a Hewlett Packard 9000 series 735 workstation. The software has been qualified and this is described in the *Software Qualification Report for ANSYS 5.1HP (CSCI# 30003 V5.1HP)*, DI Number: 30003-2006 REV 01, CRWMS M&O]. The Life Cycle Plan and the QAP-SI series procedures for the code are described in *Life Cycle Plan for ANSYS Version 5.1HP (CSCI: 30003 V5.1HP)*, DI Number: 30003-2007 REV 01, CRWMS M&O. The code was run over the range that it has been validated for and is appropriate for the application.

FLAC, Version 3.22, 1993 (CSCI #20.93.3001-AAu3.22)—The code has been verified and validated and runs on IBM PC. The code was run over the range that it has been validated for and is appropriate for the application.

RIP—Repository Integrating Program, Version 4.04, November 1995—This code runs on a PC. It has not been validated although Golder, the developer, has it under configuration control. The code was used over the range for which it was designed and it is appropriate for the application.

UNWEDGE Version 2.2 was run on a 486 base computer —The software has been qualified for use in accordance with M&O Computer Software Quality Assurance procedures. The software CSCI number is B00000000-01717-1200-30014 REV 00. The Life Cycle Plan is described in B00000000-01717-2007-30014 REV 00. UNWEDGE Version 2.2 has been used within the range of validation as specified in software qualification documentation and the code is considered appropriate for the application.

UDEC (Universal Distinct Element Code), Version 2.0—The code is run on a 486-based personal computer. The software has been qualified for use in accordance with M&O Computer Software Quality Assurance procedures. The software CSCI number is B00000000-01717-1200-30004 REV 00. The Life Cycle Plan is described in B00000000-01717-2007-30004 REV 00. UDEC Version 2.0 has been used within the range of validation as specified in software qualification documentation and the code is considered appropriate for the application.

Section 5.1

RIP—Repository Integrating Program, Version 4.04, November 1995—This code runs on a PC. It has not been validated although Golder, the developer, has it under configuration control. The code was used over the range for which it was designed and it is appropriate for the application.

TOUGH2, Version 1.0 of March 1991 developed by Pruess with T2.FOR Module replaced by T2CG1.F Version 1.1 April 1993—The code was used in conjunction with a processor code, CLIN, developed by Intera in May 1996 to include the geochemical aspects as discussed in Section 3.2. The code runs on a PC using a SALFORD compiler. The software does not currently have a configuration control number. The code is unvalidated but was used over the range for which it was designed and was appropriate for the application.

WAPDEG, version 1.0, developed by INTERA—This code runs on an HP9000 workstation. The code has not been validated nor is it configuration controlled. The code was used over the range for which it was designed and is appropriate for the applications.

Section 5.2

ANSYS Version 5.1, (CSCI #30003 V5.1 HP)—The code was run on a Hewlett Packard 9000 series 735 workstation. The software has been qualified and this is described in *Software Qualification Report for ANSYS 5.1HP (CSCI# 30003 V5.1HP)*, DI Number: 30003-2006 REV 01, CRWMS M&O. The Life Cycle Plan and the QAP-SI series procedures for the code are described in *Life Cycle Plan for ANSYS Version 5.1HP (CSCI: 30003 V5.1HP)*, DI Number: 30003-2007 REV 01,

CRWMS M&O. The code was run over the range that it has been validated for and is appropriate for the application.

DECAY—Developed by Los Alamos National Laboratory, has no version number, has not been validated, nor is it configuration controlled. The code was used over the range for which it was designed and is appropriate for the application.

FEHM (Finite Element Heat and Mass), May 7, 1996—Developed by Los Alamos National Laboratory and runs on an HP9000 workstation. This code has not been validated nor is it configuration controlled. The code was used over the range for which it was designed and is appropriate for the application.

GEOMESH, last updated March 19, 1996—Developed by Los Alamos National Laboratory, and runs on a SUN Sparc10 workstation. Some qualified data went into the development of this code but the code has not been validated. The software does not currently have a configuration control number. The code was used over the range for which it was designed and was appropriate for the application.

NUFT, Version 4-16-96b, 1996—Developed by Lawrence Livermore National Laboratory and runs on an IBM RISC6000 Powerserver Model 375. This code has not been verified nor is it configuration controlled. The code was used over the range for which it was designed and is appropriate for the applications.

RIP—Repository Integrating Program, Version 4.04, November 1995—This code runs on a PC. It has not been validated although Golder, the developer, has it under configuration control. The code was used over the range for which it was designed and it is appropriate for the application.

WAPDEG, version 1.0, developed by INTERA—This code runs on an HP9000 workstation. The code has not been validated nor is it configuration controlled. The code was used over the range for which it was designed and is appropriate for the applications.

Section 5.3

EQ3/6, version 7.2—Developed by Lawrence Livermore National Laboratory and runs on a Silicon Graphics XZ4000. This code has been validated, but it has not been configuration controlled. The code was used over the range for which it was designed and is appropriate for the applications.

OS3D/GIMRT, version 2.0—Developed at the University of Southern Florida, Department of Geology, and runs on a Silicon Graphics XZ4000. This code has not been validated nor has it been configuration controlled. The code was used over the range for which it was designed and is appropriate for the applications.

This document will not directly support any construction, fabrication, or procurement activity and therefore is not required to be procedurally controlled as TBV. In addition, the data and assumptions associated with this analysis are not required to be procedurally controlled as TBV. However, use

of any data from this analysis for input into documents supporting procurement, fabrication, or construction is required to be controlled as TBV in accordance with the appropriate procedures.

The following identifies the basic assumptions and inputs used in the study.

Thermal Loading. The thermal load employed in this study is the reference thermal load of 83 MTU/acre as defined in Key Assumption 019 of the CDA Document (CRWMS M&O 1996a).

Subsurface Concept. The reference case employed in this study is that established in the ACD Report (CRWMS M&O 1996b). Horizontal emplacement of waste packages is conducted within the emplacement drifts. The nominal diameter of the emplacement drifts is 5.0 meters. The "square" waste package spacing employed in the ACD actually varies from 9 meters to about 19 meters, depending on the waste package heat output. The drift spacings are 22.5 meters, centerline-to-centerline. Some of the analysis conducted in this study employs different waste package and drift spacings, and is identified as such in the pertinent sections.

Infiltration Rate. Section 9.2.1 of TSPA-1995 (CRWMS M&O 1995d) discusses the use of two infiltration rates used for thermohydrologic simulations which are individually associated with the TSPA repository infiltration rate scenarios. The "low" infiltration rate scenario uses thermohydrologic simulations with 0.05 mm/year with the TSPA repository infiltration rate sampled in the range 0.01 to 0.05 mm/year. The "high" infiltration rate scenario uses thermohydrologic results with an infiltration rate of 0.3 mm/year with a TSPA repository infiltration rate that is uniformly sampled in the range 0.5 to 2.0 mm/year. Many of the low infiltration rate scenarios conducted for TSPA-1995 produced no releases to the accessible environment (defined at 5 km down-gradient from the repository) over 10,000 years. For this reason, addressing whether additional barriers beyond the waste package should be added to the EBS requires looking at the high infiltration rate scenario. For the "expected-value" TSPA results presented in this report, a repository infiltration rate of 1.25 mm/year (the average of the "high" TSPA repository infiltration rate range) was employed.

Performance Standard. Until a new EPA standard is promulgated, the YMSCO is assuming a dose-based standard, referred to as the "Interim Postclosure Standard" (YMSCO, 1996, Attachment 1), which indicates that the maximum allowable peak dose rate is 15 mrem/year and must be satisfied over a 10,000 year time frame. Further, it is assumed that, associated with the "Interim Postclosure Standard" is a requirement that no more than a 50 percent probability of exceeding the maximum allowable peak dose rate will be tolerated. This is the standard assumed in this study. Dose calculations are conducted for this study assuming individuals drink two liters of water per day from a water well located about 30 km down-gradient from the repository. The "Interim Postclosure Standard" indicates that performance assessments shall be conducted past 10,000 years, out to the time of peak dose, to gain insight regarding longer-term repository performance. Primarily because of the National Research Council (NRC) report *Technical Bases for Yucca Mountain Standards* (NRC, 1995) which stated that "...the ultimate restriction on time scale is determined by the long-term stability of the fundamental geologic regime - a time scale that is on the order of 10^6 years at Yucca Mountain" (NRC, 1995, p. 55), TSPA-1995 employed a 1,000,000 year time span for longer-term repository performance. This study assumes the same. Total peak dose Complementary Cumulative Distribution Functions (CCDFs) are used in this study to assess compliance with this assumed standard.

Waste Package Containment Requirement. Key Assumption 038 of the CDA Document (CRWMS M&O 1996a) states that "The fraction of waste packages breached at 1000 years shall be less than 1%...". It is conservatively assumed that containment of radioactive waste ends when a single pit has corroded completely through the barriers of a waste package.

Modeling of Repository Performance. Recommendations regarding whether or not additional barriers should be added to the EBS beyond the waste package are partly based on the total system performance of these barriers. This study relies heavily on the capabilities and expertise of the Performance Assessment and Modeling organization in estimating the performance of the various barriers addressed in this study. Data, abstractions, and models used in TSPA-1995 are used as the basis for the TSPAs. The results and conclusions of this study are partly based on such assessments. The intent of this study was not to help in updating the fidelity of TSPA as a whole. Rather, only in those areas that were clearly deficient in addressing the specific problems associated with this study were efforts made to improve fidelity. Thus, the total system performance results presented in this study, as with those results presented in TSPA-1995, should be caveated with the statement (also expressed in Section 10 of TSPA-1995) that they are directly related to the Engineered Barrier System (EBS) and Natural Barrier System (NBS) conceptual models existing at the time the analyses were performed.

EBS Transport Model. The EBS transport model identified as "drips on waste package" in TSPA-1995 is used in the TSPAs presented in this study. This is not the nominal case EBS transport model used in TSPA-1995, but it is now thought to be a more realistic model than the "drips on waste form" model used as the nominal case in TSPA-1995. In the "drips on waste package" transport model, the corrosion pits in the waste packages are assumed to always be filled with corrosion products so that drips cannot directly contact the waste form, but can only contact the outer surface of the waste package. These corrosion-filled pits act as a barrier to advective flow such that mass-transfer of the radionuclides in the waste package occurs only by diffusion through the pits. This effectively lowers the mass of radionuclides encountered by drips at the waste package surface, compared to the mass the drips would have encountered at the waste form surface if the corrosion products did not act as a barrier to advection.

Corrosion Initiation. In the total system performance assessments presented in this study, corrosion of the outer barrier of the waste packages initiates only when both the simulated temperature at the waste package surface drops below 100°C and the relative humidity is above the threshhold values described in Appendix B.

Timing of Backfilling. All thermohydrologic, cost, and total system performance results assume that if emplacement drift backfilling is deemed necessary, it will occur at the end of the preclosure period for retrievability purposes.

3. ANALYSIS OF REPOSITORY WITHOUT EBS ENHANCEMENTS

This section of the report discusses estimations of the postclosure performance of a repository that, with regard to the EBS, consists of:

- The waste package and drift spacing concept as described in the ACD Report (CRWMS M&O 1996b)
- A waste package and drift spacing concept different from that described in the ACD.

Understanding how well the current conceptual design fares against assumed containment requirements and performance standards is crucial in establishing whether additional performance barriers are needed in the EBS.

Section 3.1 gives a brief overview of the ACD.

Section 3.1.1.1 summarizes the postclosure repository performance as indicated in TSPA-1995 (CRWMS M&O 1995d). This was the last published DOE assessment of the repository performance.

Progress has been made in many disciplines since the publication of TSPA-1995, the most relevant to this study being that of near-field thermohydrological modeling. The improvements in such models since TSPA-1995, as well as the resulting updated assessment of long-term repository performance, is described in Section 3.1.1.2.

Section 3.2 discusses the potential near-field thermohydrologic as well as total system performance benefits that could be realized if the ACD waste package-to-waste package and emplacement drift-to-emplacement drift spacings were modified to allow for very closely spaced waste packages while still maintaining the same thermal loading. This discussion is included to highlight possible improvements in long-term repository performance that could be realized without the addition of performance barriers within the EBS. There are currently thermal issues associated with this concept that have yet to be addressed, but the promising aspects of the concept presented in Section 3.2 should motivate a detailed examination of these issues.

In summary, the purpose of Section 3 is to establish the predicted performance of a repository that does not benefit from performance barriers within the EBS other than those already described in the ACD.

3.1 ADVANCED CONCEPTUAL DESIGN

The four volume ACD Report (CRWMS M&O 1996b) includes discussions of the Mined Geologic Disposal System (MGDS) concept of operations, site description, surface design description, and subsurface design description, in addition to other subject areas. The intent here is not to give an overview of the ACD as a whole, but rather to focus on the aspect of the ACD of interest to this study - the Engineered Barrier System.

The Engineered Barrier System consists of the Waste Package Subsystem and the Underground Facility Subsystem. The Waste Package Subsystem includes several waste package types for disposal of various waste forms. The Waste Package Subsystem also includes packing or other absorbent material immediately surrounding an individual waste package, filler materials, shielding, and waste package support. In addition to the waste packages, the Engineered Barrier System includes other engineered features to support the Isolate Waste function, such as emplacement drift orientation, geometry, layout and depth, drainage, backfill, and the emplacement drift invert.

Current waste package design concepts favor two-barrier waste packages for both spent nuclear fuel and defense high-level waste (DHLW). The ACD indicates that the waste packages will be placed on railcars and emplaced within the emplacement drifts in a center-in-drift (CID) emplacement mode (Figure 3.1-1a). CID emplacement requires a nominal 5 meter diameter emplacement drift.

The ACD uses the reference thermal loading of 83 MTU/acre of emplacement area (Key Assumption 019, CRWMS M&O 1996a). To satisfy this thermal loading, the ACD utilizes a "square" geometry with the spacing between emplacement drift centerlines (22.5 meters) being roughly the same as the axial center-to-center spacing between SNF WPs (19.5 meters).

3.1.1 POSTCLOSURE REPOSITORY PERFORMANCE

One of the objectives of this study is to employ the current ACD as well as the current modeling of the performance of the EBS and NBS to make a defensible assessment as to whether additional barriers in the EBS are warranted. The evaluation of the ability of the overall disposal system to meet the performance objectives specified in the applicable regulatory standards has been termed TSPA. TSPAs require the explicit quantification of the relevant processes and process interactions. In addition to providing a quantitative basis for evaluating the suitability of the site to meet regulatory objectives, such assessments are useful to help define the most significant processes, the information gaps and uncertainties regarding these processes, and the corresponding parameter, and, therefore, the additional information required to have a more robust and defensible assessment of the overall performance.

Total system performance assessments explicitly acknowledge the uncertainty in the process models and parameters and strive to evaluate the impact of this uncertainty on the overall performance. The aim of any total system performance assessment is to be as complete and reasonably conservative as possible and to ensure that the descriptions of the predictive models and parameters are sufficient to ascertain their accuracy. The EBS functions can be incorporated into a TSPA for appropriate evaluation of the impact on the performance of the system.

The overall philosophy of any assessment of total system performance is:

- To use models and parameters that are as representative as current information allows for those processes that may affect the predicted behavior of the system
- To predict the responses of the natural and engineered components of the system that are expected to result from the emplacement of wastes in the potential repository.

In those cases where representative information is not available or is very uncertain, bounding or conservative assumptions must be made, in order that the predicted performance is demonstrably worse than would be the case if more optimistic assumptions were included in the analyses. The performance assessment process requires the explicit treatment of uncertainty and variability of natural phenomena. The impact of the uncertainty is directly evaluated in the assessments themselves due to the stochastic nature of the analyses. In addition to evaluating the overall performance of the total system of engineered and natural barriers working in concert, an important objective of any predictive performance assessment modeling is to identify the significance of the current uncertainty in processes, models, and parameters on the performance. Those components that are most significant, and that are uncertain, are therefore identified as warranting additional information. This provides direct input to the site characterization and design programs to assist in prioritizing the necessary testing to develop more robust and defensible performance assessments. The results can also provide input to the evolving design of the waste package and repository design.

Repository Integration Program (RIP)

The performance assessment tool used in the analysis of EBS functions is the computer program RIP, (Repository Integration Program) which was the program used for TSPA-1995 in conjunction with detailed process-level models. The RIP was specifically developed by Golder Associates Inc. to evaluate the performance of a potential radioactive waste disposal facility at Yucca Mountain (Miller et al., 1992; Golder Associates, 1993). The program is fully documented in a Theory Manual and User's Guide (Golder Associates, 1994). The program has recently been formally verified consistent with ASME NQA-1 and ISO-9000 standards (Golder Associates, 1995).

The major features of the four component models of RIP (see Figure 3.1-2) that comprise the performance assessment model are:

- Waste package behavior and radionuclide release component model
- Radionuclide transport pathways component model
- Disruptive events model, and (4) biosphere dose/risk model.

These models are summarized briefly below.

The *waste package behavior and radionuclide release component model* input requirements are descriptions of the radionuclide inventories in the waste packages, a description of near-field environmental conditions (which may be defined as temporally and spatially variable), and subjective estimates of high-level parameters describing container failure, matrix alteration/dissolution, and radionuclide mass transfer. The waste package component model can simulate two layers of containment (i.e., outer package and zircalloy cladding). Waste package failure rates, along with matrix alteration/dissolution rates, are used to compute the rate at which radionuclides are *exposed.* Once exposed, RIP computes the rate of *mass transfer* out of and away from the waste package. Parameters describing waste package failure and radionuclide exposure and mass transfer can be described as a function of near-field environmental conditions. The output from this component (for

each system realization) consists of time histories of release for each radionuclide from the waste packages, and acts as the input for the transport pathways component.

The *radionuclide transport pathways component* model simulates radionuclide transport through the near and far field in a probabilistic mode. The RIP model uses a phenomenological approach that attempts to describe rather than explain the transport system. The resulting transport algorithm is based on a network of user defined *pathways*. The geosphere and biocell pathways reflect the major features of the hydrologic system and the biosphere, and are conduits through which transport occurs. The pathways may be used for both flow balance and radionuclide transport purposes, and may account for either gas or liquid phase transport. The purpose of a pathway is to represent large-scale heterogeneity of the hydrologic system, such as geologic structures and formation-scale hydrostratigraphy.

Geosphere pathways may be subdivided into *flow modes* that address heterogeneity at the local scale (e.g., flow in rock matrix, flow in fractures). The flow modes are primarily distinguished from one another based on flow velocity in the mode, although retardation parameters may also differ between flow modes.

The transport of radionuclides along a geosphere pathway is based on a *breakthrough curve*, which is calculated as a cumulative probability distribution for radionuclide travel times along the pathway. The breakthrough curve combines the effects of all flow modes and retardation on the radionuclide travel time, and determines the expected proportion of mass that has traversed the pathway by any specified time. The breakthrough curve is computed based on a Markov process algorithm for exchange between different flow modes.

The third performance assessment component model in RIP represents *disruptive events*. Disruptive events are defined as discrete occurrences that have some quantifiable effect on the processes described by the other two component models. Examples of disruptive events include volcanism, faulting, and human intrusion. The user first identifies all significant events (i.e., events that are both credible and consequential). Having done so, each event is assigned a rate of occurrence and, if desired, one or more descriptor parameters, which define the characteristics and magnitude of the event (e.g., length of a volcanic dike). Descriptor parameters may be described stochastically. Event occurrences are simulated as Poisson processes.

The user defines probability distributions for the event consequences (which may be functions of event descriptors). A consequence may take the form of a number of discrete responses (e.g., disrupting a number of waste packages, or moving radionuclides from some waste packages directly to the accessible environment). It is also possible for an event to directly modify parameters defined in the other two component models, and this capability can be used to specify long-term consequences (e.g., raising the water table or opening a new pathway). This capability was not used in the EBS performance assessment analyses presented herein.

The fourth performance assessment component model describes the fate and effect of radionuclides in the biosphere. The *biosphere dose/risk model* allows the user to define *dose receptors* in the system. Receptors receive radiation doses from specified geosphere (e.g., a water supply aquifer) or

biosphere (e.g., a pond, or flora, and fauna) pathways. Concentrations in these pathways are converted to radiation doses (or cancer risks) based on user-defined conversion factors.

As was indicated above, RIP was the program used for TSPA-1995 in conjunction with detailed process-level models. The next section (Section 3.1.1.1) summarizes the RIP results obtained for TSPA-1995 and compares them against several assumed requirements. Section 3.1.1.2 discusses the advances made in near-field thermohydrologic modeling since TSPA-1995, and includes RIP results that reflect these advances.

3.1.1.1 Total System Performance Assessment 1995 (TSPA-1995)

Of concern to this study are three aspects of the performance of the repository:

- Waste package containment requirement: "The fraction of waste packages breached at 1000 years shall be less than 1%..." This is currently a key assumption in the CDA (Key Assumption 038, CRWMS M&O 1996a). It is conservatively assumed that containment of radioactive waste ends when a single pit corrodes completely through the barriers of a waste package.

- 10,000 year peak dose rate requirement: This requirement results from the "Interim Postclosure Standard" (CRWMS M&O 1996c) which is assumed until a standard is promulgated for Yucca Mountain. This study will assume a 10,000 year, 15 mrem/yr peak dose rate requirement with dose calculations made for individuals drinking two liters of water per day from water wells located 30 km down gradient from the repository. These dose calculations are consistent with those employed in TSPA-1995. Furthermore, the 15 mrem/yr peak dose rate value should be shown to be met with at least a 50 percent probability.

- 1,000,000 year peak dose assessment: As indicated in the "Interim Postclosure Standard," assessments of repository performance shall be "...conducted past 10,000 years, out to the time of peak dose, in order to gain insight regarding longer-term repository performance" (CRWMS M&O 1996c). This portion of the "Interim Postclosure Standard" is being satisfied by addressing repository performance out to 1,000,000 years against a 15 mrem/year peak dose rate limit as defined by individuals drinking two liters of water per day from water wells located 30 km down gradient from the repository. Furthermore, it is assumed that the 15 mrem/year peak dose rate value should be shown to be met with at least a 50 percent probability.

The 10,000 year and 1,000,000 year peak dose performance will be indicated in terms of CCDF over the time period of interest. These plots indicate the probability of exceeding various values of peak dose rates as calculated at 30 km down-gradient from the potential repository. The following assumptions were made with regard to the 30 km case:

- A dilution factor of 25 in the saturated zone is applied, per the TSPA-1995 analysis (CRWMS M&O 1995d)

- Dispersivity in the SZ was not changed in the 30 km cases.

The following information summarizes the repository performance, as indicated in TSPA-1995 (CRWMS M&O 1995d), for the three categories of performance delineated above. In addition, the final subsection evaluates long-term repository performance against alternative hypothetical performance requirements. These alternative requirements have been selected as a means of depicting the sensitivity of long-term repository performance to variations of the "Interim Postclosure Standard." The selected alternative performance requirements apply to both 10,000 and 1,000,000 year time frames:

- No less than a 50 percent probability of not exceeding a peak dose rate of 15 mrem/year when measured from a water well located 5 km from the repository

- No less than a 90 percent probability of not exceeding a peak dose rate of 15 mrem/year when measured from a water well located 30 km from the repository.

Waste Package Containment Requirement

Corrosion of the outer barrier of the WPs is assumed to initiate only if its surface temperature is below 100°C and the relative humidity on the surface is greater than a threshhold value (usually 65-75 percent for humid air corrosion and 85-95 percent for aqueous corrosion). The corrosion of the inner barrier is always assumed to be due to aqueous corrosion. See Appendix B for additional details of the WP corrosion model employed here and in TSPA-1995 (CRWMS M&O 1995d). The waste package containment performance shown in this section and all subsequent sections was generated by use of the WAPDEG computer code.

Waste package containment performance is shown for:

- Thermal loading of 83 MTU/acre

- High infiltration rate (0.3 mm/year for thermohydrologic calculations, 1.25 mm/year for TSPA calculations)

- Corrosion initiation dependent on both the relative humidity and temperature characteristics of the waste package surface.

Figure 3.1-3 shows that for the case analyzed none of the WPs have first pit penetration until more than 2000 years after emplacement.

Figure 3.1-4 shows the benefits of cathodic (or galvanic) protection relative to performance of the waste package. Cathodic protection is protection afforded a more-noble metal or alloy by the corrosion of a less-noble metal or alloy in electrical contact exposed to the same corrosive electrolyte. This protection can eliminate or delay attack of the more-noble material. The degree of protection is a function of the differences in nobility of the materials as measured, for example, by a standard galvanic series in sea water, and the relative surface areas of the coupled materials. Also important

is the amount of polarization or passivation of the surfaces as corrosive attack progresses. The degree of protection is determined by performing prototypic tests involving material couples with the appropriate area ratios and electrolytes.

There exists a significant literature database on cathodic corrosion. However, these data were collected in short-time tests mostly under sea water, simulated sea water, or sodium chloride solutions. [See the Degradation Mode Survey - Galvanic Corrosion of Candidate Metallic Materials for High-Level Radioactive Waste Disposal Containers.] No data are available on expected repository conditions. Testing is being initiated to evaluate cathodic protection under a range of expected conditions. The emphasis will be on couples between the carbon steel corrosion-allowance outer barrier and Alloy 625, a nickel-base corrosion-resistant inner barrier. Other couples will also be tested. In advance of these tests, an elicitation (CRWMS M&O 1995h) was conducted that identified 75 percent remaining area of the less noble, corrosion-allowance material needed for cathodic protection to be viable. However, 50 percent remaining area was selected as a starting point for future total system performance calculations and sensitivity studies.

Figure 3.1-4 indicates the substantial improvement in waste package containment performance if credit is taken for the outer barrier of the waste package cathodically protecting the inner barrier until 50 percent of the outer barrier has corroded away. Figure 3.1-4 indicates that the first waste package would not breach until about 9000 years after emplacement when credit is taken for cathodic protection.

Figures 3.1-3 and 3.1-4 reflect, given our current understanding of the thermohydrology; waste package performance; and the NBS, that the ACD is predicted to satisfy the waste package containment requirement stated in Key Assumption 038 of the CDA Document (CRWMS M&O 1996a).

Repository Performance Compared to Interim 10,000 Year Peak Dose Standard

Repository performance is shown for:

- Thermal loading of 83 MTU/acre
- Infiltration rate of 0.3 mm/year for thermohydrologic calculations
- Infiltration rate uniformly sampled in the range of 0.5 to 2.0 mm/year for repository percolation
- Corrosion initiation dependent on both the relative humidity and temperature characteristics of the waste package surface.
- EBS transport conceptual model of "drips-on-waste-container" (page 9-7, CRWMS M&O 1995d) (Note: This is not the nominal TSPA-1995 case)
- Infiltration rate is affected by climatic changes (Section 7.7, CRWMS M&O 1995d).

The remaining basic inputs and assumptions are delineated in TSPA-1995 (CRWMS M&O 1995d).

Figure 3.1-5 presents a CCDF of repository performance, in terms of peak dose rate over a 10,000 year time frame. This CCDF indicates a 50 percent probability of not exceeding a peak dose rate of 0.0002 mrem/year and a 99 percent probability of not exceeding a peak dose rate of 0.08 mrem/year at 30 km from the repository. Taking credit for 50 percent cathodic protection improves repository performance such that no releases are predicted 30 km down gradient from the repository over a 10,000 year time frame (Note: Results for cathodic protection are not shown in Figure 3.1-5 due to no releases predicted). Taking performance credit for SNF cladding (CRWMS M&O 1996d) indicates an 80 percent probability of not exceeding a peak dose rate of 10^{-4} mrem/year.

In summary, current simulations indicate that the 10,000 year peak dose rate is less than the interim 10,000 year peak dose standard by just under five orders of magnitude, without taking credit for the conservative waste package performance assumption of 50 percent cathodic protection. Taking credit for this additional waste package performance results in a prediction of no release at 30 km from the repository over the 10,000 year time frame.

Repository Performance Over a 1,000,000 Year Time Frame

As with the 10,000 year time frame, repository performance is shown for:

- Thermal loading of 83 MTU/acre
- Infiltration rate of 0.3 mm/year for thermohydrologic calculations
- Infiltration rate uniformly sampled in the range of 0.5 to 2.0 mm/year for repository percolation flux
- Corrosion initiation dependent on both the relative humidity and temperature characteristics of the waste package surface
- EBS transport conceptual model of "drips-on-waste-container" (page 9-7, CRWMS M&O 1995d)
- Infiltration rate is affected by climatic changes (Section 7.7, CRWMS M&O 1995d).

Figure 3.1-6 presents a CCDF of 1,000,000 year peak dose rates. This CCDF indicates a 50 percent probability of not exceeding a peak dose rate of 1.5 mrem/year and a 99 percent probability of not exceeding a peak dose rate of 30 mrem/yr. Taking performance credit for SNF cladding (CRWMS M&O 1996d) indicates a 50 percent probability of not exceeding a peak dose rate of 0.3 mrem/year.

Repository Performance Compared to Alternative Hypothetical Performance Standards

No less than a 50 percent probability of not exceeding a peak dose rate of 15 mrem/year when measured from a water well located 5 km from the repository. Over the 10,000 year time frame the CCDF, see Figure 3.1-5, indicates a 50 percent probability of not exceeding 0.2 mrem/year. Taking performance credit for SNF cladding (CRWMS M&O 1996d) indicates a 50 percent probability of not exceeding a peak dose rate of $4x10^{-3}$ mrem/year. Over the 1,000,000 year time frame the CCDF, see Figure 3.1-6, shows only a 20 percent probability of not exceeding a peak dose rate of 15 mrem/year, and a 50 percent probability of not exceeding 45 mrem/year. Taking performance credit for SNF cladding indicates a 50 percent probability of not exceeding a peak dose rate of 6 mrem/year.

No less than a 90 percent probability of not exceeding a peak dose rate of 15 mrem/year when measured from a water well located 30 km from the repository. Over the 10,000 year time frame the CCDF, see Figure 3.1-5, indicates a 90 percent probability of not exceeding a total peak dose rate of 0.02 mrem/year and a 99 percent probability of not exceeding 0.08 mrem/year. Taking performance credit for SNF cladding (CRWMS M&O 1996d) indicates a 50 percent probability of not exceeding a peak dose rate of $3x10^{-3}$ mrem/year. Over the 1,000,000 year time frame the CCDF, see Figure 3.1-6, shows a 90 percent probability of not exceeding a total peak dose rate of 8 mrem/year and about a 95 percent probability of not exceeding 15 mrem/year. Taking performance credit for SNF cladding indicates a 50 percent probability of not exceeding a peak dose rate of 0.8 mrem/year.

Summary of Long-Term Repository Performance Results

Table 3.1-1 summarizes the repository performance against the various standards discussed above.

Table 3.1-1 Summary of Long-Term Repository Performance Results (mrem/year)

Time Frame (years)	Interim Postclosure Standard	Alternative Hypothetical Standards	
	15 mrem / 50% probability / 30 km	15 mrem/ 50% probability / 5 km	15 mrem / 90% probability / 30 km
10,000	0.0002	0.2	0.02
1,000,000	1.5	45	8

3.1.1.2 Updated Total System Performance Assessment

The results in Section 3.1.1.1 are very similar to those presented in TSPA-1995 (CRWMS M&O 1995d) for the "drips on waste package" case, with the exception that these results are for the accessible environment defined at 30 km. This section discusses the progress in modeling that has

taken place since TSPA-1995, and also gives an updated assessment of repository performance due to the recent modeling.

3-D Near-Field Thermohydrological Model

All previous studies of drift-scale (or sub-repository-scale) thermohydrological behavior [e.g., Buscheck et al. 1994; Buscheck and Nitao 1994a; Buscheck and Nitao 1994b; Buscheck et al. 1995; Ho and Francis 1996] have used two-dimensional cross-sectional models that average the heat output from rows of WPs into a uniform line-heat load. This is the type of thermohydrological analysis that has been used as input to total system performance assessments. However, this assumption can distort the representation of thermohydrological behavior in and around emplacement drifts for realistic WP emplacement scenarios, particularly those involving large axial WP spacing and/or a large variation in heat output from WP to WP. For such scenarios, three-dimensional calculations are required to adequately represent drift-scale thermal-hydrological behavior [Buscheck et al. 1996]. This is particularly true for the ACD Report case (CRWMS M&O 1996b), which has large axial WP spacing and a WP inventory with a large degree of heat output variability from WP to WP. To carry out such calculations, a three-dimensional, drift-scale, multiple-WP model, based on the NUFT code (Buscheck et al. 1996) was developed.

For all of the calculations, the atmospheric relative humidity is assumed to be 100 percent, so the model allows no loss of moisture by vapor diffusion to the atmosphere. Because actual (desert) relative humidity is much lower than 100 percent, the model under represents this loss. This neglected loss may be large for high areal mass loadings (AMLs), which can steepen the temperature gradient near the ground surface by a factor of 50 relative to ambient conditions. The effect of this assumption is offset (to some degree) by the assumption of zero percolation flux made in some of the calculations. All of the drift-scale and hybrid models used in this analysis assumed that the water table is fixed at a constant temperature, liquid saturation, and pressure. The remainder of the inputs and assumptions employed in this analysis are described in the *Near Field and Altered Zone Environment Report* (CRWMS M&O 1996n).

A mixture of WP types has been examined, ranging from those containing very hot SNF to thermally cool DHLW. The three-dimensional, multiple-WP model includes six major waste forms (Table 3.1-2), resulting in a WP inventory that is representative of that assumed for the ACD concept, including four SNF WP types:

- "Very hot" 10-yr-old "design basis fuel" WPs (comprising 10 percent of the WPs in the model)
- "relatively cool" 40-yr-old pressurized water reactor (PWR) WPs (20 percent of the WPs),
- Nominal 26-yr-old PWR WPs (20 percent of the WPs)
- Nominal 26-yr-old boiling water reactor (BWR) WPs (20 percent of the WPs), and two types of DHLW, including those from the Hanford site (10 percent of the WPs) and those from the Savannah River site (20 percent of the WPs).

Note that the ACD assumes that 27 percent of the WPs are DHLW WPs (Key Assumption 003, CRWMS M&O 1996a), while for the three-dimensional, multiple-WP model, 30 percent of the WPs are assumed to be DHLW WPs.

The spacing of the WPs, and the spacing between the emplacement drifts, is as shown in Figure 3.1-7. This is representative of that assumed in the ACD Report (see Figure 8.2.8-4, CRWMS M&O 1996b), which reflects a lineal mass loading (LML) of 0.46 MTU/m, and a spacing between emplacement drifts of 22.5 meters.

Before showing the results of the 3-D near-field thermohydrological model, the results of two relevant sensitivity studies will be presented. The purpose of presenting these study results is to indicate the relative sensitivity of the WP surface environment to variations in a few parameters. Doing this up-front will allow for solid, general conclusions to be reached employing a single set of parameters, and avoid extensive parametric studies. The parameters addressed in these sensitivity studies are:

- Emplacement drift diameter/location of WPs relative to the centerline of the emplacement drift
- Quartz sand or crushed tuff emplacement drift invert.

Sensitivity of WP Surface Environment to Emplacement Drift Diameter and WP Position Relative to Centerline of Emplacement Drift

As was discussed in Section 3.1, the emplacement drift diameter employed in the ACD is 5.0 meters, and the WP emplacement within the emplacement drift is CID. However, if a need were identified to be able to accommodate emplacement drift backfill, a larger drift diameter (discussed in Section 5.2.1) on the order of 5.5 meters as well as an off-center-in-drift (OCID) WP emplacement mode would be required. Whether the WPs are emplaced CID in a 5.0 meter diameter drift, or OCID in a 5.5 meter diameter drift, a thermal analysis (CRWMS M&O 1996d) conducted in support of this study indicates very little difference with regard to WP surface temperatures. These results, which are discussed in Section 5.2.4.1 and illustrated in Figure 5.2-9, indicate that the WP surface temperature differences between the two cases amounts to a maximum of 5°C at very early times, and diminishes to essentially 0°C by 100 years. It is judged that these small temperature differences will translate into correspondingly small relative humidity differences.

Sensitivity of WP Surface Environment to the Use of Either Quartz Sand or Crushed Tuff Invert

Figure 3.1-8 reflects the time history of relative humidity on both the upper and lower WP surfaces as a function of whether the invert is composed of TSw2 tuff or quartz sand. The calculations were performed with NUFT in a two-dimensional model that averages the heat output from a mixture of 26-yr-old BWR and 26-yr-old PWR WPs into a uniform line-heat load. This figure reflects an OCID emplacement, drift diameter of 5.5 meters, WP emissivity = 0.3, and ambient percolation flux of 0.3 mm/yr. Curves are plotted for two invert types:

- TSw2 gravel with bulk permeability (k_b) = 10 darcy, and the thermal conductivity (K_{th}) of the material = 0.6 W/mK

- Sand with k_b = 10 darcy and K_{th} = 0.6 W/mK.

The figure indicates that the invert material composition influences the WP surface relative humidity by as much as about 8.5 percent (at 400 years) and then tapers off to negligible differences by about 800 years. With respect to waste package corrosion, these maximum relative humidity differences (8.5 percent at 400 years) are inconsequential since the WP surface temperatures do not drop below 100°C until at least 1000 years (see Figure 3.1-13). Recall that this study assumes corrosion on the waste packages can only initiate when the surface temperature drops below 100°C. By the time the surface temperatures are below 100°C, the relative humidity differences are negligible.

Near-Field Thermohydrologic Results

Using the three-dimensional, multiple-WP model (using the NUFT code), the WP inventory listed in Table 3-1.1, the WP spacing as depicted in Figure 3.1-7, and an assumed ambient percolation flux of 0.3 mm/yr, Figures 3.1-9 through 3.1-12 indicate the resulting WP surface relative humidity and temperature profiles over 100, 2,000, 10,000, and 100,000 years, respectively. These results were obtained for a thermal loading of 83 MTU/acre, sand invert, 5.5 meter emplacement drift diameter, a percolation flux of 0.3 mm/year, and a WP emissivity of 0.8. Figure 3.1-13 shows the temperature and relative humidity histories for several of the WPs on a logarithmic scale.

These results indicate fairly large surface temperature differences among the WPs at early times, with these differences diminishing to very small values by 2,000 years. On the other hand, the surface relative humidity differences among the various WPs are generally large at early times and continue to be noticeably different out to 10,000 years and beyond. However, because of the way in which corrosion initiation on the WPs is currently modeled (see Section 3.1.1.1 and Appendix B), these fairly large thermohydrological differences do not cause large differences in failure rates of the WPs due to corrosion. This is discussed in more detail in the next section.

Waste Package Containment Requirement

Figure 3.1-14 depicts the predicted first pit penetration results for several of the waste forms indicated in Figure 3.1-13. The 10-yr-old "design basis fuel" PWR and the Hanford DHLW WPs were selected because they are the bounds for both the temperature and relative humidity profiles indicated in Figure 3.1-13. The average 26-yr-old BWR WP was also selected to represent an intermediate case. A comparison of Figures 3.1-13 and 3.1-14 shows that, despite the large variations among the WPs in terms of their surface relative humidity and temperature histories, there is little difference in their failure rates over time. The reason for the similar failure rates is that the WP temperature histories converge such that they reach 100°C at similar times. Since corrosion of a WP is modeled to initiate only when its surface temperature drops below 100°C, all of the large early-time variations in temperature profiles among the various WPs has no effect on overall WP performance. Thus, the WP first pit penetration results, as shown in Figure 3.1-14, are very similar for the three WP types. Furthermore, these results reveal that containment is achieved for more than 1000 years.

Table 3.1-2 Heating Characteristics of Waste Packages Represented in 3-D, Drift-Scale, Multiple-WP Model

Waste Package Type	Percentage of WP Inventory in Model	SNF Age (years)	MTU/WP	Burnup (GWD/MTU)	Enrichment (%)	Initial WP Heat Output (kW)
Hanford Site DHLW	10	N/A	2.15	N/A	N/A	1.56
Savannah River Site DHLW	20	N/A	2.15	N/A	N/A	2.84
Small 40-yr-old PWR	20	40	4.67	35,455	3.4	3.18
Large "average" 26-yr-old BWR	20	26	7.07	33,100	3.01	6.14
Large "average" 26-yr-old PWR	20	26	8.83	41,500	3.82	9.16
Design Basis Fuel 10-yr-old PWR	10	10	9.74	48,086	4.2	17.85

Repository Performance Compared to Interim 10,000 Year Peak Dose Standard

The similarities in the WP failure distributions shown in Figure 3.1-14 led to the implementation of a single failure distribution for all of the waste forms considered. The results that will be shown in this section reflect the 26-yr-old BWR failure curve as well as a blended radionuclide inventory representative of a mix of waste packages to be emplaced in the repository. The inventories were developed using revision 1 of the Characteristics Data Base Radiological (CRWMS M&O 1993), and are presented in Table 3.1-3. The percentages used for the blended inventory were as follows:

- 10 percent : DHLW - this is consistent with the value used in TSPA-1995 (CRWMS M&O 1995d)

- 90 percent : SNF - which is further broken down as follows:

  - 32 percent : 26-yr-old BWR
  - 43 percent : 26-yr-old PWR
  - 21 percent : 40-yr-old PWR
  - 4 percent : 10-yr-old PWR.

It should be noted that the TSPA-1995 inventory used for Hanford DHLW was a blended inventory of glass waste.

The results for the 10,000 year CCDF of peak dose rate for the no backfill ACD case are presented in Figure 3.1-15. These RIP analyses assume 26 yr old BWR temperatures and failure curves, and a blended inventory. The results are presented for both the 5 km and 30 km accessible environments.

For comparison, the TSPA-1995 case with similar assumptions is presented. The inventories are slightly different in the two cases as shown in Table 3.1-3. Also, the sampling sequence is different between TSPA-1995 and the current calculations which leads to slightly different results. Given the uncertainty in the overall calculations, the results differential caused by the sampling sequence is not significant. The ACD peak dose rate at the 5 km accessible environment is slightly lower than the TSPA-1995 base case at 10,000 years. Calculating the peak dose rate at 30 km instead of at the 5km boundary results in an approximately two and one-half order of magnitude decrease in the peak dose rate. This decrease is due to both the increased travel time in the SZ (6 fold longer) and the additional dilution in the SZ (factor of 25).

Figure 3.1-15 shows that, for predictions of peak dose rates at 30 km from the repository, there is a 70 percent probability of not exceeding a peak dose rate of 10^{-4} mrem/year and a 99 percent probability of not exceeding 0.04 mrem/year.

As was the case in Section 3.1.1.1, taking credit for the additional waste package performance associated with the outer barrier cathodically protecting the inner barrier until 50 percent of the outer barrier has degraded away, results in predictions of no releases at 30 km from the repository over the 10,000 year time frame.

Table 3.1-3 Radionuclide Inventories Used in Analyses (ci/pkg)

Radionuclide	TSPA-1995 SNF	TSPA-1995 DHLW	26 yr BWR	26 yr PWR	40 yr PWR	10 yr PWR	Blended Inventory
^{227}Ac	1.79e-04	6.02e-04	1.76e-05	1.71e-04	2.05e-05	2.00e-04	2.50e-05
^{241}Am	3.73e+04	8.65e+01	3.80e+03	3.70e+04	4.05e+03	3.94e+04	4.16e+03
^{242M}Am	2.16e+02	2.06e-02	2.44e+01	2.38e+02	2.33e+01	2.27e+02	1.63e+01
^{243}Am	2.48e+02	3.67e-02	2.78e+01	2.71e+02	2.92e+01	2.84e+02	2.14e+01
^{14}C	1.38e+01	0.00e+00	1.60e+00	1.56e+01	1.43e+00	1.39e+01	1.32e+00
^{36}Cl	1.11e-01	0.00e+00	1.16e-02	1.13e-01	1.20e-02	1.17e-01	1.12e-02
^{244}Cm	1.16e+04	1.14e+01	1.35e+03	1.31e+04	1.48e+03	1.44e+04	4.20e+02
^{245}Cm	3.36e+00	5.64e-05	3.96e-01	3.86e+00	4.57e-01	4.45e+00	2.39e-01
^{246}Cm	6.95e-01	6.39e-06	8.34e-02	8.12e-01	1.01e-01	9.84e-01	4.79e-02
^{135}Cs	5.13e+00	1.15e-01	5.33e-01	5.19e+00	5.85e-01	5.70e+00	4.60e-01
^{129}I	3.43e-01	1.90e-06	3.32e-02	3.23e-01	3.94e-02	3.84e-01	3.38e-02
^{93M}Nb	1.82e+01	5.48e-01	1.94e+00	1.89e+01	2.00e+00	1.95e+01	1.98e+00
^{94}Nb	8.24e+00	3.02e-05	1.02e-01	9.93e-01	1.30e+00	1.27e+01	1.12e+00
^{59}Ni	2.36e+01	2.70e-02	1.85e+00	1.80e+01	2.87e+00	2.80e+01	2.70e+00
^{63}Ni	3.10e+03	0.00e+00	2.34e+02	2.28e+03	3.83e+02	3.73e+03	3.08e+02
^{237}Np	4.35e+00	2.83e-02	3.93e-01	3.83e+00	5.34e-01	5.20e+00	4.38e-01
^{231}Pa	3.30e+04	9.74e-04	3.21e-05	3.13e-04	3.74e-05	3.64e-04	3.83e-05
^{210}Pb	6.75e-06	2.72e-08	6.30e-07	6.14e-06	7.48e-07	7.29e-06	2.52e-06
^{107}Pd	1.26e+00	0.00e+00	0.00e+00	0.00e+00	0.00e+00	0.00e+00	0.00e+00
^{238}Pu	3.05e+04	4.00e+02	2.99e+03	2.91e+04	3.87e+03	3.77e+04	2.25e+03
^{239}Pu	3.56e+03	4.73e+00	3.28e+02	3.19e+03	4.02e+02	3.92e+03	3.63e+02
^{240}Pu	5.26e+03	3.30e+00	5.06e+02	4.93e+03	6.08e+02	5.92e+03	5.26e+02
^{241}Pu	3.39e+05	1.48e+02	3.44e+04	3.35e+05	3.68e+04	3.58e+05	1.26e+04
^{242}Pu	2.01e+01	5.02e-03	2.15e+00	2.09e+01	2.23e+00	2.17e+01	1.89e+00
^{226}Ra	2.50e-05	9.37e-08	2.31e-06	2.25e-05	2.77e-06	2.70e-05	6.74e-06
^{228}Ra	3.10e-09	0.00e+00	2.84e-10	2.77e-09	3.59e-10	3.50e-09	5.72e-10
^{79}Se	4.41e+00	9.18e-02	4.18e-01	4.07e+00	5.10e-01	4.97e+00	4.37e-01
^{151}Sm	3.53e+03	0.00e+00	3.42e+02	3.33e+03	3.98e+02	3.88e+03	2.93e+02

Table 3.1-3 Radionuclide Inventories Used in Analysis (ci/pkg) (continued)

Radionuclide	TSPA-1995 SNF	TSPA-1995 DHLW	26 yr BWR	26 yr PWR	40 yr PWR	10 yr PWR	Blended Inventory
^{126}Sn	8.50e+00	0.00e+00	8.25e-01	8.04e+00	9.82e-01	9.56e+00	8.33e-01
^{99}Tc	1.40e+02	3.30e+00	1.34e+01	1.31e+02	1.60e+01	1.56e+02	1.40e+01
^{229}Th	3.54e-06	1.51e-05	3.69e-07	3.59e-06	4.63e-07	4.51e-06	4.49e-07
^{230}Th	3.59e-03	1.24e-05	3.31e-04	3.22e-03	3.99e-04	3.89e-03	6.22e-04
^{232}Th	4.35e-09	1.05e-04	3.97e-10	3.87e-09	5.04e-10	4.91e-09	7.02e-10
^{233}U	7.01e-04	5.84e-04	6.22e-05	6.06e-04	8.61e-05	8.39e-04	1.04e-04
^{234}U	1.34e+01	5.00e-02	1.25e+00	1.22e+01	1.51e+00	1.47e+01	1.50e+00
^{235}U	1.68e-01	7.93e-05	1.46e-02	1.42e-01	1.77e-02	1.72e-01	1.76e-02
^{236}U	2.72e+00	4.35e-04	2.46e-01	2.40e+00	3.14e-01	3.06e+00	2.73e-01
^{238}U	3.07e+00	3.78e-03	3.17e-01	3.09e+00	3.13e-01	3.05e+00	3.16e-01
^{93}Zr	2.38e+01	7.01e-01	2.53e+00	2.46e+01	2.61e+00	2.54e+01	2.24e+00

Notes:

SNF pkg has 9.74 MTHM/pkg.
Blended inventory percentages:
SNF: 26 yr BWR = 32%
26 yr PWR = 43%
40 yr PWR = 21%
10 yr PWR = 4%
DHLW: 10% of total repository.

WP Type	Burnup (GWd/MTU)	enrichment (%)	age (years)	# of assemblies/pkg
26 yr BWR	33.1	3.01	25.9	44
26 yr PWR	41.5	2.82	26.0	21
40 yr PWR	35.46	3.4	40	12
10 yr PWR	48.086	4.2	10.	21

Repository Performance Over a 1,000,000 Year Time Frame

For the 1,000,000 year peak dose rate results, the CCDFs for several ACD cases are presented in Figure 3.1-16. The comparable result from TSPA-1995 (83 MTU/acre; drips on WP) is also presented in the figure. The ACD results at the 5 km accessible environment show the highest dose rates, approximately an order of magnitude higher than the TSPA-1995 results. This is due to the earlier waste package failure and higher pitting rates in the ACD case compared to the TSPA-1995 case. The effect of the location of the accessible environment is again shown in this plot. Moving the AE to 30 km and calculating the dose at that location causes a reduction by a factor of 25 in the peak dose relative to the ACD case. This is exactly the dilution factor applied in the SZ. The travel time effect observed in Figure 3.1-15 is not significant over the 1,000,000 year time period.

Figure 3.1-16 shows that, for predictions of peak dose rate at 30 km from the repository and without taking any performance credit for cathodic protection, there is a 50 percent probability of not exceeding a peak dose rate of 10 mrem/year, a 90 percent probability of not exceeding 40 mrem/year, and a 99 percent probability of not exceeding 120 mrem/year. Assuming a performance credit for 50 percent cathodic protection results in a 50 percent probability of not exceeding 0.6 mrem/year, a 90 percent probability of not exceeding 2 mrem/year, and a 99 percent probability of not exceeding 5 mrem/year.

Repository Performance Compared to Alternative Hypothetical Performance Standards

As was discussed in Section 3.1.1.1, alternative hypothetical performance standards were selected to demonstrate the sensitivity of long-term repository performance to variations of the "Interim Postclosure Standard."

No less than a 50 percent probability of not exceeding a peak dose rate of 15 mrem/year when measured from a water well located 5 km from the repository. Over the 10,000 year time frame the CCDF, see Figure 3.1-15, indicates a 50 percent probability of not exceeding a total peak dose rate of 0.02 mrem/year, and about a 99 percent probability of not exceeding 15 mrem/year. Over the 1,000,000 year time frame the CCDF, see Figure 3.1-16, shows a 50 percent probability of not exceeding 270 mrem/year, and only about a 10 percent probability of not exceeding a peak dose rate of 15 mrem/year.

No less than a 90 percent probability of not exceeding a peak dose rate of 15 mrem/year when measured from a water well located 30 km from the repository. Over the 10,000 year time frame the CCDF, see Figure 3.1-15, indicates a 90 percent probability of not exceeding a total peak dose rate of 0.003 mrem/year and a 99 percent probability of not exceeding 0.04 mrem/year. Over the 1,000,000 year time frame the CCDF, see Figure 3.1-16, shows a 70 percent probability of not exceeding a total peak dose rate of 15 mrem/year and a 90 percent probability of not exceeding 45 mrem/year.

3.1.2 POSTCLOSURE PERFORMANCE CONCLUSIONS FOR ACD CONCEPT

Predicted postclosure performance of the repository is summarized here in terms of waste package containment as well as peak dose calculations at 30 km from the repository over 10,000 and 1,000,000 year time frames.

The current estimation of WP performance is that any breaches due to corrosion (breaches defined as a single corrosion pit penetrating through the outer and inner barriers) will not occur until around 1200 years (Figure 3.1-14). Therefore, WP performance is currently predicted to satisfy the WP containment requirement delineated in Key Assumption 038 of the CDA (CRWMS M&O 1996a): "The fraction of waste packages breached at 1000 years shall be less than 1%..."

Current predictions of peak dose values at 30 km from the repository over a 10,000 year time frame, taking no credit for WP cathodic protection, indicate that repository performance satisfies the "Interim Postclosure Standard" by almost five orders of magnitude. Additional assurance is obtained by recalling that the above quantitative performance assessment does not reflect benefit from cathodic protection, although substantial improvements in long-term performance are predicted for this barrier.

Current predictions of peak dose rate values at 30 km from the repository over a 1,000,000 year time frame, again taking no quantitative credit for cathodic protection, indicate satisfaction of an assumed 15 mrem/year maximum allowable peak dose rate requirement. Taking advantage and performance credit for the cathodic protection inherent in the current waste package conceptual design results in a 50 percent probability that the peak dose rate seen at 30 km from the repository will not exceed 0.6 mrem/year, and a 90 percent probability that it will not exceed 2mrem/year, better than an order of magnitude improvement in predicted repository performance over the non-cathodic protection case.

Table 3.1-4 summarizes the repository performance against the various standards discussed above.

Table 3.1-4 Summary of Long-Term Repository Performance Results (ACD) (mrem/year)

Time Frame (years)	Interim Postclosure Standard	Alternative Hypothetical Standards	
	15 mrem / 50% probability / 30 km	15 mrem/ 50% probability / 5 km	15 mrem / 90% probability / 30 km
10,000	$<<10^{-4}$	0.02	0.003
1,000,000	10	270	45

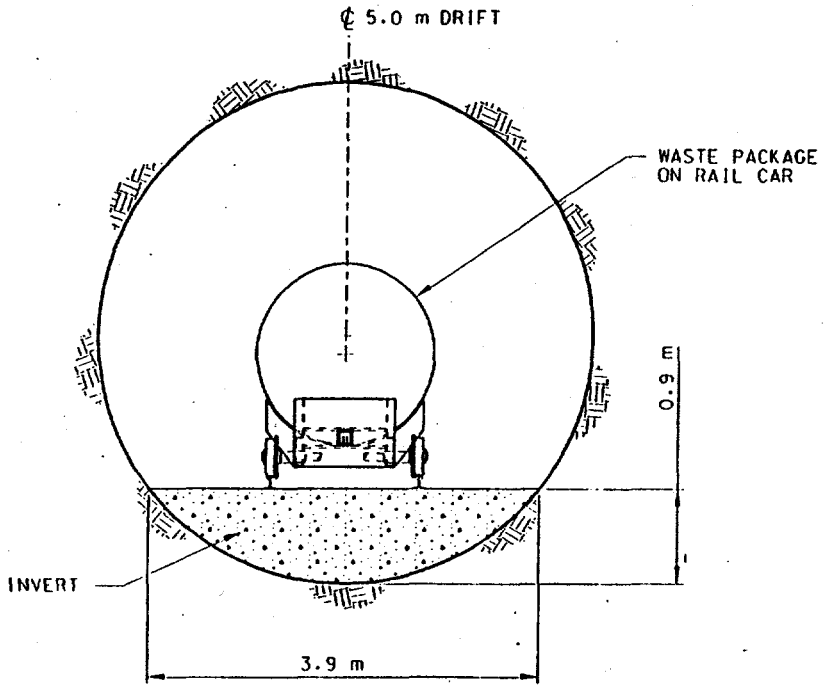

Figure 3.1-1a Center In-Drift Emplacement Mode

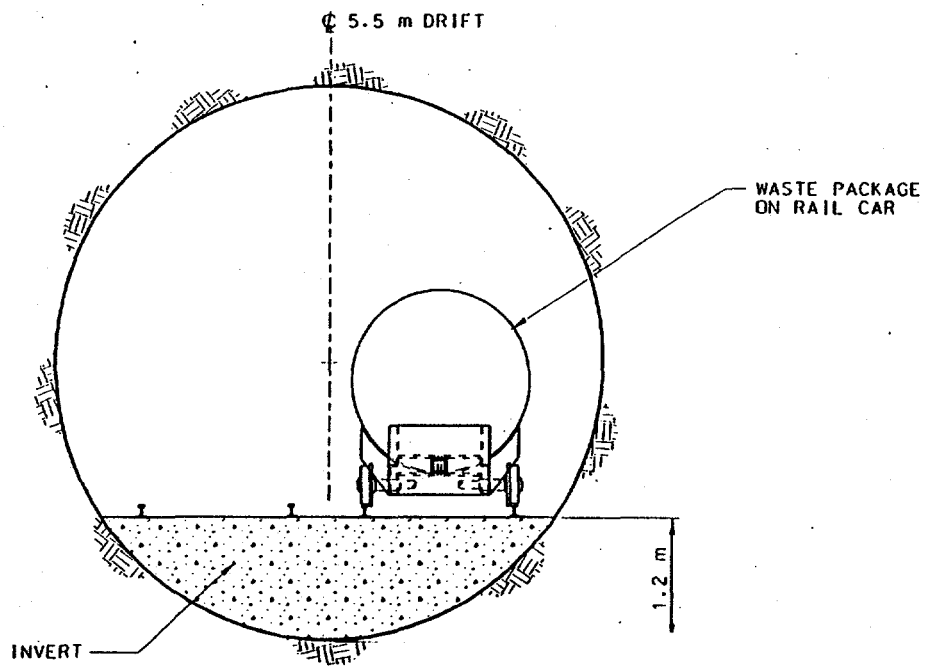

Figure 3.1-1b Off-Center-In-Drift Emplacement Mode

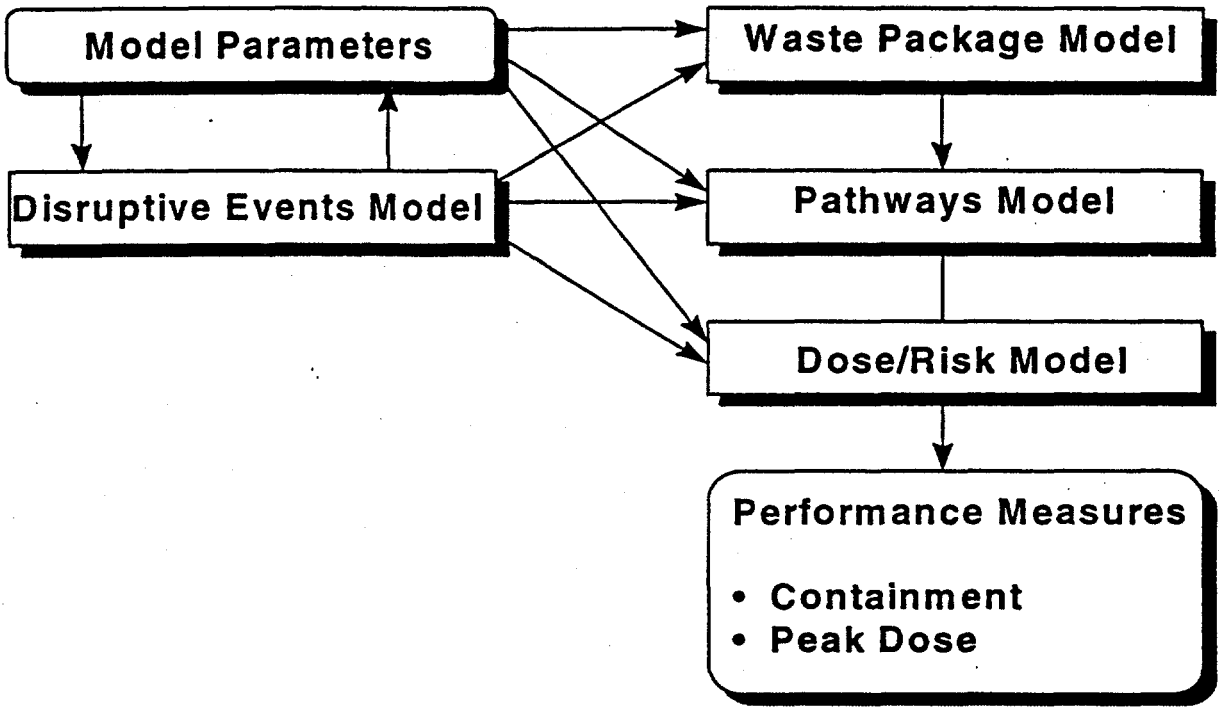

Figure 3.1-2 RIP Total System Performance Assessment Model Components

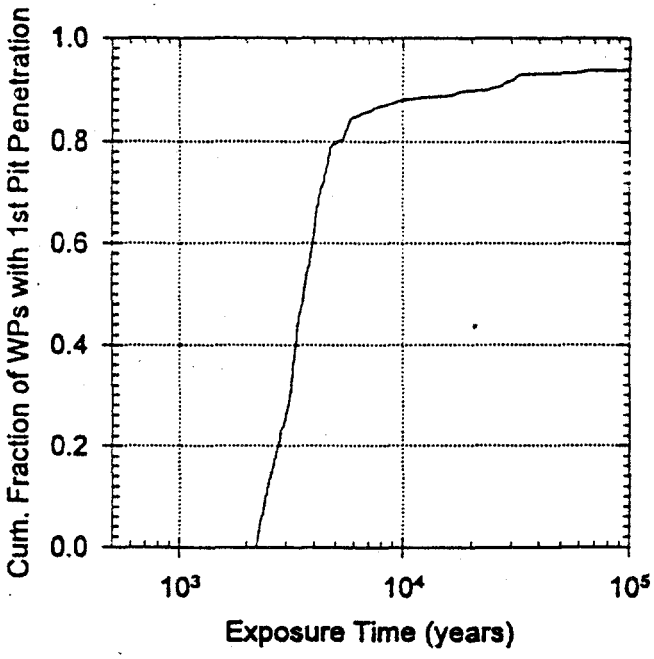

Figure 3.1-3 Waste package failure history for the case of 83 MTU/acre, high infiltration, and without backfill, using Relative Humidity (RH) and temperature switch for corrosion initiation

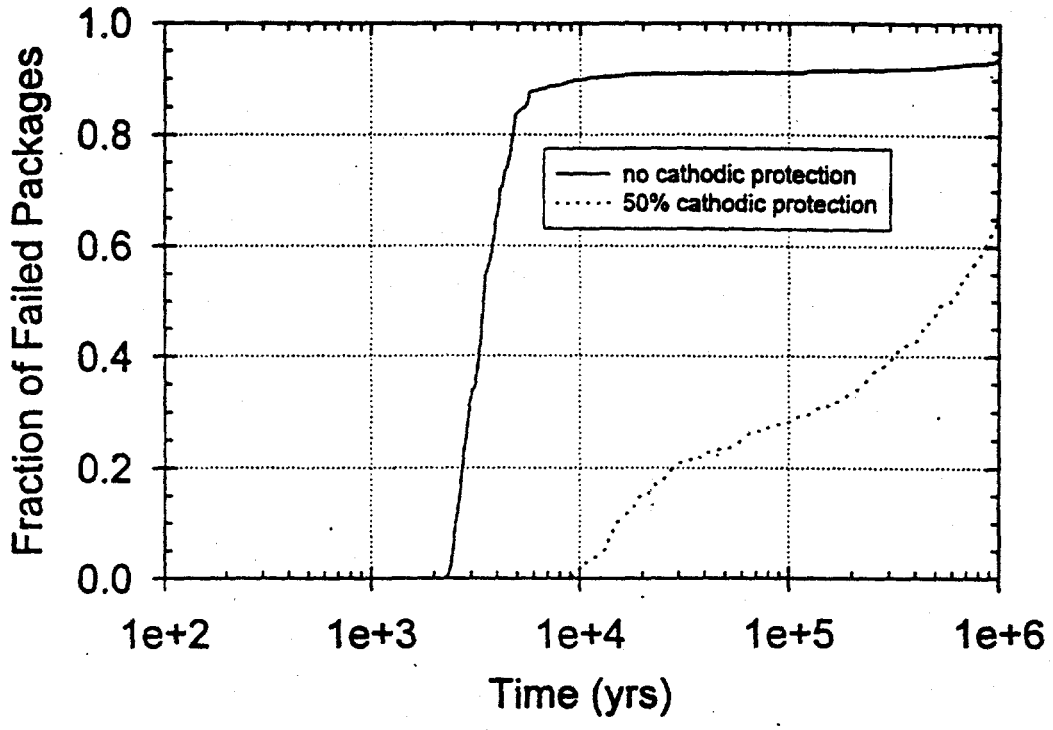

Figure 3.1-4 Waste package failure history for the case of 83 MTU/acre, high infiltration, without backfill, with 50% cathodic protection, using RH and temperature switch for corrosion initiation

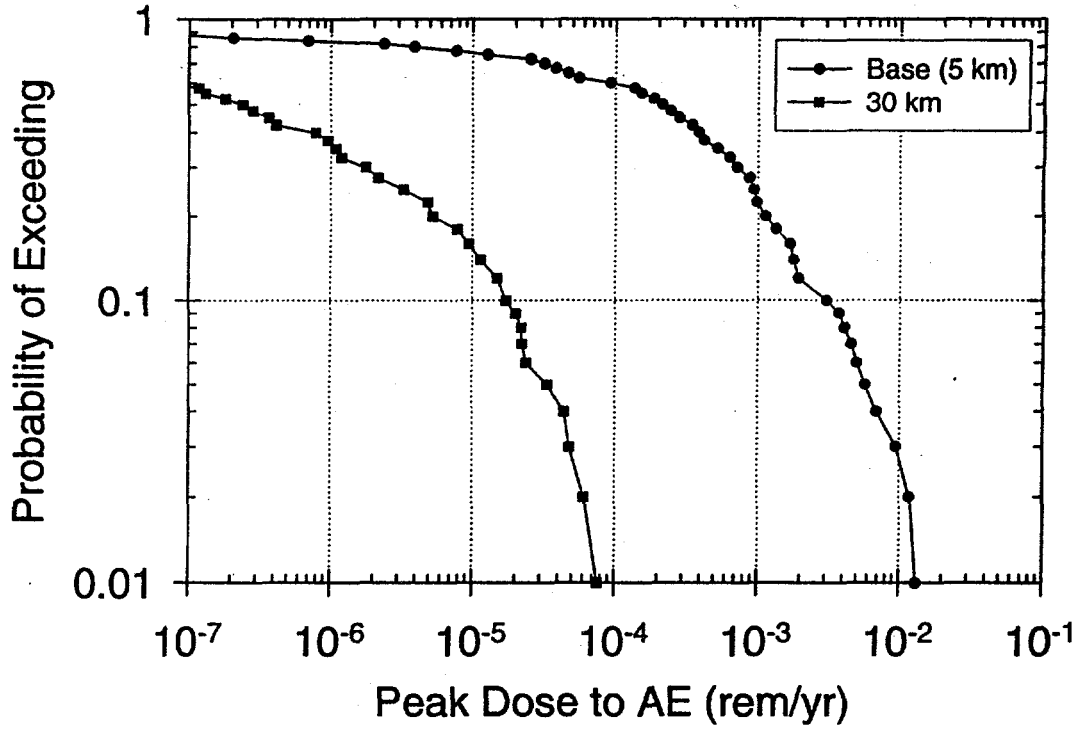

Figure 3.1-5 10,000 year total peak dose for base case at 5km and at 30 km

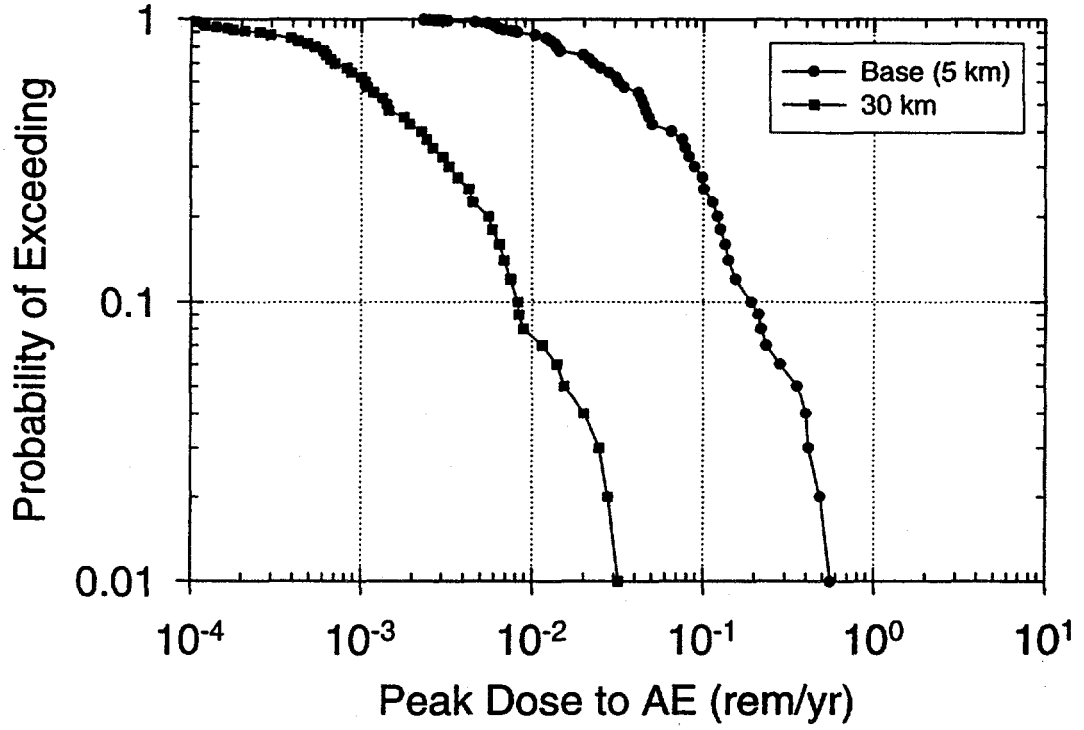

Figure 3.1-6 1,000,000 year total peak dose for base case at 5km and at 30 km

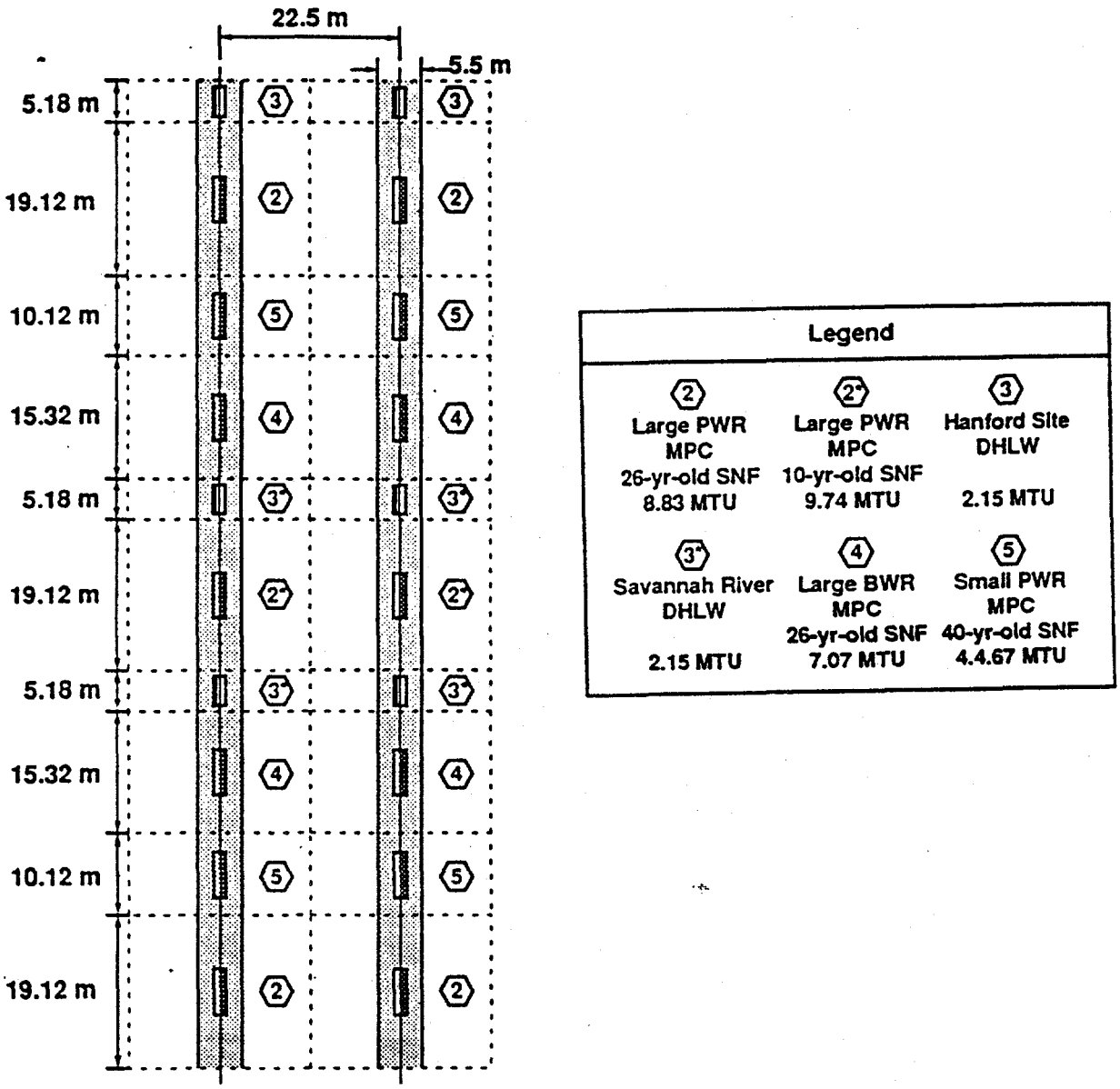

Figure 3.1-7 Plan view of waste package configuration represented by the 3-D, multiple-WP model for the ACD case

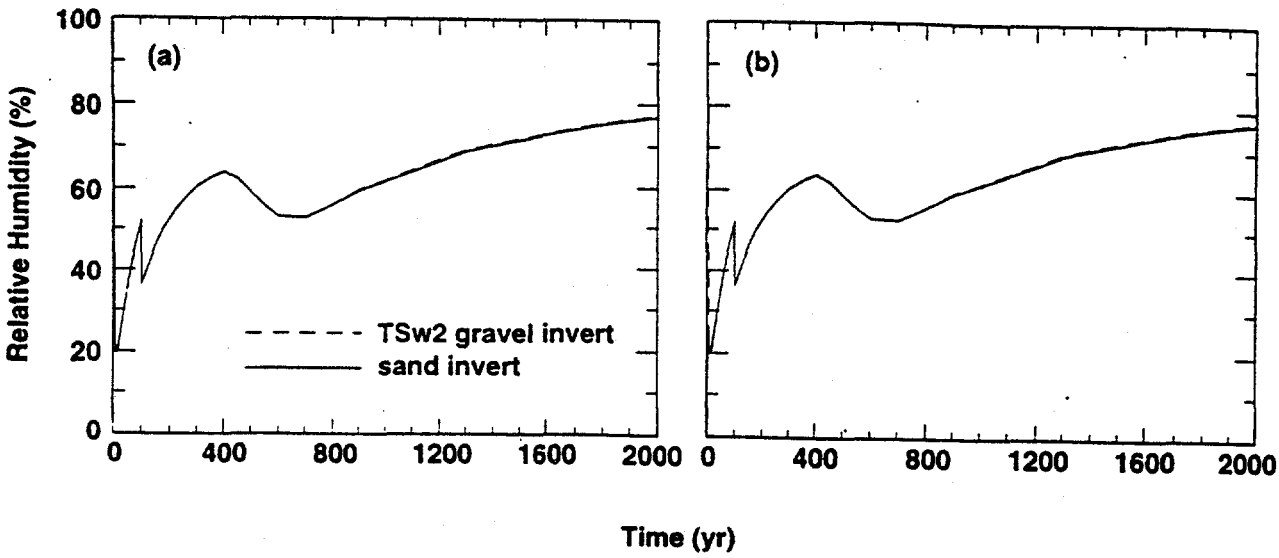

Figure 3.1-8 Relative humidity on upper (a) and lower (b) waste package surface for the ACD case with calculations performed by 2-D model that averages the heat output from a mixture of 26-yr-old BWR and PWR WPs into a uniform line-heat load

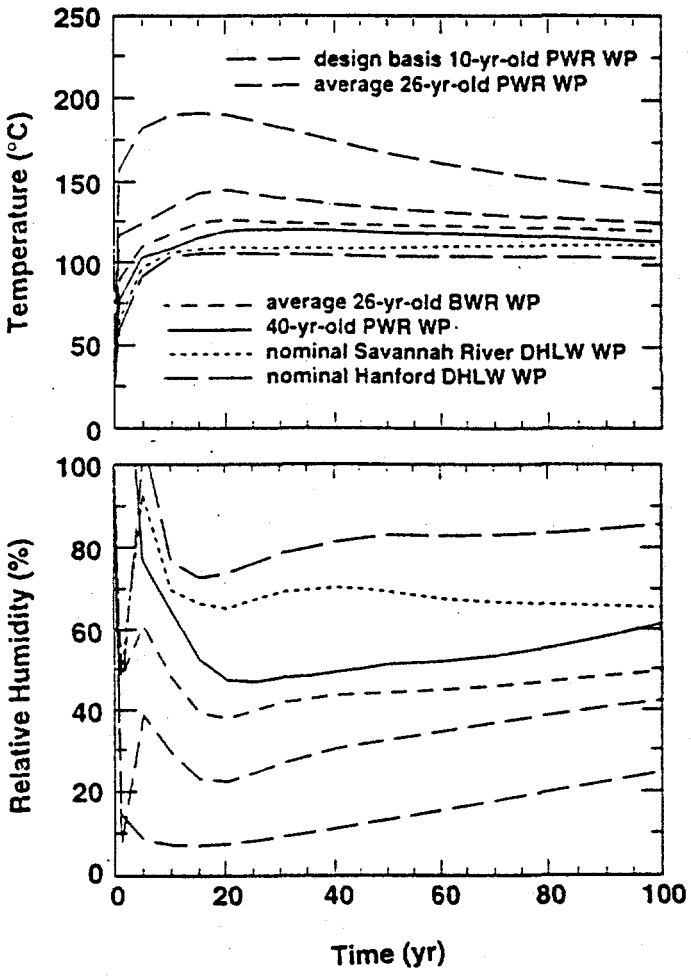

Figure 3.1-9 100 year temperature and relative humidity profiles on upper waste package surface for ACD case using 3-D, multiple-WP NUFT model

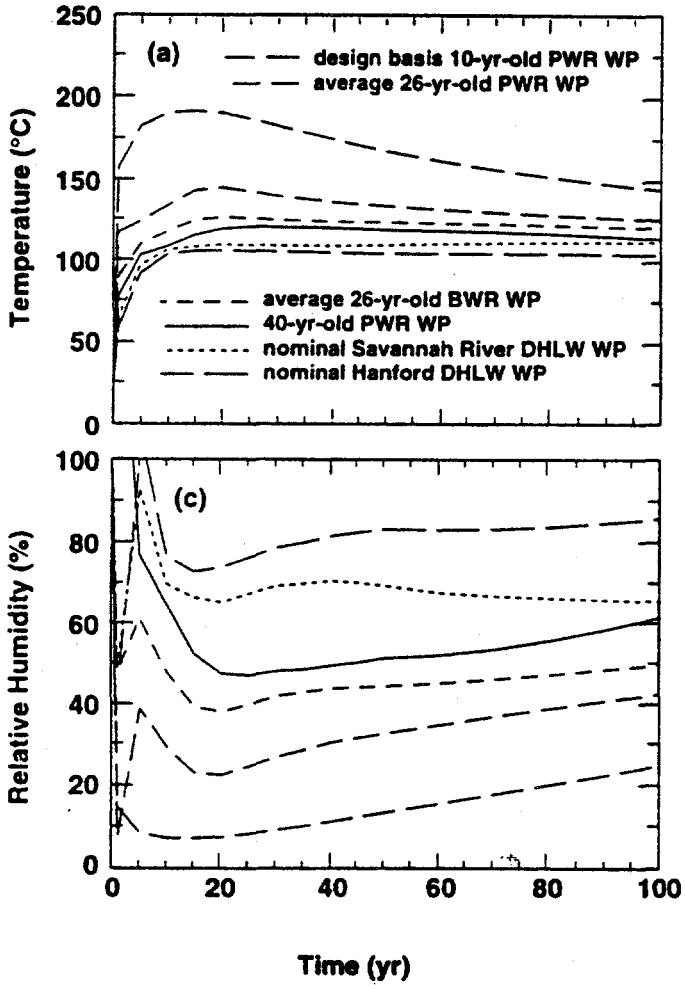

Figure 3.1-10 2000 year temperature and relative humidity profiles on upper waste package surface for ACD case using 3-D, multiple-WP NUFT model

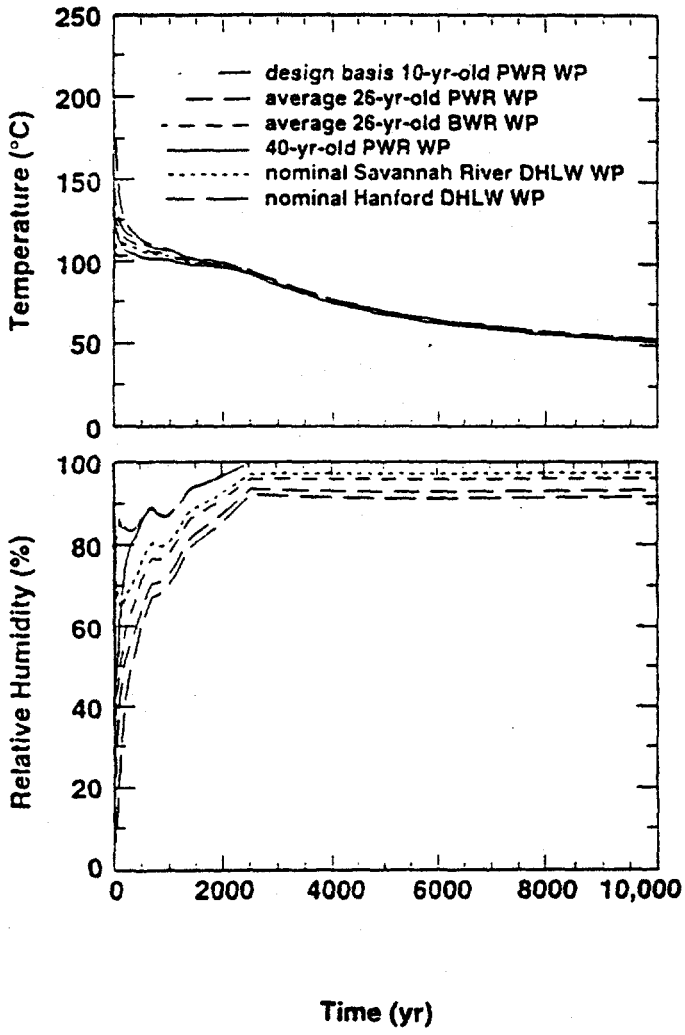

Figure 3.1-11 10,000 year temperature and relative humidity profiles on upper waste package surface for ACD case using 3-D, multiple NUFT model

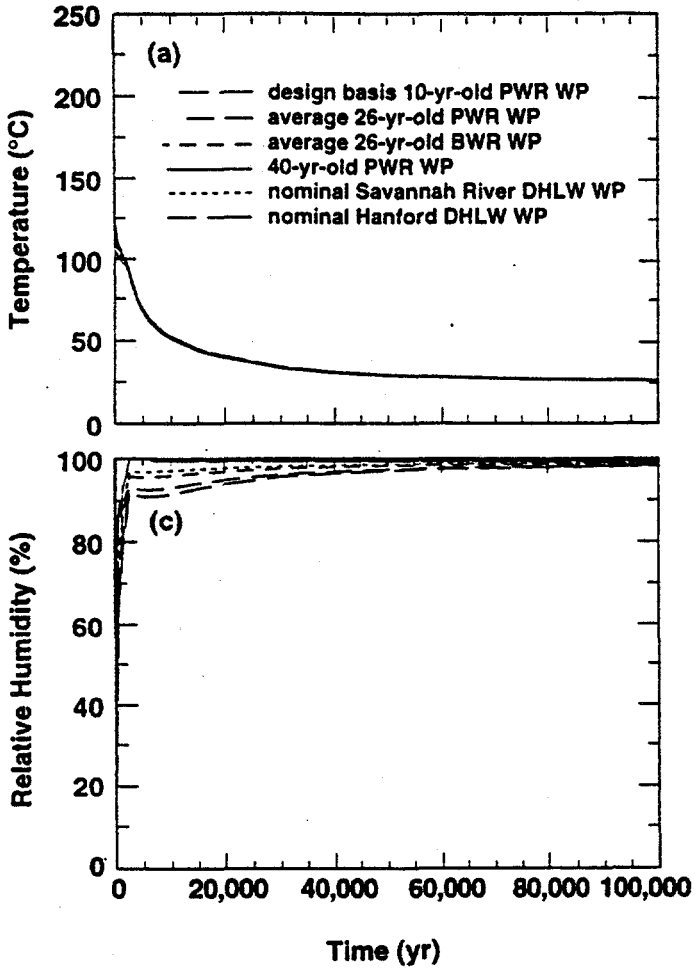

Figure 3.1-12 100,000 year temperature and relative humidity profiles on upper waste package surface for ACD case using 3-D, multiple NUFT model

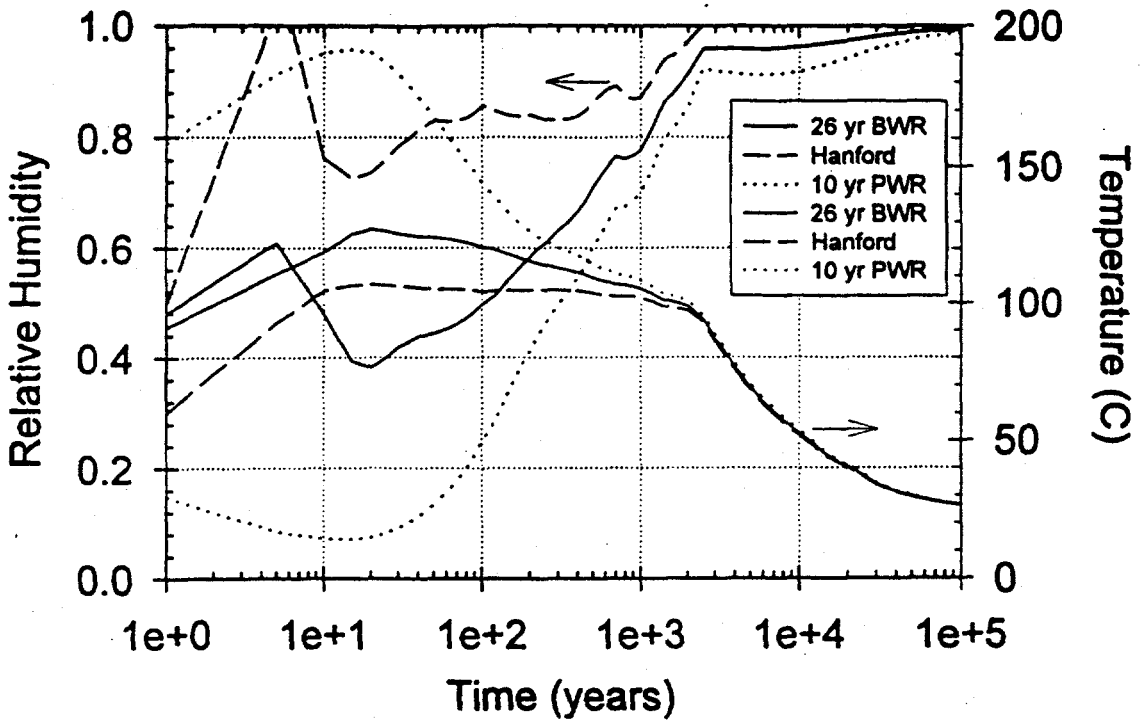

Figure 3.1-13 Temperature and relative humidity on upper waste package surface for ACD, no backfill, case using 3-D, multiple-WP NUFT model

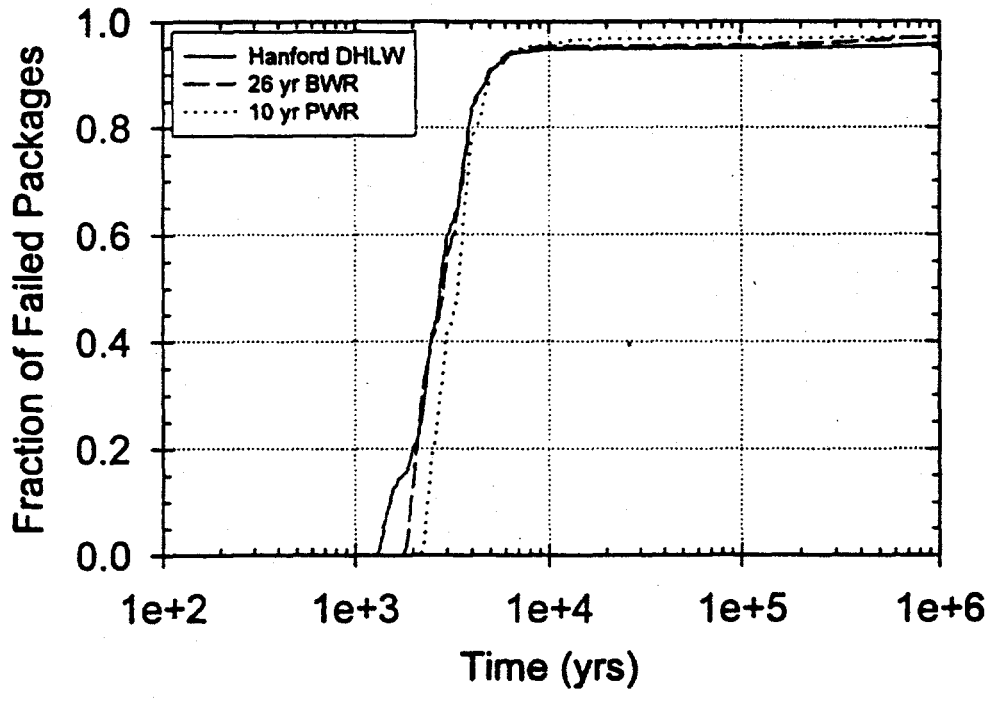

Figure 3.1-14 Waste package failure history for ACD, no backfill case using the 3-D, multiple-WP NUFT model

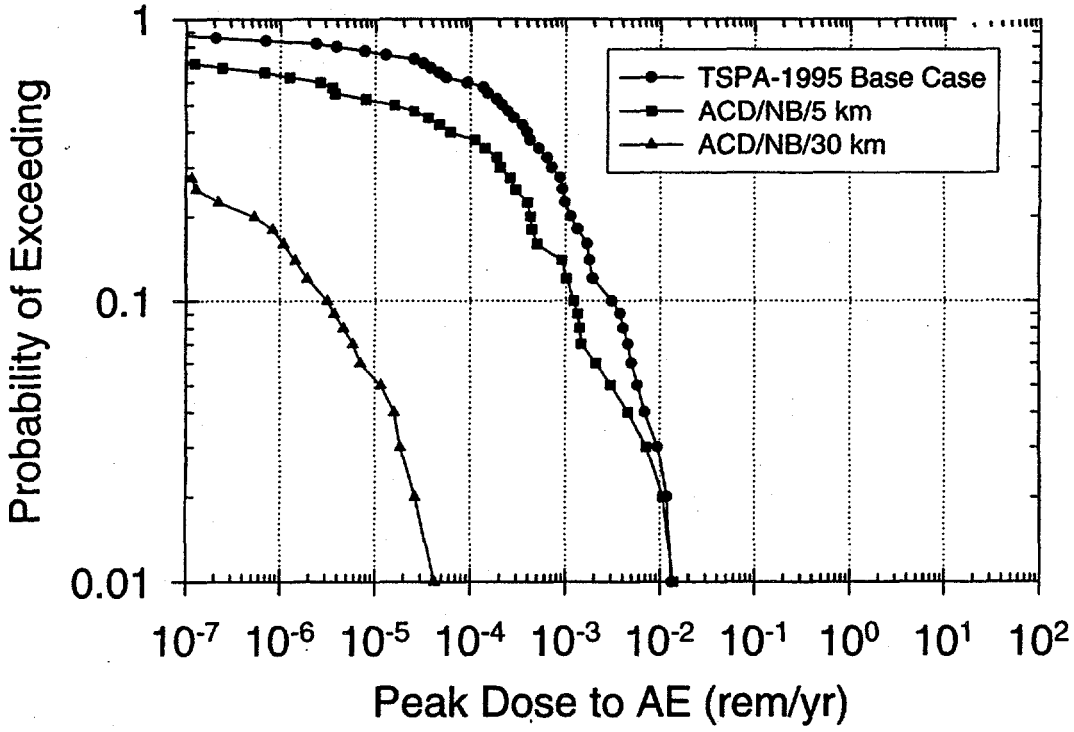

Figure 3.1-15 10,000-yr total peak dose CCDFs for the ACD cases (NB=no backfill)

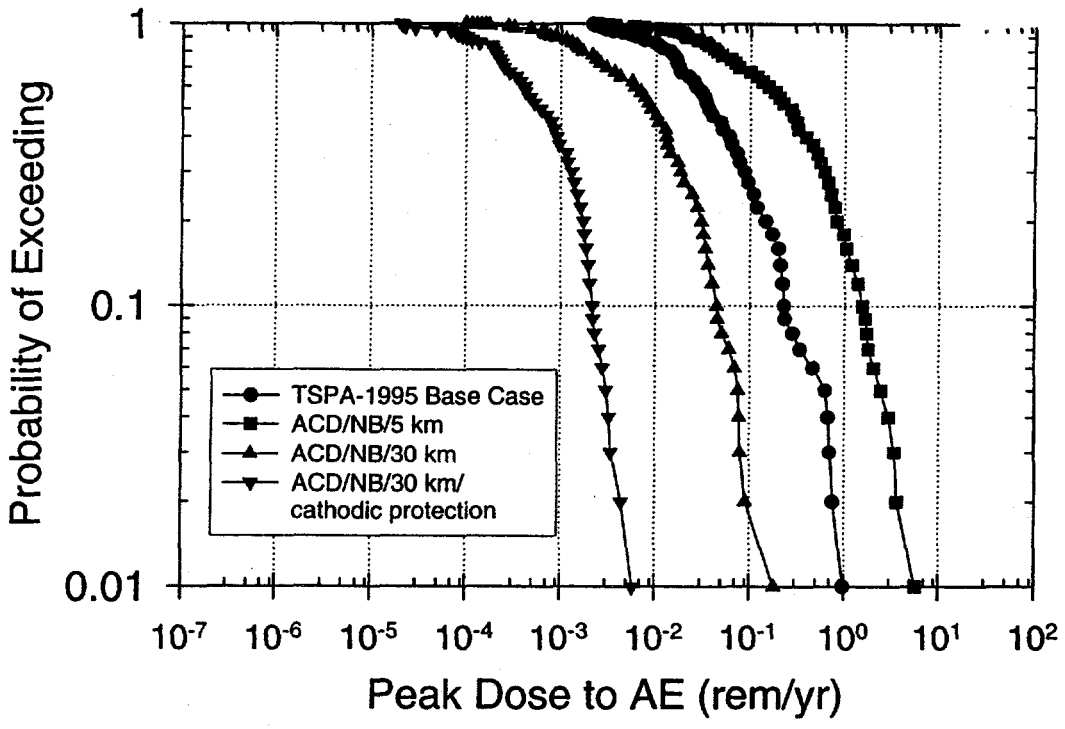

Figure 3.1-16 1,000,000-yr total peak dose CCDFs for the ACD cases (NB = no backfill, cathodic protection = 50% cathodic protection credit taken)

3.2 LINELOAD CONCEPT

The influence of axial waste package spacing and drift spacing on the thermohydrologic behavior of the potential repository is described in this section. Although this sensitivity analysis is examined and documented in the report *Thermal Loading Study for FY 1996* (CRWMS M&O 1996d), the analyses are included here since it may strongly affect estimates of long-term repository performance, and thus should be considered when addressing the question of whether additional performance barriers in the EBS are needed.

There are two fundamentally different ways that WPs can be arranged in the repository at Yucca Mountain. The ACD utilizes a "square" geometry with the spacing between drift centerlines being roughly the same as the axial center-to-center spacing between SNF WPs. The ACD has an LML = 0.46 MTU/m of emplacement drift. The lineload design places WPs nearly end-to-end (a 0.1-m gap between WPs, resulting in LML = 1.11 MTU/m); to keep the AML the same (83 MTU/acre) in the two designs, the drift spacing (53.8 m) in the lineload design is 2.4 times greater than in the ACD (compare Figure 3.2-1 with Figure 3.1-7). The lineloading thermohydrological results from the 3-D, multiple-WP model described in Section 3.1.1.2 are presented in this section.

It should be noted that there are thermal concerns associated with closely-spaced WPs (CRWMS M&O 1996d). Specifically, it is unclear whether extremely close spacing of waste packages would result in significantly increased temperatures which may violate such thermal criteria as the 200°C drift wall temperature or the SNF cladding criteria. Thus, the work presented in this section should be considered work in progress and should be investigated further when additional assurance can be developed in the calculations. This section presents the possible performance benefits of closely spaced WPs without addressing and resolving the thermal criteria issues raised in CRWMS M&O 1996d.

Figures 3.2-2 through 3.2-5 indicate the resulting WP surface relative humidity and temperature profiles over 100, 2000, 10,000, and 100,000 years, respectively. These results were obtained for a thermal loading of 83 MTU/acre, sand invert, 5.5 meter emplacement drift diameter, a percolation flux of 0.3 mm/year, and a WP emissivity of 0.8. The remainder of the inputs and assumptions employed in this analysis are described in the *Near Field and Altered Zone Environment Report* (CRWMS M&O 1996n). These results for the lineloading case can be compared directly to the ACD "square" WP spacing results shown in Figures 3.1-9 through 3.1-12. Compared to the ACD results, the lineloading results indicate much less variation among the WPs in terms of their surface relative humidity and temperature histories.

These thermohydrologic results (temperature and relative humidity) were incorporated into a performance assessment of the lineloading case. The results of this assessment are given in the next section.

3.2.1 POSTCLOSURE REPOSITORY PERFORMANCE

The results from the thermohydrologic analyses presented above were incorporated into performance assessment of the lineloading case. The temperature and relative humidity results were input directly into RIP for the analyses. The simulated temperature and relative humidity at the waste package for the lineloading concept are presented on a logarithmic scale in Figure 3.2-6. Only three of the six curves in Figure 3.2-2 were plotted because they were considered representative and bounding. These temperature and relative humidity histories were implemented in the waste package degradation model to develop first pit penetration and pitting degradation history for the particular cases. The waste package degradation results are first presented. Subsequently, assessments of 10,000 year and 1,000,000 year lineloading repository performance are provided.

Waste Package Containment Requirement

Figure 3.2-7 shows the waste package first pit penetration results using the thermohydrological results from Figure 3.2-6. The first pit penetration results for each waste form are very similar. This similarity led to an assumption that each of the waste forms within a case would be given the same first pit penetration and waste package degradation distribution. Figure 3.2-7 indicates that the earliest breach of WPs due to corrosion is predicted to occur after 2000 years. Therefore, WP performance is currently predicted to satisfy the WP containment requirement delineated in Key Assumption 038 of the CDA (CRWMS M&O 1996a): "The fraction of waste packages breached at 1000 years shall be less than 1%..." Note that the failure histories in Figure 3.2-7 reflect better waste package performance than for the comparable ACD case (Figure 3.1-14). The reason for this can be explained by comparing Figures 3.2-6 and 3.1-13. The corrosion models used in this analysis assumes that corrosion initiation does not occur on the waste packages until their surface temperatures drop below 100°C, and the relative humidity exceeds 65 percent. For some of the WPs in the ACD case (Figure 3.1-13), corrosion is initiated soon after 1000 years. However, for the lineload case (Figure 3.2-6), the WPs all stay above 100°C until about 2000 years. Therefore, corrosion initiation occurs sooner, in general, for the ACD case than for the lineload case. Furthermore, when corrosion is initiated in the ACD case, the corresponding WP surface relative humidities are higher than for the lineload case. Since corrosion rates increase for increasing relative humidity (see Appendix B), the WPs generally corrode faster in the ACD case than for the lineload case.

Repository Performance Compared to Interim 10,000 Year Peak Dose Standard

The results for the 10,000 year CCDF of peak dose for the lineloading/no backfill case are presented in Figure 3.2-8. These RIP analyses assume 26 yr old BWR temperatures and failure curves, and a blended inventory. The results are presented for accessible environments defined at both 5 km and 30 km. For the 30 km location, the assumption was made that a dilution factor of 25 would be used in the saturated zone per TSPA-1995 analysis (CRWMS M&O 1995d).

For comparison, the TSPA-1995 case with similar assumptions is also presented.

Repository Performance Over a 1,000,000 Year Time Frame

For the 1,000,000 year peak dose rate results, the CCDF's for several cases are presented in Figure 3.2-9. The comparable result from TSPA-1995 is also presented on the figure. The lineloading case at the 5 km accessible environment is nearly the same as the TSPA-1995 results. The effect of the location of the accessible environment is again shown in this plot. Moving the AE to 30 km causes an improvement in performance beyond that which was seen for the comparable ACD case (Figure 3.1-16).

Repository Performance Compared to Alternative Hypothetical Performance Standards

As was discussed in Section 3.1.1.1, alternative hypothetical performance standards were selected to demonstrate the sensitivity of long-term repository performance to variations of the "Interim Postclosure Standard."

No less than a 50 percent probability of not exceeding a peak dose rate of 15 mrem/year when measured from a water well located 5 km from the repository. Over the 10,000 year time frame the CCDF, see Figure 3.2-8, indicates a 50 percent probability of not exceeding 0.0003 mrem/year. Over the 1,000,000 year time frame the CCDF, see Figure 3.2-9, shows a 50 percent probability of not exceeding a peak dose rate of 60 mrem/year, and a 20 percent probability of not exceeding 15 mrem/year.

No less than a 90 percent probability of not exceeding a peak dose rate of 15 mrem/year when measured from a water well located 30 km from the repository. Over the 10,000 year time frame the CCDF, see Figure 3.2-8, indicates a 90 percent probability of not exceeding a total peak dose rate of 0.0002 mrem/year and a 99 percent probability of not exceeding 0.02 mrem/year. Over the 1,000,000 year time frame the CCDF, see 3.1-6, shows a 90 percent probability of not exceeding a total peak dose rate of 10 mrem/year and about a 98 percent probability of not exceeding 15 mrem/year.

3.2.2 POSTCLOSURE PERFORMANCE CONCLUSIONS FOR LINELOAD CONCEPT

Predicted postclosure performance of the repository for the lineloading case is summarized here in terms of waste package containment as well as peak dose rate calculations at 30 km from the repository over 10,000 and 1,000,000 year time frames.

The current estimation of WP performance is that any breaches due to corrosion (breaches defined as a single corrosion pit penetrating through the outer and inner barriers) will not occur until around 2000 years (Figure 3.2-7). Therefore, WP performance is currently predicted to satisfy the WP containment requirement delineated in Key Assumption 038 of the CDA (CRWMS M&O 1996a): "The fraction of waste packages breached at 1000 years shall be less than 1%..."

Current predictions of peak dose rate values at 30 km from the repository over a 10,000 year time frame, taking no credit for WP cathodic protection, indicate that repository performance satisfies the "Interim Postclosure Standard" by at least several orders of magnitude. Additional assurance is

obtained by recalling that the above quantitative performance assessment does not reflect benefit from cathodic protection, although substantial improvements in long-term performance are predicted for this barrier.

Current predictions of peak dose rate values at 30 km from the repository over a 1,000,000 year time frame, again taking no quantitative credit for cathodic protection, indicate satisfaction, by only a slight margin, of an assumed 15 mrem/year allowable peak dose rate requirement.

Table 3.2-1 summarizes the repository performance against the various standards discussed.

Table 3.2-1 Summary of Long-Term Repository Performance Results (Lineload) (mrem/year)

Time Frame (years)	**Interim Postclosure Standard**	**Alternative Hypothetical Standards**	
	15 mrem / 50% probability / 30 km	**15 mrem/ 50% probability / 5 km**	**15 mrem / 90% probability / 30 km**
10,000	$<<10^{-4}$	0.0004	0.0002
1,000,000	2	60	10

Finally, although the repository performance benefits appear promising, it needs to be reiterated that there are thermal concerns associated with very closely-spaced WPs (CRWMS M&O 1996d). The performance results shown in this section need to be strongly caveated with concerns regarding the thermal effects of very closely spaced waste packages on emplacement drift wall and SNF cladding temperatures. However, the results of this section should be regarded as motivation to continue to pursue the concept of lineloading of WPs.

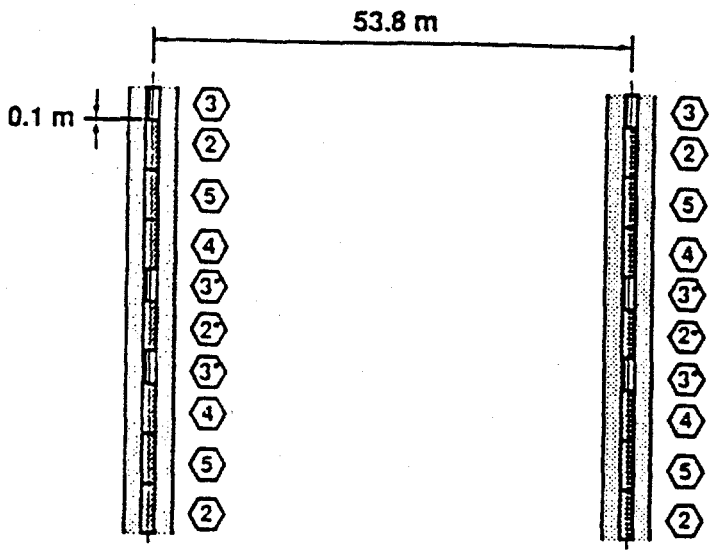

Legend		
2 Large PWR MPC 26-yr-old SNF 8.83 MTU	2* Large PWR MPC 10-yr-old SNF 9.74 MTU	3 Hanford Site DHLW 2.15 MTU
3* Savannah River DHLW 2.15 MTU	4 Large BWR MPC 26-yr-old SNF 7.07 MTU	5 Small PWR MPC 40-yr-old SNF 4.4.67 MTU

Figure 3.2-1 Plan view of the WP configuration represented by the 3-D, multiple-WP model for the lineload case

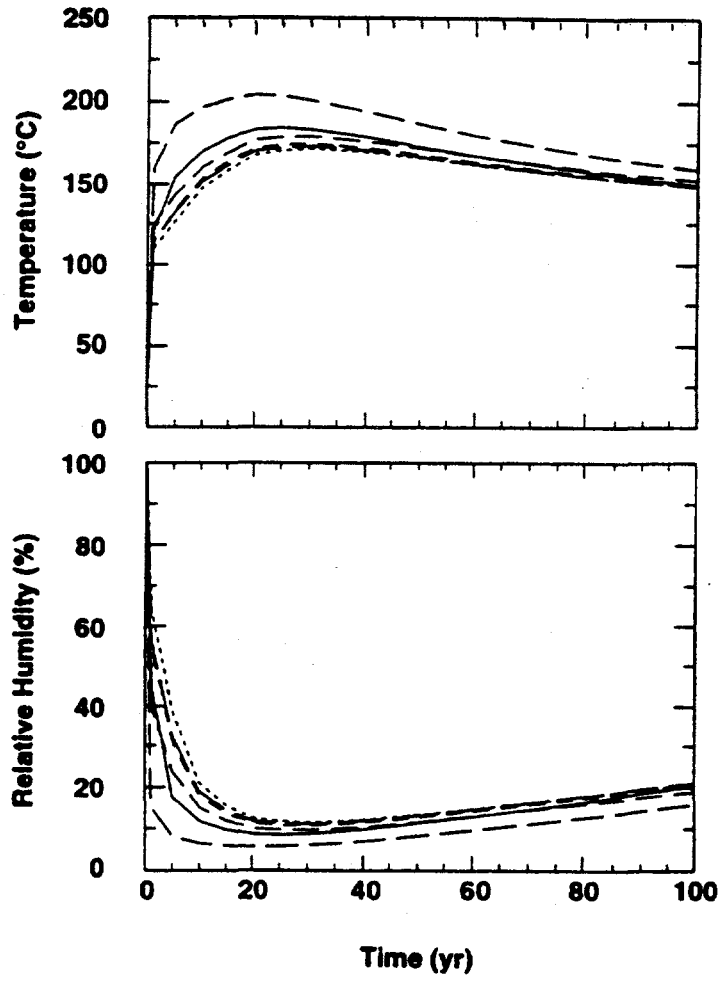

Figure 3.2-2 100 year temperature and relative humidity profiles on upper waste package surface for lineload case using 3-D, multiple-WP NUFT model

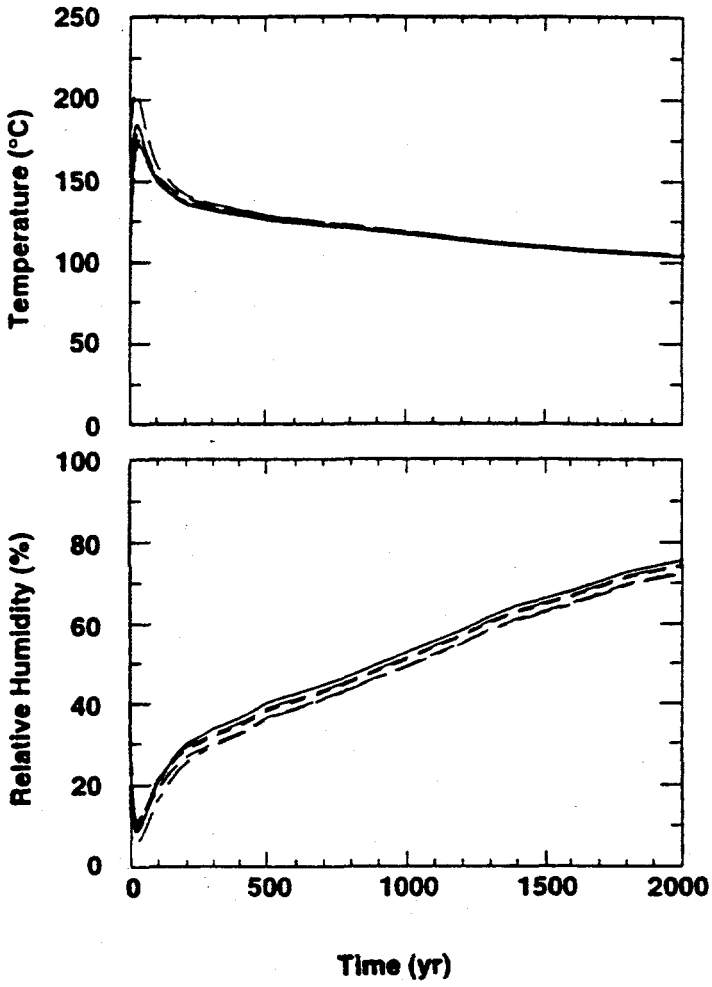

Figure 3.2-3 2000 year temperature and relative humidity profiles on upper waste package surface for lineload case using 3-D, multiple-WP NUFT model

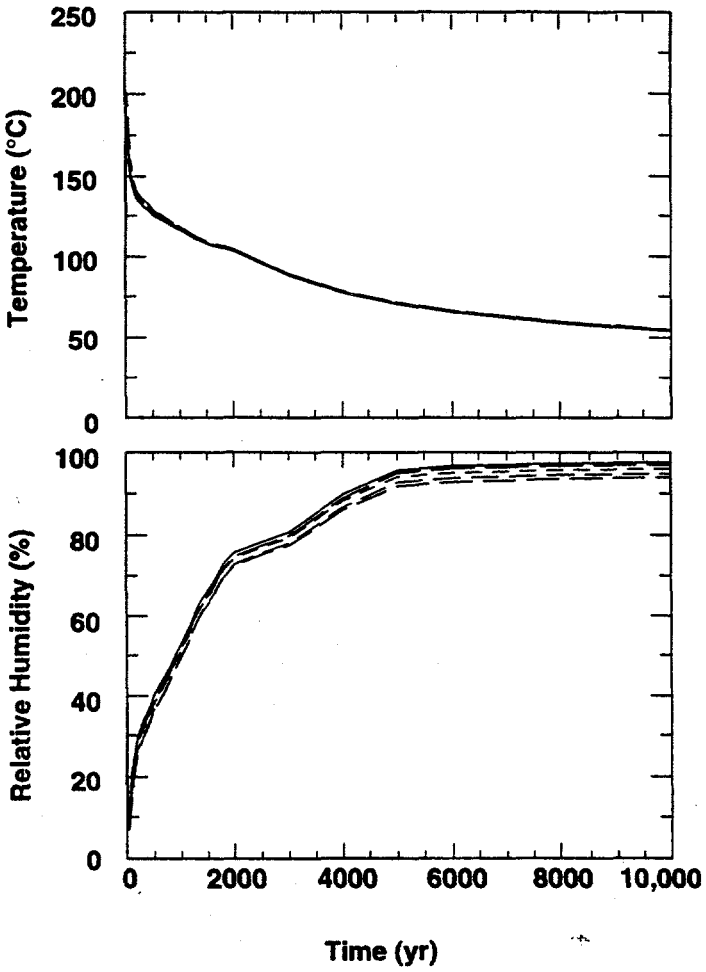

Figure 3.2-4 10,000 year temperature and relative humidity profiles on upper waste package surface for lineload case using 3-D, multiple-WP NUFT model

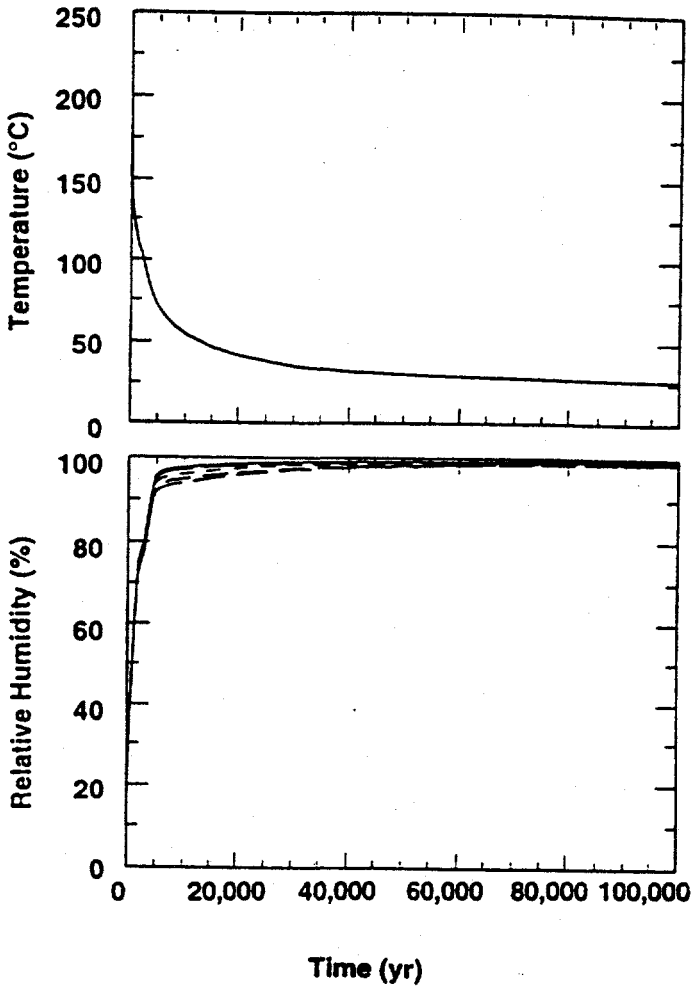

Figure 3.2-5 100,000 year temperature and relative humidity profiles on upper waste package surface for lineload case using 3-D, multiple-WP NUFT model

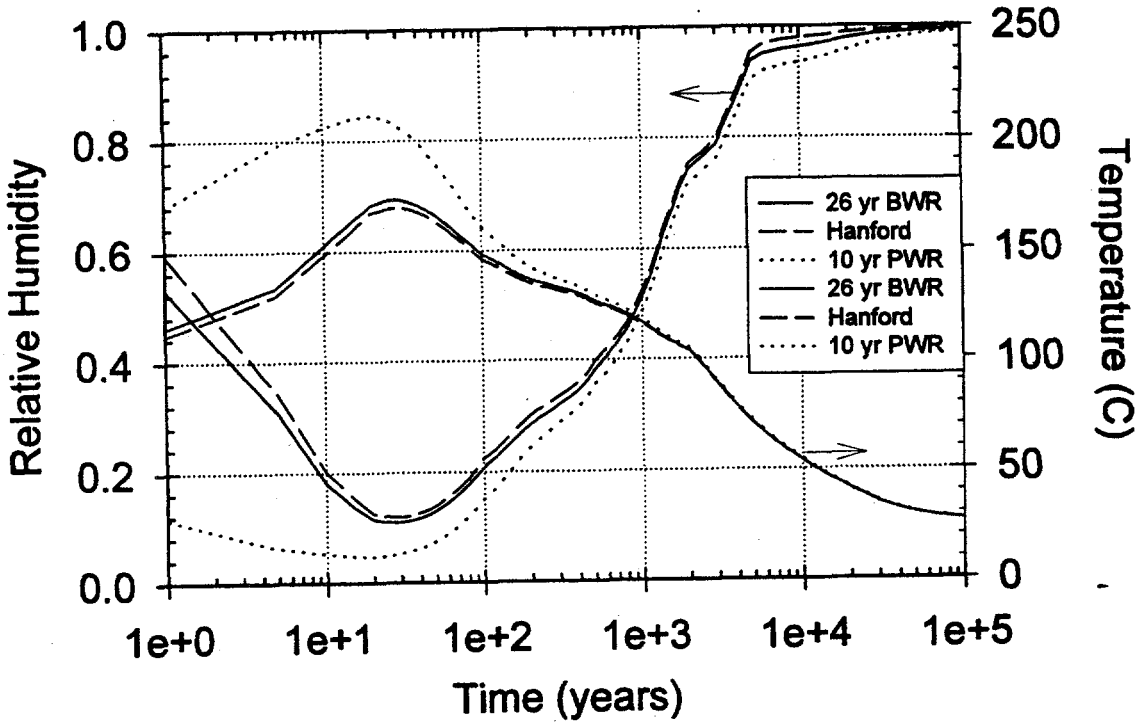

Figure 3.2-6 Temperature and RH for lineload, no backfill case

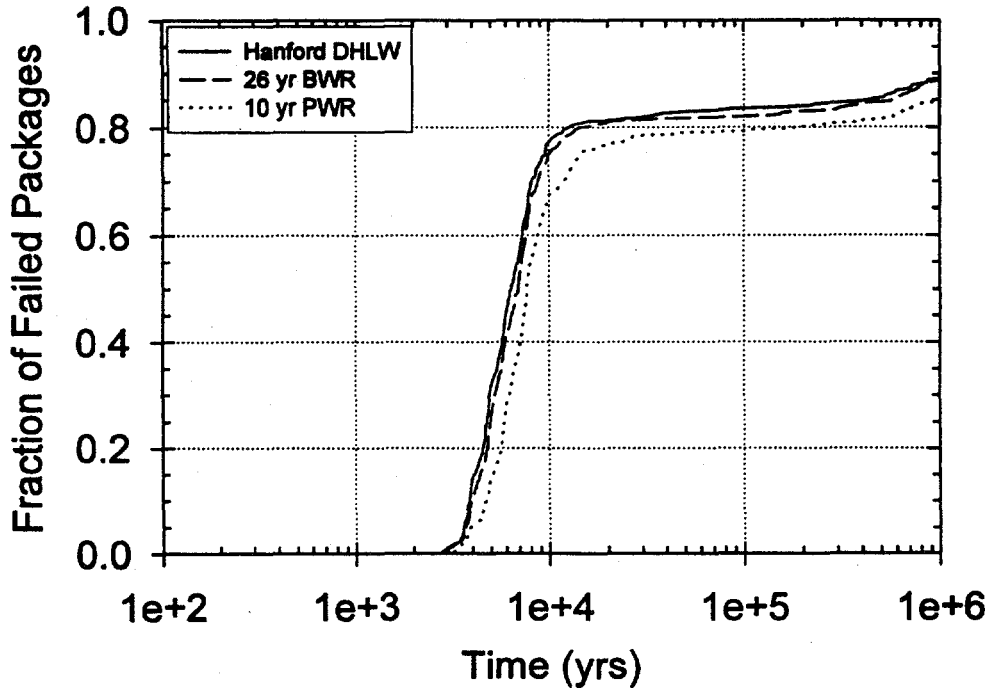

Figure 3.2-7 Waste package failure history for lineload, no backfill case

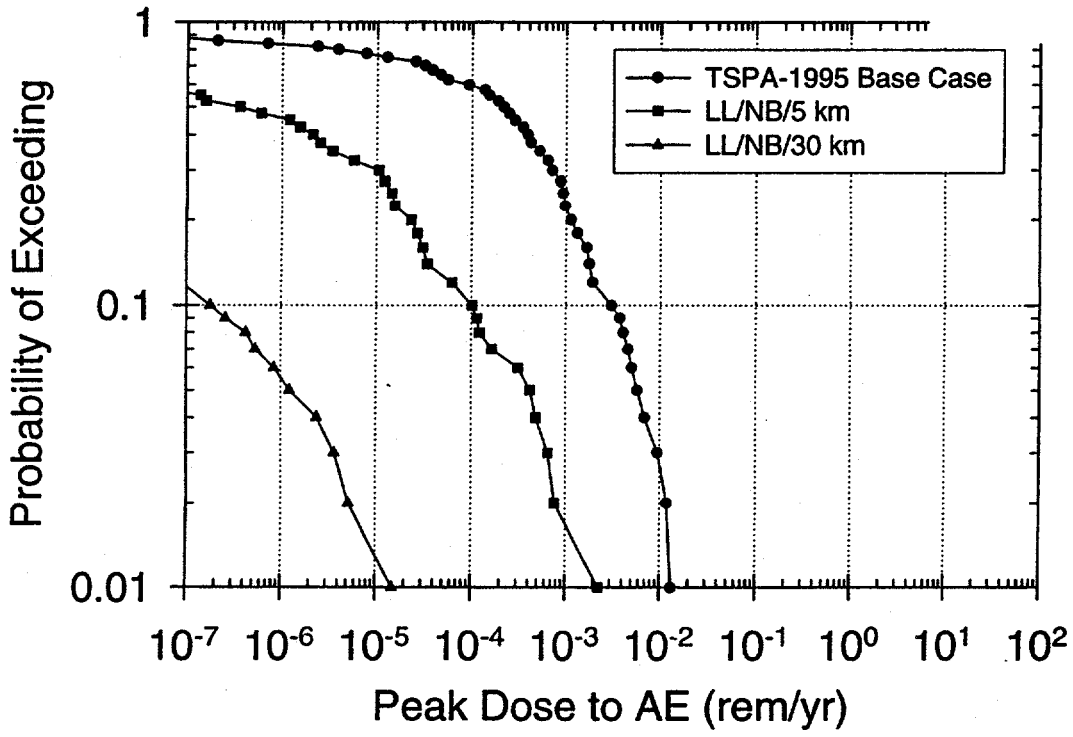

Figure 3.2-8 10,000 yr total peak dose CCDFs for lineload, no backfill cases (NB=no backfill)

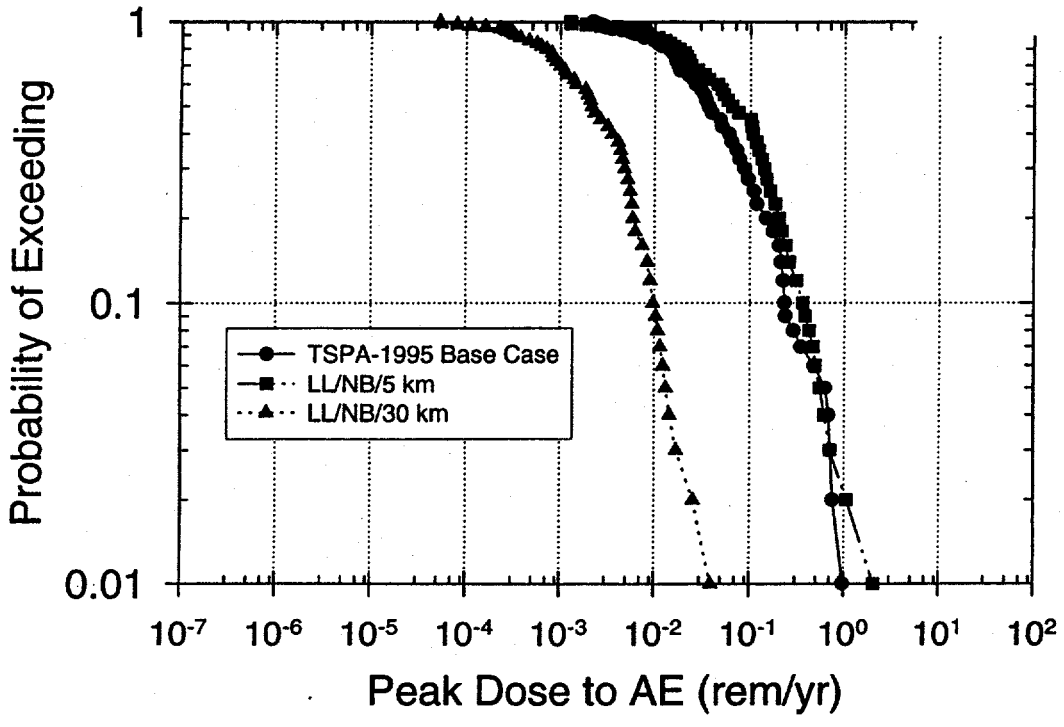

Figure 3.2-9 1,000,000 yr total peak dose CCDFs for lineload, no backfill cases (NB=no backfill)

3.3 ROCKFALL ANALYSIS

An important caveat to the total system performance results presented in Sections 3.1 and 3.2 is that those results do not reflect any possible waste package degradation in performance due to emplacement drift rockfall. This section will provide an assessment of the probable size of rocks that can be expected to fall in the emplacement drifts (Section 3.3.1), as well as an evaluation of the time-varying size of rock required to breach a waste package as the waste package degrades (Section 3.3.2). In Section 3.3.3 a set of bounding calculations will be conducted on the effects of rockfall on total system performance, over both 10,000 year and 1,000,000 year timeframes. These evaluations from Sections 3.3.1, 3.3.2, and 3.3.3 will be used as the basis for the assessments made in Section 3.3.4 regarding the effect of emplacement drift rockfall on waste package performance, and thus total system performance.

3.3.1 EVALUATION OF ROCK FALL POTENTIAL IN EMPLACEMENT DRIFTS

3.3.1.1 Preclosure Rock Mass Conditions

During excavation, repository emplacement drifts may be continuously lined with a concrete or steel support system having a maintainable preclosure service life of 150 years (CRWMS M&O 1996b). At least for the duration of the preclosure period, the support system will be designed to accommodate in situ, thermal, and seismic loads.

In response to in situ loads the drifts will deform slightly, producing a small change (inward movement) in the vertical drift diameter on the order of 10 mm and a change of about 2 mm in the horizontal diameter (CRWMS M&O 1996b). In addition, certain rock blocks (termed keyblocks), formed at the crown and sidewalls of the drifts by the intersection of joints (existing fractures and faults), will have a tendency to move into the drift. In other words, keyblocks are those joint-delineated rock blocks that have the potential to fall. The drift support system is designed to restrain the keyblocks, minimize movement along joints, and maintain the self-supporting capability of the rock mass.

In addition to the initial in situ loads at excavation, thermal loads will develop. Emplacement of waste packages a year or so after excavation will heat the rock mass, eventually producing lateral rock stresses that will cause small horizontal changes in drift diameter of about 15 mm and vertical changes that may lengthen the diameter by about 5 mm (CRWMS M&O 1996b). Keyblocks will also be acted upon by the thermally-induced stresses. However, the rock mass surrounding the drift, having been stabilized during excavation and supported by a lining system designed for the maximum thermal and seismic loads, will remain intact and retain its load-carrying capacity throughout the preclosure period. If needed, drift maintenance will be performed.

3.3.1.2 Postclosure Rock Mass Conditions

At some time after closure, portions of the ground support system will have deteriorated to the extent that keyblocks will be free to move. These rock blocks will fall due to gravity, thermal loading, and on rare occasions by the additional dynamic loading of an earthquake. As rock falls occur, a cavity will form at the crown of the drift and a zone of loosened rock (characterized by joints exhibiting

shear movement and separation) will extend some distance upward, approximating an arch-like profile. During this period, rock blocks will accumulate in the drift. Drift deterioration is progressive, but it is anticipated that the zone of block movement will eventually stabilize, due in part to the confining effect of the thermal load but also because drifts are spaced sufficiently far apart that additional load, due to the influence of adjacent drifts, is minimal. The result will be a stable zone of loosened rock with little potential for further rock mass movement. Estimates of the typical extent of this loosened rock mass will be discussed in the following sections of this report.

A potential consequence of rock fall and deterioration of emplacement drifts is damage to waste packages. Examination of this consequence involves consideration of the following:

- Rock block size—What is the distribution of keyblock sizes, the most probable rock size, and the maximum rock size?

- Drift stability—What is the geometry and extent of drift modification, overbreak, and joint movement?

These considerations are addressed below.

ANALYSIS OF ROCK BLOCK SIZE

Accurate prediction of rock block or keyblock size (weight and volume) and of size distribution (the number of rock blocks of a certain size that are likely to occur) depends on site specific data. ESF drift mapping, which shows the location, extent, and orientation of joints throughout the TSw2 rock unit (the potential host rock for all emplacement drifts), has recently become available for the first few hundred meters of the TS Main Drift. These data will allow a more detailed evaluation of keyblock distribution for emplacement drifts in the near future.

Information is not available that would enable an accurate prediction of rock fall frequency with time. Such time-distribution predictions rely on empirical databases of events, which are lacking for rockfall. One of the few estimates of the time-frequency of rock fall is from a study by Smith and Tsai (CRWMS M&O 1994), but their work is based on rock fall data from underground coal mines, which is not representative of the behavior of the TSw2 rock mass and which describes rock fall size only in a general way. The work by Gauthier et al. (1995) suggests an approach to the time distribution of rock falls. For example, they estimated that rock falls could start anytime between 100 years and 2000 years after waste emplacement.

It is noted that Chapter 8 of the Site Characterization Plan: Yucca Mountain Site, Nevada Research and Development Area (DOE 1988) lists as tentative goals, estimates of rock fall quantity (<5 ton/1000 ft/yr) and a maximum rock or slab size (< 2 ton). However, no backup is given for these numbers.

The work discussed below illustrates methods of determining keyblock geometry and size distribution and gives some estimates based on evaluation of these results.

Keyblock Analysis

A computer code developed by Stone (1994) has been used by Stone and Boontun (1995) for a preliminary keyblock analysis of the ESF North Ramp (7.6 meters in diameter) and similarly sized drifts in north/south and east/west directions. Comparing results from these drift orientations (Figures 3.3-1 and 3.3-2) indicates that the most frequent keyblock size is about 0.13 metric tons (2 cubic feet or 0.06 cubic meters). By extrapolation, a reasonable maximum keyblock size appears to be somewhat less than about 3 metric tons (40 cubic feet or 1.1 cubic meters).

The Stone/Boontun analysis gives an estimate of the number and size of blocks having the potential to fall into the drift. Only data from 140 m of the ESF North Ramp was available for the calculation, which was mainly intended as a demonstration of the technique. The data, from the portion of the North Ramp in the Tiva formation, is not completely representative, although joint orientations appear similar to those of the TSw2. The results are conservative, that is, further keyblock size-distribution analysis for emplacement drifts would not show as large a distribution of block sizes. One reason for this is the North Ramp diameter (7.6 meters) is significantly larger than the nominal diameter planned for emplacement drifts (5.0 or 5.5 meters). The maximum possible keyblock size would thus be smaller for emplacement drifts. In addition, mechanical stability (that is, the strength of the joints and the influence of confining stresses) has not been considered in the analysis by Stone and Boontun.

Analysis Based on Joint Frequency

Data on joint frequency for the TSw2 unit, given in Brechtel (Brechtel et al. 1995), allow an estimate of typical block size. These data show that 40 percent of joints are steep with dips of 80 and 90 degrees and 25 percent are shallow with dips of 10 degrees. The remaining 35 percent of joint occurrences have a frequency of 7 percent or less and are distributed uniformly between dips of 20 degrees and 70 degrees. It is assumed that the most frequent steep- and shallow-dipping joints are those most representative of block-forming joints in the TSw2. Joint spacings estimated from these data are 0.05 and 0.34 meters for the steeply dipping joints and 0.63 meters for the shallow joint set. Using the larger of these dimensions and assuming orthogonal joint intersections, resulting block sizes would not be expected to exceed about 0.17 metric tons. This is a simplified approach, which does not address keyblock formation in any way but does aid in predicting the size of typical blocks.

Also using joint frequency data, an analysis in the waste package off-normal report (CRWMS M&O 1996e) determined a distribution of block sizes (block masses) from joint frequency estimates based on measured borehole rock quality designation data. These data are preliminary and need to be verified with ESF information from drift mapping, however, the joint frequencies are, in general, within the ranges of measured data. Results indicate a 97 percent cumulative frequency of occurrence for blocks smaller than 1 metric ton and a 99 percent cumulative frequency of occurrence for blocks smaller than 10 metric tons. The mean block size from this analysis is about 0.04 metric tons. Extrapolation for the remaining 1 percent of occurrences beyond 10 metric tons gives an unrealistically high 30-metric ton maximum size.

Wedge Analysis

The UNWEDGE computer code computes the weight and size of the maximum-sized keyblocks that could occur based on the orientations of three joint sets. The keyblock failure mode, whether free-fall, sliding, or rotational is determined. A size-distribution is not calculated. Results are only for the extreme rock block size, no matter how unlikely, based on other considerations. Results are relatively insensitive to joint spacing or the frictional strength of the joints. In addition, the model is conservative in that the length of joints is considered to be infinite and results often include improbably large wedge-shaped blocks.

A range of steeply dipping joint sets and a low-angled set, representative of TSw2 joints and a 5-meter diameter drift, were analyzed to produce the data shown in Table 3.3-1. Variations in block sizes were determined for the current design orientation of emplacement drifts (N72W), plus a north/south and an east/west orientation. The range of these maximum keyblocks for the N72W and east/west drift orientations for all cases is 0.1 to 9.7 metric tons, with the typical result being 1.0 to 2.2 metric tons. The range for the north/south orientation is 0.7 to 7.7 metric tons. A 49-metric ton keyblock was also calculated, but is not likely to actually form because joint spacings and lengths will create significantly smaller blocks. Even if such a block formed, it would not likely fall because it is larger than the drift cross-section can accommodate; i.e., the width of one block dimension of the 49-metric ton wedge equals the drift diameter, and thus cannot fit in the smaller, lower half of the circular drift. Inspection of maximum wedge/keyblock sizes, such as that shown in Figure 3.3-3, indicates that blocks of greater size than about 5 metric tons are unlikely to form given the typically small joint spacings (see previous "Analysis Based on Joint Frequency" section).

Summary of Rock Block Size

The analyses cited above aid in judging a realistic maximum rock block size. A more accurate assessment can only be made based on site-specific data; i.e., ESF information from the TSw2 rock unit. Typical (most frequent) sizes of rock blocks appear to be in the range from 0.10 to 0.20 metric tons. Maximum sizes are judged to lie in the range from about 3 to 5 metric tons.

DRIFT STABILITY AND EXTENT OF ROCK BLOCK MOVEMENT

In this section examples are evaluated as a basis for estimating the extent of potential rock block loosening and fallout around an emplacement drift.

Empirical Models

A rock classification system presented by Proctor and White (1946) has been widely used to predict vertical rock loads for the purpose of designing structural steel sets for ground support. An estimate of the potential height of rock block loosening and fallout can be made by following this approach. The classification is based principally on a description of the rock condition and the examples given in the publication by Proctor and White (1946). Additional explanation is given by Rose (1982). Category 6, "completely crushed but chemically intact," could be considered a bounding condition, which Rose (1982) associates with Rock Quality Designations from 3 to 30 (corresponding to the lowest range of Rock Quality Designations for the TSw2 unit). Applying this condition for a tunnel

with a circular cross-section and taking into account the absence of groundwater at the Yucca Mountain Site, results in an estimated height of loosened rock of about 0.6 times the drift diameter, or 3 meters. With this model as a conservative estimate, rock blocks would have the potential to loosen and to progressively fall to a depth of about 3 meters in the absence of ground support and under ambient temperature conditions.

Numerical Analyses

Jointed Rock Analysis

The range of joint spacing and the attitude of typical joint sets in the TSw2 have been used in the UDEC computer code to develop a jointed rock mass model of the TSw2 rock mass. The influence of in situ, thermal, and seismic loads on the behavior of blocks at the perimeter of the emplacement drifts can be examined with this model. The model is hypothetical, but considered representative of the predominant joint geometry. The objective of the model is to aid in understanding the behavior of the jointed rock around the drift, but not necessarily to derive quantitative data. Joint properties that simulate a very weak rock mass have been used to observe block movement at the crown of the drift.

Figure 3.3-4 shows the result of progressive fallout of rock blocks at the crown following a 350-year period of heating. Block fall and enlargement of the drift profile extends up to about 3 meters into the rock mass. Joint movements in the zone of potential block fall consist of initial shear displacements ranging from 5 to 70 mm and joint separations greater than 1 mm. Joint movements for the falling block exceeded a shear of 170 mm and separation of 18 mm. Joint movement also showed a maximum extent of about 10 meters above and below the drift but eventually stabilized, showing little movement beyond 250 years. Much of this joint movement was of small magnitude (typically less than 10 mm for shear displacement and less than 1 mm for separation) and did not significantly affect mechanical stability.

Continuum Analysis

A continuum model does not explicitly model joints but can help to define the portion of the rock mass where stresses may exceed the strength. Either rock block movement or fracturing, or both, could occur in such an overstressed zone. A 5-meter diameter emplacement drift, subjected to representative in situ, thermal, and seismic loads, was modeled using the FLAC computer code. Joints were not modeled but the full range of expected rock properties were used. Results showed that the ratio of strength-to-stress (which can be thought of as a safety factor against rock fracture) is at least 2.0 close to the drift. A zone, varying from 0.5 to 1.0 meters in depth, of potential rock fracturing and/or joint movement and loosening can be conservatively estimated from these results.

Summary of Extent of Rock Block Movement

The analyses given above can be used as approximations of the extent of fallout and loosening that could develop above an unsupported emplacement drift. Judging from these results, a zone of potential fallout and loosening could extend about 3 meters above the crown. Small joint movements

also extend from 3 to 10 meters above and below the drift but these movements are not detrimental to stability.

3.3.1.3 Conclusions

Conclusions for this preliminary rockfall analysis include the following:

- Rock falls will occur at some time during postclosure following deterioration of the ground support system.
- A keyblock analysis based on ESF drift joint-mapping data will provide the most accurate prediction of a rock block size-distribution. Information on rock-fall histories, that is, an empirical database, that would enable an accurate prediction of a time-distribution of rock fall is not available.
- Typical (most frequent) sizes of rock blocks appear to be in the range from 0.10 to 0.20 metric tons. Maximum sizes are judged to lie in the range from about 3 to 5 metric tons.
- Zones of rock block loosening and fallout that may develop following loss of ground support during postclosure will eventually stabilize. A zone of potential rock block loosening and fallout could extend 3 meters above the crown before stabilizing. Some renewed movement may occur following sufficient cooling of the rock mass or periodically due to earthquakes.

Table 3.3-1 Rock Block Sizes estimated by UNWEDGE Computer Code

Drift Orientation	Fail Mode	Location	Weight (tonnes)	Comment
E-W	Fall	Crown	0.4 - 6.6 (2.2 typical)	
	Slide	Wall	0.2 - 2.3 (1.0 typical)	Upper wall: SF=0 Lower wall: SF>1
	Rotation	Upperwall/Crown	2.3	
N72W	Fall	Crown	0.4 - 9.7	
	Slide	Wall	0.1 - 2.0	SF>2
	Rotation	Upperwall/Crown	0.1 - 2.0	
N-S	Fall	Crown	0.7 - 7.7	
	Slide	Wall	0.9	SF>3
	Rotation	Upperwall/Crown	8.9	

NOTE: SF = Safety Factor

3.3.2 ANALYSIS OF WASTE PACKAGE STRUCTURAL CAPABILITY THROUGH TIME

3.3.2.1 Introduction

The objective of this section is to present the Advanced Uncanistered Fuel Design WP resistance to rock falls at different levels of degradation. Analyses have been performed on waste packages with degradation levels ranging from no degradation to degradation levels at which three-fourths of the outer barrier is degraded. The outputs of the analyses performed are reported in terms of the percent degradation in the waste package materials.

The rock impact loading on the waste package has been simulated by a commercially available finite-element analysis (FEA) code (ANSYS). The finite-element model developed to obtain solution for this accident condition is a three-dimensional solid model which is solved by a transient dynamic analysis. Degradation of the outer barrier is modeled as uniform general material thinning, which results in weakening of the waste package component.

The results of the rock fall analyses do not relate degradation to time. However, these results will provide the basis for time dependent structural analyses and serve as inputs in determining the expected time of failure of the waste package barriers. Determination of the expected time of failure of the barriers provides basis for determining the probability of SNF release for performance assessment.

The models described and the analysis results given in Sections 3.3.2.2 through 3.3.2.7 are included in *Rock Size Required to Cause a Through Crack in Containment Barriers* (CRWMS M&O 1996l)

3.3.2.2 Waste Package Description

The advanced uncanistered fuel WP consists of two containment barriers which hold a basket assembly. The basket assembly is composed of carbon steel tubes in an array of interlocking stainless steel boron plates. Around the outside of the basket assembly, there are carbon steel side guides and corner guides. The carbon steel tubes protect the fuel assemblies from damage in the case of accidents and maintain the configuration of the stainless steel-boron plates which are used for criticality control. The side guides and corner guides hold the basket in place in the inner barrier, providing structural support and a conduction path for temperature control. The inner barrier is made of a corrosion resistant material for long life. The thick outer barrier is made of a corrosion allowance material, initially providing high strength and protection for the inner barrier. Figure 3.3-5 is an exploded view of the 21 PWR fuel assembly advanced uncanistered fuel WP.

3.3.2.3 Description of Model Employed in Analysis

A three-dimensional finite-element model of the 21 PWR advanced uncanistered fuel Tube WP (including inner and outer barriers) has been developed in accordance with the WP conceptual designs. The finite-element solution is obtained from a transient dynamic analysis with gravitational acceleration as the load on the system. The bottom of the WP is aligned with the invert, providing maximum rock fall height for conservatism. Displacement constraints placed along the WP section

length prevent vertical and horizontal translational motion of the WP. These boundary conditions provide a conservative approach for the simulation of the WP used in this analysis.

For the present WP conceptual designs, the outer and inner barriers of 21 PWR WP are fabricated as one piece. However, material properties are unique to each specific material. The materials called out for the barriers are as follows:

- Outer barrier: ASTM A 516 carbon steel (grade 70)
- Inner barrier: Alloy 625

The 21 PWR WP outer and inner barrier dimensions used in the finite-element model are as follows:

- Outer barrier, outer diameter = 1661.9 mm
- Outer barrier, inner diameter = Inner barrier, outer diameter = 1461.9 mm
- Inner barrier, inner diameter = 1421.9 mm

A spherical geometry was selected for the rock because the impact of a sphere will result in a global distribution of stress onto the WP, whereas a sharp-wedge geometry would fail at the pointed region of the rock as a result of high stress concentration. The spherical rock provides a bounding approach to the problem since the most severe effect of impact on the WP will be determined without any failure on the rock surface; i.e., crumbling of the rock. In order to perform the FEA evaluations, the radius of the rock was varied to simulate different rock sizes.

To determine the effect of WP static weight in the FEA, the maximum bending moment and resulting stress magnitudes are calculated on the 21 PWR advanced uncanistered fuel WP due to its own weight which is conservatively applied as a point load at the center of the span. The summation of the resulting stress magnitude with the stress obtained from the finite-element solutions for dynamic loading on the waste packages shows that the static loads are negligible compared to the dynamic loads.

Degradation of the outer barrier is treated as general thinning of the material. Furthermore, degradation of the inner barrier does not begin until the outer barrier is completely degraded.

The fall height of the rock is calculated from the given dimensions of the emplacement drift tunnel. Figure 3.3-6 depicts the emplacement drift tunnel geometry. For conservatism, the rock fall height is maximized by placing the WP directly on the invert. Fall height is the distance from the top surface of the degraded WP to the bottom of the rock.

The geometry of the rock and emplacement drift tunnel is defined by the parameters indicated in Figure 3.3-6.

The parameters listed in Figure 3.3-6 are calculated for different barrier thickness values. Detailed calculations of these parameters are provided in *Rock Size Required to Cause a Through Crack in Containment Barriers* (CRWMS M&O 1996l).

The structural integrity of the inner and outer barriers in terms of their resistance to fracture is also discussed in (CRWMS M&O 1996l). The finite-element model of the containment barriers was described previously. As the rock bottom surface contacts the waste package outer surface, a nonlinear local deformation takes place in the vicinity of the impact region. When the transient response of the impact region is observed in small time frames, a question of potential crack growth through the inner and outer barrier thickness can be raised.

Fracture toughness is an essential material property for the fracture mechanics analyses. The inner barrier material is Alloy 625 which shows excellent fracture toughness as annealed. Because of exceptionally high fracture toughness of Alloy 625, an instantaneous fracture due to an unstable crack growth is not anticipated to be observed in the inner barrier.

The rock fall analysis reported here determines the critical rock sizes which could cause a through crack in both inner and outer barriers of the waste package. A through crack in the outer barrier in terms of the material fracture causes an increased load on the inner barrier. However, because of high fracture toughness of Alloy 625, the containment barrier is capable of keeping its structural integrity after being impacted by a rock of critical size. Therefore, the release of radionuclides through the containment barrier does not occur as long as the inner barrier is intact even though it is likely to have a fractured outer barrier after the rock fall event. For this reason, a fracture mechanics evaluation on the outer barrier was not performed, for final decision it is intended to include a fracture mechanics review.

3.3.2.4 Modeling Assumptions

In the course of performing these analyses, several assumptions were made regarding the rock fall finite-element model. These assumptions are identified below:

- The rock is assumed to have a spherical shape. This geometry was selected because the impact of a sphere will result in a global distribution of stress onto the WP, whereas a sharp-wedge geometry would fail the pointed region of the rock as a result of high stress concentration. This assumption provides a bounding approach to the problem since the most severe effect of impact on the WP will be determined without any failure on the rock surface.

- Levels of degradation have not been related to the time at which they will occur, therefore, the temperatures of waste package components at various levels of degradation cannot be specified. For this reason, room temperature (20°C) material properties are used in these analyses. The impact of using room temperature material properties is small because, while allowable stresses would decrease with increasing temperature, stress results would also decrease due to the decrease in the elastic modulus. Therefore, for this initial set of calculations, use of room temperature properties is adequate.

- The stress-strain curve used in the analysis is an approximation to the real material behavior. The materials are assumed to reach the ultimate tensile strength at the maximum percent elongation. The basis for this assumption is that the criteria for a through crack development in a material are based on the ultimate tensile strength of the materials, and not on the path followed by the curve in the plastic region of the stress-strain diagram. Hence, the results are bounding in this analysis.

- The WP consists of the outer and inner barriers. The weights of the WP internals (basket assembly and the fuel assemblies) are not included in this analysis. Impact occurs on the surface of the outer barrier in the middle of the WP length. Since the stiffness of the system will not be considerably affected by absence of the WP internals, the load is not incorporated in the model.

- There is no structural damping in the materials used for this simulation. Attenuation of stress waves is not of interest because the criteria for a through crack development in a material are based solely on the comparison of maximum stress with the allowable stress. However, absence of structural damping also provides bounding results to the FEA since the peak stress magnitudes will be larger.

- For conservatism, it is assumed that all of the kinetic energy of the falling rock is imparted onto the WP as mechanical energy. Furthermore, the rock does not shatter and deflection of the rock, as compared to deflection of the WP, is negligible.

- It is assumed that the outer barrier degrades completely prior to any pitting on the inner barrier. This assumption is made because the outer barrier is a less noble material, so it will degrade faster and also provide protection to the inner barrier. While this assumption is somewhat less conservative than the cathodic protection assumption used elsewhere in this report, this assumption only becomes relevant after 10,000 years (approximately the time at which half of the outer barrier has corroded away), and so is of no consequence with regard to the conclusions of Section 3.3.

3.3.2.5 Criteria for a Through Crack

The criteria assumed for developing a through crack in the containment barriers were based on the failure criteria in Section III of the ASME Boiler and Pressure Vessel Code. S_u is defined as the ultimate tensile strength of the materials and the criteria for the plastic analysis are described in the ASME Boiler and Pressure Vessel Code as follows:

The general primary membrane stress intensity shall not exceed $0.7S_u$ and the maximum primary stress intensity at any location shall not exceed $0.90S_u$. Therefore,

- Maximum Membrane Stress $< 0.7\ S_u$

- Maximum Membrane + Bending Stress $< 0.9\ S_u$

will be satisfied for both outer and inner barriers of the WP in order to prevent a through wall crack from developing.

For the outer barrier material, A 516 carbon steel, S_u = 485 MPa. Therefore, the criteria for the outer barrier are specified as follows:

- Maximum Membrane Stress < 0.7*(485) = 339.5 MPa
- Maximum Membrane + Bending Stress < 0.9*(485) = 436.5 MPa

For the inner barrier material, Alloy 625, S_u = 758 MPa. Therefore, the criteria for the inner barrier are specified as follows:

- Maximum Membrane Stress < 0.7*(758) = 530.6 MPa
- Maximum Membrane + Bending Stress < 0.9*(758) = 682.2 MPa

The margin of safety for the stress magnitudes is defined as follows:

- margin of safety = $(S_{allowable} / \sigma) - 1$, where σ is the maximum stress on the containment barriers.

3.3.2.6 Results of Analysis

The maximum membrane and membrane plus bending stress magnitudes are obtained for each degradation level and rock size by a two step procedure. First, a post-processing file is used to determine the location of the maximum stress intensity throughout the containment barriers. Then, the node numbers for these critical stress locations are used to define linearized stress paths through the thickness of inner and outer barriers. As a result, the linearized stresses are obtained along these paths for each time-step used in the simulation.

The criteria for developing a through crack in the containment barriers were explained in Section 3.3.2.5. Thus, the maximum stresses from the ANSYS solution are compared to the stress allowables in order to determine the critical rock sizes for different degradation levels in the WP containment barriers. Table 3.3-2 presents the maximum values of the membrane stress, membrane plus bending stress, and allowable stress magnitudes. Rock sizes were increased in the FEA until a comparison of allowable stresses with the maximum stresses indicated that a through crack developed in the outer barrier. The rock sizes at which this occurred are reported in Table 3.3-2 for the various degradation levels. The margin of safety values were calculated according to the relation given in Section 3.3.3.5 and provided in the same table. Since the margin of safety values are small for the membrane stresses in the inner barrier for the no degradation and 50 percent degradation levels, and for the membrane plus bending stress of the 75 percent degradation level, any further increase in the rock mass causes a through crack in the inner barrier also. Therefore, the rock mass and sizes given in Table 3.3-2 are used as the bounding results of this analysis.

Table 3.3-2 Emplacement Drift Rock Fall Results

Barrier Analysis at Different Degradation Levels	**Percent Degradation (General Thinning of Outer Barrier). It is assumed that the outer barrier degrades completely prior to any pitting on the inner barrier.**		
Outer Barrier Degradation	0%	50%	75%
Inner Barrier Degradation	0%	0%	0%
Membrane Stress in Outer Barrier	208	233	301
Membrane Stress Allowable in Outer Barrier	339.5	339.5	339.5
Margin of safety	0.632	0.457	0.128
Membrane Plus Bending Stress in Outer Barrier	636	655	495
Membrane Plus Bending Stress Allowable in Outer Barrier	436.5	436.5	436.5
Margin of safety	Limit Exceeded	Limit Exceeded	Limit Exceeded
Membrane Stress in Inner Barrier	518	510	497
Membrane Stress Allowable in Inner Barrier	530.6	530.6	530.6
Margin of safety	0.024	0.040	0.068
Membrane Plus Bending Stress in Inner Barrier	584	583	671
Membrane Plus Bending Stress Allowable in Inner Barrier	682.2	682.2	682.2
Margin of safety	0.168	0.170	0.017
Critical Rock Mass (kg)	38,000	24,000	3,500
Rock Size Diameter for Critical Rock Mass Values (m)	3.16	2.71	1.43

*All stresses in MPa

3.3.2.7 Time-Dependent Results

The membrane plus bending stress magnitudes in the outer barrier exceed the allowable stress limit, resulting in a through crack in this component for each degradation level in Table 3.3-2. Table 3.3-2 also shows that the stresses in the inner barrier are nearly equal to the stress limit. Thus, it is concluded that the critical rock size that the barriers are capable of withstanding during a rock fall in the emplacement drift has been determined.

No time-dependency has been associated with the data presented so far. If the approximate time is estimated at which the waste package outer barrier is expected to degrade by 50 percent and by 75 percent, then the critical rock mass necessary to breach the waste package can be determined as a function of time. Figure 3.3-7 indicates the average remaining thickness versus time of the outer barrier of the 26-yr-old BWR waste packages emplaced in the repository with the other waste packages in a "square" spacing at a thermal loading of 83 MTU/acre. This figure indicates that the 95th percentile of these waste packages experience roughly half of their outer barrier corroded away after about 10,000 years. About 75 percent of their outer barrier has corroded away after 20,000 years. Given this information and the information in Table 3.3-2, the time-dependency of the critical rock mass necessary to breach a waste package can be established, as summarized in Table 3.3-3.

Table 3.3-3 Variation of Critical Rock Mass with Time

Time (years)	Critical Rock Mass (metric tons)
0	38
10,000	24
20,000	3.5

3.3.3 SENSITIVITY OF TOTAL SYSTEM PERFORMANCE TO BOUNDING ROCKFALL EVENTS

A conservative approach to the problem of defining the effect of rockfall would be to assume a certain portion of the repository incurred rockfall strong enough to breach some bounding percentage of waste packages at 100 years. For this case, 1 percent of the waste packages were assumed to incur significant rockfall. These waste packages were assumed to be breached at 100 years, and the percentage of the waste packages with dripping fractures were assumed to initiate advective release from the waste form at that time. Approximately 50 percent (consistent with the percentage of waste packages assumed to see drips at an infiltration rate of 1.25 mm/yr; see Figure ES.5-4 in CRWMS M&O 1995d) of the packages breached by rockfall were assumed to follow the EBS transport release model noted as "drips on waste form" because the rockfall was assumed to create a breach large enough for dripping water to flow into the waste package. The 99 percent of the waste packages which did not incur rockfall were assumed to follow the EBS transport conceptual model of "drips on waste package" with only diffusive release out of the waste package, followed by advective release outside the waste package. This EBS transport conceptual model leads to lower releases than the drips on waste form conceptual model.

Results for 10,000 year peak dose rate CCDF's are presented in Figure 3.3-8. The TSPA-1995 results are presented for comparison. Due to computer limitations, the 99 percent and 1 percent cases were simulated separately. The CCDFs can be visually combined to evaluate the comparison of the rockfall case with the no rockfall case. The rockfall case will be approximately an order of magnitude worse than the TSPA-1995 case at the 50 percent probability of exceeding the calculated dose.

The significance of the rockfall is also shown by comparing the 1 percent of waste packages with no rockfall with the 1 percent rockfall case. The 1 percent of the waste packages with rockfall case is about a factor of 2 higher than the no rockfall case. This is important when comparing the other analyses in the report because an increase of a factor of 2 to the 30 km results for either ACD or lineloading design will still not increase the peak dose rates above the 10,000 year standard. CCDF results for the 1,000,000 year peak dose rockfall case are presented in Figure 3.3-9. The results are presented similar to the 10,000 year case. They indicate that the effect of 1 percent of the waste packages breaching due to rockfall at the beginning of the postclosure period degrades long-term repository peak dose rate performance by two to five-fold.

3.3.4 ASSESSMENT OF ROCKFALL ON TOTAL SYSTEM PERFORMANCE

The analysis in Section 3.3.1 concluded that the typical (most frequent) sizes of rock blocks appear to be in the range from 0.1 to 0.2 metric tons. The maximum sizes are judged to lie in the range from about 3 to 5 metric tons. Furthermore, Section 3.3.1 indicates that a relevant analysis in the waste package off-normal report (CRWMS M&O 1996e) employed joint frequency data in finding a 99 percent cumulative frequency of occurrence for blocks smaller than 10 metric tons.

The analysis in Section 3.3.2 concluded that the weight of a rock necessary to breach a waste package that had not yet degraded by corrosion effects is 38 metric tons. Furthermore, the same analysis shows that after fully half of the outer barrier of the waste package has corroded away, a 24-metric ton rock is required to breach the waste package. As indicated in Table 3.3-3, for 95 percent of the waste packages this is predicted to occur no earlier than 10,000 years. Furthermore, Section 3.3.1 indicates that there is at most a 1 percent likelihood of rock blocks of such size.

If the likelihood of rockfall is evenly distributed throughout all emplacement drifts, and the emplacement drifts are tightly packed with waste packages such that there are no gaps between waste packages, then a 1 percent likelihood of rock blocks greater than 10 metric tons translates into 1 percent of the waste packages impacted by these large rocks. In this conservative scenario, at most 1 percent of the waste packages would be breached by rockfall. The fact that over a 10,000 year time frame the size of rock necessary to breach a waste package is significantly greater than 10 metric tons is additional reason to regard as conservative the estimation that at most 1 percent of the waste packages would be breached by rockfall. The results in Section 3.3.3 indicate that this would increase the peak dose rate seen 30 km from the repository by about two-fold.

Finally, although the size of rock necessary to breach a waste package decreases with time (Table 3.3-3), the effects of such rocks on waste package performance also decreases. Figure 3.1-14 depicts the time-dependent fraction of waste packages that breach due to corrosion:

- By 4000 years approximately 80 percent of the waste packages have been breached by corrosion.

- By about 7000 years, fully 95 percent of the waste packages have been breached.

As more and more waste packages are breached by corrosion, the likelihood is greater that the very small percentage of waste packages that are impacted by significant rockfall would have already been breached due to corrosion.

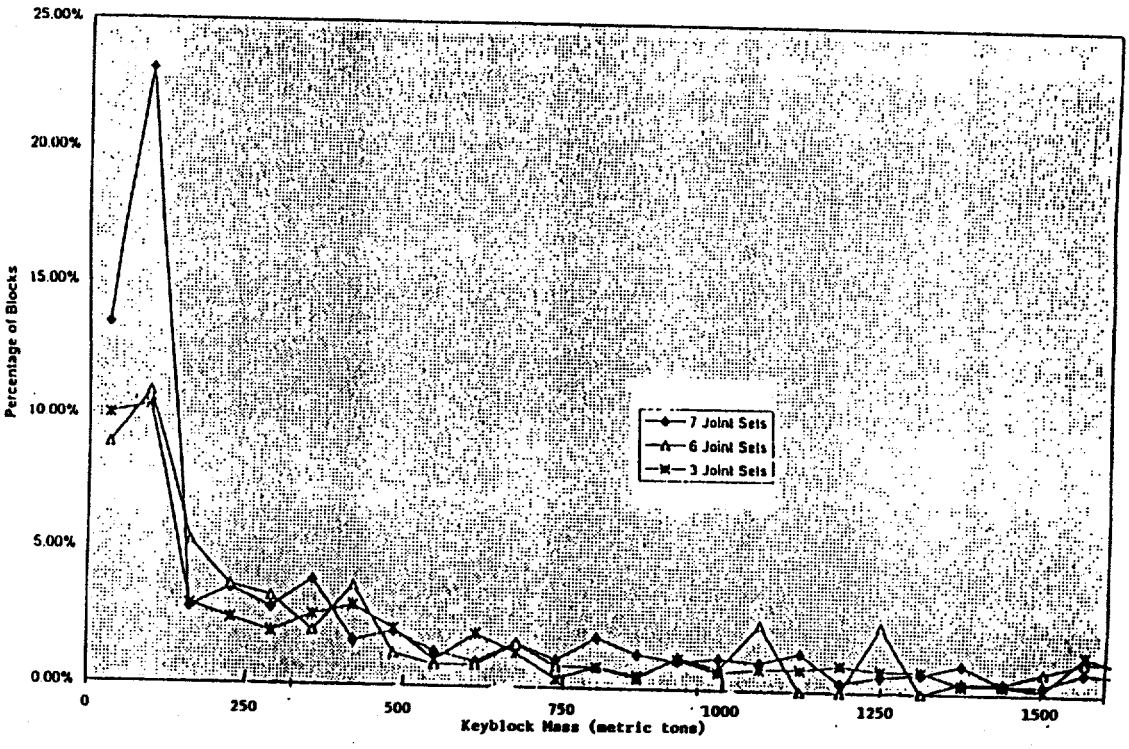

Figure 3.3-1 Keyblock size distribution, north-south orientation

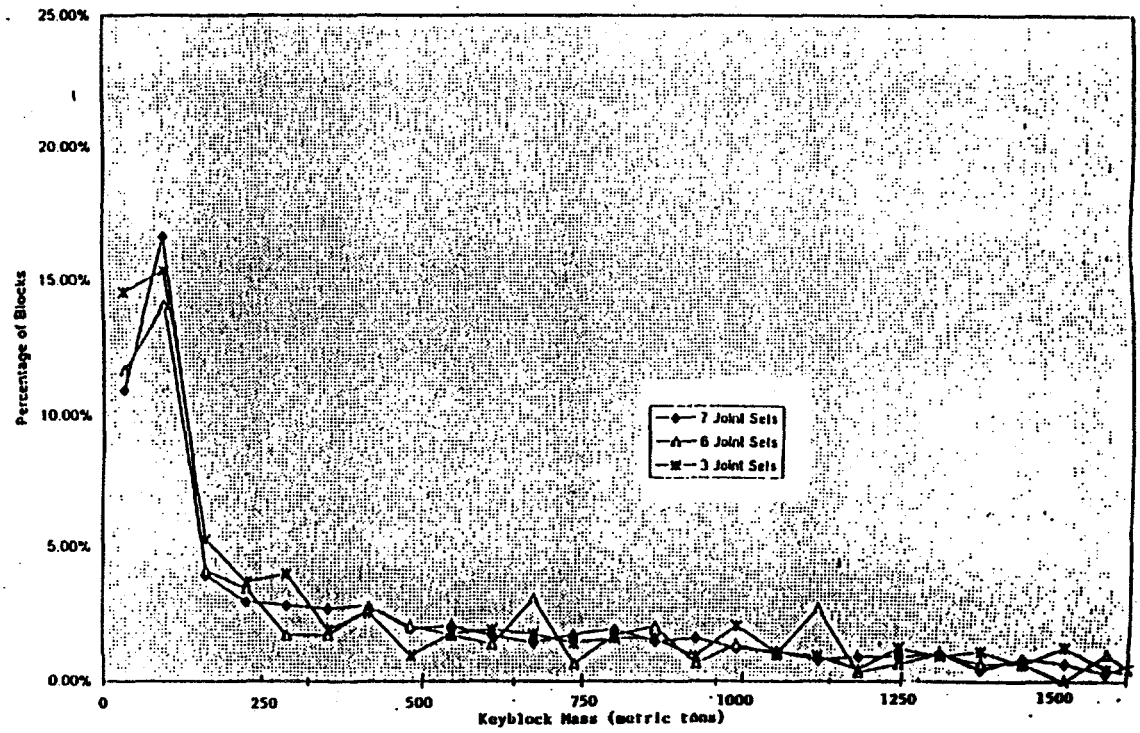

Figure 3.3-2 Keyblock size distribution, east-west orientation

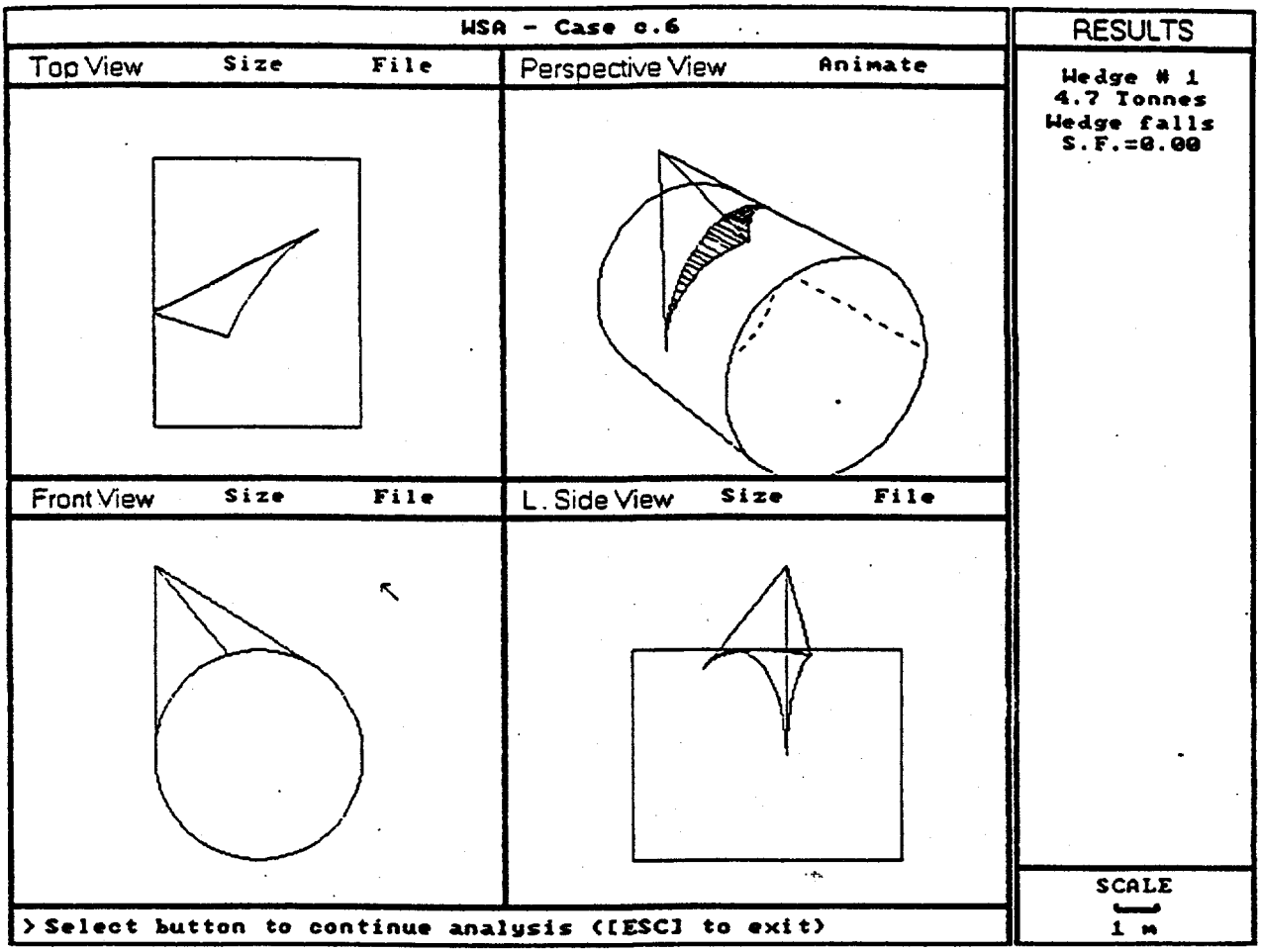

Figure 3.3-3 Example of rock wedge from UNWEDGE analysis

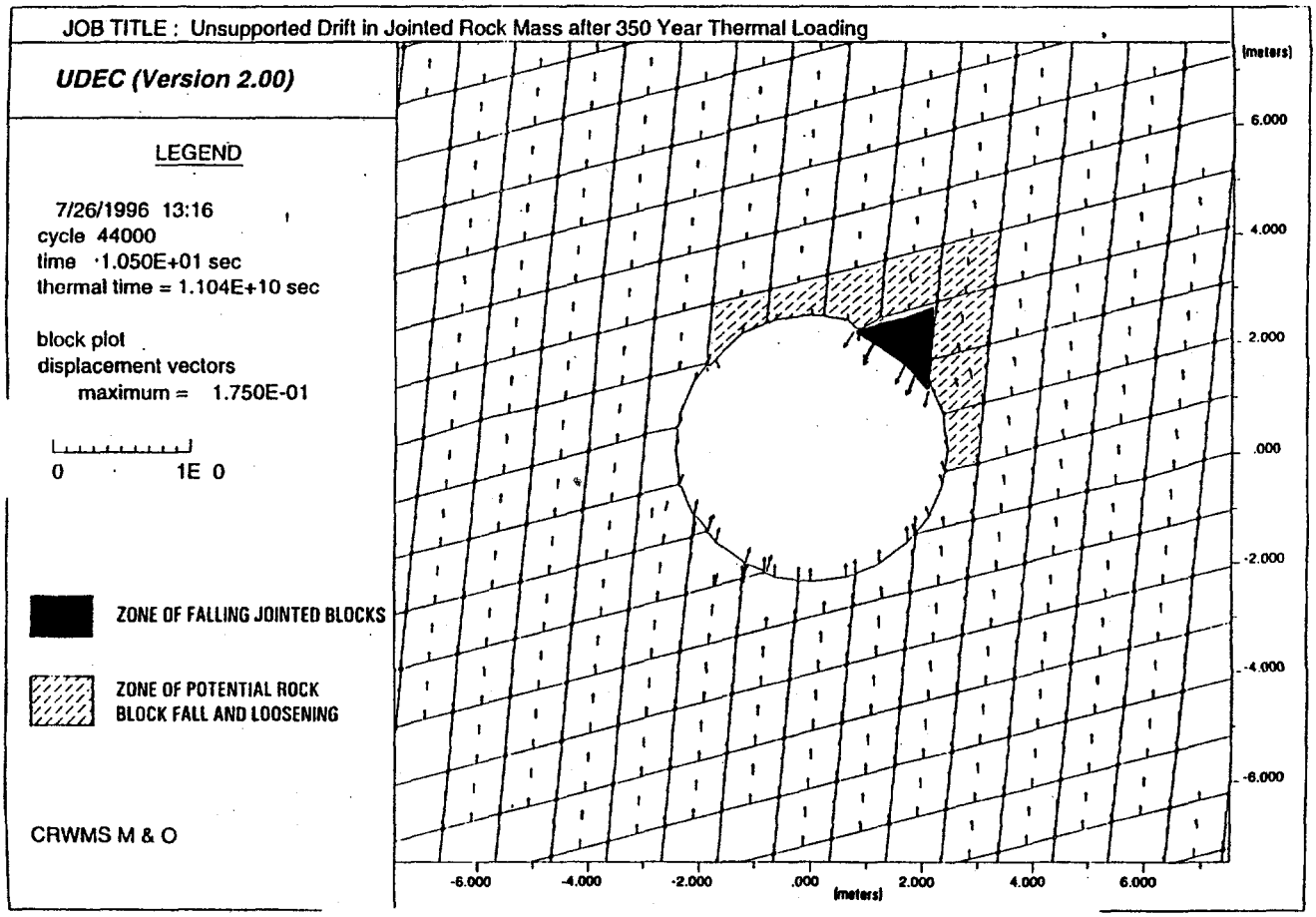

Figure 3.3-4 Example of rock keyblock formation from UDEC analysis

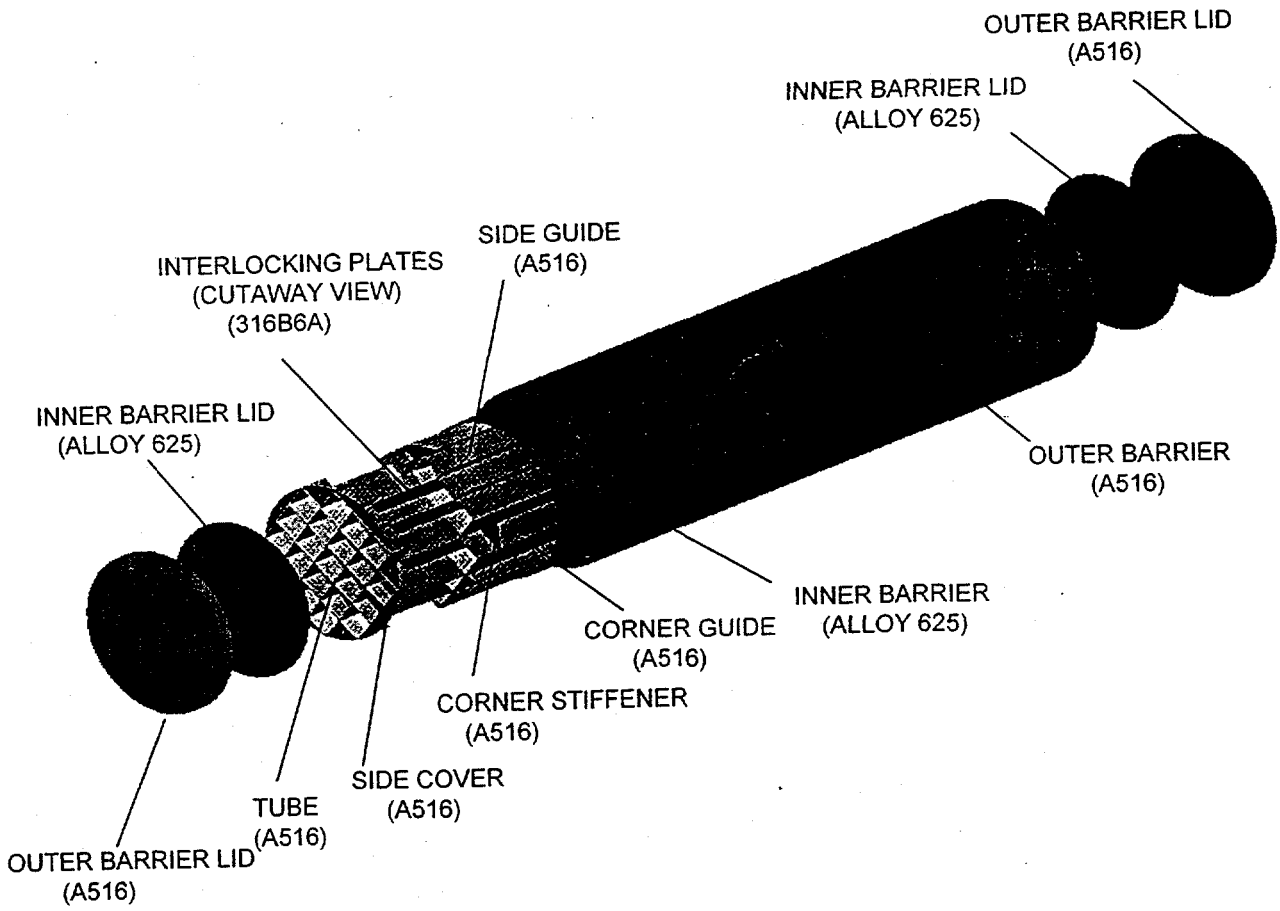

Figure 3.3-5 21-PWR advanced uncanistered fuel waste package

D = Emplacement drift tunnel diameter
r_1 = WP containment barrier outer radius
r_2 = Rock radius (determined by finite-element analysis for different levels of degradation in the WP)
k = Invert
h = Rock fall height = Tunnel height - $2*(r_1)$ - k
y = Distance from the WP center to the rock center = $h + r_1 + r_2$

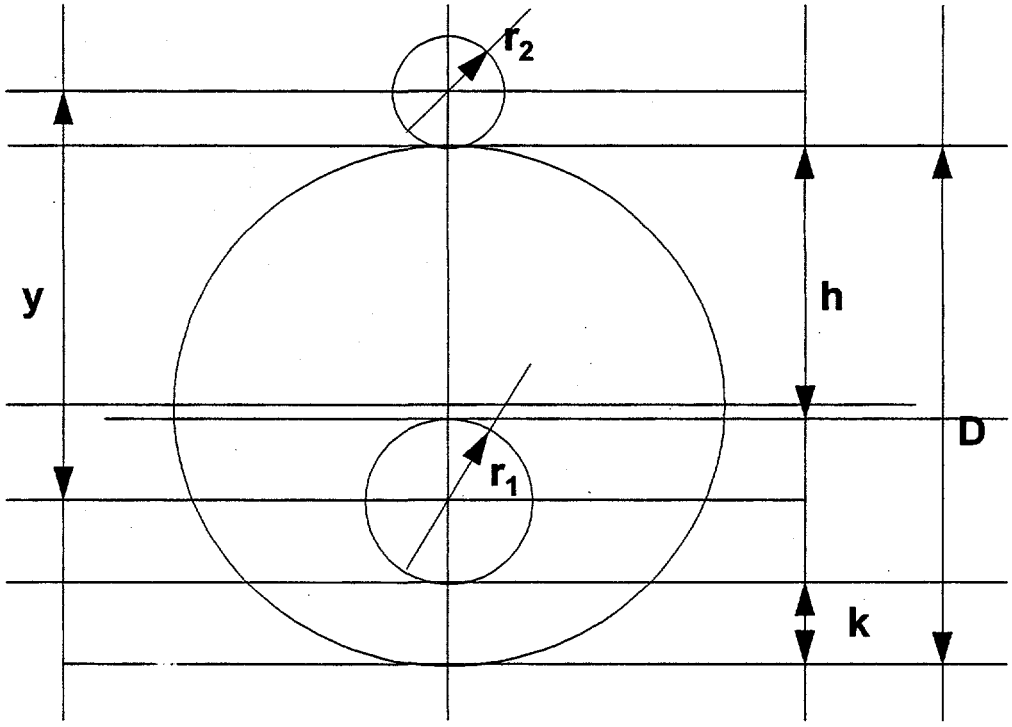

Figure 3.3-6 Emplacement Drift Tunnel Geometry

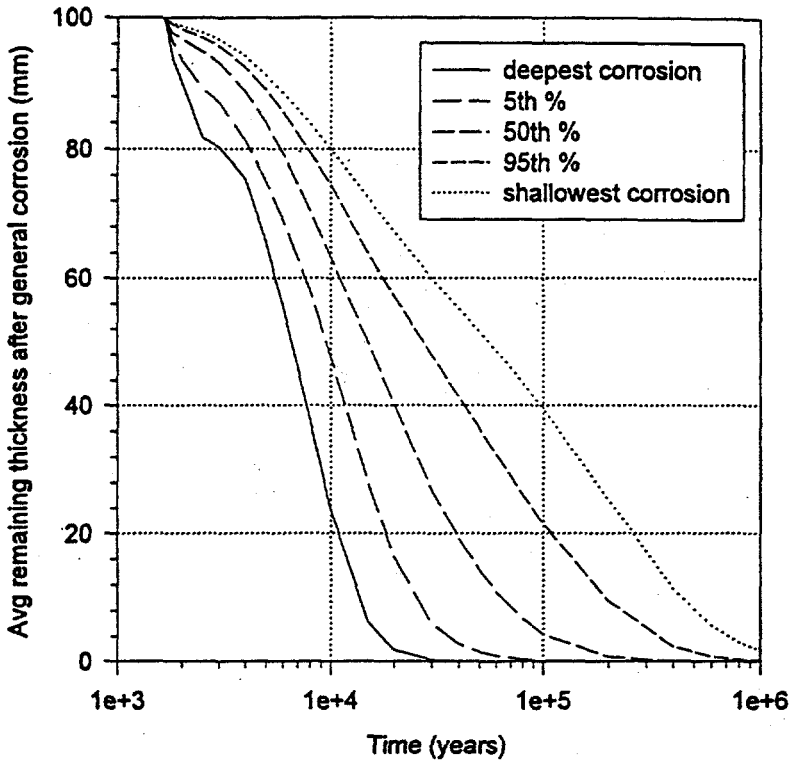

Figure 3.3-7 Depth of general corrosion for ACD, no backfill, 26-yr-old BWR case

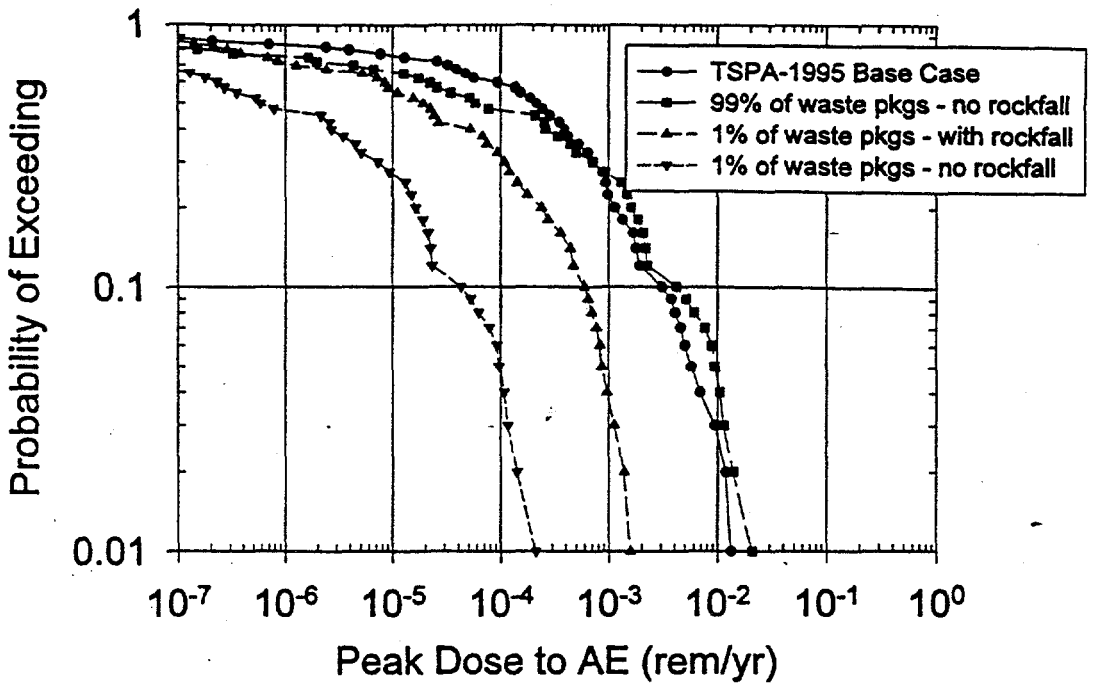

Figure 3.3-8 10,000 yr total peak dose CCDFs for rockfall evaluation (1% of waste packages breached due to rockfall)

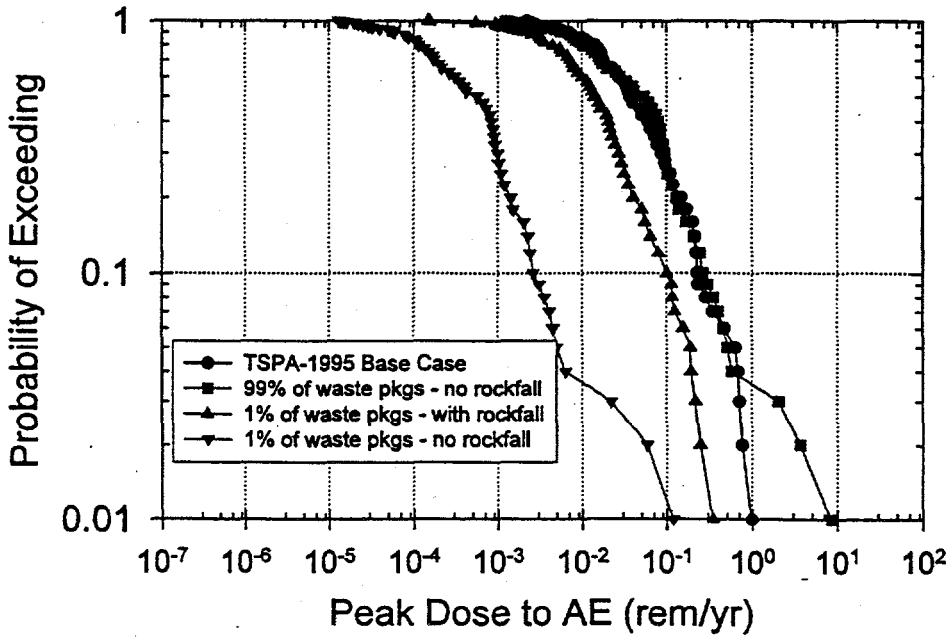

Figure 3.3-9 1,000,000 yr total peak dose CCDFs for rockfall evaluation (1% of waste packages breached due to rockfall)

3.4 IMPLICATIONS OF ^{36}Cl FINDINGS

This section summarizes ^{36}Cl data, including that collected in the ESF as of March 1996, and implications for conceptual models of the unsaturated zone under Yucca Mountain. This discussion formed part of a white paper on ^{36}Cl issues prepared by the CRWMS Management & Operating Contractor (CRWMS M&O 1996m). It is also important to note that work is continuing on these issues and more data and modeling will be available in FY 1996 Level 3 Deliverables, as well as work planned to continue in FY 1997.

Based on our conceptual model of unsaturated zone flow at Yucca Mountain, it is expected that the PTn will constitute a major barrier to infiltration into the TSw, and elevated $^{36}Cl/Cl$ ratios to be indicative of zones of rapid flow below the PTn (but not necessarily high fluxes). However, above the PTn we may expect the occurrence of elevated ^{36}Cl to be fairly common, if variable. High $^{36}Cl/Cl$ ratios have been discovered at several meters depth in alluvium at the site, whereas in other locations the $^{36}Cl/Cl$ ratios have been more like background (several tens of samples total). In some boreholes, both elevated and background ratios have been observed in the same well. This illustrates that infiltration processes are heterogeneous, even within the alluvial cover of Yucca Mountain. Similarly, variable $^{36}Cl/Cl$ ratios are found within both the TCw and PTn at the site, reinforcing our notion of the heterogeneity of the shallow hydrologic system. Saturated zone and perched waters have rather uniform $^{36}Cl/Cl$ ratios toward the low end of what is considered to be background.

In general, elevated ratios have not been found below the PTn unit in boreholes (several tens of samples), especially in the 15-20 samples that have been analyzed between the PTn and the CHn. Some borehole samples have reported $^{36}Cl/Cl$ ratios that are lower than background, but it is uncertain whether the low ratios are due to radioactive decay of the ^{36}Cl during long residence or travel times of pore water, or to the dilution of the porewater $^{36}Cl/Cl$ ratios by Cl released from the rock during drilling. The latter is a distinct possibility.

It is difficult to perform planned lateral sampling or feature-specific sampling based on boreholes; thus, the ESF affords a unique opportunity for uniform lateral sampling and sampling fractures and faults which appear to have favorable characteristics for fracture flow. As of March 1996, the ESF sampling (16 of 52 samples) detected elevated or bomb-pulse ^{36}Cl in five locations along with background values. Three of the five locations recorded multiple elevated occurrences. The two that did not may be an artifact of sampling density.

First, four samples showed an elevated signal near the entrance of the ESF (station 2) within the Bow Ridge Fault. In this case, it appears that the fault itself was a direct conduit for water flow. Second, between stations 12 and 13, a single occurrence of high ^{36}Cl was recovered from a cooling fracture. This sample is in the vicinity of the western limit of the Imbricate Fault Zone; however, its correlation to a specific fault is not as obvious. Third, four elevated samples were found within a 45 meter interval near the Drill Hole Wash Fault. Fourth, as the North Ramp comes out of the turn into the Main Drift, another single elevated sample was detected. At this occurrence, there is not an obvious correlation with a known fault. However, the sample is described as being taken from a shear zone and it is located fairly close to a fault mapped at the surface that could have provided a pathway for water. Fifth, over a length of about 120 meters, six samples with bomb-pulse ^{36}Cl were found. These samples all occur near the intersection of the Sundance Fault with the ESF.

Three of the five occurrences of bomb-pulse ^{36}Cl are clearly associated with faults known to penetrate the PTn. The correlation of the remaining two sample locations with major faults is not known, but they are in reasonable proximity to features that could have allowed fast flow through fractures. The significant lateral spread (45 m and 120 m) in two of the occurrences are consistent with our conceptual model that a fault typically is required to disrupt the PTn and allow the flow of water. Once water penetrates the PTn and enters the TSw, it will take whatever fracture or feature is hydrologically favorable. In other words, water does not discriminate between faults, cooling joints, shear zones, or lithophysae. Although occurrences of bomb-pulse ^{36}Cl are expected to be concentrated near faults that transect the PTn unit, some spread in the distribution of ^{36}Cl at depth also is expected.

It is important to note that the ^{36}Cl results are generally consistent with the conceptual model of the unsaturated zone under Yucca Mountain. The data do suggest that there are certain preferential flow pathways, but do not necessarily mean that these pathways are zones of high flux. In addition, even if some or all of these are high flux zones, that does not necessarily translate to a spatially uniform high flux over the entire repository area. It is for these reasons that the assumed percolation fluxes in the process model and TSPA simulations in this and subsequent sections are considered reasonable based on our present understanding. The Project will continue to test these assumptions and refine our conceptual model as data collection and modeling continue through FY 1996 and into FY 1997.

4. POTENTIAL EBS FUNCTIONS AND ASSOCIATED CONCEPTS

Section 3 makes a strong case that there is no need to supplement the EBS with additional barriers beyond the waste package. However, the "Interim Postclosure Standard" (YMSCO, 1996, Attachment 1) mandates that "engineering measures that have potential for significantly reducing the peak dose rate, and could be implemented at reasonable cost, will be evaluated for possible inclusion in the reference design." Implementation of this mandate will help identify cost-effective means of adding confidence to total system performance assessments.

However, rather than haphazardly and inefficiently identifying a multitude of "engineering measures" or concepts that may significantly improve repository performance at reasonable cost, a methodical approach is defined and implemented. This approach is three-fold:

- First, to identify the various postclosure performance functions that can be performed by the Engineered Barrier System, both in terms of extending the waste package lifetime as well as in delaying the transport of radionuclides once the waste packages have been breached. Mechanisms that allow each of the functions to be realized will be identified, as well as one or more concepts that may satisfy each identified mechanism. This is performed here in Section 4.

- Second, to perform preliminary performance assessment sensitivity analyses wherein the concepts identified in the previous step are each given finite lifetimes to establish whether they have any noticeable or significant impact on total system performance. This step is conducted in Section 5.1.

- Third, to examine more closely those concepts that have initially shown an ability to improve total system performance. This examination will entail conducting a more in-depth assessment of the ability of the concept to achieve the function(s) desired. If it becomes clear that the concept cannot achieve the intended function for the length of time deemed necessary in step 2, then examination of the concept will not be pursued any further. The costs, uncertainties, and risks associated with the concept will be addressed, if appropriate. This step is conducted in Sections 5.2 through 5.5.

4.1 POTENTIAL POSTCLOSURE EBS FUNCTIONS

A clear delineation of the various postclosure performance functions that can be performed by the Engineered Barrier System (EBS), both in terms of extending the waste package lifetime as well as delaying the transport of radionuclides once the waste package has been breached, will be conducted in this section. Furthermore, other function(s) that the EBS may be able to perform will also be described. The mechanisms that allow each of the performance functions to be realized will be identified, as well as one or more concepts that satisfy each identified mechanism.

A total of seven postclosure performance EBS functions have been identified, as shown in Table 4.1-1. These functions fall into two categories: functions that extend waste package lifetimes, and functions that delay the transport of radionuclides once the waste packages have been breached.

As a preface to the discussion of the various potential EBS functions, mechanisms, and concepts, it is important to note how they were developed. This is important because the majority of the work conducted within this study followed from this determination of functions, mechanisms, and concepts. Therefore, it is important that there is a defensible basis for such a starting point. Soon after the inception of this system study, a kickoff meeting was held with attendance from representatives from the Performance Assessment and Modeling, Repository Design, Scientific Program, Systems Engineering, Waste Package Development, and Waste Package Materials organizations, as well as representatives from Los Alamos National Laboratory, Lawrence Livermore National Laboratory, and Sandia National Laboratories. The second day of the kickoff meeting was comprised of a "brainstorming" session in which the majority of the EBS functions, mechanisms, and associated concepts were identified and discussed. Subsequent to this meeting, the work conducted during the brainstorming session was refined and expanded upon.

Four postclosure EBS functions (see Table 4.1-1) were identified that could extend the waste package lifetime, depending on how long the functions are realized. The first few functions all deal with the impact water (in either a vapor or aqueous form) would have on the life of a waste package that has a corrosion allowance material outer barrier. Preventing liquid water contact with the waste package would reduce to some degree the corrosion rate and thus extend the life of the waste package. Reducing the relative humidity at the waste package surface for some period of time would delay the inception of either humid-air and/or aqueous corrosion, thus extending the life of the waste package. As opposed to delaying or reducing the corrosion rates by keeping water (either liquid water or films of condensate) off the waste package, another possible means of extending the waste package lifetime would be to reduce the corrosion properties of water that come in contact with the waste package. Finally, the waste package lifetime could possibly be extended if the EBS were to act so as to structurally protect the waste package from rockfall.

Three potential EBS functions were identified that would delay the transport of radionuclides once the waste package has been breached. The first of these would occur if the EBS were to function as an aqueous diffusion barrier to released radionuclides. That is, if the transport of radionuclides through the EBS were forced to be caused by diffusive rather than advective transport, radionuclide travel times through the EBS would increase. The second function identified in this group of functions is that which would retard transport of released radionuclides. Although one could argue that the previous function which causes diffusive transport of released radionuclides is also a form of retardation, this latter function more specifically relates to the sorption of radionuclides while still within the EBS. The third function in this group is that which would reduce the radionuclide solubility properties of incoming water and/or reduce the waste form dissolution rate. Treating any incoming water before it contacts the waste form within the breached waste package such that important radionuclides are less soluble or such that the dissolution rate of the waste form is reduced would serve to delay the transport of radionuclides through the EBS.

In the following section, mechanisms and their associated concepts will be identified for each of the potential EBS functions listed in Table 4.1-1. This is done for two reasons:

- To show how the concepts are tied to particular EBS functions, and
- To demonstrate that various concepts may be able to satisfy more than one potential EBS function.

Although it is arguable that those concepts that satisfy the largest number of EBS functions should be the ones deserving a closer look, this should be tempered with information that indicates the importance of each of the EBS functions to the total system performance (peak dose rate at the accessible environment). That is, it is conceivable that a concept satisfies perhaps only one or two EBS functions but that the achievement of those EBS postclosure performance functions are more important than any of the others in terms of impacts on total system performance. In this case it is not so much how many functions a concept may satisfy, but rather the importance of those functions to total system performance. An assessment of the relative importance of the various potential EBS postclosure performance functions will be conducted in Section 5.

Table 4.1-1 Potential Postclosure EBS Functions

FUNCTIONS THAT EXTEND WASTE PACKAGE LIFETIME
Prevent Liquid Water Contact with Waste Package
Reduce the Relative Humidity at the Waste Package Surface
Reduce Corrosion Properties of Incoming Water
Act as Structural Protection from Rockfall
FUNCTIONS THAT DELAY TRANSPORT OF RADIONUCLIDES ONCE WASTE PACKAGE HAS BEEN BREACHED
Act as a Barrier to Advective Flow
Retard Transport of Released Radionuclides
Reduce Radionuclide Solubility Properties And/Or Reduce Waste Form Dissolution Rate

4.2 POTENTIAL POSTCLOSURE EBS PERFORMANCE FUNCTIONS, THEIR MECHANISMS AND ASSOCIATED CONCEPTS

Section 4.2.1 will delineate the mechanisms and associated concepts for each of the EBS functions identified in Table 4.1-1. Section 4.2.2 contains a description of those concepts that appear to hold promise of satisfying multiple EBS functions.

4.2.1 IDENTIFICATION OF MECHANISMS AND ASSOCIATED CONCEPTS

4.2.1.1 Function : Prevent Liquid Water Contact With the Waste Package

Two mechanisms have been identified by which it would be possible to prevent liquid water contact with a waste package. The first mechanism is flow diversion, and the second is evaporation. Diverting any water that makes its way into the emplacement drift and toward the waste package can be achieved by either a Richards Barrier or a drip shield. Evaporation of liquid water before it comes in contact with the waste package can be accomplished by means of a single layer backfill covering the waste package.

4.2.1.2 Function : Reduce the Relative Humidity at the Waste Package Surface

Two mechanisms have been identified to achieve this function. Developing a positive DT between the drift wall and waste package surface is one mechanism, and allowing for vapor pressure equilibrium throughout the drift is the second. Both of these mechanisms can be explained by looking at the equation for the relative humidity on the waste package surface (CRWMS M&O 1996n):

$$RH_{wp} = RH_{dw}\left(\frac{P_{sat}(T_{dw})}{P_{sat}(T_{wp})}\right)\left(\frac{P_{v_{wp}}}{P_{v_{dw}}}\right)$$

where,

RH_{wp} = relative humidity at the waste package surface
RH_{dw} = relative humidity at the drift wall
P_{sat} = local saturated vapor pressure
T_{dw} = drift wall temperature
T_{wp} = waste package surface temperature
P_v = local vapor pressure

The relative humidity on the waste package surface depends on the RH_{dw}, the ratio of the saturated vapor pressures, and the ratio of the local vapor pressures. For a given RH_{dw}, that depends primarily on the AML and the thermal properties of the mountain, the way to reduce the relative humidity on the waste package surface is to decrease the value of the ratio of the saturated vapor pressures and to decrease the value of the ratio of the local vapor pressures. Reducing the value of the first ratio is performed by increasing the temperature of the waste package surface over that of the drift wall; that is, developing a positive DT between the drift wall and waste package surface. This will cause the saturated vapor pressure at the waste package surface to be higher than that at the drift wall. The ratio of the local vapor pressures will be unity if the P_v at the waste package surface is in equilibrium with the P_v at the drift wall.

Several concepts have been identified to satisfy the first mechanism listed; including a single-layer backfill or a Richards Barrier. These concepts were identified because, whether a single-layer backfill

or a multi-layer backfill such as the Richards Barrier, they would satisfy this mechanism to varying degrees by essentially insulating the waste package and thus causing its surface temperature to rise.

Achieving vapor pressure equilibrium between the waste package surface and the drift wall can be managed by means of:

- A low matric potential single-layer backfill or Richards Barrier, or
- No type of barrier at all between the waste package surface and the drift wall.

4.2.1.3 Function : Reduce Corrosion Properties of Incoming Water

Three mechanisms were identified as a possible means of achieving this function. They are high pH, low oxygen fugacity, and low microbial content.

High-pH water may produce passivation (corrosion-impeding) films on the outer barrier of the waste packages, possibly increasing waste package lifetimes. Reducing the oxygen content of any water that comes in contact with the waste packages could be another means of delaying or reducing the rate of corrosion of the waste packages by reducing the rate of oxidation of the metal. MIC occurs due to the metabolic activity of micro-organisms. Although the extent to which MIC can influence waste package lifetimes is currently not well known, indications are that micro-organisms may indeed have a detrimental effect on waste packages (Horn and Meike, 1995). Reducing the quantity and diversity of micro-organisms in any water that comes in contact with waste packages may also be a means of helping extend the waste package lifetime.

A couple of concepts have been identified that may increase the pH of any water that comes in contact with the waste packages. These concepts are a chemically conditioned backfill, and a shotcrete liner. These same concepts were also considered applicable for the mechanism of reducing the oxygen content of any water contacting the waste packages. The final mechanism of reducing the microbial content of incoming water was determined possible only if the surface of the waste package was maintained hot (>120°C) and dry (Horn and Meike, 1995). A low thermal conductivity backfill was considered one means of extending the time during which such conditions would prevail.

4.2.1.4 Function: Act as Structural Protection From Rockfall

Two mechanisms have been identified which may allow this function to be achieved. Not allowing any falling rocks to impart any dynamic load on the waste packages is one mechanism, and reducing the load experienced by the waste packages due to rockfall is the second mechanism. The use of a rigid shield (such as a rigid drip shield) over the waste packages would be one way of keeping the waste packages from feeling any effects of rockfall. Completely filling the emplacement drifts with backfill could also be a means of eliminating any dynamic load imparted on a waste package due to rockfall by essentially eliminating the possibility of rockfall within the emplacement drifts. The use of a backfill which does not completely fill the void space within the emplacement drifts could be a means of distributing the load imparted to a waste package due to rockfall.

4.2.1.5 Function: Act as a Barrier to Advective Transport of Released Radionuclides

Radionuclides may be transported from the waste packages by advective and/or diffusive mechanisms. A drip shield or a Richards Barrier have been identified as concepts that could prevent advective flow past the waste packages leading to only diffusive release from the waste packages. The drip shield would do this by means of a rigid barrier whereas the Richards Barrier would divert advective flow by means of a capillary barrier. Lower advective flow into the EBS would also lead to lower saturations and even reduced diffusion from the waste packages. Diffusive releases from the waste packages are expected to be significantly lower than advective releases.

4.2.1.6 Function: Retard Transport of Released Radionuclides

The specific meaning of this function is to retard the transport of radionuclide independent of whether they are transported by advection or diffusion. Sorption is the single mechanism associated with this function. The concept identified as appropriate for such a mechanism is a highly sorptive invert that retards long-lived radionuclides such as ^{237}Np.

4.2.1.7 Function: Reduce Radionuclide Solubility/Waste Form Dissolution Rate

The mechanism identified to achieve such a function is to reduce the oxygen fugacity of the water that comes in contact with the waste form. A single layer backfill that has been chemically conditioned might be one means to accomplish this. A second concept could involve a shotcrete liner that essentially seals the emplacement drift such that no oxygen is permitted to ingress.

4.2.2 MULTI-FUNCTIONAL EBS CONCEPTS

It is evident from the analysis conducted in Section 4.2.1 that several EBS concepts are identified as being able to potentially satisfy multiple postclosure EBS performance functions. They include:

- Single Layer Backfill (possibly chemically conditioned)
- Drip Shield
- Richards Barrier.

As these concepts potentially can satisfy a multitude of postclosure EBS performance functions, focus is initially on them. However, simply selecting concepts because they may to be able to satisfy multiple EBS functions is not necessarily correct, especially if it happens that the functions, given finite and reasonable lifetimes, have no significant effect on total system performance. Therefore, in Section 5.1, the functions identified in this section are examined in more detail in that they are assigned finite lifetimes and their impact to total system performance is assessed.

Although the highly sorptive emplacement drift invert concept appeared under only one function, previous research conducted holds promise that a chemically conditioned invert may have a significant impact on total system performance. Therefore, the sorptive invert concept will remain a consideration.

5. EBS CONCEPTS EVALUATION

A preliminary performance assessment is presented in this section (Section 5.1) in which the sensitivity of the long-term repository performance is determined relative to specific EBS functions with finite lifetimes. In most cases, very long lifetimes are first provided to the functions as a way of determining whether there is any potential for the function to have an effect on total system performance. If a function is given an implausible lifetime, such as 500,000 years, and there is no impact to total system performance, then it becomes quickly clear that there is no need to pursue such a function any further. On the other hand, a significant improvement in repository performance would be incentive to further investigate the function by first reducing the lifetime associated with it.

In Section 5.1 all but two of the functions identified in Table 4.1-1 are examined. The first function not examined in Section 5.1, "Prevent liquid water contact with the waste package," is considered a potential function that could extend the waste package lifetime. The assumption here is that liquid water contact (rather than the thin or thick films associated with high relative humidities on the waste package surface) would enhance the corrosion rates. Diverting the aqueous water from contacting the waste packages would then aid in extending waste package performance by reducing corrosion rates. However, the TSPA-1995 corrosion model already assumes that liquid water is not required to contact the waste packages for corrosion to occur. The current corrosion models employed reflect corrosion initiation and corrosion rates of waste package surface conditions in terms of relative humidity and temperature only. This is consistent with conditions expected at low infiltration rates, in which a very small percentage of waste packages would expect to see drips. At higher infiltration rates (1.25 mm/year), however, the current abstraction in TSPA-1995 (CRWMS M&O 1995d, pg. ES-37) indicates about 50 percent of the waste packages would see drips. What is currently not known is the additional degradation of the waste packages that may occur on those 50 percent of the waste packages that do see drips.

The second function not examined in Section 5.1, "Reduce the relative humidity at the waste package surface," is considered a potential function that could extend the waste package lifetime. This particular function was determined to be too complicated and cumbersome for a simple sensitivity analysis. However, although a sensitivity analysis of this function is not addressed in Section 5.1, the concept associated with this function, a single layer backfill, is the focus of this report and so will be addressed in detail in Section 5.2.

Additional analyses are included in Section 5.2.8 that incorporate recent thermohydrologic calculations by Lawrence Livermore National Laboratory for alternative waste package spacing design (ACD and lineloading). These analyses evaluate the performance in terms of peak dose rate over 10,000 years and 1,000,000 years for the case with backfill at alternative accessible environment locations. A brief discussion on the effect of cathodic protection on the dose rate results is also included.

5.1 PRELIMINARY PERFORMANCE ASSESSMENT OF SOME POTENTIAL EBS FUNCTIONS

As identified in Section 4, several potential EBS functions are being evaluated to determine their impact on repository performance (i.e., change in dose rate at the accessible environment). These functions are grouped into two main categories:

- Functions that extend waste package lifetime and reduce advective transport, and
- Functions that delay radionuclide transport after waste package failure.

The assessment of the impact of the EBS functions on performance in comparison with the "Interim Postclosure Standard" (YMSCO, 1996, Attachment 1) is provided in this section.

The evaluation of the ability of the overall disposal system to meet the performance objectives specified in the applicable regulatory standards has been termed TSPA. TSPAs require the explicit quantification of the relevant processes and process interactions. In addition to providing a quantitative basis for evaluating the suitability of the site to meet regulatory objectives, such assessments are useful to help define the most significant processes, the information gaps and uncertainties regarding these processes and the corresponding parameters, and therefore the additional information required in order to have a more robust and defensible assessment of the overall performance.

Total system performance assessments explicitly acknowledge the uncertainty in the process models and parameters and strive to evaluate the impact of this uncertainty on the overall performance. The aim of any total system performance assessment is to be as complete and reasonably conservative as possible and to ensure that the descriptions of the predictive models and parameters are sufficient to ascertain their accuracy. The EBS functions can be incorporated into a TSPA for appropriate evaluation of the impact on the performance of the system.

The specific goals of the EBS performance assessment are to:

- Evaluate the total system performance (expected value and peak dose rate at the accessible environment over 10,000 and 1,000,000 years) for the alternative EBS functions
- Provide comparisons of performance at alternative accessible environment locations (i.e., 5 km and 30 km from repository)
- Utilize recent alternative waste package spacing designs in the analyses
- Utilize recent process level modeling and laboratory data for the TSPA analyses.

Case Description

The performance assessment of the EBS functions and their impact on the overall performance of the repository are described in the following. A variety of cases were analyzed to evaluate the impact

on expected value dose rate at the AE and peak dose rate over specified time periods (e.g., 10,000 and 1,000,000 years). The cases are generally grouped according to EBS function (Table 5.1-1). The two major EBS functions were extend waste package lifetime and reduce advective transport, and delay radionuclide transport after waste package failure.

Case Extend Waste Package Lifetime/Reduce Advective Transport

1) Capillary barrier/drip shield with a limited lifetime to delay the onset of advective release,
2) Decrease the corrosion of the waste packages by preconditioning the water that flows into the repository, and
3) Protect the waste packages from rockfall.

Delay Radionuclide Transport

4) Condition the transport characteristics of the invert to retard transport of the radionuclides,
5) Condition the solubility of ^{237}Np to delay its transport, and
6) Condition the spent fuel waste form to decrease the dissolution rate using pH and direct intervention in the dissolution rate.

Each of the cases was based on the TSPA-1995 case of high thermal load, backfill, and high infiltration (initial q_{inf} =1.25 mm/yr) (Figure 9.3-40, CRWMS M&O 1995d). In some of the cases, both high and low thermal conductivity in the backfill were simulated to evaluate the impact of the proposed EBS enhancement. The high thermal conductivity backfill case was the Lingineni analysis presented in TSPA-1995 (calculated using the Finite Element Heat and Mass (FEHM) code). The low thermal conductivity backfill case was the Buscheck analysis presented in TSPA-1995 (calculated using TOUGH2). There were some conceptual differences in these two cases aside from the conductivity of the backfill which led to significantly different temperature and relative humidity histories (Buscheck and Blink, 1995). Also, for each of the cases additional sensitivity analyses were conducted to further evaluate the impact of the proposed EBS enhancement. The base case EBS release model was the "drips-on-waste-container" EBS transport model (i.e., only diffusive release from the waste package and both advective and diffusive release from EBS) (see Figure 6.5-10, CRWMS M&O 1995d).

The sensitivity analyses conducted with this section are illustrated by means of "expected value" dose rate histories (see Figure 5.1-1 as an example). An expected value dose rate history is the breakthrough curve for dose rate exposure (rem/year) for a single RIP realization that uses the expected values for all stochastic parameters modeled in RIP. The total dose at any given time in an expected value dose history plot can be determined by summing the contributions from the individual radionuclides.

5.1.1 EXTENSION OF WASTE PACKAGE LIFETIME

Case 1: Limited-lifetime capillary-barrier/drip shield (and evaporative effects of backfill).

In this case, the effect of a limited lifetime capillary barrier/drip shield on the dose rate at the accessible environment is presented. Diffusive release from the WP is assumed for the entire period

of simulation. From the EBS, diffusive release is assumed for a limited time (the lifetime of the capillary-barrier/drip shield), followed by both advective and diffusive release. This is simulated in RIP by setting the advective flow to 0 for a limited period of time when the capillary barrier/drip shield is assumed to be functioning, and then setting the advective flow to the nominal infiltration of 1.25 mm/yr. This conceptualization also effectively represents the impact of evaporation in eliminating advective flow past the waste package. Corrosion of the outer container is assumed to occur only if temperature is below 100°C and RH is greater than a threshhold value (usually 65-70 percent initiation threshhold for humid air corrosion and a switch at 85-95 percent for aqueous corrosion). The corrosion of the inner container is always assumed to occur as aqueous corrosion, not humid air corrosion. For additional details of the waste package corrosion model, see Appendix B.

The detailed drift scale modeling analyses in Section 5.2.7 indicate that advective flow will not occur into the drift even for relatively high percolation rates (5 mm/yr). In the modeling, the fracture flow is imbibed into the matrix and redirected around the drift. Alternative mechanisms and conditions not included in the modeling (e.g., coated fractures, unconnected fractures, and different matrix capillary pressure curves) may allow advective flow or dripping into the drift. In the cases presented herein, dripping is assumed to occur on approximately 50 percent of the packages, which is consistent with the current abstraction in TSPA-1995 (CRWMS M&O 1995d, pg. ES-37). If the simulation results presented in Section 5.2.7 can be substantiated by field testing or incorporates additional realism and still concludes that no dripping occurs, the releases from the repository will decline substantially because the only release will be by diffusive mechanisms.

High Thermal Conductivity Backfill

Base case (note: this is the base case for these analyses, but incorporates a different EBS transport model than that in the nominal TSPA-1995 base case):

The base case 1,000,000 year expected value dose history at the AE is shown in Figure 5.1-1. This case was presented in TSPA-1995 (Figure 9.3-40, CRWMS M&O 1995d) and assumes "drips-on-waste-container" EBS transport model (i.e., only diffusive release from the waste package and both advective and diffusive release from EBS for the entire simulation period).

The temperature and RH history, the first pit penetrating time cumulative distribution function (CDF), and humid air and aqueous corrosion initiation time CDFs for this case are shown in Figure 5.1-2a. Note that approximately 10 percent of the waste packages do not fail in 1,000,000 years, and approximately 15 percent of the waste packages initiate aqueous corrosion without first having humid air corrosion.

Figure 5.1-2b presents the pitting curves for the waste package groups of this case. The fraction of pits through the waste package is an indicator of the area available for diffusive release from the waste packages. This represents the waste package failure discretization used in RIP, since individual waste package failures are not simulated.

Case 1a:

An alternative case to simulate a capillary barrier/drip shield that provides protection from drips for 100,000 years was evaluated. This conceptualization simulates any physical configuration (e.g., drip shield, capillary barrier, evaporative effect of backfill) which eliminates advective flow past the waste packages. While it may be argued that a backfill system could last for an indefinite period of time, we chose to evaluate a 100,000 year, and in case 1b a 500,000 year lifetime of the advective flow barrier. The case assumed diffusive release from the waste package for the entire period of the simulation and diffusive release from the EBS for 100,000 years, followed by both advective and diffusive release only from the EBS. The schematic of the conceptual model is shown in Figure 5.1-3. This case effectively keeps dripping or flowing water off of the waste packages for 100,000 years, though waste packages will be failing earlier due to relative humidity effects on corrosion.

As previously indicated, the analyses of Section 5.2.7 indicate that advective flow will not occur into the drift even for relatively high percolation rates. The fracture flow is imbibed into the matrix and redirected around the drift. Mechanisms and conditions (e.g., coated fractures, unconnected fractures, different matrix capillary pressure curves) may allow advective flow or dripping into the drift.

The 1,000,000 year expected value dose history for this case is shown in Figure 5.1-4. In this case, the release of ^{99}Tc, ^{237}Np, ^{229}Th, and ^{233}U to the accessible environment is delayed by 100,000 years, though the peak at 1,000,000 years is almost identical with the base case (Figure 5.1-1) which had no such delay. The delay is caused by turning off advective flow (to simulate the drip shield, or Richards barrier, or evaporative effect of backfill) for 100,000 years so that diffusion is the only transport mechanism for these radionuclides. No change is seen in the dose of ^{129}I because it is assumed to be released in a gaseous form and thus unaffected by changes in the advective flow through the EBS. The 100,000 year delay has reduced the peak dose of ^{99}Tc by 20 percent as a result of decay of the ^{99}Tc source term prior to release to the AE (the decay half-life of ^{99}Tc is 2.15E5 years).

Case 1b:

Another case was analyzed with a capillary barrier/drip shield effect that was assumed to last 500,000 years. The conditions are identical to Case 1a, except the advective flow is zero for 500,000 years. The 1,000,000 year expected value dose history for this case is shown in Figure 5.1-5. Compared with Figure 5.1-1 (base case), the release of ^{99}Tc, ^{237}Np, ^{229}Th, and ^{233}U to the accessible environment is delayed by 500,000 years as a result of the capillary barrier effect and the peak dose of ^{99}Tc is reduced by approximately a factor of 5 due to decay. It is expected that the peak dose of ^{237}Np, ^{229}Th, and ^{233}U will eventually reach the same value as the base case 1,000,000 year value. Again, no effect is seen on the peak dose of ^{129}I because it is assumed to release from the EBS in a gaseous form, which is unaffected by the flow rate in the EBS.

Low Thermal Conductivity Backfill

Base Case:

For the low thermal hydraulic conductivity backfill, the 1,000,000 year expected value dose history base case is shown in Figure 5.1-6. These doses are lower and start at a later time than the doses from the case with high thermal conductivity backfill (Figure 5.1-1). This is due to the difference in the waste package failure history between the two cases as shown in Figures 5.1-2a and 5.1-7. A fewer total number of waste packages fail, and they fail at later times than those in the high thermal conductivity backfill case.

The temperature and relative humidity history, the first pit penetrating time CDF, and humid air and aqueous corrosion initiation time CDFs for this case are shown in Figure 5.1-7. The temperature is already low (~40 deg C) when the RH reaches the corrosion threshhold; thus, the corrosion rate is quite low.

Case 1c:

For the case with a capillary barrier/drip shield assumed to last 100,000 years and using the low thermal conductivity model, the 1,000,000 year dose history is presented in Figure 5.1-8. The schematic of the conceptual model was shown in Figure 5.1-3.

No effect of the capillary barrier/drip shield on the dose at the accessible environment is seen in this case compared to the base case in Figure 5.1-6, because all the releases occur after 100,000 years.

Gradual Failure of Capillary Barrier/Drip Shield

Case 1d:

To evaluate the effect of gradual failure of the capillary barrier/drip shield, Case 1a was modified. The advective flow was modified so that from 0 to 100,000 years the flow was 0, and then the flow was gradually increased to the expected value at 500,000 years. The 1,000,000 year expected value dose history is presented in Figure 5.1-9. The results are nearly identical to Case 1a (Figure 5.1-4) because both the waste package failure and the waste form alteration proceeded independent of the drip shield performance. When advective flow was allowed through the repository, the releases proceeded as they had in Case 1a because the advective flow was high enough to dissolve and transport the radionuclides from the waste package.

Case 1e:

Another case of gradual capillary barrier/drip shield failure from 100,000 years until significant failure at 500,000 years was implemented in RIP. The advective flow was modified so that from 0 to 100,000 years the flow was 0, and then the flow was gradually increased to .001 times the expected value at 500,000 years, then remained there from 500,000 years to 1,000,000 years. This resulted in a slight reduction in the dose at 1,000,000 years, as well as a noticeable reduction of dose at early

time (Figure 5.1-10), compared to Figure 5.1-9, because the dissolution limited radionuclides were not transported as rapidly for this low flow case.

Case 2: Pre-conditioning incoming water (repository flow) to decrease corrosion of waste packages

In this case, repository flow/incoming water was assumed to be pre-conditioned to decrease the corrosion of the waste packages. The effect of this EBS alteration on the dose at the A is evaluated. This is implemented by changing the corrosion initiation criteria in the waste package degradation model external to RIP. Three cases with different corrosion initiation criteria are presented below and compared with TSPA-1995 results.

The three cases can be summarized as follows:

2a) Backfill conditioning to reduce corrosion: start of aqueous corrosion is delayed 10,000 years beyond RH threshhold,

2b) Backfill conditioning to reduce corrosion: start of aqueous corrosion is delayed 100,000 years beyond the RH threshhold, and

2c) Backfill conditioning to reduce corrosion: start of corrosion (whether humid air or aqueous corrosion) is delayed 10,000 years beyond RH threshhold.

High Thermal Conductivity Backfill

Cases 2a, 2b and 2c look at the effect of a layer of iron ("grits") placed in the backfill, which would condition the near-field environment in such a way that the iron "grits" consume the oxygen and the near-field environment maintains a substantially reducing environment for a period of time. While it exists, the reducing environment is assumed to significantly reduce (or "stop") the corrosion of the waste package. Two scenarios for the near-field conditioning are considered:

- The conditioner affects only the (dripping) bulk water and effectively blocks aqueous corrosion, or
- The conditioner affects the humid-air and (dripping) bulk water effectively blocking both humid air and aqueous corrosion.

Table 5.1-1 Performance Assessment of EBS Functions

Function	Case		Description
Extend WP Lifetime	1		Capillary barrier/drip shield to delay onset of advective release (base case for **high** thermal conductivity backfill)
		1a	100,000 yr advective flow barrier
		1b	500,000 yr advective flow barrier
	1		Capillary barrier/drip shield to delay onset of advective release (base case for **low** thermal conductivity backfill)
		1c	100,000 yr advective flow barrier
		1d	100,000 yr advective flow barrier, then gradual failure until 500,000 years (high thermal conductivity backfill)
		1e	100,000 yr advective flow barrier, then modified advective flow (high thermal conductivity backfill)
	2		Pre-condition incoming percolation to decrease corrosion of waste packages
		2a	Delay aqueous corrosion initiation 10,000 years beyond RH threshhold
		2b	Delay aqueous corrosion initiation 100,000 years beyond RH threshhold
		2c	Delay all corrosion initiation 10,000 years beyond RH threshhold
	3		Rockfall on 1% of waste packages
Delay Radionuclide Transport	4		Condition transport characteristics of invert to retard transport for 100,000 years for two ^{237}Np K_d's
	5		Condition EBS materials to reduce solubility of ^{237}Np radionuclides to delay transport
		5a	100,000 yr solubility conditioning
		5b	500,000 yr solubility conditioning
	6		Condition EBS materials to slow the dissolution rate of spent fuel waste form to delay the release of radionuclides
		6a	Increase pH to 9 for 100,000 years, then revert to pH=7
		6b	Reduce dissolution rate by 2 orders of magnitude for 100,000 years
		6c	Reduce dissolution rate by 2 orders of magnitude for 500,000 years
		6d	Reduce dissolution rate by 4 orders of magnitude for 100,000 years

Cases 2a and 2b refer to the first scenario in which a conditioning time of 10,000 or 100,000 years are assumed. In Case 2c, the second scenario is investigated with a conditioning time of 10,000 years. Finally, a case similar to 2c, with the conditioning period extended to 100,000 years, was examined, but very few packages failed during the period of one million years, so no results are presented.

Case 2a:

This case assumes humid air corrosion is initiated as in the base case, but aqueous corrosion initiation is delayed by 10,000 years after the threshhold RH for aqueous corrosion is reached. The 1,000,000 year expected value dose history is presented in Figure 5.1-11.

The temperature and relative humidity history, the first pit penetrating time CDF, and humid air and aqueous corrosion initiation time CDFs for this case are shown in Figure 5.1-12. 30 percent less packages fail in this case compared to the base case (Figure 5.1-2a) due to assuming no aqueous corrosion for a 10,000 year period, at which time the temperature has significantly decreased. The pitting curves (not shown) also are significantly lower than the base case.

Compared to the high thermal conductivity backfill base case (Figure 5.1-1), the peak dose of ^{99}Tc, ^{129}I, ^{237}Np, ^{229}Th and ^{233}U has decreased by a factor of 3 to 5. Unlike the base case, the dose of ^{129}I takes an upward slope around 175,000 years till about 250,000 years and then stabilizes. This is due to the method of simulating the increase in waste package failures around 150,000 years, and is a modeling artifact.

Case 2b:

This case is identical to case 2a, except there is an assumed delay of 100,000 years after humid air corrosion ends and before aqueous corrosion is initiated. The 1,000,000 year expected value dose history is presented in Figure 5.1-13.

The temperature and relative humidity history, the first pit penetrating time CDF, and humid air and aqueous corrosion initiation time CDFs for this case are shown in Figure 5.1-14. Compared with Figure 5.1-12, there are fewer package failures and they fail slightly later in this case. The pitting curves are also lower than the base case.

Here again, compared to the high thermal conductivity backfill base case (Figure 5.1-1), the peak dose of all the major radionuclides reduced significantly. Again ^{129}I dropped below 1e-7 rem/yr at 175,000 years and then increased at 250,000 years due to modeling discretization. Compared with Case 2a, the decrease in peak dose is about 30 percent due to the difference in package failure times.

Case 2c:

The 1,000,000 year expected value dose history, shown in Figure 5.1-15a, is for the high thermal conductivity in backfill case, with the initiation of waste package corrosion delayed for an additional period of 10,000 years after the RH reaches the threshhold for aqueous corrosion.

The temperature and relative humidity history, the first pit penetrating time CDF, and aqueous corrosion initiation time CDFs for this case are shown in Figure 5.1-15b. The first pit penetration is significantly later and the total number of waste packages which fail is ~50 percent less than the base case (Figure 5.1-2a). Also, the pitting curves for this case (not shown) are significantly lower than the base case.

In this case the release of ^{99}Tc and ^{129}I were delayed by 50,000 years, and ^{237}Np, ^{229}Th, and ^{233}U releases were delayed by 100,000 years. Also, the peak dose of all the radionuclides is reduced by over 1 order of magnitude compared to the high thermal conductivity backfill base case (Figure 5.1-1). Compared to Case 2a, the doses are also reduced, confirming delaying both aqueous and humid air corrosion obviously has a greater impact than just blocking aqueous corrosion.

Figure 5.1-16a gives an indication of the effect on WP performance for corrosion delay times less than 10,000 years. These results indicate that a delay in corrosion initiation on the order of 7,000 years will provide similar WP performance as a delay time of 10,000 years. Furthermore, if credit can be taken for 50 percent cathodic protection, Figure 5.1-16b shows that just a 3,000 year delay in corrosion initiation will provide the same level of WP performance as a 10,000 year delay when no cathodic protection credit is assumed.

Case 3. Rockfall Analysis

Another feature of backfill which is expected to prolong waste package lifetime is that the protection backfill provides against rockfall from the ceiling of the drift. The estimation of the timing of rockfall events and the size of rocks that may fall on the waste packages in the emplacement drifts is still preliminary, as discussed in Section 3.3. However, expert judgement can provide some reasonable bounding of the size of rockfall. This bounding analysis, used in conjunction with estimates of the size of rock necessary to breach a waste package (also provided in Section 3.3), can be used as input in evaluating the sensitivity of total system performance to emplacement drift rockfall.

A single case was analyzed which showed the potential results of a rockfall on repository performance if the following assumptions were made. These assumptions will be reconsidered in the future as to their acceptability when additional rockfall-related information becomes available.

Assumptions:

- Use the same base case as in Case 1 of Section 5.1 as a starting point.
- Develop modified waste package failure curves based on the assumption that 1 percent of the waste packages will be breached by rockfall at the beginning of the postclosure period. This assumes that ground support fails, and rocks large enough to breach the waste packages fall directly onto 1 percent of the waste packages.
- Assume that the waste packages breached by rockfall are susceptible to dripping on waste form (i.e., advective flow through the waste package rather than around the waste package), rather than dripping on the waste package if there are drips in the repository at the location of the waste package. According to the dripping model used in TSPA-1995, slightly more

than 50 percent of the packages breached by rockfall will experience dripping on the waste form, which leads to greater releases than are expected from similar waste packages with only dripping on waste packages conceptual model.

- The waste packages will follow the same pitting degradation curves as the base case. This means that the potential for accelerated corrosion due to scuffing of the waste package from rockfall is not included in these analyses.

The results for the case are presented in Figure 5.1-17. Due to computer limitations, two runs were required:

- 99 percent of waste packages with no rockfall and EBS transport model of drips on waste package, and

- 1 percent of waste packages with rockfall and EBS transport model of drips on waste form.

These two curves can be visually added together to evaluate the increase in peak dose over the base case shown in the figure. The overall performance for the case that considers the effects of rockfall is worse by approximately a factor of 2 than for the base case, which neglects the effects of rockfall. This is not a significant effect given uncertainty in other parameters in the system.

Clearly, there are many uncertainties in this rockfall effects analysis. Additional rock mechanics analysis could lead to improvement in the reliability of the analyses.

5.1.2 DELAY RADIONCULIDE TRANSPORT

Case 4: Conditioning the transport characteristics of the invert

In this case, the transport of ^{237}Np through the invert is delayed or retarded by increasing the distribution coefficient (K_d) in the invert for the first 100,000 years. The K_d is incorporated in the retardation of the radionuclide transport in the following equation:

$$R_f = 1 + \frac{\rho_s}{n} K_d$$

where
n = porosity,
ρ_s = bulk mass density (g/cm^3), and
K_d = distribution coefficient for reversible adsorption: (mass of solute on the solid phase per unit mass of solid phase)/(concentration of solute in solution) (cm^3/g).

This delay is implemented only in the 1 m thick invert. The delay is not permanent, only a retardation of the transport rate.

High Thermal Conductivity Backfill

The schematic of the conceptual model for this case is presented in Figure 5.1-18, indicating the invert K_d is modified for 10,000 years of the simulation, followed by a return to the original invert K_d of 0 cm^3/g.

The base case invert K_d was 0 cm^3/g. This analysis was conducted for two cases:

- K_d of 15 cm^3/g for 100,000 years then K_d of 0 cm^3/g, and
- K_d of 1000 cm^3/g for 100,000 years then K_d of 0 cm^3/g.

The effect of increasing the K_d of the invert to 15 and 1000 cm^3/g for the first 100,000 years is shown in Figure 5.1-19. With a K_d of 15 cm^3/g for the first 100,000 years then reverting to 0 cm^3/g, the release of ^{237}Np to the AE is delayed by approximately 20,000 years to reach a dose of about 1E-7 rem/yr compared to the base case (shown on the figures as $K_d = 0$ cm^3/g). When K_d is increased to 1000 cm^3/g for the first 100,000 years then reverted to 0 cm^3/g, the time required to reach a dose of 1E-7 at the AE is delayed by approximately 80,000 years. Since the effect of K_d is prevalent for only 100,000 years the release is seen after 100,000 years, but if the K_d was high enough and effective for the entire period of simulation, then there would have been no significant release to the AE.

Case 5: Condition solubility of radionuclides

In this case, the effect of conditioning the ^{237}Np solubility in the system such that it is reduced to a very low value (~ 1e-5 g/m^3) for some period of time (100,000 or 500,000 years) then reverting to the expected value of 78 g/m^3 is investigated.

High Thermal Conductivity Backfill

Case 5a:

The 1,000,000 year expected value dose history for ^{237}Np using ^{237}Np solubility of 1E-5 g/m^3 for the first 100,000 years is shown in Figure 5.1-20. The stochastic solubility range for TSPA-1995 base case Figure 5.1-1 was mean = 79.86 g/m^3, standard deviation = 119.703 g/m^3, minimum = 1.2 g/m^3, and maximum = 2.4E+3 g/m^3. So, the Np solubility for this case is nearly 7 orders of magnitude lower.

The release of ^{237}Np is delayed by 100,000 years compared to the base case due to the low value of solubility during this period. However, peak dose at 1,000,000 years is unaffected by the solubility conditioning.

Case 5b:

Analysis of a case identical to case 5a except using an ^{237}Np solubility of 1E-5 g/m^3 for the first 500,000 years is shown in Figure 5.1-21. Similar to Case 5a, the release of ^{237}Np is delayed by

500,000 years. Peak dose at 1,000,000 years is lower, but is expected to reach the base case peak dose at later time (~1.5 million years).

Case 6: Condition dissolution rate of waste form

The sensitivity of the spent fuel dissolution rate on the dose at the AE is studied in this case. The effect of changing the pH for a limited amount of time, as well as the effect of directly changing the spent fuel dissolution rate used in TSPA-95 to a smaller value are presented below.

High Thermal Conductivity Backfill

Case 6a:

The effect of increasing the pH for 100,000 years then reverting to the base case pH was evaluated in this case. In the RIP simulations, this change impacts spent fuel and glass waste dissolution rates. The 1,000,000 year expected value dose history with a pH of 9 for the first 100,000 years and 7 for the remaining period is presented in Figure 5.1-22. In TSPA-1995, pH of 7 was used for 1,000,000 years. The spent fuel dissolution and glass dissolution in this case are pH dependent. In Figure 5.1-23, the spent fuel dissolution rate as a function of pH is presented. The dissolution rate is generally lower for higher pH values. Note that data are only available for pH up to 10.1. All information beyond that on the figure is extrapolation.

The change of pH value for the first 100,000 years has no effect on the dose at the accessible environment (Figure 5.1-22) compared to the high thermal conductivity backfill base case (Figure 5.1-1). Changing pH may increase the solubility thus counteracting the decrease in dissolution rate. This effect is not explicitly modeled in the RIP simulations.

Case 6b:

This case evaluates the effect on dose of reducing the dissolution rate by two orders of magnitude. The 1,000,000 year expected value dose history with a dissolution rate of 1 percent of the base case value (TSPA-95) for the first 100,000 years is shown in Figure 5.1-24.

Compared to the high thermal conductivity backfill base, the peak dose of ^{99}Tc and ^{129}I are delayed by 100,000 years. There is no significant effect on the release of other radionuclides, because they are solubility limited, and thus decreasing the dissolution rate to 1 percent of the value used in TSPA-95 does not show any effect on the releases. This is demonstrated in Figures 5.1-25 and 5.1-26 for ^{237}Np and ^{99}Tc respectively.

Case 6c:

This case is identical to case 6b, except the reduced dissolution rate is assumed for 500,000 years. The 1,000,000 year expected value dose history for this case is shown in Figure 5.1-27. The peak dose of ^{99}Tc and ^{129}I is delayed by 500,000 years. However, there is no significant effect on the release of other radionuclides in comparison with the base case.

Case 6d:

This case is identical to case 6b, except the dissolution rate is reduced by two more orders of magnitude. The 1,000,000 year expected value dose history, using a dissolution rate of 0.001 percent of the base case value (TSPA-95) for the first 100,000 years is shown in Figure 5.1-28.

Compared to the high thermal conductivity backfill case, the peak dose of ^{99}Tc and ^{129}I is delayed by 100,000 years. The release of ^{237}Np, ^{229}Th, and ^{233}U is delayed by 15,000, 30,000, and 90,000 years respectively because the dissolution rate is finally below the Np solubility limit (see Figure 5.1-25).

5.1.3 CONCLUSIONS

One of the more interesting aspects of the sensitivity analysis conducted in Section 5.1 is that some of the EBS functions that delay releases also delay doses seen at the accessible environment, whereas other functions delay releases but have no effect on peak doses seen at the accessible environment. For example, this section has shown that capillary barriers and/or drip shields delay the release of ^{237}Np to the accessible environment, but have no effect on the contribution of ^{237}Np to the peak dose (see Figure 5.1-4). On the other hand, a chemically treated backfill that delays corrosion initiation on the waste packages not only delays the releases of ^{237}Np to the accessible environment, it also reduces the contribution of ^{237}Np to the peak dose (Figure 5.1-15a). The reason for such behavior will now be explained.

Figure 5.1-1 in the report gives one an idea of the key radionuclides contributing to the peak dose calculations at 30 km from the repository. After a couple of hundred thousand years, ^{237}Np is the key radionuclide in peak dose calculations. Figure 5.1-4 shows that promoting diffusive release through the EBS for 100,000 years (or 500,000 years as shown in Figure 5.1-5) only succeeds in delaying the releases of ^{237}Np to the AE because the only function the capillary barrier/drip shield is assumed to achieve is to promote diffusive release out of the EBS, but not to delay the breaching of WPs. Therefore, the rate at which WPs breach is still assumed to be the same as the solid curve shown in Figure 5.1-2a. Therefore, the amount of ^{237}Np available for transport from breached WPs is the same whether or not we are using some type of barrier that promotes diffusive transport throughout the EBS. Unless that barrier works for 750,000 years or more, the ^{237}Np contribution to peak dose will be the same. However, if we are able to significantly delay the breaches of waste packages - as shown by the solid curve in Figure 5.1-15b for chemically conditioned backfill - then not only do the WPs start to breach much later than that indicated by the solid curve in Figure 5.1-2a, but also much less of the WPs breach over the 1,000,000 year time frame and so much less of the ^{237}Np inventory is available for transport to the AE. Delaying the time at which the WPs start to breach, as well as reducing the total number of WPs that breach over 1,000,000 years, not only delays the release of ^{237}Np, it also reduces the amount of ^{237}Np available for release.

Results from the sensitivity analyses conducted in Sections 5.1.1 and 5.1.2 indicate that a chemically treated backfill with a lifetime on the order of several thousand years may provide a substantial improvement in long-term repository performance, and is worth evaluating in greater detail. This is done in Section 5.3.

The function "Reduce the relative humidity at the waste package surface" was not addressed in Section 5.1 because this function is not amenable to a simple sensitivity analysis and because the concept associated with this function, a single layer backfill, is a focus of this study and as such is to be examined in detail anyway. This is done in Section 5.2

The remaining "extend waste package lifetime" function is "Act as a structural protection from rockfall." The sensitivity analysis conducted in this section is considered conservative, as discussed in some detail in Section 3.3. Current estimations (Section 3.3) are that less than 1 percent of the waste packages would be expected to receive rockfall significant enough to cause a breach. Furthermore, the degradation in long-term repository performance due to 1 percent of the waste packages breaching at the beginning of the postclosure period is expected to be about a two-fold increase in peak dose over a 1,000,000 year time frame. For the 10,000 year time frame, the current predictions also indicate about a two-fold increase in peak dose.

The functions investigated in Section 5.1 that deal with delaying the transport of radionuclides once the waste package has been breached appear to require very long lifetimes to significantly affect repository performance over 1,000,000 years. For example, the function "Act as a barrier to advective release of radionuclides" would have to last at least tens of thousands of years to reduce peak doses, and even then has no effect on one of the dominant radionuclides, ^{129}I, which is assumed to be transported through the EBS in gaseous form. However, since the concepts associated with this function, the drip shield and the Richards Barrier, have been widely discussed outside of this study as potential enhancements to the EBS, they are both examined in some detail in Section 5.4.

Of the remaining two functions associated with delaying the transport of radionuclides once the waste package has been breached, the function "Retard the transport of released radionuclides" will be examined in more detail in Section 5.5. Although the lifetime of this function has to be very long (hundreds of thousands of years) to significantly affect peak dose, there have been indications as a result of research done independent and previous to this study that the use of a sedimentary apatite ore in the emplacement drift invert may actually retard the transport of an important and dominant radionuclide, ^{237}Np, for extremely long periods of time. Therefore, the concept of a chemically treated invert is discussed in detail in Sections 5.2.7.7, 5.2.7.9, and 5.5.

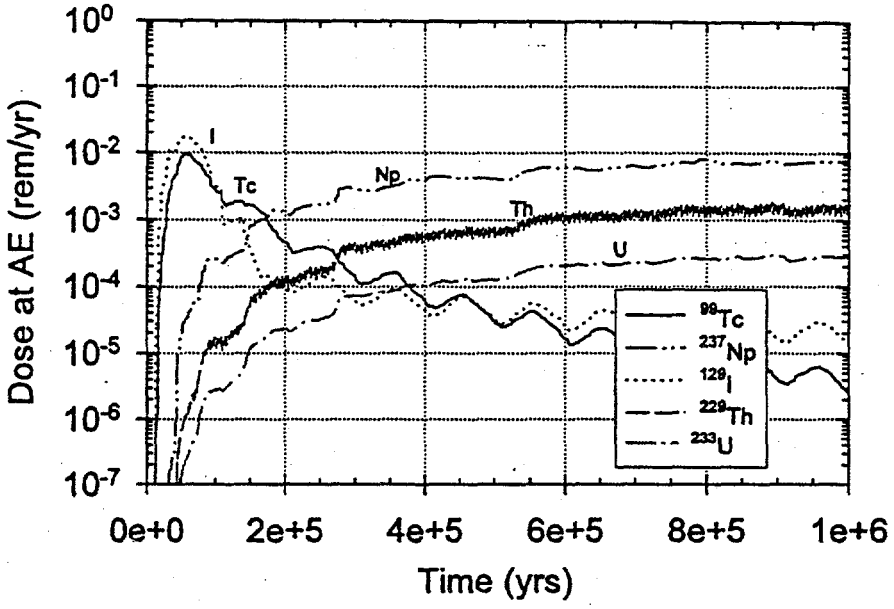

Figure 5.1-1 1,000,000 yr expected value dose history for the high thermal conductivity backfill base case. Use for comparison with other engineered barriers

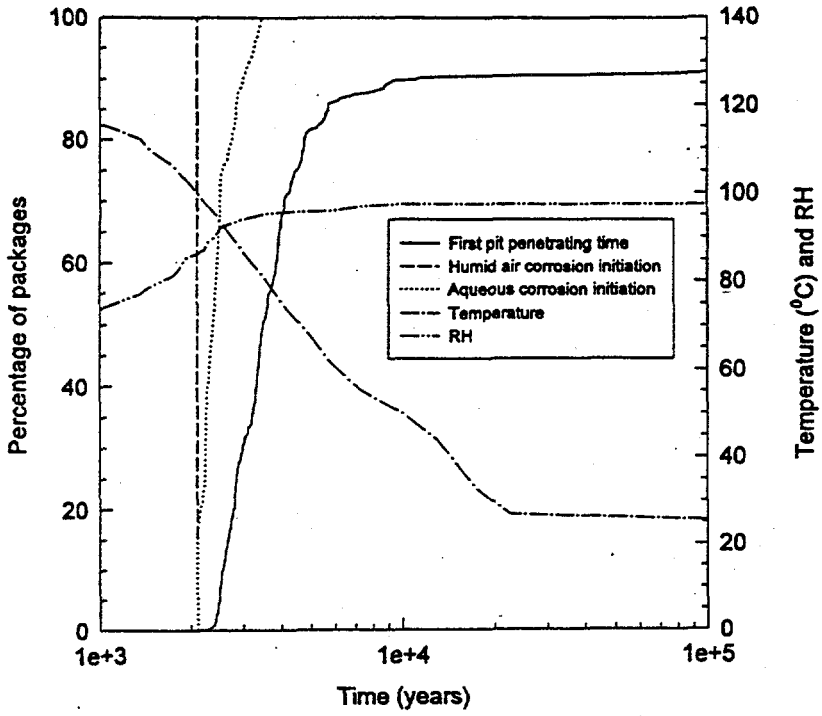

Figure 5.1-2a Temperature, RH, and pitting information for the high thermal conductivity backfill base case

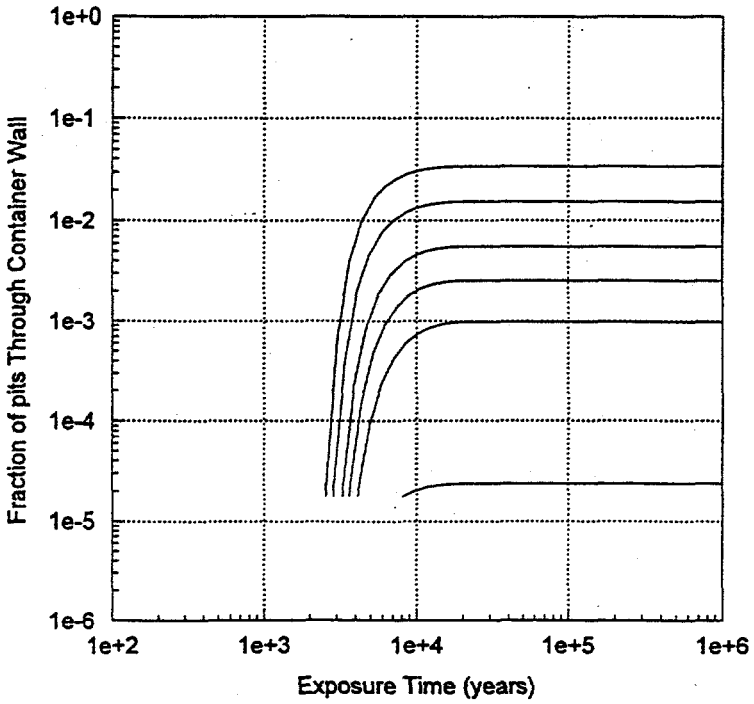

Figure 5.1-2b Abstraction of the pitting history for the high thermal conductivity backfill base case

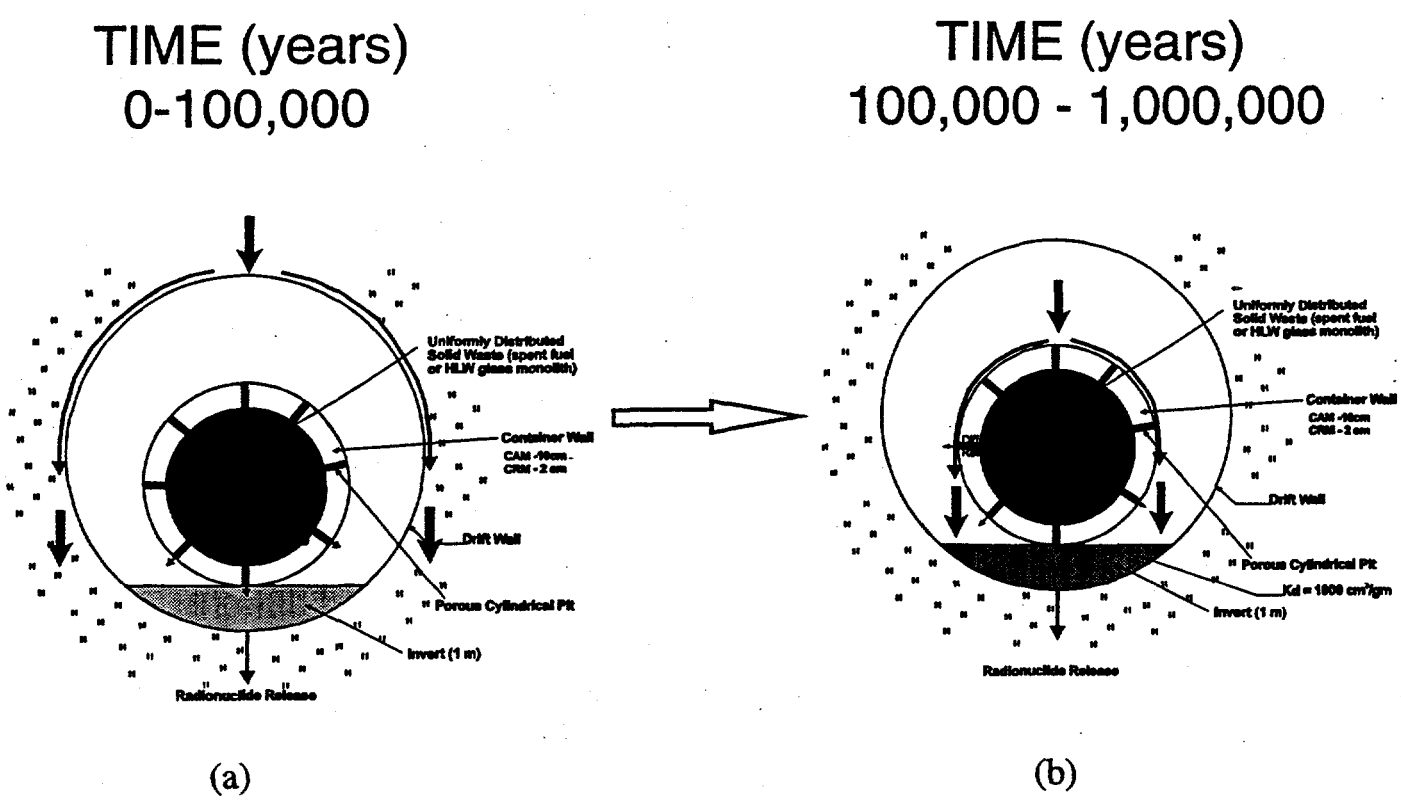

Figure 5.1-3 Schematic of the conceptual model for cases 1a and 1c

(a) capillary barrier effect: only diffusive release from both waste package and other EBS components

(b) no capillary barrier effect: diffusive release from waste package and diffusive plus advective release from other EBS components

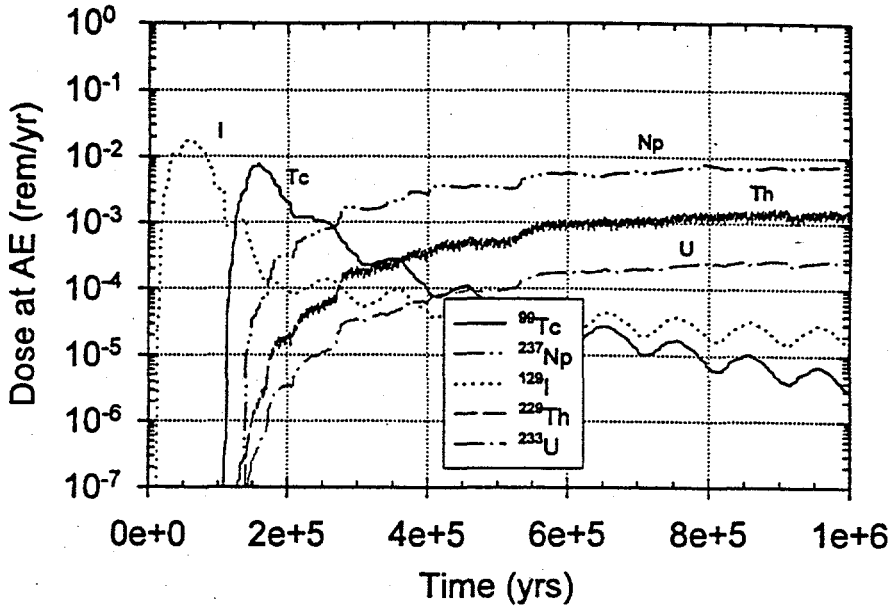

Figure 5.1-4 1,000,000 yr expected value dose history for a limited lifetime (100,000 years) capillary barrier using the high thermal conductivity backfill

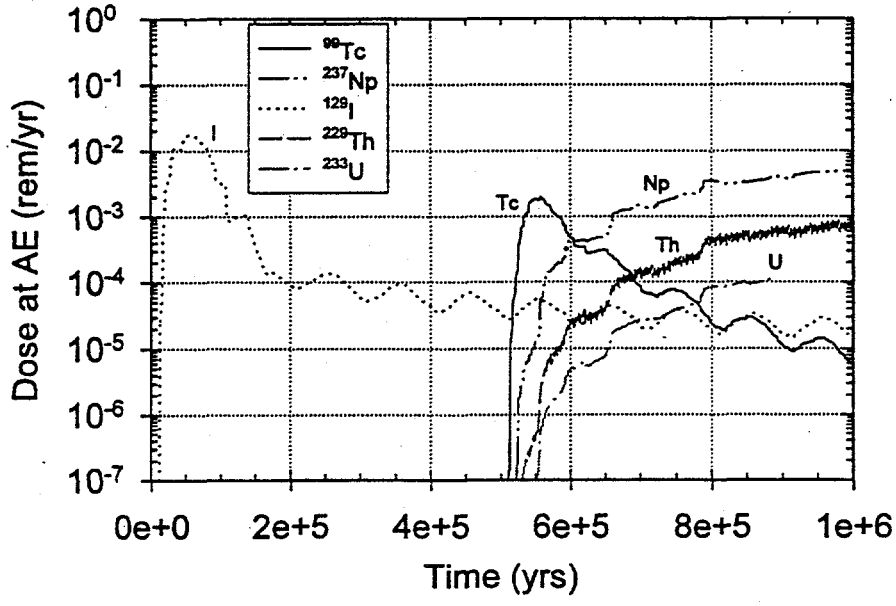

Figure 5.1-5 1,000,000 yr expected value dose history for a limited lifetime (500,000 years) capillary barrier using the high thermal conductivity backfill

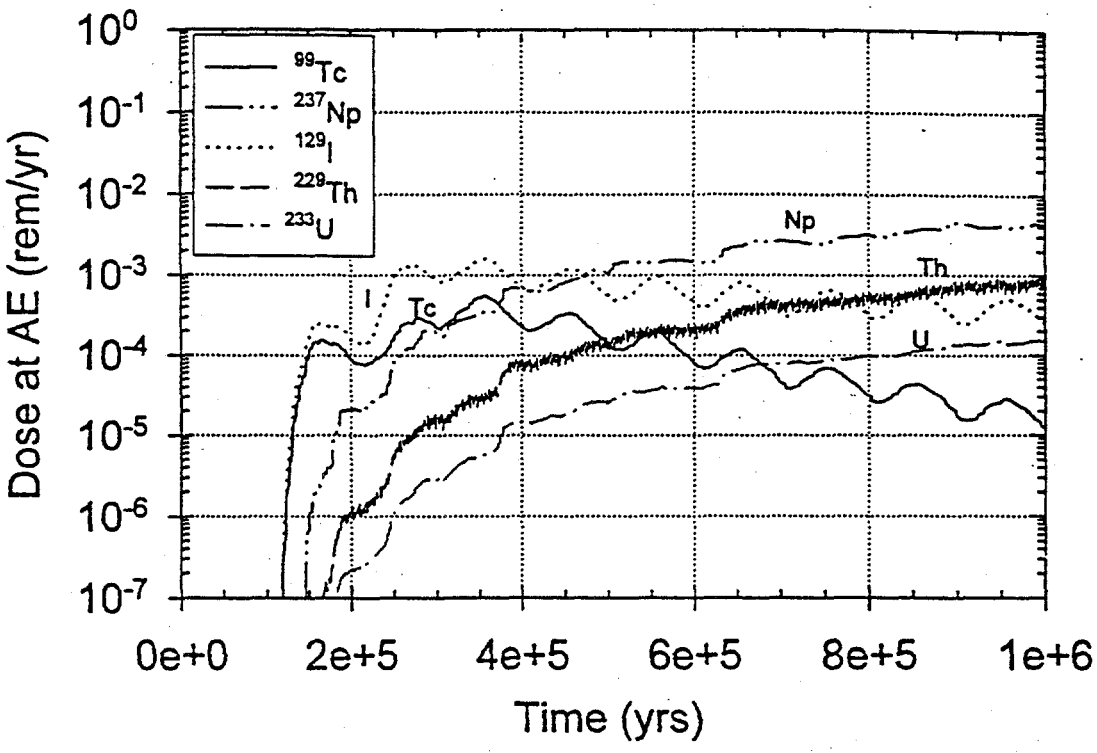

Figure 5.1-6 1,000,000 yr expected value dose history for the low thermal conductivity backfill base case

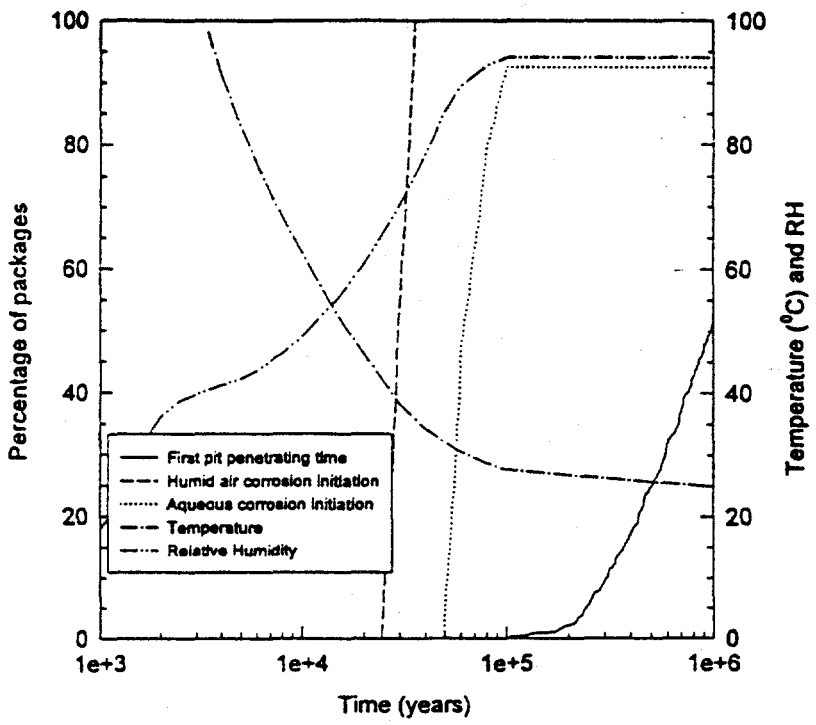

Figure 5.1-7 Temperature, RH, and pitting information for the low thermal conductivity backfill base case

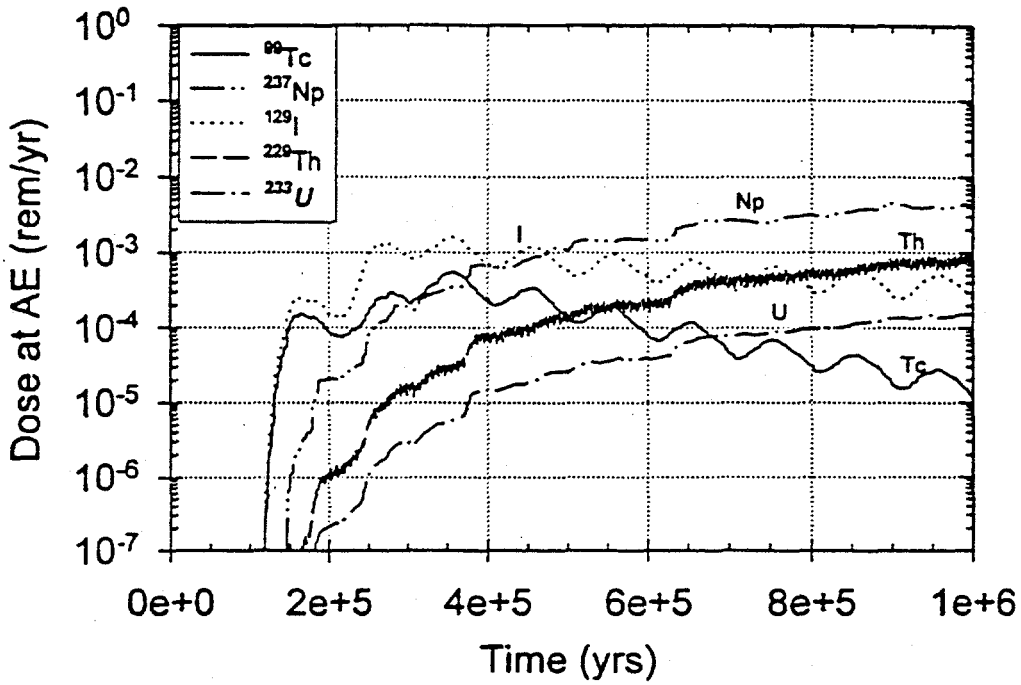

Figure 5.1-8 1,000,000-yr expected value dose history for a limited lifetime (100,000 years) capillary barrier using the low thermal conductivity backfill

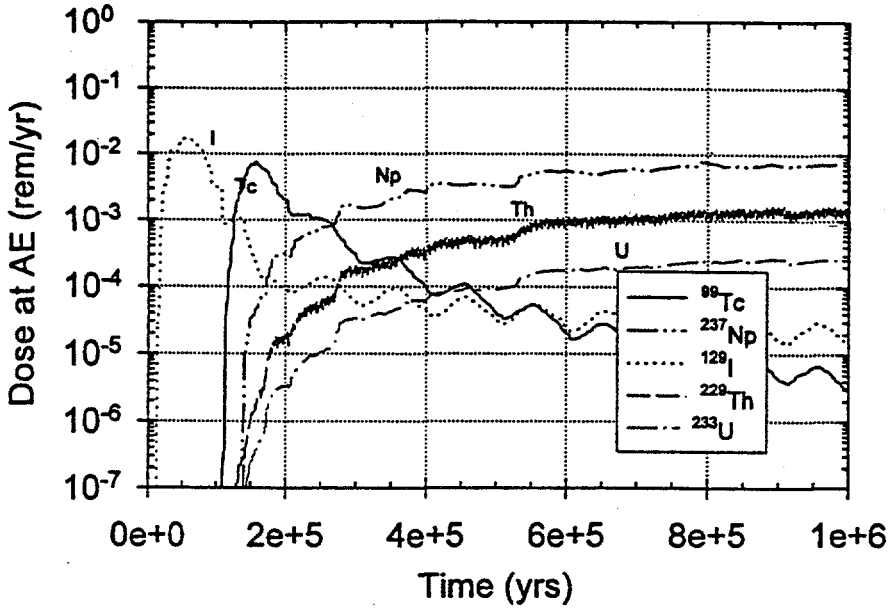

Figure 5.1-9 1,000,000 yr expected value dose history for the gradual capillary barrier/drip shield failure for Case 1d

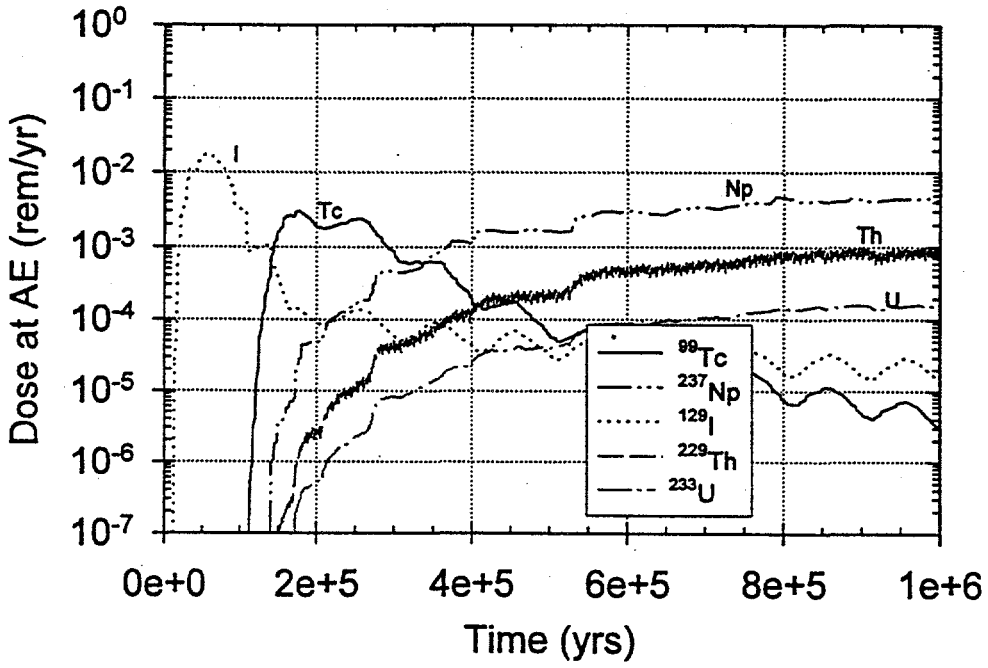

Figure 5.1-10 1,000,000 yr expected value dose history for the gradual capillary barrier/drip shield failure fc Case 1e

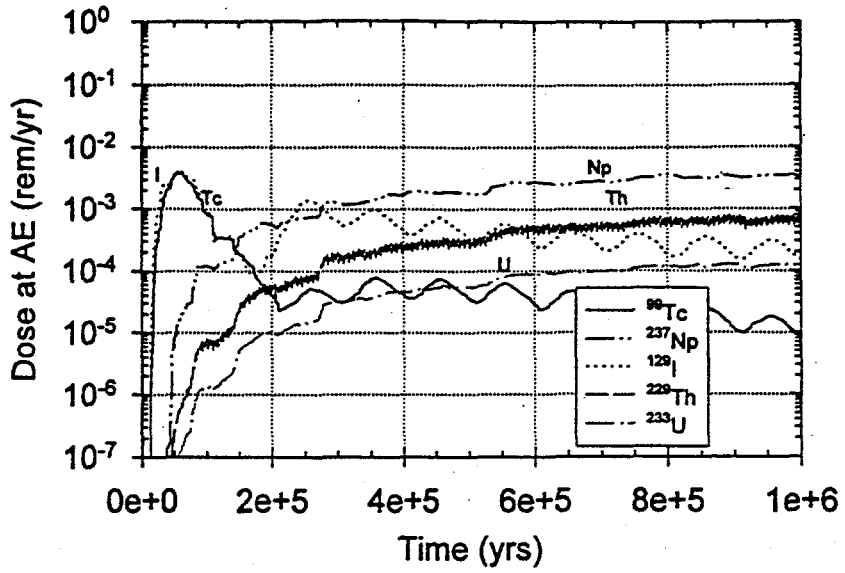

Figure 5.1-11 1,000,000 yr expected value dose history results for humid air corrosion followed by a 10,000 year delay in aqueous corrosion initiation with high thermal conductivity backfill

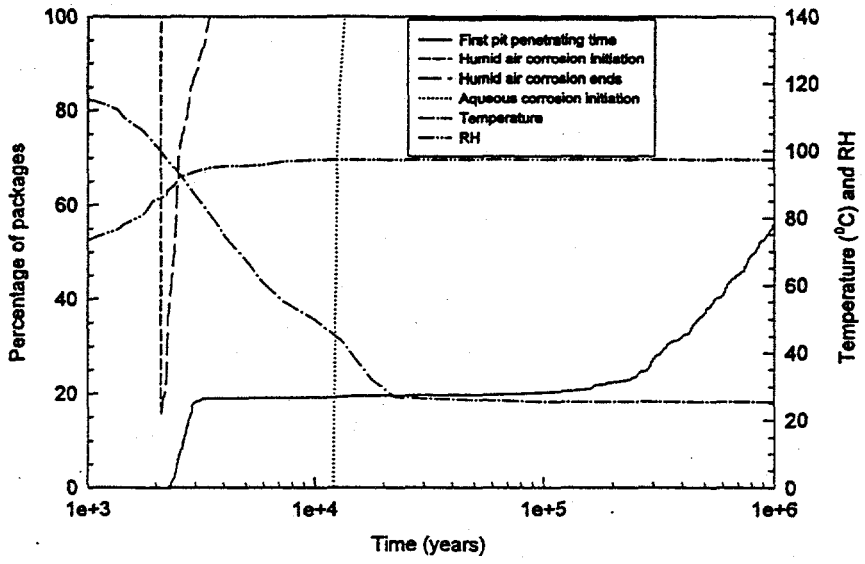

Figure 5.1-12 Temperature, RH, and pitting information for case presented in Figure 5.1-11

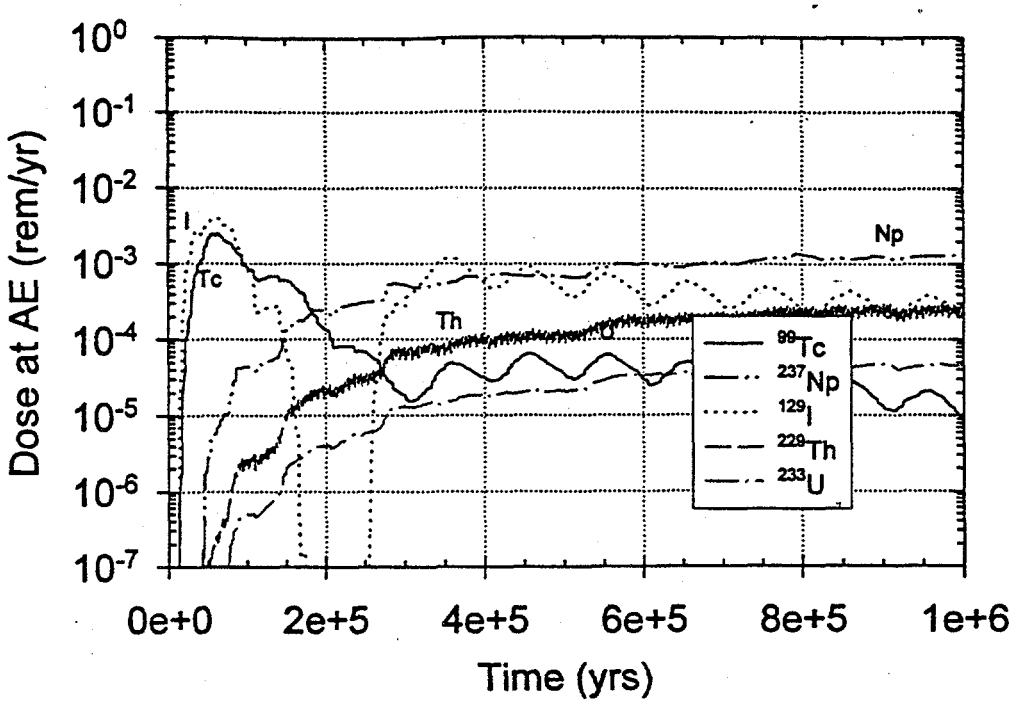

Figure 5.1-13 1,000,000 yr expected value dose history for case with humid air corrosion followed by 100,000 year delay in aqueous corrosion initiation, using the high thermal conductivity backfill

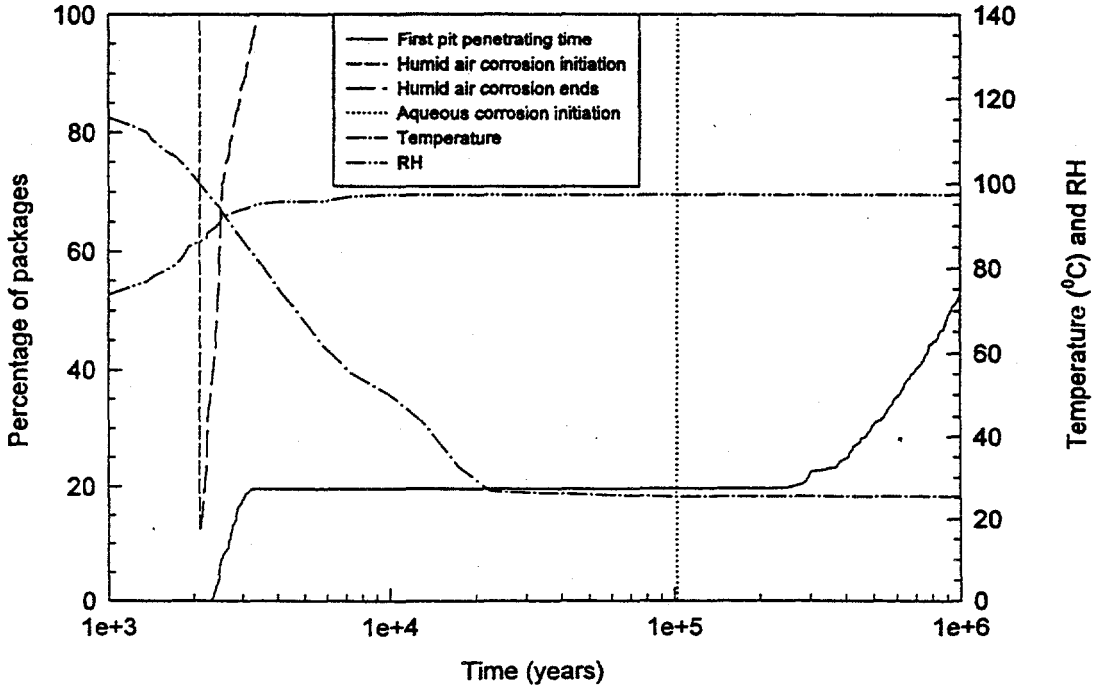

Figure 5.1-14 Temperature, RH, and pitting information for case presented in Figure 5.1-13

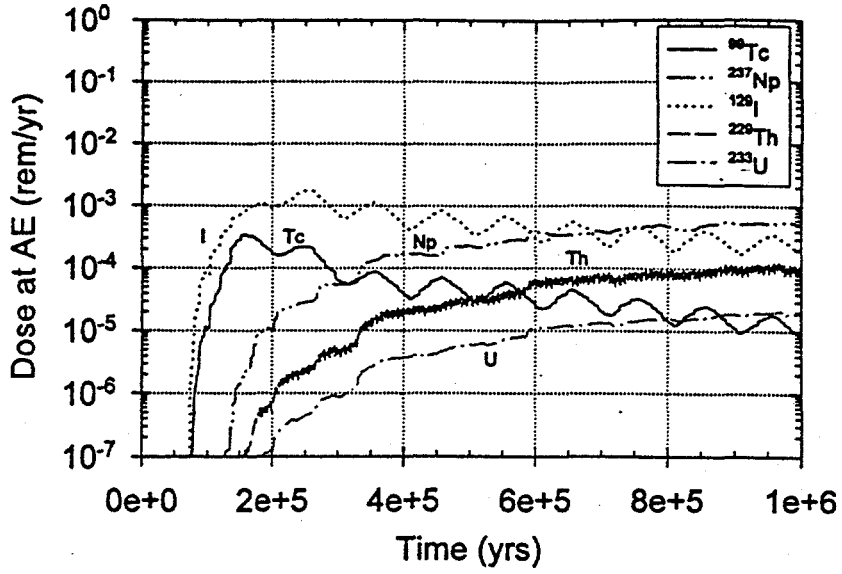

Figure 5.1-15a 1,000,000 yr expected value dose history for a 10,000 year delay in corrosion initiation with the high thermal conductivity backfill

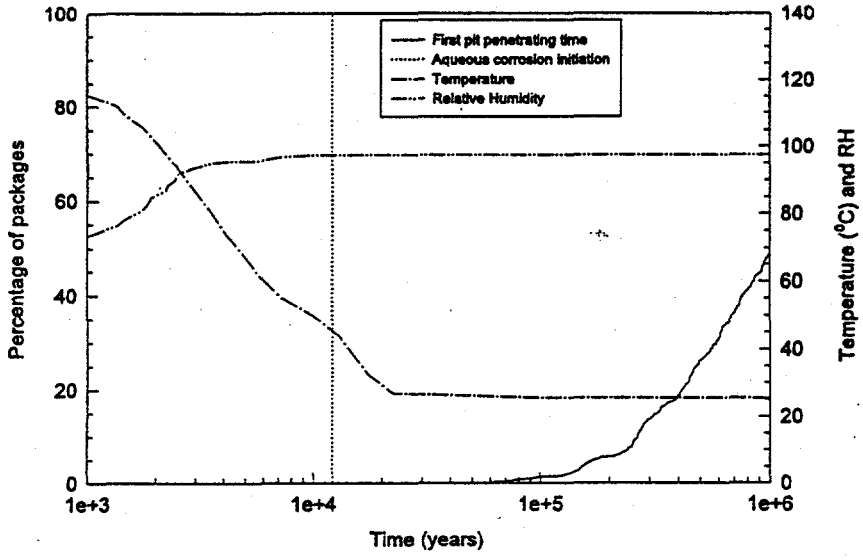

Figure 5.1-15b Temperature, RH, and pitting information for case presented in Figure 5.1-15a

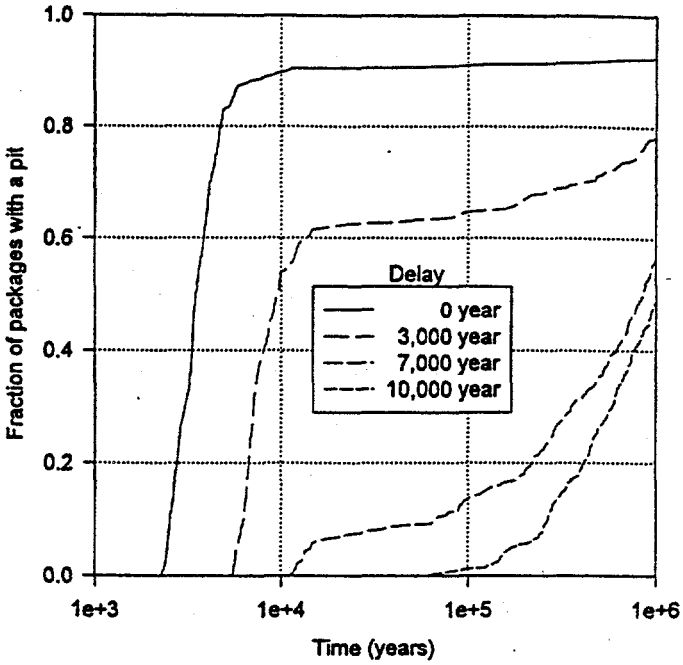

Figure 5.1-16a Waste package failure history sensitivity to delay in corrosion initiation

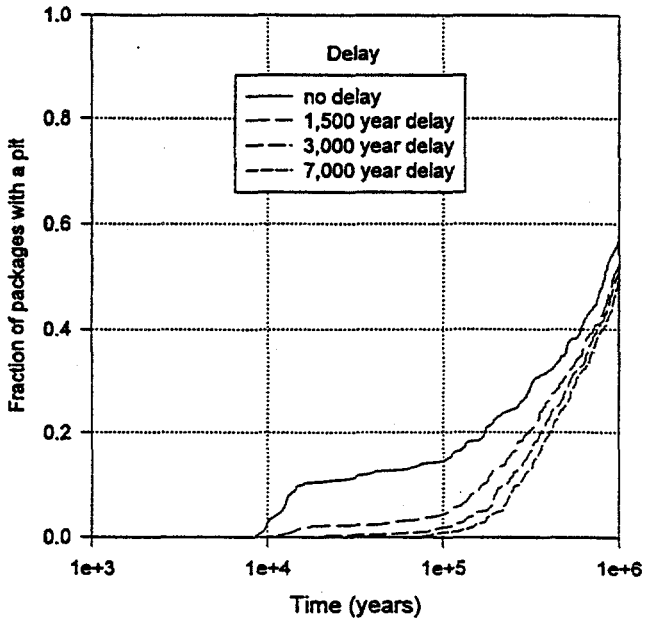

Figure 5.1-16b Waste package failure distribution sensitivity to delay in corrosion initiation with 50% cathodic protection

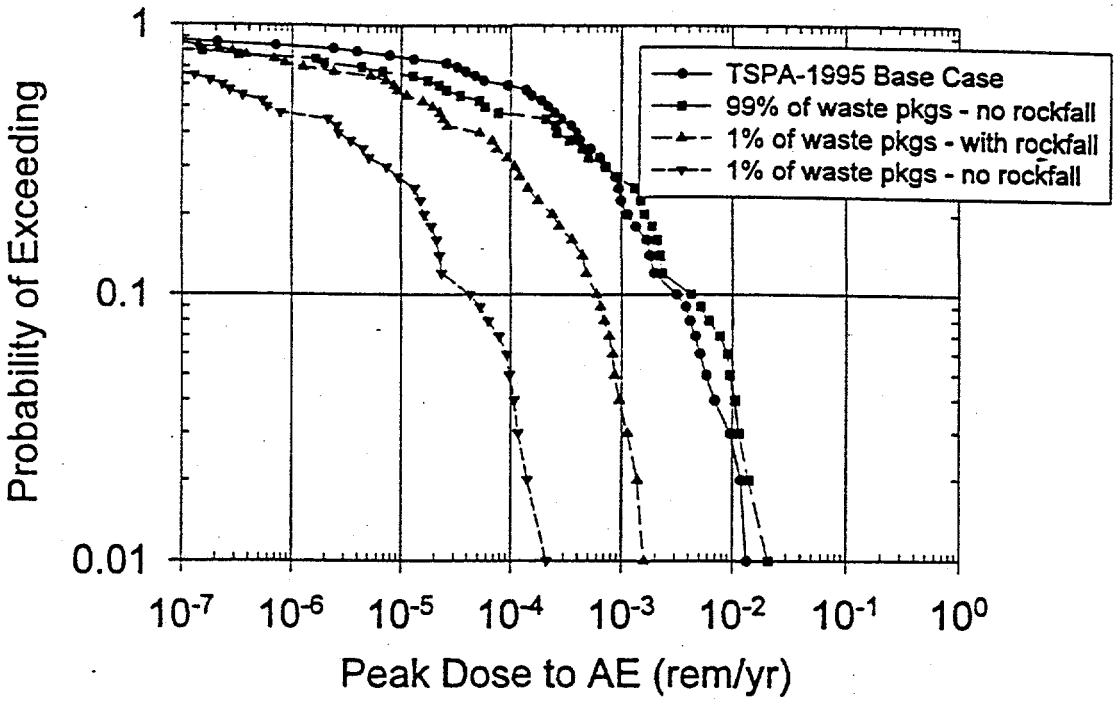

Figure 5.1-17 1,000,000 yr total peak dose CCDFs for rockfall analysis (1% of waste packages breached due to rockfall)

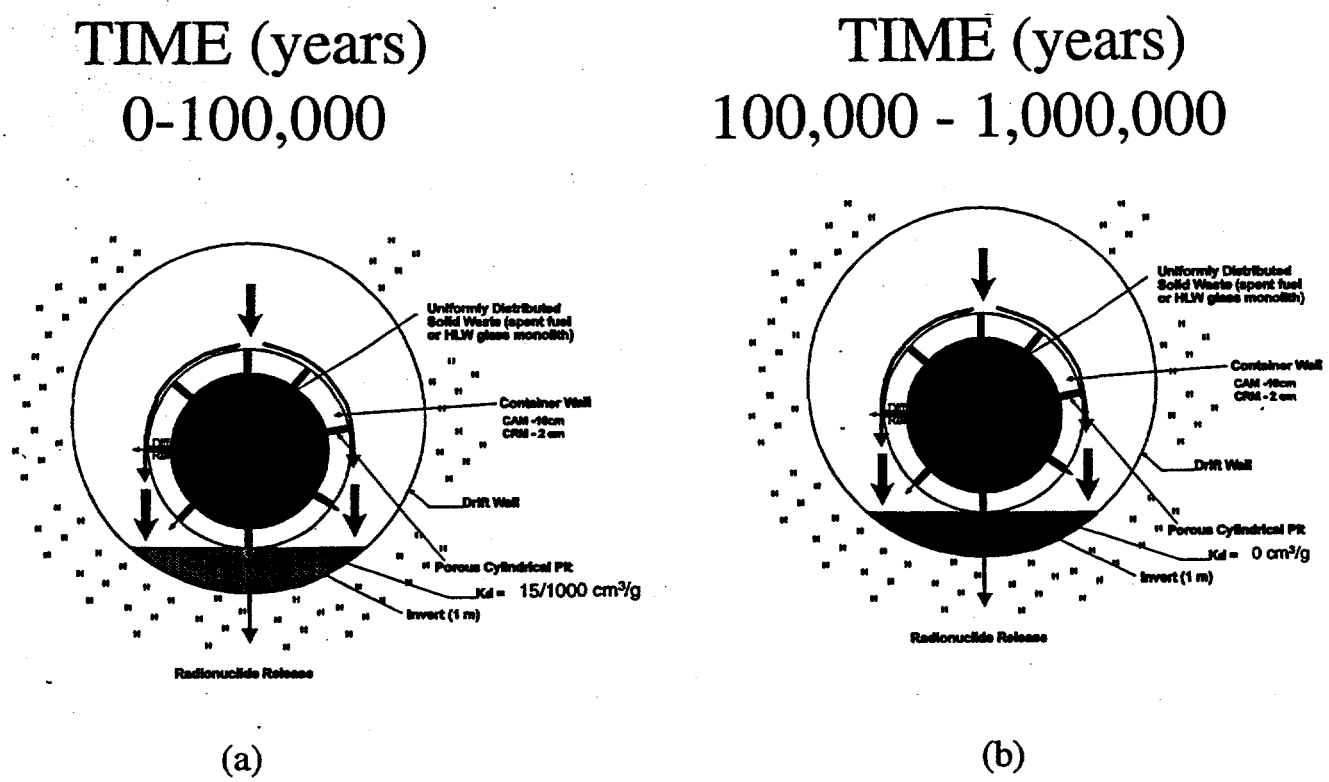

Figure 5.1-18 Schematic of the conceptual model for Case 4

(a) high K_d invert: diffusive release from waste package and diffusive plus advective release from other EBS components ($K_d > 0$ cm^3/g)

(b) low K_d invert: diffusive release from waste package and diffusive plus advective release from other EBS components ($K_d = 0$ cm^3/g)

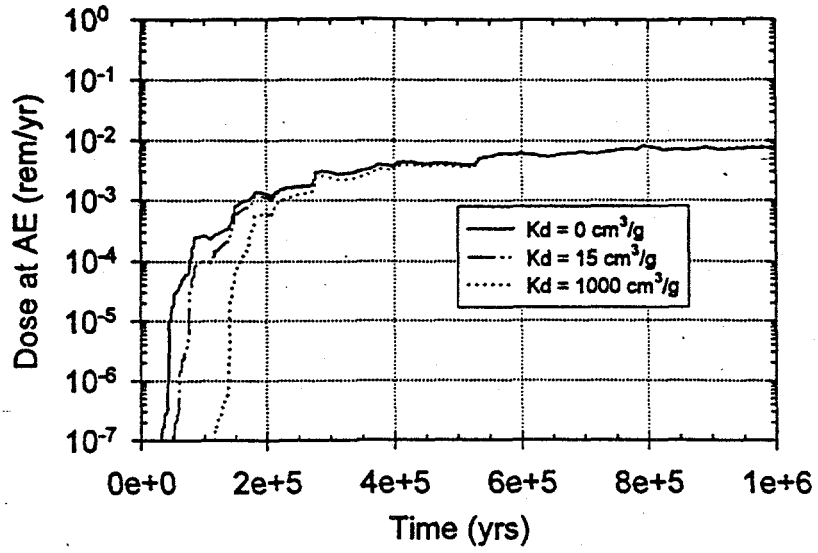

Figure 5.1-19 1,000,000 yr expected value 237Np dose history results from conditioning the transport characteristics of the invert by increasing the K_d for 100,000 years

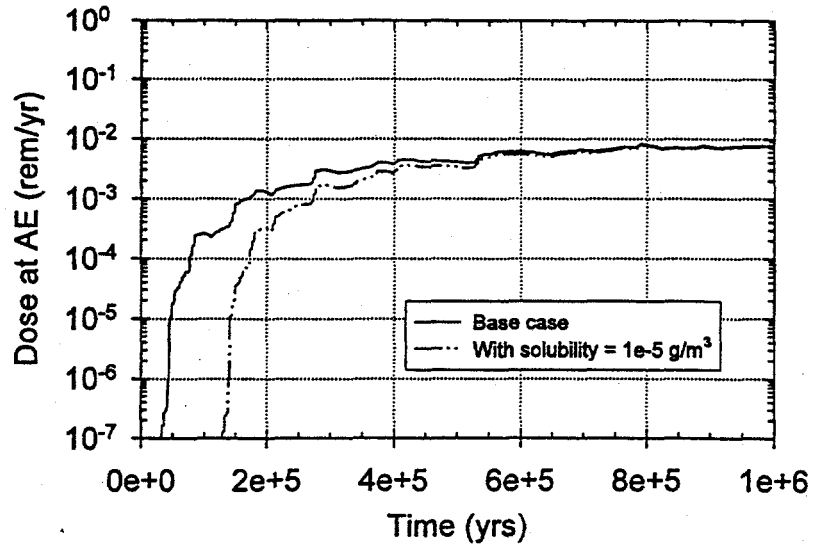

Figure 5.1-20 1,000,000 yr expected value 237Np dose history results from conditioning the 237Np solubility for 100,000 years

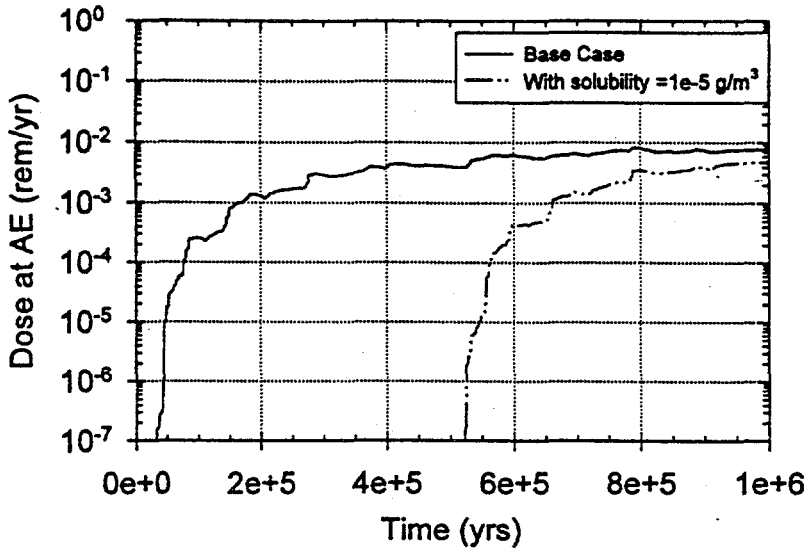

Figure 5.1-21 1,000,000 yr expected value 237Np dose history results from conditioning the 237Np solubility for 500,000 years

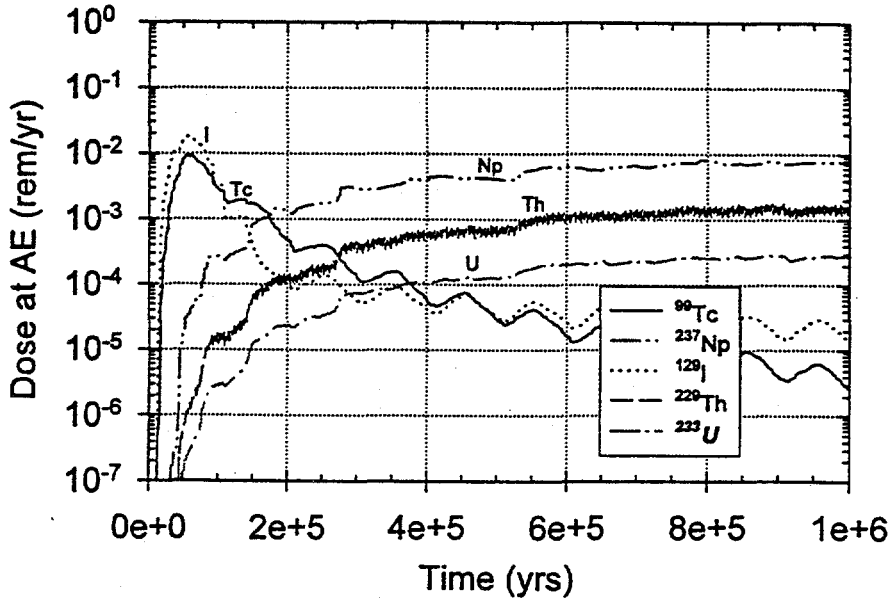

Figure 5.1-22 1,000,000 yr expected value dose history results from conditioning the waste form dissolution rate by changing pH to 9 for 100,000 years

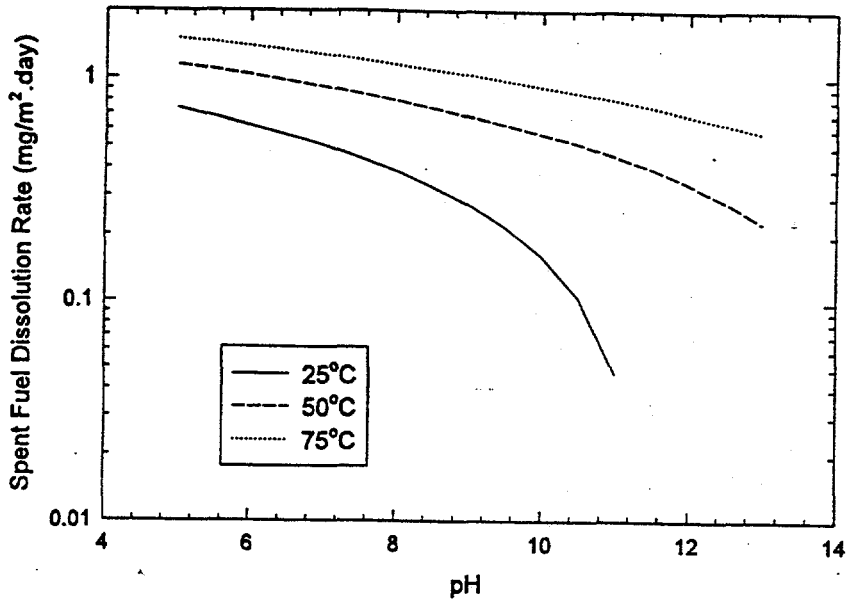

Figure 5.1-23 Spent fuel dissolution rate as a function of pH and temperature

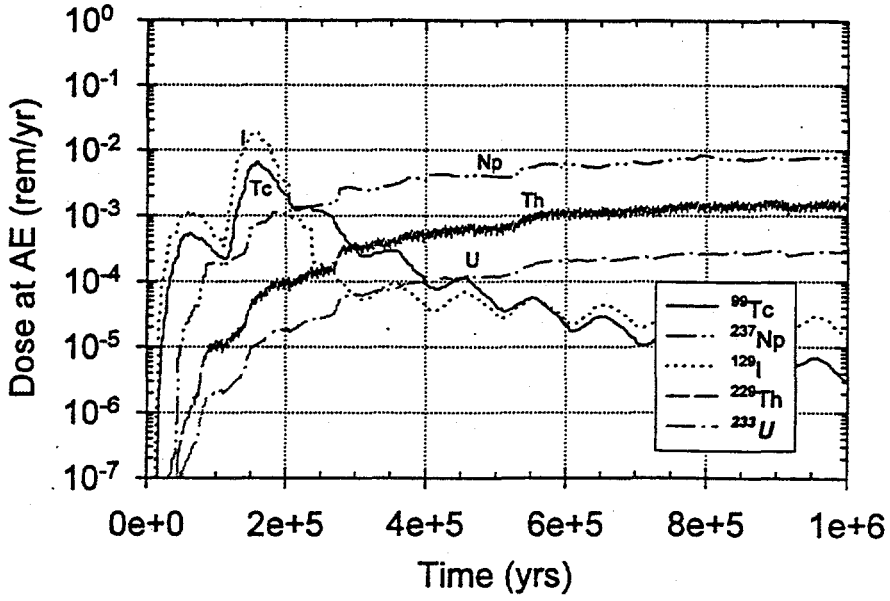

Figure 5.1-24 1,000,000 yr expected value dose history for case with dissolution rate reduced to 1% of the TSPA-1995 value for 100,000 years

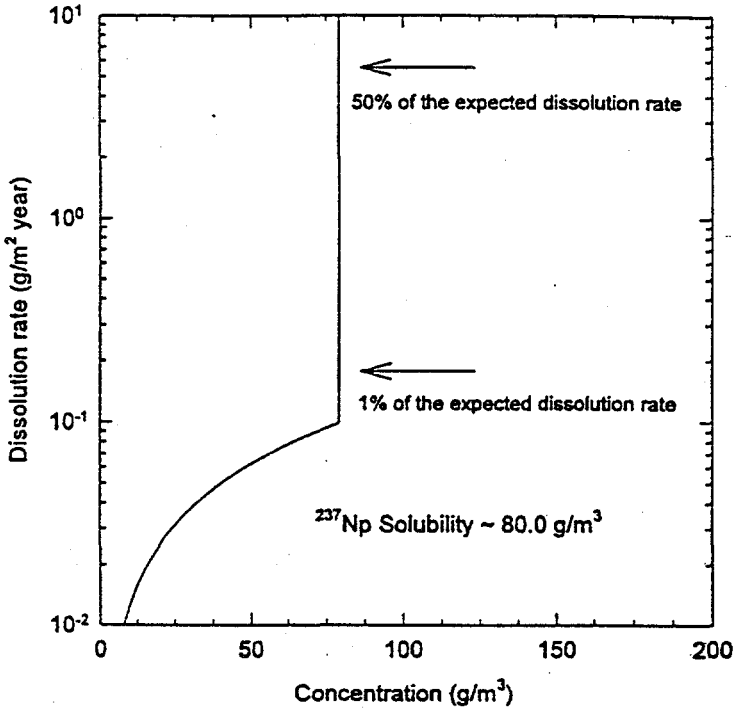

Figure 5.1-25 Dissolution rate as a function of concentration and solubility

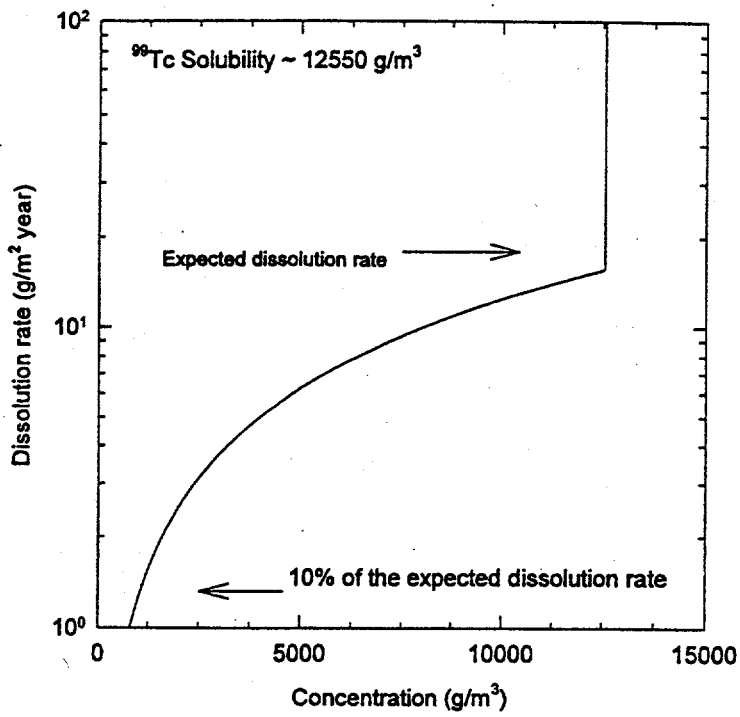

Figure 5.1-26 Dissolution rate as a function of concentration and solubility

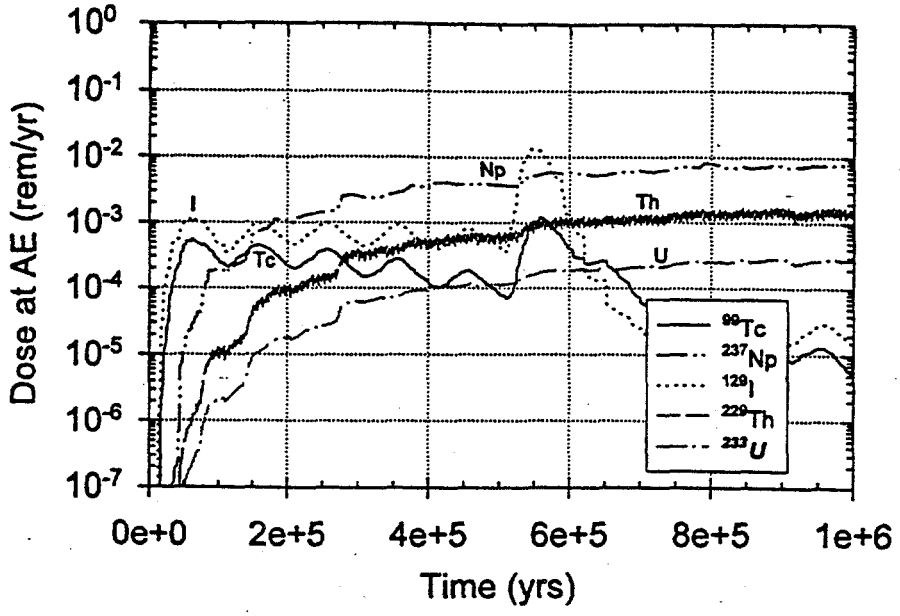

Figure 5.1-27 1,000,000 yr expected value dose history results for dissolution rate reduced to 1% of the TSPA-1995 value for 500,000 years

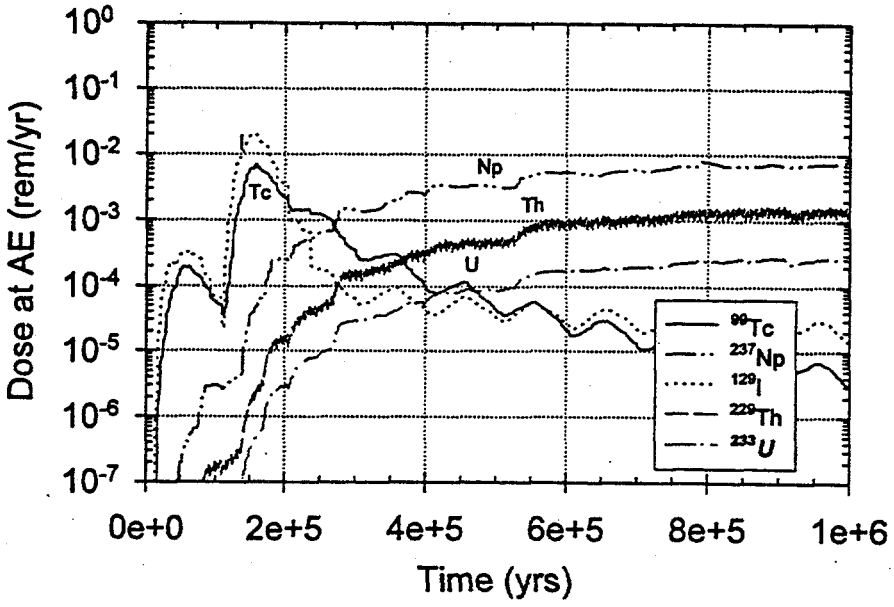

Figure 5.1-28 1,000,000 yr expected value dose history results for dissolution rate reduced to 0.001% of the TSPA-1995 value for 100,000 years

5.2 SINGLE LAYER BACKFILL

This concept will be looked at to address its ability to satisfy the EBS function of reducing the relative humidity at the waste package surface as a means of delaying corrosion initiation on the waste package surface. Backfilling of the waste packages in a square spacing scenario (ACD) as well as in a lineload scenario will be addressed in this section. Both a quartz sand backfill as well as a crushed TSw2 tuff backfill are discussed to varying degrees throughout this section. The thermohydrologic advantages of quartz sand (see Section 5.2.5.1) is the primary motivation for investigating it, and the obvious availability and cost advantages of crushed TSw2 make it an attractive material to investigate.

The stowing methods as well as the modifications necessary to the repository to accommodate emplacement drift backfill are discussed in Section 5.2.1. In Section 5.2.3, the effective thermal conductivities of the backfill materials are discussed. Section 5.2.4 deals with the impacts of emplacement drift backfilling on the SNF cladding temperature criteria. Significant improvement in the backfill thermohydrologic models employed in TSPA-1995 has been realized and this is discussed in detail in Section 5.2.5. Hydrologic properties of the various potential backfill and invert materials are determined by tests, with the results provided in Section 5.2.6. Improvements in the modeling of ambient flow and transport through and around an emplacement drift have been developed and are discussed in Section 5.2.7. The total system performance estimates of a repository that employs emplacement drift backfill is presented and discussed in Section 5.2.8. In Section 5.2.9, the repository costs and schedule impacts are addressed. Finally, in Section 5.2.10 the uncertainties and risks associated with the use of emplacement drift backfill are delineated.

5.2.1 EMPLACEMENT METHODS AND MODIFICATIONS TO REPOSITORY

5.2.1.1 Backfill Operations

If backfill is determined necessary, stowing of backfill would not be feasible for the CID waste emplacement mode which is currently the conceptual method of emplacement of waste packages (CRWMS M&O 1996b). In the CID mode, each rail carrier-mounted waste package would be spaced on a predetermined interval along the complete length of each waste emplacement drift. Each emplaced waste package would occupy most of the available cross-sectional area of each drift. With the inability to move around each waste package and the inability to move over the waste packages, access to the inner portions of the emplacement drifts beyond the first waste packages would be eliminated. Backfill for such an emplacement mode could not be placed beyond a few meters distance into each drift. The off-center in-drift (OCID) mode, however, would permit passage along the complete length of each emplacement drift. In the OCID mode, two sets of parallel track would be placed within each waste emplacement drift. The waste packages would be emplaced in a line on one track while backfilling could be performed at a later time from the other track. The drift diameter for the CID waste package emplacement mode is currently defined as 5.0 meters. However, the minimum diameter required to accommodate an OCID emplacement mode is currently considered to be 5.5 meters. If emplacement drift backfill was deemed necessary, one fairly significant result would be the need to bore 5.5 meter, rather than 5.0 meter, diameter emplacement drifts.

As currently conceived, backfilling equipment would consist of a rail-mounted train of material supply cars and a locomotive that would transport the material underground to either the individual waste emplacement drifts being backfilled or to sidetracks for holding until the material is needed for backfilling. Within a waste emplacement drift, one or more rail cars would be coupled to the self-propelled backfill stower and moved to the end of the drift. An additional material supply car with locomotive would shuttle material from the entrance of the waste emplacement drift to the stower. The stower would slowly retreat to the drift entrance as the stowing of backfill is performed. Additional equipment which supports backfilling would be located on the surface. This equipment would be primarily involved in material handling.

Hostile thermal and radiation conditions existing within the emplacement drifts would necessitate the use of remote control of all backfilling within the emplacement drifts. Remote-controlled equipment would include operator control stations, wireless communication networks, video monitors, and various sensing devices.

Backfilling labor would consist of work crews and operators located mainly on the surface for material handling. As currently conceived, backfilling operations would be directed by operators located within shielded control stations outside of the waste emplacement drifts.

The preliminary backfilling design (see Figure 5.2-1) reflects the utilization of a cantilevered belt conveyor and support boom. This system would transport loose material to an elevated point beyond the stower and dump the material as shown in Figure 5.2-1. When centered over the alignment of the waste packages, a continuous "windrow" extending from one end of an emplacement drift to the other would be formed as shown in the cross-section in Figure 5.2-2. The "windrow" concept permits continuous stowing while the stower unit retreats to the access end of the typical emplacement drift. This "windrow" concept results in a partial sloping backfill outline, as depicted in Figure 5.2-2.

An alternative to the "windrow" concept is the "side-to-side" concept in which stowing is conducted by swivelling the stowing boom from side-to-side across the typical emplacement drift opening. The side-to-side stowing concept, which produces a level partial backfill outline as depicted in Figure 5.2-3, is also addressed because of seismic issues identified with the sloping partial backfill (see Section 5.2.2). This concept would result in not only backfill coverage of the waste packages but also coverage of much of the open space adjacent to the waste packages, as shown in Figure 5.2-3. The combination of haulage and stowing alternatives are shown in the flowsheet in Figure 5.2-4. Other stowing alternatives such as mechanical slinging and pneumatic stowing were not considered in this study.

5.2.1.2 Equipment Limitations

Emplacement drifts will have to be cooled down for backfilling operations within the emplacement drifts, as stated on page 8-301 of the ACD Report (CRWMS M&O 1996b):

> Heat and dust are potential conditions which may affect equipment performance. The temperature in unventilated drifts 100 years after waste emplacement has been estimated at 170°C. The high temperature exceeds the maximum recommended temperature for an electrical

drive unit. High temperatures are likely to adversely affect hydraulic over electric or compressed air drives if used on stowing equipment. Therefore, if backfill is to be applied in emplacement drifts, the drifts will first have to be cooled down for equipment access.

5.2.2 SENSITIVITY OF BACKFILL TO SEISMIC EVENTS

This section addresses the sensitivity of emplacement drift backfill to seismic activity. In addition to cost and schedule impacts of backfilling the emplacement drifts (discussed in Section 5.2.9), if deemed necessary, an additional consideration is the functional performance of backfill after it has experienced seismic activity. Both the "level partial" (also referred to as "side-to-side" in Section 5.2.1) concept as well as the "sloping partial" (referred to as "windrow" in Section 5.2.1) concept are addressed. Figures 5.2-3 and 5.2-2, respectively, depict these two concepts. This section will address the possibility of backfilled waste packages becoming uncovered due to seismic effects, and based on this analysis will indicate a preference for the "level partial" backfill concept.

The following factors were considered in this analysis:

- Pertinent backfill design features:
  - loose cohesionless materials -- Both sand and crushed tuff are granular materials with low shear strength; no compaction is envisioned.
  - partial backfill limitation -- Each of the two backfill cross-sections (sloping and level partial backfill concepts) includes a significant void space (approximately 1.2 m at centerline of crown) and two slopes due to the conceptual backfill placement method.
  - position of waste package relative to the position of the upper backfill surface -- Each of the two backfill cross sections includes an invert layer, which raises the waste package to the upper half of the emplacement drift.
- Potential failure modes due to earthquakes:
  - displacement of backfill slopes due to shaking
  - minor rockfall due to loosening or spalling, causing displacement of backfill
- Complexity of the two failure modes. Earthquake induced backfill failure is controlled by a variety of parameters, including the following:
  - potential activity of various faults in the Yucca Mountain area, each with different types of displacement, distances to the site, and recurrence intervals
  - intensity and duration of shaking
  - attenuation of ground motion with distance and direction from the source fault

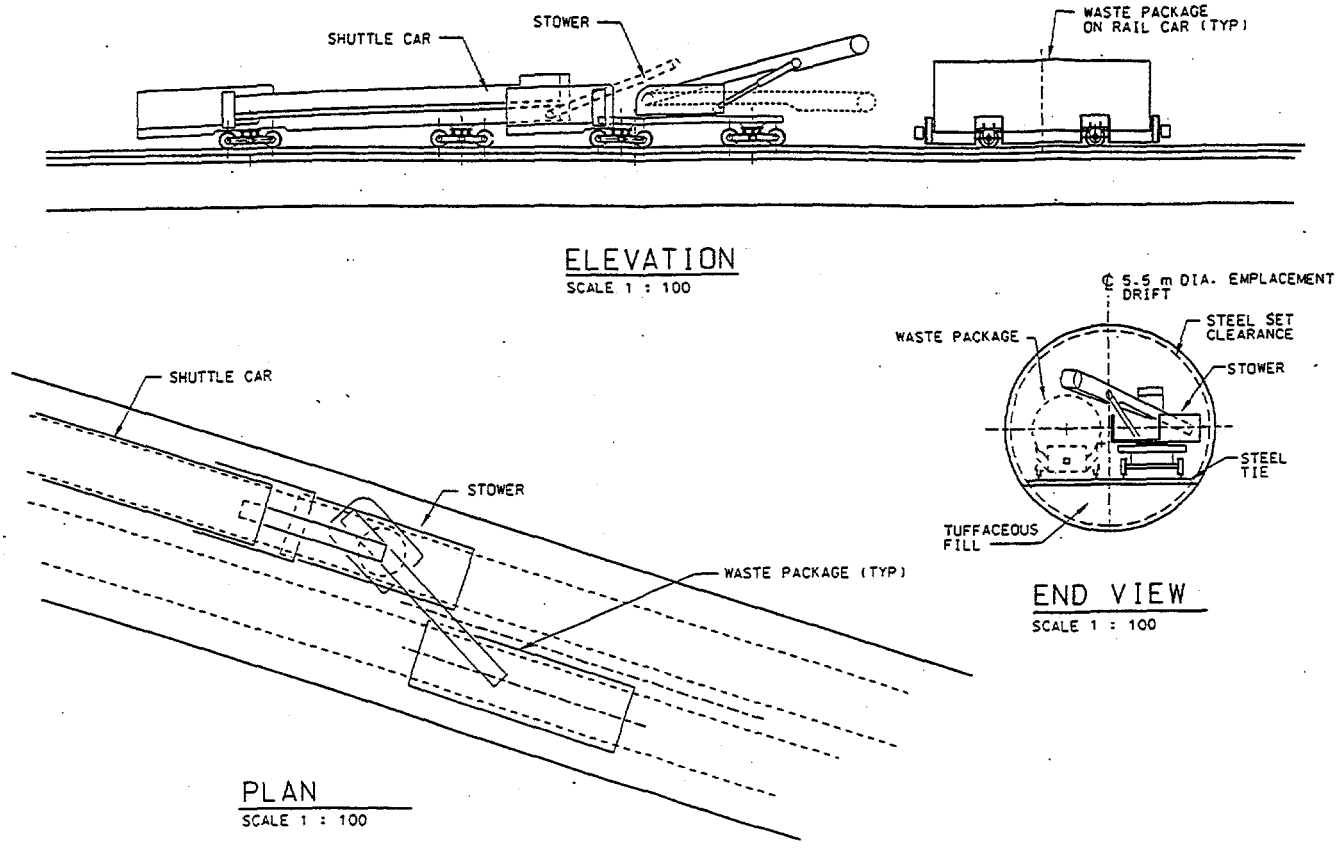

Figure 5.2-1 Conceptualized backfilling equipment for the off-center-in-drift waste emplacement mode

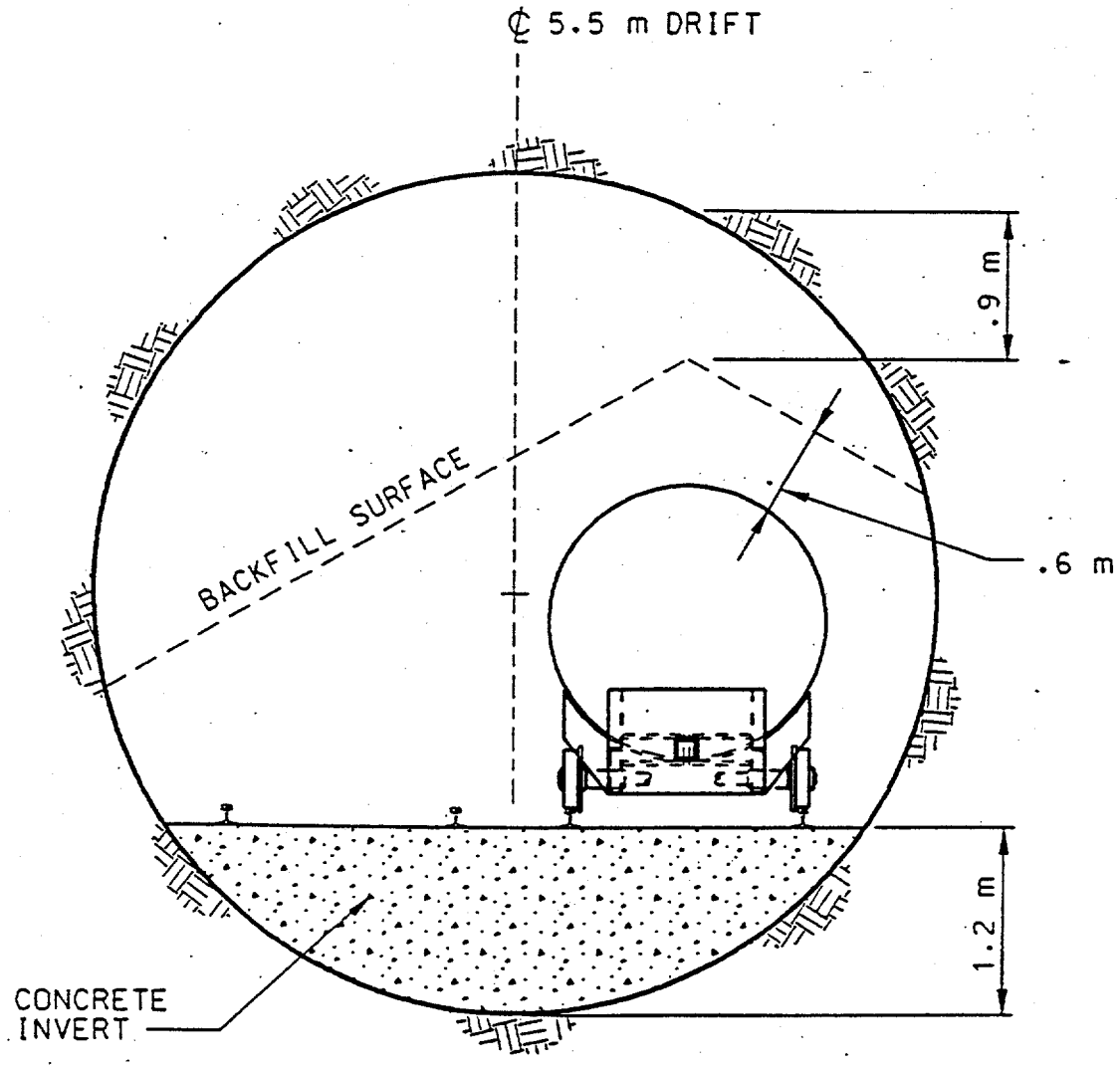

Figure 5.2-2 Wind row (also referred to as "sloping partial") backfill cross-section

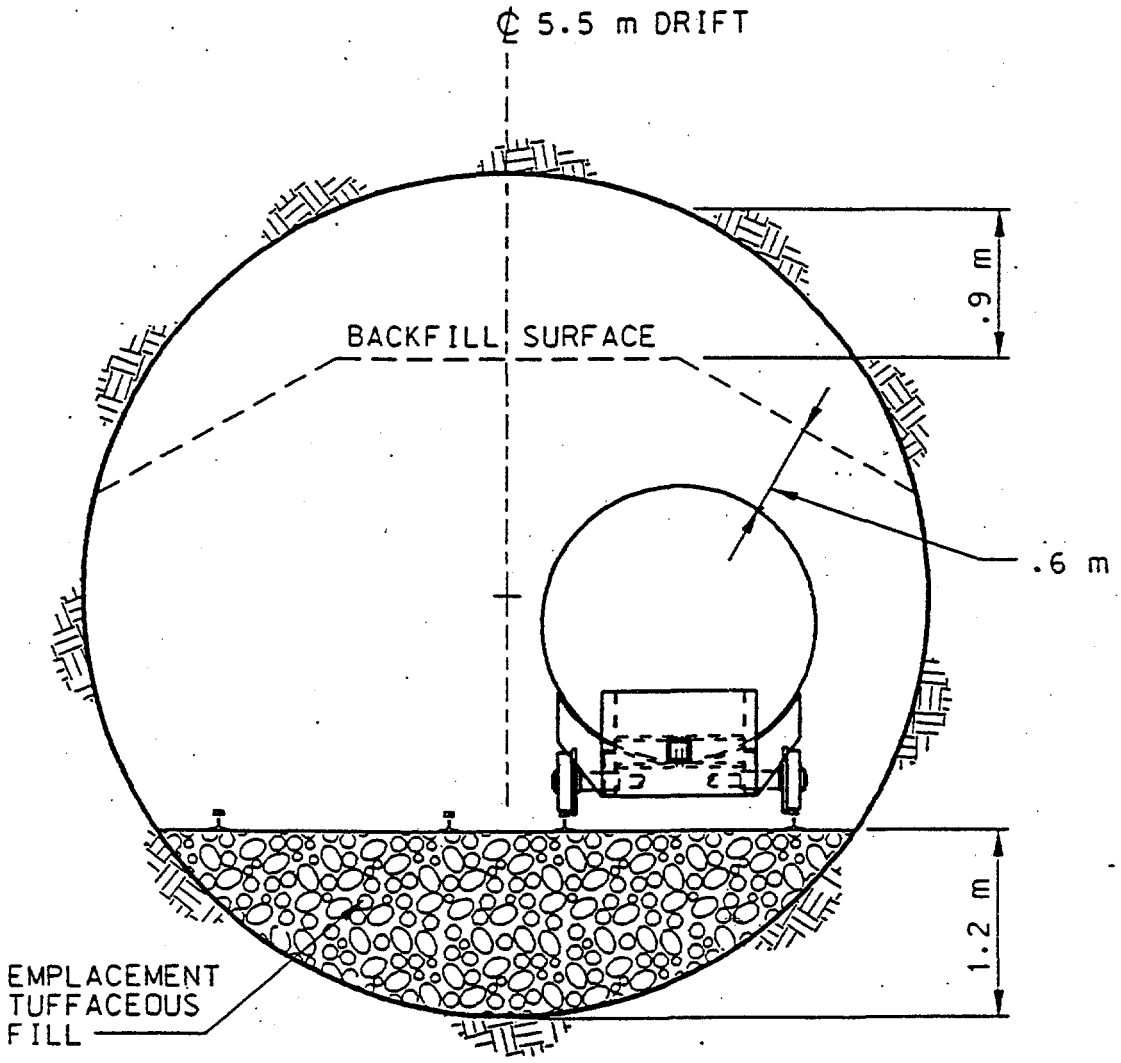

Figure 5.2-3 Side-to-side (also referred to as "level partial") backfill cross section

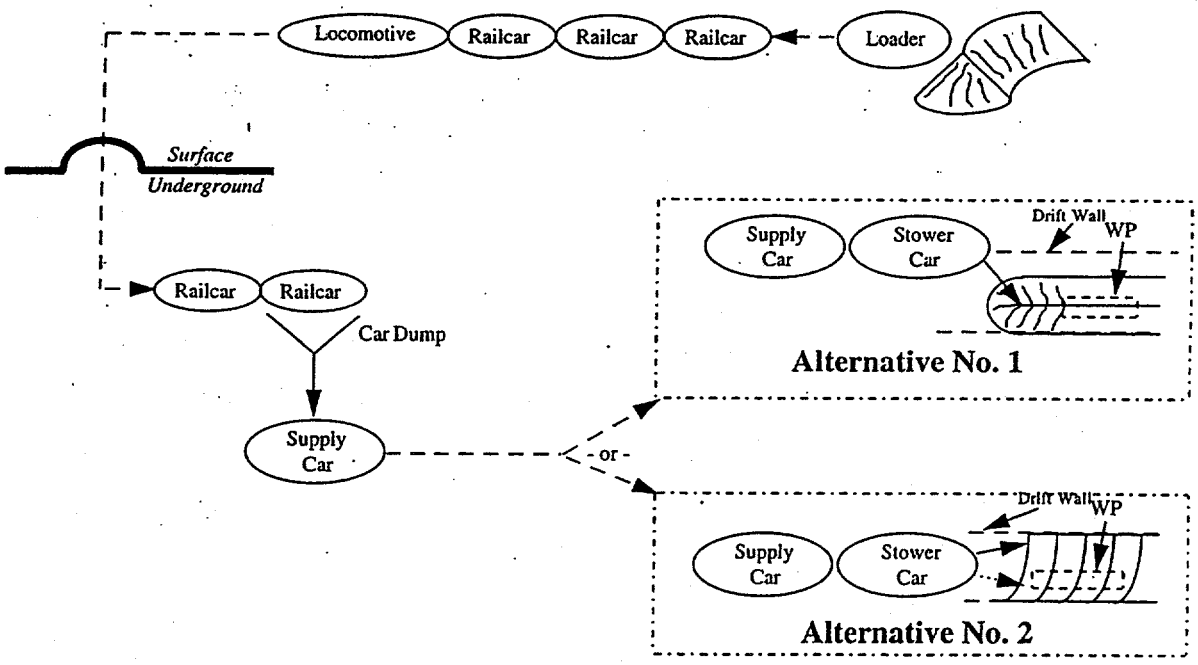

Figure 5.2-4 Backfill material haulage and stowing flowsheet

- geologic structure (discontinuities and layering)

- ground and backfill response characteristics.

5.2.2.1 Evaluation of Seismic Stability of Backfill

One concern with the behavior of backfill under seismic activity results from an unfavorable, but seemingly necessary, combination of features. Due to the fact that the backfill material is granular (essentially no fines and no cohesion) and would probably be robotically dumped (without mechanical compaction) on the waste packages, any amount of shaking will result in horizontal and vertical displacements. As the backfill grains move to a more stable configuration, these displacements will result in loss of backfill cover above the waste package.

A simplified approach was considered appropriate for this study. A more sophisticated approach, including consideration of the backfill response behavior and time history of shaking, would be warranted for design applications.

Using estimated ranges of soil properties for uniformly graded sand and for a well-graded sand and gravel mixture (based on Lambe and Whitman, 1969 and Department of the Navy DM-7, 1982), the following stability analyses were applied to the sloping partial backfill concept, shown in Figure 5.2-2:

- infinite slope displacement analysis

- simple pseudostatic stability analysis for top of backfill pile under horizontal earthquake load

- pseudostatic stability analysis for circular failure wedge (Department of the Navy 1982)

The infinite slope method, based on shallow slope failures, gives the most useful results of the three methods. A more sophisticated simplified dynamic stability analysis method by Makdisi and Seed (1978) was investigated, but was not applied, due to a concern that the assumption of a circular failure surface is nonconservative and may not be compatible with the level of sophistication of this method. The Navy DM-7 method assumes a circular failure surface, but was easily performed by hand calculations and was considered sufficient for a preliminary stability evaluation.

- Assumed backfill material properties are summarized at the bottom of Table 5.2-1.

The following analyses were applied to the level partial backfill concept, shown in Figure 5.2-3, using the same estimated ranges of soil properties as those used in the analysis of the sloping partial backfill:

- infinite slope displacement analysis

- maximum settlement estimate.

5.2.2.2 Results of Seismic Evaluation

Results of the slope analysis for the sloping and partial level backfill concepts are summarized in Tables 5.2-1 and 5.2-2.

Results of the seismic analysis for the sloping partial backfill design concept include the following:

- The most likely earthquake induced failure of the sloping partial backfill will be by downslope displacement along shallow failure surface(s), resulting in leveling of the upper backfill surface.

- The use of a sloping partial backfill of quartz sand will probably result in significant displacement of the slope under a single earthquake induced acceleration of only 0.1g. An earthquake producing this level of ground motion has an annual probability of approximately 7×10^{-3}, corresponding to a recurrence interval of 150 years (based on Wong et al., 1995).

- The use of a sloping partial backfill of quartz sand will result in very significant displacement of the slope under a single earthquake induced acceleration of 0.2g. This analysis indicates a decrease of approximately 40 percent of the thickness of backfill cover over the waste package. An earthquake producing this level of ground motion has an annual probability of approximately 2×10^{-3}, corresponding to a recurrence interval of 500 years (based on Wong et al, 1995).

- The use of a sloping partial backfill of well-graded crushed tuff will result in very significant displacement under a single earthquake induced acceleration of 0.2g. This analysis indicates a decrease of approximately 35 percent of the thickness of backfill cover over the waste package. An earthquake producing this level of ground motion has an annual probability of approximately 2×10^{-3}, corresponding to a recurrence interval of 500 years (based on Wong et al, 1995).

- The use of a sloping partial backfill of well-graded crushed tuff will result in very significant (probably excessive) displacement of the slope under a single earthquake induced acceleration of 0.4g (the current design earthquake, from CRWMS M&O 1996a). This analysis indicates a decrease of approximately 75 percent of the thickness of backfill cover over the waste package. An earthquake producing this level of ground motion has an annual probability of approximately 5×10^{-4}, corresponding to a recurrence interval of 2000 years (based on Wong et al, 1995).

Figure 5.2-4a is an illustration of the sloping partial backfill surfaces of quartz sand and crushed tuff before and after a single shaking event of 0.4g acceleration.

Results of the seismic analysis for the level partial backfill concept include the following:

- The long term settlement due to the weight of the backfill and severe seismic shaking for the level partial backfill concept is conservatively estimated to be in the range from 5 percent to

10 percent of the overall backfill thickness, or approximately 0.15 to 0.3 m. The overall backfill thickness is defined from the emplacement drift invert to the top of the backfill.

- The use of a level partial backfill of quartz sand will result in flattening of the backfill side slopes under a single earthquake induced acceleration of 0.2g to 0.4g. This flattening of the side slopes has an insignificant effect on the thickness of backfill cover over the waste package.

- The use of a level partial backfill of crushed tuff will result in little or no displacement of the backfill side slopes under a single earthquake induced acceleration of 0.2g to 0.4g.

Figure 5.2-4b is an illustration of the level partial backfill surfaces of quartz sand and crushed tuff before and after a single shaking event of 0.4g acceleration.

5.2.2.3 Conclusions

The results and conclusions presented are based on highly simplified methods using single event, peak ground accelerations in a horizontal or near-horizontal direction. Multiple accelerations with greater vertical components would cause greater settlements, further leveling of the upper backfill surface, and losses of backfill cover depth.

The slope stability and displacement analyses led to the following conclusions:

- For earthquake resistance of a sloping partial backfill, the use of crushed tuff would be a better backfill material than clean sand, due to the anticipated gradation ranging from sand to gravel, angular particle shape, and resulting increased frictional characteristics.

- For consideration of earthquake resistance, the use of a sloping partial backfill is undesirable, unless a structural retaining wall is added to provide lateral confinement, or the quantity of the backfill material is increased until lateral confinement is provided by the repository drift walls.

- Due to the increased volume of a level partial backfill and commensurate decrease in void space within the drift, any amount of shaking causes little flattening of the original backfill side slopes, and the volume of backfill would be sufficient to provide a cover thickness of at least 50 percent to 75 percent of the original thickness after long term settlement.

- The post-earthquake cover thickness of level partial backfill consisting of clean quartz sand, crushed tuff, or any other granular material would be based primarily on the long term settlement behavior of the material.

The seismic evaluations performed for this study show that maximizing the backfill volume by using the level partial backfill concept decreases the probability of waste package exposure and increases the probability of maintaining the backfill thickness required for thermal and rockfall protection.

5.2.2.4 Recommendations for Future Work on Backfill-Related Seismic Analysis

In the event that backfill is pursued as a means of providing improvements in repository performance at reasonable cost, recommendations for further seismic analyses include the following:

- An empirical approach to long term settlement evaluation, based on laboratory testing, is required for further evaluation of the level partial backfill concept.
- The minimum backfill cover depths for the beneficial thermal functions of the backfill need to be evaluated and compared to the estimated post-earthquake cover depths.
- Future backfill seismic evaluations should include characterization of various proposed backfill materials by soil mechanics laboratory testing, including the following tests:
  - triaxial compression tests to determine internal friction angle and cohesion
  - grain size distribution
  - static physical model testing (in-place density, relative density)
  - dynamic physical model testing (shaking table).

Table 5.2-1 Summary of Results for Seismic Analysis of Sloping Partial Backfill Concept

Method & Assumed Failure Geometry	Backfill Material*	Assumed Acceleration & Direction, Single Shaking Event	Estimated Factor of Safety	Comments
Simple pseudostatic, horiz failure plane across top of backfill pile	qtz SAND, fine to med grained	0.4g horiz	1.2 to 1.4	Significant horiz displacement across top of slope is unlikely under horiz acceleration only
Simple pseudostatic, horiz failure plane across top of backfill pile	crushed TUFF, well-graded	0.4g horiz	1.6 to 2.1	Significant horiz displacement across top of slope is unlikely under horiz acceleration only
Pseudostatic, circular failure wedge	qtz SAND, fine to med grained	0.4g downslope	0.3 to 0.5	Slope is unstable; Excessive displacement (exposure or near exposure of WP) is likely
Pseudostatic, circular failure wedge	qtz SAND, fine to med grained	0.1g downslope	0.6 to 0.9	Slope is unstable; Excessive displacement (exposure or near exposure of WP) is likely
Pseudostatic, circular failure wedge	crushed TUFF, well-graded	0.4g downslope	0.9	Slope is unstable; Significant displacement is likely
Pseudostatic, circular failure wedge	crushed TUFF, well-graded	0.2g downslope	1.0	Significant displacement is possible
Infinite slope displacement	qtz SAND, fine to med grained	0.4g horiz	< 1.0	Est. cover depth after earthquake induced displacement: 0.1 m
Infinite slope displacement	qtz SAND, fine to med grained	0.2g horiz	< 1.0	Est. cover depth after earthquake induced displacement: 0.3 to 0.4 m
Infinite slope displacement	crushed TUFF, well-graded	0.4g horiz	< 1.0	Est. cover depth after earthquake induced displacement: 0.1 to 0.2 m
Infinite slope displacement	crushed TUFF, well-graded	0.2g horiz	< 1.0	Est. cover depth after earthquake induced displacement: 0.4 m

* Assumed Properties of Backfill Materials:

Quartz sand: cohesion = 0; friction angle = 26 to 30 degrees; unit weight = 83 to 92 pcf
Crushed tuff: cohesion = 0; friction angle = 32 to 40 degrees; unit weight = 100 pcf

Table 5.2-2 Summary of Results for Analysis of Partial Level Backfill

Method & Assumed Failure Geometry	Backfill Material*	Assumed Acceleration & Direction, Single Shaking Event	Comments
Infinite slope displacement	qtz SAND, fine to med grained	0.4g horiz	Est. cover depth after earthquake induced displacement: 0.58 m
Infinite slope displacement	qtz SAND, fine to med grained	0.2g horiz	Est. cover depth after earthquake induced displacement: 0.59 to 0.60 m
Infinite slope displacement	crushed TUFF, well-graded	0.4g horiz	Est. cover depth after earthquake induced displacement: 0.59 to 0.60 m
Infinite slope displacement	crushed TUFF, well-graded	0.2g horiz	Est. cover depth after earthquake induced displacement: 0.58 m

* Assumed Properties of Backfill Materials:

Quartz sand: cohesion = 0; friction angle = 26 to 30 degrees; unit weight = 83 to 92 pcf
Crushed tuff: cohesion = 0; friction angle = 32 to 40 degrees; unit weight = 100 pcf

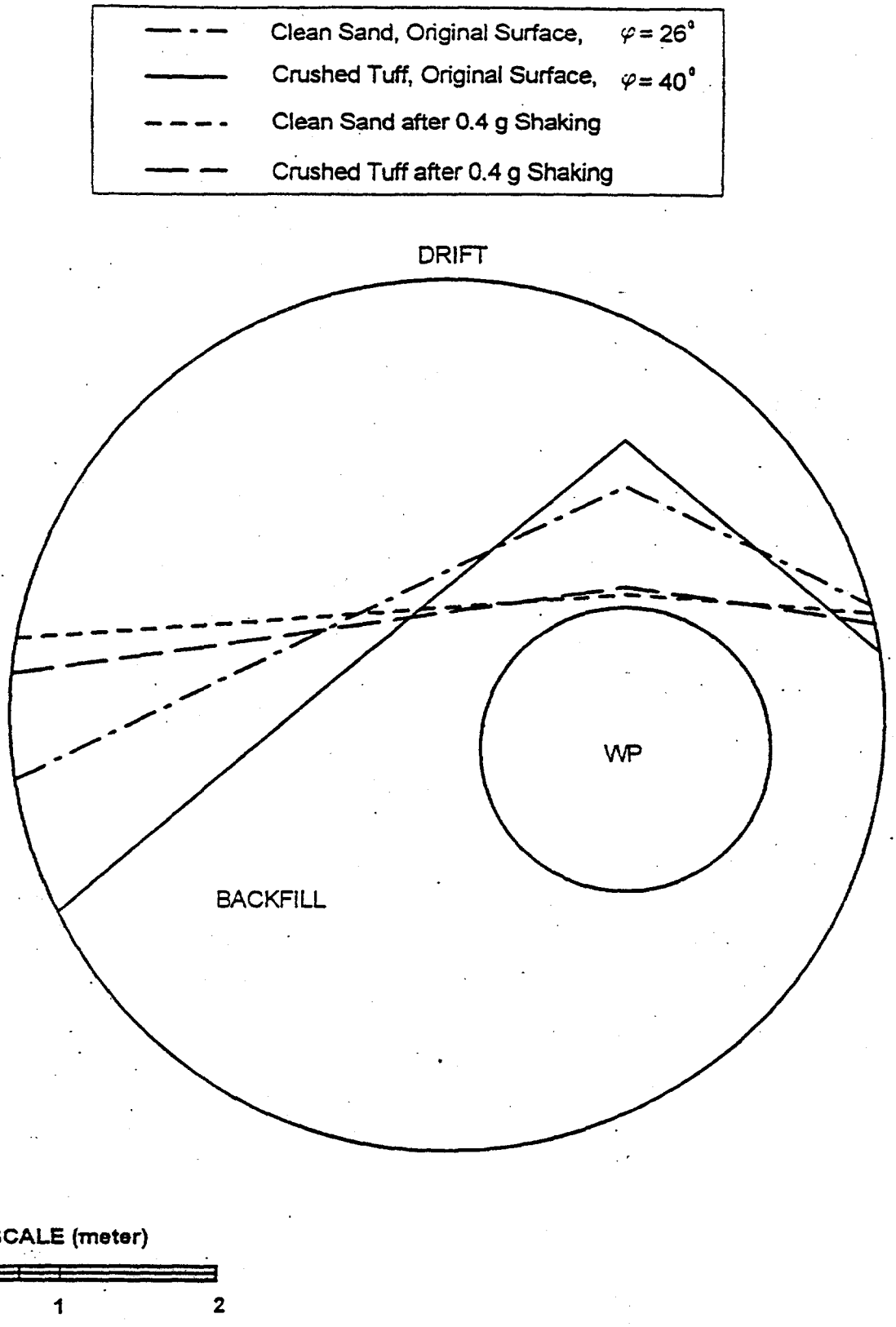

Figure 5.2-4a Effects of a single shaking event on the sloping partial backfill

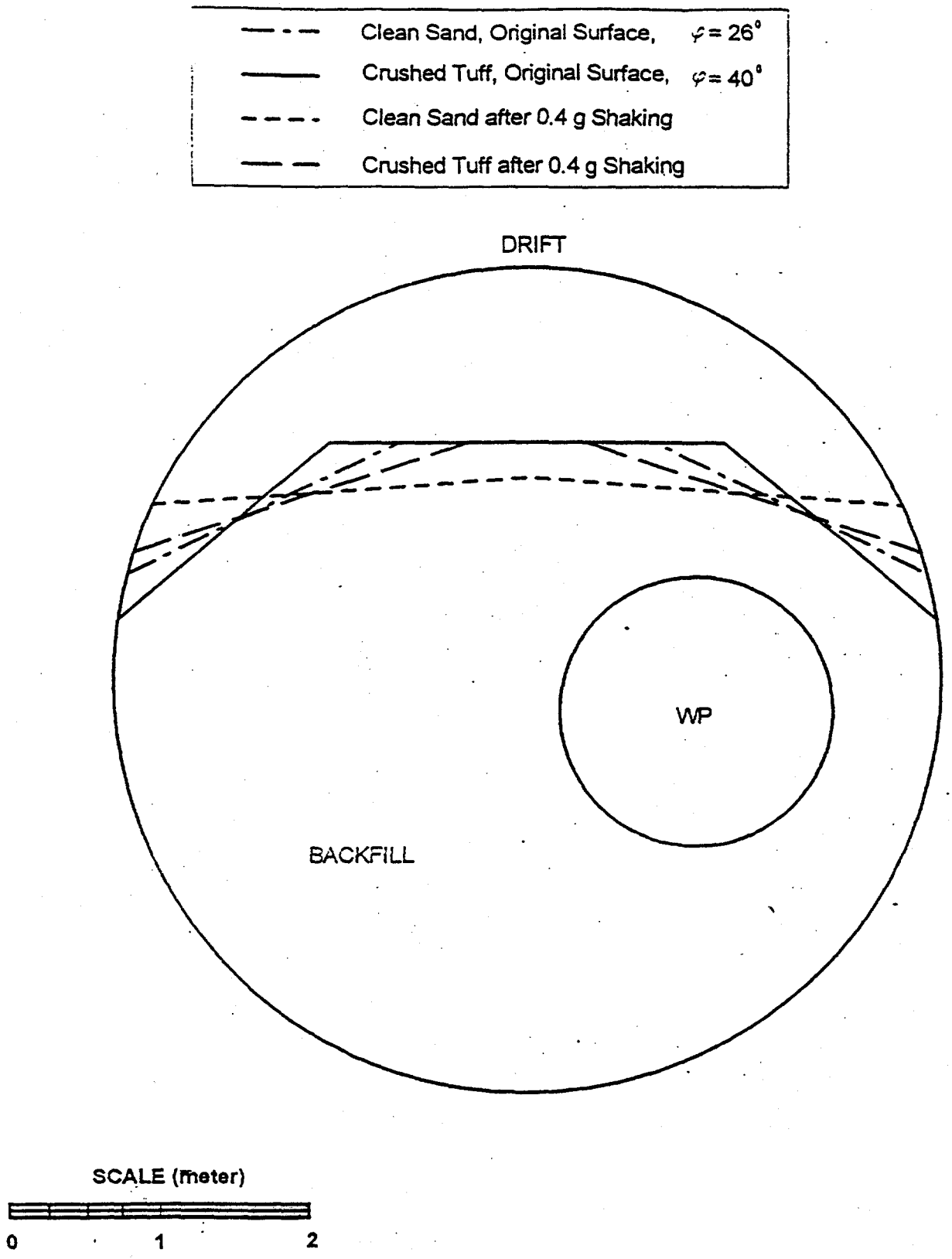

Figure 5.2-4b Effects of a single shaking event on a level partial backfill

5.2.3 ESTIMATES OF THERMAL CONDUCTIVITY OF BACKFILL

5.2.3.1 Quartz Sand

Quartz sand has been used as a test medium for numerous experimental investigations of the effective thermal conductivity of two-phase systems (e.g., Luikov et al., 1968; Woodside and Messner, 1961; Krupiczka, 1967; Crane and Vachnon, 1977; Middleton, 1994). One of the most recent studies on quartz sand-air mixtures is also one of the most comprehensive. Middleton (1994) performed experiments on seventeen samples of quartz sand-air mixtures with aggregate porosities ranging from approximately 0.2 to 0.5. Based on these experimental data, Middleton developed the following relationship for the effective thermal conductivity of a quartz sand-air mixture:

$$\lambda_{eff} = -0.699 \ln(\phi) + \lambda_{air}$$

where λ_{eff} is the effective thermal conductivity of the two-phase quartz sand-air system, ϕ is the aggregate porosity, and λ_{air} is the thermal conductivity of air. Depending upon the particle size distribution, a quartz sand is likely to exhibit a porosity ranging from 0.35 to 0.40 (e.g., Tidwell and Glass, 1994). Based on the assumption that sand grains can be represented by uniform spheres, the upper limit of porosity is 0.48 (assuming a cubic packing arrangement). Assuming the thermal conductivity of air to be 0.03 W/m-K and an upper limit on porosity of 0.48, the lower bound on effective thermal conductivity can be calculated as 0.54 W/m-K. Taking 0.35 as a lower bound on porosity, the upper bound on effective thermal conductivity is 0.76. A value between 0.54 and 0.76 W/m-K is therefore assumed to represent a reasonable approximation of the effective thermal conductivity of a dry, unconsolidated quartz sand.

5.2.3.2 Crushed TSw2 Tuff

For crushed TSw2 tuff with an effective porosity of 0.48, estimates for effective thermal conductivity of 0.58 to 0.74 W/m-K have been reported (CRWMS M&O 1995c).

5.2.4 IMPACTS OF BACKFILL ON SNF CLADDING TEMPERATURES

5.2.4.1 ACD Waste Package Spacing Concept

Introduction

Evaluations were conducted of the thermal effects of the introduction of a relatively insulating backfill at 100 years after WP emplacement for the reference thermal loading (CRWMS M&O 1996b) of 83 MTU/acre and a limiting thermal loading of 100 MTU/acre. Parametrics were performed for several different assumed backfill thermal conductivities to determine the minimum allowable backfill conductivity while maintaining emplacement thermal goals. The effects of waste stream variability were also considered including comparisons of average and design basis SNF, youngest fuel first (YFF) and oldest fuel first (OFF) scenarios, and PWR and BWR SNF. Temperature effects comparisons were performed for CID and OCID emplacements, full and partial (sloped) drift backfilling, and two-dimensional (2-D) and three-dimensional (3-D) modeling approaches.

Model Description

The 3-D emplacement thermal model used for these analyses is similar to the model described in detail in *Emplacement Scale Thermal Evaluations of Large and Small WP Designs* (CRWMS M&O 1995a), which is a CRWMS M&O QAP-3-9 design analysis. The emplacement scale model represents a pillar section of an infinite repository with one nominal (assumed average) WP positioned in the drift. The thermal loading of the repository determines the size of the "unit cell" of rock around each WP (the lower the thermal loading, the more rock around each WP). Rock layers are modeled from the ground surface to a depth of 1300 meters with the sides of the pillar assumed adiabatic. Heat is transported from the WP to the rock walls using an explicit treatment of thermal radiation (view factors calculated by the ANSYS code) and is conducted away through the rock. Water and water vapor transport are not modeled. The key parameter in this finite element model is the time-dependent heat generation in the single WP which depends on assumptions for waste receipt and averaging methods.

Waste Stream Parametrics

By assuming average SNF heat productions, the emplacement scale model can predict the average expected temperatures in the emplacement drift. These average temperatures represent the nominal case from which temperature variations due to waste stream variability can be bounded or extrapolated. Figure 5.2-5 depicts the decay heat of different design basis SNF types plotted as a function of time. The initial heat of the MGDS PWR design basis (bounding 97 percent of the PWR assemblies) can be almost twice that of an assumed average PWR assembly. Because of the variability in expected assembly heats, the average will depend on assumptions in waste receipt. Figure 5.2-6 provides a comparison of PWR and BWR average assembly heats. There is also a difference between the average of all assembly heats and the calculated heat of an assembly with average characteristics. While the base case analyses here use the former (from Key Assumption 004, CRWMS M&O 1996a), many previous evaluations have assumed the latter average. The difference is subtle, as seen in Figure 5.2-6; however, the effect can be significant when integrated over thousands of years.

Before the analysis of drift backfilling was performed, several Parametrics related to waste stream averaging and emplacement geometry were performed. Figure 5.2-7 depicts an emplacement temperature comparison of the YFF with a minimum SNF age of 10 years (YFF10) scenario and the OFF scenario of (CRWMS M&O 1996a). Two thermal loadings, 83 and 100 MTU/acre, were considered. Peak temperatures at the WP surface and drift wall were around 10°C cooler with the OFF SNF. Previous emplacement scale thermal calculations (CRWMS M&O 1996b) had conservatively assumed the YFF10 average PWR SNF. Figure 5.2-8 gives an emplacement temperature comparison of average (OFF) PWR SNF and average BWR SNF. Peak temperatures at the WP surface and drift wall were 13 to 18°C cooler with the BWR SNF compared to the more conservative (with respect to peak temperatures) results with PWR SNF.

Some thermal loading calculations have attempted to include both PWR and BWR heat by using a weighted average of both, however, the only way to truly capture the waste stream variability in the near field is to model each package individually -- a task beyond the scope of this analysis. An analysis including many individual packages was performed at Sandia National Laboratories

(CRWMS M&O 1995b) and modeled the waste packages emplaced in three years. The impact of that analysis on the backfill evaluations performed here are discussed later.

A final waste stream parametric compared a CID emplacement to OCID. The comparison between CID and OCID for two thermal loadings can be seen in Figure 5.2-9. The difference for the maximum WP surface dropped from 5°C during the first few years to 2°C at the peak time of around 50 years.

Backfill Parametrics

A parametric analysis of the effect of backfilling the emplacement drift at repository closure was performed using the three-dimensional emplacement model described above. Two thermal loadings were considered: the reference 83 MTU/acre (CRWMS M&O 1996a) and a bounding high case at 100 MTU/acre. This parametric analysis evaluates the thermal impact of the addition of backfill material; however, it does not consider the "performance" of the backfill against any of the potential functions of backfill (see Section 4). It is expected that the addition of backfill will insulate the WP such that WP temperatures increase. In an open emplacement drift, radiation heat transfer is the primary heat transfer path from the WP surface to the drift wall. If thermal radiation were replaced by an equivalent "imaginary" material, it might have an effective thermal conductivity of about 20 W/m•K. This can be contrasted to crushed TSw2 tuff with an effective porosity of 0.48, for which estimates for effective thermal conductivity of 0.58 to 0.74 W/m•K have been reported (CRWMS M&O 1995c). Table 5.2-3 provides a comparison of typical material conductivities (at around 27°C).

As a means of constraining the type of backfill materials that may be considered, a parametric was devised to determine what value of thermal conductivity is needed to maintain peak cladding temperatures below the cladding thermal goal of 350°C. For the large WP, peak cladding temperatures generally occur within the first ten years. For the purpose of this evaluation it was assumed that backfilling of the emplacement drifts is not performed until a repository closure time of 100 years after emplacement. To evaluate the thermal response to backfill, the following range of backfill conductivities was considered: 0.2, 0.3, 0.4, 0.5, 0.6, 0.8, and 1.0 W/m•K. Other parameters assumed in the model are listed below:

Waste Package:	21 PWR Emplaced OCID	
Outer Diameter:	1.629 m	
Outer Length:	5.335 m	
Drift Diameter:	5.5 m	
Drift Invert:	1.2 m of Concrete	
Area Mass Loading:	100 MTU/acre (24.7 kg/m^2),	83 MTU/acre (20.5 kg/m^2)
Drift Spacing:	22.5 m,	22.5 m
WP Spacing:	16.166 m,	19.477 m
Drift Backfill:	Sloping partial fill with crest over WP	
Average SNF:	26.4 years old, 39.65 GWd/MTU burnup, 0.428 MTU/assembly	

Design Basis SNF: 10 years old, 48.086 GWd/MTU burnup, 0.464 MTU/assembly

Peak cladding, WP surface, and drift wall temperature results at 100 MTU/acre are displayed in Figures 5.2-10, 5.2-11, and 5.2-12, respectively. Peak cladding temperatures are estimated based on predicted WP surface temperatures and a heat load and temperature dependent correlation (typically between 12 and 24°C/kW) derived from the detailed thermal evaluation of the 21 PWR MPC with disposal container described in the ACD Report (CRWMS M&O 1996b). While WP surface temperatures are derived based on nominal heat loads (Key Assumption 004 in CRWMS M&O 1996a), the temperature drop from center to edge of the WP is based on the design basis PWR SNF. Using a WP temperature drop based on design basis SNF will bound the temperature drop within the WP with respect to waste stream variability. Waste stream variability may also result in higher WP surface temperatures for some packages; this is discussed later. As seen in Figure 5.2-10, a backfill conductivity of no less than approximately 0.3 W/m•K is required to maintain cladding temperatures below 350°C when backfill is added at 100 years for a thermal loading of 100 MTU/acre.

Figure 5.2-12 displays the temperature history of the emplacement drift wall adjacent to the WP with and without backfill. At the time of backfilling (100 years), drift wall temperatures drop because the backfill material is assumed to start at the ground surface average temperature of 18.7°C. However, temperatures quickly rise as the backfill absorbs heat from the WP and the drift wall. Drift wall temperatures near the WP actually increase after backfilling because the backfill prevents thermal radiation heat transfer which would otherwise spread the WP heat over several meters of drift wall surface. Figure 5.2-13 provides a graphical description of this effect. Although drift wall temperatures increased, thermal goals for TSw2 rock were not exceeded. Also, the magnitude of the second drift wall peak temperature after backfilling was not seen to depend on backfill conductivity.

Table 5.2-3 Thermal Conductivities of Various Materials

Material	**Thermal Conductivity (W/m•K)**
Pure Copper	401
Aluminum 6063	218
Carbon Steel A516	41.0
Stainless Steel 316	13.4
Intact TSw2 Rock	2.1
Concrete (stone mix)	1.4
Crushed Tuff (0.48 porosity)	0.58 - 0.74
Fiberglass Insulation	0.038

Peak cladding, WP surface, and drift wall temperature results at 83 MTU/acre are displayed in Figures 5.2-14, 5.2-15, and 5.2-16, respectively. As seen in Figure 5.2-14, a backfill conductivity of no less than about 0.3 W/m•K is required to maintain cladding temperatures below 350°C when backfill is added at 100 years for a thermal loading of 83 MTU/acre. However, this result does not include the effects of waste stream variability on the emplacement near-field. An evaluation of this variability was performed in (CRWMS M&O 1995b) for a thermal (mass) loading of 78.2 MTU/acre. At 100 years after the start of emplacement, the maximum reported difference between the case with discretely modeled WPs and the base case was 44.5°C (p. 16, CRWMS M&O 1995b). As a check, an analysis was performed using design basis (97 percent) SNF heat loads instead of the nominal WP heat loads used above in the emplacement scale model with 0.6 W/m·K backfill. This analysis was only evaluated out to a few years so that the repository thermal loading would not be affected by the design basis SNF assumption. The resulting WP surface temperatures were 49°C hotter than the nominal case, and the cladding temperatures were 44°C hotter than nominal (remember that design basis SNF, not average, was already used here to estimate cladding temperatures given average WP surface temperatures). These two analyses indicate that, due to waste stream variability, some WPs could be as much as 50°C hotter than the nominal case (average). Accounting for this variability can be done by biasing the curves in Figure 5.2-14 upwards by 50°C, which results in a minimum acceptable backfill conductivity in the range of 0.4 to 0.5 W/m·K.

Tabulated temperature results for two backfill conductivities (0.6 and 0.3 W/m·K) for the 83 MTU/acre case are included here as Appendix A. The positions reported in the attachment are graphically displayed on page 1 of Appendix A. For each cross-sectional position (A, B, C, etc.), temperatures are reported for three axial positions: the WP mid-length, WP end, and halfway between two WPs.

Sensitivity to Backfilling at 50 Years

If the backfill was added earlier after emplacement, a more conductive backfill would be needed. A sensitivity analysis was conducted for drift backfill 50 years after emplacement for 83 MTU/acre. Peak cladding, WP surface, and drift wall temperature results for this case are displayed in Figures 5.2-17, 5.2-18, and 5.2-19, respectively. As seen in Figure 5.2-17, a backfill conductivity of no less than about 0.65 W/m•K is required to maintain cladding temperatures below 350°C when backfill is added at 50 years for a thermal loading of 83 MTU/acre. And given likely variations in WP waste stream heat loads, the required backfill conductivity may be 1.0 W/m·K or greater which is higher than typical crushed tuff rock conductivities.

Sensitivity to Emplaced Backfill Geometry

A sensitivity study was also performed for the emplaced backfill geometry. A partial drift backfill with a sloping surface (the case assumed above) is compared to a case with the drift completely filled. Figures 5.2-20 and 5.2-21 show the cladding and WP surface temperature, respectively for 0.6 W/m·K backfill added at 100 years for 100 MTU/acre. Peak cladding and WP surface temperatures were 18°C and 20°C higher, respectively, for the case with the drift completely filled. By 1000 years, these differences diminish to negligible amounts. A level partial backfill (see Section 5.2.1) can be expected to generate a thermal history between the two cases depicted in Figures 5.2-20 and 5.2-21. Furthermore, at several hundred years after backfill emplacement and beyond it can be inferred that

the SNF cladding temperature and WP surface temperature values are fairly independent of whether the backfill is a sloping partial, level partial, or full.

Conclusions

The backfill analysis (using an OFF waste stream) indicates that backfill with an effective thermal conductivity greater than 0.4 to 0.5 W/m·K can be emplaced at 100 years after WP emplacement without violating SNF cladding thermal goals. These values reflect the fact that variability in the waste stream could lead to single WP temperatures 50°C higher than the nominal, thus requiring thermal conductivity values greater than those indicated in Figure 5.2-14 as needed to satisfy the 350°C SNF cladding limit. A comparison of backfill geometry was found to impact peak temperatures by no more than 20°C. Furthermore, waste package surface temperature differences due to backfill geometry rapidly diminish after a few hundred years. Generally, issues of geometry were secondary to backfill conductivity and time of backfilling. Backfill added earlier than 100 years would require the use of backfill materials with much higher effective thermal conductivities.

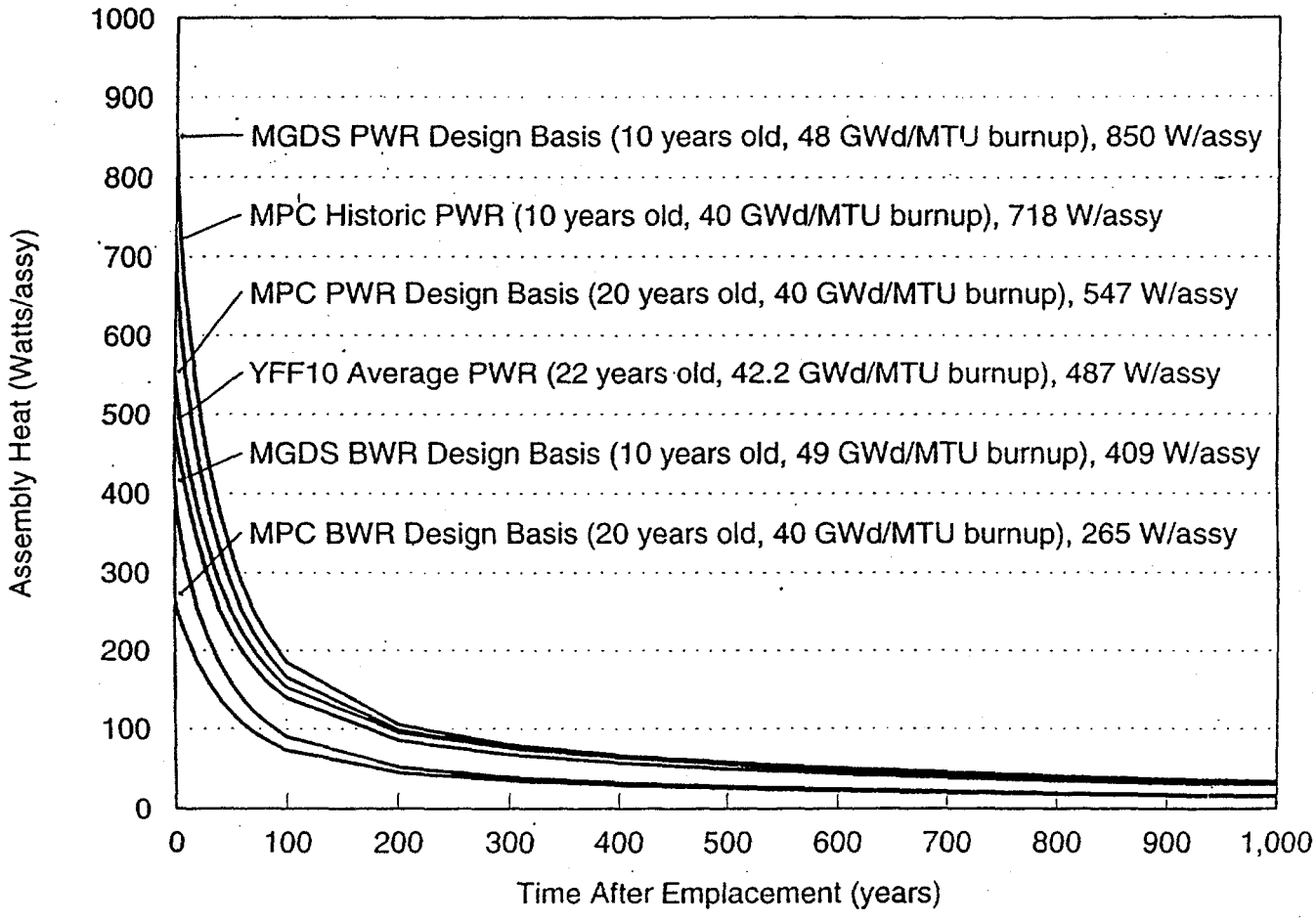

Figure 5.2-5 Decay of SNF heat over time

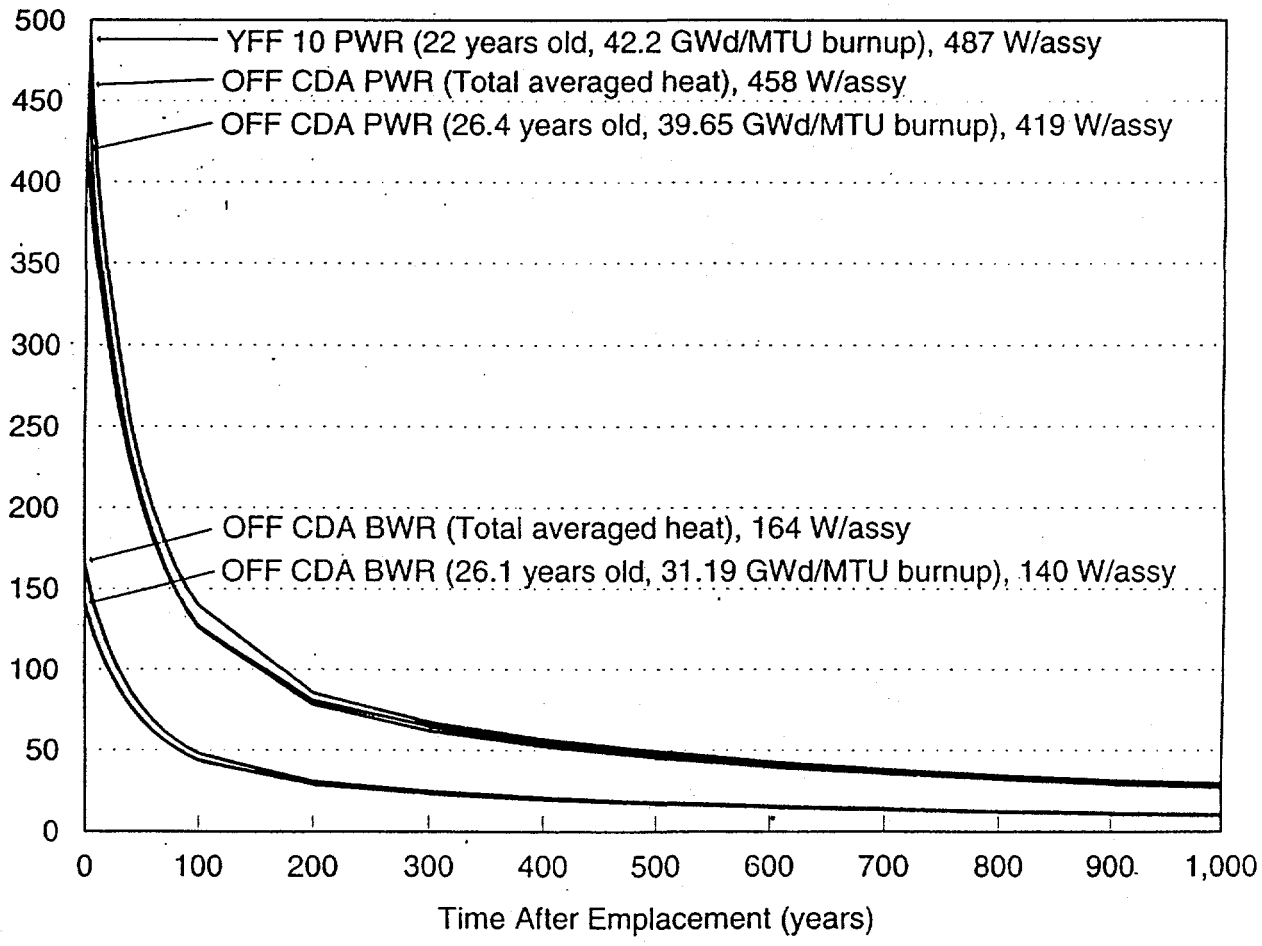

Figure 5.2-6 Decay of average SNF heat over time

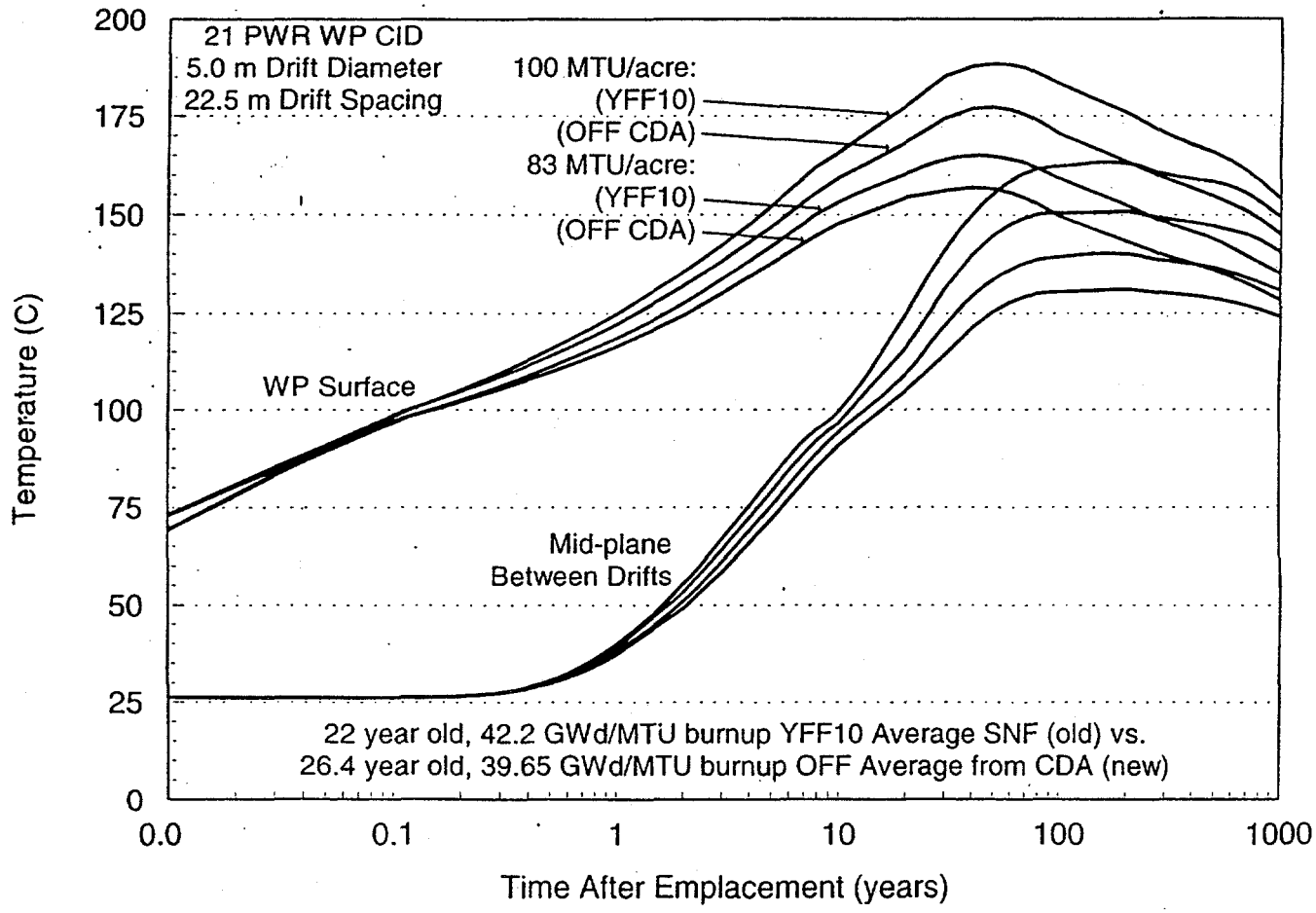

Figure 5.2-7 Temperature comparison for waste stream averages

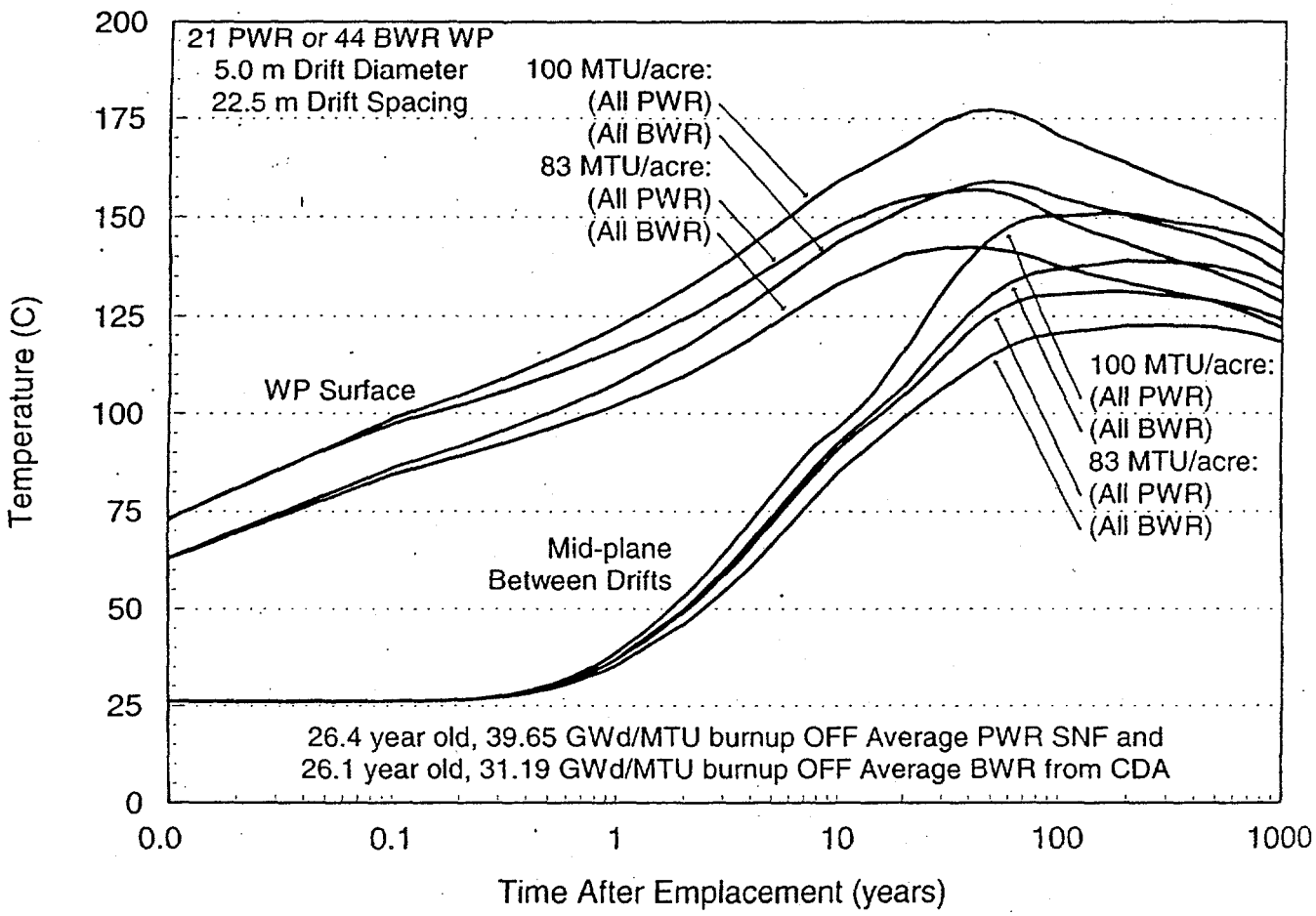

Figure 5.2-8 Average PWR and BWR SNF temperature comparison

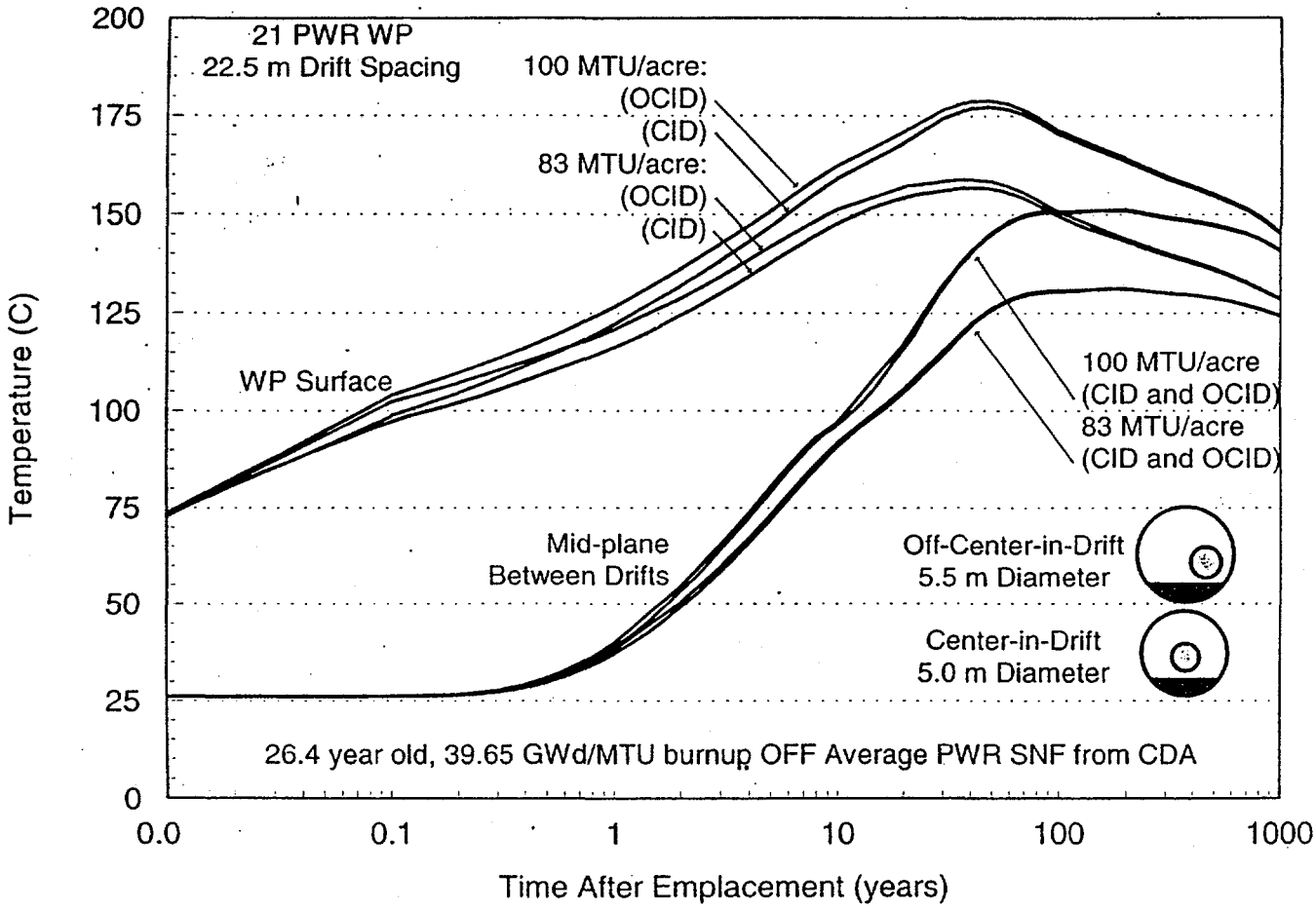

Figure 5.2-9 Temperature comparison for off-center-in-drift waste package

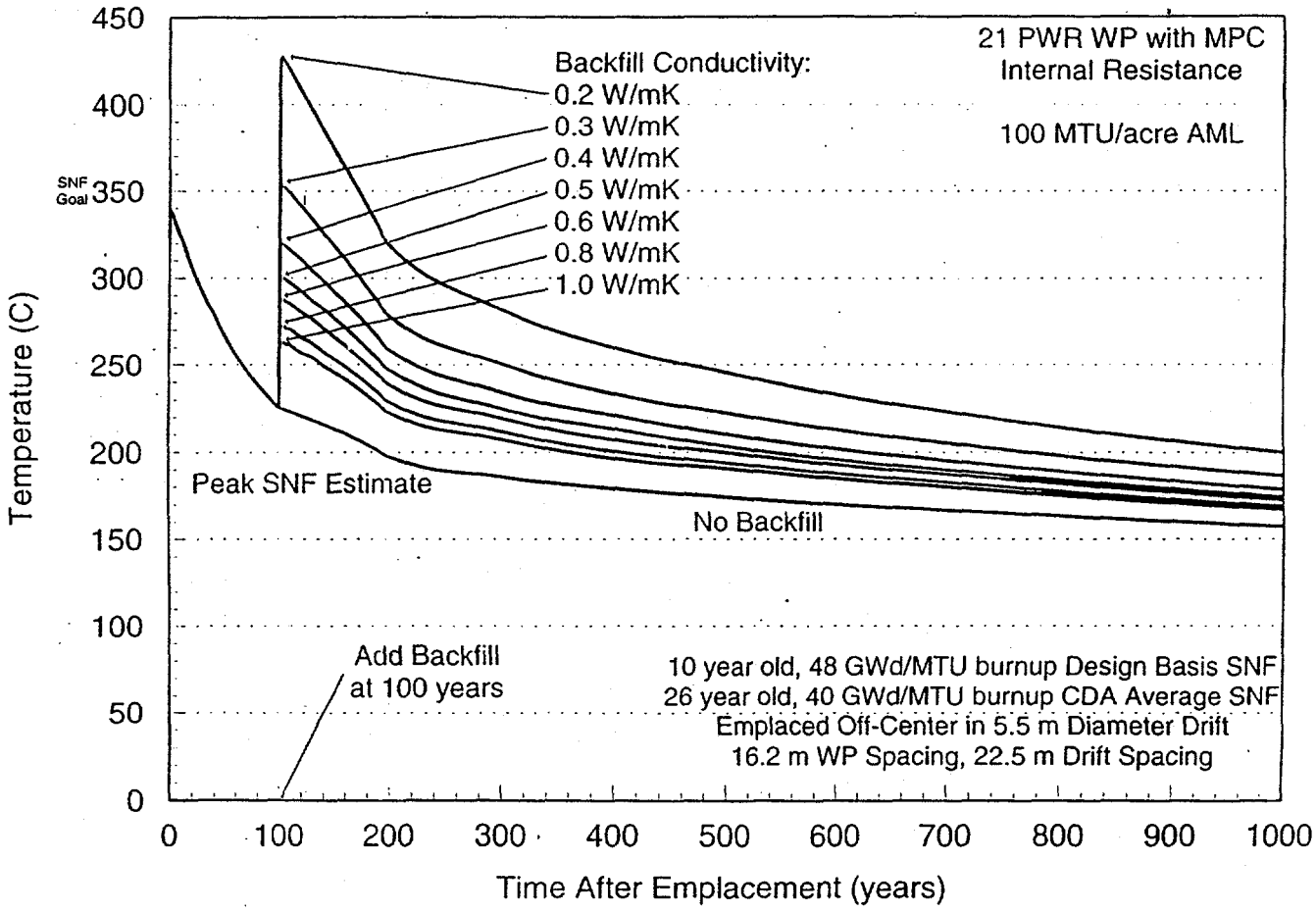

Figure 5.2-10 Effect of drift backfill on cladding temperature (100 MTU/acre)

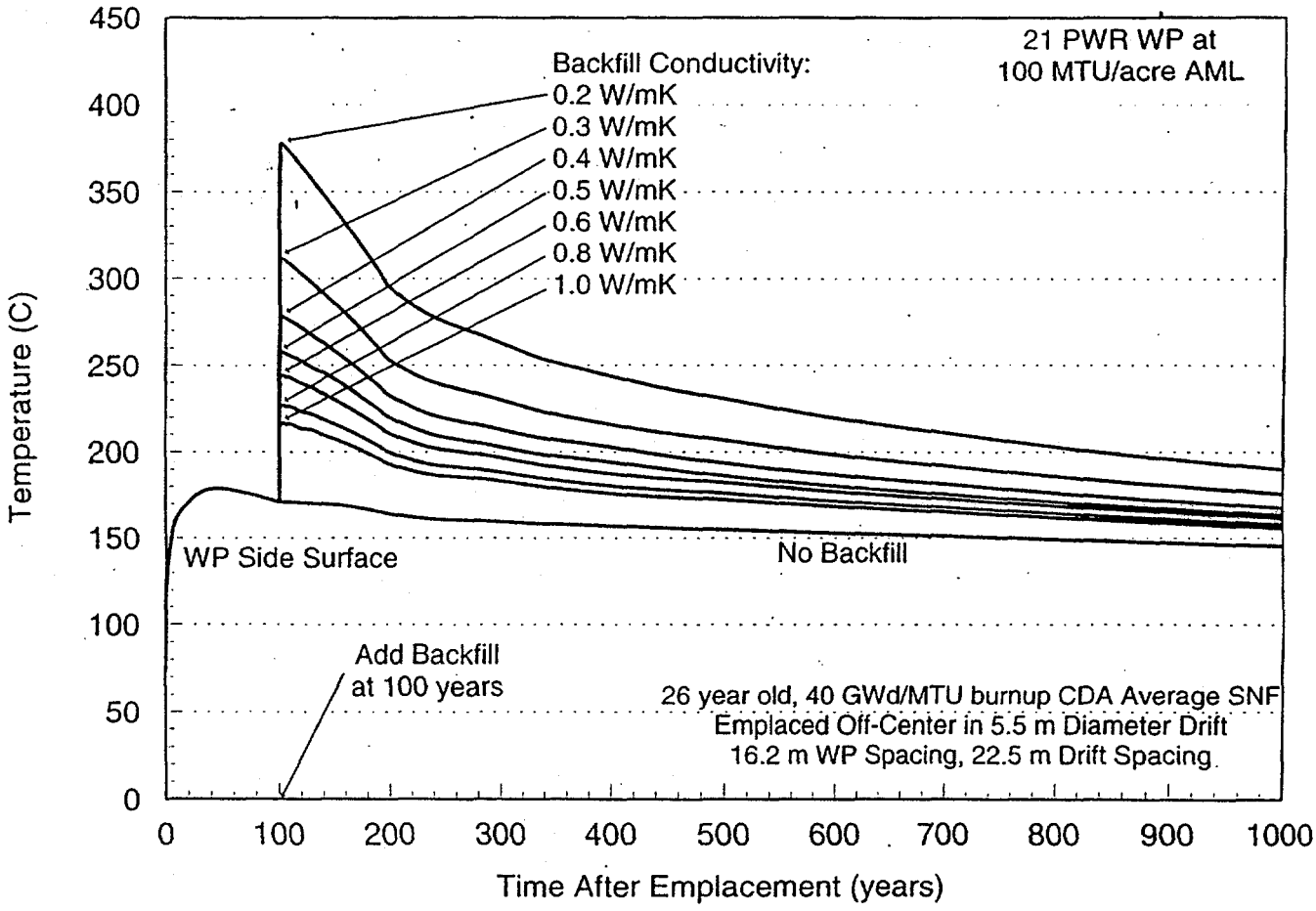

Figure 5.2-11 Effect of drift backfill on waste package surface temperature (100 MTU/acre)

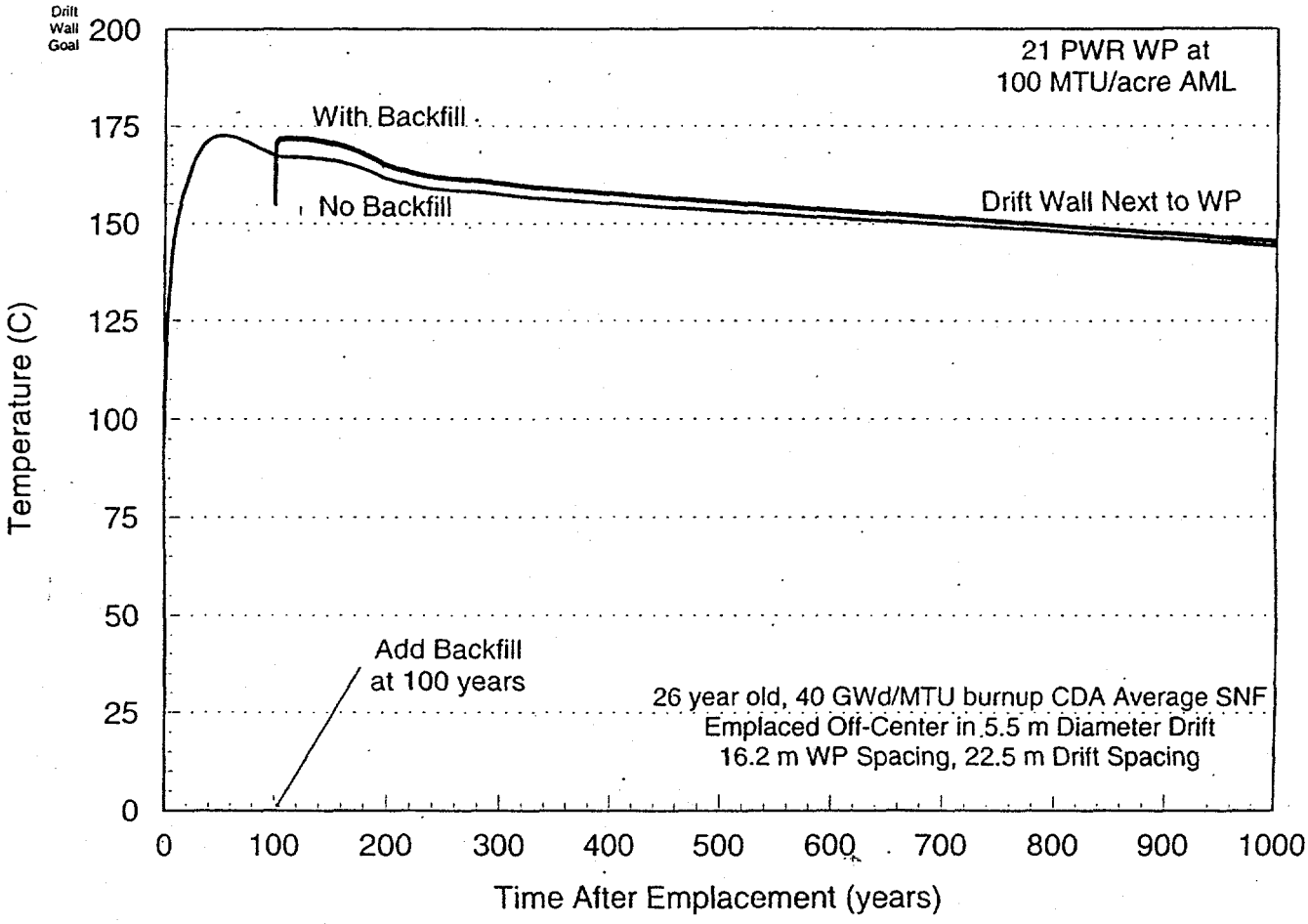

Figure 5.2-12 Effect of drift backfill on drift wall temperature (100 MTU/acre)

Drift Wall Temperature Rise Due to the Addition of Drift Backfill Material

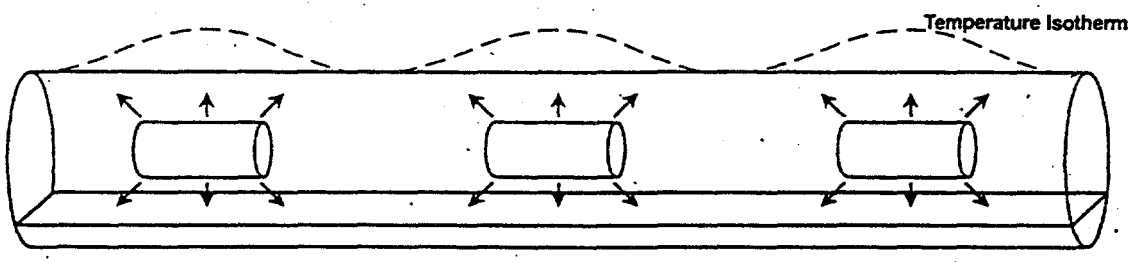

In an open drift, WP heat is transferred down the drift faster than it is conducted through the rock.

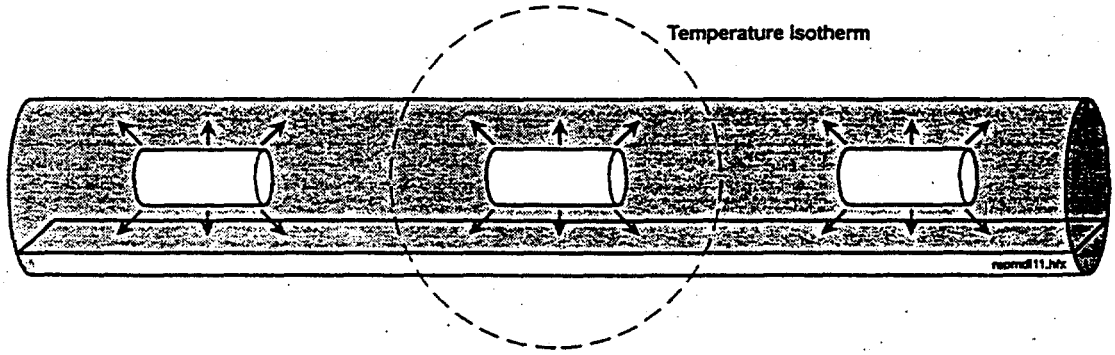

After backfill, the WPs are more isolated from each other and heat is conducted evenly resulting in more spherical isotherms.

Figure 5.2-13 Drift wall temperature rise due to the addition of drift backfill material

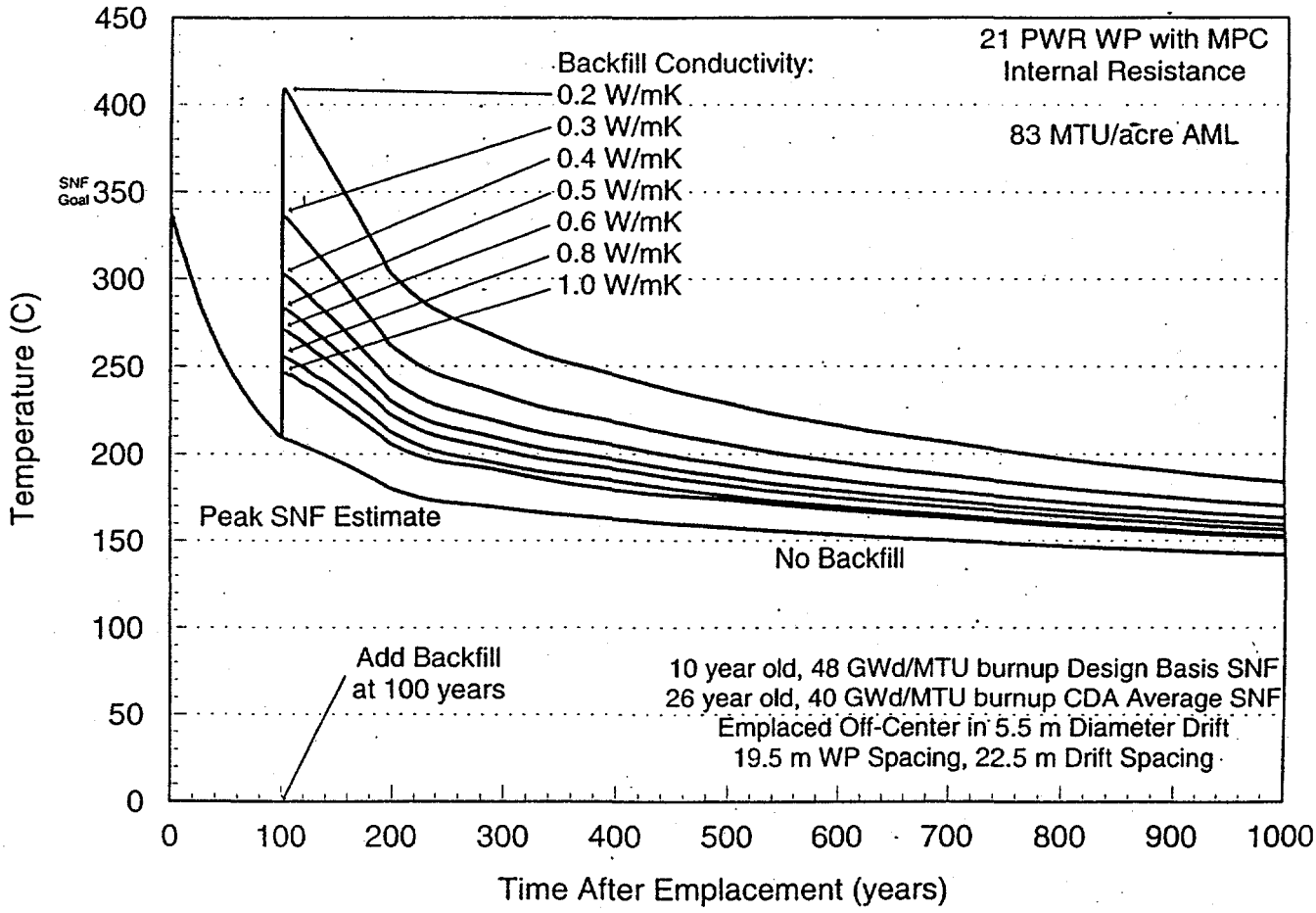

Figure 5.2-14 Effect of drift backfill on cladding temperature (83 MTU/acre)

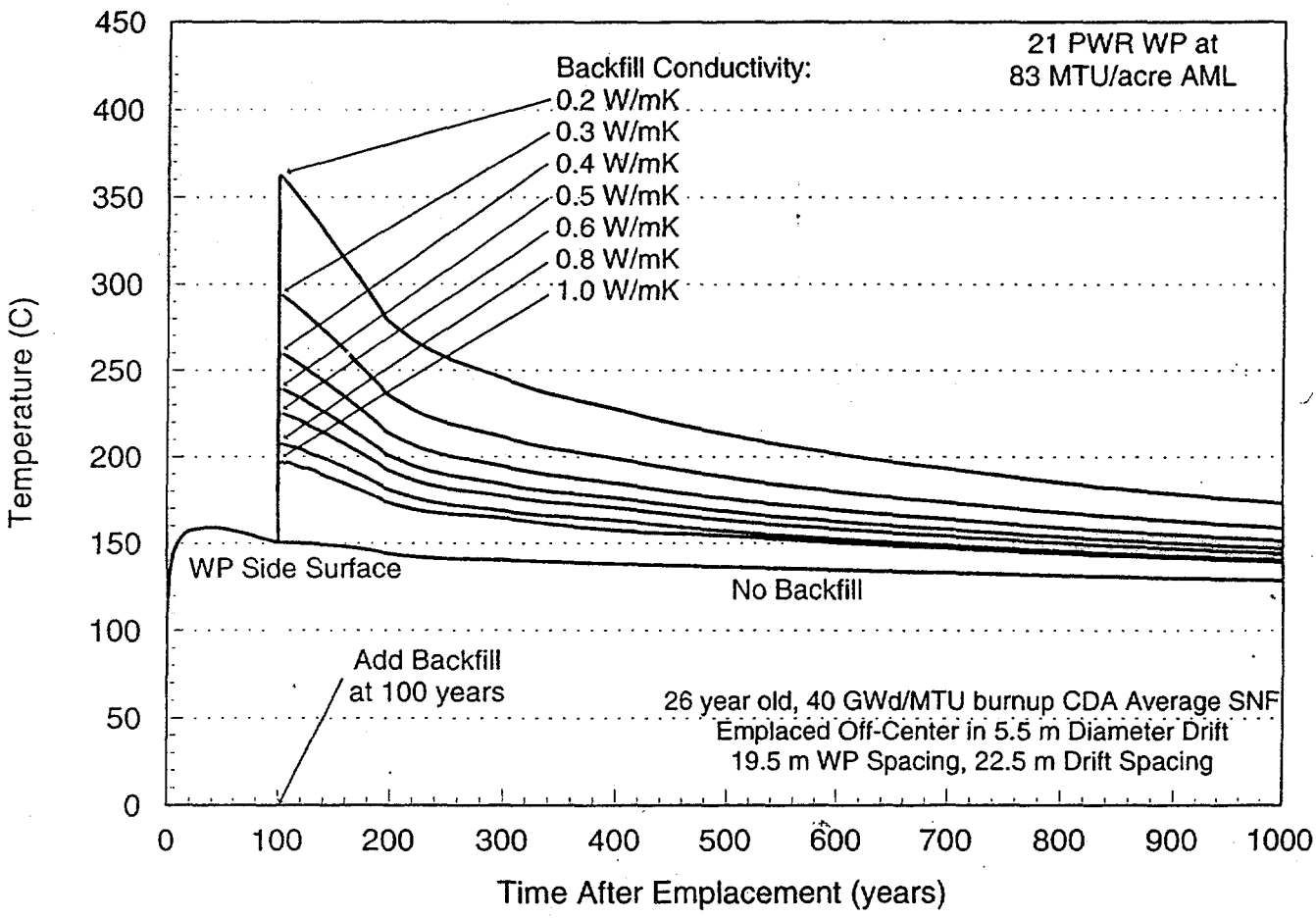

Figure 5.2-15 Effect of drift backfill on waste package surface temperature (83 MTU/acre)

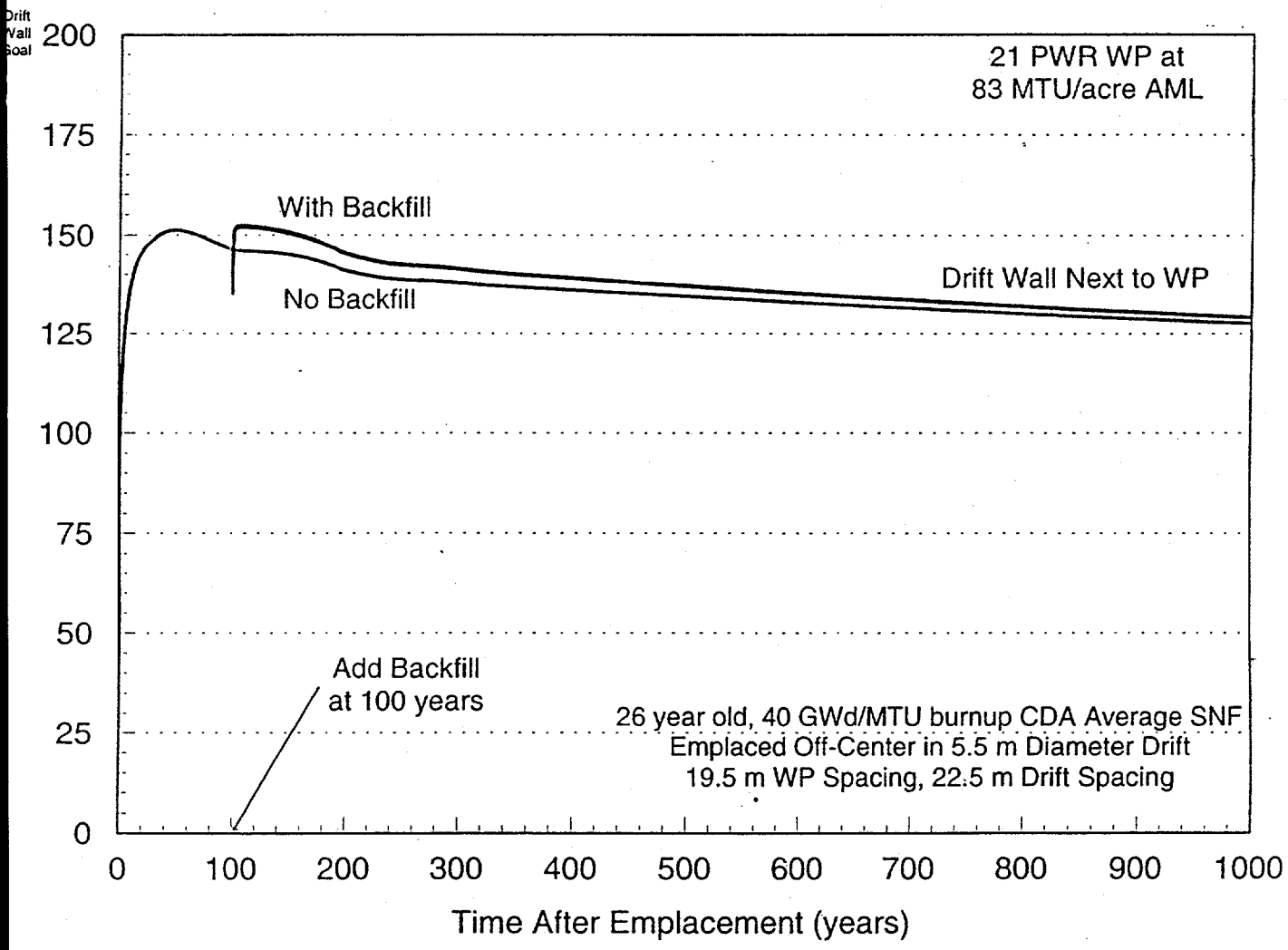

Figure 5.2-16 Effect of drift backfill on drift wall temperature (83 MTU/acre)

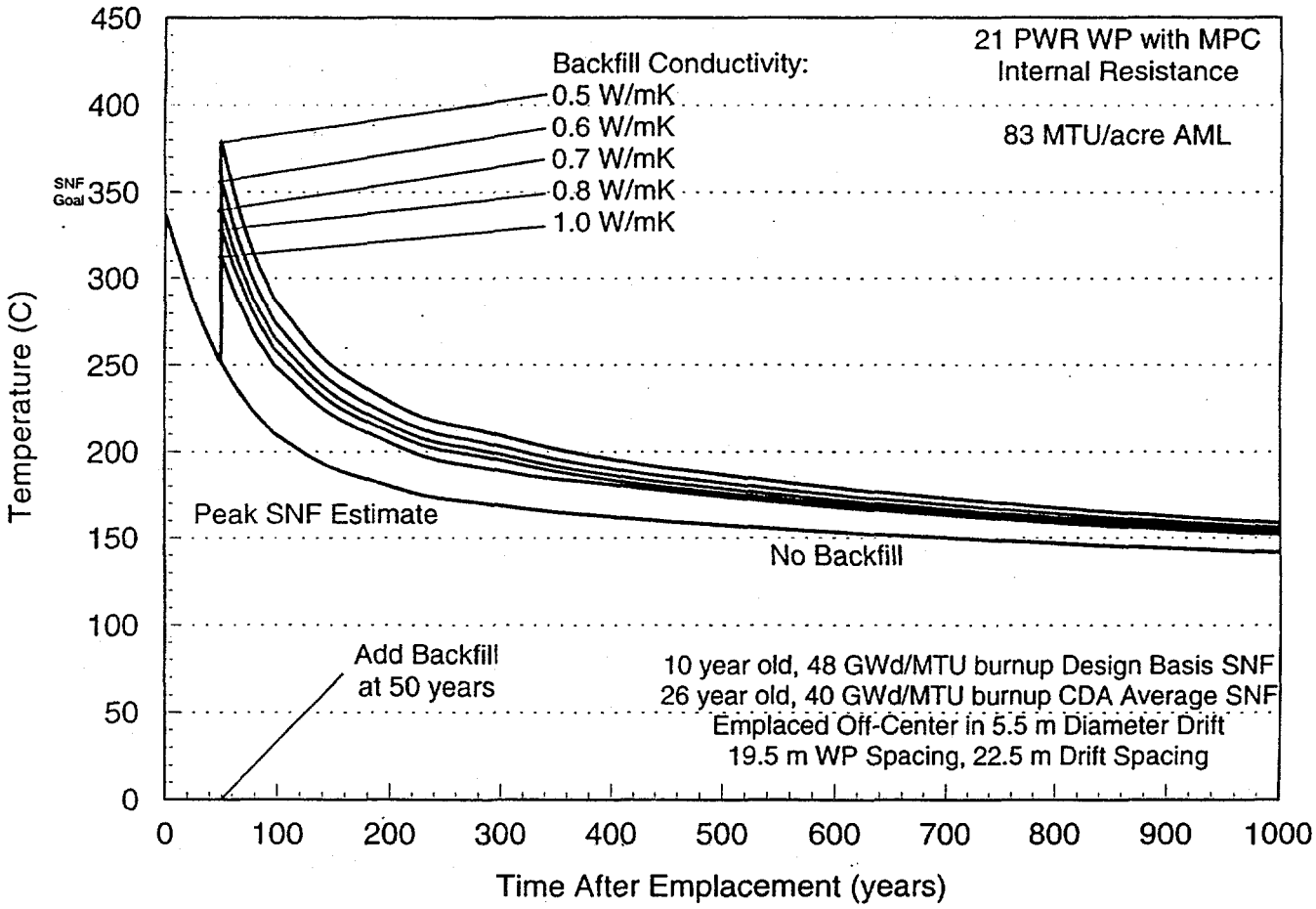

Figure 5.2-17 Effect of drift backfill on cladding temperature (83 MTU/acre, backfill at 50 years)

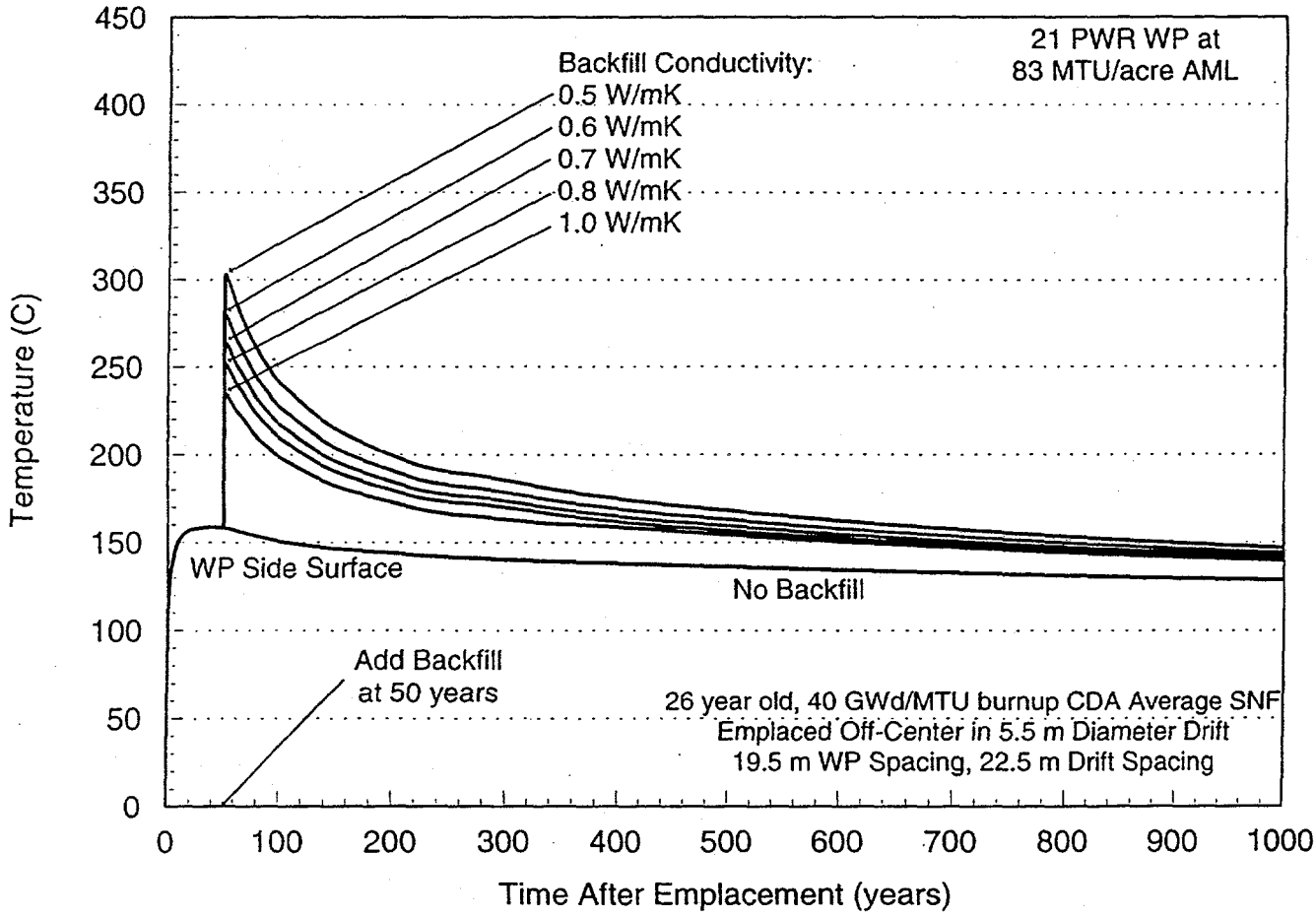

Figure 5.2-18 Effect of drift backfill on waste package surface temperature (83 MTU/acre, backfill at 50 years)

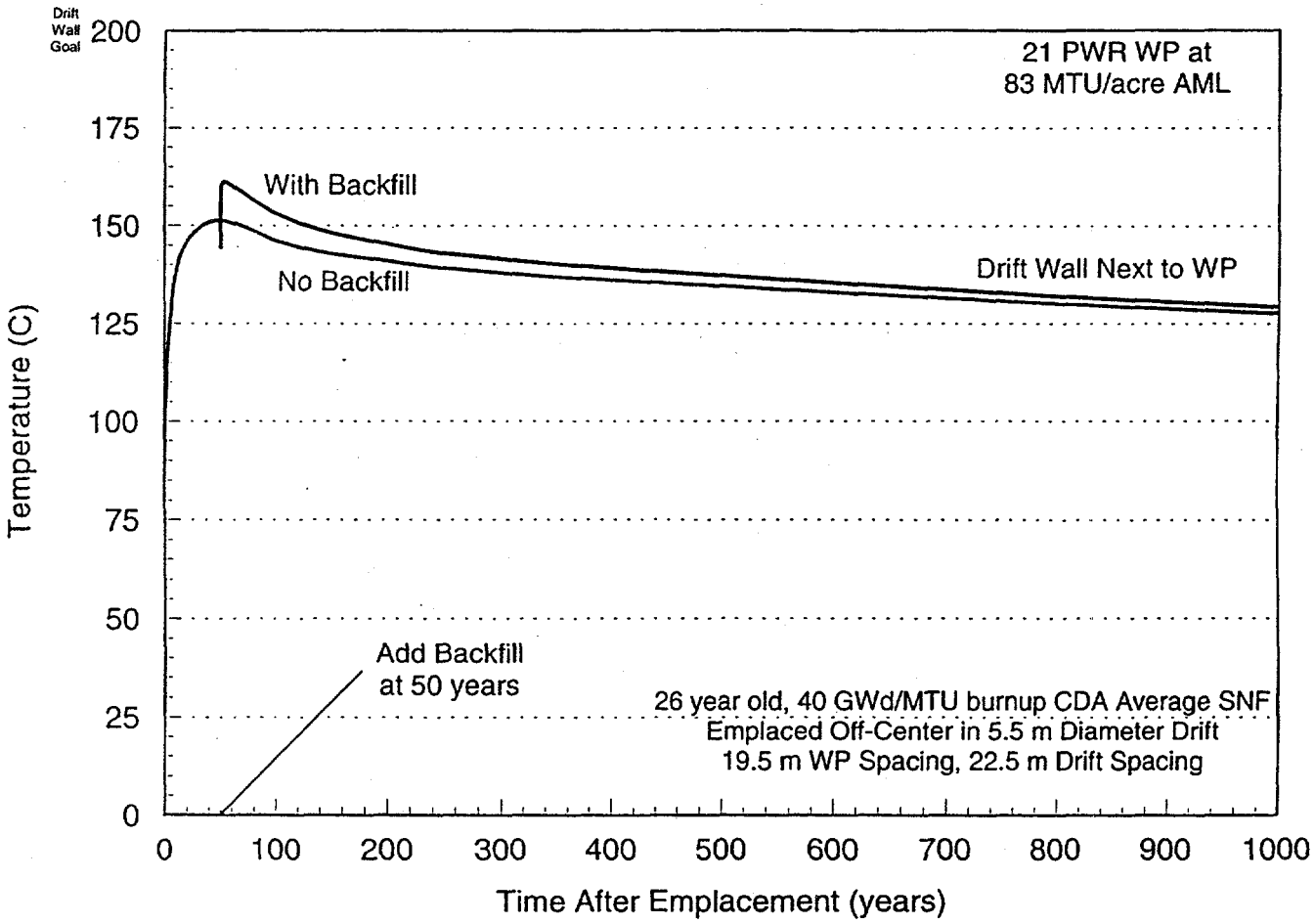

Figure 5.2-19 Effect of drift backfill on drift wall temperature (83 MTU/acre, backfill at 50 years)

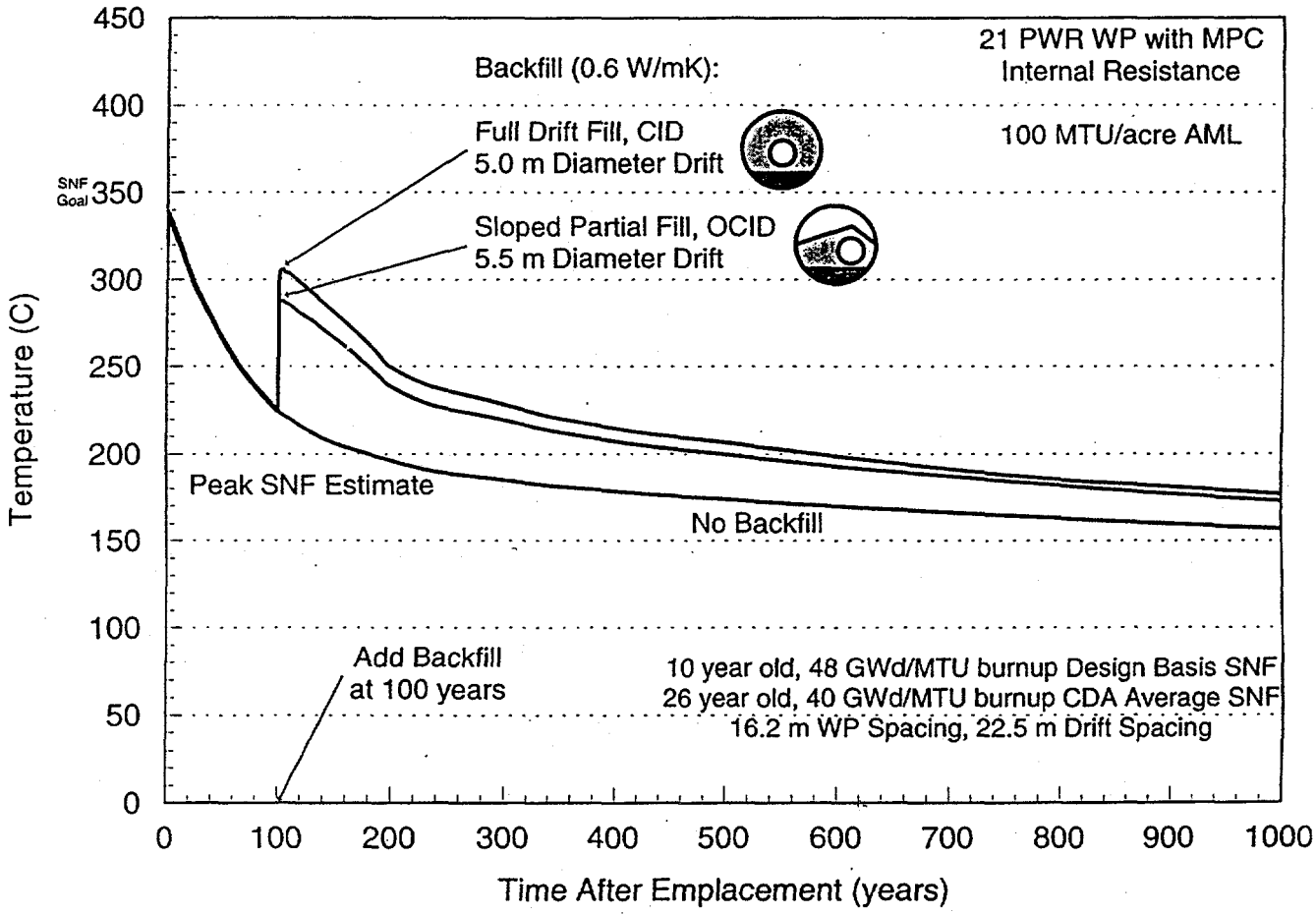

Figure 5.2-20 Effect of backfill geometry on cladding temperature (100 MTU/acre)

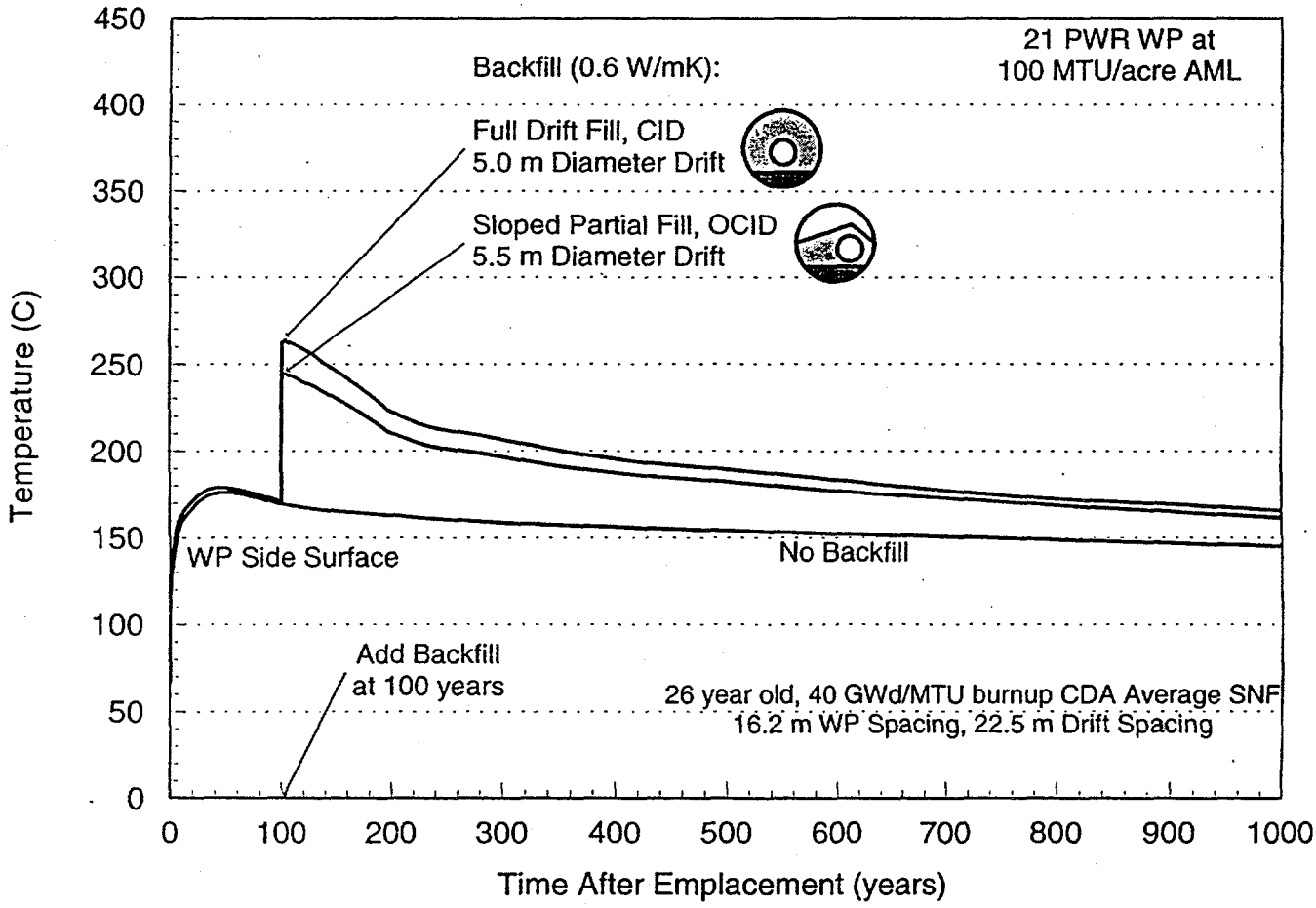

Figure 5.2-21 Effect of backfill geometry on waste package surface temperature (100 MTU/acre)

5.2.4.2 Lineload Concept

As reported in the "Thermal Loading Study for FY 1996," (CRWMS M&O 1996d) it is not yet clear whether close spacing of the waste packages would not result in significantly increased temperatures which may violate such thermal criteria as the 200°C wall temperature or the cladding criteria. Although total system performance and repository cost results within this report will show this to be a promising concept, the current concern regarding thermal criteria (CRWMS M&O 1996d) requires that the lineloading concept be considered work in progress, with additional work still necessary to establish whether this is indeed a viable concept.

5.2.5 3-D NEAR-FIELD THERMOHYDROLOGICAL ANALYSIS

5.2.5.1 Introduction

One of the important thermohydrologic considerations for engineered backfill concerns the magnitude and duration of the RH reduction on the WP, relative to RH conditions in the adjacent near-field rock. The reduction in RH is affected by three key factors:

Drift-ΔRH effect: This effect is based on the relationship: $RH_{wp}/RH_{dw} = P_{sat}(T_{dw})/P_{sat}(T_{wp})$, which holds if the partial pressure of water vapor P_v on the WP is in equilibrium with P_v in the rock at the drift wall (see Section 4.2.1.2). Therefore, this effect is governed by the magnitude and duration of the temperature difference DT_{drift} between the WP and cooler drift wall. The extent to which P_v on the WP is greater than P_v at the drift wall, RH reduction on the WP is negated.

Net moisture flux into the drift: This is the net result of mechanisms that cause water to enter the drift (drift seepage and wicking) and mechanisms that cause water to leave the drift (drainage and evaporation). If the net flux of moisture into the drift is high enough, P_v on the WP will be higher than P_v in the rock at the drift wall, thereby negating some (or possibly all) of the drift-DRH effect.

Axial vapor flow and condensation within the drift: This effect is driven by axial variations in temperature and P_v along the drift. Water vapor is transported (by gas-phase advection and diffusion) from areas of higher temperature and P_v to areas of lower temperature and P_v where it condenses, which causes RH to increase (even as high as 100 percent). Large condensation rates can arise in the cooler areas if the following three conditions are met:

- High RH in the rock at the drift wall
- WP heat output varies substantially from WP to WP
- WPs are thermally isolated from one another.

The following are the two primary mechanisms that cause water to enter the drift:

Drift seepage: Advective liquid-phase flow of water that enters the drift (and flows through the backfill) as a result of ambient percolation or decay-heat driven condensate flow. This can include episodic nonequilibrium fracture flow or a steady weep.

Wicking: Transport of moisture driven by matric potential gradients (i.e., capillary pressure gradients). This is primarily considered to be an advective liquid-phase transport process (called imbibition); however, binary gas-phase diffusion can also play a role. Because wicking can occur as two-phase flow, it does not necessarily require a continuous liquid phase.

The following are the two primary mechanisms that cause water to leave the drift:

Drainage: Advective liquid-phase flow of water that leaves the drift. Net drainage will be affected by:

A. The rate at which water enters the drift (e.g., episodically verses a steady weep).

B. The capillary properties of the intragranular and intergranular porosity of the backfill (in particular, how strongly capillary forces tend to retain moisture).

C. Whether fractures at the bottom of the drift readily drain or cause water to pond.

Evaporation: Heat flow through the backfill will be capable of maintaining an evaporation rate (or evaporative capacity). This evaporative capacity depends on the WP heat generation rate, which will decay with time. The water vapor generated by this evaporation will be transported out of the drift by gas-phase advection, driven by gas-phase pressure gradients, and by the gas-phase diffusion of water vapor and air, possibly including enhanced diffusion. While the backfill is above the boiling point, gas-phase advection will be an important means of transporting vapor out of the drift. After the backfill has dropped below the boiling point, gas-phase diffusion may be the primary means of transporting vapor out of the drift.

If the combined effects of the evaporative capacity and drainage exceed the combined effects of drift seepage and wicking, then the backfill will be maintained in a state in which P_v in the backfill (and on the WP surface) tends to be in equilibrium with P_v in the near-field rock adjacent to the drift. If drift seepage occurs episodically, the net moisture gain in the backfill will be minimized if the backfill and the fractures at the base of the drift (i.e., base of the invert) facilitate rapid drainage.

If the backfill has intragranular porosity, wicking can occur as a result of the matric suction potential gradients that occur within the porous grains. Minimal asperity contact area between grains does not prevent wicking, because it can occur as a two-phase flow process, involving vapor transport in the air between grains and liquid flow within grains. These grains do not need to be in solid-phase contact with one another for this process to occur because water can evaporate from the wetter grain, be transported by vapor diffusion through the air gap between the grains from the wetter to the drier grain, and then condense on the drier grain.

If the backfill has no intragranular porosity, then wicking is limited to film flow along the surfaces of the grains. If the intragranular porosity is effectively zero, and the intergranular porosity is sufficiently coarse, then water retention in the backfill will be limited to the asperity contacts. Unless RH in the backfill is high enough to cause continuous surface films of water to exist on the surfaces of the grains, then liquid-phase will be discontinuous, limited to the pendular water at the asperities. The discontinuous liquid phase that will be incapable of supporting a wicking flux from the relatively

wetter near-field rock, through the relatively drier backfill, and onto to the WPs. As seen in the experimental testing of backfill (Section 5.2.6), the relative permeability for this discontinuous saturation condition can be extremely low. It should also be pointed out that hysteresis effects in the capillary pressure and relative permeability characteristics of the backfill will make it easier for water to drain from the backfill than for water to wick back (i.e., rewet) from the wetter near-field rock, through the backfill, and onto the WP (CRWMS M&O 1996n, section 1.10). Because of hysteresis effects, it is important that data obtained under drainage conditions not be applied to rewetting behavior of the backfill. The combination of minimized water retention in the drift, rapid drainage of episodic fracture flow, and extremely low relative permeability of the backfill all tend to favor having P_v on the WP being in equilibrium with P_v in the adjacent near-field rock.

5.2.5.2 Modeling Discussion

Selection of Quartz Sand as the Backfill Material

The cases analyzed in Sections 5.2.5.3 and 5.2.5.4 utilize the same assumptions and computer codes as in Section 3.1.1.2, with the exception that the emplacement drifts are backfilled at 100 yr with a full sand overfill. The hydrological properties of the backfill are representative of a fine to medium sand. However, other backfill materials, such as crushed tuff or basalt gravel, may be found to exhibit similar hydrological properties. The important hydrological feature of sand or "sand-like" backfill that was assumed in these calculations is that it does not wick moisture in from the near-field rock unless the matric suction potential of the adjacent rock is nearly zero (nearly saturated conditions). This arises largely from the sand having zero intragranular porosity (i.e., the sand grains are essentially nonporous). It is assumed that when the backfill is emplaced, its moisture content (matrix suction potential and relative humidity (RH)) will be drier than ambient pre-emplacement conditions at the repository horizon. Moreover, as was shown in Section 3.2 for the lineload, conditions in the drift will be extremely dry when backfill is emplaced at 100 yr. Therefore, for some time after the emplacement of backfill, the backfill will be subjected to RH conditions that are much drier than ambient pre-emplacement conditions at the repository horizon. Moreover, after backfill is emplaced, temperature in the backfill will abruptly rise to well above the nominal boiling point. Altogether, these effects tend to cause the backfill RH to be much drier than ambient pre-emplacement conditions.

Assumptions

As was mentioned, the results presented in this section reflect backfilling of the emplacement drifts at 100 years with full sand backfill. That is, the drift is modeled as having the sand occupy all void space not occupied by the waste package. Modeling of a level partial backfill (see Figure 5.2-3), rather than a full backfill, in addition to modeling multiple WPs is currently beyond the capability of the three-dimensional, drift-scale, multiple-WP model based on the NUFT code (Buscheck et al., 1996). However, as is discussed in Section 5.2.2, if backfill is needed, a level partial backfill configuration is preferred because of its relative insensitivity to seismic events. Therefore, results obtained in this section for the full sand backfill were used to estimate the thermohydrologic behavior of a partial level backfill.

Estimates of the thermohydrologic effects of varying amounts of backfill over the WPs were determined by making use of a two-dimensional, drift-scale model based on the NUFT code in which

the heat output from multiple WPs is averaged into a uniform lineload. By not explicitly modeling the heat output of each individual WP in a portion of an emplacement drift, the two-dimensional model is capable of modeling varying amounts of backfill over a WP. Figures 5.2-22 and 5.2-23 indicate the sensitivity of the WP surface RH and temperature profiles to variations in the amount of backfill over the waste packages. These results reflect the modeling of a 40 darcy TSw2 gravel invert, a 10 darcy sand backfill, and a percolation flux of 0.3 mm/year. This information was used along with the data associated with the "no backfill" case to establish formulas for converting from "full backfill" results to "level partial backfill" approximations :

$$T_p=(T_f-T_n)*0.85+T_n \qquad (5.2\text{-}1)$$

$$RH_p=(RH_f-RH_n)*0.82+RH_n$$

where T_p = temperature profile for "level partial backfill" case
T_f = temperature profile for "full backfill" case
T_n = temperature profile for "no backfill" case
RH_p = relative humidity profile for "level partial backfill" case
RH_f = relative humidity profile for "full backfill" case
RH_n = relative humidity profile for "no backfill" case

The total system performance calculations performed for backfilled emplacement drifts (Section 5.2.8) employ the results presented in this section and modified according to the above calculations.

As was discussed in Section 5.2.1, the eventual use of emplacement drift backfill would require that the WPs be emplaced in an OCID mode so that the backfill stowing equipment would be able to reach all WPs in an emplacement drift. However, due to the additional complexity of this non-symmetric case, this OCID mode was not able to be simulated in the three-dimensional, drift-scale, multiple-WP model. Rather, the symmetric CID emplacement mode was used in the model as an approximation to the OCID mode. Again, the two-dimensional, drift-scale, lineload model was employed to estimate the thermohydrologic error incurred in simulating the CID emplacement mode rather than the OCID emplacement mode. Figure 5.2-24 shows the differences obtained, in terms of WP surface temperature and relative humidity profiles, when one compares an OCID to a CID emplacement mode (these results reflect the use of a 5.5 meter drift diameter, a sand invert, full sand backfill at 100 years with thermal conductivity (K_{th}) = 0.6 W/mK, a WP emissivity = 0.3, and a percolation flux of 0.3 mm/year). These differences from the two-dimensional model are considered insignificant. It is expected that similar results would be obtained with the three-dimensional model if it was capable of simulating such, and so the CID three-dimensional model results given in this section should be considered representative of OCID results.

Both ACD "square" WP spacing as well as closely spaced (lineload) results are presented in this section. For most of the lineload cases, it is assumed that measures are taken to prevent backfill from filling in between the gaps separating the WPs. This is done to maintain small variations in peak WP surface temperatures for the various WPs within an emplacement drift. Such measures might involve

the use of a "skirt" or an overhang at one end of the WPs. The effect of filling these gaps with backfill is discussed in Section 5.2.5.4.

The thermal conductivity of the backfill is assumed to be 0.6 W/mK. This is consistent with the minimum allowable backfill thermal conductivity calculated in Section 5.2.4, and it is also consistent with estimates made for materials such as course quartz sand and TSw2 crushed tuff (Section 5.2.3).

5.2.5.3 Thermohydrologic Results

Figures 5.2-25 through 5.2-27 indicate the results obtained when backfill is emplaced at 100 years, for both the ACD "square" WP spacing ((a) and (c)) and the lineload case ((b) and (d)) (these results were obtained using a 5.5 meter drift diameter, a sand invert, full sand backfill at 100 years with K_{th} = 0.6 W/mK, WP emissivity = 0.8, and percolation flux = 0.3 mm/year). The large axial WP spacing in the ACD case (LML = 0.46 MTU/meter) thermally isolates the WPs from one another, and this isolation is magnified once the backfill is emplaced. The left-side of Figure 5.2-28 graphically depicts the thermal isolation of WPs 400 years after backfill has been emplaced. On the other hand, the small axial spacing in the lineload case (LML = 1.11 MTU/meter) takes advantage of the high thermal conductivity of the WPs and allows for efficient thermal-radiative WP-to-WP heat transfer. This allows heat flow to be efficiently distributed along the line of WPs, as depicted on the right-side of Figure 5.2-28. A very large axial heat flux occurs from WP-to-WP; in effect, relatively cool WPs function like "cooling fins" or heat flow conduits, receiving the heat generated by hotter neighboring WPs, and distributing that heat to adjacent drift wall surfaces and (in some cases) to the next WP along the drift.

The result of backfilling the widely spaced WPs in the ACD concept is to produce a wide range of WP surface relative humidity and temperature profiles for the various WPs considered, as shown in Figure 5.2-25. The cooler WPs have the lower temperature profiles, and the higher relative humidity profiles. In the lineload case, the improved thermal communication between WPs because of their relatively close spacing allows for a much more consistent set of relative humidity and temperature profiles among the assorted WPs. Note too that although the cooler WPs see an increase in their temperature profile (and a resulting decrease in their relative humidity profile) in the lineload case, the hotter WPs see a resulting decrease in their overall temperature profile (and a resulting increase in their relative humidity profile). The range in WP surface temperatures just after backfill is emplaced is 236°C for the ACD case, and only 16°C for the lineload case (Lineload A in Table 5.2-4). The range of WP surface relative humidities is 56 percent for the ACD case at 120 years, and decreases slightly thereafter. At 120 years, the Lineload A case shows a range of WP surface relative humidities of 1 percent, and this increases to only 4 percent by 10,000 years. As indicated in Table 5.2-4, for the lineload cases the WP-to-WP variability in relative humidity grows slowly with time because the declining WP temperatures result in somewhat less efficient thermal-radiative WP-to-WP heat transfer, which modestly reduces the effectiveness of thermal homogenization along the line of WPs.

It is worth repeating that the temperature and relative humidity profiles indicated in Figure 5.2-25, and all subsequent figures in this section, reflect the full backfill case. Modifications to these profiles, per equation 5.2-1, will be conducted prior to their use in establishing total system performance (Section 5.2.8).

Table 5.2-4 Waste Package Surface Temperature (T) and Relative Humidity (RH) Comparisons for Backfill at 100 Years

Repository Design	ACD	Lineload A	Lineload B	Lineload C
Lineal Mass Loading	0.46 MTU/m	1.11 MTU/m	1.11 MTU/m	0.94 MTU/m
Drift Spacing	22.5 m	53.8 m	53.8 m	46.1 m
Gap between WPs	varies	0.1 m	0.1 m	1.0 m
Gap Between WPs	backfilled at 100 years	remains empty	backfilled at 100 years	remains empty
T_{peak} (t<100 years)	107-192°C	172-203°C	172-203°C	149-197°C
RH (t<100 years)	25-86%	16-21%	16-21%	20-32%
T_{peak} (t>100 years)	117-353°C	250-266°C	231-314°C	194-221°C
RH (t=120 years)	1-57%	2-3%	1-4%	5-8%
RH (t=2000 years)	43-98%	49-51%	44-57%	59-66%
RH (t=10,000 years)	60-99.7%	73-77%	68-81%	78-86%

5.2.5.4 Sensitivity Analyses

Variations on the previously described lineload case are presented here. Although the effects of these variations on total system performance will not be addressed in Section 5.2.8, it is nevertheless considered important to understand, at least from a thermohydrologic sense, the effects of filling in the gaps between the WPs with backfill, and spacing the WPs with more than a 0.1 meter gap.

So far, it has been shown that axial homogenization of temperature and RH along the drift works if the WPs are axially spaced very close together (0.1-m gaps), and if backfill is not allowed to fill the gaps between the WPs. Does effective axial homogenization depend on the 0.1-m gaps being free of backfill? How much WP-to-WP thermal isolation occurs if the 0.1-m gap is filled with backfill? Figures 5.2-29 through 5.2-31 summarize the temperature and RH on the upper drift wall and upper WP surface for a 1.11-MTU/m lineload in which the 0.1 meter gaps between the WPs are filled with 0.6 W/m°C backfill at 100 yr. These results reflect the use of a 5.5 meter drift diameter, sand invert, full sand backfill at 100 years with K_{th} = 0.6 W/mK, WP emissivity = 0.8, and percolation flux = 0.3 mm/year.

At the time that backfill is emplaced at 100 yr, the range in peak WP temperature is only 16°C if the 0.1-m gaps between the WPs are free of backfill (Table 5.2-4), whereas backfilling these gaps causes the post-emplacement peak WP temperature range to increase to 83°C (Table 5.2-4). Note that this is still much less than the 236°C peak WP temperature range for the ACD concept.

So far, it has been shown that axial homogenization of temperature and RH along the drift can be readily achieved if the WPs are placed very close together (0.1-m gaps). Does axial homogenization require that the WPs be that close together? What if the WPs are placed with a 1.0-m gap between them – what happens to thermal homogenization? Figures 5.2-32 through 5.2-34 summarize the temperature and RH on the upper drift wall and upper WP surface for a 0.94-MTU/m lineload case in which the 1.0-m gaps between the WPs are not filled with backfill at 100 years. These results reflect the use of a 5.5 meter drift diameter, sand invert, full sand backfill at 100 years with K_{th} = 0.6 W/mK, WP emissivity = 0.8, and percolation flux = 0.3 mm/year.

At the time that backfill is emplaced at 100 yr, the range in peak WP temperature is only increased slightly (from 16 to 27°C) if the 1.0-m gaps between the WPs are used instead of 0.1 m (Table 5.2-4). Because of the lower LML (0.94 MTU/m), all post-emplacement peak WP temperatures are decreased.

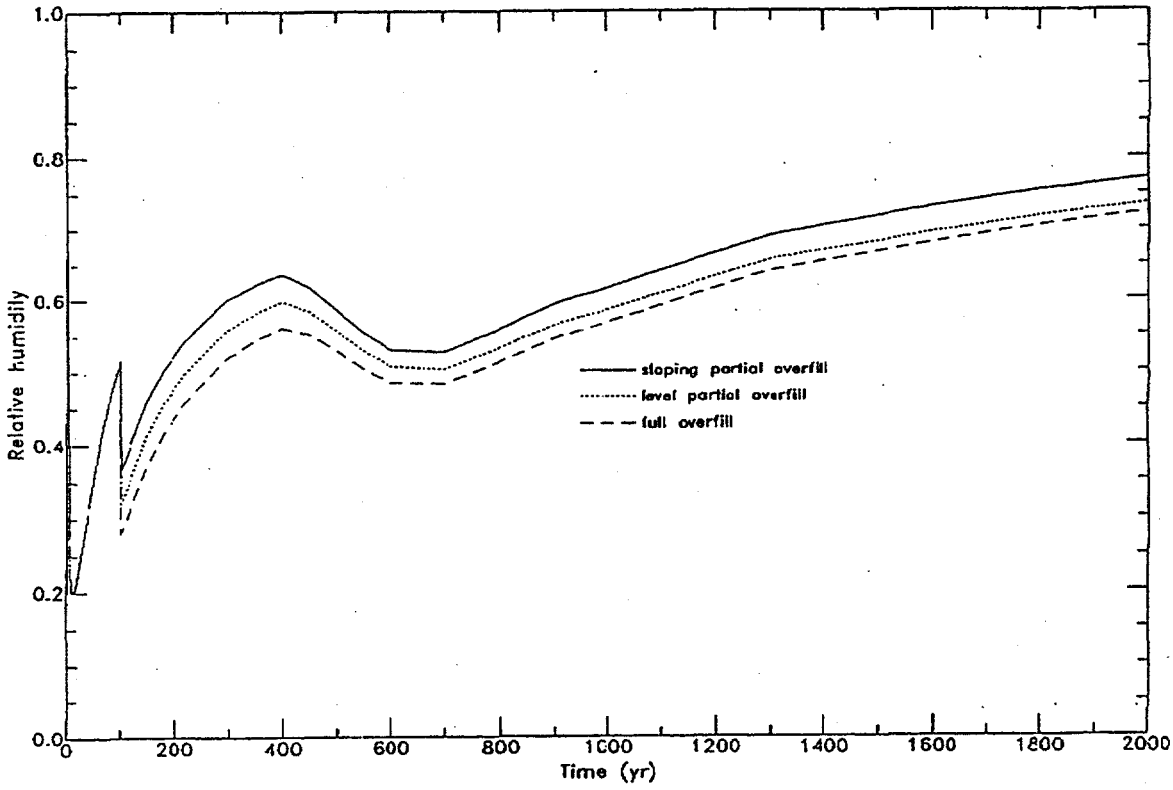

Figure 5.2-22 Comparison of relative humidity profiles on upper waste package surface for various backfill geometries

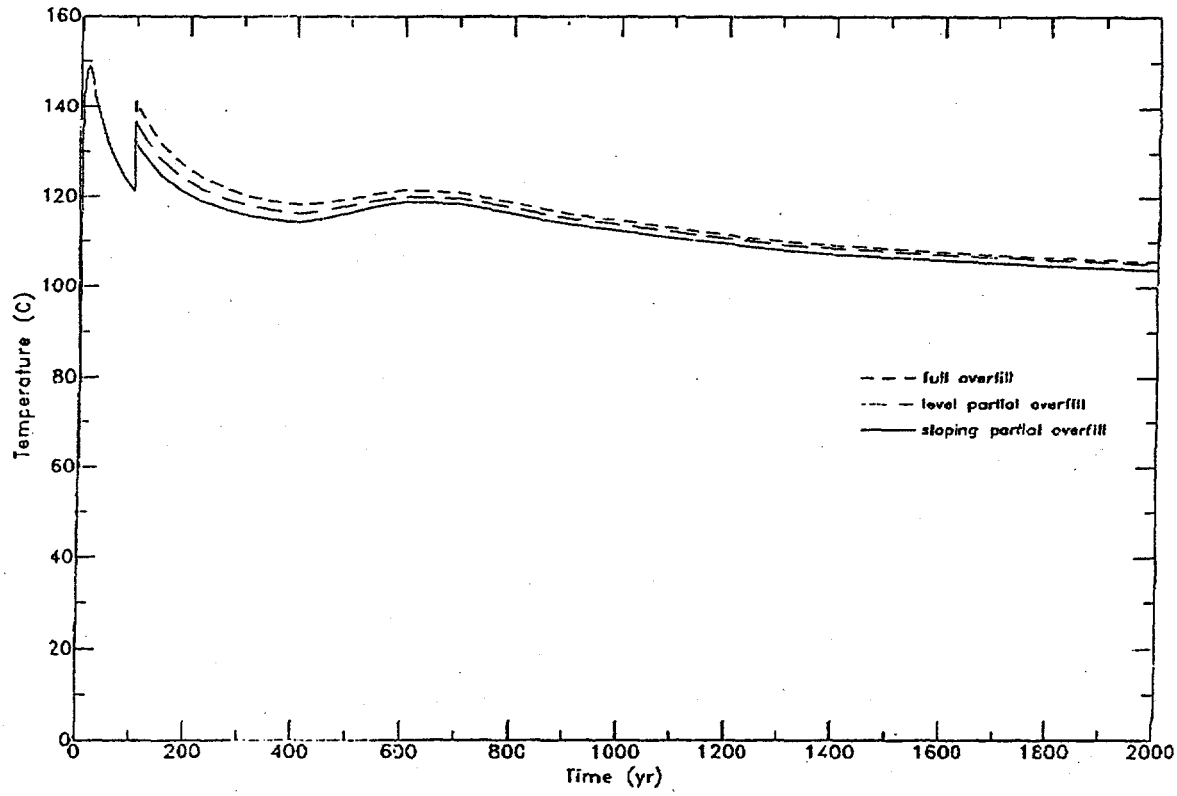

Figure 5.2-23 Comparison of temperature profiles on upper waste package surface for various backfill geometries

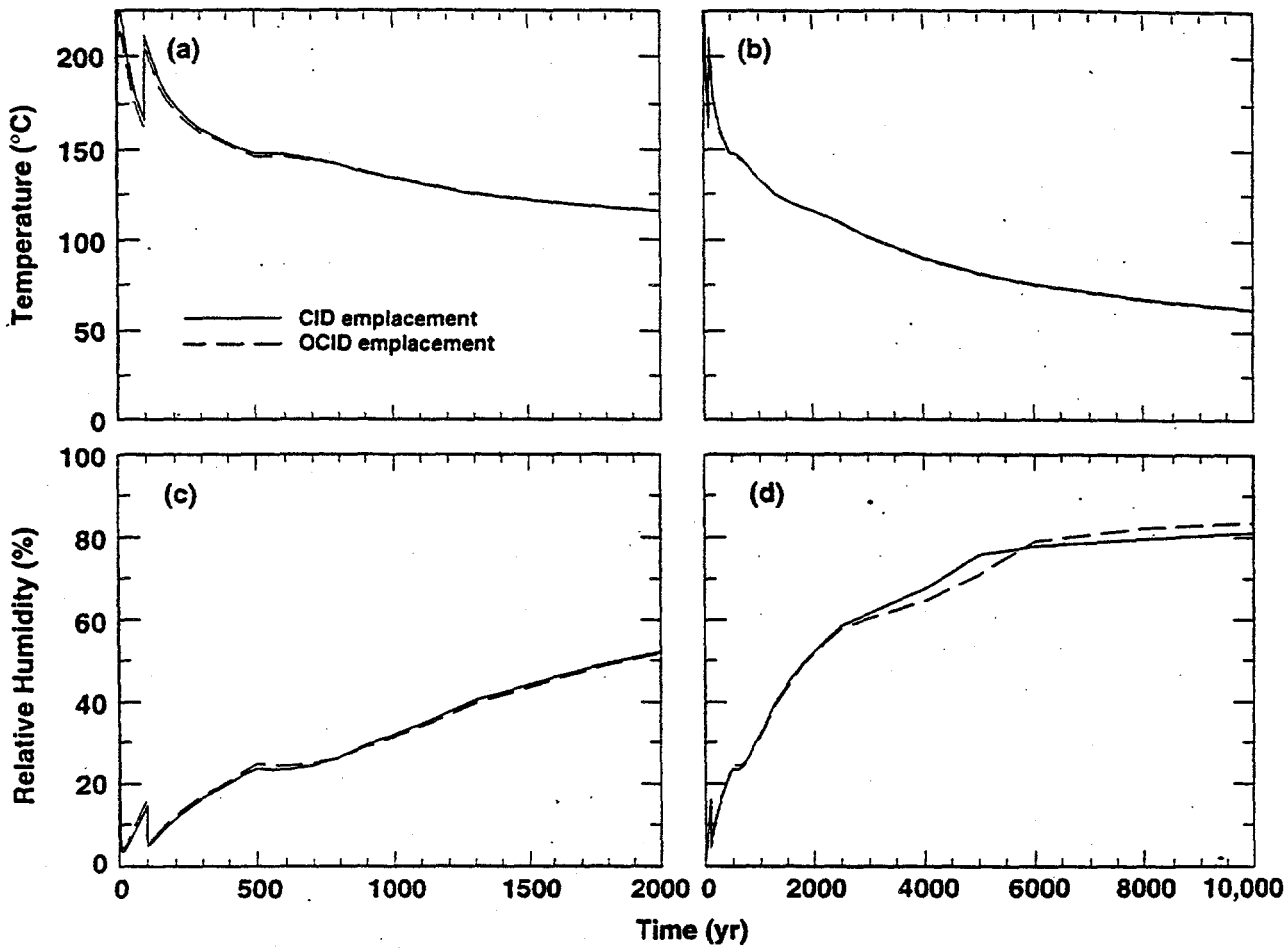

Figure 5.2-24 Temperature and relative humidity profiles on upper waste package surface for lineload case of 0.94 MTU/meter, full sand backfill, and for two different emplacement modes

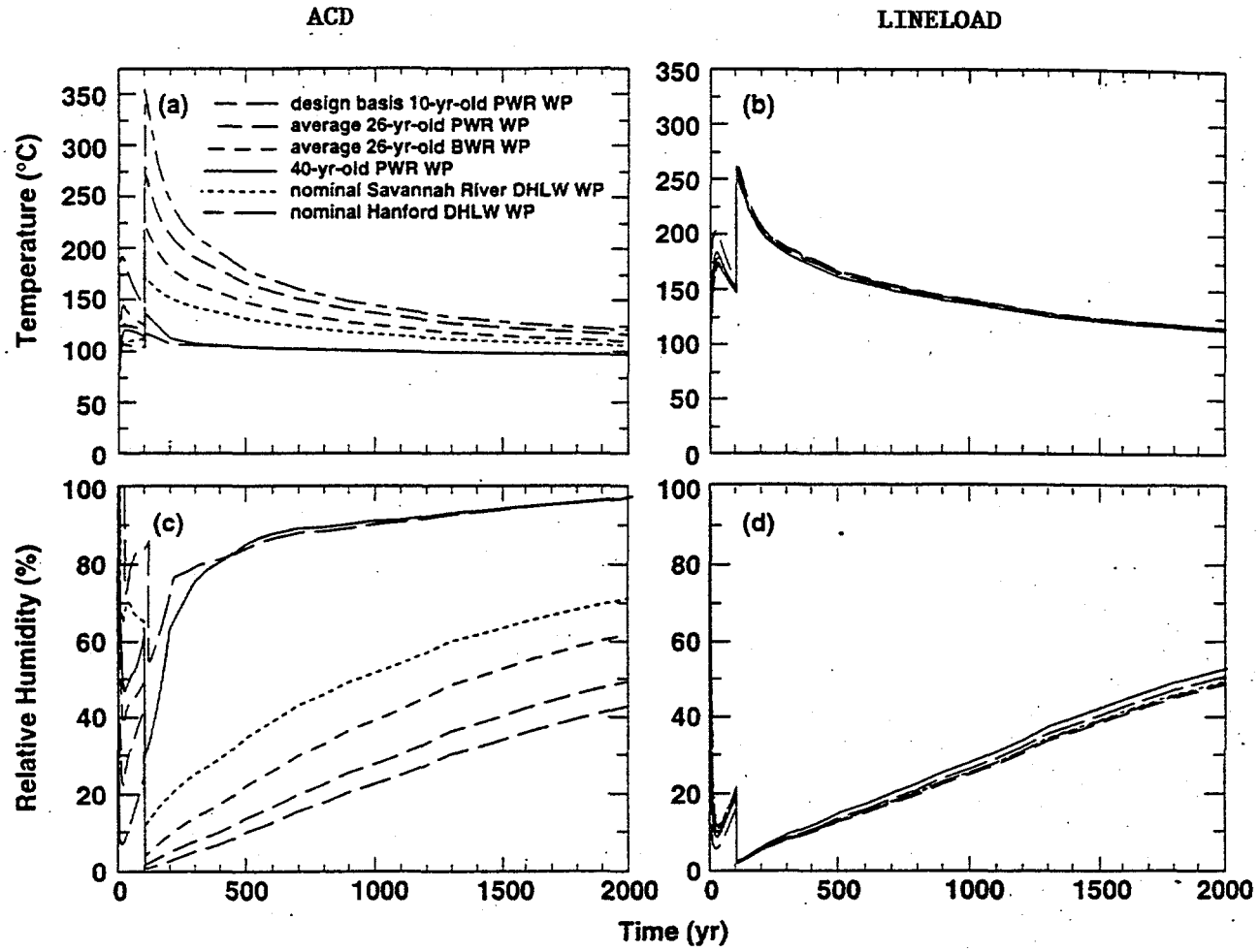

Figure 5.2-25 Temperature and relative humidity profiles on upper surface of several waste packages for full sand backfill, and two different spacing concepts (ACD and lineload) over a 2,000 year period

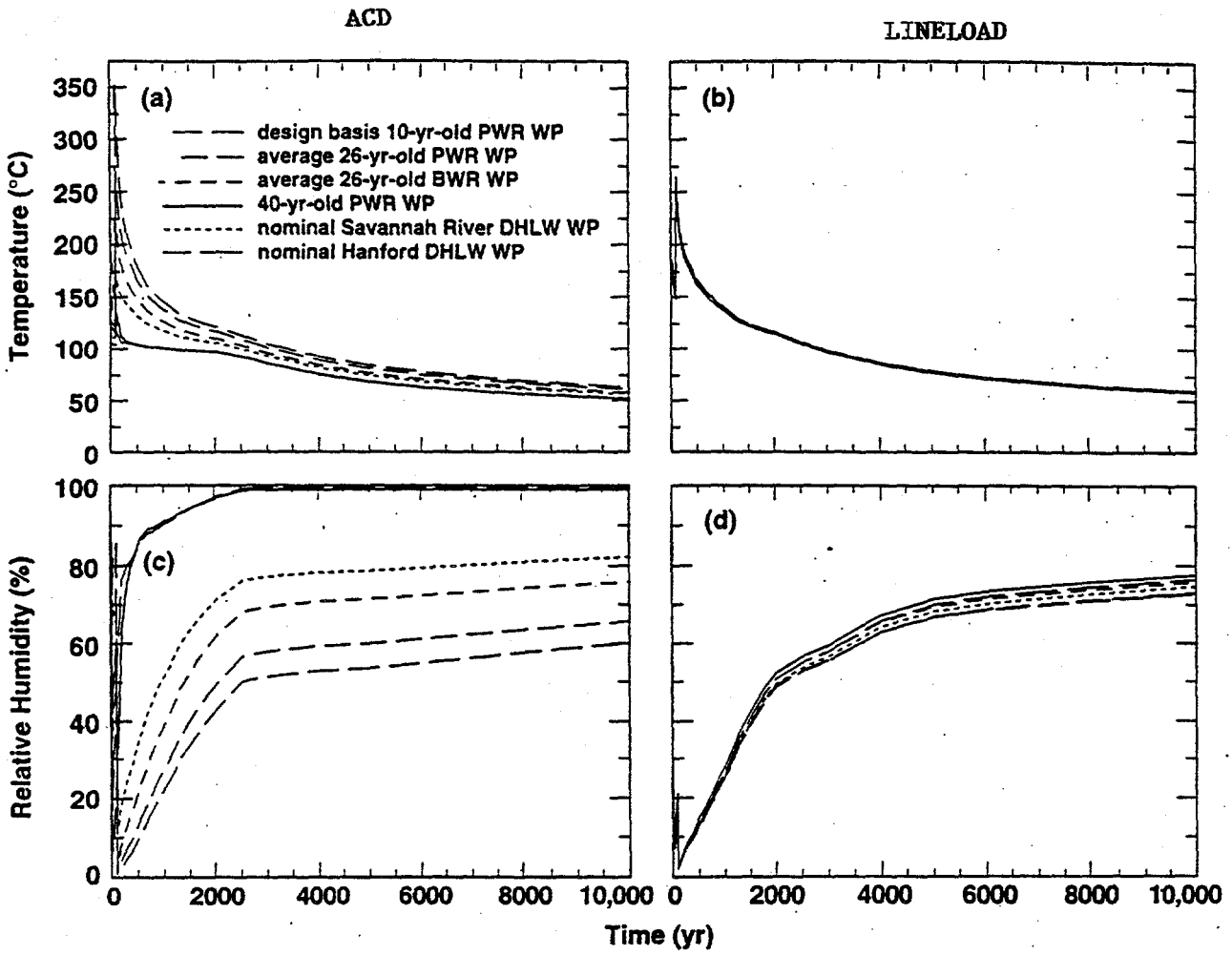

Figure 5.2-26 Temperature and relative humidity profiles on upper surface of several waste packages for full sand backfill, and two different spacing concepts (ACD and lineload) over a 10,000 year time period

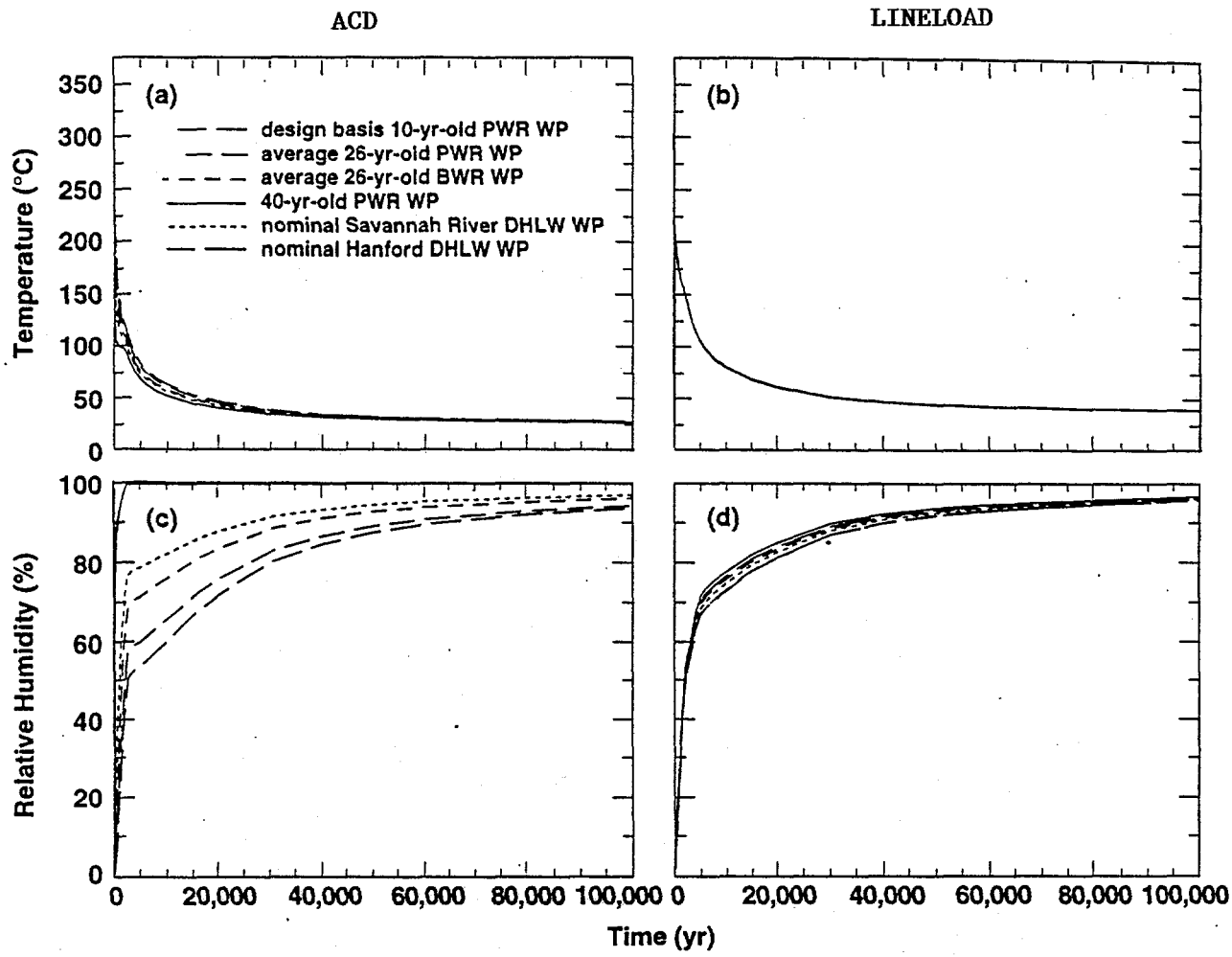

Figure 5.2-27 Temperature and relative humidity profiles on upper surface of several waste packages for full sand backfill, and two different spacing concepts (ACD and lineload) over a 100,000 year time period

Advanced Conceptual Design
LML = 0.46 MTU/m

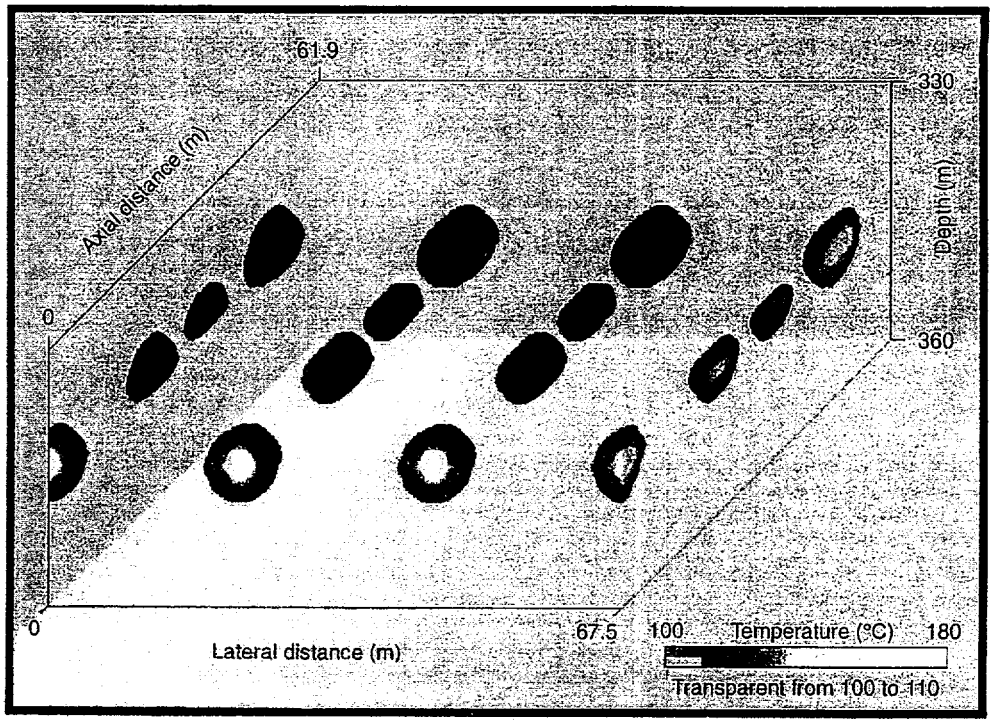

Localized Dryout Design
LML = 1.11 MTU/m

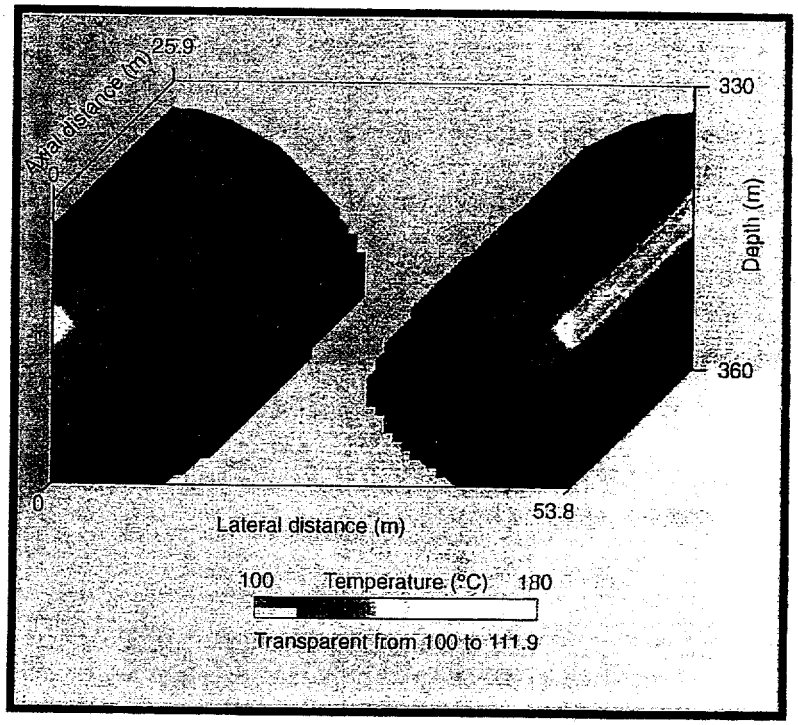

Figure 5.2-28 Thermal comparisons of backfilling waste packages in an ACD or lineload spacing scenario

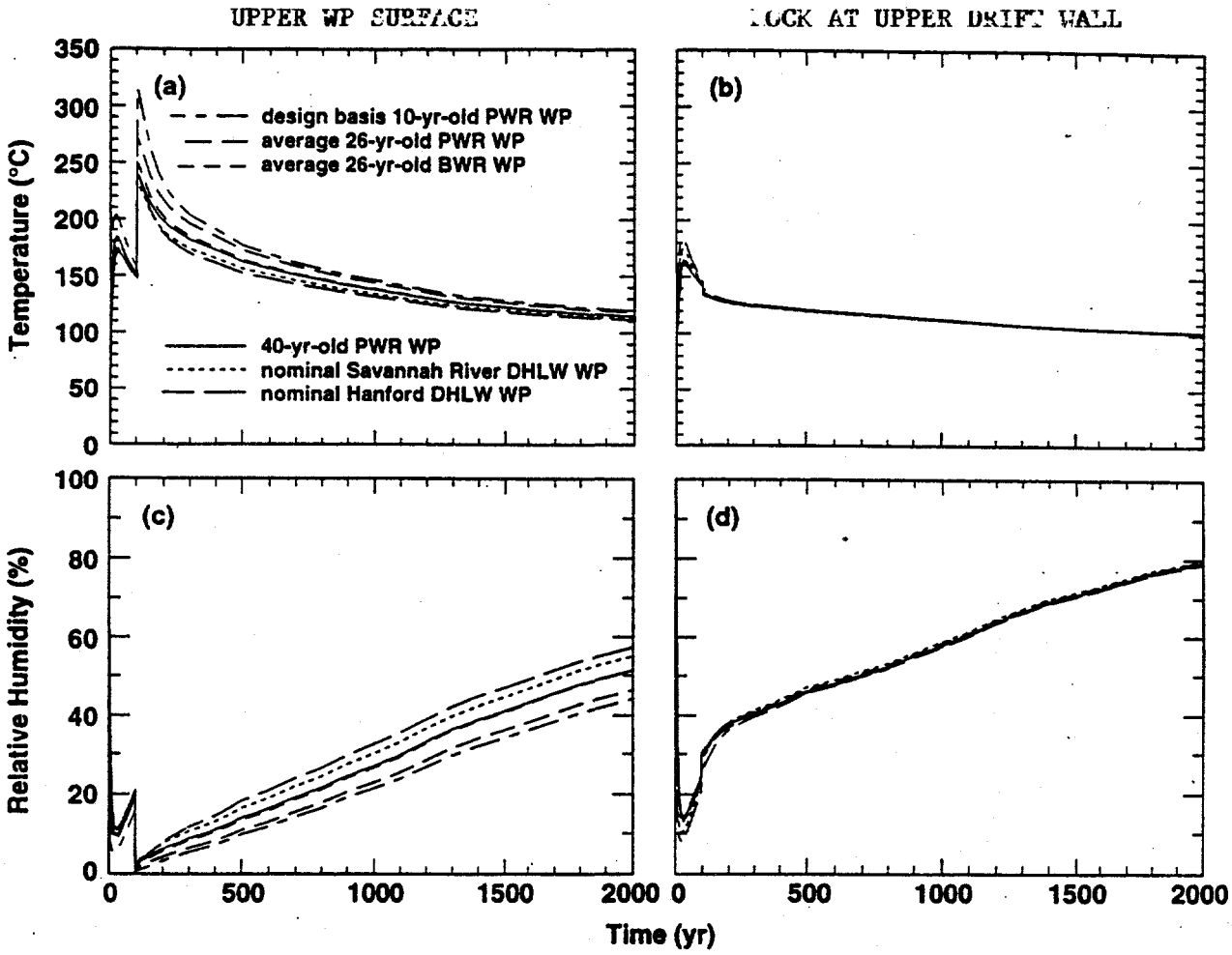

Figure 5.2-29 Temperature and relative humidity profiles for full sand backfill, lineload concept, and where sand is allowed to fill gap separating waste packages (over 2000 years)

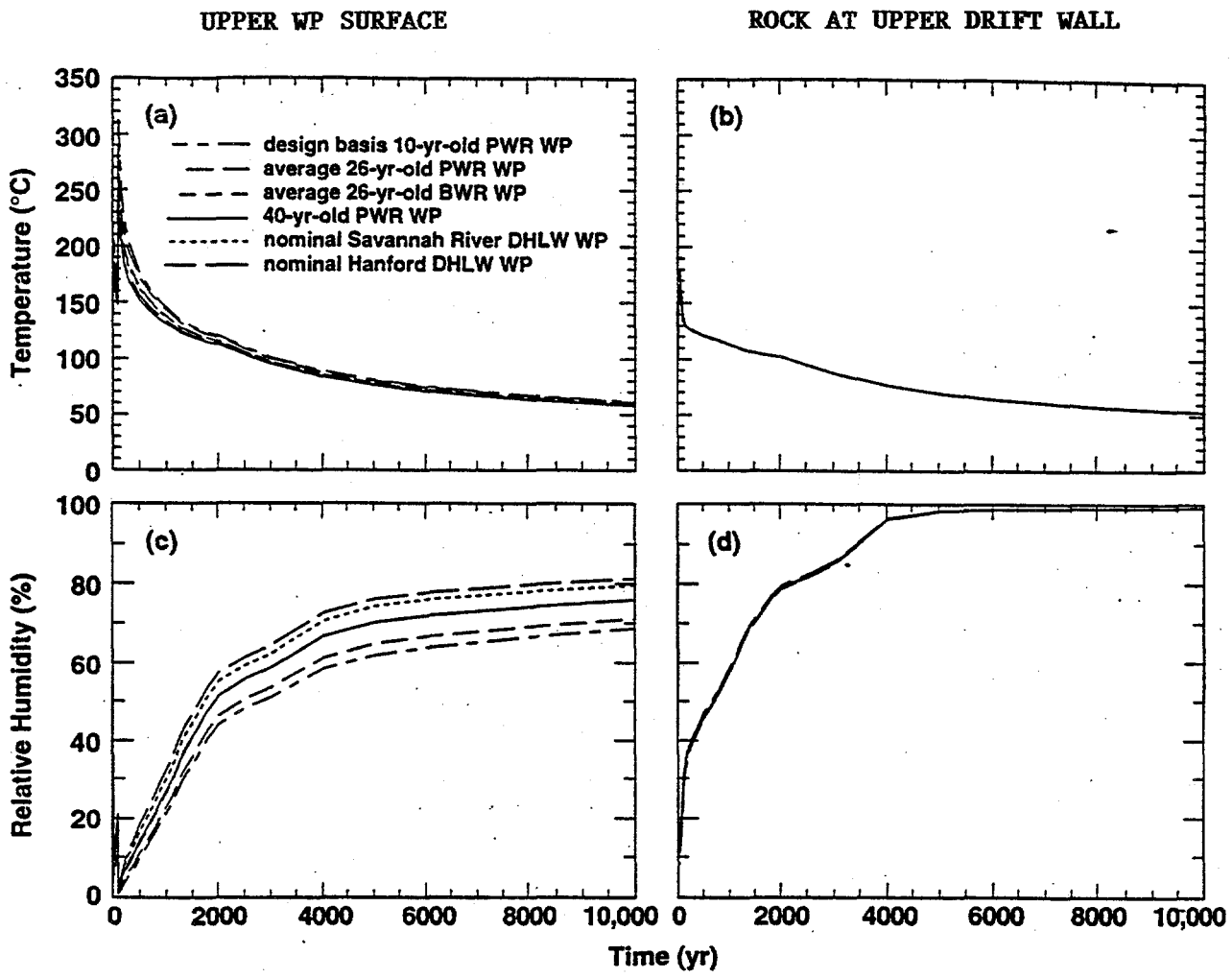

Figure 5.2-30 Temperature and relative humidity profiles for full sand backfill, lineload concept, and where sand is allowed to fill gap separating waste packages (over 10,000 years)

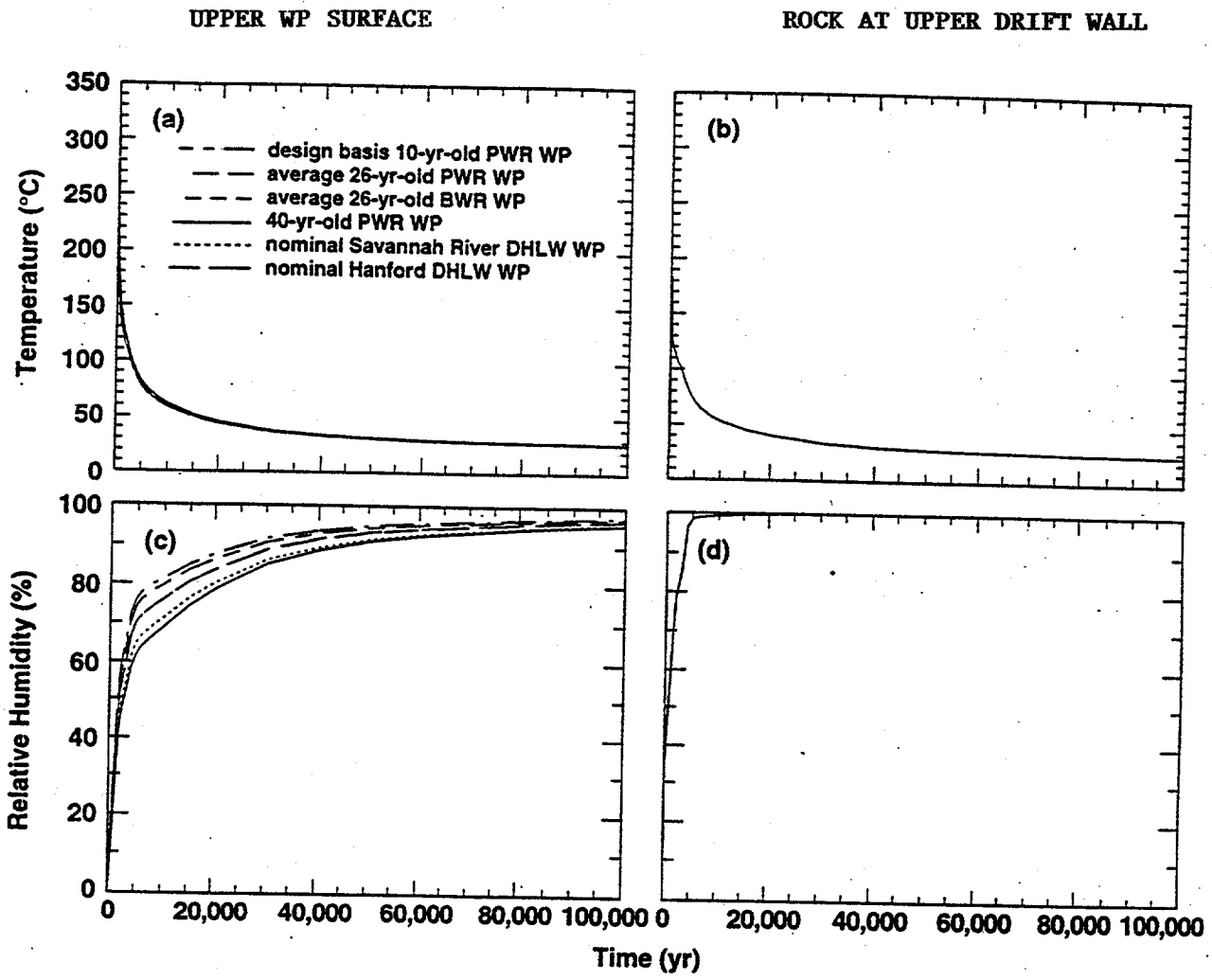

Figure 5.2-31 Temperature and relative humidity profiles for full sand backfill, lineload concept, and where sand is allowed to fill gap separating waste packages (over 100,000 years)

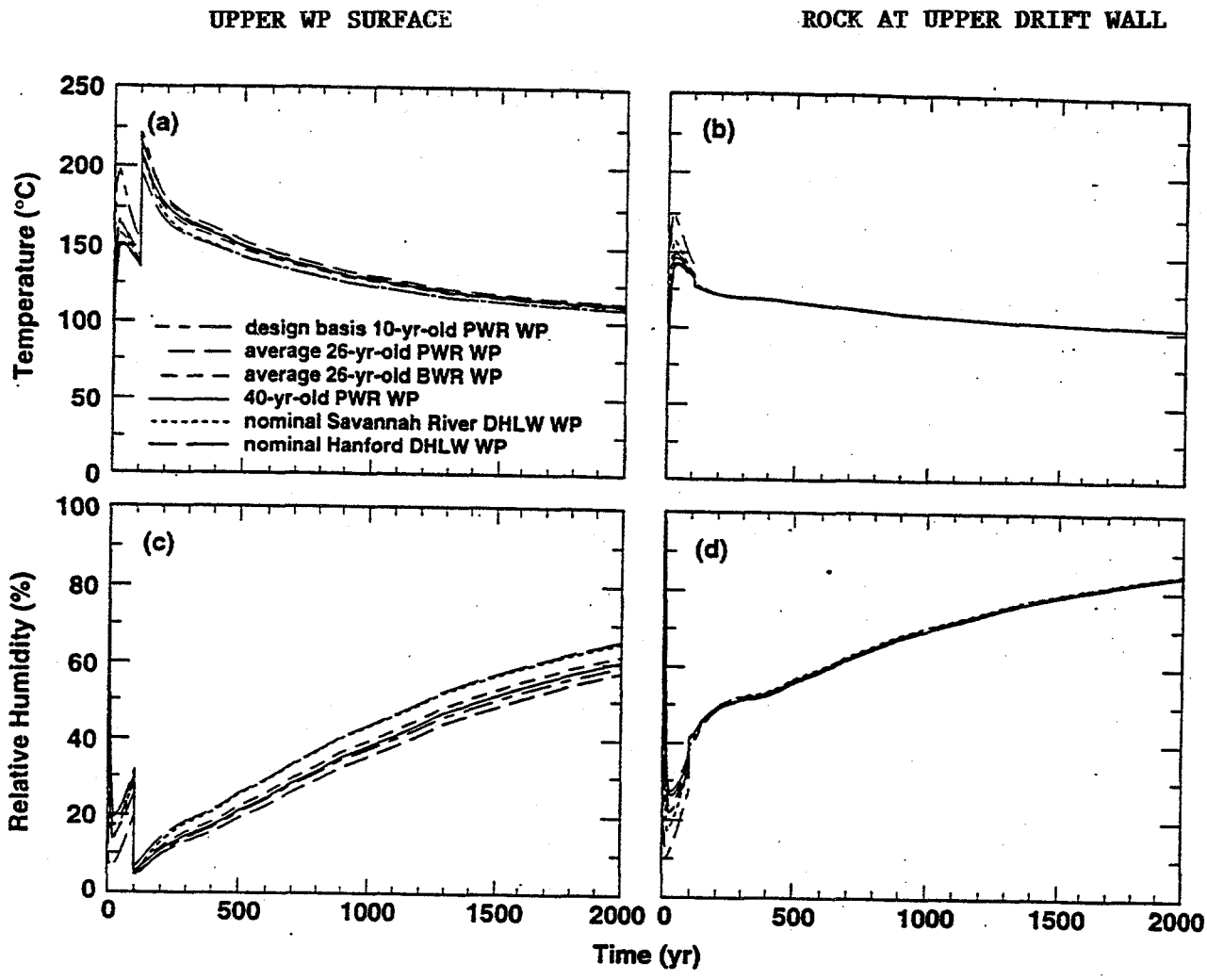

Figure 5.2-32 Temperature and relative humidity profiles for full sand backfill and lineload concept where waste packages are spaced one meter apart (over 2000 years)

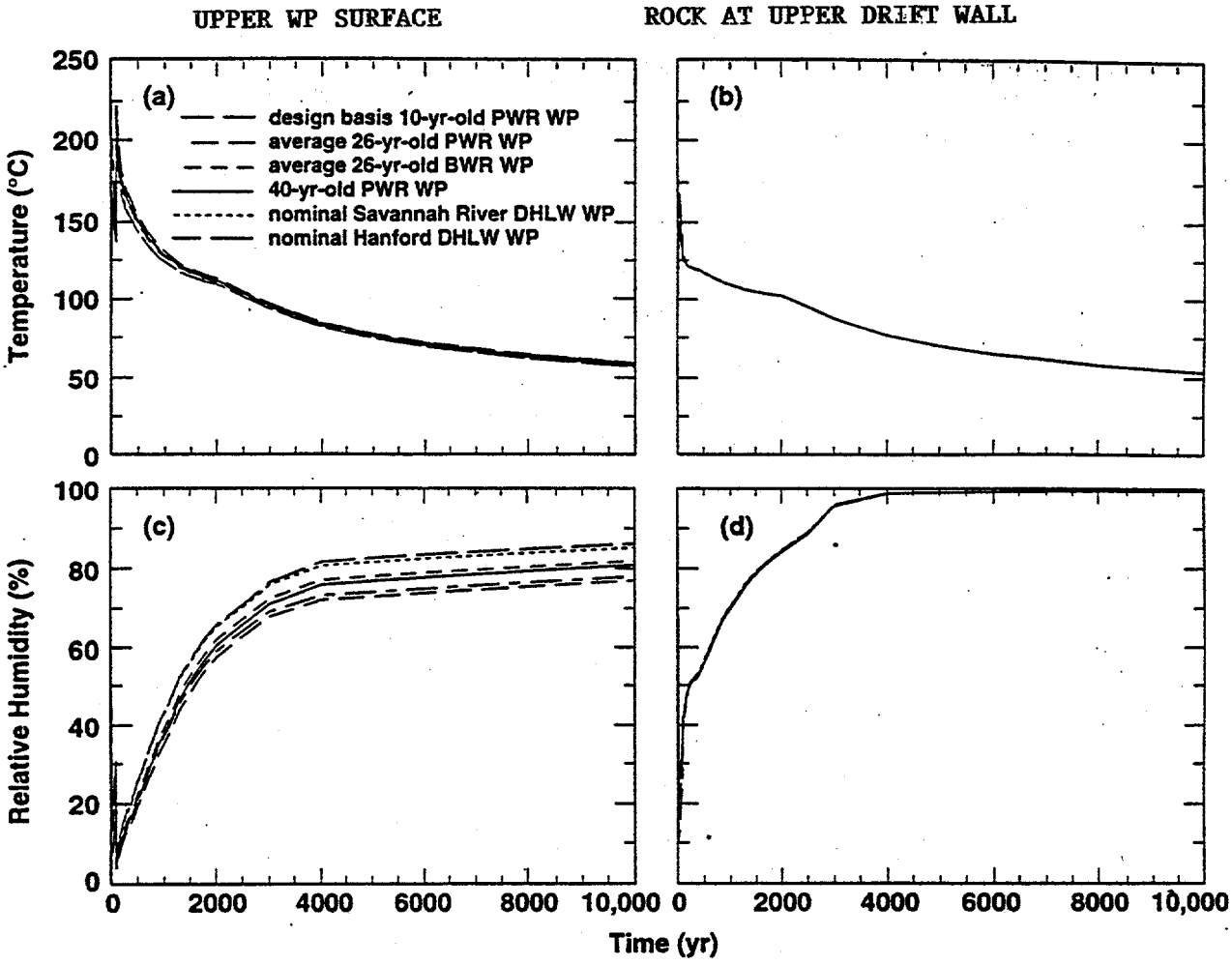

Figure 5.2-33 Temperature and relative humidity profiles for full sand backfill and lineload concept where waste packages are spaced one meter apart (over 10,000 years)

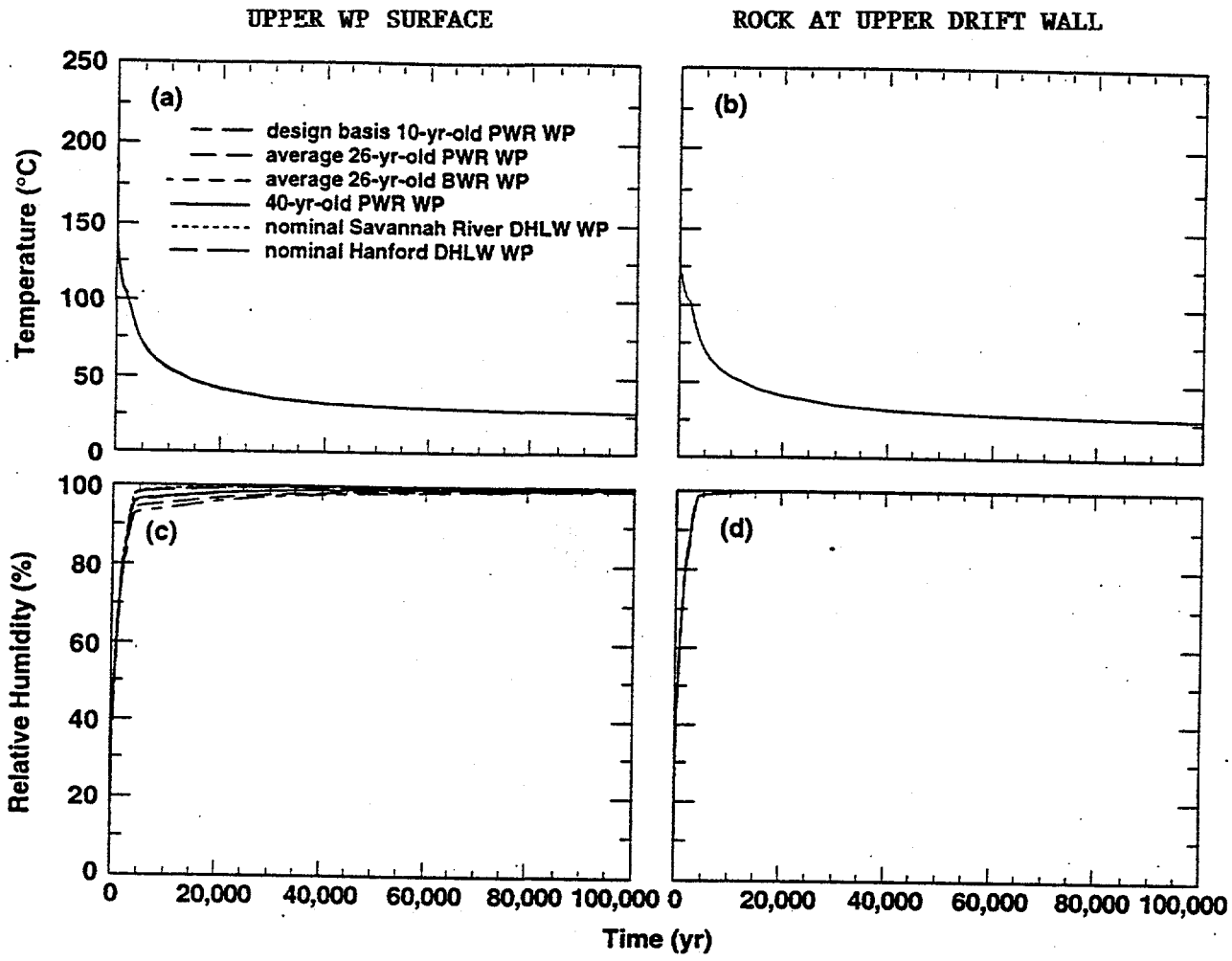

Figure 5.2-34 Temperature and relative humidity profiles for full sand backfill and lineload concept where waste packages are spaced one meter apart (over 100,000 years)

5.2.6 MATERIAL PROPERTIES TEST RESULTS

5.2.6.1 Introduction

Imperative in determining the effects of backfill on total system performance is an improvement in the understanding of flow and transport through and around a partially backfilled emplacement drift. A necessary ingredient in assessing the effects of backfill on flow and transport is to establish the unsaturated transport properties of the various backfill and invert materials being considered. This section documents the collection of such data.

Because liquid transport is generally much slower in the unsaturated zone matrix relative to the saturated zone, transport through the vadose zone is usually the rate limiting step for contaminant release from the site. In the EBS, unsaturated transport will provide the source term for contaminant release to the near-field. Vadose zone regulations that will soon be released by the EPA will govern most activities in the unsaturated zone and will require measurement of the unsaturated transport parameters for each geologic unit, soil horizon, and engineered component for modeling and performance assessment needs. Unfortunately, these parameters are strong, non-linear functions of the volumetric water content, q. The most important factor affecting these functional relationships is the pore-size distribution, which is determined by the grain-size or fracture aperture distribution, bulk density, and the pore connectivity factor.

The Unsaturated Flow Apparatus (UFA) Method was used to measure the unsaturated transport parameters, hydraulic conductivity, matric potential, vapor diffusivity, and diffusion coefficient on seven samples of backfill and invert materials that were selected for characterization: fractured whole rock Topopah Spring tuff (Tsp rock), 3/8 inch crushed Topopah Spring tuff gravel (Tsp gravel), 3/8 inch crushed basalt gravel (basalt gravel), Yucca Mountain Split Wash Alluvium, fine and coarse clean quartz sands, and North Carolina apatite (NC apatite). The apatite is being investigated for its potential benefits as a retardant of ^{237}Np and ^{99}Tc. The modeling of apatite in the emplacement drift invert will be discussed in Section 5.2.7, and the rationale for the selection of apatite will be discussed in Section 5.5.

Transport parameters have been difficult to obtain as a function of the volumetric water content. Traditional methods of investigating unsaturated systems require very long times to attain homogeneous distributions of water because normal gravity does not provide a large enough driving force relative to the low hydraulic conductivities that characterize unsaturated conditions. Pressure techniques can often bypass portions of the sample because pressure is not a whole body force like gravity and will seek the path of least resistance, usually the sandy areas and macro pores. Also, high pressures can induce structural changes in the sample, especially by collapsing clay interlayers and by affecting pressure-dependent chemical reactions and phase stabilities in hydrated phases, carbonates, and soluble salts.

To address these problems, an unsaturated flow apparatus based on open-flow centrifugation was developed in which hydraulic steady-state is achieved rapidly in any porous media by using an adjustable, whole-body driving force in combination with precision fluid flow (Conca, 1993 ; Conca and Wright, 1992; Wright et al., 1994). The UFA achieves hydraulic steady-state rapidly, in hours, even at very low water contents, and is actually a Darcy's Law machine in that the operator adjusts

both the flux and the driving force, and attains any desired hydraulic steady-state within the operating range. For this study, the operating range was from saturated down to 10^{-10} cm/s (10^{-7} darcy; 10^{-15} cm^2). Sample volumes ranged between 40 cm^3 and 92 cm^3. A detailed description of the UFA Method is in Appendix C (Conca and Wright, 1996, Appendix).

Because the UFA is an advective machine, it can isolate and separate advection from other processes such as diffusion or vapor flow. This means that the advective residual water content can be attained and used in advective codes and numerical routines. The evaporative residual water content as determined using water retention methods is not suitable for advective codes and numerical routines and is always much lower than the advective residual water content. In addition to the pore connectivity factor, the choice of residual water content is the greatest source of error in applying hydraulic parameter estimation models such as van Genuchten/Mualem or Brooks-Cory, to any material other than sands (Stephens and Rehfeldt, 1985; van Genuchten et al., 1992).

The primary transport parameters include hydraulic conductivity, K, intrinsic permeability, k_a, diffusion coefficient, D, matric potential, y, distribution coefficient, K_d, and retardation factor, R_f, and vapor diffusivity, D_v. D_v, or any other non-wetting fluid conductivity, is the only primary transport parameter that increases with decreasing water content. Related properties include electrical conductivity, G, thermal conductivity, κ, and dispersivity, α. All of these properties are required to effectively describe subsurface transport and behavior, especially with respect to migrating fluids and contaminants in the extreme thermal conditions expected in the high-level waste repository. An important parameter describing the migration of dissolved aqueous contaminants in most subsurface environments is the hydraulic conductivity. The critical parameter for gaseous contaminant migration (e.g., $^{14}CO_2$ or ^{129}I) is the vapor diffusivity at specific water contents. However, engineered barrier systems designed to prevent advection are being considered for the Yucca Mountain repository. In the absence of advection, the diffusion coefficient becomes the critical parameter for the transport of dissolved aqueous contaminants.

5.2.6.2 Summary of Results

Detailed results, in the form of plots and tables, can be found in Appendix C (Conca and Wright, 1996, Appendix).

Because all of the samples were engineered materials chosen for specific characteristics, their transport properties were well-defined and reflected end-member characteristics. Transport within the whole rock core of Topopah Spring tuff was dominated by a single small fracture with an aperture of about 20 microns. The hydraulic conductivity curve, $K(\theta)$, is almost a vertical line. At saturation, when the fracture is filled, the volumetric water content is 15 percent, the hydraulic conductivity is 10^{-7} cm/s, the matric potential is effectively zero, the vapor diffusivity is effectively zero, and the aqueous diffusion coefficient is 8×10^{-7} cm^2/s. A slight desaturation to a volumetric water content of 14 percent drops the hydraulic conductivity to 10^{-10} cm/s, raises the matric potential to over 2 bars, increases the vapor diffusivity to 3×10^{-4} cm/s (a coefficient of air permeability of 3×10^{-8} cm^2), and leaves the aqueous diffusion coefficient almost unchanged at 6×10^{-7} cm^2/s. At matric potentials above 2 bar, $\psi(\theta)$ becomes a steadily decreasing function up to 47 bars as the finer and finer pores desaturate.

The gravels exhibit equally extreme behavior. For the tuff gravel at saturation, the volumetric water content is 56 percent, the hydraulic conductivity is 10.4 cm/s, the matric potential is effectively zero, the vapor diffusivity is effectively zero, and the aqueous diffusion coefficient is 10^{-5} cm^2/s. However, the gravel cannot be saturated in the subsurface environment at Yucca Mountain and even a slight non-zero matric potential causes the following:

- the volumetric water content drops to 8 percent (approximately that portion of the total porosity internal to the gravel particles themselves),
- the hydraulic conductivity falls to below 10^{-1} cm/s (in fact, whatever the recharge rate is at that point),
- $\psi(\theta)$ becomes a vertical line,
- the vapor diffusivity increases to 0.1 cm/s (a coefficient of air permeability of 10^{-5} cm^2), and
- the aqueous diffusion coefficient falls to 10^{-7} cm^2/s.

The basalt gravel has similar behavior except that the volumetric water content is lower at any point, about 4 percent lower, because the basalt particles have no internal porosity. It is not yet unknown what effect the tuff gravel internal porosity will have on the rewetting phase after drying out of the repository.

For the coarse quartz sand at saturation, the volumetric water content is 42 percent, the hydraulic conductivity is 2.09 cm/s, the matric potential is effectively zero, the vapor diffusivity is effectively zero, and the aqueous diffusion coefficient is 10^{-5} cm^2/s. However, like the gravels, the sand cannot be saturated in the subsurface environment at Yucca Mountain and even a slight non-zero matric potential causes similar dramatic changes; i.e., the volumetric water content drops to below 6 percent, the hydraulic conductivity to below 10^{-1} cm/s (in fact, whatever the recharge rate is at that point), makes $\psi(\theta)$ a near-vertical line, increases the vapor diffusivity to 0.1 cm/s (a coefficient of air permeability of 10^{-5} cm^2), and drops the aqueous diffusion coefficient to 10^{-7} cm^2/s. The fine quartz sand used in this study reached an even lower water content than the coarse sand, and one explanation is that the purity of the quartz sand was greater, and the surface roughness was less, than the coarse sand.

The Split Wash Alluvium from the site was too fine-grained and clay-rich making its hydraulic conductivity and matric potential relationships completely inappropriate for any barrier application. The apatite and the two clean sands were all very well-sorted materials, except that the fine sand is too fine for the backfill layer, and would create local Richards Barriers if overlying any of the other backfill materials. The apatite is appropriate as an additive to the invert material, but should not be added to the backfill above the invert as it also could create local Richards Barriers if overlying any of the other backfill materials. From these results, the gravels and coarse sand are adequate as backfill materials over an invert of apatite.

5.2.7 IMPROVED MODELING OF FLOW AND TRANSPORT THROUGH AND AROUND AN EMPLACEMENT DRIFT

Development of a process-level model simulation of the flow and transport through and around a partially backfilled emplacement drift is described in this section. The process-level model simulation, along with the appropriate materials test results from Section 5.2.6, are used to establish an improved understanding of the effects of backfill and a chemically treated invert on flow and transport about an emplacement drift.

With regard to the chemically treated invert, a sensitivity analysis was conducted in Section 5.1.2 to establish whether a sorptive invert would have any significant effect on total system performance. Those results indicated that the invert would have to be highly sorptive for very long periods of time to have any significant effect on repository performance. As Section 5.5 will discuss, one particular material, sedimentary apatite, was deemed to have sufficient promise to satisfy such requirements. Therefore, this section includes both test results establishing the retardation properties of apatite as well as the incorporation of the test results to establish the near-field benefits of a sorptive invert. The radionuclides addressed in this section are ^{237}Np and ^{99}Tc. These radionuclides are thought to be among the most problematic radionuclides because of their large inventories, high solubilities and low sorption coefficients on the Yucca Mountain tuffs. ^{129}I is another important radionuclide for peak dose at early time, but it is not considered in these analyses because it produces results similar to ^{99}Tc. As a result, the scientists studying the geochemical processes of the chemical system consisting of the Yucca Mountain groundwater, rock, and radionuclides have performed comprehensive studies of solubility, speciation, sorption, and transport for ^{237}Np. The solubility, speciation, and sorption behavior of ^{99}Tc is not as well studied because it has been determined that under the oxidized conditions likely to be present in the unsaturated zone, this radionuclide is probably extremely soluble (e.g. CRWMS M&O 1995d) and very poorly sorbed to the Yucca Mountain tuffs. Thus the source term will be governed by the rate of dissolution of the waste form rather than by the solubility of the radionuclide once it leaves the near-field environment, and the hydrologic conditions and the extent of matrix diffusion alone will determine the transport behavior. Under conditions in which significant fracture flow is likely to occur at the potential repository horizon, the nature of the hydrologic conditions in the vicinity of emplacement drifts will have a strong influence on the rate of release of radionuclides in the near field. It is important to characterize the hydrologic and transport conditions over the entire time frame of interest (up to one million years) to generate a source term for subsequent unsaturated zone and saturated zone transport models. In this section, the hydrologic and transport behavior of key radionuclides under ambient (isothermal) conditions are examined. The time-varying rate of release of radionuclides is examined for several different hydrologic conditions consistent with the current understanding of site unsaturated zone hydrology. The dissolution rate of the waste form and the solubility of the radionuclide in question also play an important role in the estimation of the release rate once the waste package is breached. This section examines these factors in detail for the two radionuclides determined in the latest Total Systems Performance Assessment (CRWMS M&O 1995d) to be the most important: ^{237}Np and ^{99}Tc.

5.2.7.1 Hydrologic Model Assumptions

A complete hydrologic and transport model of the near-field environment at Yucca Mountain would capture the important processes of fracture and matrix flow, the influence of a drift of zero capillary pressure in the midst of a host rock with variable hydrologic properties, and the time-varying and spatially varying infiltration rates known to occur at the site, all in the presence of radioactive waste decay heat that exerts a strong influence on the hydrologic conditions near the emplacement drifts. Currently, our state of understanding and ability to simulate all of these processes is limited. Therefore, reasonable assumptions are required to make the problem tractable. Since the focus is on radionuclide migration away from the near-field environment, several simplifications are possible that will result in conservative calculations of the radionuclide source term from the near field environment. Assumptions employed in this section related to hydrology are:

Isothermal conditions in the vicinity of the emplacement drift is conservative. In the first 10 to 100 years after waste emplacement, the rock around the drift should become completely dry, as water is driven away as steam, condensing when it reaches the cooler rock a greater distance away. During this time, it is unlikely that significant quantities of liquid water will be able to percolate through the rock without vaporizing. Dry rock and low relative humidity in the vicinity of the waste packages is favorable from the standpoint of corrosion (e. g. Buscheck et al., 1996), and the lack of liquid water to transport the soluble radionuclides will minimize transport even if waste package failure occurs. When the declining waste heat load is no longer capable of maintaining a boiling condition in the rock near the drift, liquid water will begin to re-invade the drift area as the temperatures slowly return to their ambient values. At long times (conservatively estimated to be greater than about 10,000 years after waste emplacement), the hydrologic conditions present before waste emplacement are assumed to be present in the near field. Failure of the waste packages is assumed to have occurred, and radionuclides can migrate from the near field in the percolating fluid. By assuming isothermal conditions from the start of these simulations, we conservatively ignore all of the favorable conditions (prolonged lifetime of the canisters, low liquid flux through the near field environment, dry, unsaturated backfill material of effectively 0 aqueous diffusion coefficient) that should take place in the presence of radioactive decay heat.

Hydrologic parameter values are unchanged from their pre-waste-emplacement values. Vaporization of water near the emplacement drift and condensation at the outskirts could cause mineral precipitation and dissolution in various locations, thereby changing the hydrologic properties of the fractured tuff. In particular, precipitation in a fracture would result in a sharp decrease in permeability that would probably be irreversible. Such changes in the rock mass due to the effect of waste heat and thermohydrologic processes is beyond the scope of this study. It remains an uncertainty in model predictions of near-field behavior.

Steady state flow conditions apply. As already mentioned, the actual time-varying thermohydrologic conditions brought about by the input of waste heat are being neglected. Even after the heat has dissipated, there is a transient effect brought about by the time-varying, episodic infiltration conditions known to be present at Yucca Mountain. Recent studies of episodic infiltration (Robinson et al. 1996) show that a large influx of water for short periods of time, followed by zero infiltration, result in ^{36}Cl responses similar to those found in the ESF. However, the transient flow effects do not extend into the Topopah Spring welded unit. This is due to the ability of the PTn to dampen pulses

of infiltration such that the flux into the Topopah Spring welded (TSw) unit is more closely approximated by a constant, average infiltration rate. Since this near-field transport study is carried out in the TSw, this approximation is considered to be valid. Longer term changes in infiltration rate brought about by a change in climate are assumed to be captured in this study by examining a range of infiltration rates from 0.3mm/y to 3mm/y, even though they are held constant within a simulation. This same infiltration rate variation is also assumed to capture the uncertainty in this parameter both in a temporal and spatially average sense.

A dual permeability model can be used to represent flow and transport through the fractured rock mass. In this model conceptualization, the fractures and matrix form individual continua through which fluid can flow, with an interaction term to represent transport of mass (water or radionuclide) from one continuum to the other. This conceptual model is superior to one that assumes that a single continuum with one set of properties applies to the rock mass (Robinson et al., 1995) because the rapid transport times through fractures can be simulated, and the fractures can transmit fluid without requiring that the matrix be completely saturated and at low capillary pressure.

Fluid flow from the host rock into the air-filled drift can be modeled using Darcy's law in the drift. The physics of flow from either fractures or matrix into an empty cavity such as an emplacement drift is a complex, transient process. The codes used in this study apply Darcy's law to capture the fluid flow behavior throughout the model domain. In this study, this includes the empty air space in an emplacement drift. Clearly, this is an expedient used to facilitate the computation of flow and transport results that does not capture the actual process of individual drips of water that pass from the rock mass into the drift. As a result, this type of analysis should not be used to predict details of the hydrology at the interface between the host rock and the drift. In the present study, we assume different hydrologic parameters for the air space above the backfill and the backfill itself in an attempt to bracket the rate of advective flux through the drift. This allows us to determine how significant the details of the hydrologic processes acting in the near field are to the predicted radionuclide source term.

5.2.7.2 Hydrologic Model Geometry and Numerical Grids

To study the hydrologic and transport processes acting in the near field, it is necessary to reproduce the geometry of the emplacement drift, backfill, and canister for the current proposed design. Figure 5.2-35 is a finite element grid for the two-dimensional slice through a SNF waste package. This geometry was constructed from Figure 5.2-3. The model domain consists of a waste package, backfill and invert regions, an air gap above the backfill, and the host rock. Note that due to the need for separate rail systems for loading the waste packages and emplacing the backfill, the waste package is not placed in the center of the drift (see Section 5.2.1 for more details). The grid generation software X3D was used to build the grid. The high grid resolution shown in Figure 5.2-35 is needed to minimize numerical dispersion in the radionuclide transport simulations. To construct this grid, a regular point distribution is first defined with points on the material boundaries to achieve a well-defined set of nodes and interfaces. The points are then connected in such a way as to honor the Delaunay criterion for numerical grids. Finally, to achieve a uniform point distribution within a material, a grid smoothing algorithm is applied within the materials while holding the interface points fixed. The resulting finite element grid produces very accurate simulation results because of the care

taken to adhere to numerical criteria regarding the shapes of elements on a high resolution grid. The grid shown in the figure contains 6024 node points.

5.2.7.3 Hydrologic Property Values

Critical indicators of the acceptability of a backfill material, in terms of its ability to retard radionuclide migration, are its diffusion coefficient and hydraulic conductivity. For a variety of potential backfill materials, characteristic curves were measured by Conca and Wright (1996) and are reported in Section 5.2.6. Among the materials investigated were Tsw gravel, basalt gravel, Japanese fine sand, and Japanese coarse sand. Rather than employ the van Genuchten functions (van Genuchten, 1980) to fit the characteristic curves of every material examined and then perform multiple transport simulations alternately using each material as backfill in the emplacement drift, it is fitting to first examine the diffusion coefficient and hydraulic conductivity of the various materials to determine whether a single material can be used as a bounding case.

This examination is done by first asserting that the capillary pressure in the backfill will approach the value in the whole rock, which is about 0.5 MPa for the conditions of the site. Then, Conca and Wright's data are used to estimate the volumetric water content at 0.5 MPa capillary pressure, followed by estimates of hydraulic conductivity and diffusion coefficient (conductivity from the characteristic curve data, and diffusion coefficient from Figure A3 of Appendix C (Conca and Wright, 1996, Appendix)). The results are indicated in Table 5.2-5.

Table 5.2-5 Volumetric Water Content and Hydraulic Conductivity of Potential Backfill Materials

Backfill Material	**Volumetric Water Content (%)**	**Hydraulic Conductivity (cm/s)**	**Diffusion Coefficient (m^2/s)**
TSw Gravel	6.7	0	2×10^{-11}
Basalt Gravel	2.1	0	2×10^{-12}
Japanese Fine Sand	1.6	0	1×10^{-12}
Japanese Course Sand	4.1	1×10^{-5}	5×10^{-12}

First, note that except for Japanese coarse sand, the hydraulic conductivity is found to be low at this capillary pressure. So, regardless of the type of backfill used, this model predicts low advective flux through the drift, except for Japanese coarse sand, which perhaps could support advective flow under these conditions.

The diffusion coefficients of the basalt gravel and the sands are generally lower than the value for TSw gravel because of the lower volumetric water content at 0.5 MPa capillary pressure; however, they never go completely to zero. There is probably a predicted performance benefit to using Japanese fine sand, in that the diffusive flux to the edge of the drift would be 20-times lower than that of TSw gravel used in the simulations. However, Conca and Wright (1996) conclude that "...the fine

sand is too fine for the backfill layer, and would create local Richards Barriers if overlying any of the other backfill materials." Thus, of the acceptable backfill materials, the rate of diffusion and thus release rates are conservatively, yet not overly so, represented by the calculations performed assuming TSw gravel. Given this information, the calculations carried out in the remainder of this section pertain to the TSw gravel and should be considered not unlike the results that would be obtained with the other materials.

Figures 5.2-36 and 5.2-37 show, for TSW gravel, the measured capillary pressure versus fluid saturation curve, and the hydraulic conductivity versus fluid saturation curve, respectively. The van Genuchten functions (van Genuchten, 1980) were used to fit the data shown in the figures.

The model equations are (Robinson and Triay, 1996):

$$R_l = \begin{cases} \left[1.0 - \left(1.0 - \hat{S}^{\frac{1}{\lambda}} \right)^{\lambda} \right]^2 \sqrt{\hat{S}}, & \hat{S}_l < S_{lmax} \\ 1.0, & \hat{S}_l \geq S_{lmax} \end{cases} \qquad (5.2\text{-}2)$$

$$R_v = 1.0 - R_l \qquad (5.2\text{-}3)$$

where $\hat{S} = \frac{S_l - S_{lr}}{S_{lmax} - S_{lr}}$ and $\lambda = 1 - \frac{1}{n}$, where n is an experimentally determined parameter. The capillary pressure is described by the following equation:

$$P_{cap} = \begin{cases} P_{capmax}, & P_{capl} \geq P_{capmax} \\ P_{capl}, & P_{capl} < P_{capmax} \\ 0.0, & S_l \geq S_{lmax} \end{cases} \qquad (5.2\text{-}4)$$

where $P_{cap} = P_0 \left[\hat{S}^{\frac{1}{\lambda}} - 1.0 \right]^{1.0-\lambda}$, $\hat{S} = \frac{S_l - S_{lr}}{S_{lmax} - S_{lr}}$ and $P_0 = \frac{1.0}{\alpha_G}$, and $\lambda = 1 - \frac{1}{n}$,

where n and α_G are experimentally determined parameters. The van Genuchten capillary pressure curves approach an infinite value as S_l approaches 0 and 1. This requires the use of extrapolation techniques. At these extremes, linear fits were used.

The resulting parameter values from the fitting exercise are given in Table 5.2-6.

Table 5.2-6 Parameter Values from Fitting Exercise

Parameter	Value
S_{lr}	0.12
S_{lmax}	0.2
α_G	50 m^{-1}
n	3

A different view of this data is presented in Figure 5.2-38, a plot of capillary pressure versus relative permeability for the TSw rock matrix, fractures, and the fit to the TSw crushed gravel. To understand the hydrologic simulation results presented below, we must recognize that for a gravel in contact with an intact rock mass, the steady state solution is one in which the capillary pressures in the two media attempt to approach one another. Taking a capillary pressure of 0.5 MPa as a typical value in the matrix rock at the infiltration rates present at Yucca Mountain, the saturation in the backfill consistent with this pressure is low enough that the relative permeability in the backfill is vanishingly small, in this example on the order of 10^{-25}. Thus for the hydrologic conditions present at the site, the permeability in the backfill will be extremely low, and water will be forced around the drift rather than through it. Thus, under any feasible infiltration rate, there will be no advective flux through the backfill in this model.

As mentioned above, the physics of the hydrology at the interfaces of the rock and air space is not properly captured in a porous medium model. In addition, dripping water on a crushed material is unlikely to behave locally as a porous medium with property values as measured using the UFA employed in the work of Conca and Wright (1996). An averaged model is not capable of capturing this detail, and thus the model result in which no water percolates through the drift must be considered to be a limiting case. At the other extreme, the drift and backfill provide no resistance to percolating fluid. This end-member case is simulated in the present study by assuming that the emplacement drift (air gap and backfill) has hydrologic properties identical to those of the host rock. Examination of the two extremes allows us to assess the impact of this uncertainty on the radionuclide source term from the near field. In the present study, simulations assuming the measured properties of the crushed TSw gravel apply in the drift are called "Gravel Properties" simulations, while the runs that set the properties equal to those of the host rock are called "Host Rock Properties" simulations.

The hydrologic properties of the rock surrounding the emplacement drift are those of the TSw unit at the potential repository horizon, as assumed by Robinson et al. (1995), taken from Wittwer et al. (1995). The air space above the backfill was assumed to have hydrologic properties identical to those of the host rock, so that the presence of an empty cavity is assumed to have no impact on the downward movement of fluid when it reaches the emplacement drift. This assumption is considered to be conservative, since in the actual case, there may be a tendency for percolating fluid to travel around the drift due to the higher capillary pressure in the rock.

The waste package is assumed to be a porous medium with 0 permeability, so that if fluid is allowed to percolate through the drift, it will travel around the waste package rather than through it.

5.2.7.4 Numerical Model Assumptions

The FEHM computer code was used for the hydrologic and transport simulations. The dual permeability option was employed to capture the fracture flow and transport more accurately than can be done using a continuum model approach. The mean fracture spacing, the one additional parameter in the dual permeability model, was assumed to be 0.5 m in the TSw rock. Since FEHM requires that the entire medium be represented as dual permeability, the backfill and invert were represented using a "fracture" porosity of 0.5, identical "fracture" and "matrix" hydrologic parameter values, and an extremely small fracture spacing (10^{-3}m). In all simulation results, the two continua attained identical values for fluid saturation, pressure, and fluid velocity within the backfill and invert, thus verifying the validity of the approach.

The boundary conditions used were a fixed infiltration rate along the top set of fracture nodes, and a fixed fluid saturation in the fracture nodes at the bottom boundary. No flow conditions were assumed along the sides of the model domain. An important constraint on the model was the choice of an appropriate saturation in the fractures along the bottom. Since the entire model domain is only 22.5 m in height, setting a fracture saturation on the bottom results in a capillary rise through the medium to the point where all fluid saturations reach the value used at the bottom. If the value is too high, corresponding matrix saturations at steady state are also unrealistically high. To eliminate this problem, a two-step process was used. First, a simulation was performed at a bottom saturation boundary that was lower than the eventual fracture saturations throughout the model. The steady state value reached within the model was then used as the bottom boundary in a second simulation. This method resulted in saturations in the fractures that differed by no more than 0.007 throughout the model domain. This approach prevented the model from achieving a steady state in which there is an unrealistic gradient in capillary pressure through the model (if the bottom saturation is set too low) or an unrealistic fluid saturation in the rock (if the bottom saturation is set too high).

5.2.7.5 Hydrologic Model Results

Background steady state flow simulations were carried out at infiltration rates of 0.3, 1.0, and 3.0 mm/year. Figure 5.2-39 shows the saturation distribution in the fractures and drift material at 1 mm/year infiltration rate for the "Gravel Properties" assumption. The saturation in the drift reaches a value of slightly less than 0.12, consistent with a capillary pressure close to that in the host rock. As described in Section 5.2.7.3, the corresponding permeability through the backfill is extremely low, and water travels around the drift. The positions labeled A, B, and C in Figure 5.2-39 are locations at which the downward component of percolation flux was recorded. As shown in Table 5.2-7, flux through the drift is extremely low (effectively zero to within the accuracy of the simulation).

Table 5.2-7 Fluid Velocities Around and Through an Emplacement Drift

Position	Downward Fluid Velocity (mm/year)
A	1×10^{-9}
B	1.1
C	2.4

Note also that the nominal percolation flux is the infiltration rate of 1 mm/year. Away from the emplacement drift the value is only slightly greater than 1 mm/year, but near the drift the value is greater than 1 mm/year, a consequence of diversion of flux around the drift.

At the other two infiltration rates, this qualitative picture still applies, with only the magnitude of flow velocity changing. The "Host Rock Properties" simulations yield the expected result of advective flux through the drift equal to that in the host rock, since there are no capillary forces acting to keep water out of the drift.

5.2.7.6 Radionuclide Transport Model Assumptions

The radionuclide transport simulations in the present study are carried out using the steady state flow simulations just presented. Thus the model assumptions relating to the hydrologic properties of the rock and backfill apply to the transport simulations as well. The convective dispersion equation is the fundamental relation governing the transport of a solute in a flowing fluid. Advection, dispersion, diffusion, and possibly sorption on the porous medium are assumed in the advection-dispersion model. Assumptions specific to the transport model are:

Dispersion is governed by a model in which the components of the dispersion coefficient tensor are aligned with the direction of fluid velocity. This is the assumption commonly made in porous medium transport models (e.g. Freeze and Cherry, 1979), with the ratio of longitudinal to transverse dispersion coefficient usually of order 10. In the present study, the longitudinal dispersivity was taken to be 2 m, and the transverse dispersivity was assumed to be 0.2 m. Lower or higher values will change the shape of a solute breakthrough curve at a downstream location, but to a first approximation the rate of solute movement will remain constant.

Transport out of the drift in the absence of advective water flow is by molecular diffusion through an unsaturated medium. The rate of movement from the drift under these conditions is controlled by the a diffusion coefficient, measured to be a function of volumetric water content by Conca (1990). FEHM has a transport option in which the diffusion coefficient is a function of water content: Figure 5.2-40 shows the relationship for the parameter values used in the present study. This curve, based on the work of Conca (1990), shows that for the volumetric water content of the backfill material in these simulations (about 6.7 percent), the diffusion coefficient is 1.6×10^{-11} m^2/s, roughly 60 times lower than the free diffusion coefficient of dissolved ions in water. Thus the diffusion coefficient is small, but definitely not 0, so that radionuclides will eventually diffuse to the advecting fluid and escape the near-field environment. The steady state, isothermal assumption is a particularly conservative one in this case, as the fluid saturation in the drift, and thus the diffusion coefficient, is

likely to be lower than the steady state value for a significant time period during the period when decay heat is important. The simulations presented here should be considered to be valid only after the backfill has rewetted, with negligible transport by diffusion until the volumetric water content rebounds to at least 2 to 3 percent.

Sorption of radionuclides on the invert material is governed by a linear isotherm model. This is the so-called "Kd" model used in most simulations of transport through porous media. The values reported from laboratory measurements simply reflect the relative partitioning of solute on the rock and in the water, neglecting kinetics effects and the possibility of nonlinear sorption behavior caused by the exhausting of all available sorption sites. The Kd model represents a best case assumption for the possible benefit of a sorptive invert material such as apatite. It was decided that before embarking on a comprehensive experimental program to fully characterize the sorption process on a potential invert material, calculations placing the benefits in the best possible light would be useful to assess whether it is useful to further pursue the idea of an engineered sorptive barrier.

Two dimensional simulations can be employed to represent the three dimensional system. A two-dimensional slice normal to the axis of the waste package is assumed to have a thickness of 1 m. The liquid flow rate and the amount of radionuclide in the inventory (discussed in Section 5.2.7.8 below) are then scaled accordingly. The actual situation is one in which fluid passing through or around the drift in between waste packages will pick up less radionuclide, and then mix with and dilute the fluid that passes directly by a waste package. Thus the dilution factor will be underestimated in a two-dimensional simulation. Future work will use three-dimensional models to provide the best possible estimate of the dilution effect. Fortunately, the two-dimensional assumption is likely to be conservative, since the waste package is effectively present throughout the entire drift in the two-dimensional domain, whereas in three dimensions there will be fluid encountering sections of the drift with no packages.

5.2.7.7 Transport Property Values

The values of diffusion and dispersion coefficients were discussed in the previous section. For sorption on the invert material, the values for K_d of ^{237}Np and ^{99}Tc on apatite measured by Los Alamos National Laboratory (Triay and Thornton, 1996) are used. The measurements at 25°C on apatite were conducted twice and are summarized in the Table 5.2-8 (K_d values reported in cm^3/g).

Table 5.2-8 K_d Measurements for ^{237}Np and ^{99}Tc

Conditions	^{237}Np K_d	^{99}Tc K_d
pH 4	535	0.69
	660	0.74
pH 6	646	0.45
	576	0.44
pH 8	512	1.2
	653	0.61
pH 10	432	0.59
	334	0.44

Similar sets of measurements at 60°C and 80°C yielded K_d values in this same range, with the ^{237}Np exhibiting a drop-off in sorption coefficient to values of 100 to 200 cc/g at lower pH and higher temperature. However, the pH of the Yucca Mountain unsaturated zone fluid is about 7, and could possibly be higher in the presence of cement materials present in the repository. Therefore, the higher K_d values are probably representative of the values that would be encountered at the time of radionuclide release. In summary, a significant sorption coefficient of roughly 500 cc/g was determined for ^{237}Np, whereas ^{99}Tc exhibited little or no sorption on apatite (approximately 1 cc/g). This value is sufficiently close to 0 to be negligible; therefore ^{99}Tc is assumed to be a conservative, nonsorbing radionuclide in these simulations.

5.2.7.8 Radionuclide Source Term

Under various conditions, the rate of removal of a radionuclide from the waste package can be a function of either the rate of dissolution of the waste form or the solubility of the radionuclide. The initial dissolution is generally considered to be one congruent dissolution, such that the rate of dissolution of a given radionuclide is proportional to the fraction of the waste form that is that radionuclide. However, for sparingly soluble radionuclides, the rate of dissolution of the waste form will result in a flux of the radionuclide that results in oversaturation in the fluid. It is then generally assumed that the radionuclide forms a solid precipitate such that the fluid concentration reaches the solubility of the radionuclide in water. Thus, to assess whether rate-limited or solubility-limited dissolution applies, we must compare the rate leached from a waste form undergoing congruent dissolution to the rate predicted from a transport calculation based on solubility-limited dissolution. The smaller of the radionuclide source rates is then used in subsequent calculations.

For an estimate of the rate of waste form dissolution, we assume a nominal value of 10 mg/m^2/day (CRWMS M&O 1995d, Figure 6.2-2) and a waste form surface area of 500 m^2 per package (CRWMS M&O 1996d, p. 8-18). This rate (5000 mg/day), applied to 9.74 MTU (or, as UO2, 11.05 metric tons of solid waste) of waste, results in a time of 6050 years for complete dissolution. Since

there is a range of uncertainty of about an order of magnitude on either side of the nominal dissolution rate, the complete dissolution could take from 605 years to 60,500 years. Any solubility-limited transport simulation that predicts a complete depletion of radionuclide in less than this time is overestimating the rate of dissolution. When this happens, a dissolution-rate-limited model should be used instead.

For a solubility-limited dissolution simulation, the concentration is held constant at the solubility of the radionuclide at the waste package. As fluid passes by the waste package, it sweeps radionuclide from the package. For conditions of zero advective flux through the drift, diffusion through the backfill takes place, and the flowing water at the drift-rock interface picks up radionuclide. Thus for these conditions the boundary at which advective transport occurs changes and there are potential diffusional transport limitations within the drift, but otherwise the processes are similar.

From the above discussion, it is obvious that the solubility of the radionuclide under the thermal and chemical conditions after failure of the waste canister is crucial for predicting the source term of a given radionuclide. Since the solubility is typically estimated only within loose bounds, the resulting radionuclide source versus time will only be known imprecisely. The effect that this uncertainty has on system performance must then be studied to quantify the uncertainty.

A final consideration is that there is not an unlimited supply of radionuclide available for transport, so that if these results are to provide source-term input to larger scale calculations, the time of complete dissolution of the waste must be identified, and the source term must be turned off at this time. This time is the larger of the time required for complete dissolution of the waste form and the time computed from a solubility-limited calculation. The amount of radionuclide present in a waste package is obtained from a straightforward calculation of the inventory after converting from radiation units (Ci) to moles of radionuclide. For example, a 21 assembly PWR waste package contains approximately 13.5 Ci/MTU of ^{99}Tc, or 13.5 Ci/MTU x 9.74 MTU/Pkg = 131.5 Ci/Pkg. Then, the conversion from Ci to moles is based on the half-life of the material, so that for ^{99}Tc, the result is 131.5 Ci/Pkg x 2.13 x10^5 y / 3.574 x 10^5 = 78.5 moles of ^{99}Tc/Pkg, where 3.574 x 10^5 is the conversion factor in the above expression when the half-life is expressed in years.

For ^{237}Np, the situation is complicated by the fact that the initial inventory of this radionuclide is augmented by radioactive decay of parent radionuclides ^{241}Am, ^{241}Pu, and ^{245}Cm. Figure 5.2-41 shows the time-varying inventory of ^{237}Np as computed by the computer code DECAY to track the quantities of all radionuclides in the inventory. Taking as a starting condition the initial inventory reported by Wilson et al. (1994), the simulation shows the ingrowth of ^{237}Np over about the first 10,000 years from the decay of the aforementioned parents, especially ^{241}Am. Thus an additional constraint on the source term model of ^{237}Np is the finite production rate of the radionuclide in the first 10,000 years, which could limit the source rate of the radionuclide under rapid dissolution, high solubility scenarios. Instead of building this complexity into the transport calculations, we will compare the results assuming the initial inventory of ^{237}Np is the value at 10,000 years, and then assess whether this assumption was valid after performing the calculation.

5.2.7.9 Transport Model Results

The release rates and concentrations for a specific radionuclide are dependent on many processes and parameter values, including infiltration rate, solubility, waste form dissolution rate, and the nature of the hydrology near the emplacement drift. To study the influence of backfill on performance, it is instructive to examine the transport in a generic way before presenting results for specific radionuclides. We do this by taking a single infiltration rate (1 mm/y) and examining the predicted release rate under solubility-limited conditions. The "Gravel Properties" hydrologic model will be presented in this development. Before considering the effect of a limited supply of radionuclide, we present results based on an assumed large amount of radionuclide, as would be the case for a sparingly soluble radionuclide.

Figure 5.2-42 shows the release rate versus time from the waste package and from the bottom of the model domain for a solubility of 10^{-3} moles/l (probably an upper bound on the solubility of ^{237}Np at Yucca Mountain). The release curve for the bottom of the model is assumed to be an appropriate source term for site-scale unsaturated zone calculations, since this detailed model is intended to capture the detail that is occurring within a single source node of a site scale simulation. The difference at early times (less than about 1000 years) represents the finite time required for radionuclide to migrate from the waste package to the bottom of the model. If releases are presumed to occur for times much greater than 1000 years, then this transient can be ignored in favor of a simpler constant source rate.

It has generally been assumed that under conditions in which no advective flux travels through the drift, the release rates are vanishingly small (e.g. CRWMS M&O 1995d, Fig. 9.3-43). The present study shows this to be a nonconservative result of assuming a low value for the volumetric water content, rather than the value of about 7 percent as measured by Conca and Wright (1996). This value results in a diffusion coefficient of 1.6×10^{-11} m^2/s, large enough to result in significant mass transport by molecular diffusion. Of course, in the presence of even a small amount of decay heat, the backfill would remain much drier than is predicted in these isothermal calculations, with a resulting delay in the time at which molecular diffusion through the backfill would become significant. In the present study, we chose to take the conservative assumption of 7 percent volumetric water content. Use of the results of this work is appropriate beginning at the time at which the volumetric water content of the backfill rebounds to a large enough value for diffusion to become important.

A comparison of the release rates from the near field environment for the two different hydrologic model assumptions is shown in Figure 5.2-43. Advective flux through the drift results in a more rapid release of radionuclide to the bottom boundary of the model, as expected. The magnitude of this difference may not be as pronounced as has been previously assumed, as discussed above. At times on the order of 1000 years, the release rate has approached a steady state value after the initial transient representing the time required for diffusion through the backfill and transport to the bottom of the model.

The actual magnitude of the curves in Figure 5.2-42 are directly proportional to the solubility of the radionuclide. Figure 5.2-44 shows the release rate curves from the canister for solubilities ranging from 10^{-3} to 10^{-5} mol/l, a reasonable range for ^{237}Np. The horizontal lines on the figure are the release rates of ^{237}Np assuming the range of waste form dissolution rates assumed in Section 5.2.7.8. These

horizontal curves are the maximum possible release rates of ^{237}Np at the waste form dissolution rate chosen. If the curve predicted based on solubility-limited dissolution exceeds the waste form dissolution rate curve, the assumption of solubility-limited dissolution is not valid, and the maximum value should instead be the horizontal curve. If the solubility of ^{237}Np is 10^{-3} mol/l, the analysis shows that unless the highest waste form dissolution rate is selected, the dissolution rate is not solubility limited, as is currently assumed in most analyses. However, for solubilities 10^{-4} mol/l or lower, solubility-limited dissolution is a good assumption over almost the entire time history of the simulation as long as the waste form dissolution rate is 10 mg/m^2/day (the nominal value) or lower. Thus, ^{237}Np release, which is usually taken to be solubility-limited, is actually close to the cut-off between solubility-limited dissolution and release that is limited by the kinetics of waste-form dissolution.

Note that a similar analysis for ^{99}Tc results in a clear-cut conclusion that the release is kinetically limited. This is due to the orders of magnitude higher solubility of Tc (of order 1 mol/l). This result is expected, and is in agreement with all previous analyses of the system.

Since the concentration, rather than the release rate itself, is the important result from the standpoint of a dose calculation, it is desirable to compute an effective concentration leaving the near-field environment. This concentration will be less than the solubility due to dilution of fluid near the waste package with fluid that passes between drifts and between canisters. In these calculations, an effective concentration can be computed simply as the total flux of radionuclide leaving the model (moles/s) divided by the total liquid flux leaving the model (kg water/s). The concentration profile near the potential repository is very non-uniform, with high concentrations near waste packages and lower values in between. And although the actual concentration varies with position across the bottom boundary of the model due to incomplete transverse dispersion across the model, it is likely that this fluid will fully mix over the much larger length scales of a unsaturated zone transport simulation. Transverse dispersion within the unsaturated zone is expected to provide the mixing needed to homogenize the concentration distribution. Under these conditions, the average concentration obtained using this abstraction is the average value across the individual plumes. Thus the calculation abstracts the results of a complex calculation into a term that is easy to recognize.

Figure 5.2-45 shows the effective concentration versus time exiting the model domain for the two hydrologic models. The concentrations are normalized with respect to the solubility of the radionuclide, so that the value is actually a dilution factor (the concentration is diluted by this factor from the solubility limited value assumed to occur immediately adjacent to the waste package). For the "Gravel Properties" case, the diffusional limitations through the backfill are sufficiently great to lower the effective concentration leaving the near field by an order of magnitude below the solubility at the waste package. The dilution effect is less pronounced for the "Host Rock Properties" case because flowing fluid comes in direct contact with the waste package. However, there is still a tendency for some dilution by fluid that does not contact the package. Sorption in the invert reduces the effective concentration somewhat in the time frame of interest, but the effectiveness of sorption is limited if it is assumed to occur only in the invert.

This dilution effect is likely to be more pronounced in three dimensions than is predicted here (see discussion in Section 5.2.7.6). Until three-dimensional calculations are performed, these results can be considered to be conservative.

Of course, there is not an unlimited supply of radionuclide present in the waste package, as has been assumed in the presentation above. The actual rate of release from the near field is directly proportional to the solubility, so that the time required for complete release of a radionuclide is inversely proportional to the solubility, assuming there are no kinetic limitations resulting from dissolution of the waste form. Figure 5.2-46 shows the quantity of radionuclide released from the waste package versus time assuming solubilities ranging from 10^{-3} to 10^{-5} mol/l (typical values for ^{237}Np) for the "Host Rock Properties" model. Also shown is the quantity of ^{237}Np predicted to be present in the inventory from the ingrowth calculation. When the released mass crosses the inventory curve, the entire inventory of ^{237}Np is depleted, except for any additional radionuclide that would be produced by ingrowth. At the lower solubilities, the time for complete release is large enough for the impact of ingrowth to be minimal (for example, the time for complete depletion is 12,500 years at 10^{-4} mol/l and 129,000 years at 10^{-5} mol/l solubility). Since there is a significant inventory of ^{237}Np present initially and most of the ingrowth occurs within the first 1000 years, there does not seem to be a regime in which the source term becomes controlled by the rate of ingrowth rather than by the solubility. This may not be strictly valid at the highest solubility selected (10^{-3} mol/l), or at higher infiltration rates than 1 mm/y, but is certainly true for solubilities of order 10^{-4} mol/l or less.

The source term rate for ^{237}Np under solubility-limited conditions will follow the simulation results shown in Figure 5.2-46 up until the time that the entire inventory is depleted, after which time the source rate at the waste package abruptly drops to 0. Figure 5.2-47 shows this behavior for an infiltration rate of 1 mm/y and solubility of 5×10^{-4} mol/l ("Gravel Properties" model). Since the time scale for the transients is on the order of 1000 years for the assumption of no sorption on the invert material, the source term from the near field in larger scale simulations is adequately approximated by a square wave that starts at the initial time of release and ends after the inventory is completely dissolved. The case for sorption of ^{237}Np on an invert material consisting of apatite is somewhat different. The time scale for the radionuclide to exit the model is considerably greater with sorption, so that the effective concentration no longer resembles a square wave. Figure 5.2-47 shows that in this case, the effective source concentration is more broadly distributed at lower concentrations. The impact this difference has on larger scale simulations will have to be analyzed in unsaturated zone transport models to assess the impact of a sorbing invert material on system performance.

We now examine the impact of infiltration rate on the release of radionuclide to the far field for the two hydrologic models. For the "Host Rock Properties" hydrologic model, advective flux travels immediately adjacent to the waste package, and the steady state rate at which radionuclide is leached from the near field is therefore approximately proportional to the infiltration rate, as shown in Figure 5.2-48. As expected, at higher infiltration rates, the approach to steady state occurs more rapidly than for lower fluxes. The presence of apatite as an invert material that sorbs ^{237}Np impacts the results similarly at lower and higher infiltration rates than the 1 mm/yr rate shown earlier. For the "Gravel Properties" case (Figure 5.2-49), there is a significant diffusion limitation through the backfill that limits somewhat the rate of release at any infiltration rate. Therefore, the steady state release rate is less dependent on infiltration rate. The effective concentration plots for these cases are shown in Figure 5.2-50 ("Host Rock Properties" model) and Figure 5.2-51 ("Gravel Properties" model). The "Gravel Properties" case, with diffusion limitations in the backfill, show a larger dilution effect with increasing infiltration rate. In other words, the impact of increased infiltration rate is to lower the effective concentration leaving the near field, rather than increasing the release rate.

5.2.7.10 Summary and Conclusions

A series of near-field radionuclide transport calculations examining the impact on performance of various design assumptions concerning the use of backfill have been conducted in this section. No attempt is made here to examine the many issues related to waste package thermohydrologic environment in the presence of radioactive decay waste heat. Corrosion of the waste package is critically dependent on the moisture distribution at the waste package, and must be studied by simulating the transport of heat, moisture, and air throughout the lifetime of the repository. Such thermohydrologic analysis can be found in Section 5.2.5. The conclusions reached in this section pertain only to radionuclide release from the near field. The working assumption is that most radionuclides will be released from the waste package only after the most vigorous thermohydrologic processes have dissipated, allowing the diffusion coefficient of the backfill material to reach sufficiently large values to permit radionuclide transport. Therefore, the analyses presented here assume isothermal conditions.

The hydrologic calculations of the present study use a porous medium flow assumption throughout the model domain. It was felt that the assumption of porous medium flow does not necessarily apply at the interface between the host rock, and therefore the resulting flow solution may not capture the actual flow processes very well. Specifically, even without backfill, the low capillary pressure in the drift results in a capillary barrier in a porous medium simulation that would not be present in reality if a *flowing* fracture intersects the drift. With regard to backfill, at a capillary pressure similar to that in the host rock, the unsaturated liquid permeability of the backfill is exceedingly small, resulting in no flow through the backfill even at infiltration rates of 3 mm/y. The detailed physics of these processes could be examined with explicitly gridded fractures in the host rock and a finely discretized, heterogeneous porous medium to represent the backfill. However, this level of detail is beyond the scope of the present work. Instead, the range of hydrologic conditions are bracketed by the two extremes of gravel properties in the backfill (resulting in no advective movement of liquid through the drift) and rock properties in the backfill and air gap (thereby providing no impediment to downward flow of water that intercepts the emplacement drift).

The two extremes in hydrologic behavior result in relatively minor differences in the transport of radionuclides from the near field. Release rates (moles of radionuclide per unit time) are lower for the case of zero liquid flux through the drift, but not by the orders of magnitude that have been obtained in the past (e.g., CRWMS M&O 1995d) for the case of diffusion through a gravel backfill. The reason for the difference is that at the volumetric water content predicted under steady state conditions (about 7 percent, the water content at which capillary pressure begins to rise dramatically in the TSw crushed tuff gravel studied by Conca and Wright (1996)), the aqueous diffusion coefficient is predicted by measurements of Conca (1990) to be of order 1.6×10^{-11} m^2/s, lower than under saturated conditions, but clearly not as low as would be obtained assuming an extremely low water content such as the residual saturation of 1 percent used in the TSPA-95 analyses. The present study is a more conservative approach to predicting the long term release from the near field environment. It suggests that after the thermohydrology has rebounded to ambient conditions, the backfill will rewet to water content values consistent with a condition of capillary pressure equilibration with the surrounding rock. The results of this work become valid at such a time as when the volumetric water content in the backfill rebounds sufficiently to allow the backfill aqueous diffusion coefficient to return to significant values (about 3 percent volumetric water content).

The predicted impact of utilizing an invert consisting of apatite is to lower the release rate of ^{237}Np from the near field environment by roughly a factor of two, although the details of this result depend on the specific assumptions of infiltration rate, solubility, and hydrologic conditions. Since the mass of radionuclide leached from the waste package is independent of the type of invert used, the resulting effective concentration exiting the near field environment for the apatite case is roughly approximated as a source at one-half the concentration for twice the time. It is doubtful that this difference is significant from a performance assessment point of view, but this conclusion should be tested by simulating site scale unsaturated zone transport of ^{237}Np under the different release rate scenarios (sorbing invert versus no sorption). Although not specifically simulated here, a potentially more effective sorption strategy would be to place a sorber in the backfill as well as the invert. This would delay the transport from the drift of radionuclide that attempts to escape via lateral diffusion to edge of the drift, thereby avoiding the invert.

The release of ^{99}Tc is apt to be controlled by the rate of waste form dissolution, rather than by a solubility-limited mechanism. Thus it can be assumed to enter the groundwater over a time period governed by the time for complete dissolution of the waste form. Based on TSPA-95 (CRWMS M&O 1995d), the estimate of this time ranges from 600 years to 60,000 years, depending on dissolution rate. Once it is dissolved from the waste form, ^{99}Tc is found to undergo very little sorption even on a sorptive material such as apatite. The source rate for ^{99}Tc can be abstracted as a constant rate (or, perhaps as a temperature-dependent rate governed by the temperature-time history obtained from a thermohydrologic simulation) for enough time to completely dissolve the waste. Even for the "Gravel Properties" hydrologic case, the transport time from diffusion through the backfill is on the order of only 1000 years. Therefore, for dissolution times greater than about 5000 years, the influence on the source rate leaving the near field of diffusion is minimal, and can be neglected.

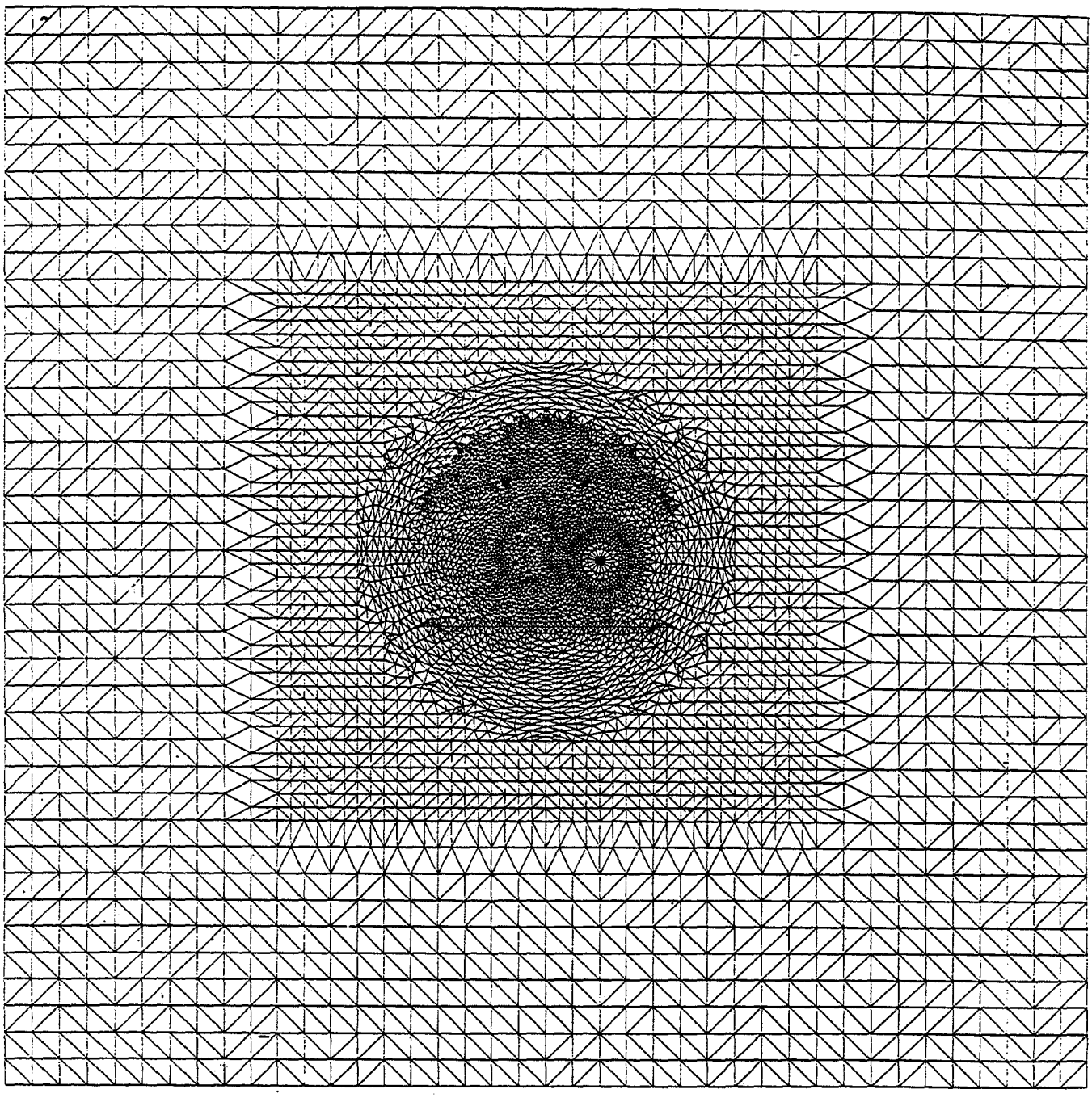

Figure 5.2-35 Finite element grid of the two-dimensional near-field hydrologic and radionuclide transport model

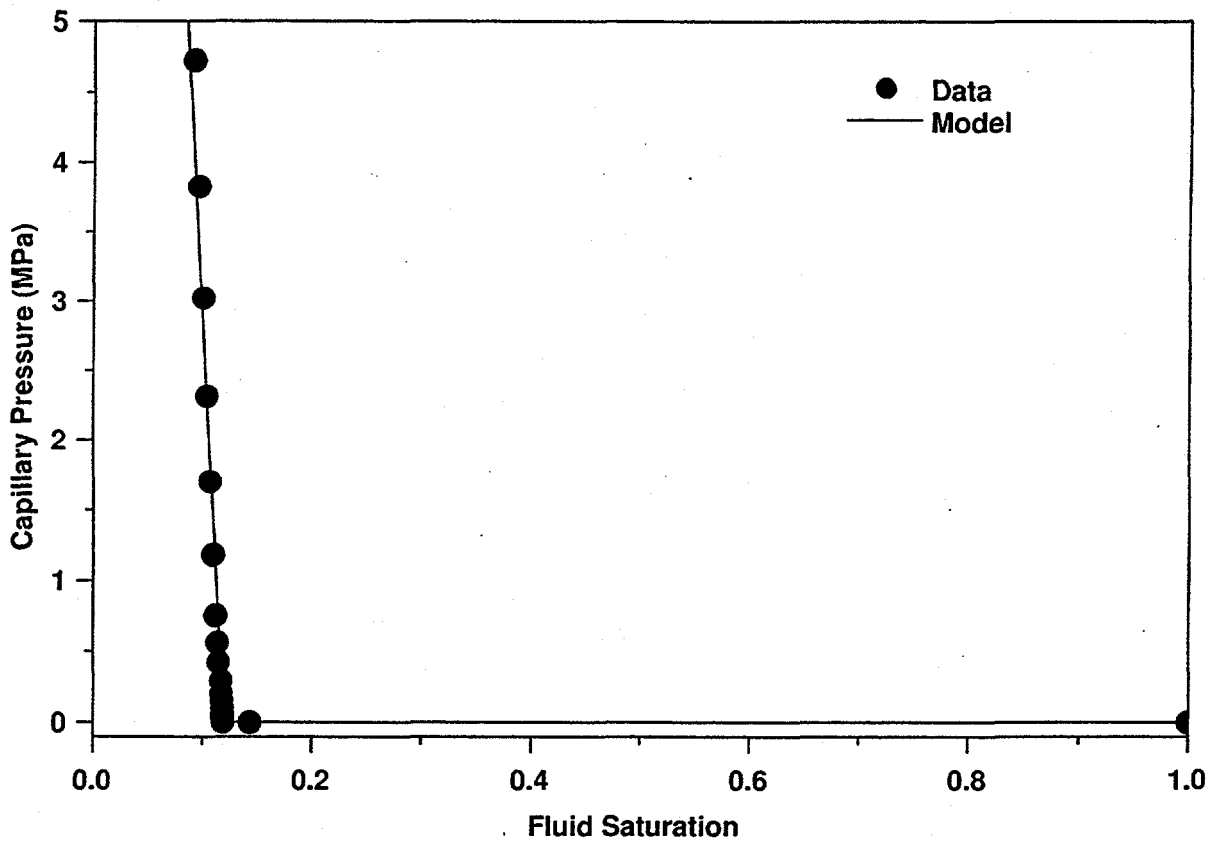

Figure 5.2-36 Capillary pressure versus fluid saturation for the crushed TSW gravel backfill

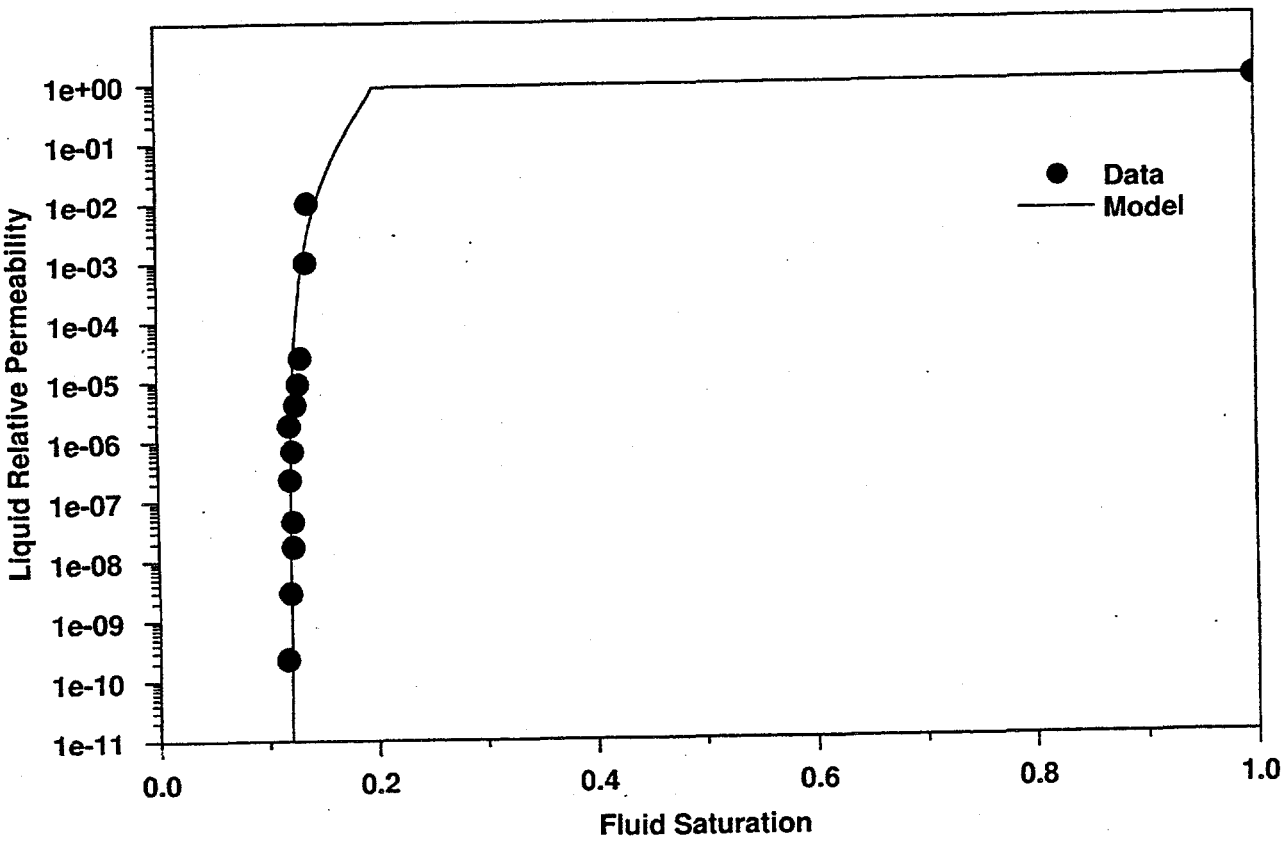

Figure 5.2-37 Liquid relative permeability versus fluid saturation for the crushed TSW gravel backfill

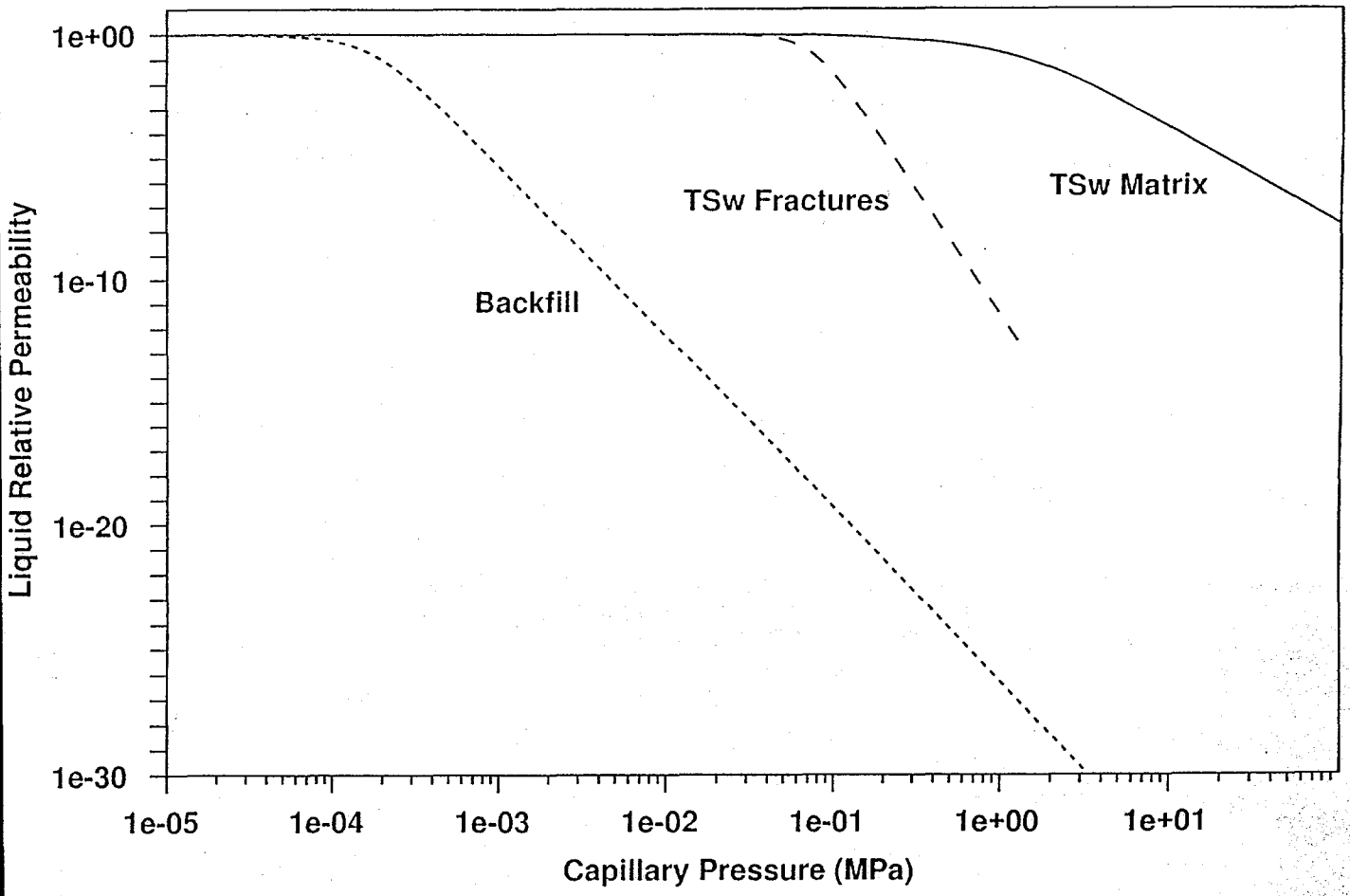

Figure 5.2-38 Liquid relative permeability versus capillary pressure for the crushed TSW gravel backfill and the TSW fractures and matrix rock

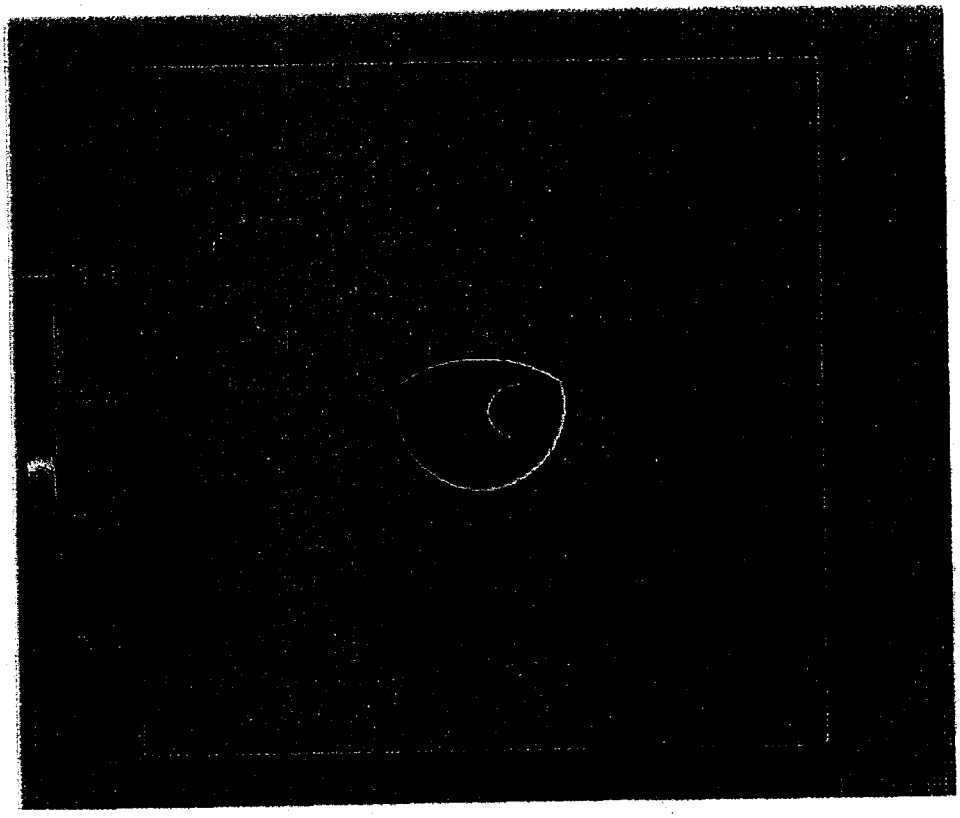

Figure 5.2-39 Simulated liquid saturation distribution in the rock fractures and emplacement drift: 1 mm/yr, "Gravel Properties" hydrologic assumption

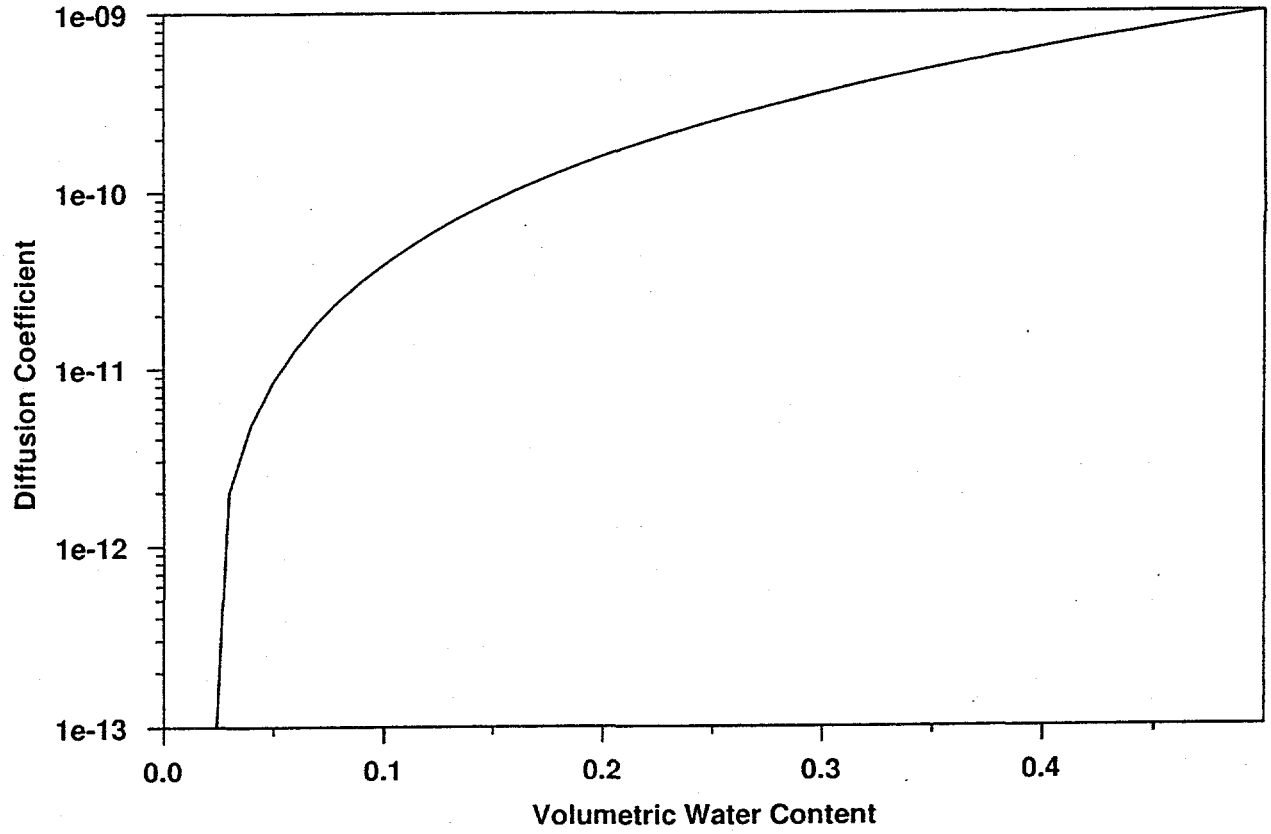

Figure 5.2-40 Aqueous diffusion coefficient versus volumetric water content. This curve is generated from a correlation implemented in FEHM based on measurements of Conca (1990)

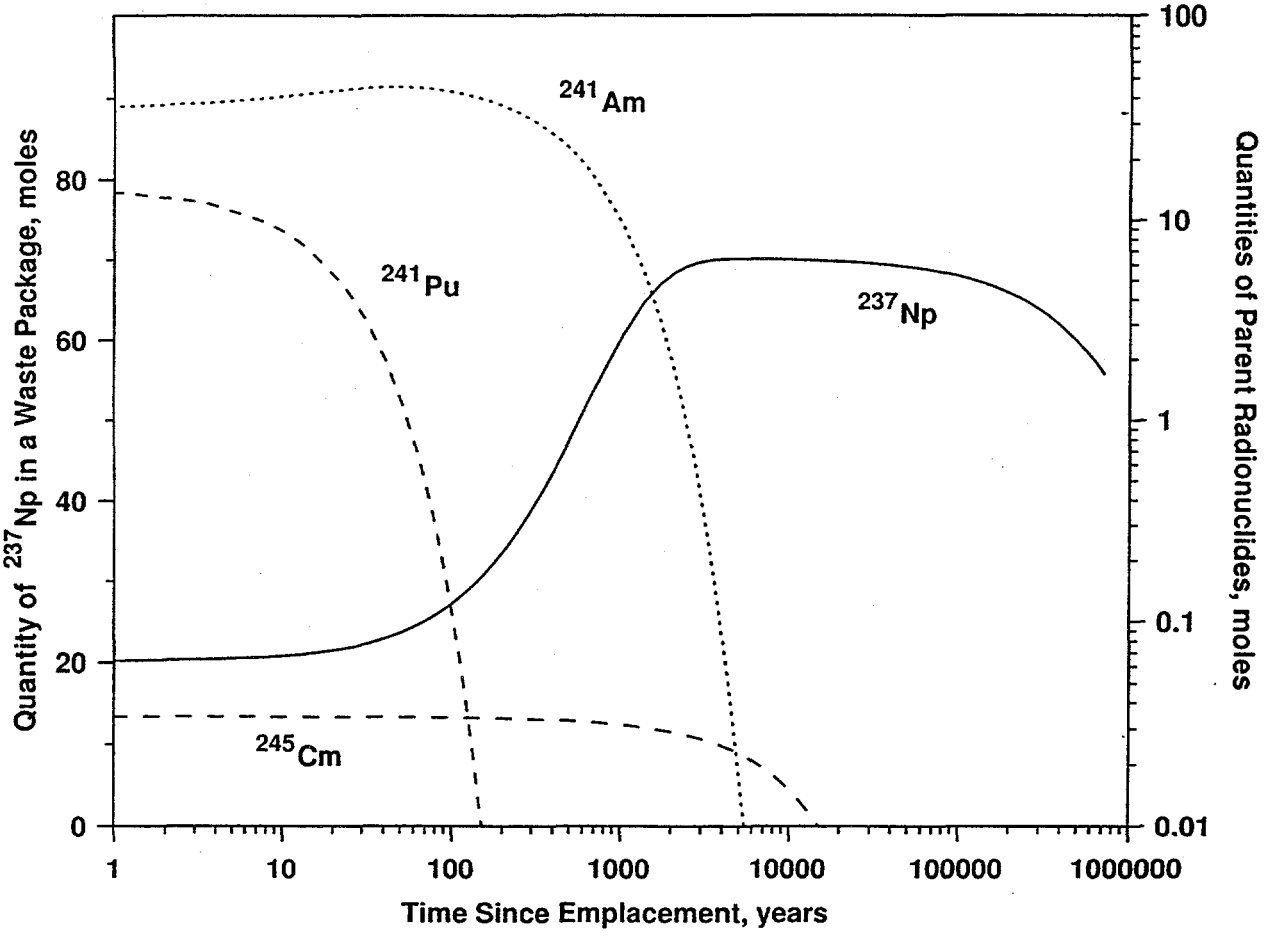

Figure 5.2-41 Quantity of 237Np in a waste package versus time, illustrating the effect of ingrowth of the inventory. Also shown are the time histories of the parent radionuclides of 237Np

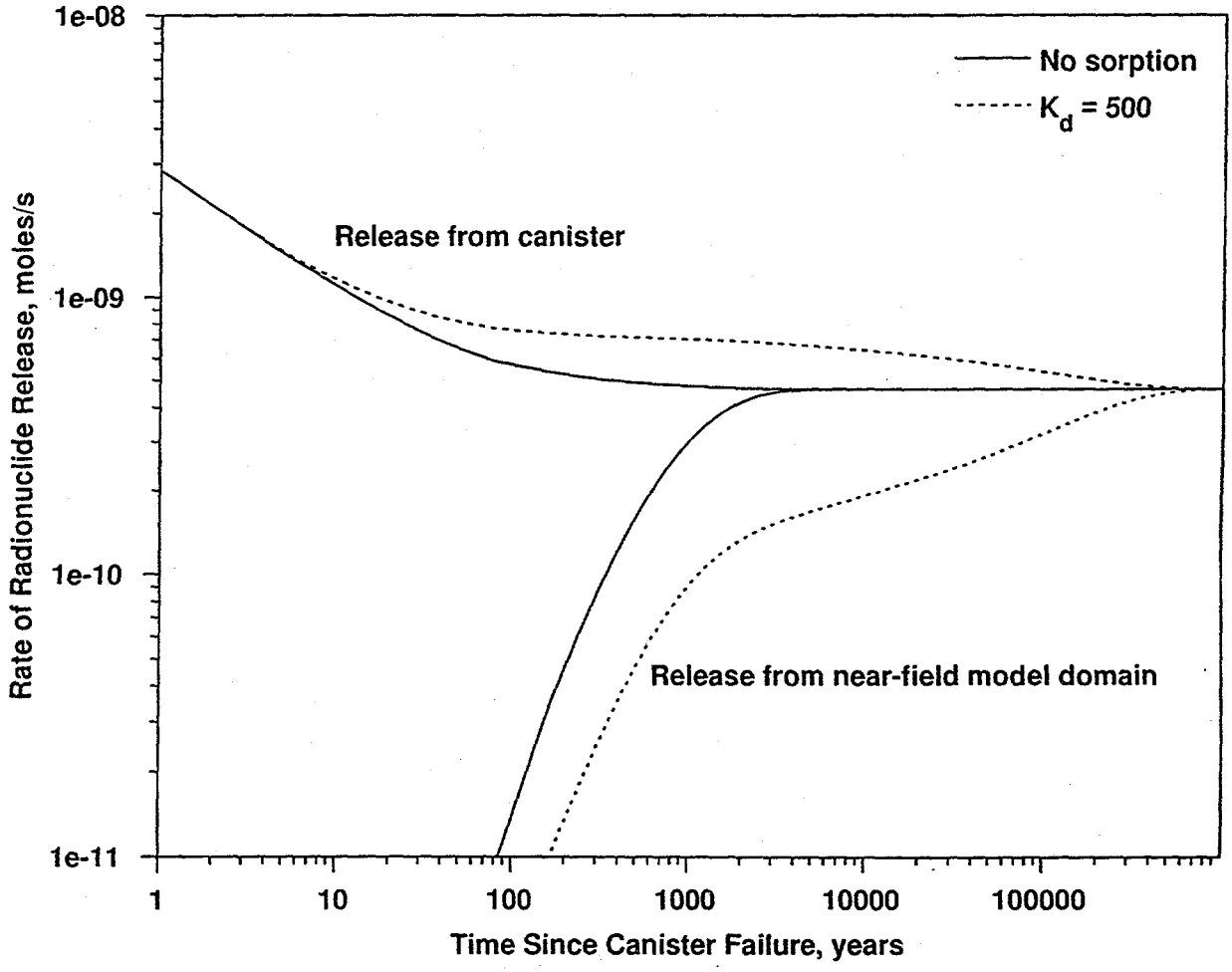

Figure 5.2-42 Release rate versus time from the canister and from the bottom of the near-field model domain. Infiltration rate: 1 mm/yr, "Gravel Properties" model

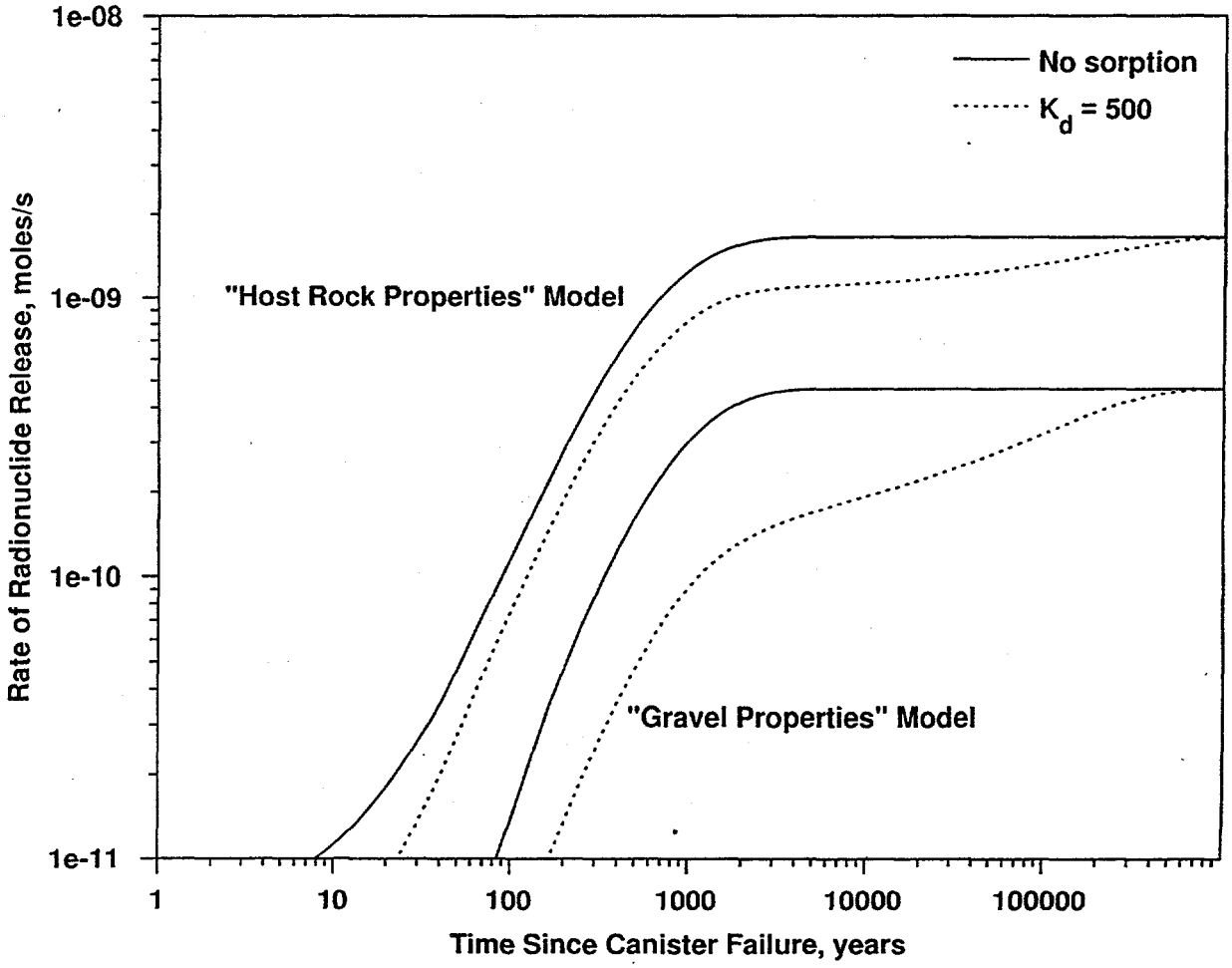

Figure 5.2-43 Release rate versus time from the bottom of the near-field model domain comparing the "Gravel Properties" and "Host Rock Properties" models. Infiltration rate: 1 mm/yr

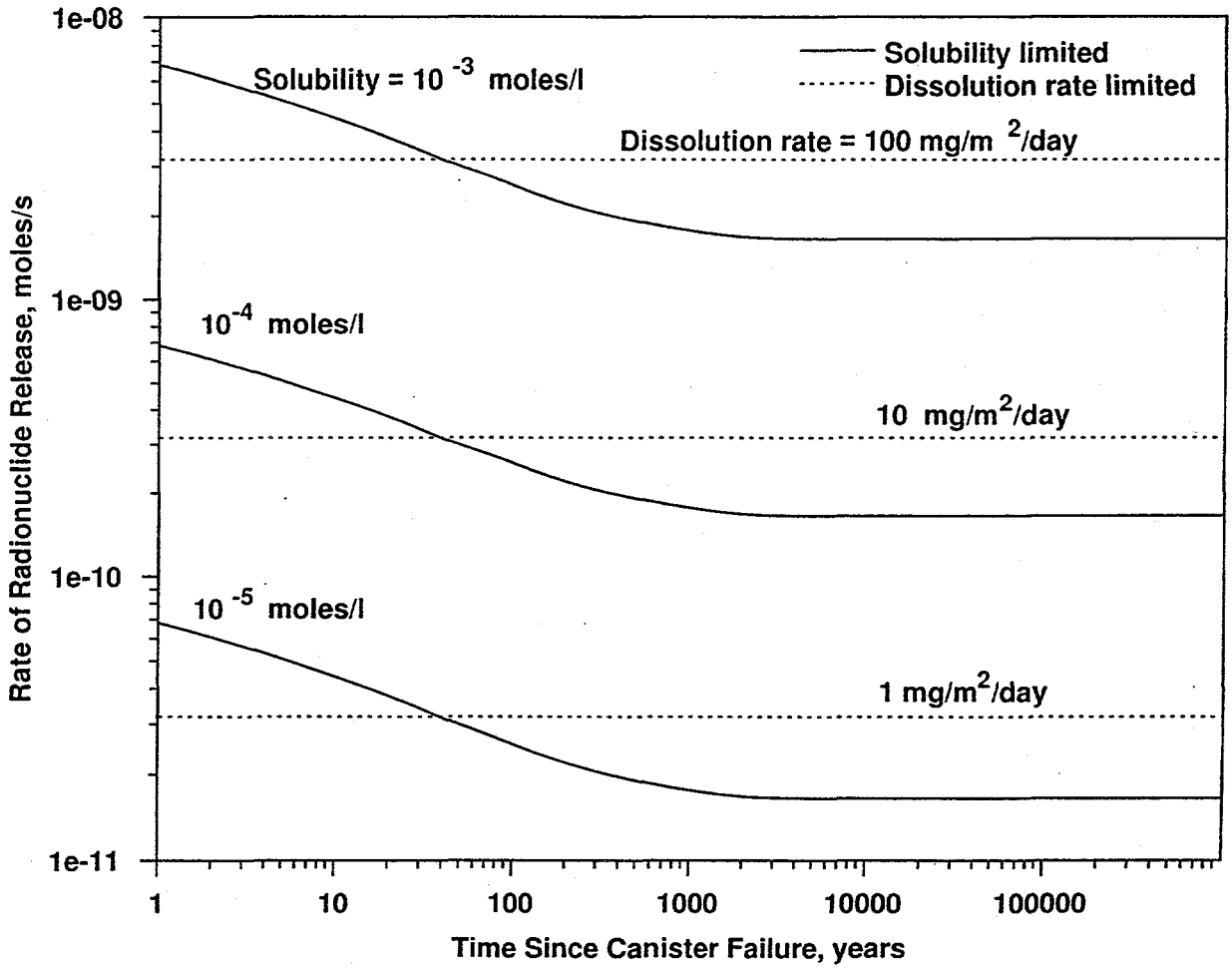

Figure 5.2-44 Release rate versus time from the canister for different assumed radionuclide solubilities. Infiltration rate: 1 mm/yr, "Host Rock Properties" model

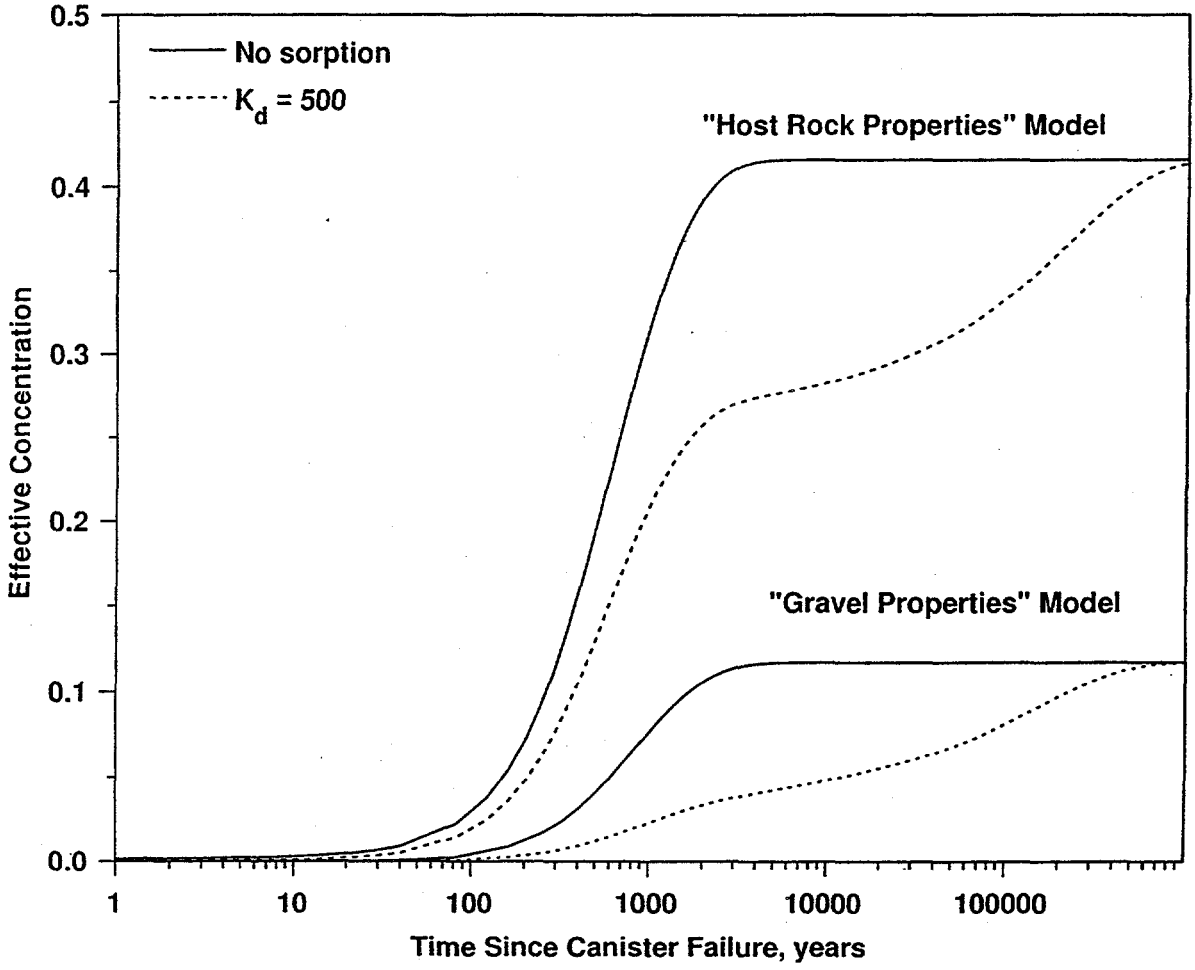

Figure 5.2-45 Effective concentration versus time exiting the near-field model domain. Infiltration rate: 1 mm/yr

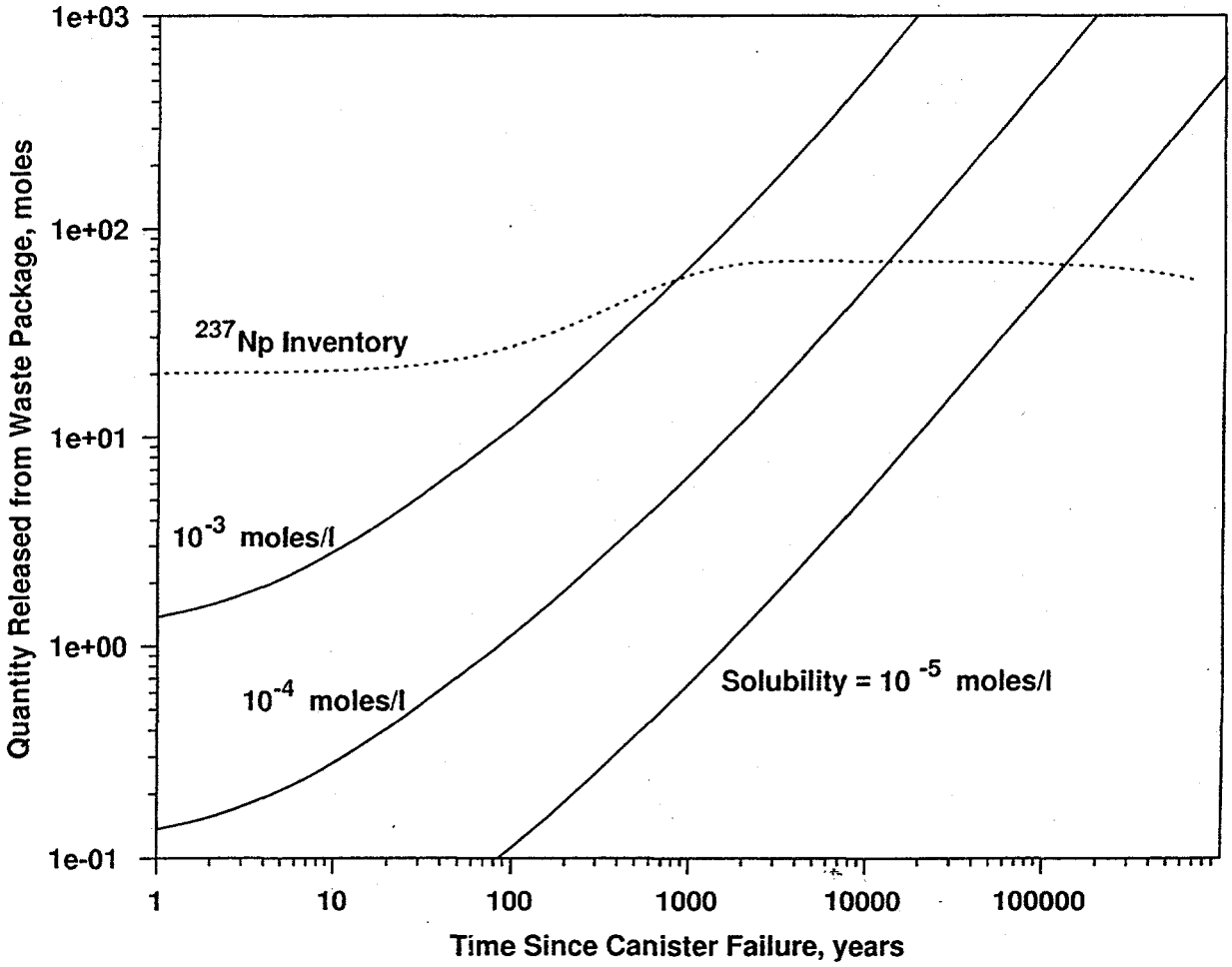

Figure 5.2-46 Total release from canister versus time for different assumed solubilities. Infiltration rate: 1 mm/yr. Also shown is the total inventory of ^{237}Np predicted from the model for ingrowth from parent radionuclides

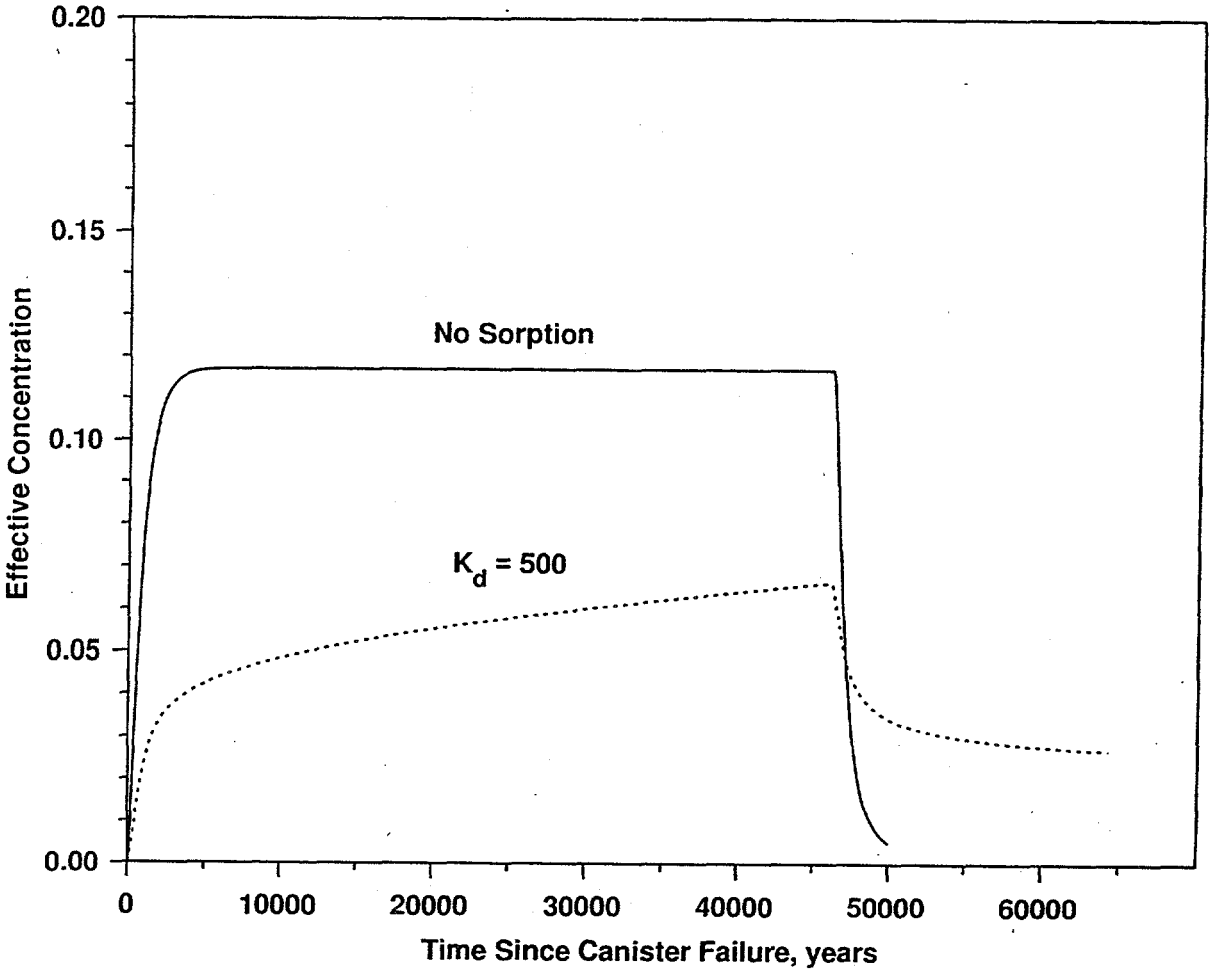

Figure 5.2-47 Effective concentration versus time of 237Np exiting the near-field model domain, considering the complete dissolution of all of the radionuclide. "Gravel Properties" model. Infiltration rate: 1 mm/yr, solubility: 5 x 10^{-4} moles/l

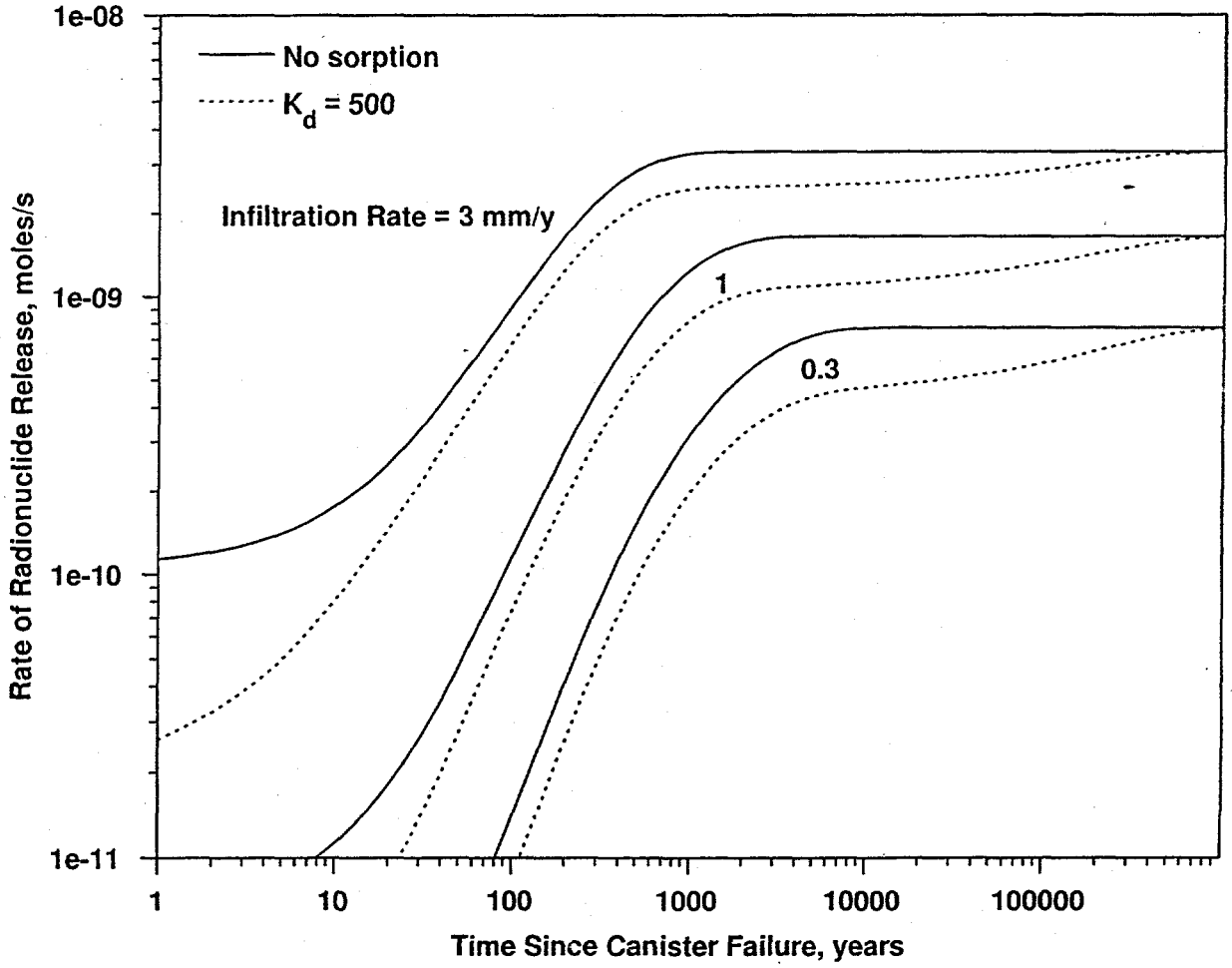

Figure 5.2-48 Release rate versus time from the bottom of the near-field model domain for different infiltration rates. "Host Rock Properties" model.

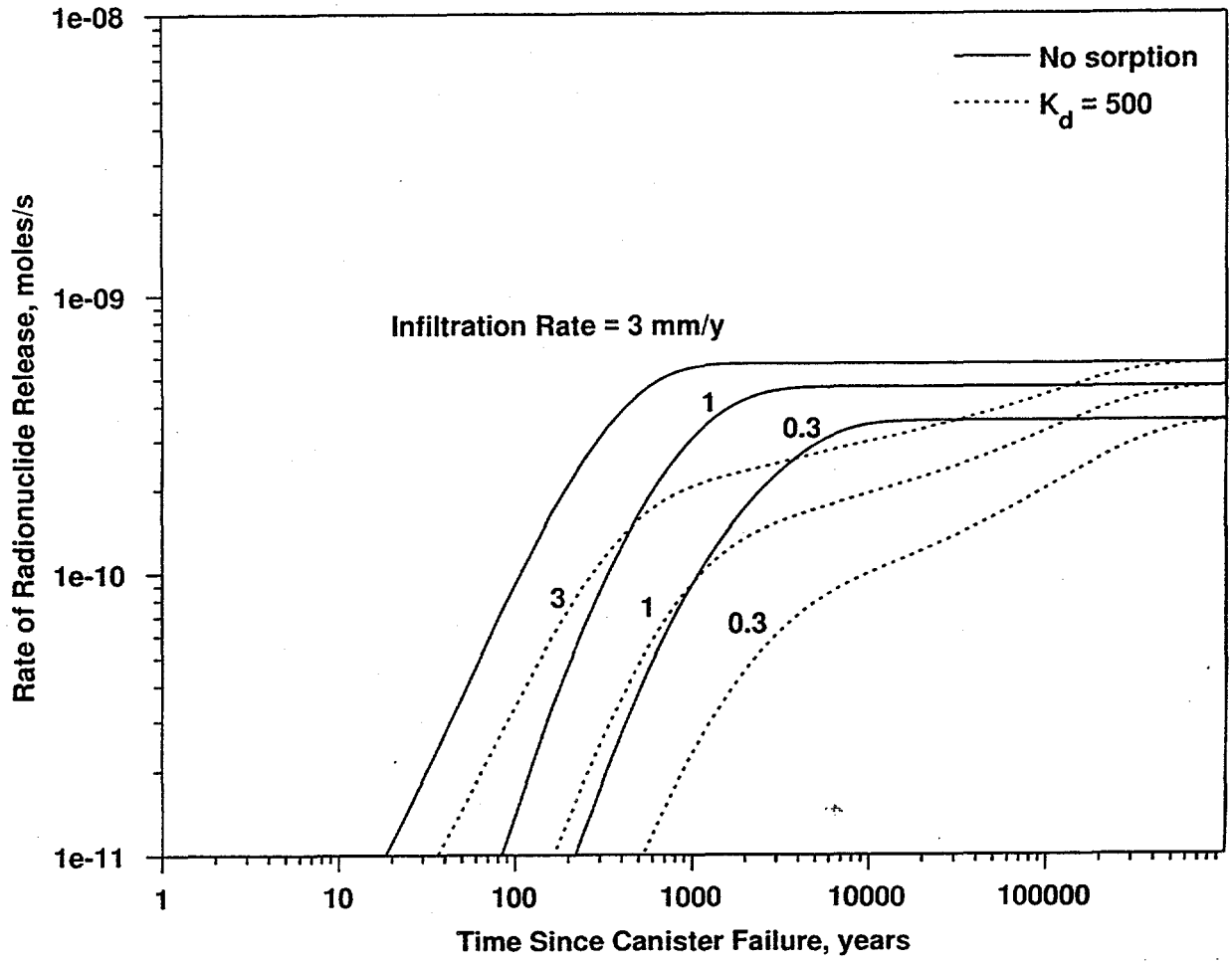

Figure 5.2-49 Release rate versus time from the bottom of the near-field model domain for different infiltration rates. "Gravel Properties" model

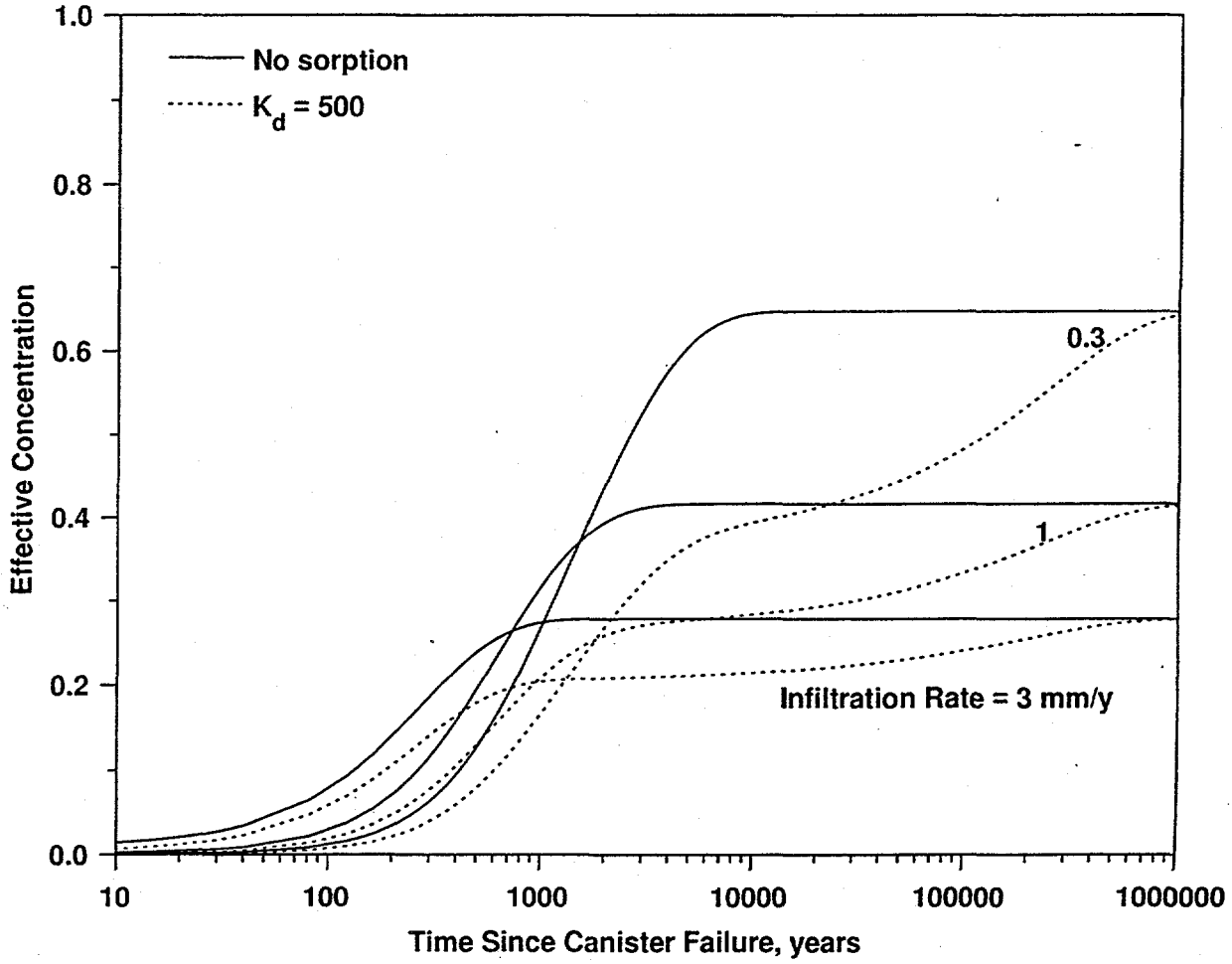

Figure 5.2-50 Effective concentration versus time from the bottom of the near-field model domain for different infiltration rates. "Host Rock Properties" model.

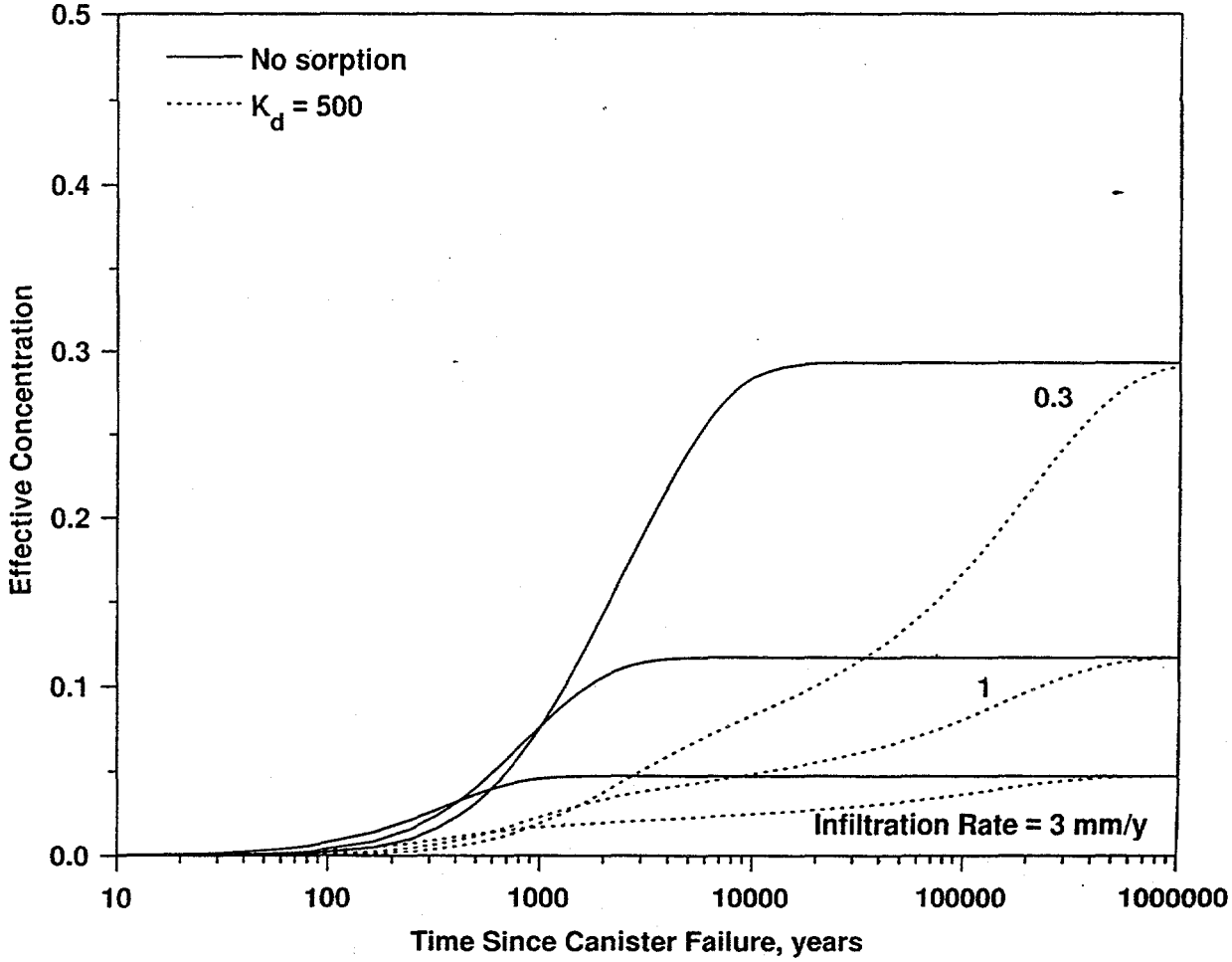

Figure 5.2-51 Effective concentration versus time from the bottom of the near-field model domain for different infiltration rates. "Gravel Properties" model.

5.2.8 TOTAL SYSTEM PERFORMANCE ASSESSMENT WITH BACKFILL

The effect of the inclusion of backfill on the performance of the repository can be analyzed using a total system performance assessment. Previous sections have described the near-field thermohydrologic effects of backfill (Section 5.2.5) as well as the effects of backfill on flow and radionuclide transport (Section 5.2.7). This section incorporates the thermohydrologic analysis included in Section 5.2.5 into a performance assessment model which uses many of the inputs and assumptions stated in TSPA-1995 (CRWMS M&O 1995d).

The thermohydrologic modeling evaluated the ACD "square" waste package spacing concept (LML = 0.46 MTU/meter), as well as the lineload concept for waste package spacing in which the waste packages are axially spaced relatively close together (LML = 1.11 MTU/meter). The waste package containment requirement, the interim 10,000 year peak dose standard, and a 1,000,000 year peak dose evaluation are conducted for the two waste package spacing cases with backfill.

The temperature and relative humidity profiles at the waste packages' surface for the full backfill cases were presented in Figures 5.2-25 through 5.2-27. Modifying these profiles to reflect "level partial" backfill was conducted using equation 5.2-1, and the results are presented in Figures 5.2-52 (ACD) and 5.2-53 (lineload).

The ACD results vary significantly between the various waste forms, while the temperature and relative humidity results for the different waste forms in the lineload configuration fall within a narrow band. This leads to similar WP failure distributions for the lineload case and widely different failure distributions for the ACD case.

5.2.8.1 Waste Package Containment Requirement

The critical relative humidities for corrosion initiation discussed in Appendix B and employed for the "no backfill" cases in Section 3 are also conservatively applied here. Although preliminary Lawrence Livermore National Laboratory thermogravimetric analysis humid air testing corrosion results for carbon steel (CRWMS M&O 1996o) indicate slightly higher critical relative humidity values than used in this study, those results were for a "clean" carbon steel sample. The critical relative humidity values used in TSPA-1995 and in this study were developed from atmospheric corrosion data for which any major salt deposits, except sulfate-iron salts from sulfate sources in mostly industrial areas, were not expected nor reported (see Section 5.3 of CRWMS M&O 1995d). The use of backfill and the stowing methods associated with backfill are expected to produce scratches on the waste package surface as well as contact points of the backfill with the waste package surface, thus providing sites for water condensation and a possible lowering of the critical relative humidity. Further work is certainly needed in this area, and so because of the relative uncertainty in whether the use of backfill will result in higher or lower critical relative humidities, the same values used in TSPA-1995 will be used here.

An important backfill-related aspect of waste package containment is the ability of the waste package to withstand the static load of backfill. A Design Analysis (CRWMS M&O 1996i) was conducted in which the ability of a waste package to withstand the static loads of a "sloping-partial" backfill (see Figure 5.2-2) was established. The analysis concluded that the waste package barrier would begin

to fail due to static loading when the outer barrier had corroded completely away and the inner barrier had thinned to 9.5 mm of its original 20 mm thickness (CRWMS M&O 1996i, p. 80, Vol. 1). The time required to completely corrode away the outer barrier alone, without considering the corrosion-related benefits of backfill, is estimated to be hundreds of thousands of years (see Figure 3.3-7). And although the static loading analysis was not conducted for the "level partial" backfill (the preferred concept if backfill is employed), even if all of the inner barrier were needed to keep the waste package from failing under the static load of backfill, this would still not occur for hundreds of thousands of years. A Design Analysis of the "level partial" backfill concept would be needed to confirm this.

Nevertheless, it is concluded that the static loads of backfill, whether "sloping partial" or "level partial," have no effect on a waste package containment requirement that is concerned with only the first 1000 years of waste package performance.

ACD Waste Package Spacing Concept

The failure curve indicating the first pit penetration times for this case is presented in Figure 5.2-54. Note that the Hanford DHLW WP failure curve in Figure 5.2-54 with backfill is very similar to its failure curve when no backfill is employed (Figure 3.1-14). The lifetime of this relatively cold WP does not appear to benefit from the use of backfill. However, the lifetime of the hotter SNF WPs is substantially improved with the use of backfill. These results indicate no waste package failures prior to 1,000 years, and so are currently determined to meet the waste package containment requirement of less than 1 percent waste package failure prior to 1,000 years. Figure 5.2-55 presents the failure curves when the outer barrier of the waste package is assumed to cathodically protect the inner barrier until 50 percent of the outer barrier has corroded away. These results indicate a substantial improvement in the predicted lifetimes of the various waste packages when compared to the non-cathodic protection case.

Lineload Concept

The failure curves showing the first pit penetration times for the lineload waste package spacing case are presented in Figure 5.2-56. The WP performance benefits of placing backfill over closely spaced WPs is evident here when compared to the no-backfill lineloading WP failure results presented in Figure 3.2-7. The predicted thermal communication among the various WPs provides that even the initially cool Hanford DHLW WP will not breach due to corrosion until 4,900 years after emplacement. As with the ACD case, the lineload case appears to meet the waste package containment requirement.

A caveat to these lineload results must be included here. While the lineload concept appears promising, it has just recently begun to be investigated in earnest, and there is currently large uncertainty in the ability to meet certain thermal goals - such as maximum allowable emplacement drift wall temperature and SNF cladding temperature criteria - when WPs are spaced closely together. This analysis needs to be concluded before any recommendations can be made with regard to lineload of WPs.

5.2.8.2 Repository Performance Compared to Interim 10,000 year Peak Dose Standard

The analyses conducted thus far indicated that the interim 10,000 year peak dose standard was met for the cases without backfill at 30 km from the repository (see Sections 3.1.2 and 3.2.2). Thus, no additional analyses for the ACD or lineload concepts were conducted for the case with backfill.

5.2.8.3 Repository Performance Over a 1,000,000 Year Time Frame

The 1,000,000 year peak dose results for the ACD and lineload cases with backfill are presented in this section. TSPA-1995 results are presented for comparison in the figures in this section.

ACD Waste Package Spacing Concept

The thermohydrologic results produced from analysis of the ACD design led to unique failure curves for each waste form (Figure 5.2-54). The 26-yr-old and 10-yr-old PWR fuel have similar failure curves, so they were treated as one group with a blended inventory. Each of the other waste forms was considered separately in the RIP implementation. Due to computer limitations, the simulations for this ACD/backfill were conducted in two individual RIP runs. The first run consisted of 26-yr-old BWR and 40-yr-old PWR WPs, and the second run consisted of DHLW, 26-yr-old PWR and 10-yr-old PWR WPs. The first RIP run indicated a peak dose rate approximately one order of magnitude higher than that in the second run; thus, combining the results of the two runs would not have a significant effect on the overall results. Figure 5.2-57 shows the results of the first run. The ACD/backfill result at 30 km from the repository is significantly lower than the 5 km accessible environment result due to the dilution assumed during transport to the more distant location. The ACD/no backfill case result is presented for comparison with the ACD/backfill case in Figure 5.2-58. The ACD/no backfill peak dose rate CCDFs are over one order of magnitude greater than the corresponding ACD/backfill cases. The ACD/backfill/30 km case results in Figure 5.2-58 show a 50 percent probability of not exceeding a peak dose rate of approximately 0.6 mrem/year, a 90 percent probability of not exceeding about 2 mrem/year, and a 99 percent probability of not exceeding approximately 11 mrem/year.

Lineload Concept

The thermohydrologic results produced using the lineload concept led to the failure curves presented in Figure 5.2-56. For the assessment of 1,000,000 year peak dose rate, the middle failure curve for the 26-yr-old BWR WP was used to represent all WPs in this case. This failure curve starts later and is generally below the Hanford, 40-yr-old PWR, and 26-yr-old BWR failure curves for the ACD/backfill case (Figure 5.2-54). This leads to lower releases for the lineload/backfill case than were simulated in the ACD/backfill case (Figure 5.2-59). The results from the lineload concept for the backfill case at 30 km from the repository are presented in Figure 5.2-59. The peak dose rates are significantly below the TSPA-1995 case results and a factor of 2 lower than the ACD/backfill case. The differences are due primarily to the failure distributions and pitting degradation which are lower for the lineload case (see Figure 5.2-56).

5.2.8.4 Repository Performance Compared to Alternative Hypothetical Performance Standards

The analyses summarized in Table 3.1-4 of Section 3.1.2 indicate that, without the use of extra performance barriers in the EBS, over the 10,000 year time frame both the "Interim Postclosure Standard" as well as the alternative hypothetical standards are satisfied. The repository performance with the use of backfill is assumed to be no worse than that without backfill, and may be better. Therefore, it is concluded that, over the 10,000 year time frame, the performance of the repository with backfill will be satisfactory compared with the alternative hypothetical performance standards.

No less than a 50 percent probability of not exceeding a peak dose rate of 15 mrem/year when measured from a water well located 5 km from the repository. Over the 1,000,000 year time frame the CCDF, see Figure 5.2-57, shows a 50 percent probability of not exceeding a peak dose rate of approximately 18 mrem/year for the ACD case, and, as shown in Figure 5.2-59, a 50 percent probability of not exceeding about 4 mrem/year for the lineload case.

No less than a 90 percent probability of not exceeding a peak dose rate of 15 mrem/year when measured from a water well located 30 km from the repository. Over the 1,000,000 year time frame the CCDF, see Figure 5.2-27, shows a 90 percent probability of not exceeding a total peak dose rate of 3 mrem/year for the ACD case, and a 90 percent probability of not exceeding 0.8 mrem/year for the lineload case (Figure 5.2-59)

5.2.8.5 Summary of Repository Performance Compared to Various Standards

Table 5.2-9 summarizes the repository performance against the various standards discussed above, for both the ACD and lineload cases, with backfill. "N/A" in the table means that an assessment was not conducted for that case. However, estimates of performance are given assuming that performance would be no worse than for the comparable "no backfill" case.

Table 5.2-9 Summary of Long-Term Repository Performance Results (ACD/Lineload/Backfill) (mrem/year)

Time Frame (years)	Interim Postclosure Standard	Alternative Hypothetical Standards	
	15 mrem / 50% probability / 30 km	**15 mrem/ 50% probability / 5 km**	**15 mrem / 90% probability / 30 km**
10,000	ACD : N/A ($<<10^{-4}$) Lineload : N/A ($<<10^{-4}$)	ACD : N/A (<0.02) Lineload : N/A (<0.0004)	ACD : N/A (<0.003) Lineload : N/A (<0.0002)
1,000,000	ACD : 0.6 Lineload : 0.2	ACD : 18 Lineload : 4	ACD : 3 Lineload : 0.8

5.2.8.6 Cathodic Protection

The total system performance results presented thus far in Section 5.2.8 do not include any performance credit for the effect of cathodic protection on delaying or preventing corrosion of the waste packages, leading to slower failure of the waste packages. Additional WP failure analyses were conducted to determine the impact of 50 percent cathodic protection on the waste package failure. A discussion of cathodic protection was provided previously in Section 3.1.1.1, but will also be provided here for completeness. Cathodic protection is protection afforded a more-noble metal or alloy by the corrosion of a less-noble metal or alloy in electrical contact exposed to the same corrosive electrolyte. This protection can eliminate or delay attack of the more-noble material. The degree of protection is a function of the differences in nobility of the materials as measured, for example, by a standard galvanic series in sea water, and the relative surface areas of the coupled materials. Also important is the amount of polarization or passivation of the surfaces as corrosive attack progresses. The degree of protection is determined by performing prototypic tests involving material couples with the appropriate area ratios and electrolytes. There exists a significant literature database on cathodic corrosion. However, these data were collected in short-time tests mostly under sea water, simulated sea water, or sodium chloride solutions. [See the Degradation Mode Survey - Galvanic Corrosion of Candidate Metallic Materials for High-Level Radioactive Waste Disposal Containers.] No data are available on expected repository conditions. Testing is being initiated to evaluate cathodic protection under a range of expected conditions. The emphasis will be on couples between the carbon steel corrosion-allowance outer barrier and Alloy 625, a nickel-base corrosion-resistant inner barrier. Other couples will also be tested. In advance of these tests, an elicitation (CRWMS M&O 1995h) was conducted that identified 75 percent remaining area of the less noble, corrosion-allowance material needed for cathodic protection to be viable. However, 50 percent remaining area was selected as a starting point for future total system performance calculations and sensitivity studies. This leads to a significant delay in initiation of corrosion of the inner barrier, during which time the temperature of the waste packages diminishes. Figure 5.2-55 presents the failure curves for the case when the outer barrier of the waste package is assumed to cathodically protect the inner barrier until 50 percent of the outer barrier has corroded away. These results indicate a substantial improvement in the predicted lifetimes of the various waste packages. Thus, when corrosion of the inner barrier is initiated, it proceeds at a slower rate than if corrosion was initiated at earlier times and at higher temperatures.

Figure 5.2-60 presents the fraction of packages with a fully penetrating pit for the case of 26-yr-old BWR fuel in an ACD/backfill configuration as well as a 26-yr-old BWR fuel in a lineloading/backfill configuration, assuming either no cathodic protection or 50 percent cathodic protection. The comparison of results for no cathodic protection with the 50 percent cathodic protection failure curves demonstrate that the performance of the repository with cathodic protection will be significantly better over 10,000 years than the case without the cathodic protection assumptions (i.e., there will be no releases). Figure 5.2-61 shows the performance benefits of backfill used in conjunction with cathodic protection. Due to computer limitations, the simulations for this ACD/backfill were conducted in two individual RIP runs. The first run consisted of 26-yr-old BWR and 40-yr-old PWR WPs, and the second run consisted of DHLW, 26-yr-old PWR and 10-yr-old PWR WPs. Combining the second RIP run with the first would shift the first RIP run slightly to the right, closer to the "ACD/B/30 km" curve. These results indicate that the performance benefits of backfill are negligible if performance credit is already taken for cathodic protection. This is evident

if one compares the "ACD/NB/30 km/cathodic protection" curve in Figure 3.1-16 with the cathodic protection curves of Figure 5.2-61.

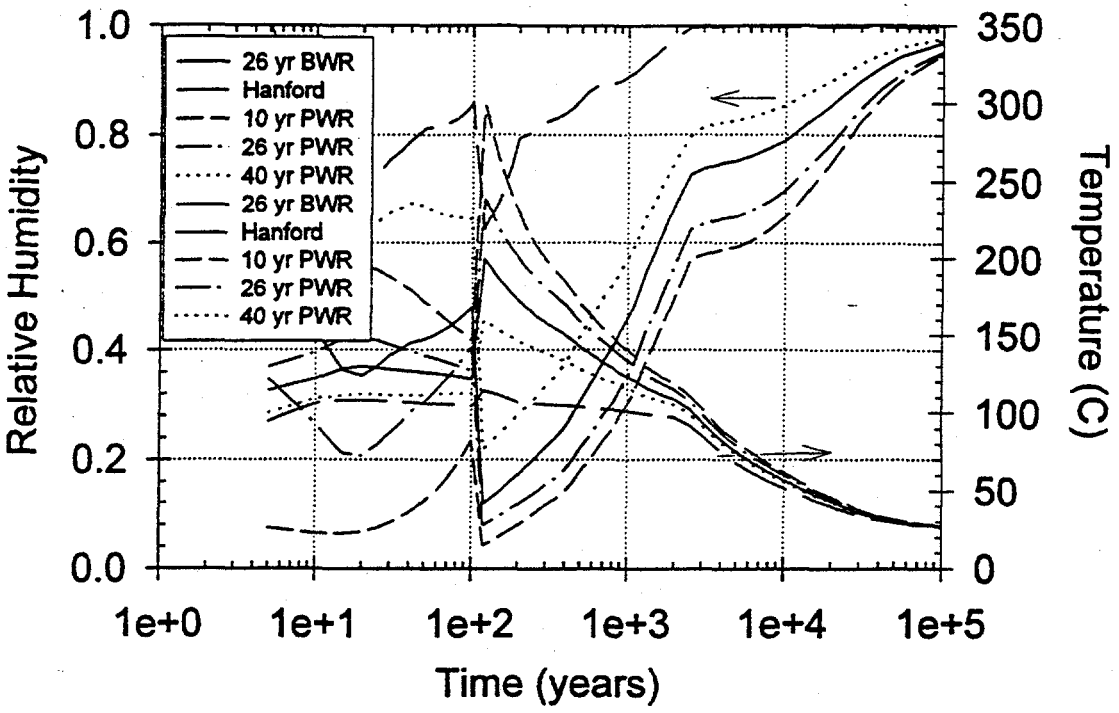

Figure 5.2-52 Temperature and RH on waste package surface for ACD, backfill case (partial level backfill)

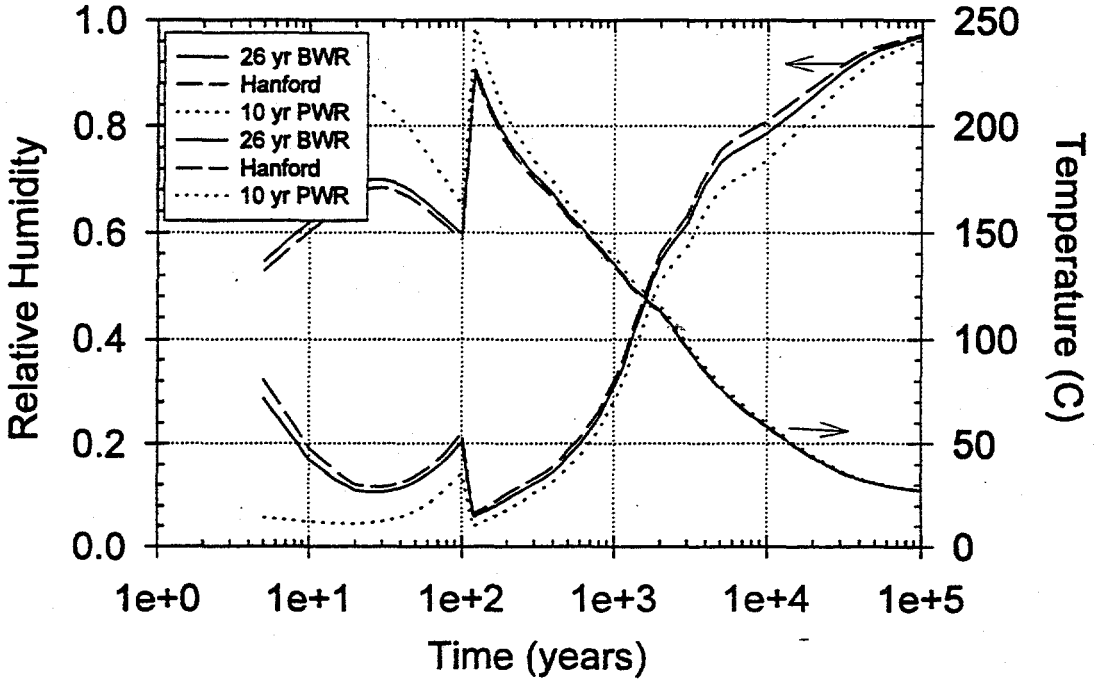

Figure 5.2-53 Temperature and RH on waste package surface for lineload, backfill case (partial level backfill)

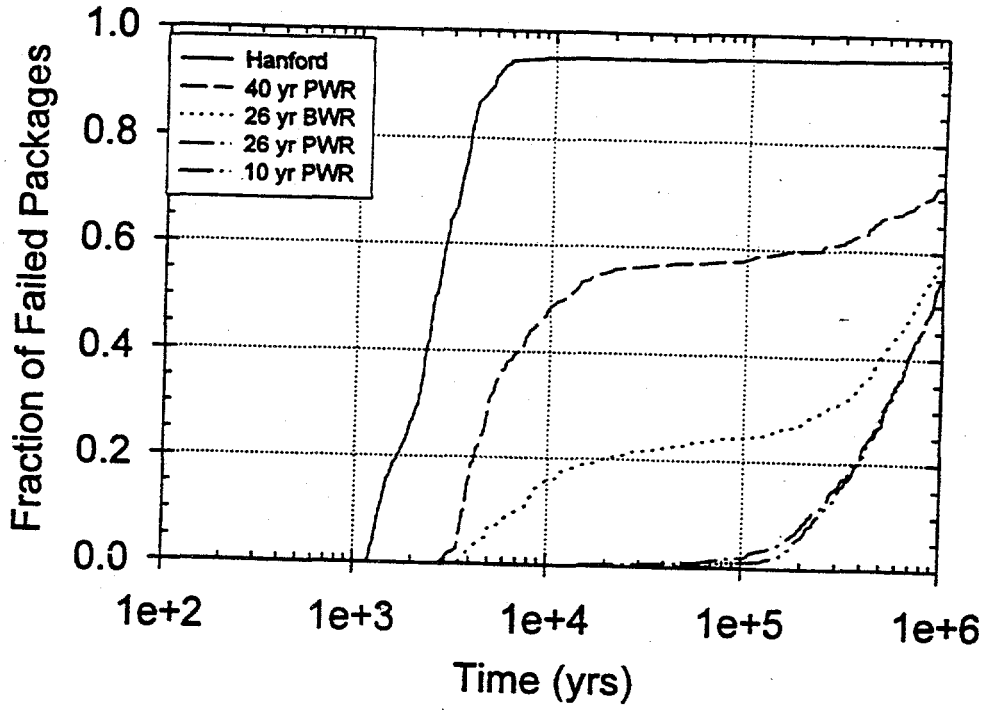

Figure 5.2-54 Waste package failure histories for ACD, backfill case (partial level backfill)

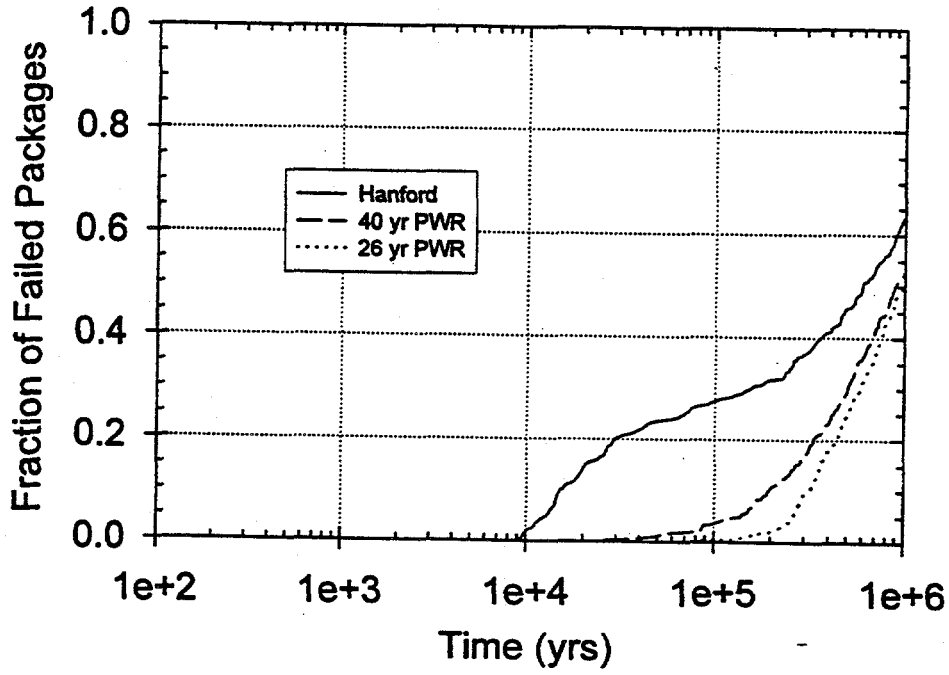

Figure 5.2-55 Waste package failure histories for ACD, backfill (partial level backfill) with 50% cathodic protection

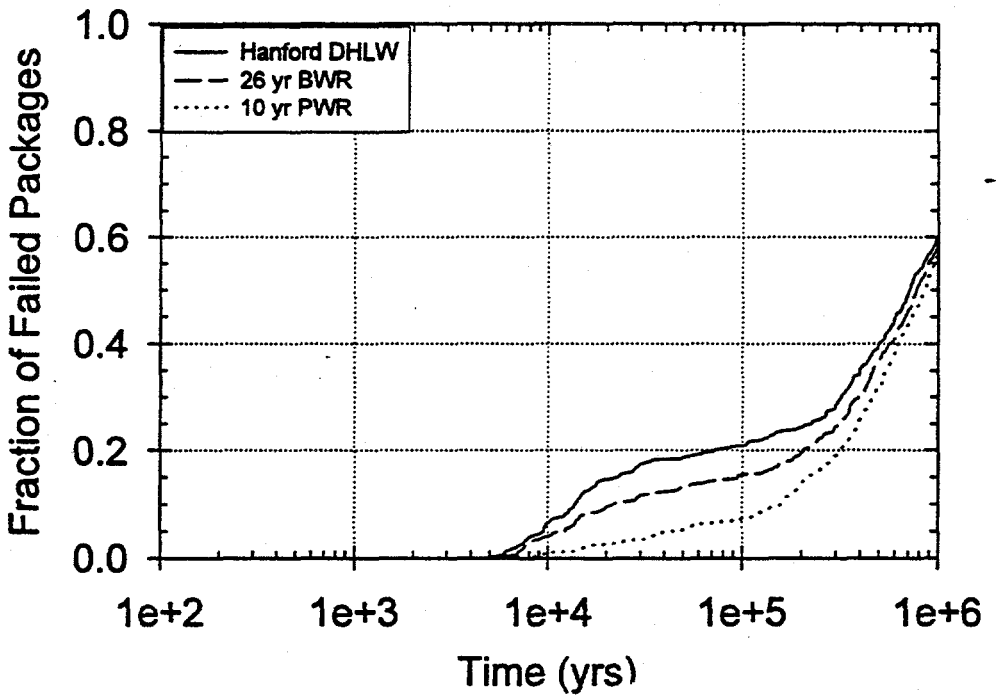

Figure 5.2-56 Waste package failure histories for lineload, backfill case (partial level backfill)

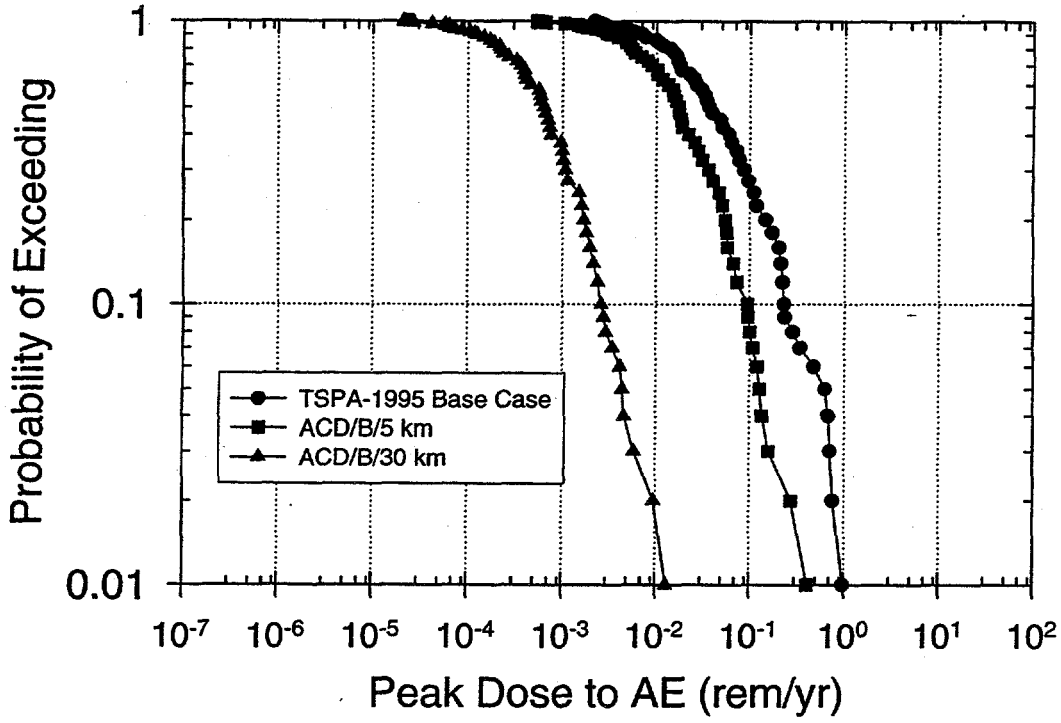

Figure 5.2-57 1,000,000 yr total peak dose CCDFs for ACD, backfill cases

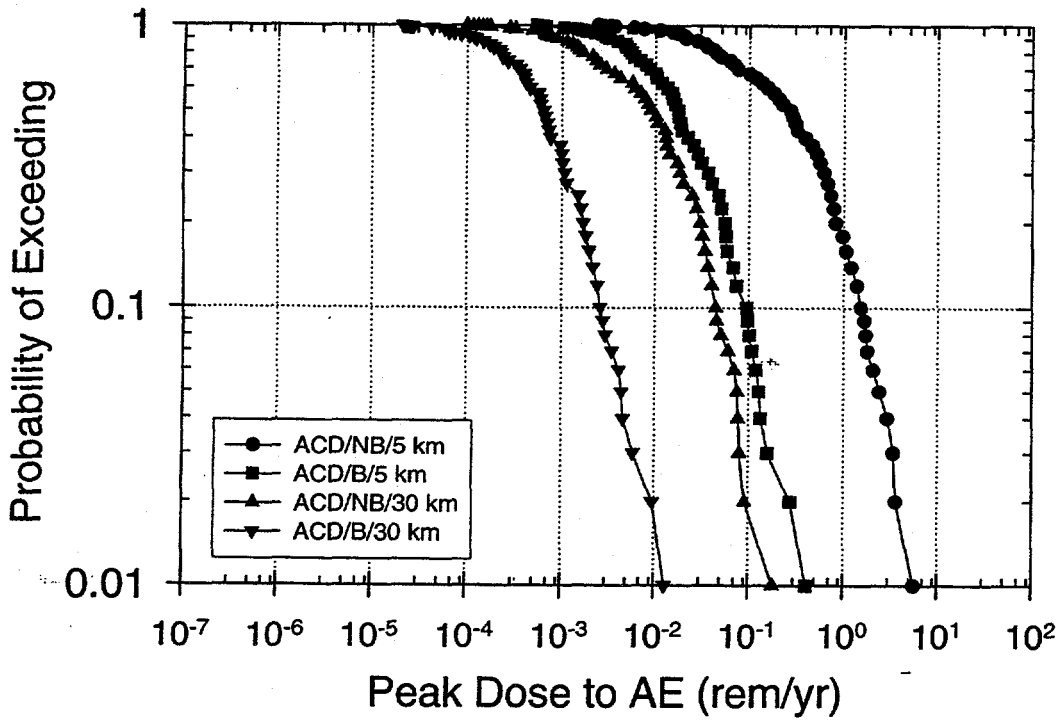

Figure 5.2-58 1,000,000 yr total peak dose CCDFs for ACD with and without backfill cases

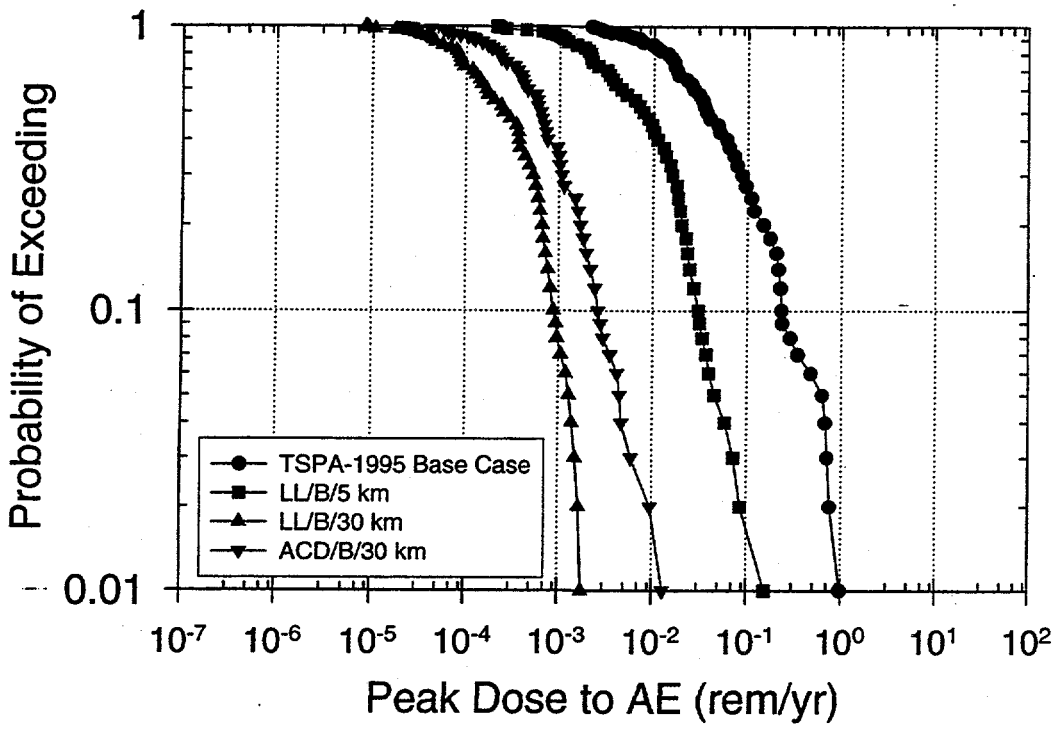

Figure 5.2-59 1,000,000 yr total peak dose CCDFs for lineload, backfill cases

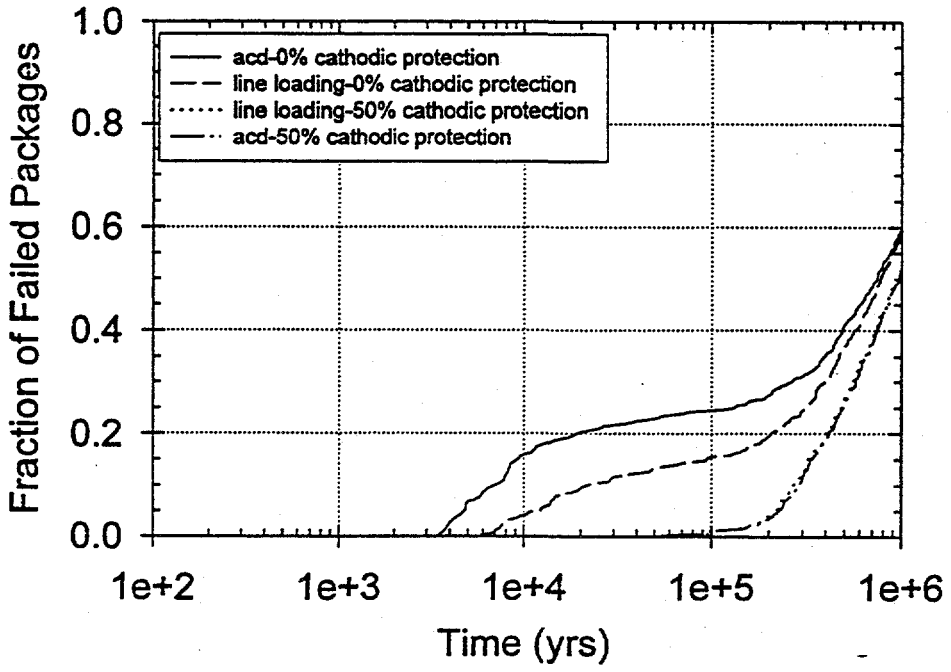

Figure 5.2-60 Waste package failure histories for 50% cathodic protection applied to ACD and lineload cases for 26-yr-old BWR WP

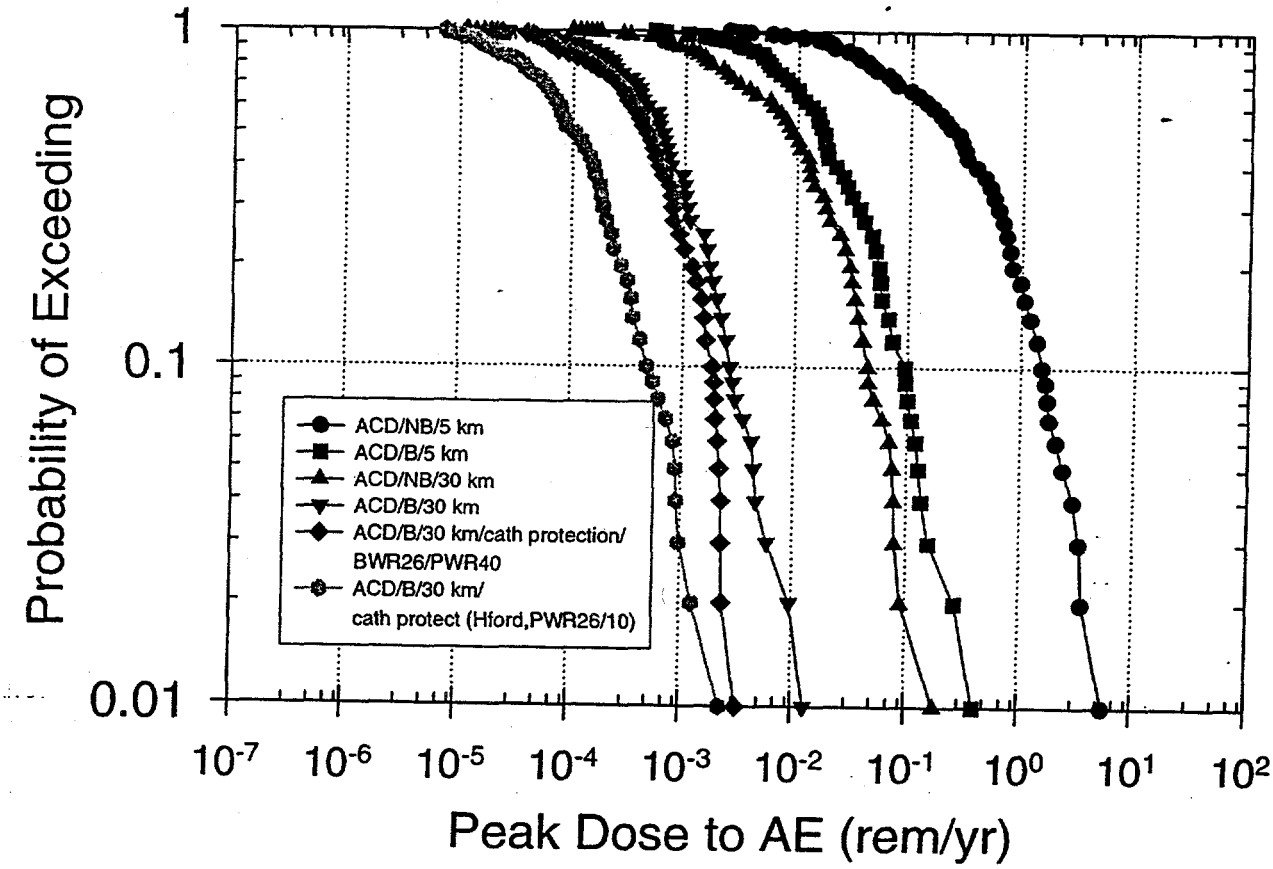

Figure 5.2-61 1,000,000 yr total peak dose CCDFs for ACD cases with and without backfill, for two defined accessible environments, and with and without 50% cathodic protection

5.2.9 COSTS AND SCHEDULE IMPACTS OF BACKFILL

The cost estimating methodology which was used for the ACD Report (CRWMS M&O 1996b) has also been used here. DOE Order 5700.2, *Cost Estimating and Standardization*, (DOE 1992), the DOE *Cost Estimating Guide* (DOE 1994a), and the DOE/Nevada *Cost Estimating Guide* (DOE 1993) provide the standards by which cost estimation is performed for the Yucca Mountain Site Characterization Project. These standards define the potential cost items and activities that are included in this report. The development of conceptual cost estimates for the implementation of labor, equipment, supplies, and materials are based on:

A. The *Cost Reference Guide for Construction Equipment* (CRG, 1994) which provides hourly operating costs on a wide range of construction equipment that has been adjusted to local conditions;

B. Specific pricing which has been obtained from equipment manufacturers inquiries; and

C. Inputs on labor rates, cost of materials, and sundry items by suppliers and ESF experience.

The primary costing categories in this report include Direct Costs (Labor, Equipment Operating, Supplies, Permanent Materials), Indirect Costs (Equipment Purchase), and Other Costs (Contingency, General and Administrative (G&A), and Fees for CRWMS M&O contractor support).

The cost estimates have been expressed in constant October 1995 dollars for each year in which the work is performed, spread over the years in which the costs will be incurred, and totaled for the duration of invert construction and backfill emplacement. In the "Other Costs" category, the 25 percent contingency is applied to the sum of capital and operating costs. The 20 percent CRWMS M&O G&A is applied to the sum of the capital cost, operating cost, and contingency. The 15 percent CRWMS M&O fees are applied to the sum of all of the above. See the example provided in Table 5.2-10.

The following determinations of costs attributed to backfilling of the emplacement drifts have been performed on the basis that the waste emplacement drifts are 5.5 meters in diameter, utilize railcar-mounted waste packages which are emplaced off-center in-drift, have a dual set of tracks, and require an invert which is 1.2 meters in depth at the center of the drift. At the time the ACD Report (CRWMS M&O 1996b) was being prepared, these features were required to accommodate the only practical means of backfilling that was available at that time. The total project costs for a repository with backfill (5.5 meter diameter waste emplacement drifts) and of a repository without backfill (5.0 meter diameter waste emplacement drifts) are compared in this analysis.

Cost estimates are provided in some detail for the ACD waste package spacing concept as described in the ACD Report (CRWMS M&O 1996b). For the lineload concept, in which waste packages are closely spaced such that there is only a 0.1 meter gap between adjacent packages, costs are estimated based on the information gained in conducting the ACD waste package spacing cost analysis. Detailed cost estimates (CRWMS M&O 1996h) have been developed and serve as a basis for the summary costs presented in this report.

It is important to note that the costs given in this report do not include performance confirmation costs. Performance confirmation costs associated with backfill could not be conducted in the FY 1996 *Performance Confirmation Concepts Study Report* (CRWMS M&O 1996j) since not enough information was available at the time to make defensible cost estimates. The following few paragraphs indicate the cost-relevant observations made by the *Performance Confirmation Concepts Study Report* with regard to emplacement drift backfill.

10 CFR 60.142(a) describes an in situ testing program used to assess the effects of backfill. This test is prescribed to start "During the early or developmental stages of construction..." Subsequently, 10 CFR 60.142(c) describes a "backfill test section" which is intended to "... test the effectiveness of backfill placement and compaction procedures..." This test, however, must only be completed "...before permanent backfill placement is begun." Two backfill tests are described, which may occur 90 years or so apart. The earlier test is likely to be conducted on a reasonably small scale (tens of meters) in a test alcove-type environment.

The second test is more for constructability, and will likely be conducted more on something approaching an emplacement drift scale (hundreds of meters). As noted, it does not need to be conducted until just prior to backfill placement. If emplacement drift backfill is utilized in the MGDS, it would not be emplaced until just prior to closure. This test would likely involve filling all or part of an empty emplacement drift to test the material handling equipment and concept.

The initial backfill test could be conducted in an alcove along the south ramp extension. It is assumed that an arrangement similar to that being used for the ESF heated drift would suffice for this testing activity. A "U" shaped alcove layout with one leg of the "U" serving as the backfilled drift and the other leg as the observation area should be adequate for the test. Heaters to simulate emplaced waste would be covered with backfill material. Instrumentation for data acquisition would be placed in the backfill and in boreholes drilled from the observation drift.

It is noted that the configuration and size of the testing areas described here are estimates made only for purposes of developing a feel for their associated construction costs and operational impacts. Additional input will be needed to produce complete testing configurations.

An estimate of the excavation required for this test area is approximately 100-130 meters of drift. The backfill test area will likely be driven to resemble the emplacement drift size and shape, while the balance of the drifting could be very similar to the ESF heated drift test access.

Data acquisition could be handled by either a local data logger which is downloaded on a regular basis, or by a permanently installed data acquisition, transfer and storage system. In either case, the information would be acquired and stored on-site and subsequently retrieved and transferred to the appropriate scientific personnel located off-site.

On-site scientific presence would be needed to monitor the test, and construction support would be needed to install the test initially and to assist with maintenance over the test duration.

If a decision is made to employ emplacement drift backfill, then performance confirmation costs would have to be developed.

5.2.9.1 ACD Waste Package Spacing

Repository Costs of 5.5 Meter Diameter Emplacement Drifts

The total construction cost of the repository as given in the ACD Report (CRWMS M&O 1996b) was $1,783,500,289. This cost covered both the development and emplacement phases of the repository for 5.0 meter diameter waste emplacement drifts. In the ACD, the CID, rail carrier mounted waste package emplacement mode was adopted. As was mentioned above, this method did not provide a favorable means of backfilling and so the off-center in-drift, rail carrier mounted waste emplacement mode was offered as means to overcome the difficulties to backfilling. The total construction cost of the repository for OCID waste emplacement is estimated at $1,899,738,588, or an increase of about $116,200,000.

Table 5.2-10 Example of Costs Breakdown

Cost Item	Costs ($M)		
	Capital & Operating	**Material**	**Total**
Capital	11.0		
Operating	69.1		
Material		68.6	
Subtotal	80.1	68.6	148.7
25% Contingency	20.0	N/A	
Subtotal	100.1	68.6	168.7
20% M&O G&A	20.0	13.7	
Subtotal	120.1	82.3	202.4
15% M&O Fees	18.0	12.3	
Subtotal	138.1	94.6	232.7

This cost differential of $116.2M does not include the costs associated with the actual backfilling of the emplacement drifts. These backfilling costs will be subsequently discussed, but first the costs associated with the OCID emplacement mode will be addressed.

The major differences between the CID and OCID emplacement mode cost estimates are derived from increasing the drift diameter, deepening the invert, and requiring a second track for each waste emplacement drift. By changing these aspects of the waste emplacement drifts, five cost centers are affected including excavation of the waste emplacement drifts, placement of the inverts and finishing the waste emplacement drifts, disposal of the rock debris, surface crushing of the invert material, and

capital expenditure for equipment. A comparison of the cost centers for the two estimates is shown in Table 5.2-11.

The invert for both the 5 meter and 5.5 meter diameter drifts are costed for tuffaceous material without additives. The cost differences as related to the invert impact to some degree all the above cost centers except excavation.

Table 5.2-11 Effects of Emplacement Drift Diameter on Total Construction Costs

Cost Center	Cost ($M)		
	5.5 m ϕ Drift	5 m ϕ Drift	Difference
Excavation	295.3	276.2	19.1
Invert and Drift Finish	254.6	205.4	49.2
Rock Debris Disposal	27.7	26.6	1.1
Surface Crushing	5.2	4.3	0.9
Equipment Capital Cost	118.0	117.4	0.6
Cont., G&A, Fees	650.9	605.6	45.3
Other common costs	548.0	548.0	0.0
Total Estimated Cost	1,899.7	1,783.5	116.2

Schedules Associated with Backfilling

For the windrow stowing method, a stowing rate of 75 m^3/hr per stowing unit has been calculated. Given this rate, and assuming the use of two stowing units, an estimated eight years would be required to complete backfilling of the emplacement drifts. For the side-to-side stowing method, a reduced stowing rate of 68 m^3/hr per stowing unit has been calculated. Assuming the use of two stowing units, an estimated twelve[1] years would be required to complete backfilling of the emplacement drifts. The reduced production rate is explained by the stop-and-go manner of backward advance by each stowing unit for side-to-side stowing while windrow stowing continues non-stop backfilling from one end of the typical waste emplacement drift to the other.

[1]An estimate of ten years was provided in the ACD Report (pg 8-304, CRWMS M&O 1996b) and was based on a two shift-per-day operation at 2000 hours per year per shift. This amounts to 4000 hours per year. In Nevada, however, only 3250 hours per year is allowed, so the estimate of total time required to backfill the emplacement drifts was increased accordingly.

Costs of Backfilling with TSw2 Tuff

The cost estimate for crushed tuff has been prepared for both windrow stowing and side-to-side stowing. The windrow stowing is representative of the sloping partial backfill, and the side-to-side stowing represents level partial backfill. Detailed cost elements have been summarized in Tables 5.2-12 and 5.2-13. Both tables have been structured to show the following:

A. Capital Cost. The initial capital investment for equipment occurs at the onset of backfilling operation for the complement of equipment required. Replacement cost is shown to indicate the magnitude of equipment items that are replaced before the end of backfilling. For windrow stowing, five batteries for 25 ton locomotives are replaced during the third, fifth, and seventh year at a total cost of $160,630 per year of replacement. In side-to-side stowing the same replacement is extended into the ninth and eleventh year with all other equipment components replaced in the ninth year. Note that for windrow stowing backfilling is completed prior to the ninth year and major recapitalization is not required.

B. Operating Cost. Labor, equipment, and supplies are consistent for a seven year period with a one year lead-in for windrow stowing while side-to-side stowing will have ten years of consistent costs, a one year lead-in, and a one year step-down to complete backfilling operations.

C. Material Cost. No acquisition expenses will be incurred with the use of crushed tuff. All material handling costs, including crushing and screening, are included as operating cost items.

D. Other Costs. Contingency is applied to the sum of capital and operating costs. CRWMS M&O G&A is applied to the sum of the capital cost, operating cost, and contingency. CRWMS M&O fees are applied to the sum of all of the above.

Table 5.2-12 Wind Row Backfilling Costs With Crushed TSw2 Tuff

Capital Equipment Cost			**Total**
• Initial • Replacement			$ 8,070,507 481,890 **$ 8,552,397**
Operating Cost‡	**Year 2110**	**Years 2111-2117***	
• Labor • Equipment & Supplies	$ 492,086 420,459 $ 912,545	$ 6,151,060 5,265,884 $ 11,416,944	$ 55,021,605 25,809,548 **$ 80,831,153**
Material Cost			
Crushed Tuff	$ 0	$ 0	**$ 0**
Other			
• 25% Contingency • 20% M&O G&A • 15% M&O Fees			$ 22,345,888 22,345,888 20,111,299 **$ 64,803,075**
Total			**$154,186,625**

* Cost per year
‡Total Calculated Backfill Volume: 1,869,986 m^3 (sloping partial backfill)

Table 5.2-13 Side-to-Side Stowing with Crushed TSw2 Tuff

Capital Cost				Total
Tuff Only Total • Initial • Replacement Total Capital Cost				$ 8,070,507 7,287,358 **$ 15,357,865**
Operating Cost‡	Year 2110	Years 2111-2120*	Year 2121	Total
Labor, Equipment, and Supplies	$ 1,321,560	$ 11,401,710	$ 4,337,884	**$ 119,676,544**
Material Cost				
Crushed Tuff	$ 0	$ 0	$ 0	**$ 0**
Other				
• Contingency • M&O G&A • M&O Fees				$ 33,758,602 33,758,602 30,382,742 **$ 97,899,946**
Total				**$232,934,355**

* Cost per year
‡Total Calculated Backfill Volume: 2,496,664 m^3 (level partial backfill)

Costs of Backfilling with Quartz Sand

In this section costs are indicated for a backfill material composed solely of quartz sand which is stowed either in a continuous windrow or stowed across the drift in sweeping side-to-side placement. General size distribution of particles is assumed to be included within a range that passes a #14 U.S. Standard screen and is retained on a #200 screen; that is, 1.19 mm to 0.074 mm. Except for minor variations, cost estimates for quartz sand only and for crushed tuff only are similar. The appropriate adjustments include:

A. Deletion of crush/screen plant capital and operating costs and crusher liner operating costs from the Tuff Only estimate.

B. Addition of washed quartz sand to the Tuff Only estimate.

The crushed tuff only cost estimate totals as shown in Tables 5.2-12 and 5.2-13 have been carried over into Tables 5.2-14 and 5.2-15, respectively, and adjusted as indicated above.

Summary

Table 5.2-16 summarizes the additional estimated repository costs for backfilling. Additional repository costs of developing a repository with 5.5 meter diameter emplacement drifts, rather than 5.0 meter diameter drifts, is estimated to be $116.2M. The cost of conducting side-to-side stowing of backfill is greater than the windrow stowing costs because of the additional backfill material used and the additional time required to conduct the backfilling of the emplacement drifts.

Table 5.2-14 Wind Row Backfilling Cost with Quartz Sand

Capital Equipment Cost			**Total**
Tuff Only Total			$ 8,552,397
Crush/Screen Plant			
• Initial			(-) 291,685
• Replacement			0
Adjusted Capital Cost			**$ 8,260,712**
Operating Cost	Year 2110	Years 2111-2117*	
Total Labor, Equip., Sup'l	$ 912,545	$ 11,416,944	$ 80,831,153
Crush/Screen Plant	(-) 22,726	(-) 284,072	
Crusher Liner	(-) 12,864	(-) 163,176	
Adjusted Operating Cost	$ 876,955	$ 10,969,696	**$ 77,664,827**
Material Cost			
Quartz Sand	$ 731,876	$ 9,283,612	**$ 65,717,160**
Other			
• 25% Contingency			$ 21,481,385
• 20% M&O G&A			34,624,817
• 15% M&O Fees			31,162,335
			$ 87,268,537
Total			**$238,911,236**

* Cost per year

‡Total Calculated Backfill Volume: 1,869,986 m^3 (sloping partial backfill)

Table 5.2-15 Side-to-Side Backfilling Costs with Quartz Sand

Capital Cost				Total
Tuff Only Total				$ 15,357,865
Crush/Screen Plant				
• Initial				(-) 291,685
• Replacement				(-) 240,032
Adjusted Capital Cost				**$ 14,826,148**
Operating Cost	Year 2110	Years 2111-2120*	Year 2121	Total
Tuff Only Total	$ 1,321,560	$ 11,401,710	$ 4,337,884	$ 119,676,544
Crush/Screen Plant	(-) 32,953	(-) 284,072	(-) 88,631	
Crusher Liner	(-) 17,181	(-) 147,942	(-) 46,166	
Adj. Operating Cost	$ 1,271,426	$ 10,969,696	$ 4,203,087	**$ 115,171,473**
Material Cost				
Quartz Sand	$ 977,109	$ 8,413,791	$ 2,625,589	**$ 87,740,604**
Other				
• 25% Contingency				$ 32,499,405
• 20% M&O G&A				50,047,526
• 15% M&O Fees				45,042,774
				$127,589,705
Total				**$345,327,930**

* Cost per year

‡Total Calculated Backfill Volume: 2,496,664 m^3 (level partial backfill)

Table 5.2-16 ACD Waste Package Spacing - Additional Costs and Total Repository Costs of Construction and Backfilling Emplacement Drifts (in Millions of Dollars)

	Backfill Stowing Method			
	Wind Row (Sloping Partial Backfill)		Side-to-Side (Level Partial Backfill)	
	Crushed Tuff	Quartz Sand	Crushed Tuff	Quartz Sand
5.0 m diameter to 5.5 m diameter emplacement drifts	$116.2M	116.2	116.2	116.2
Stowing	154.2	238.9	232.9	345.3
Total Additional Costs	270.4	355.1	349.1	461.4
Other Costs of Construction	1783.5	1783.5	1783.5	1783.5
Total Repository Costs	2053.9	2138.6	2132.6	2244.9

5.2.9.2 Lineload Concept

The aforementioned backfilling methods have all utilized a waste emplacement spacing which averages 12.76 m, centerline to centerline of waste packages, as stated in the ACD Report (CRWMS M&O 1996b). Lineloading would position the waste packages nearly end-to-end with as little as a 0.1m gap between each waste package, which equates to a LML of 1.11 MTU/meter. The impacts of such an option would include reducing the required underground drift development and backfilling quantity. The estimated backfill quantity would be reduced from 1.87 million m^3 (see Table 5.2-14) to about 0.72 million m^3 for backfilling in a windrow, or a reduction of 61.5 percent. For side-to-side stowing, the estimated backfill quantity would decrease from 2.5 million m^3 (see Table 5.2-15) to 0.96 million m^3.

Lineloading is estimated to reduce backfilling costs for quartz sand stowing in windrows from $238.9M to $88.4M and for side-to-side stowing from $345.3M to $138.1M. Also, backfilling costs for crushed TSw2 tuff stowing in windrows are estimated to be reduced from $154.2M to $57.1M, and for side-to-side stowing from $232.9M to $93.2M. The construction cost of a repository with 5.0 m diameter emplacement drifts, assuming lineloading of waste packages, is estimated to be $1,065M. This estimate is $719M less than that given for the ACD repository with 5.0 m diameter emplacement drifts. The construction cost of a repository with 5.5 m diameter waste emplacement drifts is estimated to be $1,105.2M. This estimate is $794M less than that given for the ACD repository with 5.5 m diameter emplacement drifts.

Summary

Table 5.2-17 summarizes the total repository costs associated with backfilling in a lineload scheme.

Table 5.2-17 Lineloading - Total Repository Costs of Construction and Backfilling Emplacement Drifts (in Millions of Dollars)

	Backfill Stowing Method			
	Wind Row (Sloping Partial Backfill)		Side-to-Side (Level Partial Backfill)	
	Crushed Tuff	Quartz Sand	Crushed Tuff	Quartz Sand
Total Repository Costs	$1162.3	$1193.6	$1198.4	$1243.3

5.2.10 UNCERTAINTIES AND RISKS ASSOCIATED WITH BACKFILL

Several areas of uncertainty have been identified with the use of emplacement drift backfill. They are:

Backfill Thermohydrologic Results. The near-field thermohydrologic results presented in Section 5.2.5 for backfill are recently obtained results that have not yet been independently verified. The impact of emplacement drift backfill on waste package performance, and thus total system performance, is inextricably tied to these results. Therefore, as (or if) this analysis matures, an examination of its effects on waste package and total system performance should be conducted.

Microbial-Influenced Corrosion. Probably the least-examined area of investigation is the effect backfill may have in producing conditions such as microenvironments in which crevicing or pitting can occur, and in the development of a substrate for the migration and re-entry of microbes once conditions are favorable. MIC occurs due to the metabolic activity of micro-organisms. The micro-organisms usually work synergistically to create an environment in which they can grow. This requires a combination of moisture, a suitable substrate, and a source of energy. The energy is derived from electrochemical reactions which are similar to aqueous corrosion cells. Thus, when the repository is hot and dry, MIC is not possible. Existing microbes in the crushed tuff backfill or invert will die or go dormant as they are dried out with decay heat. However, when the repository cools and the relative humidity rises, these existing or new airborne microbes may colonize and grow. The microbes create a biofilm that can contain both anaerobic and aerobic bacteria. The anaerobes, such as sulfate reducing bacteria, attack the corrosion-allowance carbon steel outer barrier. The conditions that will allow MIC to occur are similar to those that are conducive to aqueous corrosion - temperatures below boiling and relative humidities above about 60 percent. Although the extent to which MIC can influence waste package lifetimes is currently not well known, indications are that micro-organisms may indeed have a detrimental effect on waste packages (Horn and Meike, 1995).

Long-Term Settlement. The thermohydrologic benefits of backfill are dependent on the amount of backfill surrounding the waste packages, as discussed in Section 5.2.5 of this report. What is currently not known is the effect that long-term settlement of the backfill will have on the thermohydrology near the waste package, and thus waste package performance as well as long-term repository performance.

5.2.11 CONCLUSIONS

The efforts conducted within this study indicate that the use of emplacement drift single-layer backfill is an engineering feat that appears to be technically feasible at this point in time, which is more than 100 years prior to when backfilling would actually occur.

There are promising performance benefits associated with backfill, and there are fewer issues associated with the backfilling of waste packages when spaced as described in the ACD Report (CRWMS M&O 1996b) than are associated with the lineload concept. However, the apparent cost and performance advantages of the lineload concept are attractive enough to warrant additional analyses to better assess the impacts of very closely spaced waste packages on the drift wall temperature and SNF cladding criteria.

Given our current conceptual models of both the EBS and the NBS, it is clear that the use of emplacement drift backfill is unnecessary if repository performance is assessed over 10,000 years. The repository performance is currently estimated to easily satisfy the assumed performance standard, without need for any additional performance barriers beyond the waste package.

Over the 1,000,000 year time frame, repository peak dose rates are improved by about an order of magnitude when backfill is employed. Further, the use of backfill aids in allowing the repository to satisfy all of the performance criteria delineated in the alternative hypothetical standards. As indicated in Table 3.1-4, without the use of backfill two of the alternative hypothetical standards is violated over the 1,000,000 year time frame.

5.3 CHEMICALLY TREATED BACKFILL

5.3.1 INTRODUCTION

Section 5.1, which conducted a preliminary performance assessment of some potential EBS functions, indicated that there could be significant benefits in performance by delaying initiation of corrosion. Figures 5.1-15 and 5.1-16 show, depending on the amount of credit taken for cathodic protection, that perhaps only a relatively short period of time in delaying corrosion initiation is required to see large improvements in total system performance. The significant improvement in waste package performance results because the WPs are thermally much cooler after several thousand years and so when corrosion is initiated the temperature-dependent corrosion rates (see Appendix B, "Additional Details of Waste Package Degradation Simulation") are much less and more time is required to breach the WPs.

The primary focus of this section is to provide information on the effectiveness of specific backfill formulations for chemical conditioning of the waste package environment . The purpose has been

to determine whether the material options will provide the desired design effect and for how long. The option under consideration is intended to have a twofold effect: first, to reduce oxygen in the waste emplacement drift, thereby reducing corrosion rates, and second, to increase pH which would provide a beneficial environment for certain waste package materials at some later time (e.g., mild steels). The merits of this chemical conditioning option need to be considered from both a microbial point of view, and from the point of view of the waste form. The material options presently under consideration are combinations of metallic iron (to control oxidation potential), lime (to control pH), and quartz sand (because of its thermohydrologic benefits). The modeling effort is intended to provide insight into the long term evolution of the backfill through a given thermal and relative humidity history which are based on hydrological modeling.

The simulations that have been conducted to date have examined the following backfill options: 1) iron metal only, 2) iron metal and lime, and 3) iron metal, lime and quartz sand, in equal volume ratios. Each of the backfill options was simulated under two environments, that for which air exchange with the atmosphere is limited and that for which air exchange is unlimited. The geometry of the backfill is such that it completely covers the canister but does not completely fill the drift. It should be noted that this set of chemical simulations is not to be taken as "realistic" or "conservative," but rather as a tool for determining whether a specific concept (chemically treated backfill) is worth pursuing further. Note that these simulations do not consider the impacts of microbial activity. Although the chemical models used in these simulations apply to saturated systems, the results can also be applied to scenarios in which liquid water is present. This could therefore apply to chemical processes within a water film, or situations in which saturated steam is present. The simulations conducted using these modeling codes are limited by the absence of high quality data for a number of amorphous and crystalline phases in the Ca- Si - H_2O system that may be involved in the chemical processes under consideration. These phases occur in situations where the concentration of Ca is high with respect to Si. Many of these phases are sensitive to CO_2 partial pressure, and may form a range of calcium carbonate and hydrous calcium silicate phases as well as silica polymorphs. The ability to model chemistry in the absence of data for these phases is limited and may affect the simulation of scenarios for high lime content backfill.

The results of the simulations suggest that the most important variable in the chemical conditioning effect is the amount of air exchange that occurs in the emplacement drift. The desired chemical conditioning (both oxidation potential and pH) will be far less effective in an emplacement drift that experiences an unlimited exchange of air with the atmosphere. In fact, the simulations conducted demonstrate that a backfill composed of quartz sand, magnetite, and lime will not control oxygen fugacity or pH unless the drifts are completely sealed. Even then, the chemical conditioning effects would be minor, and would probably not achieve the engineering goals. A candidate backfill should be further tested over prolonged periods of time and various temperature gradients. However, the simulations conducted here are sufficient to demonstrate that this backfill option does not sufficiently improve the robustness of the repository concept to warrant further consideration. All of the chemical evolutions shown here, including the desired chemical conditioning, takes place and are expended within a matter of decades, which is a significantly shorter time frame than that determined in Section 5.1.1 to be needed to have any effect on total system performance.

5.3.2 COMPUTER MODELS EMPLOYED

5.3.2.1 EQ3/6

The EQ3/6 geochemical modeling package is a first principles chemical modeling package which uses a database of fundamental thermodynamic parameters, and user-supplied reaction rate parameters to describe the chemical evolution of a system. The output of the simulations are pH, Eh mineral assemblages, and water chemistry (chemical speciation), as a function of time (reaction progress). These simulations provide important information to establish:

- Whether the desired conditioning effect is achieved during the approach to steady state (transient), steady state, or equilibrium conditions.

- The mechanisms responsible for contrasts in chemical properties of different systems (e.g. why pH differences are observed between "fixed" fO_2 / fCO_2 and " unfixed" fO_2 /fCO_2 cases), and

- Steady state conditions between the water chemistry and solid phase assemblage, which represents an "endpoint" for the evolution of the system.

Physically, the exposure of the waste packages to oxygen and other atmospheric gases is limited by two possibilities. Either the drifts are ventilated by an engineered ventilation system or naturally through rock fractures, or the drifts are unventilated. The implication of this distinction is profound because it means the distinction between a system in which the gas composition and fugacities remain constant over time, and a system in which the gas composition evolves. These physical possibilities are simulated by setting two modeling options. First, the system parameters are set using the terminology "open" and "closed", implying that precipitated minerals do not remain in the system in the former case or remain in the system and continue to react with the aqueous phase in the latter case. Second, the gas fugacity parameters are set as either "fixed", which means the fugacity remains constant throughout the simulation (equivalent to a ventilated system) or "unfixed," which allows the fugacities to evolve over time.

The results of the EQ3/6 simulations are used to select the significant chemical properties of the system. These properties are then used in the OS3D/GIMRT reactive transport code, which has simplified chemical modeling capabilities.

5.3.2.2 OS3D/GIMRT

The OS3D/GIMRT reactive transport package is a first principles reactive transport code (Steefel and Lasaga, 1994; Steefel and Yabusaki, 1995) that simulates chemical changes in an aqueous fluid as it moves through a porous medium. It also determines the evolution of mineralogy and porosity as the aqueous fluid reacts with the porous medium, thus providing a model of the time-dependent evolution of the flow field. As mentioned above, the simulations rely on first principles chemical modeling (e.g., EQ3/6) for the selection of appropriate input parameters. The output of the simulations shows spatial and temporal chemical and mineralogical changes due to the reactive transport of water through a saturated permeable material. Spatial simulation shows reaction fronts and time sequence evolution

as a function of flow rate, thermal gradient, and water chemistry. The formation of a crust may have a great impact on hydrology. This is not shown in these simulations and depends on grain size, ratio of the components, and reaction rates.

In general, it is possible to recognize three distinct regions of chemical evolution that are illustrated by the cartoon representation in Figure 5.3-1. The three regions are: the initial condition (represented in light gray), the input condition (represented in dark gray), and the transition zone, (which with time moves through the system and is represented in black). It is important to note that the transition zone itself evolves toward a stable (mature) chemical profile over time. The length of the transition zone and the speed at which it travels through the system depend on infiltration rate and water chemistries. This simple visualization demonstrates that understanding the chemical process responsible for the conditioning effect is fundamental to determining its timing and its potential duration. Clearly, if the chemical effect occurs within the transition zone, then the engineering objective would be to make the transition zone as wide as possible and move it as quickly as possible to contact the waste package (at 1.0 m). If the chemical conditioning effect occurs within the initial state, then the object would be to slow the rate of the transition zone movement to the extent possible.

5.3.3 SIMULATION STRATEGY

A complete analysis of the chemical conditioning effects of candidate backfill materials involves a series of simulations that test a number of composition parameters over a range of temperatures, grain sizes, and water chemistries. Ideally, one would pursue a simulation strategy in which the overall chemical characteristics of selected systems would be defined using EQ3/6, which would establish the detailed chemical behavior of the system in the absence of fluid flow. The chemical characteristics that should be most thoroughly considered would be the ability of the Fe-phase to maintain low oxygen partial pressures, the ability of the CaO-phase to buffer the pH at high values, the impact of interactions between the backfill components on the overall buffering capacity, as well as the sensitivity of the backfill system to the degree of drift ventilation.

Information developed through these simulations would then be used to select the significant chemical species to be considered in simulations that account for the effects of fluid flow, and the simulations would be carried out using the OS3D/GIMRT reactive transport code package. The results of these simulations would define the spatial distribution of reaction fronts, fluid chemistries, and steady state conditions as a function of time. A thorough analysis of reactive transport would include simulations of at least two flow rates and two thermal gradients, for one selected water chemistry, and one flow rate and one thermal gradient for the other two waters. Sensitivity studies are required for physical variables such as particle size and porosity, as well as variations in the proportion of backfill components. Ultimately, this information would establish the extent to which the conditioning goals would be met for a given backfill emplacement scenario.

For a complete parametric analysis, several fluid chemistries that could be considered include 1) J-13 water, which is a naturally occurring dilute, bicarbonate water that has chemical characteristics which approximate those of waters in contact with tuffs similar to those of the proposed repository horizon, 2) water that equilibrates with concrete, which was selected based on the possibility that concrete may be a common material used within emplacement drifts, and 3) a brine equilibrated with concrete,

which was considered, based on the possibility that salts and carbonates of various chemical elements are expected to be deposited in the vicinity of emplacement drifts, as a result of evaporation and boiling of pore waters during the heating phase of the repository.

Table 5.3-1 is a summary of all of the cases described above. Since not all of the 28 delineated cases could be conducted, a carefully chosen subset of the cases was employed to establish the functional usefulness of the selected backfill chemical composition. Those cases investigated are indicated by an asterisk in the table.

Table 5.3-1 Compete List of Simulation Conditions

Chemical System and Water Type	O_2 and CO_2 Uncontrolled	O_2 Fixed at Atmospheric Value, CO_2 Uncontrolled	O_2 and CO_2 Fixed at Atmospheric Values	O_2 Fixed at Atmospheric Value, CO_2 Fixed at High Value
Fe° or Magnetite				
J-13 Water	X*	X*	X	X
Concrete Water	X	X	X	X
Fe° or Magnetite				
J-13 Water	X*	X*	X*	X
Concrete Water	X	X	X	X
Fe° or Magnetite + CaO + SiO_2				
J-13 Water	XO*	XO*	XO*	XO
Concrete Water	XO	XO	XO	XO
Concrete Water + Brine	XO	XO	XO	XO

EQ3/6 run - X
OS3D/GIMRT run - O
cases actually run - *

5.3.3.1 Completed EQ3/6 Simulations

The EQ3/6 simulations were conducted in three parts (Table 5.3-2). The first part was conducted to test aspects of fO_2 conditioning. The simulated system consisted of a solid Fe species (Fe^0, magnetite) and J13 water. Each case was simulated for both fixed and unfixed fO_2 cases and at a constant temperature (90°C). No significant difference was observed between simulations using magnetite and those that used Fe^0. However, differences in reaction rates suggest that the chemical system would evolve at slightly different rates. In addition, the thermodynamic database (Table 5.3-2) appears to contain data for the relevant oxides and hydroxides of iron found in corrosion experiments. Thus, barring redox scenarios that cannot be simulated at this time, it is concluded that the Fe^0 simulations are relevant to both elemental iron and magnetite bearing backfill, and so the magnetite case was omitted in the remaining simulations. The second part consisted of a sensitivity study of the system with respect to fCO_2. The simulated system consisted of solid Fe^0 and CaO, in a molar ratio of 1:1, and J13 water. In this case, a simulation in which both fCO_2 and fO_2 were fixed was compared to a simulation in which both were unfixed. In the third part of the EQ3/6 simulation exercises, the complete matrix of fO_2 and fCO_2 values, and J13 water was tested for a molar ratio of 80 : 15 : 5 quartz sand, Fe^0, and lime, respectively.

The following set of assumptions were made for the EQ3/6 computations:

- all backfill materials are 7/16 in. diameter,
- 40 percent porosity,
- calculated cross section for backfill model = 3.1138 m^2 (using angle of repose geometry, and subtracting invert and WP), and
- a backfill volume = 7.78×10^5 m^3 was calculated using the cross section above and an estimated length, L = 2.5×10^5 m (Sassani, 1995), for estimating surface area.

Table 5.3-2 Data for Solid Fe Phases Contained in the Thermodynamic Database

Mineral Name	Chemical Formula	Reaction	Temperature Range
iron	Fe^0	$Fe^0 + 2H^+ + 0.5\ O_{2(g)} <=> Fe^{++} + H_2O$	all
iron	$Fe(OH)_2$	$Fe(OH)_2 + 2H^+ <=> Fe^{++} + 2H_2O$	all
iron	$Fe(OH)_3$	$Fe(OH)_3 + 3H^+ <=> Fe^{++} + 3H_2O$	all
iron	FeO	$FeO + 2H^+ <=> Fe^{++} + H_2O$	all
goethite	FeO(OH)	$FeO(OH) + 3H^+ <=> Fe^{+++} + 3H_2O$	0 - 200°C
hematite	a - Fe_2O_3	a - $Fe_2O_3 + 6H^+ <=> 2Fe^{+++} + 3H_2O$	all
magnetite	Fe_3O_4	$Fe_3O_4 + 8H^+ <=> Fe^{++} + 2Fe^{+++} + 4H_2O$	all
wustite	$Fe_{0.9478}O$	$Fe_{0.9478}O + 2H^+ <=> 0.106Fe^{++} + 0.841Fe^{+++} + 4H_2O$	all

5.3.3.2 Completed OS3D/GIMRT Simulations

Unidimensional OS3D/GIMRT simulations were run using an initially saturated system 1.0 m in length. The conditions defined for the simulations were as follows: 1) the water composition of the initial system was given a very low ionic strength, 2) the speciation of this water was calculated using EQ3/6 to approximate a water composition that was as close as possible to equilibrium with the initial backfill composition; however, given that the phases themselves are not in equilibrium, especially in the presence of water, the mineral assemblage that has not contacted J13 water evolves over time, and 3) J13 water, initially introduced into the first 0.2 meters of the system is allowed to flow further into the system at a given infiltration rate (10 mm/yr).

The resultant qualitative picture of reactive transport develops. Backfill exposed to both J13 water and low ionic strength water evolves toward a steady state, but not necessarily along the same chemical path or toward the same mineral assemblage endpoint. Between the two water chemistries is an active reaction zone, which itself evolves to a mature state with a stable chemical profile. This reaction zone is mobile and moves through the system and ultimately disappears at the outlet (1.0m). Clearly, a waste package located at the outlet will experience different chemistries through time. Spatial simulations, showing reaction fronts, and time simulations have been conducted for a single flow rate and a constant temperature (90°C). No temperature gradient simulations have been conducted. All simulations are for the SiO_2: CaO: FeO molar ratio 80:15:5 and J13 water. The reaction rates are based on values obtained from the literature as described in Table 5.3-3.

5.3.4 RESULTS

The results of EQ 3/6 simulations of magnetite, lime, quartz sand system (80:15:5 molar ratio, are shown in Figure 5.3-2. Both pH and Eh are illustrated as a function of reaction progress for both a closed (unventilated) system (no gas control; i.e., "unfixed" fO_2) and an open (ventilated) system (gas control; i.e., "fixed" fO_2). From these results it is clear that the equilibrium pH of a system that allows free exchange with the atmosphere (open system), and reaction in the presence of lime (until the lime is reacted), is 8.64 until quartz saturation is reached, at which time it becomes 8.02 (Figure 5.3-2c). In contrast, a closed system achieves an equilibrium pH of around 10 (Figure 5.3-2a). In the open system pH is maximized during the transient period, that is, while the system is evolving. In the closed system pH is maximized during the steady state condition in which lime is present. Once lime is consumed the pH effect disappears. The iron phase only effects oxygen availability in the closed system, and even then the effect is relatively short. The composition of the final mineral assemblage is independent of ventilation conditions. The composition consists of calcite, quartz (which is relatively unaffected during the simulation), and hematite. Although qualitatively any scenario for this backfill composition simulated at 90°C will produce similar results, the time required to achieve a complete evolution to the final assemblage and the movement of the transition zone will depend on the rate of water influx and passivation of reactive phases. This observation is critical to the present case, in which the desired chemical conditioning effect is achieved during the evolution of the system.

Table 5.3-3 Reaction Rates used in OS3D/GIMRT Calculations

Phase	Rate (moles/m^2/sec)	Source
lime	1×10^{-8}	"scientific judgement" (real value is probably larger).
quartz	3.3×10^{-14}	Data from van Lier et al. (1960) at 90°C are consistent with Knauss and Wolery (1988) at 70°C and near neutral pH
magnetite	4.0×10^{-10}	Extrapolated from data from White et al. (1994) pH 5.0, who measure values in the range of 2 - 65.0°C.
hematite	9.93×10^{-11}	Calculated from Bruno et al. (1992) for a system at 25°C containing elevated concentrations of carbonate. Calculated value was modified (increased) by an order of magnitude to account for the elevated temperature.
calcite	9.3×10^{-8}	Calculated value for system far from equilibrium and at 70°C based on data from Gutjahr et al. (1996)

The results of the OS3D/GIMRT simulations are shown in Figures 5.3-3 through 5.3-6. Simulations of reactant consumption (Figures 5.3-3a and 5.3-3b) demonstrate that quartz and magnetite are unaffected through time and that changes in porosity are dependent on lime consumption (Figure 5.3-3a for the closed system, and Figure 5.3-5 for the open system) and calcite and portlandite generation (Figure 5.3-4c for the closed system, and Figure 5.3-6 for the open system). This is true of both ventilated and unventilated cases.

A few engineering considerations become clear from these results. First, for the defined hydrological scenario, the system will probably have evolved to a hematite + portlandite + quartz assemblage before it contacts water. Second, the formation of a crust may have a great impact on hydrology. This is not shown in these simulations and depends on grain size, ratio of the components and reaction rates. Third, reaction rate is a function of grain size and water availability, which remained constant for these simulations. Fourth, completeness of the reaction may be a function of grain size (passivation may occur in larger grains). These simulations were conducted assuming that the reaction is complete.

5.3.5 CONCLUSIONS

These simulations demonstrate that a backfill composed of quartz sand, magnetite, and lime will not control oxygen fugacity or pH unless the drifts are completely sealed. Even then the chemical conditioning effects would be minor, and would probably not achieve the engineering goals. A candidate backfill should be further tested over prolonged periods of time and various temperature gradients. However, the simulations conducted here are sufficient to demonstrate that this backfill option does not sufficiently improve the robustness of the repository concept to warrant further consideration. All of the chemical evolution shown here, including the desired chemical conditioning, take place and are expended within a matter of decades, which is a significantly shorter time frame than that determined in Section 5.1.1 to be needed to have any effect on total system performance.

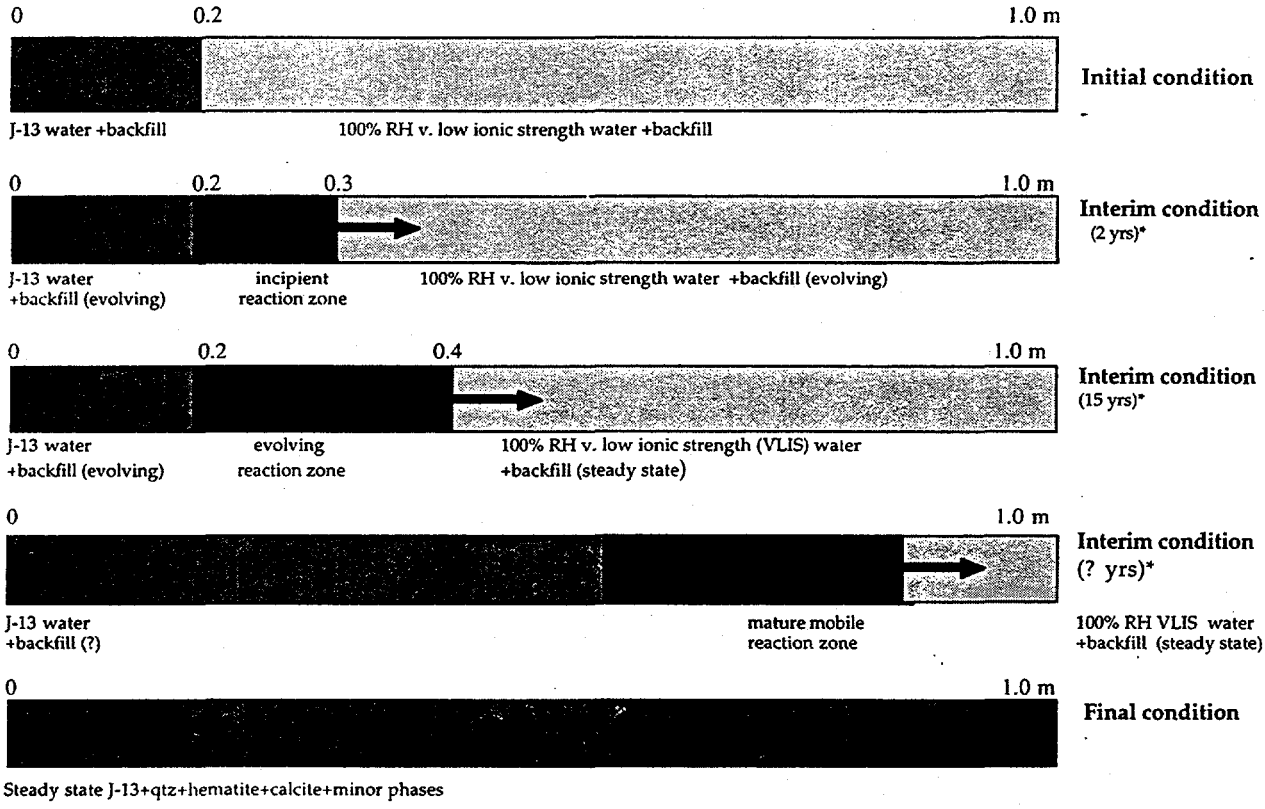

Figure 5.3-1 Illustration of one-dimensional reaction progress using OS3D/GIMRT

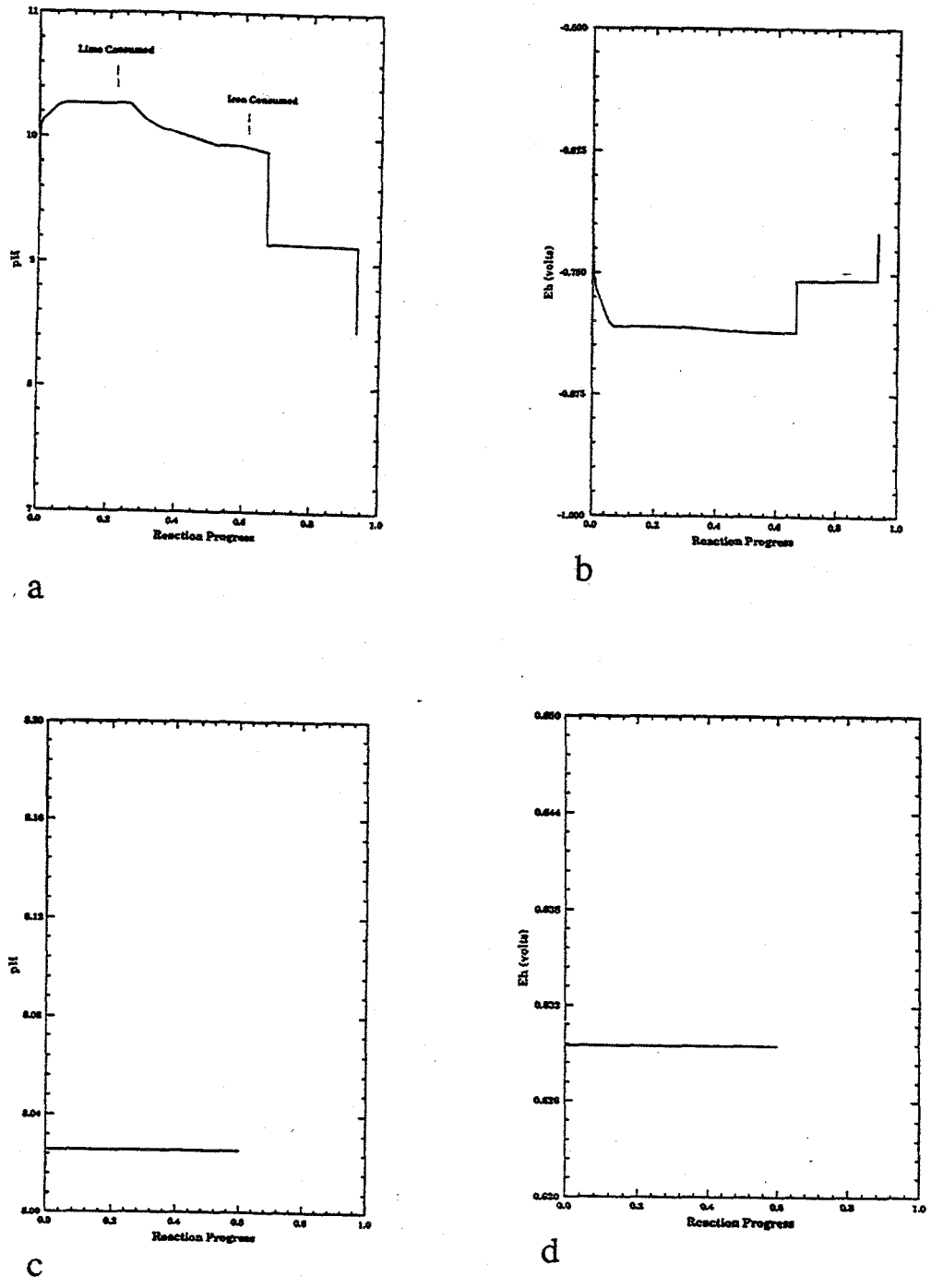

Figure 5.3-2 EQ3/6 simulations of the magnetite/lime/quartz sand backfill (80:15:5 molar ratio). a) pH versus reaction progress for a closed system (no gas control, i.e "unfixed" fO_2), b) Eh versus reaction progress for a closed system (no gas control, i.e "unfixed" fO_2), c) pH versus reaction progress for an open system (gas control, i.e "fixed" fO_2), d) Eh versus reaction progress for an open system (gas control, i.e "fixed" fO_2)

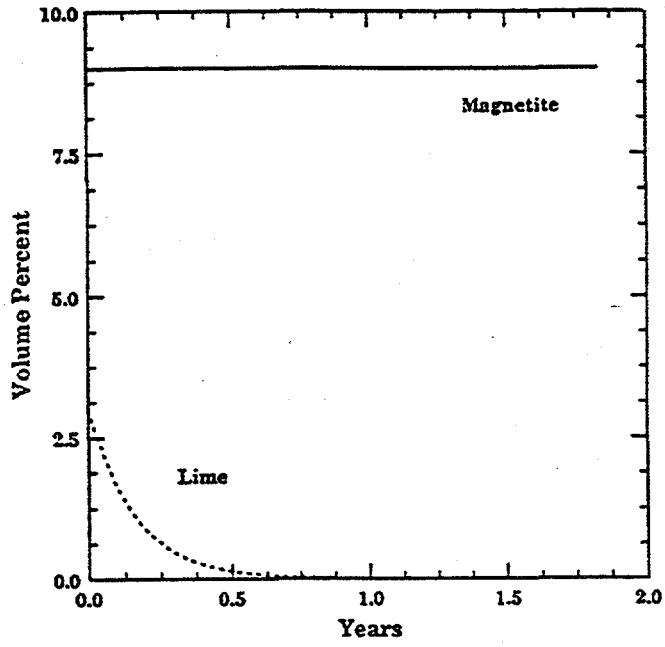

a

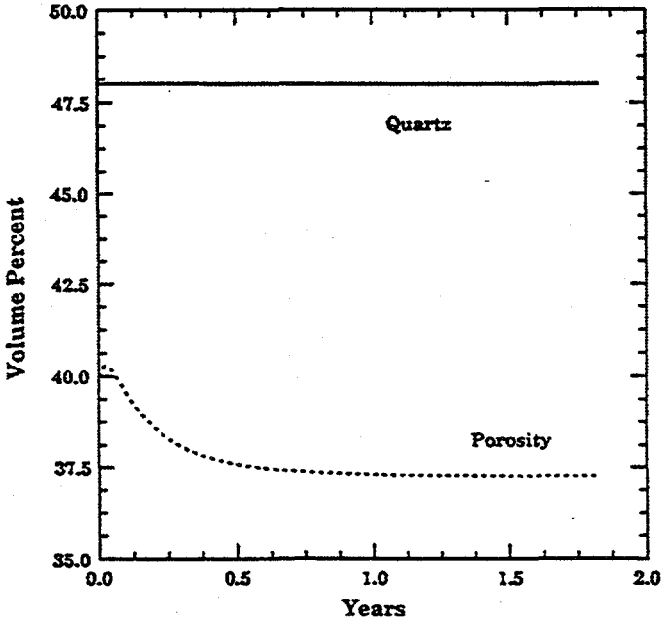

b

Figure 5.3-3 OS3D/GIMRT simulations of reactant consumption and porosity at the inlet (0m) for the magnetite/lime/quartz sand backfill system (80:15:5 molar ratio) for the closed ("unfixed") system. a) Volume percent of magnetite and lime as a function of time (2 year duration). b) Volume percent of quartz and porosity as a function of time (2 year duration)

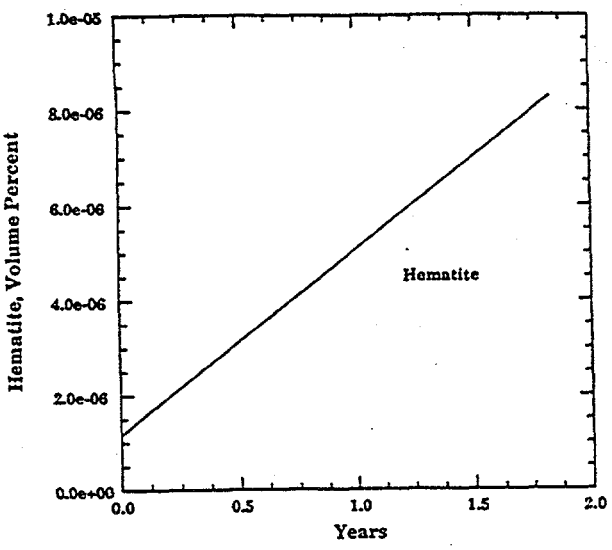

a

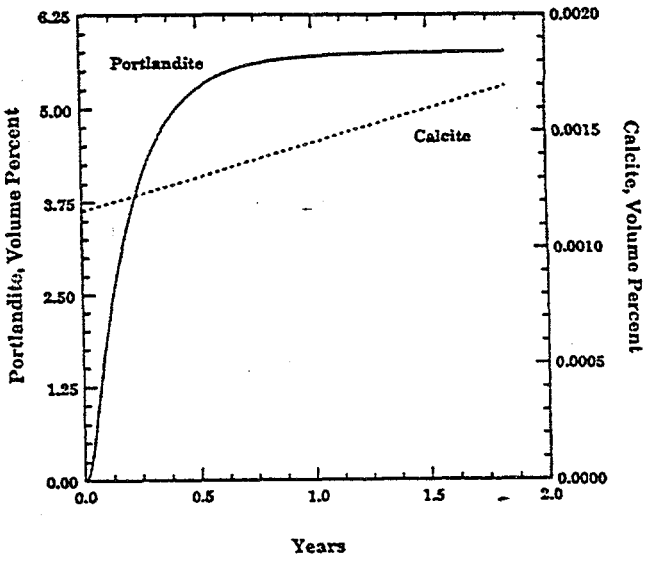

c

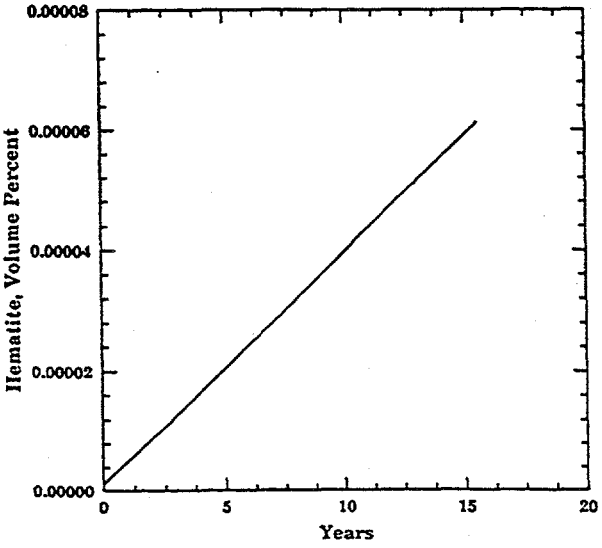

b

Figure 5.3-4 OS3D/GIMRT simulations of product evolution at the inlet (0m) for the magnetite/lime/quartz sand backfill system (80:15:5 molar ratio) for the closed ("unfixed") system. a) Hematite evolution as a function of time (2 yr. duration), b) Hematite evolution as a function of time (20 yr. duration), c) Portlandite and calcite evolution as a function of time (2 yr. duration)

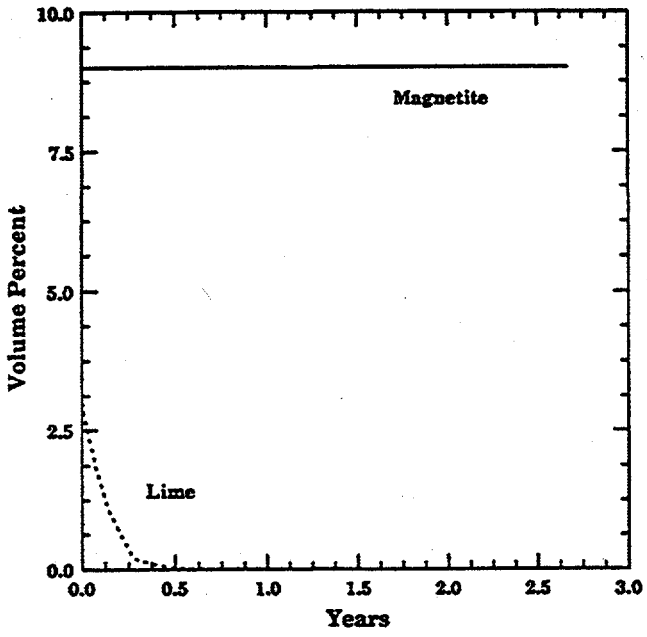

Figure 5.3-5 OS3D/GIMRT simulations of reactant consumption and porosity at the inlet (0 m) for the magnetite/lime/quartz sand backfill system (80:15:5 molar ratio) for the open ("fixed") system. Volume percent of magnetite and lime as a function of time (3 year duration)

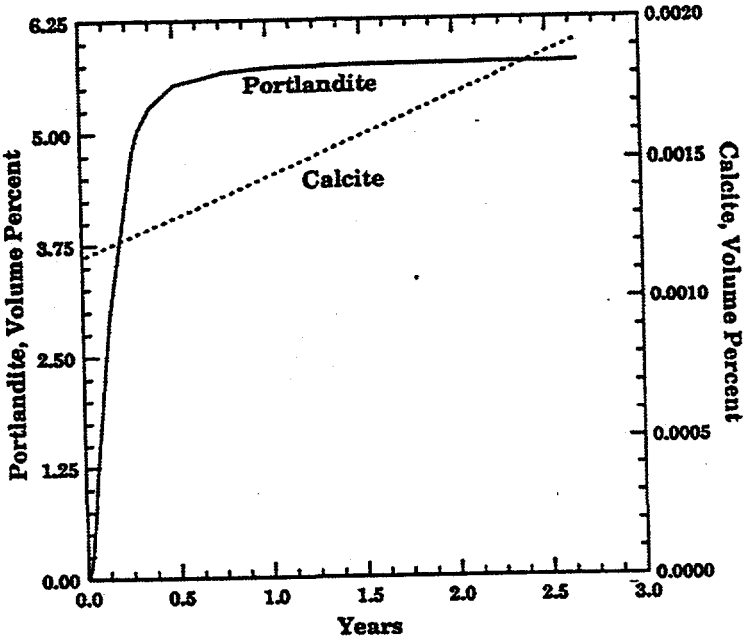

Figure 5.3-6 OS3D/GIMRT simulations of product evolution at the inlet (0m) for the magnetite/lime/quartz sand backfill system (80:15:5 molar ratio) for the open ("fixed") system. Portlandite and calcite evolution as a function of time (3 year duration)

5.4 DRIP SHIELD AND CAPILLARY BARRIER

Both the drip shield and the capillary barrier are addressed in this section since the primary potential EBS function they could perform is to delay the advective transport of radionuclides once the waste package has been breached. This would be accomplished by providing a barrier to the advective transport of released radionuclides. As depicted in Figure 5.1-3(a), the idea is to divert any advective flow around the waste package such that diffusion is the only transport mechanism for radionuclides out of the waste package and the emplacement drift.

5.4.1 TOTAL SYSTEM PERFORMANCE ASSESSMENT

A performance assessment sensitivity analysis was conducted in Section 5.1.1 in which the effect on long-term performance of a limited-lifetime drip shield or capillary barrier was examined. This sensitivity study was conducted by employing information available at the time of TSPA-1995 with the accessible environment defined at 5 km. The sensitivity analysis gives some very useful results regarding the effect of a drip shield on performance. Specifically, the expected-value results of Figure 5.1-4, when compared to Figure 5.1-1, shows that for a drip shield/capillary barrier lifetime of 100,000 years, the doses due to aqueous radionuclides (all but the ^{129}I) are delayed in reaching the accessible environment by about 100,000 years. Similar results are obtained (see Figure 5.1-5) when a 500,000 year lifetime is assumed.

Of most import to this discussion is the trend seen in the ^{237}Np breakthrough curve as one progresses from a 0 year lifetime drip shield/capillary barrier (Figure 5.1-1) to a 500,000 year lifetime (Figure 5.1-5). The ^{237}Np breakthrough curve shifts to the right as the lifetime of the drip shield/capillary barrier increases, but the peak dose realized due to ^{237}Np does not diminish over the 1,000,000 year time frame until extremely long lifetimes are assumed for the drip shield/capillary barrier. This information will be made use of in the next discussion.

The analysis presented in this study is somewhat different than that presented in TSPA-1995, primarily because the capillary barrier (and drip shield) results presented in TSPA-1995 (CRWMS M&O 1995d) assume aqueous transport of the ^{129}I radionuclide through the EBS, rather than the current assumption of gaseous transport. Thus, the results shown in TSPA-1995 (see Section 9.3.3 of TSPA-1995) reflect great improvements in 1,000,000 year repository performance for capillary barriers that last 1,000,000 years. As can be inferred from the following sensitivity analysis, since the capillary barrier has no effect on gaseous radionuclides (see Section 5.4.3) such as ^{129}I, the improvement in repository performance is not expected to be as pronounced as that seen in TSPA-1995.

Figure 5.4-1 presents expected-value breakthrough curves of the important radionuclides over a 1,000,000 year time frame where the doses are calculated at 30 km from the repository, no backfill is employed, and the near-field thermohydrologic results of Section 3.1.1.2 are implemented in the total system performance assessment. The peak dose rate occurs at 1,000,000 years and amounts to about 6 mrem/yr. This is approximately the same as the dose rate at the 50 percent probability point in Figure 3.1-16. Figure 5.4-1 would indicate that the ^{237}Np curve would have to be biased to the right by at least 700,000 years before even a 5 rem/year reduction in peak dose rate would be realized. Employing the same logic as was used in the sensitivity analysis in Section 5.1.1 (Figures

5.1-1, 5.1-3, and 5.1-4), this could be accomplished with a drip shield/capillary barrier with a lifetime of at least 700,000 years. It is quite unlikely that a defensible, sensible, argument can be made supporting a drip shield or capillary barrier concept that functions as intended for 700 millennium.

Therefore, the first argument for discounting the use of either a drip shield or capillary barrier to act as an aqueous diffusion barrier to released radionuclides is the extremely long time frame (750,000 years) required for such barriers to operate to see a noticeable reduction in peak dose rate. In addition to this argument, there are additional specific arguments that help bolster the conclusion that neither a drip shield nor a capillary barrier should be further considered as possible barriers in the Engineered Barrier System. These arguments are delineated first for the drip shield and then the capillary barrier.

5.4.2 ISSUES ASSOCIATED WITH THE DRIP SHIELD

During the process of developing waste package and drip shield conceptual designs, a range of materials were evaluated, including metals and ceramics (CRWMS M&O 1996f). In looking at ceramics it was determined that since ceramics are fairly brittle, their exposure to eventual rockfall in the emplacement drifts would render them potentially useless in performing their intended function. On the other hand, a thin, corrosion resistant metal such as Titanium could fit closely to the outer containment barrier, be supported by it, and thus have possibly greater resistance to rockfall. This assessment was considered valid as long as any rockfall impact is normal to the drip shield and the drip shield is supported on the inside by the containment barrier. However, if the rock strikes with a glancing blow, it would be possible for the drip shield to be gouged or torn. This is especially true on the ends of the waste package since the skirts of the package leave hollows that would be spanned by the drip shield. A second cause for concern in the use of a drip shield is that corrosion of the corrosion allowance barriers will result in a volume expansion because the corrosion products are larger than the original metal. The result effectively would be an increase in the volume of the waste package. This anticipated volume increase could distort and damage the waste package.

Chemical interactions with the waste package may also degrade the drip shield. From an industrial point of view, "Titanium and its alloys are fully resistant to water, all natural waters, and steam to temperatures in excess of 315°C." (Corrosion 1987). However, significant reductions in long-term dose rate will require an extremely long-lived drip shield, and thus one that is quite compatible with the corrosion allowance barrier. One mechanism that has been identified for degradation of titanium alloys by the corrosion allowance material is smeared surface iron pitting (Corrosion 1987). To achieve pit initiation times that are of interest to industry, this form of corrosion appears to require exposure to hot brines, and "Titanium grades 7 and 12 appear to be much more resistant [than unalloyed titanium] to this form of localized attack." "Titanium grade 12" refers to ASTM B 265 Grade 12, and "titanium grade 7" refers to ASTM B 265 Grade 7. The former is a candidate material for the corrosion resistant barrier; the latter is similar to a candidate material (ASTM B 265 Grade 16) though somewhat richer in palladium. Nevertheless, the drip shield would be in contact with or in close proximity to carbon steel over a large area for a very long time.

Of course, one way to reduce the likelihood of any chemical interaction with the waste package would be to space the drip shield away from the waste package. However, a preliminary analysis valid for small air gaps indicates (CRWMS M&O 1996g) that to maintain the SNF cladding goal of

350°C (Assumption Identifier DCWP 001 in CRWMS M&O 1996a), the air gap between the waste package and drip shield should be less than 8 mm. Significantly increasing the air gap to tens of centimeters may have less impact on the SNF cladding temperature, but it would also make the rockfall problem more intractable as well as significantly increasing the costs associated with drip shields.

5.4.3 ISSUES ASSOCIATED WITH THE CAPILLARY BARRIER

The combination of unsaturated soil/gravel layers in the unsaturated, or vadose, zone that act as a hydraulic barrier to inflow of water from the surrounding environment, is referred to by various names (e.g., diversion barrier, wick layer, capillary barrier, gravel barrier, gravel cocoon, advective barrier, and Richards Barrier). A Richards Barrier can also function as a diffusion barrier to the transport of radionuclides away from the waste packages. A Richards Barrier, however, provides no barrier to vapor or gas, such as the gaseous ^{129}I.

A traditional Richards Barrier consists of a sloped layer of gravel below a layer of finer-grained material such as sand or silt. Figure 5.4-2 illustrates the components of a Richards Barrier as applied to a geologic repository located in volcanic tuff. A positive pressure in the direction of flow is necessary for flow across the boundary from the sand into the gravel, a condition requiring the bottom of the sand layer to become completely or nearly saturated. If the hydraulic conductivity of the sand is sufficiently high, even a slight slope will conduct water away in the sand very rapidly, preventing the boundary from ever saturating. The fluxes or recharge rates required to saturate an ordinary sand or coarse silt are greater than that which occurs in almost any vadose zone; i.e., fluxes of over 10^5 cm/yr (Conca 1995). The exact size and nature of the gravel and sand are not critical to performance as long as the relative grain sizes are different enough to provide a capillary break.

This concept does require that perturbations in the interface between the two materials not be greater than 5 to 10 centimeters, and that the sand-size material does not penetrate deeper than three to four gravel-size particles into the lower layer.

However, these conditions will be extremely difficult to replicate in the underground environment of a geologic repository. The aspect of the Richards Barrier concept that makes it infeasible is that multiple layer backfills cannot be constructed within the context of the current underground repository concept. The problem is two-fold, the exacting requirements outlined above cannot be met and access to perform the operations required to emplace a Richards Barrier is not provided. For various stowing methods, such as dumping described in Section 5.2.1, as well as slinging or pneumatic stowing, the emplacement of backfill is too energetic and too erratic for the requirements of a Richards Barrier. The available backfilling techniques will likely invalidate the effectiveness of a two-component, stacked backfill. For example, the rail track that runs parallel to the emplaced waste packages in the OCID mode, and which provides access for the backfill equipment (see Figure 5.2-1), would be covered by the first layer of backfill so that the equipment would have no access to apply the second layer. If consideration is given to slinging or pneumatic stowing of the second layer from the entrance of the emplacement drift, the following problems would arise:

- Perturbations along the interface between two distinct fill materials will likely be the greatest for pneumatic and slung placement due to the force of the material striking previously placed

material. For both methods solids are likely to be traveling at a high rate of speed which will not only compact some previously placed material but will also dislodge other material causing furrowing and gouging. Even for dumped material, the boundary between the two fills will be roughened as one material cascades over another.

- Sand-sized material is likely to penetrate into the gravel-sized material due to the force of placement, seismic activity, and consolidation of the loose material. Non-uniform fingering or piping is a probable result which would reduce the efficacy of the Richards Barrier.

- Particle segregation will be the greatest for pneumatically placed and slung material with the most dense and largest particles falling short of finer graded material. Particles which are only a few microns in size will tend to travel great distances as dust. Particle segregation for dumped material is likely lessened. For all backfilling techniques, some degree of segregation is likely for particles representing a wide range of screen fractions.

5.4.4 CONCLUSIONS

For the reasons discussed in Section 5.4.2, the drip shield cannot be considered an engineered barrier that has the potential to significantly reduce the peak dose. Also, for the reasons discussed in Section 5.4.3, a double-layered backfill meeting the Richards Barrier criteria is not considered a viable alternative for use in the underground environment of a geologic repository.

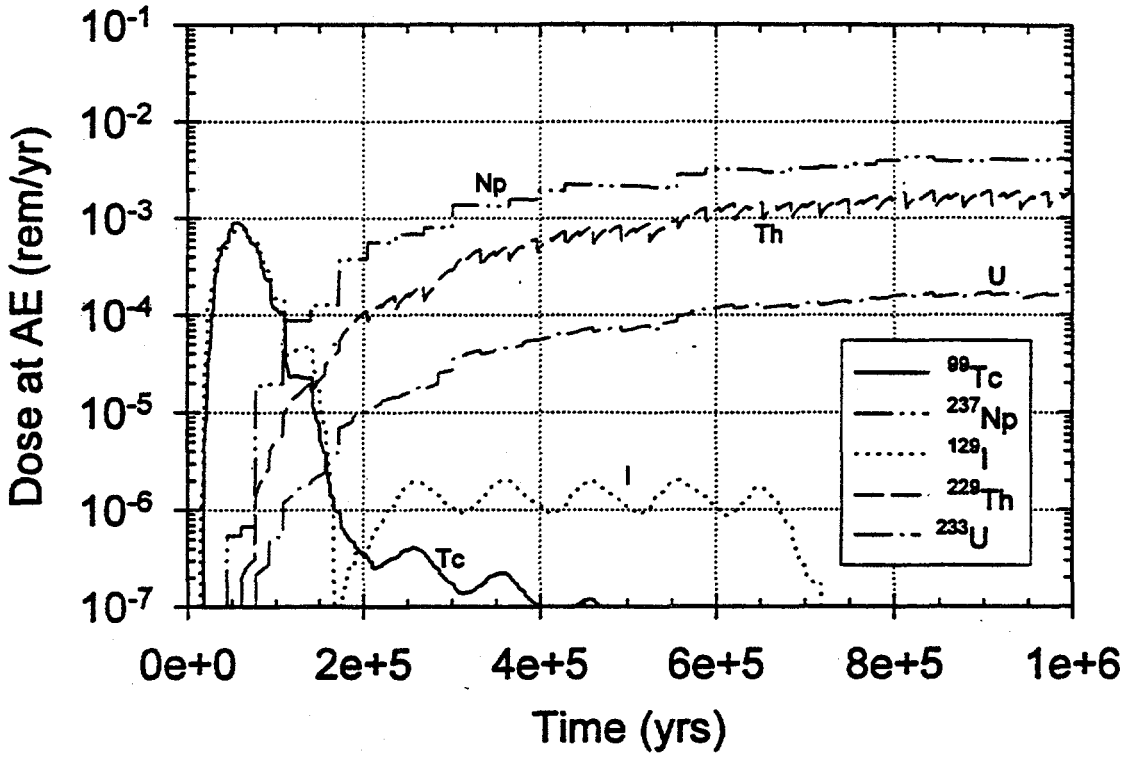

Figure 5.4-1 1,000,000 yr expected-value total dose history for the ACD, no backfill, 30 km case

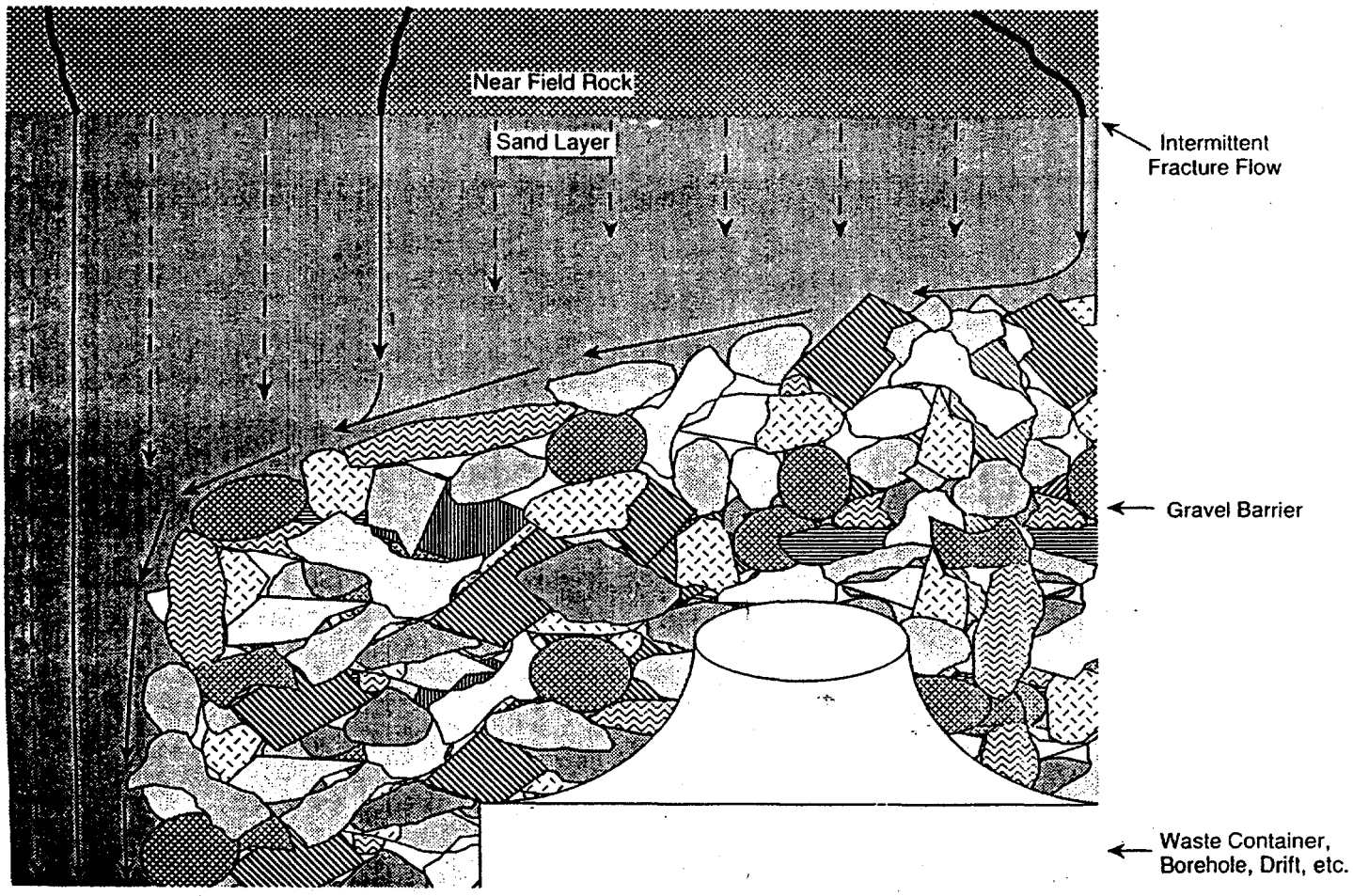

Figure 5.4-2 Features of a Richards Barrier applied to conceptualized high level waste

5.5 CHEMICALLY TREATED INVERT

5.5.1 INTRODUCTION

A sensitivity analysis was conducted in Section 5.1.2 to establish whether a sorptive invert would have any significant effect on total system performance. Those results indicated that the invert would have to be highly sorptive for very long periods of time to have any significant effect on repository performance.

Sedimentary apatite ore was first mentioned in the context of this study during the kickoff meeting held at the beginning of FY 1996. Of course, much previous research has been conducted with regard to apatite, as will soon be discussed. However, first the qualitative attributes of apatite will be discussed that led to its selection within this study as a possible addition to the emplacement drift invert.

The problem of contaminant metals in soils and groundwater is presently identified by the EPA as one of the most critical environmental risks. Metals readily leach from waste containers, contaminated tailings, soils, and sediments and serve as a constant source of metal contamination to groundwater. The objective of previous efforts has been to determine how well specific metals are immobilized by apatite, the capacity and efficiency of the apatites used relative to the inventory of metal contaminants, and which apatites perform best under environmental conditions of interest.

Metals most affected by this treatment are the lanthanides and actinides, especially uranium, plutonium, and thorium, as well as lead, zinc, copper, cadmium, nickel, barium, cesium, and strontium. An important aspect of this treatment is that the metal stabilization is nearly irreversible. It is not a simple sorption that can later desorb, it is not a reduction that can later oxidize, and it is not a mineral phase that can later leach. Metals sequestered in apatites have great durability and leach resistance that significantly exceed other chemically stabilized waste forms because the apatite mineral structure is very stable over a wide range of environmental conditions (e.g., pH 2.5 to 13.5) to over 1000°C, in the presence of aqueous and non-aqueous phase liquids, in fresh water and in brines, and under disruptions such as earthquakes or ground subsidence, for geologically long time periods (hundreds of millions of years).

The reaction between the apatite and the metal is rapid (Ma et al., 1993; Moody and Wright, 1995), and so the treatment is effective immediately, requiring no time for the material to "set up." Previous results indicate that the efficiency of apatite is well over 20 percent; i.e., the apatite can sequester over 20 percent of its weight in metals.

The primary advantage of this system is its potential for rendering metals into a non-hazardous waste form that will not leach under any anticipated environmental conditions over geologically long time scales.

5.5.2 BACKGROUND AND PREVIOUS WORK

The groundwork for this research has been laid by previous studies in widely divergent disciplines, including 1) phosphate mineralogy and crystal chemistry (Skinner, 1987, 1989; Skinner and Burnham,

1968); 2) scavenging and sequestration of minor and trace elements such as uranium, metals, and the rare earth elements, in natural phosphate deposits (McArthur et al., 1990); 3) remediation studies of phosphate/lead systems (Ma et al., 1993; Ruby et al., 1994; Xu and Schwartz, 1994; Stanforth and Chowdhury, 1994); 4) the impact and accessibility of phosphorus fertilizers to crops (Adepoju et al., 1986); 5) natural analogues in metallic mineral deposits (Koeppenkastrop and DeCarlo, 1988, 1992); 6) phosphate diagenesis during the formation and evolution of phosphorite deposits (McArthur, 1985) and 7) the evidence of changes in the paleochemical evolution of oceans, atmospheres, and climates evidenced by metals, lanthanides, and actinides incorporated into fossil teeth that have apatite composition (Wright, 1990a,b).

Apatite minerals form naturally and are stable across a wide range of geologic conditions for hundreds of millions of years. Work by Wright, Conca, and others (Wright et al., 1987 and 1990) investigated the trace element composition of apatite in fossil teeth and bones and in sedimentary phosphorite deposits through geologic time. They found that apatite deposited in seawater concentrates metals and radionuclides from the seawater to millions of times the ambient concentration, and locks them into the apatite structure for up to a billion years with no subsequent desorption, leaching, or exchange, even in the face of extreme diagenetic changes in the pore water chemistry and pH, extreme temperatures, and geologic or tectonic disruptions.

In summary, previous research indicated reasonable cause to find that apatite might prove to be a valuable radionuclide retardant additive in the emplacement drift invert. Indeed, as the test results in Section 5.2.7.7 show, at least for ^{237}Np the phosphate material (which has the apatite mineral in its composition) obtained from North Carolina has excellent retardant properties.

What this means in terms of total system performance will be discussed in the next section, with the repository costs associated with placing apatite in the emplacement drift inverts discussed in Section 5.5.4.

5.5.3 TOTAL SYSTEM PERFORMANCE ASSESSMENT

The test results of the ability of apatite to retard ^{237}Np and ^{99}Tc were described in section 5.2.7.6. The results indicated that ^{237}Np exhibited a great deal of sorption on apatite, with a sorption coefficient (K_d) of 500 cc/g, whereas ^{99}Tc exhibited little tendency to sorb on apatite. The analysis conducted in the previous section and Section 5.2.7 assumes that there is enough apatite in the invert for sorption of all of the ^{237}Np, as well as any of the other actinides that may sorb to apatite. This is the bounding case. The expected-value TSPA case for the ACD configuration (does not reflect backfill nor the use of apatite in the invert) shown in Figure 5.4-1 indicates the dominant radionuclide over the 1,000,000 year period is ^{237}Np.

Figure 5.5-1 gives the expected value results if the emplacement drift invert transport characteristics are modeled as if the invert is treated with a layer of apatite and has a sorption coefficient (K_d) of 500 cm^3/g which is functioning for the entire 1,000,000 year time period. These results indicate a significant potential reduction in the ^{237}Np doses at the accessible environment. However, since apatite has no retardation effect on ^{99}Tc or ^{129}I, a peak dose rate due to these two radionuclides occurs at about 50,000 years, and amounts to approximately 2 mrem/year. This is a factor of 3 reduction from the case presented in Figure 5.4-1, and is about half the reduction attributed to backfill

over the 1,000,000 year time frame (see Section 5.2.8 for total system performance results regarding the use of backfill).

5.5.4 COSTS AND SCHEDULE IMPACTS

The analysis conducted in this section assumes 5.5 meter diameter emplacement drifts. In the conceptual repository design this equates into an invert 1.2 meters in thickness. The corresponding invert thickness in a 5.0 meter diameter emplacement drift would be 0.9 meters. Thus, the repository costs in this section can be considered conservative as they would be somewhat less for 5.0 meter diameter emplacement drifts.

The emplacement drift invert has a structural function to support the dual tracks in the OCID waste emplacement drifts. Two basic invert conceptual designs are being considered for the typical 5.5 m diameter waste emplacement drift. These include an invert constructed of crushed tuff (TSw2 material initially removed as part of ESF and repository development) and a cast-in-place concrete and crushed tuff invert. For this study, invert construction costs for varying thicknesses of apatite or phosphate are conducted for the crushed tuff invert.

While the thicknesses of the various layers within the invert may vary, the total thickness of the invert will be 1.2 m as described for the typical backfilled waste emplacement drift in the ACD Report (CRWMS M&O 1996b). Invert construction will occur concurrently with other functions following excavation of waste emplacement drifts. The surface facilities for invert material utilizing crushed tuff will require crushing and screening process steps as shown in the flowsheet in Figure 5.5-2. If phosphate is added, the crushed tuff will be hauled underground by railcar and dumped over the other material. The addition of the phosphate to the emplacement drift invert is judged to not have any effect on the invert construction schedule.

The handling and placement of phosphate involves some difficulty beyond that of crushed tuff. The phosphate is very fine grained and without significant cohesion. No additional equipment or labor has been provided to mitigate potential problems arising from the use of phosphate. Additional study will be required to examine the impacts of this material on repository operations.

The same cost estimating methodology which was used for the ACD Report (CRWMS M&O 1996b) as well as for Section 5.2.9, is applied here. The cost estimates have been expressed in constant October 1995 dollars for each year in which the work is performed, spread over the years in which the costs will be incurred, and totaled for the duration of invert construction. As a basis for comparison, the cost estimate for a crushed tuff invert is indicated in Table 5.5-1. This and subsequent cost tables have been structured to show the following:

- Capital Cost. The initial capital investment for equipment occurs at the onset of invert emplacement operation for the complement of equipment required. Replacement cost is shown to indicate the magnitude of equipment items that are replaced before the end of invert emplacement.

- Operating Cost. Labor, equipment, and supplies are shown in lump-sum form.

- Material Cost. No acquisition expenses will be incurred with the use of crushed tuff. The material cost of phosphate will be subsequently discussed. All material handling costs are included as operating cost items.

- Other Costs. Contingency is applied to the sum of capital and operating costs. CRWMS M&O G&A is applied to the sum of the capital cost, operating cost, and contingency. CRWMS M&O Fees are applied to the sum of all the above.

As the specific amount of phosphate that may be needed under a waste package is yet an unknown, costs are estimated for varying thicknesses of crushed tuff and phosphate in a 1.2 m thick non-rigid invert of a 5.5 m diameter waste emplacement drift, with the cost in Table 5.5-1 reflecting that of all crushed tuff and no phosphate. Detailed (bottom-up) cost estimates (CRWMS M&O 1996h) were conducted for two cases, a 1.2 meter thick invert of crushed tuff and an invert with 0.7 meters of crushed tuff overlying 0.5 meters of phosphate. The capital costs for both cases were equal while a few specific items caused a change in comparative total operating costs. The total operating costs were \$71,149,152 and \$69,163,996 for the total crushed tuff and layered crushed tuff-phosphate cases, respectively. The total volume of the invert was calculated at 685,200 cubic meters which was based on 179,051 linear meters of 5.5 m diameter drifts. The operating cost was calculated at \$103.84/m^3 for an invert of crushed tuff only and \$100.94/m^3 for an invert of layered crushed tuff and phosphate.

The specific operating items which varied between the two estimates were within the general categories of Labor, Equipment, and Supplies as given below.

Labor:	Bull Gang Welder
Equipment:	Air Plate Compactor, Air Tamper
Supplies:	Crusher Liner, Cost for Supply Personnel

It is apparent that the cost for these items decreases with a decrease in the thickness of crushed tuff while the material cost increases with the use of phosphate to maintain a constant invert depth of 1.2 meters. The increase in material cost due to the added use of phosphate appears to have a smaller effect than reducing the amount of tuffaceous material has on the labor, equipment, and supplies operating costs. For labor, equipment, and supplies the individual operating incremental costs per unit (such as \$/shift or \$/hour) remain constant for the range of unit quantities given in the detailed cost estimate (CRWMS M&O 1996h). It is reasonable to assume that the rising material cost of using additional amounts of phosphate will, at least in part, offset the decreasing costs of labor, equipment, and supplies with the use of less tuffaceous material; although, the downward trend in overall operating cost with using less tuff will likely decrease in a linear relationship.

Table 5.5-2 gives the invert quantities for variable crushed tuff/phosphate thicknesses. Table 5.5-3 reflects the invert operating cost estimates for various phosphate thicknesses. A linear regression analysis was conducted to estimate the costs for phosphate thicknesses other than 0.0 and 0.5 meters. Table 5.5-4 summarizes the total costs associated with emplacing varying thicknesses of phosphate in the emplacement drift invert. These total costs need to be considered relative to the total cost of emplacing a crushed tuff-only invert (\$141.8M).

5.5.5 UNCERTAINTIES ASSOCIATED WITH CHEMICALLY TREATED INVERT

The results in Section 5.5.4 indicate a *potential* gain in total system performance over the 1,000,000 year time frame, approximately half that associated with backfill. However, recall that the results in Section 5.5.4 reflect a bounding case in which it is assumed that enough apatite is below each waste package to ensure sorption of the available ^{237}Np. What is still unknown is the approximate amount of apatite that would actually be needed to ensure sorption of all of the available ^{237}Np. It may be that only a thin layer of apatite is needed in the crushed tuff emplacement drift, or, more likely, a very large amount may be needed. In the current emplacement drift conceptual design where the waste package and rail carriage are supported by rails sitting on the emplacement drift invert, only a limited amount of the very fine apatite may be allowed to be layered in the invert as the invert is also and primarily acting as structural support for the waste package and rail carriage.

5.5.6 CONCLUSIONS

If the amount of apatite deemed necessary for sorption purposes is sufficiently small to not thwart the ability of the invert to act as a structural support for the waste package and rail carriage, the cost of the apatite would have to be estimated from the cost data given in Section 5.5.4 to determine if a chemically treated invert produces a significant reduction in peak dose at a reasonable cost. Further work should be conducted in this area to determine if a chemically treated invert is a viable addition to the Engineered Barrier System.

Table 5.5-1 Invert Cost with Crushed Tuff Only

Capital Equipment Cost		**Total**
• Initial • Replacement		$ 3,821,038 7,214,988 **$ 11,036,026**
Operating Cost		
• Labor • Equipment & Supplies		$ 63,187,289 7,961,863 **$ 71,149,152**
Material Cost		
Crushed Tuff		**$ 0**
Other		
• 25% Contingency • 20% M&O G&A • 15% M&O Fees		$20,546,295 20,546,295 18,491,665 **$59,584,255**
Total		**$141,769,433**

Table 5.5-2 Invert Quantities for Variable Crushed Tuff/Phosphate Thicknesses

Thickness (m)		Area (m^2)		Volume (m^3)*	
Tuff	**Phosphate**	**Tuff**	**Phosphate**	**Tuff**	**Phosphate**
1.2	0.0	3.827	0.000	685,200	0
1.0	0.2	3.550	0.277	635,600	49,600
0.8	0.4	3.054	0.773	554,000	131,200
0.7	0.5	2.752	1.075	492,700	192,500
0.6	0.6	2.423	1.404	433,800	251,400
0.4	0.8	1.691	2.136	302,700	382.500
0.2	1.0	0.879	2.948	157,400	527,800
0.0	1.2	0.000	3.827	0	685,200

*Note: Total Drift Length = 179,051 meters; Drift Diameter = 5.5 meters

Table 5.5-3 Invert Operating Cost Estimates for Various Phosphate Thicknesses

Phosphate Thickness (m)	Operating Cost ($/m^3)	Operating Cost ($ million)
0.0	103.84	71.1*
0.2	102.68	70.4
0.4	101.52	69.6
0.5	100.94	69.2*
0.6	100.36	68.8
0.8	99.20	68.0
1.0	98.04	67.2
1.2	96.88	66.4

* From by Detailed Cost Estimates (CRWMS M&O 1996h)

Table 5.5-4 Invert Costs for Variable Phosphate Thicknesses

Phosphate Thickness (m)	$ Million				
	Capital Cost	Operating Cost	Material* Cost	Other Cost	Total Cost‡
0.0	11.0	71.1	0	59.5	**141.8**
0.2	11.0	70.3	17.7	65.6	**164.6**
0.4	11.0	69.5	46.7	76.0	**203.2**
0.5	11.0	69.1	68.6	84.0	**232.7**
0.6	11.0	68.7	89.6	91.7	**261.0**
0.8	11.0	67.9	136.3	108.9	**324.1**
1.0	11.0	67.1	188.1	127.1	**393.3**
1.2	11.0	66.3	244.2	149.0	**470.5**

* Unit Material Cost: $356.32/m^3 of phosphate

‡ Total Cost Calculation

Example: 0.5 m thick phosphate layer and 0.7 m thick crushed tuff layer. No material cost assigned to crushed tuff.

Cost Item					
Capital:	11.0				
Operating:	69.1				
Material:			68.6		
Subtotal:	80.1		68.6		
25% Contingency	20.0		-na-		
Subtotal:	100.1		68.6		
20% M&O G&A	20.0		13.7		
Subtotal:	120.1		82.3		
15% M&O Fees	18.0		12.3		Total Cost
Subtotal:	138.1	+	94.6	=	232.7

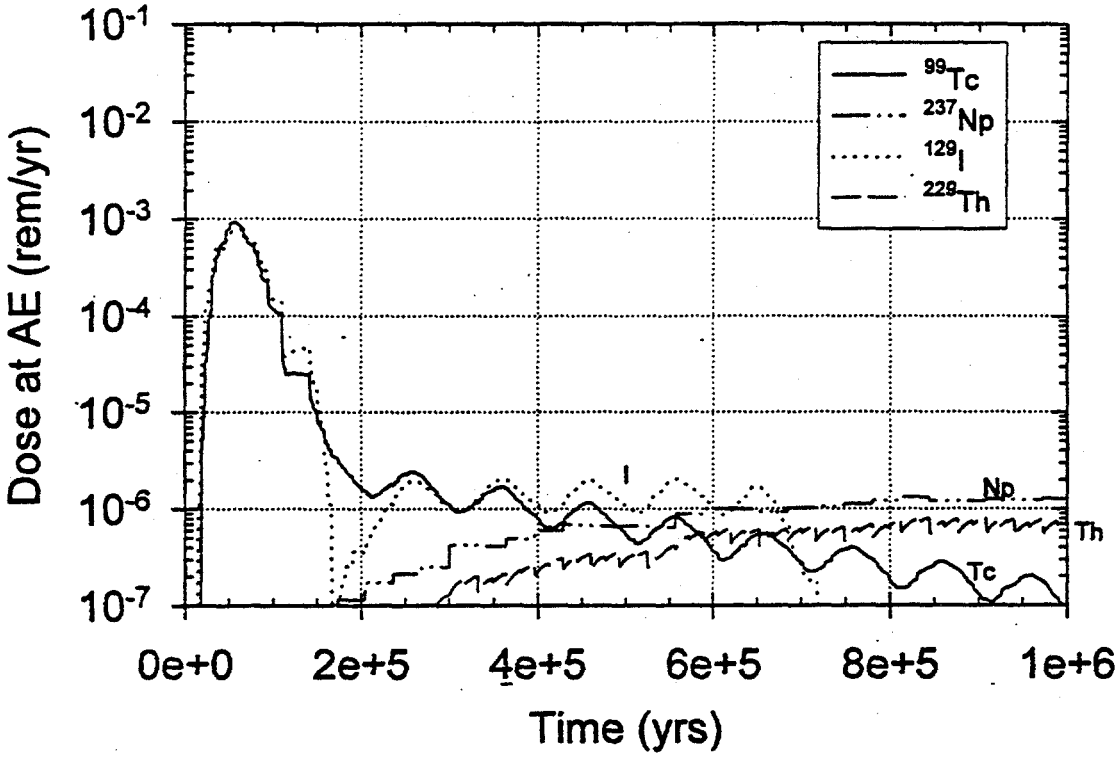

Figure 5.5-1 1,000,000 yr expected-value total dose for ACD, no backfill, 30 km case, with sorption coefficient (K_d) of 500 cm^3/g in the emplacement drift invert for all time

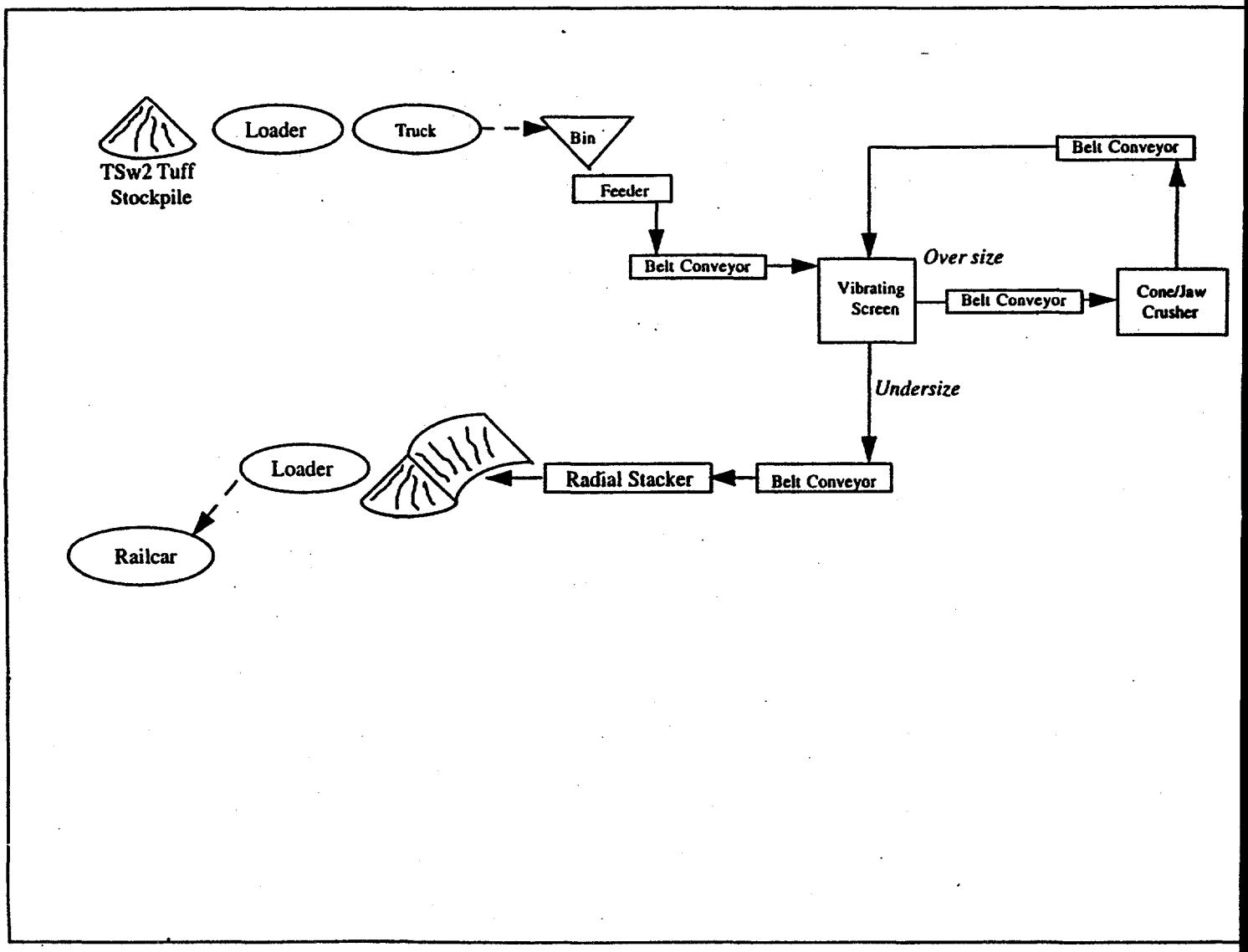

Figure 5.5-2 Backfill material haulage and stowing TSw2 tuff flowsheet

6. STUDY RESULTS, CONCLUSIONS, AND RECOMMENDATIONS

6.1 RESULTS

The following results reflect the outcome of the latest modeling used in support of this study. In the case of predictions of long-term repository performance, these results do not reflect TSPA-1995 (although many of the TSPA-1995 inputs and assumptions are used in this analysis) but rather are generated from performance assessments conducted since then.

Waste Package Containment Requirement

Current estimates of EBS performance, excluding the use of backfill, drip shields, or any other additional performance barriers beyond the EBS, indicate no breaches of waste packages within the 1,000 year time frame. Additional assurance is obtained since this result does not account for the potential performance benefits of cathodic protection. In the current waste package conceptual design, some degree of cathodic protection of the Alloy 625 corrosion-resistant inner barrier will be provided by the carbon steel outer barrier. Significant waste package performance benefits are realized when some credit is taken for this phenomenon.

10,000 Year Time Frame :

- The repository as currently envisioned (see the Advanced Conceptual Design report), that is without backfill, drip shields, or any other additional EBS barrier beyond the waste package, and at a thermal loading of 83 MTU/acre, is calculated to satisfy the allowable peak dose rate as described in the "Interim Postclosure Standard" by more than four orders of magnitude in the methodology used for the 1995 total system performance assessment. These calculations give a 70 percent probability that peak dose rates at 30 km from the repository will not exceed 10^{-4} mrem/year. Further, the same analysis gives a 99 percent probability of not exceeding 0.04 mrem/year.

- The above results neglect the potential performance benefits of cathodic protection and SNF cladding. If credit is taken for the performance of the cladding, the predicted peak dose rates at 30 km from the repository show several orders of magnitude improvement over that already indicated above. Furthermore, if credit is taken only for the ability of the outer barrier of the SNF waste packages to cathodically protect the inner barrier, and no credit is taken for the SNF cladding, the calculations give essentially no releases at the AE over the 10,000 year time frame.

- Tightly packing (lineloading) the waste packages while increasing emplacement drift spacing to maintain a constant thermal load (83 MTU/acre) has been, and is continuing to be, considered and debated as another means of extending waste package lifetimes. Lineloading may reduce waste package corrosion initiation by reducing the relative humidity on the waste package surface by way of maintaining a large temperature difference between the waste package and drift wall. This alternative spacing concept, which is also discussed in the Thermal Loading Study for FY 1996 (CRWMS M&O 1996d), is included in this study so that an evaluation of its performance with and without backfill can be assessed. Without the

use of emplacement drift backfill, lineloading results in a repository that is calculated to meet the peak dose rate requirements delineated in the "Interim Postclosure Standard." Yet uncertain is whether the SNF cladding or the drift wall temperature thermal goals would be violated in this scenario. Calculations of the long-term performance of the repository give about a 90 percent probability that dose rates at 30 km from the repository will not exceed 10^{-4} mrem/year. Further, the same analysis gives a 99 percent probability of not exceeding 0.02 mrem/year. Again, taking credit for the outer barrier of the SNF waste packages cathodically protecting the inner barrier, the calculations give no releases to the accessible environment over the 10,000 year time frame.

- Over this time frame, the effect of rockfall on the performance of the waste packages, and thus the performance of the repository, is estimated to result in a two-fold degradation in peak dose rate performance. This estimate was established by assuming that one percent of the waste packages would be breached by rockfall at the beginning of the postclosure period. Current judgements are that this would occur over a significant period of time rather than immediately upon closure of the repository. Nevertheless, a two-fold degradation in peak dose rate performance still reflects a repository that satisfies the maximum allowable peak dose rate if the calculations are valid.

1,000,000 Year Time Frame

- The repository as currently envisioned is calculated to passably satisfy the allowable peak dose rate as described in the "Interim Postclosure Standard." The calculations of long-term performance of the repository give a 50 percent probability that peak dose rates at 30 km from the repository will not exceed 10 mrem/year. Further, the same analysis gives a 99 percent probability that peak dose rates will not exceed 180 mrem/year.

- As was found to be the case for the 10,000 year time frame, if performance credit is taken for one of the additional existing barriers in the EBS (50 percent cathodic protection), the calculated performance of the repository improves noticeably. Specifically, credit for this additional barrier results in a 50 percent calculated probability of not exceeding 0.6 mrem/year, a 90 percent probability of not exceeding 2 mrem/year, and a 99 percent probability of not exceeding 5 mrem/year peak dose rate. This is about the same as the performance calculated when a single-layer backfill is employed (see below). Further, these estimates do not account for any performance credit due to SNF cladding. Indications are that the benefits of SNF cladding on total system performance could result in over an order of magnitude decrease in peak dose rates at the AE (CRWMS M&O 1996d).

- Over this time frame, the effect of rockfall on the performance of the waste packages, and thus the performance of the repository, is estimated to result in about a two-fold degradation in peak dose rate performance. This estimate was established by assuming that one percent of the waste packages would be breached by rockfall at the beginning of the postclosure period. As indicated previously, current judgements are that this would occur over a significant period of time rather than immediately upon closure of the repository. Furthermore, the longer the time frame over which repository performance is assessed, the less the overall impact of rockfall on performance. Therefore, it is estimated, given current

available information, that rockfall will have a two-fold degradation in peak dose rate performance.

- For near-field thermohydrologic reasons, the use of a quartz sand backfill would be preferred over that of crushed TSw2 tuff (see Section 5.2.5.2 of this report). The emplacement of a quartz sand backfill over the waste packages at the end of the preclosure period allows for estimates of a 50 percent probability of not exceeding 0.6 mrem/year peak dose rate at 30 km from the repository. The same analysis indicates a 99 percent probability of not exceeding 11 mrem/year. The employment of the appropriate backfill after 100 years (end of preclosure period) is not calculated to cause the violation of any current thermal goals. Tightly packing (lineloading) the waste packages and backfilling after 100 years reflects a 50 percent probability of not exceeding 0.1 mrem/year at 30 km from the repository. However, there is still significant uncertainty in whether the SNF cladding or drift wall temperature thermal goals would be violated in this scenario.

- If it were possible to chemically condition the quartz sand backfill such that corrosion initiation on the waste packages is delayed for several thousand years, and taking the 50 percent cathodic protection credit, results demonstrate a substantial improvement in predicted long-term repository performance. However, the set of chemicals considered in this study as additives to the quartz sand backfill were calculated in computer simulations to be ineffectual.

- Use of a capillary barrier, such as a Richards Barrier, or a drip shield to noticeably affect total system performance over 1,000,000 years, requires that the barriers perform their EBS function for approximately 750,000 years. In addition to this extremely long time frame, emplacement concerns associated with the Richards Barrier, and issues with the drip shield/waste package interface, make these two concepts impractical as EBS performance barriers.

- Use of an emplacement drift invert chemically treated with sedimentary apatite ore has been found, in bounding calculations, to severely retard the transport of ^{237}Np to the AE. The calculations predict about half the improvement in repository performance as is realized with the use of emplacement drift backfill. However, the bounding calculations assumed a sufficient amount of apatite under a waste package to sequester all the ^{237}Np, as well as any of the other actinides that may sorb to apatite, in a waste package. What is not yet known is the actual amount of apatite needed and whether this amount is compatible with the need of the drift invert to structurally support the waste package and rail carriage. Depending on the amount of apatite required, additional repository construction costs could range from tens of millions to hundreds of millions of dollars. Further work needs to be conducted in this area if this concept is deemed to be of interest.

- The additional repository costs (relative to those costs found in the ACD Report, CRWMS M&O 1996b) associated with backfilling of emplacement drifts include both the cost of constructing 5.5 meter, rather than 5.0 meter, diameter emplacement drifts as well as the cost of stowing the backfill over the waste packages. The additional repository costs amount to approximately $461M, which is about 25 percent of the currently estimated repository

construction costs ($1,783.5M). Of this $461M, $116M is due to construction of the 5.5 meter diameter emplacement drifts and the remainder ($345M) results from the stowing of the backfill. Current estimates of repository construction costs, as indicated in the ACD Report (CRWMS M&O 1996b), could be reduced by 30 percent, even if backfill were employed, if lineloading of the waste packages was conducted. However, again it must be stated that there is yet significant uncertainty in the thermal implications of closely-spaced waste packages. It is currently estimated that twelve years would be required to backfill all of the emplacement drifts. In the lineloading scheme roughly half that amount of time would be required.

6.2 CONCLUSIONS

Given the information and models available at this time, this study has reached the following conclusions regarding both 10,000 and 1,000,000 year time frames.:

10,000 Year Time Frame:

- Calculations of repository performance, even accounting for the effects of rockfall on waste package performance, show results indicating the "Interim Postclosure Standard" would be met by a wide margin. Therefore, if these calculations can be shown to represent the repository system at Yucca Mountain, there would be no need to supplement the Engineered Barrier System with any additional barriers.

1,000,000 Year Time Frame:

- Without taking performance credit for existing barriers such as cathodic protection and SNF cladding, and without employing additional performance barriers external to the waste package, over the 1,000,000 year time frame repository performance is calculated to meet the 15 mrem/yr maximum peak dose rate. Including currently-considered conservative credit for cathodic protection allows for an order of magnitude improvement in peak dose rates at the AE. Furthermore, the performance of SNF cladding, which is not explicitly included in these calculations, would only serve to benefit peak dose rates or at a minimum add assurance to current performance assessment results.

- Including the effects of rockfall, it is estimated that repository performance will be degraded by about two-fold, without the use of backfill, in terms of peak dose rates at the AE. This modest degradation in performance, along with the current estimates of satisfactory repository performance excluding the effects of rockfall, leads to the conclusion that, if the performance calculations prove to be valid, there would be no compelling reason to supplement the currently conceived EBS with emplacement drift backfill. Although an emplacement drift backfill is calculated to improve peak dose rate performance at the AE by about an order of magnitude at a repository cost of ~$461M, current estimates of repository performance without backfill do not compel the implementation of any additional performance barriers to the EBS. Also, although a chemically treated emplacement drift invert shows the potential of having about half the effect on repository performance as backfill, there is no compelling need at this point in time for the use of such an invert.

The EBS functions and barriers addressed in this study should continue to be considered during the design process to not preclude opportunities for cost effective design solutions

6.3 UNCERTAINTIES

The ultimate foundation for the results and conclusions presented is our scientific understanding of the behavior of the EBS and the NBS, which is still evolving; the results and conclusions outlined in this study report are based on the information available at this time. Associated with some of the information is a high degree of confidence, and with other information, less confidence. The intent in this section is not to identify all uncertainties associated with the performance of the NBS and EBS. Rather, only those uncertainties are highlighted that have been identified as having a possible impact on the conclusions of this study.

Regulatory Framework. As previously stated, there is currently no EPA standard applicable to protection of the public and the accessible environment from unacceptable release of radioactive material from the potential repository at Yucca Mountain. This study has used assumed dose rate limits and time periods of regulatory concern (15 mrem/year and 10,000 years, respectively) in developing conclusions about the need for backfill and other potential variations to the ACD design for the EBS. The study also assumes that no more than a 50 percent probability of exceeding the standard is acceptable, and it assumes a location and water consumption rate for the limiting population group. The study results are sensitive to changes in these assumptions, none of which correspond to an existing regulation or standard.

The EPA is expected to issue new standards for Yucca Mountain in the near future. Although the standards are likely to be dose- and risk-based to be consistent with National Academy of Sciences recommendations on the subject, the exact nature of the standards and the quantitative limits are presently not known. To the extent the standards, required assumptions, and limits as promulgated vary from those assumed for this study, the conclusions of the study could change significantly. In particular, a lower limit on dose rate than that assumed for the study could require reconsideration of the conclusion that use of emplacement drift backfill is not warranted.

The NRC is required by law to revise 10 CFR Part 60 to address the EPA's new standards. In addition to use of a dose-based performance objective for the repository, other changes may occur. For example, subsystem performance objectives, such as limits on radioactive material release rate and the requirement for essentially complete containment, may be revised or deleted. The NRC is considering broad-based changes, possibly including a new, site-specific Part that would apply only to Yucca Mountain, to address the new EPA standards as well as other issues and concerns with the existing Part 60. These changes to Part 60, if implemented, also could require reconsideration of the conclusions of this report.

Rockfall Analysis. The rockfall analysis conducted in Section 3.3 of this report must be considered preliminary in nature. It is an analysis conducted with the information available at this time, and so as additional rockfall information is accrued and compiled the conclusions reached in this report should be re-examined. This is most important since the recommendations regarding backfill are closely tied to the effects of rockfall on long-term repository performance.

Backfill Thermohydrologic Results. The near-field thermohydrologic results presented in Section 5.2.5 for backfill are recently obtained results that have not yet been independently verified. The impact of emplacement drift backfill on waste package performance, and thus total system performance, is inextricably tied to these results. Therefore, as (or if) this analysis matures, an examination of its effects on waste package and total system performance should be conducted. Further, because of the distinct availability and cost advantages of a crushed TSw2 tuff backfill versus that of a quartz sand backfill (Section 5.2.9 of this report), an investigation of the thermohydrologic deficiencies of crushed TSw2 tuff should be conducted at greater depth, and the significance of such on total system performance.

Microbial-Influenced Corrosion. Probably the least-examined area of investigation is the effect backfill may have in producing conditions such as microenvironments in which crevicing or pitting can occur, and in the development of a substrate for the migration and re-entry of microbes once conditions are favorable. MIC occurs due to the metabolic activity of micro-organisms. The micro-organisms usually work synergistically to create an environment in which they can grow. This requires a combination of moisture, a suitable substrate, and a source of energy. The energy is derived from electrochemical reactions which are similar to aqueous corrosion cells. Thus, when the repository is hot and dry, MIC is not possible. Existing microbes in the crushed tuff backfill or invert will die or go dormant as they are dried out with decay heat. However, when the repository cools and the relative humidity rises, these existing or new airborne microbes may colonize and grow. The microbes create a biofilm that can contain both anaerobic and aerobic bacteria. The anaerobes, such as sulfate reducing bacteria, attack the corrosion-allowance carbon steel outer barrier. The conditions that will allow MIC to occur are similar to those that are conducive to aqueous corrosion - temperatures below boiling and relative humidities above about 60 percent. Although the extent to which MIC can influence waste package lifetimes is currently not well known, indications are that micro-organisms may indeed have a detrimental effect on waste packages (Horn and Meike, 1995).

Modeling of Repository Performance. Recommendations regarding whether or not additional barriers should be added to the EBS beyond the waste package are partly based on the total system performance of these barriers. This study relies heavily on the capabilities and expertise of the Performance Assessment and Modeling organization in estimating the performance of the various barriers addressed in this study. Currently available abstractions and models are used in the total system performance assessments. The results and conclusions of this study are partly based on such assessments. The intent of this study was not to help in updating the fidelity of TSPA as a whole, and so such was not done. Rather, only in those areas that were clearly deficient in addressing the specific problems associated with this study were efforts made to improve fidelity. Thus, the total system performance results presented in this study, as with those results presented in TSPA-1995, should be caveated with the statement (also expressed in Section 10 of TSPA-1995) that they are directly related to the Engineered Barrier System (EBS) and Natural Barrier System (NBS) conceptual models existing at the time the analyses were performed.

Modifications to the Waste Stream. Modifications to the input waste stream other than that assumed for the ACD Report (CRWMS M&O 1996b), such as DOE SNF, could have a significant effect on the calculations of peak dose rates at the accessible environment. Only when the inventories of the important radionuclides and the appropriate alteration/dissolution models for new waste types become available and are implemented in RIP will the specific effects on long-term repository

performance be known. At that time it would be prudent to re-evaluate the need for additional EBS performance barriers.

Long-Term Settlement. The thermohydrologic benefits of backfill are dependent on the amount of backfill surrounding the waste packages, as discussed in Section 5.2.5 of this report. What is currently not known is the effect that long-term settlement of the backfill will have on the thermohydrology near the waste package, and thus waste package performance as well as long-term repository performance.

6.4 RECOMMENDATIONS

As a result of considering the uncertainties described in the previous section, the small margins available with current concepts against the 1,000,000 year time frame, and the potential for significant total system performance improvements with EBS performance enhancements, several recommendations are made. Use of any of these recommendations as input to documents supporting procurement, fabrication, or construction is required to be controlled as TBV in accordance with the appropriate procedures.

- Currently, the project-level technical baseline does not require emplacement drift backfill. The current findings of this study indicate that no technical basis can be established for imposing a requirement for the use of backfill, chemically conditioned inverts, drip shields, or other EBS performance enhancements. However, it should be noted that a recent interpretation (CRWMS M&O 1996p) of the ^{36}Cl bomb-pulse findings in the Exploratory Studies Facility leading to higher fluxes (approximately 7 mm/yr) at the repository horizon was not considered in this FY 1996 study. At this time it is not known if this information would have changed either the previous conclusions or the following recommendations to carry the option for backfill; further analysis is required and recommended to assess the impact of such interpretations. In light of the unexplored impact of such uncertainties on repository performance, as well as current repository performance margins, a design requirement should be levied on the underground repository layout to provide a sufficient envelope such that a reasonable backfill emplacement system could be designed and backfit at a later date. As a contingency, this requirement should be demonstrated at the time of the Viability Assessment through an appropriate design study based primarily on analysis of emplacement drift design coupled with minimal backfill system concept development. For the license application design, if the decision is still to only maintain the option to backfill, the backfill concept should be further developed to address the licensing requirements for the use of reasonably available technology and safe constructibility for the placement of backfill.

- It is recommended that the following requirement be placed in the EBDRD:

  "Backfill in emplacement drifts is not required. However, the repository design should not preclude the use of emplacement drift backfill at the end of the preclosure period. The specifications for the emplacement drift envelope to accommodate are: 1) level single layer backfill (quartz sand, crushed tuff, or other material of similar favorable thermohydrologic properties), and 2) waste packages should be covered with at least 0.6 meters of material."

However, the Department of Energy Level I Program Change Control Board has recommended that the requirements document hierarchy be streamlined in areas, and at this time it is not obvious that the EBDRD and RDRD will any longer be a part of the document hierarchy. As the *Mined Geologic Disposal System Requirements Document* (DOE 1996) is developed to replace those documents, it will be evaluated to determine if any of the requirements coming out of this study are appropriate to capture in that document. In the interim, these requirements will be tracked in the CDA. The following modifications are suggested for implementation in the CDA Document:

Key assumption 046 of the CDA Document (CRWMS M&O 1996a) states:

Statement of Assumption : Current design assumes no backfill in emplacement drifts. Options for backfill will be considered based on ongoing and future backfill studies.

This Key Assumption should be modified to state the following:

"Statement of Assumption: Backfill in emplacement drifts is not required. However, the repository design should not preclude the use of emplacement drift backfill at the end of the preclosure period. The specifications for the emplacement drift envelope to accommodate are: 1) level single layer backfill (quartz sand, crushed tuff, or other material of similar favorable thermohydrologic properties), and 2) waste packages should be covered with at least 0.6 meters of material.

Rationale: TSPA calculations show that the Interim Postclosure Performance Standard (see assumption RDRD 3.2.1.6.c) is satisfied without requiring an additional EBS barrier. However, in light of the current repository performance margins and uncertainties, the underground repository layout should provide a sufficient envelope such that a reasonable backfill emplacement system could be designed and backfit at a later date. Further discussion of this conclusion can be found in the "Engineered Barrier System Performance Requirements Systems Study Report", DI # BB0000000-01717-5705-00001, Rev. 02."

- Testing required as a result of the previous recommendation includes tests of quartz sand, or material of similar favorable thermohydrologic properties in the repository environment and the relationship between such material(s) and microbial-induced corrosion. Further, because of the distinct availability and cost advantages of a crushed TSw2 tuff backfill versus that of a quartz sand backfill (Section 5.2.9 of this report), an investigation should be conducted at greater depth of the thermohydrologic deficiencies of crushed TSw2 tuff, and the significance of such on total system performance. As the understanding of the expected environment to be experienced by the waste package and the ability to meet post closure performance standards increases, it may be necessary to expand the backfill testing program to include testing to understand the potential materials interaction issues concerning the use of backfill material in emplacement drifts. However, at this time testing beyond what is described above is not recommended.

- Use of an emplacement drift invert chemically treated with a phosphate containing sedimentary apatite ore has been found, in bounding calculations, to severely retard the

transport of ^{237}Np to the AE. If subsequent evaluations of long-term repository performance (such as TSPA-VA) indicate the need for additional performance barriers within the EBS, the use of a chemically treated invert should be considered as an option and should be investigated in more detail. Specifically, the approximate amount of apatite beneath a waste package to ensure that all of the ^{237}Np is sequestered should be determined, along with the resulting assessment of whether it is feasible to place such an amount beneath a waste package.

- One of the potential attributes of emplacement drift backfill is its ability to protect waste packages from the effects of rockfall. However, the preliminary rockfall analysis conducted within this study has indicated that rockfall would have very little effect on overall waste package, and thus repository, performance. Therefore, the use of backfill as a means of protecting waste packages from rockfall is currently considered unnecessary. As additional information is accrued from the ESF, the results of this rockfall analysis, and the ensuing benefits of backfill in mitigating the effects of rockfall on long-term repository performance, should be re-examined.

- As part of the overall license strategy, a regulatory compliance strategy should be adopted for this issue at the time of the Viability Assessment. This strategy should take advantage of the repository's predicted performance being compliant with established limits, acknowledge the small calculated margin to the limits, acknowledge the uncertainties in the performance models, and identify contingency activities that need to be carried out to better quantify the performance benefits of the EBS enhancements (e.g., activities related to MIC, thermohydrologic value of backfill, long-term settlement of backfill, and feasibility of chemically conditioned invert). The strategy should also take advantage of a long term performance confirmation program for monitoring the need for an additional EBS performance barrier and the ability to backfit the repository with backfill (for example) if additional performance margin is required. This issue could potentially be monitored and tracked as a potential license condition to be resolved during the performance confirmation period after repository operations have commenced.

INTENTIONALLY LEFT BLANK

7. REFERENCES

Adepoju, A. Y.; Mattigod, S. V.; and Pratt, P. F. 1986. "Relationship Between Probable Dominant Phosphate Compound in Soil and Phosphorus Availability to Plants." *Plant and Soil*, Vol. 92, pp. 47-54.

Brechtel, C. E.; Kessel, D. S.; Lin, M.; and Martin, E. 1995. *Geotechnical Characterization of the North Ramp of the Exploratory Studies Facility*, Vol. I. Data Summary. SAND95-0488/1. Albuquerque, New Mexico: Sandia National Laboratories.

Bruno, J.; Brandberg, F.; Stumm, W.; and Wersin, P. 1992. "On the Influence of Carbonate in Mineral Dissolution. 1. The Thermodynamics and Kinetics of Hematite Dissolution in Bicarbonate Solutions at T = 25°C." *Geochimica et Cosmochimica Acta*, Vol. 56, pp. 1139-1147.

Buscheck, T. A. and Blink, J. 1995. "Thermal-Hydrological Analysis of Backfill." *Nuclear Waste Technical Review Board Presentation*, November 28, 1995. Las Vegas, Nevada.

Buscheck, T. A.; Nitao, J. J.; and Ramspott, L. D. 1996. "Localized Dryout: An Approach for Managing the Thermal-Hydrological Effects of Decay Heat at Yucca Mountain." *Proceedings of Material Research Society Symposium*, Vol. 412, pp. 715-722.

Conca, J., 1990. *Diffusion Barrier Transport Properties of Unsaturated Paintbrush Tuff Rubble Backfill*, Vol. 1, pp. 394-401. Location not given: High Level Radioactive Waste Management.

Conca, J. L. and Wright, J. V. 1992. "Diffusion and Flow in Gravel, Soil, and Whole Rock." *Applied Hydrogeology*, Vol. 1, pp. 5-24.

Conca, J. L. 1993. *Measurement of Unsaturated Hydraulic Conductivity and Chemical Transport in Yucca Mountain Tuff*, 28 p. Technical Report LA-12596-MS. Los Alamos, New Mexico: Los Alamos National Laboratory.

Conca, J. L. 1995. *The Ability of a Richards Barrier to Completely Divert Recharge in the Unsaturated Zone*, December 1995. Affiliate Report to Los Alamos National Laboratory.

Conca, J. and Wright, J. 1996. *Transport Property Testing of Engineered Barrier Materials for the Yucca Mountain Project*. NESTT Interim Report, Subcontract No. 215BA0016-3Y. Los Alamos, New Mexico: Los Alamos National Laboratory.

Corrosion 1987. *Metals Handbook*, 9th Ed., Vol. 13, p. 676 "Corrosion." Metals Park, Ohio: ASM International, 1987.

Crane, R. A. and Vachon, R. I. 1977. "A Prediction of the Bounds on the Effective Thermal Conductivity of Granular Materials." *International Journal of Heat and Mass Transfer*, Vol. 30, pp. 711-723.

CRG 1994. *Cost Reference Guide for Construction Equipment*. Dataquest.

CRWMS M&O 1993. *CDB_R.* CSCI ID A00000000-02268-1200-20002 Vol. 1.1, REV 1. Vienna, Virginia: Civilian Radioactive Waste Management System Management and Operating Contractor.

CRWMS M&O 1994. *Preclosure Radiological Safety Assessment for the ESF.* BAB000000-01717-2200-00006 REV 00. Las Vegas, Nevada: Civilian Radioactive Waste Management System Management and Operating Contractor.

CRWMS M&O 1995a. *Emplacement Scale Thermal Evaluations of Large and Small WP Designs.* BB0000000-01717,0200-00009 REV 00. Las Vegas, Nevada: Civilian Radioactive Waste Management System Management and Operating Contractor.

CRWMS M&O 1995b. *Repository Thermal Response: A Preliminary Evaluation of the Effects of Modeled Waste Stream Resolution.* SLTR 95-0002. Albuquerque, New Mexico: Sandia National Laboratories.

CRWMS M&O 1995c. *Bench-Scale Experimental Determination of the Thermal Diffusivity of Crushed Tuff.* SAND94-2320, UC-814. Albuquerque, New Mexico: Sandia National Laboratories.

CRWMS M&O 1995d. *Total System Performance Assessment-1995: An Evaluation of the Potential Yucca Mountain Repository.* B00000000-01717-2200-00136 REV 01. Las Vegas, Nevada: Civilian Radioactive Waste Management System Management and Operating Contractor.

CRWMS M&O 1995f. *Perform System Studies.* B00000000-01717-2200-00086 REV 02. Las Vegas, Nevada: Civilian Radioactive Waste Management System Management and Operating Contractor.

CRWMS M&O 1995g. *Status Report on Systems Study to Evaluate Technical Basis for Project Decision on Use of Backfill in Emplacement Drifts at the Potential High-Level Nuclear Waste Repository at Yucca Mountain, Nevada.* BB0000000-01717-5703-00003 REV 00. Las Vegas, Nevada: Civilian Radioactive Waste Management System Management and Operating Contractor.

CRWMS M&O 1995h. "Galvanic Effects in Multi-Barrier Waste Package Containers," LLYMP.9507060 Letter, Daniel McCright to Joon Lee, July 12, 1995.

CRWMS M&O 1996a. *Controlled Design Assumptions Document.* B00000000-01717-4600-00032 REV 03. Las Vegas, Nevada: Civilian Radioactive Waste Management System Management and Operating Contractor.

CRWMS M&O 1996b. *Mined Geologic Disposal System Advanced Conceptual Design Report.* B00000000-01717-5705-00027 REV 00. Las Vegas, Nevada: Civilian Radioactive Waste Management System Management and Operating Contractor.

CRWMS M&O 1996c. *Test Model Abstractions for Total System Performance Assessment.* B00000000-01717-2200-00173. Las Vegas, Nevada: Civilian Radioactive Waste Management System Management and Operating Contractor.

CRWMS M&O 1996d. *Thermal Loading Study for FY 1996.* B00000000-01717-5705-00044 REV 01. Las Vegas, Nevada: Civilian Radioactive Waste Management System Management and Operating Contractor.

CRWMS M&O 1996e. *Waste Package Off-Normal And Accident Scenario Report.* BBA000000-01717-5705-00008 REV 00. Las Vegas, Nevada: Civilian Radioactive Waste Management System Management and Operating Contractor.

CRWMS M&O 1996f. "Material Selection for Design," LV.WP.DS.03/96-051. Letter, A. M. Segrest to D. C. Haught, March 1, 1996. Las Vegas, Nevada: Civilian Radioactive Waste Management System Management and Operating Contractor.

CRWMS M&O 1996g. "Waste Package Temperature Increase Due to Addition of Drip Shield." LV.WP.HW.06/96.127. Internal Office Communication, H. Wang to M. Balady, June 3, 1996. Las Vegas, Nevada: Civilian Radioactive Waste Management System Management and Operating Contractor.

CRWMS M&O 1996h. "Detailed Analyses for Backfill and Invert Cost Estimates for EBS Study." LV.RD.KKB.07/96-036. Internal Office Communication (with enclosures), K. K. Bhattacharyya to M. Balady, July 23, 1996. Las Vegas, Nevada: Civilian Radioactive Waste Management System Management and Operating Contractor.

CRWMS M&O 1996i. *Static Structural Analysis of Waste Packages in Degraded States.* BBAA00000-01717-0200-00014 REV 00. Las Vegas, Nevada: Civilian Radioactive Waste Management System Management and Operating Contractor.

CRWMS M&O 1996j. *Performance Confirmation Concepts Study Report.* B00000000-01717-5705-00035 REV 00A. Las Vegas, Nevada: Civilian Radioactive Waste Management System Management and Operating Contractor.

CRWMS M&O 1996k. *Technical Document Preparation Plan for the Engineered Barrier System Performance Requirements Systems Study Report.* BB0000000-01717-4600-00023 REV 01. Las Vegas, Nevada: Civilian Radioactive Waste Management System Management and Operating Contractor.

CRWMS M&O 1996l. *Rock Size Required to Cause a Through Crack in Containment Barriers.* BBAA00000-01717-0200-00015 REV 00. Las Vegas, Nevada: Civilian Radioactive Waste Management System Management and Operating Contractor.

CRWMS M&O 1996m. "Important Aspects of ^{36}Cl Studies at Yucca Mountain." LV.SI.SLE.05/96-034. Internal Office Communication (with enclosure), C. Thomas Statton to D. Williams, May 29, 1996. Las Vegas, Nevada: Civilian Radioactive Waste Management System Management and Operating Contractor.

CRWMS M&O 1996n. *Near Field and Altered Zone Environment Report.* UCRL-LR-124998, Vol. 2. Livermore, California: Lawrence Livermore National Laboratory.

CRWMS M&O 1996o. *Engineered Materials Characterization Report.* UCRL-ID-119564, Vol. 3, REV 3. Livermore, California: Lawrence Livermore National Laboratory.

CRWMS M&O 1996p. *Development and Calibration of the Three-Dimensional Site-Scale Unsaturated Zone Model of Yucca Mountain, Nevada.* Ernest Orlando Lawrence Berkeley National Laboratory, August 1996.

Department of the Navy 1982. *Soil Mechanics Design Manual 7.1.* Naval Facilities Engineering Command, Chapter 7.

DOE 1988. *Site Characterization Plan: Yucca Mountain Site, Nevada Research and Development Area.* DOE/RW-0199. Oak Ridge, Tennessee: U.S. Department of Energy Office of Scientific and Technical Information.

DOE 1992. *Cost Estimating and Standardization.* U.S. Department of Energy. DOE Order 5700.2D. September 1992.

DOE 1993. *Cost Estimating Guide.* U.S. Department of Energy. Nevada: Nevada Operations Office.

DOE 1994a. *Cost Estimating Guide.* DOE/MA-0065, Vol. 6. U.S. Department of Energy. Office of Infrastructure Acquisition (FM-50).

DOE 1994b. *Repository Design Requirements Document.* YMP/CM-0023. Las Vegas, Nevada: Civilian Radioactive Waste Management System Management and Operating Contractor.

DOE 1994c. *Engineered Barrier Design Requirements Document.* YMP/CM-0024. Las Vegas, Nevada: Civilian Radioactive Waste Management System Management and Operating Contractor.

DOE 1994d. *Q-List,* YMP/90-55Q, REV 3. Las Vegas, Nevada: Civilian Radioactive Waste Management System Management and Operating Contractor.

DOE 1996. Mined Geologic Disposal System Requirements Document. DOE/RW-0404P, B00000000-00811-1708-00002. U.S. Department of Energy: Vienna, Virginia.

Fontana, M. G. 1986. *Corrosion Engineering.* 3rd Ed. New York: McGraw-Hill.

Freeze, R. A. and Cherry, J. A. 1979. *Groundwater.* Englewood Cliffs, New Jersey: Prentice-Hall, Inc.

Fyfe, D. 1994. "The Atmosphere." *Corrosion,* Vol. 1-Metal/Environment Reactions, 3rd Ed. Burstein, G. T.; Jarman, R. A.; and Shreir, L. L., Eds. Butterworth-Heinemann, pp. 2:31-2:42.

Gauthier, J. H.; Borns, D. J.; Dockery, H. A.; and Wilson, M. L. 1995. "Incorporating Tectonic Effects in Total-System Performance Assessment of Yucca Mountain." *Methods of Seismic Hazards*

Evaluation, Proceedings of Focus '95. Location not given: American Nuclear Society and the Geological Society of America.

Golder Associates, Inc. 1993. *Application of the RIP (Repository Integration Program) to the Proposed Repository at Yucca Mountain: Conceptual Model and Input Data Set*. Redmond, Washington: Golder Associates.

Golder Associates, Inc. 1994. *RIP Performance Assessment and Strategy Evaluation Model: Theory Manual and User's Guide, Version 3.20*. Redmond, Washington: Golder Associates.

Golder Associates, Inc. 1995. *Verification Report for the Repository Integration Program (RIP)*. Location not given: U.S. Department of Energy, WIPP Technical Assistance Contractor (WTAC).

Gutjahr, A.; Dabringhaus, H.; and Ladmann, R. 1996. "Studies of the Growth and Dissolution Kinetics of the $CaCO_3$ Polymorphs Calcite and Aragonite." *Journal of Crystal Growth*, Vol. 158, pp. 296-309.

Hassler, G. L. and Brunner, E. 1945. "Measurement of Capillary Pressures in Small Core Samples." *Transactions of the American Institute of Mining and Metallurgical Engineering*, Vol. 160, pp. 114-123.

Haynie, F. H.; Spence, J. W.; and Upham, J. B. 1978. "Effects of Air Pollutants on Weathering Steel and Galvanized Steel: A Chamber Study." *Atmospheric Factors Affecting the Corrosion of Engineering Metals*, pp. 30-47. ASTM STP 646. S. K. Coburn, Ed. Location not given: American Society for Testing and Materials.

Hoffman, R. N. A. 1963. "A Technique for the Determination of Capillary Pressure Curves Using a Constantly Accelerated Centrifuge." *Society of Petroleum Engineering Journal*, Vol. 3, pp. 227-235.

Horn, J. M. and Meike, A. 1995. *Microbial Activity at Yucca Mountain*. UCRL-ID-122256. Livermore, California: Lawrence Livermore National Laboratory.

Klute, A. and Dirksen, C. 1986. "Hydraulic Conductivity and Diffusivity: Laboratory Methods." *In Methods of Soil Analysis, Part 1, Physical and Mineralogical Methods*, pp. 687-734. 2nd Ed. A. Klute, Ed. Madison, Wisconsin: American Society of Agronomy, Inc., and Soil Science Society of America, Inc.

Knauss, K. G. and Wolery, T. J. 1988. "The Dissolution Kinetics of Quartz as a Function of pH and Time at 70°C." *Geochimica et Cosmochimica Acta*, Vol. 52, pp. 43-53.

Koeppenkastrop, D. and De Carlo, E. J. 1988. "Adsorption of Rare Earth Elements From Seawater onto Synthetic Mineral Phases." *EOS Transactions of American Geophysical Union*, Vol. 69, p. 1254.

Koeppenkastrop, D. and De Carlo, E. J. 1992. "Sorption of Rare Earth Elements From Seawater onto Synthetic Mineral Phases; An Experimental Approach." *Chemical Geology*, Vol. 95, pp. 251-263.

Krupiczka, R. 1967. "Analysis of Thermal Conductivity in Granular Materials." *International Chemical Engineering*, Vol. 7, No. 1, pp. 122-144.

Lambe, T. William and Whitman, R. V. 1969. *Soil Mechanics*, Chapter 11. New York: John Wiley & Sons.

Luikov, A. V.; Fraiman, Y. E.; Shashkov, A. G.; and Vasilev, L. L. 1968. "Thermal Conductivity of Porous Systems." *International Journal of Heat and Mass Transfer*, Vol. 7, pp. 117-140.

Ma, Q. Y.; Logan, T. J.; and Traina, S. J. 1993. "In Situ Lead Immobilizaton by Apatite." *Environmental Science Technology*, Vol. 27, pp. 1803-1810.

Makdisi, F. I. and Seed, H. B. 1978. "A Simplified Method for Measuring Earthquake-Induced Deformations in Dams and Embankments." *Journal of Soil Mechanics & Foundation Engineering of ASCE*, Vol. 104GT7, pp. 849-867.

Marsh, G. P. and Taylor, K. J. 1988. "An Assessment of Carbon Steel Containers for Radioactive Waste Disposal." *Corrosion Science*, Vol. 28, pp. 289-320.

Marsh, G. P.; Sooi, Z.; and Taylor, K. J. 1988. *The Kinetics of Pitting Corrosion of Carbon Steel.* SKB Technical Report 88-09, Stockholm, Sweden.

McArthur, J. M. 1985. "Francolite Geochemistry—Compositional Controls on Formation, Diagenesis, Metamorphism, and Weathering." *Geochimica et Cosmochimica Acta*, Vol. 49, pp. 23-35.

McArthur, J. M.; Hamilton, P. J.; Osborn, A. O.; Salami, A. R.; and Thirwall, M. 1990. "Dating Phosphogenesis with Sr Isotopes." *Geochimica et Cosmochimica Acta*, Vol. 54, pp. 1343-1352.

Middleton, M. F. 1994. "Determination of Matrix Thermal Conductivity from Dry Drill Cuttings." *American Association of Petroleum Geologists (AAPG) Bulletin*, Vol. 78, No. 11, pp. 1790-1799.

Miller, I.; Cunnane, M.; and Kossik, R. 1992. "*A New Methodology for Repository Site Suitability Evaluation.*" *Proceedings of the Third International Conference for High Level Radioactive Waste Management*, April 12-16, 1992. Las Vegas, Nevada.

Moody, T. E. and Wright, J. 1995. "Adsorption Isotherms: North Carolina Apatite Induced Precipitation of Lead, Zinc, Manganese and Cadmium from Bunder Hill 4000 Sndel." *The System of Mineralogy*, 7th Ed. Location not given: John Wiley and Sons.

Nimmo, J. R.; Hammermeister, D. P.; and Rubin, J. 1987. "Unsaturated Flow in a Centrifugal Field: Measurement of Hydraulic Conductivity and Testing of Darcy's Law." *Water Resources Research*, Vol. 23, pp. 124-134.

Nimmo, J. R. and Akstin, K. C. 1988. "Hydraulic Conductivity of a Sandy Soil at Low Water Content After Compaction By Various Methods." *Soil Science Society of America Journal*, Vol. 52, pp 303-310.

Nimmo, J. R. and Mell, K. A. 1991. "Centrifugal Techniques for Measuring Saturated Hydraulic Conductivity." *Water Resources Research*, Vol. 27, pp. 1263-1269.

Nimmo, J. R.; Akstin, K. C.; and Stonestrom, D. A. 1994. "The Feasibility of Recharge Rate Determination Using Steady-State Centrifuge Method." *Soil Science Society of America Journal*, Vol. 58, pp. 49-56.

NRC 1995. *Technical Bases for Yucca Mountain Standards*. Washington, D.C.: National Research Council.

Orlando, E. 1996. *Development and Calibration of the Three-Dimensional Site-Scale Unsaturated Zone Model of Yucca Mountain, Nevada*. Berkeley, California: Lawrence Berkeley National Laboratory.

Phipps, P. B. and Rice, D. W. 1979. "The Role of Water in Atmospheric Corrosion." *Corrosion Chemistry*, pp. 235-261. G. R. Brubaker and P. B. Phipps, Eds. Location not given: ACS Symposium Series 89, American Chemical Society.

Proctor, R. V. and White, T. L. 1946. *Rock Tunneling with Steel Supports*. Location not given: Commercial Shearing & Stamping Company.

Robinson, B. A.; Gable, C. W.; Wolfsberg, A. V.; and Zyvoloski, G. A. 1995. *An Unsaturated Zone Flow and Transport Model of Yucca Mountain*. YMP Milestone Number 3468.

Robinson, B. A.; Gable, C. W.; Wolfsberg, A. V.; and Zyvoloski, G. A. 1996. *An Unsaturated Zone Flow and Transport Model of Yucca Mountain: 1996 Revision*. YMP Milestone 3672.

Robinson, B. A. and Triay, I. R. 1996. "Near-Field Radionuclide Transport Calculations." Draft Report. Los Alamos, New Mexico: Los Alamos National Laboratory.

Rose, D. 1982. "Revising Terzaghi's Tunnel Rock Load Coefficients." *Issues in Rock Mechanics*, pp. 953-960. Twenty-Third Symposium on Rock Mechanics. University of California, Berkeley, California: Society of Mining Engineers of AIME.

Ruby, M. V.; Davis, A.; and Nicholson, A. 1994. "In situ Formation of Lead Phosphates in Soils as a Method to Immobilize Lead." *Environmental Science and Technology*, Vol. 28, pp. 646-654.

Ruijini, G.; Ives, M. B.; and Srivastava, S. C. 1989. "Pitting Corrosion Behavior of UNS No. 8904 Stainless Steel in a Chloride/Sulfate Solution." *Corrosion*, Vol. 45, No. 11, pp. 874-882.

Sassani, D. 1995. LV.PA.DCS.7/95.053. Oral Presentation. Location not given: Civilian Radioactive Waste Management System Management and Operating Contractor.

Skinner, H. C. W. 1987. "Bone: Mineral and Mineralization." *The Scientific Basis of Orthopaedics*. J. A. Albright and R. Brand, Eds., Norfolk, Connecticut: Appleton and Longe.

Skinner, H. C. W. 1989. "Low Temperature Carbonate Phosphate Materials For the Carbonate-Apatite Problem." *Origin, Evolution and Model Aspects of Biomineralization in Plans and Animals*. Rex Crick, Ed. Proceedings of the 5th International Symposium on Biomineralization, Arlington, Texas. New York: Plenum Press.

Skinner, H. C. W.; Griswold, J.; and Hunt, H. T. 1980. "Automatic Scanning of Multiple Sample Guinier X-ray Power Diffraction Films." *Journal Of Physics E:Scientific Instruments*, Vol. 13, pp. 74-79.

Skinner, H. C. W. and Burnharn C. W. 1968. "Hydroxyapatite, Annual Report of the Director, Geophysical Laboratory." Carnegie Institute, Washington, D. C.

Stanforth, R. and Chowdhury, A. 1994. "In Situ Stabilization of Lead-Contaminated Soil." *Federal Environmental Restoration III and Waste Minimization II Conference Proceedings*. New Orleans, Louisiana.

Steefel, C. I. and Lasaga, A. C. 1994. "A Coupled Model for Transport of Multiple Chemical Species and Kinetic Precipitation/Dissolution Reactions with Application to Reactive Flow in Single Phase Hydrothermal Systems." *American Journal of Science*, Vol. 294, pp. 529-592.

Steefel, C. I. and Yabusaki, S. B. 1995. *OS3D/GIMRT: Software for Modeling Multicomponent-Multidimensional Reactive Transport: User's Manual and Programmer's Guide*, Ver. 1.0, 58 p.

Stephens, D. B. and Rehfeldt, K. R. 1985. "Evaluation of Closed-Form Analytical Models to Calculate Conductivity in a Fine Sand." *Soil Science Society of America Journal*, Vol. 49, pp. 12-19.

Stone, C. A. 1994. "A Matrix Approach to Probabilistic Key Block Analysis." *Ph.D. Dissertation*. Michigan: Michigan Technological University.

Stone, C. A. and Boontun, A. 1995. *Probabilistic Assessment of Keyblock Size in the ESF Main Drift*. Las Vegas, Nevada: Agapito Associates, Inc.

Strutt, J. E.; Barbier, B.; and Nichols, J. R. 1985. "The Prediction of Corrosion by Statistical Analysis of Corrosion Profiles," *Corrosion Science*, Vol. 25, pp. 305-315.

Szklarska-Smialowska, Z. 1986. "Pitting Corrosion of Metals." Houston, Texas: National Association of Corrosion Engineers.

Tidwell and Glass, 1994. "X-ray and Visible Light Transmission for Laboratory Measurement of Two-Dimensional Saturation Fields in Thin-slab Systems." *Water Resources Research*, Vol. 30, No. 11, pp. 2873-2882.

Triay, I. and Thornton, S. 1996. *Sorption of Radionuclides by Apatite as a Backfill Material.* Los Alamos, New Mexico: Los Alamos National Laboratory.

van Genuchten, M. T. 1980. "A Closed Form Equation for Predicting Hydraulic Conductivity of Unsaturated Soils," *Soil Science Society of America Journal*, Vol. 44, pp. 892-898.

van Lier, J. A.; de Bruyn; and Overbeek, J. Th. G. 1960. "The Solubility of Quartz." *Journal of Physical Chemistry*, Vol. 64, pp. 1675-1682.

Vernon, W. H. 1933. "The Role of the Corrosion Product in the Atmospheric Corrosion of Iron." *Transactions of the Electrochemical Society*, Vol. 64, pp. 31-41.

Wilson, M. L., et al. 1994. *Total-System Performance Assessment for Yucca Mountain - SNL Second Iteration.* Report SAND93-2675. Albuquerque, New Mexico: Sandia National Laboratories.

White, A. F.; Hochella, Jr., M. F.; and Peterson, M. L. 1994. "Electoro Chemistry and Dissolution Kinetics of Magnetite and Ilmenite." *Geochimica et Cosmochimica Acta*, Vol. 58, pp. 1859-1875.

Wittwer, C.; Bodvarsson, G. S.; Chen, G.; Chornack, M.; Flint, A.; Flint, L.; Kwicklis, E.; and Spengler, R. 1995. "Preliminary Development of the LBL/USGS Three-Dimensional Site-Scale Model of Yucca Mountain, Nevada." Technical Report LBL-37356/UC-814. Berkeley, California: Lawrence Berkeley National Laboratory.

Wong, I.; Menges, C.; Pezzopane, S.; and Quittmeyer, R. 1995. "Probabilistic Seismic Hazard Analysis of the ESF at Yucca Mountain, NV." *5th DOE Natural Phenomena Hazards Mitigation Symposium Presentation.* Denver, Colorado.

Woodside, W. and Messmer, J. H. 1961. "Thermal Conductivity of Porous Media I. Unconsolidated Sands." *Journal of Applied Physics*, Vol. 32, No. 9, pp. 1688-1699.

Wright, J. 1990a. "Conodont Apatite: Structure and Geochemistry." *Metazoan Biomineralization: Patterns, Processes and Evolutionary Trends, 28th International Geological Congress*, pp. 445-459. Joseph Carter, Ed. Washington, D.C.: Paleontological Society and American Geophysical Union.

Wright, J. 1990b. "Conodont Geochemistry, a Key to the Paleozoic." *1st International Senckenberg Conference and 5th European Conodont Symposium (ECOS V) Contributions III*, pp. 277-305. Willi Ziegler, Ed. Germany: Courier Forschungsinstitut Senchenberg.

Wright, J.; Holser, W. T.; and Miller, J. F. 1987a. "Chemostratigraphy of Conodonts Across the Cambrian-Ordovician Boundary: Western United States and Southeast China." *Conodonts: Investigate Techniques and Applications*, pp. 259-286. Ronal L. Austin, Ed. London, England: Ellis Horwood, Ltd.

Wright, J.; Holser, W. T.; and Scrader, H. 1987b. "Paleoredox Variations in Ancient Oceans Recorded by Rare Earth Elements in Fossil Apatite." *Geochimica et Cosmochimica Acta*, Vol. 51, pp. 631-644.

Wright J.; Clark, J.; Conca, J. L.; and Repetski, J. 1990. "Geochemistry and Microstructure of Conodonts from Jilin Province, China." *1st International Senckenberg Conference and European Conodont Symposium Contributions III*, Vol. 118, pp. 307-332. Frankfurt, Germany: Courier Forschunginstitut Senckenberg.

Wright, J. V.; Chen, X.; and Conca, J. L. 1994. *Hydrostratigraphy and Recharge Distributions from Direct Measurements of Hydraulic Conductivity Using the UFA™ Method*, 150 p. PNL Technical Report PNL-9424. Richland, Washington: Pacific Northwest Lab.

Xu, Y. and Schwartz, F. W. 1994. "Lead Immobilization by Hydroxyapatite in Aqueous Solutions." *Journal of Contaminant Hydrology*, Vol. 15, pp. 187-206.

YMSCO 1996. "Fiscal Year (FY) 1997 Planning Guidance (SCPB: N/A)." Letter (with enclosures), Wesley E. Barnes to L. Dale Foust, July 5, 1996.

8. ACRONYMS

ACD	Advanced Conceptual Design
AE	Accessible Environment
AML	Areal Mass Loading
BWR	Boiling Water Reactor
CCDF	Complementary Cumulative Distribution Function
CDA	Controlled Design Assumptions
CDF	Cumulative Distribution Function
CFR	Code of Federal Regulations
CID	Center-In-Drift
CRWMS	Civilian Radioactive Waste Management System
DHLW	Defense High Level Waste
DOE	Department of Energy
EBDRD	Engineered Barrier Design Requirements Document
EBS	Engineered Barrier System
EPA	Environmental Protection Agency
ESF	Exploratory Studies Facility
FEA	Finite-Element Analysis
LML	Lineal Mass Loading
M&O	Management and Operating contractor
MGDS	Mined Geologic Disposal System
MIC	Microbial-Influenced Corrosion
MTU	Metric Tons of Uranium
NAS	National Academy of Sciences
NBS	Natural Barrier System
NRC	National Research Council
NRC	Nuclear Regulatory Commission
OCID	Off-Center-In-Drift
OFF	Oldest Fuel First
PTn	Non-welded vitric tuff
PWR	Pressurized Water Reactor

QA	Quality Assurance
QAP	Quality Administrative Procedure
RDRD	Repository Design Requirements Document
RIP	Repository Integrating Program
SNF	Spent Nuclear Fuel
SZ	saturated zone
TSPA	Total System Performance Assessment
TSw	Topopah Spring welded unit
TSw2	Topopah Spring welded unit
UFA	Unsaturated Flow Apparatus
WP	Waste Package
YFF	Youngest Fuel First
YMSCO	Yucca Mountain Site Characterization Office
2-D	two dimensional
3-D	three dimensional

APPENDIX A

ANSYS Temperature Results for Backfilling at 100 Years

Temperature Results for Backfill at 100 years

Temperature Location Key

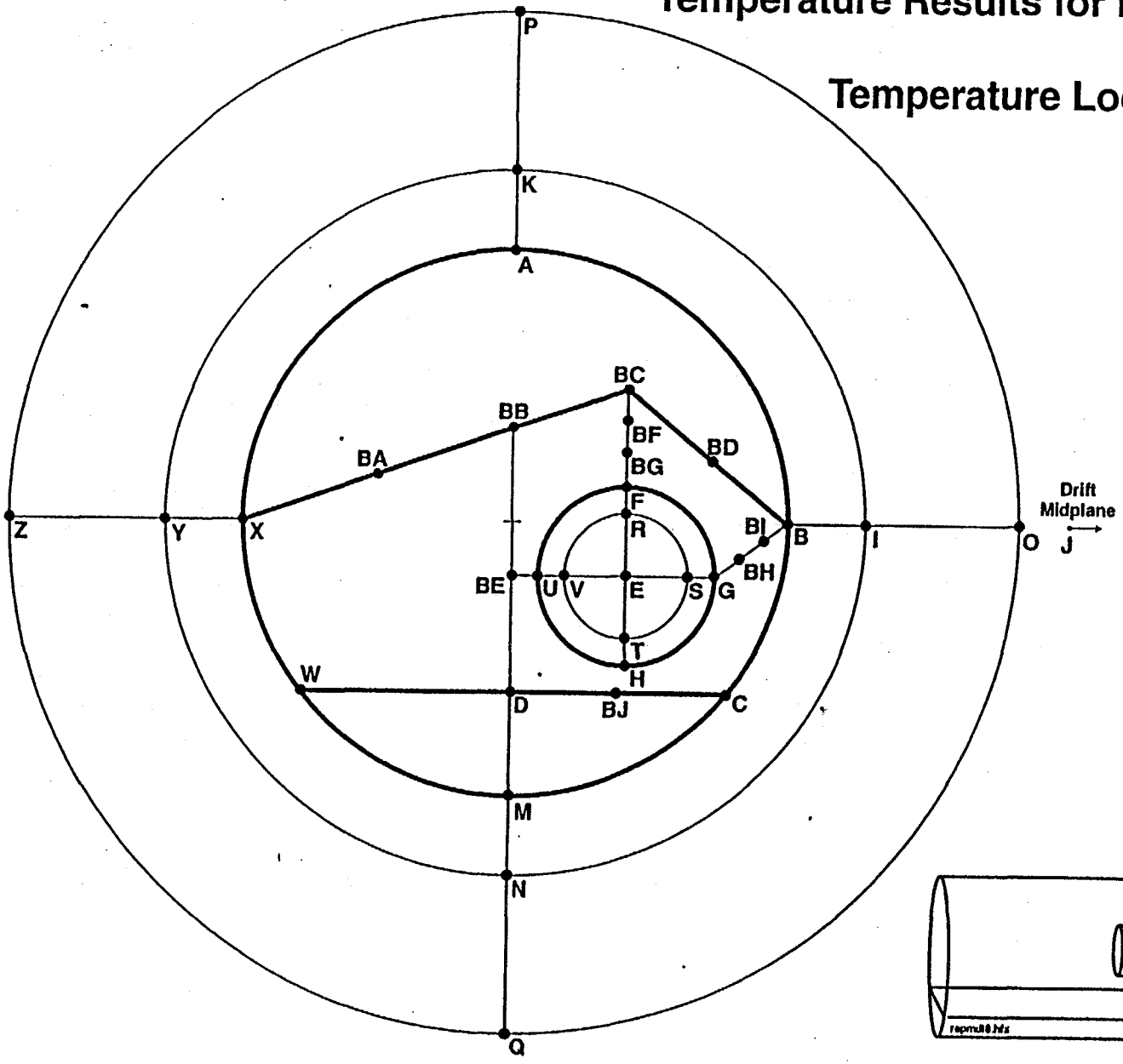

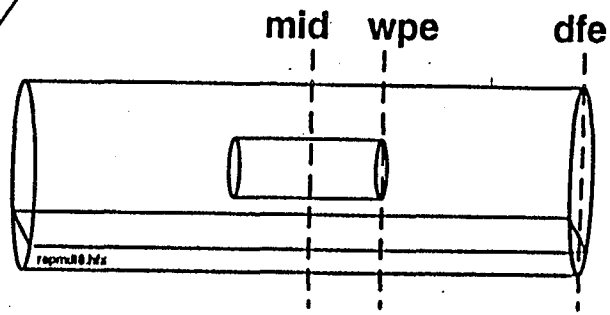

Temperature Results for Backfill at 100 years

Temperatures at WP Midlength (Axial Position: mid) for NO backfill

21 PWR Waste Package Emplaced OCID at 83 MTU/acre with 39.65 GWd/MTU burnup Average SNF (ly95cdaO-P), Sloped Backfill

Peak internal temp. (E) based on Deg C/kW from WP-CDR MPC WPs and 10 year old, 48 GWd/MTU burnup Design Basis SNF

Time (years)	A	B	C	E	F	G	H	I	M	O	U	X	BC	BF	BG	BH	BI	BJ
0.0	26	26	26	323	73	73	73	26	26	26	73	26						26
0.1	59	76	73	334	96	102	102	51	43	31	95	57						81
0.2	66	83	80	335	101	107	107	58	50	36	100	64						87
0.3	70	87	84	336	104	110	110	62	55	40	103	68						90
0.4	73	89	87	336	106	113	112	65	58	42	105	71						93
0.5	76	92	89	336	108	114	114	68	60	45	107	74						95
0.6	78	94	91	336	110	116	116	70	63	47	109	76						97
0.7	80	95	93	336	111	117	117	72	65	49	110	78						99
0.8	81	97	94	336	113	119	119	73	66	51	111	80						100
0.9	83	98	96	336	114	120	120	75	68	52	112	81						102
1.0	84	100	97	336	115	121	121	76	69	54	113	83						103
2.0	95	109	107	334	123	129	128	87	80	66	121	94						112
3.0	102	116	114	332	128	134	134	95	88	74	127	101						119
4.0	108	121	119	330	133	138	138	101	94	81	132	107						124
5.0	113	125	123	328	136	142	142	105	99	87	135	112						128
6.0	117	129	127	325	139	144	144	109	103	91	138	116						131
7.0	120	131	130	323	141	147	146	113	106	95	140	119						134
8.0	123	134	132	321	143	148	148	116	109	98	142	122						136
9.0	125	136	134	319	145	150	150	118	112	101	144	124						138
10.0	127	137	136	318	146	151	151	120	114	103	145	126						139
20.0	137	146	145	297	153	157	157	131	126	117	152	137						147
30.0	142	149	148	280	155	158	158	137	132	125	154	141						150
40.0	145	151	150	265	156	159	159	140	136	130	155	144						152
50.0	146	151	150	252	156	158	158	142	138	133	155	145						152
60.0	146	151	150	241	155	157	157	143	139	134	154	146						152
70.0	145	150	149	231	153	156	155	143	140	135	153	145						151
80.0	145	149	148	223	152	154	154	142	139	135	151	144						149
90.0	144	147	147	216	150	152	152	141	139	135	150	144						148
100.0	143	146	146	209	149	151	151	141	138	135	149	143						147
200.0	139	141	141	180	143	144	144	138	136	134	143	139						141
300.0	136	138	138	169	140	140	140	135	134	132	139	136						138
400.0	135	136	136	162	137	138	138	134	133	131	137	135						136
500.0	133	135	134	158	136	136	136	133	132	130	136	133						135
600.0	132	133	133	153	134	135	135	131	130	129	134	132						133
700.0	131	132	131	150	132	133	133	130	129	128	132	130						132
800.0	129	130	130	147	131	131	131	129	128	127	131	129						130
900.0	128	129	129	144	130	130	130	127	127	126	129	128						129
1000.0	127	128	127	142	128	129	129	126	126	125	128	127						128
1500.0	125	126	125	136	126	126	126	125	124	124	126	125						126
2000.0	117	118	118	126	118	119	119	117	117	117	118	117						118
2500.0	112	112	112	120	113	113	113	112	112	111	113	112						112
3000.0	107	108	108	114	108	108	108	107	107	107	108	107						108
3500.0	104	105	104	111	105	105	105	104	104	103	105	104						105
4000.0	101	102	102	108	102	102	102	101	101	101	102	101						102
4500.0	98	98	98	104	99	99	99	98	98	97	99	98						98
5000.0	95	95	95	101	96	96	96	95	95	94	95	95						95
5500.0	92	93	92	98	93	93	93	92	92	92	93	92						93
6000.0	90	90	90	95	90	90	90	90	90	89	90	90						90
6500.0	88	88	88	93	88	88	88	87	87	87	88	88						88
7000.0	86	86	86	91	86	86	86	86	86	85	86	86						86
7500.0	84	84	84	89	84	85	85	84	84	83	84	84						84
8000.0	82	82	82	87	83	83	83	82	82	82	83	82						82
8500.0	81	81	81	85	81	81	81	80	80	80	81	81						81
9000.0	79	79	79	84	80	80	80	79	79	79	80	79						79
9500.0	78	78	78	82	78	78	78	78	78	77	78	78						78
10000	76	76	76	81	77	77	77	76	76	76	77	76						77

Temperature Results for Backfill at 100 years

Temperatures at WP End (Axial Position: wpe) for NO backfill

21 PWR Waste Package Emplaced OCID at 83 MTU/acre with 39.65 GWd/MTU burnup Average SNF (ly95cdaO-P), Sloped Backfill
Peak internal temp. (E) based on Deg C/kW from WP-CDR MPC WPs and 10 year old, 48 GWd/MTU burnup Design Basis SNF

Time (years)	A	B	C	E	F	G	H	I	M	O	U	X	BC	BF	BG	BH	BI	BJ
0.0	26	26	26	65	60	61	60	26	26	26	60							26
0.1	53	61	59	85	80	83	83	44	39	30	79							64
0.2	59	68	65	90	85	88	88	51	46	34	84							70
0.3	64	72	69	93	89	92	91	55	51	38	88							74
0.4	67	75	73	96	91	94	93	59	54	41	90							77
0.5	70	77	75	98	93	96	95	61	56	43	92							80
0.6	72	79	77	100	95	98	97	63	59	45	94							82
0.7	74	81	79	101	96	99	99	65	61	47	95							84
0.8	76	83	81	102	98	101	100	67	62	49	97							85
0.9	77	84	82	104	99	102	101	69	64	51	98							87
1.0	79	86	84	105	100	103	102	70	65	52	99							88
2.0	90	96	95	113	109	112	111	82	77	64	108							98
3.0	98	104	102	120	115	118	117	90	85	73	114							106
4.0	104	110	108	124	120	123	122	96	91	80	119							111
5.0	108	114	113	128	124	127	126	101	96	85	123							116
6.0	112	118	116	131	127	130	129	105	100	90	126							119
7.0	116	121	119	134	130	132	132	108	104	94	129							122
8.0	119	124	122	136	132	134	134	111	107	97	131							125
9.0	121	126	125	138	134	136	136	114	109	99	133							127
10.0	123	128	127	139	136	138	138	116	111	102	135							129
20.0	134	138	137	147	144	146	146	128	124	116	144							139
30.0	139	143	142	150	147	149	149	134	131	124	147							143
40.0	143	145	144	152	149	151	151	138	135	129	149							146
50.0	144	146	146	152	150	151	151	140	137	132	150							147
60.0	144	147	146	151	150	151	151	141	138	134	149							147
70.0	144	146	145	150	149	150	150	141	139	135	149							146
80.0	143	145	145	149	148	149	148	141	138	135	147							146
90.0	143	144	144	148	147	147	147	140	138	135	146							145
100.0	142	143	143	147	146	146	146	139	138	135	145							144
200.0	138	139	139	141	141	141	141	137	136	134	140							139
300.0	136	136	136	138	138	138	138	135	134	132	138							137
400.0	134	135	135	136	136	136	136	133	133	131	136							135
500.0	133	133	133	135	134	135	135	132	131	130	134							134
600.0	131	132	132	133	133	133	133	131	130	129	133							132
700.0	130	131	131	132	131	132	132	130	129	128	131							131
800.0	129	129	129	130	130	130	130	128	128	127	130							129
900.0	128	128	128	129	129	129	129	127	127	126	129							128
1000.0	127	127	127	128	127	128	128	126	126	125	127							127
1500.0	125	125	125	126	125	126	126	124	124	124	125							125
2000.0	117	118	117	118	118	118	118	117	117	117	118							118
2500.0	112	112	112	112	112	112	112	112	111	111	112							112
3000.0	107	108	107	108	108	108	108	107	107	107	108							108
3500.0	104	104	104	105	104	105	105	104	104	103	104							104
4000.0	101	101	101	102	102	102	102	101	101	101	102							101
4500.0	98	98	98	98	98	98	98	98	98	97	98							98
5000.0	95	95	95	95	95	95	95	95	95	94	95							95
5500.0	92	92	92	93	92	93	93	92	92	92	92							92
6000.0	90	90	90	90	90	90	90	90	90	89	90							90
6500.0	87	88	88	88	88	88	88	87	87	87	88							88
7000.0	86	86	86	86	86	86	86	85	85	85	86							86
7500.0	84	84	84	84	84	84	84	84	84	83	84							84
8000.0	82	82	82	82	82	82	82	82	82	82	82							82
8500.0	80	81	81	81	81	81	81	80	80	80	81							81
9000.0	79	79	79	79	79	79	79	79	79	79	79							79
9500.0	78	78	78	78	78	78	78	77	77	77	78							78
10000	76	76	76	77	77	77	77	76	76	76	76							76

Temperature Results for Backfill at 100 years

Temperatures Between WPs (Axial Position: dfe) for NO backfill

21 PWR Waste Package Emplaced OCID at 83 MTU/acre with 39.65 GWd/MTU burnup Average SNF (ly95cdaO-P), Sloped Backfill

Peak internal temp. (E) based on Dog C/kW from WP-CDR MPC WPs and 10 year old, 48 GWd/MTU burnup Design Basis SNF

Time (years)	A	B	C	E	F	G	H	I	M	O	U	X	BC	BF	BG	BH	BI	BJ
0.0	26	26	26					26	26	26		26						26
0.1	40	39	38					32	32	27		40						40
0.2	46	45	44					38	37	30		46						46
0.3	50	50	48					41	40	33		50						51
0.4	54	53	51					45	44	35		54						54
0.5	57	56	54					47	46	37		56						57
0.6	59	58	57					50	49	39		59						60
0.7	61	61	59					52	51	41		61						62
0.8	63	62	61					54	52	43		63						64
0.9	65	64	63					55	54	45		65						65
1.0	67	66	64					57	56	46		66						67
2.0	79	78	77					70	68	59		79						79
3.0	87	87	86					79	76	68		88						88
4.0	94	94	92					86	83	75		94						95
5.0	99	99	98					91	89	81		100						100
6.0	104	104	102					95	93	86		104						104
7.0	107	107	106					99	97	90		107						108
8.0	110	110	109					102	100	93		111						111
9.0	113	113	112					105	103	96		113						114
10.0	115	115	114					107	105	98		116						116
20.0	128	128	127					121	120	113		129						129
30.0	134	134	133					129	127	121		134						135
40.0	138	138	137					133	131	127		138						139
50.0	140	140	140					136	134	131		140						141
60.0	141	141	140					137	136	132		141						141
70.0	141	141	141					138	136	133		141						141
80.0	141	141	140					138	136	134		141						141
90.0	140	140	140					137	136	134		140						140
100.0	139	139	139					137	136	134		140						140
200.0	137	137	136					135	134	133		137						137
300.0	135	135	134					133	133	132		135						135
400.0	133	133	133					132	132	131		133						133
500.0	132	132	132					131	131	130		132						132
600.0	131	131	131					130	130	129		131						131
700.0	129	129	129					129	128	128		130						130
800.0	128	128	128					128	127	127		128						128
900.0	127	127	127					126	126	126		127						127
1000.0	126	126	126					125	125	125		126						126
1500.0	124	124	124					124	124	123		124						124
2000.0	117	117	117					117	117	116		117						117
2500.0	112	112	112					111	111	111		112						112
3000.0	107	107	107					107	107	107		107						107
3500.0	104	104	104					104	104	103		104						104
4000.0	101	101	101					101	101	100		101						101
4500.0	98	98	98					98	98	97		98						98
5000.0	95	95	95					94	94	94		95						95
5500.0	92	92	92					92	92	92		92						92
6000.0	89	89	89					89	89	89		89						89
6500.0	87	87	87					87	87	87		87						87
7000.0	85	85	85					85	85	85		85						85
7500.0	84	84	84					83	84	83		84						84
8000.0	82	82	82					82	82	82		82						82
8500.0	80	80	80					80	80	80		80						80
9000.0	79	79	79					79	79	79		79						79
9500.0	77	77	77					77	77	77		77						77
10000	76	76	76					76	76	76		76						76

Temperature Results for Backfill at 100 years

Temperatures at WP Midlength (Axial Position: mid) for 0.3 W/mK backfill

21 PWR Waste Package Emplaced OCID at 83 MTU/acre with 39.65 GWd/MTU burnup Average SNF (ly95cdaO-P), Sloped Backfill
Peak internal temp. (E) based on Deg C/kW from WP-CDR MPC WPs and 10 year old, 48 GWd/MTU burnup Design Basis SNF

Time (years)	A	B	C	E	F	G	H	I	M	O	U	X	BC	BF	BG	BH	BI	BJ
100.0	143	146	146	209	149	151	151	141	138	135	149	143	19	19	19	19	19	147
100.1	130	137	139	274	228	228	229	134	132	133	229	128	138	145	175	184	154	149
100.2	134	143	146	309	267	267	268	137	137	132	269	132	142	157	199	210	169	163
100.3	137	146	151	324	282	281	283	140	141	133	285	134	140	162	208	220	175	170
100.4	138	148	153	330	288	288	290	141	143	134	291	136	141	165	212	224	178	174
100.5	139	149	155	332	291	290	293	142	144	134	294	136	142	166	214	227	179	176
100.6	139	150	156	334	292	292	294	143	145	135	296	137	143	167	216	228	180	177
100.7	140	150	156	335	293	293	295	143	146	135	296	137	143	167	216	229	181	178
100.8	140	150	157	335	294	293	296	144	146	135	297	138	143	167	217	229	181	178
100.9	140	151	157	336	294	294	296	144	147	135	297	138	143	168	217	229	181	179
101.0	140	151	157	336	294	294	296	144	147	136	297	138	144	168	217	230	182	179
102.0	141	152	158	336	295	294	297	145	148	136	298	139	144	168	218	230	182	180
103.0	141	152	159	336	294	294	296	145	148	137	298	139	145	169	218	230	182	180
104.0	142	152	159	335	294	294	296	145	148	137	297	139	145	169	218	230	183	180
105.0	142	152	159	334	293	293	296	146	148	137	297	139	145	169	217	230	182	180
106.0	142	152	159	334	293	293	295	146	148	137	296	139	145	169	217	230	182	180
107.0	142	152	159	333	292	292	295	146	149	137	296	139	145	169	217	229	182	180
108.0	142	152	159	332	292	292	294	146	149	138	295	139	145	169	217	229	182	180
109.0	142	152	159	332	291	291	293	146	149	138	295	140	145	169	217	229	182	180
110.0	142	152	159	331	291	291	293	146	149	138	294	140	145	169	216	228	182	180
120.0	142	152	158	323	285	285	287	146	149	138	288	140	145	168	214	225	181	178
130.0	142	152	158	316	279	279	281	146	148	138	282	140	145	167	211	222	179	177
140.0	142	151	157	308	273	273	275	146	148	138	276	140	145	166	208	218	177	175
150.0	142	151	156	301	267	267	269	145	148	138	270	140	144	164	205	215	176	174
160.0	141	150	155	293	261	261	263	145	147	138	264	140	144	163	201	211	174	172
170.0	141	149	154	285	255	255	257	144	146	138	257	139	143	161	198	207	172	170
180.0	140	148	153	277	248	248	250	143	145	137	251	139	143	160	194	203	169	168
190.0	139	147	151	269	242	242	243	142	144	137	244	138	142	158	191	199	167	166
200.0	139	145	150	261	235	235	236	141	143	136	237	137	141	156	187	195	165	163
300.0	136	141	145	234	212	212	213	138	139	134	214	135	138	150	174	180	157	155
400.0	134	139	142	218	199	199	200	136	137	133	200	133	136	146	167	172	152	151
500.0	133	137	139	206	189	189	190	135	136	132	190	132	134	143	161	166	148	147
600.0	132	135	137	196	181	181	181	133	134	130	182	131	133	141	156	160	145	144
700.0	130	134	135	188	174	174	175	132	132	129	175	130	131	138	152	156	142	142
800.0	129	132	134	181	168	168	169	130	131	128	169	128	130	136	149	152	140	139
900.0	128	130	132	176	164	163	164	129	130	127	164	127	129	134	146	149	138	137
1000.0	127	129	130	171	159	159	160	128	128	126	160	126	127	133	143	146	136	135
1500.0	125	127	128	159	150	150	151	126	126	124	151	124	125	129	138	140	132	131
2000.0	117	119	120	142	135	135	136	118	118	117	136	117	118	121	126	128	122	122
2500.0	112	113	114	134	128	128	128	112	113	111	128	112	112	115	120	121	116	116
3000.0	107	108	109	127	121	121	121	108	108	107	122	107	108	110	114	116	111	111
3500.0	104	105	106	123	117	117	117	104	105	104	118	104	104	106	111	112	108	108
4000.0	101	102	103	119	114	114	114	102	102	101	114	101	101	103	107	109	105	105
4500.0	98	99	100	115	110	110	110	98	99	98	110	98	98	100	104	105	101	101
5000.0	95	96	96	111	106	106	107	95	96	95	107	95	95	97	101	102	98	98
5500.0	92	93	94	108	103	103	103	92	93	92	103	92	92	94	98	99	95	95
6000.0	90	91	91	105	100	100	101	90	91	89	101	89	90	92	95	96	93	93
6500.0	87	88	89	102	98	98	98	88	88	87	98	87	88	89	93	94	90	90
7000.0	85	86	87	100	96	96	96	86	86	85	96	85	86	87	91	91	88	88
7500.0	84	85	85	98	93	93	94	84	85	84	94	83	84	85	89	89	86	87
8000.0	82	83	83	96	91	91	92	82	83	82	92	82	82	84	87	88	85	85
8500.0	80	81	82	94	90	90	90	81	81	80	90	80	81	82	85	86	83	83
9000.0	79	80	80	92	88	88	88	79	80	79	88	79	79	81	83	84	81	82
9500.0	78	78	79	90	86	86	86	78	79	78	87	77	78	79	82	83	80	80
10000	76	77	77	89	85	85	85	77	77	76	85	76	76	78	80	81	79	79

Temperature Results for Backfill at 100 years

Temperatures at WP End (Axial Position: wpe) for 0.3 W/mK backfill

21 PWR Waste Package Emplaced OCID at 83 MTU/acre with 39.65 GWd/MTU burnup Average SNF (ly95cdaO-P), Sloped Backfill
Peak Internal temp. (E) based on Deg C/kW from WP-CDR MPC WPs and 10 year old, 48 GWd/MTU burnup Design Basis SNF

Time (years)	A	B	C	E	F	G	H	I	M	O	U	X	BC	BF	BG	BH	BI	BJ
100.0	142	143	143	147	146	146	146	139	138	135	145		19	19	19	19	19	144
100.1	129	133	136	217	213	214	215	132	129	133	213		132	139	170	147	147	143
100.2	133	138	142	256	251	252	253	135	134	132	253		136	151	194	164	164	156
100.3	135	141	146	271	266	267	268	137	137	132	269		138	156	204	171	171	163
100.4	137	143	148	277	272	273	275	139	139	133	275		139	158	208	175	175	166
100.5	137	144	149	280	275	275	277	139	141	133	278		140	160	210	176	176	168
100.6	138	145	150	281	276	277	279	140	142	134	279		141	160	211	177	177	169
100.7	138	145	151	282	277	278	280	141	142	134	280		141	161	211	178	178	170
100.8	139	145	151	283	278	278	280	141	143	134	281		141	161	212	178	178	170
100.9	139	146	151	283	278	279	281	141	143	134	281		142	161	212	179	179	170
101.0	139	146	152	283	278	279	281	141	143	135	281		142	162	212	179	179	171
102.0	140	147	153	284	279	279	281	142	144	136	282		143	162	213	180	180	172
103.0	140	147	153	283	278	279	281	143	144	136	282		143	163	213	180	180	172
104.0	140	147	153	283	278	279	281	143	144	136	281		143	163	213	180	180	172
105.0	140	147	153	283	278	278	280	143	145	136	281		143	163	213	180	180	172
106.0	140	147	153	282	277	278	280	143	145	136	280		143	163	213	180	180	172
107.0	140	147	153	282	277	277	280	143	145	137	280		143	163	212	180	180	172
108.0	141	147	153	281	276	277	279	143	145	137	280		143	163	212	180	180	172
109.0	141	147	153	281	276	277	279	143	145	137	279		143	163	212	180	180	172
110.0	141	147	153	280	275	276	278	143	145	137	279		143	163	212	179	179	172
120.0	141	147	153	275	270	271	273	143	145	137	273		144	162	209	178	178	171
130.0	141	147	153	270	265	266	268	143	145	137	268		143	161	207	177	177	170
140.0	141	147	152	264	260	261	262	143	145	138	263		143	160	204	175	175	168
150.0	141	146	151	259	254	255	257	143	144	138	257		143	159	201	174	174	167
160.0	140	146	151	253	249	249	251	142	144	137	252		143	158	198	172	172	165
170.0	140	145	150	247	243	244	245	142	143	137	246		142	157	194	170	170	164
180.0	139	144	149	241	237	238	239	141	142	137	240		141	155	191	168	168	162
190.0	139	143	147	235	231	232	233	140	142	136	234		140	154	188	165	165	160
200.0	138	142	146	228	225	226	227	139	140	135	227		139	152	184	163	163	158
300.0	135	139	142	207	205	205	206	137	138	133	206		137	147	172	155	155	151
400.0	134	137	139	194	192	193	193	135	136	132	194		135	143	165	151	151	147
500.0	133	135	137	185	183	184	184	134	134	131	184		134	141	159	147	147	144
600.0	131	134	136	177	176	176	177	132	133	130	177		132	139	155	144	144	142
700.0	130	132	134	171	170	170	171	131	131	129	171		131	137	151	142	142	139
800.0	129	131	132	166	164	165	165	129	130	128	165		129	135	148	139	139	137
900.0	127	129	131	161	160	160	161	128	129	127	161		128	133	145	137	137	135
1000.0	126	128	129	157	156	156	157	127	127	126	157		127	131	142	135	135	133
1500.0	125	126	127	149	148	148	148	125	125	124	148		125	128	137	131	131	130
2000.0	117	118	119	134	134	134	134	118	118	117	134		118	120	126	122	122	121
2500.0	112	113	113	127	126	126	126	112	112	111	126		112	114	119	116	116	115
3000.0	107	108	109	120	120	120	120	108	108	107	120		108	109	114	111	111	110
3500.0	104	105	105	116	116	116	116	104	105	104	116		104	106	110	107	107	107
4000.0	101	102	102	113	112	112	113	101	102	101	113		101	103	107	104	104	104
4500.0	98	98	99	109	109	109	109	98	98	98	109		98	100	104	101	101	101
5000.0	95	95	96	106	105	105	105	95	95	94	105		95	96	100	98	98	97
5500.0	92	93	93	103	102	102	102	92	93	92	102		92	94	97	95	95	95
6000.0	89	90	91	100	99	99	99	90	90	89	100		90	91	95	92	92	92
6500.0	87	88	89	97	97	97	97	88	88	87	97		88	89	92	90	90	90
7000.0	85	86	87	95	95	95	95	86	86	85	95		86	87	90	88	88	88
7500.0	83	84	85	93	92	93	93	84	84	83	93		84	85	88	86	86	86
8000.0	82	82	83	91	91	91	91	82	83	82	91		82	83	86	84	84	84
8500.0	80	81	81	89	89	89	89	81	81	80	89		80	82	85	83	83	83
9000.0	79	79	80	87	87	87	87	79	80	79	87		79	80	83	81	81	81
9500.0	77	78	79	86	85	86	86	78	78	78	86		78	79	82	80	80	80
10000	76	77	77	84	84	84	84	76	77	76	84		76	77	80	78	78	78

Temperature Results for Backfill at 100 years

Temperatures Between WPs (Axial Position: dfe) for 0.3 W/mK backfill

21 PWR Waste Package Emplaced OCID at 83 MTU/acre with 39.65 GWd/MTU burnup Average SNF (ly95cdaO-P), Sloped Backfill

Peak internal temp. (E) based on Deg C/kW from WP-CDR MPC WPs and 10 year old, 48 GWd/MTU burnup Design Basis SNF

Time (years)	A	B	C	E	F	G	H	I	M	O	U	X	BC	BF	BG	BH	BI	BJ
100.0	139	139	139	19				137	136	134		140	19					140
100.1	126	126	125	88				128	124	131		127	126					117
100.2	130	130	126	117				129	125	130		130	131					123
100.3	132	132	128	126				130	126	130		131	133					126
100.4	134	134	129	130				131	127	130		133	134					128
100.5	135	134	130	131				132	128	130		133	135					129
100.6	135	135	130	132				132	128	130		134	136					129
100.7	135	135	130	133				133	129	130		134	136					130
100.8	136	136	131	133				133	129	131		134	136					130
100.9	136	136	131	134				133	129	131		135	136					130
101.0	136	136	131	134				133	129	131		135	137					131
102.0	137	137	132	135				134	130	132		135	137					132
103.0	137	137	132	135				134	131	132		136	138					132
104.0	137	138	133	135				135	131	132		136	138					132
105.0	137	138	133	136				135	131	133		136	138					132
106.0	138	138	133	136				135	131	133		136	138					132
107.0	138	138	133	136				135	131	133		136	138					133
108.0	138	138	133	136				135	131	133		136	138					133
109.0	138	138	133	136				135	131	133		136	138					133
110.0	138	138	133	136				135	132	133		136	138					133
120.0	138	138	134	136				136	132	134		137	139					134
130.0	138	139	134	137				136	133	134		137	139					134
140.0	138	139	135	137				136	133	134		137	139					134
150.0	138	139	135	137				136	133	134		137	139					134
160.0	138	138	135	137				136	133	134		137	139					134
170.0	138	138	134	136				136	133	134		137	138					134
180.0	137	137	134	136				136	133	134		136	138					134
190.0	137	137	134	135				135	132	133		136	137					133
200.0	136	136	133	135				134	132	133		135	136					133
300.0	134	134	132	133				133	131	131		133	134					131
400.0	133	133	131	132				132	130	131		132	133					131
500.0	131	132	130	131				131	129	130		131	132					130
600.0	130	130	129	130				130	128	129		130	130					129
700.0	129	129	128	129				128	127	128		129	129					128
800.0	128	128	127	127				127	126	127		128	128					127
900.0	127	127	126	126				126	125	126		126	127					126
1000.0	126	126	125	125				125	124	125		125	126					125
1500.0	124	124	123	124				124	123	123		124	124					123
2000.0	117	117	116	117				117	116	116		117	117					116
2500.0	111	111	111	111				111	111	111		111	111					111
3000.0	107	107	107	107				107	107	107		107	107					107
3500.0	104	104	103	104				103	103	103		103	104					103
4000.0	101	101	101	101				101	101	100		101	101					101
4500.0	97	98	97	97				97	97	97		97	97					97
5000.0	94	94	94	94				94	94	94		94	94					94
5500.0	92	92	92	92				92	92	91		92	92					92
6000.0	89	89	89	89				89	89	89		89	89					89
6500.0	87	87	87	87				87	87	87		87	87					87
7000.0	85	85	85	85				85	85	85		85	85					85
7500.0	83	83	83	83				83	83	83		83	83					83
8000.0	82	82	82	82				82	82	82		82	82					82
8500.0	80	80	80	80				80	80	80		80	80					80
9000.0	78	79	79	79				79	79	78		79	79					79
9500.0	77	77	77	77				77	78	77		77	77					78
10000	76	76	76	76				76	76	76		76	76					76

Temperature Results for Backfill at 100 years

Temperatures at WP Midlength (Axial Position: mid) for 0.6 W/mK backfill

21 PWR Waste Package Emplaced OCID at 83 MTU/acre with 39.65 GWd/MTU burnup Average SNF (fy95cdaO-P), Sloped Backfill

Peak Internal temp. (E) based on Deg C/kW from WP-CDR MPC WPs and 10 year old, 48 GWd/MTU burnup Design Basis SNF

Time (years)	A	B	C	E	F	G	H	I	M	O	U	X	BC	BF	BG	BH	BI	BJ
100.0	143	146	146	209	149	151	151	141	138	135	149	143	19	19	19	19	19	147
100.1	131	139	142	247	197	197	199	135	133	133	199	129	134	144	164	170	151	153
100.2	136	145	149	262	215	215	217	139	138	133	218	134	139	151	176	184	160	165
100.3	138	148	152	267	220	220	223	141	141	133	223	136	141	154	180	188	164	169
100.4	139	149	154	268	222	222	225	142	143	134	225	137	142	155	182	190	165	171
100.5	140	150	155	269	223	223	226	143	144	135	226	137	143	156	182	191	166	172
100.6	140	150	155	270	224	224	227	143	145	135	227	138	143	157	183	191	167	173
100.7	140	151	156	270	224	224	227	144	145	135	227	138	144	157	183	192	167	174
100.8	141	151	156	271	224	225	227	144	145	135	228	138	144	157	184	192	167	174
100.9	141	151	156	271	224	225	227	144	146	136	228	138	144	157	184	192	167	174
101.0	141	151	156	271	225	225	228	144	146	136	228	139	144	158	184	192	168	174
102.0	142	152	157	271	225	225	228	145	146	136	228	139	145	158	184	193	168	175
103.0	142	152	157	271	225	225	228	145	147	137	228	139	145	158	185	193	168	175
104.0	142	152	158	270	225	225	228	145	147	137	228	140	145	158	185	193	168	175
105.0	142	152	158	270	225	225	228	145	147	137	228	140	145	159	184	193	168	175
106.0	142	152	158	270	224	225	227	145	147	137	228	140	145	159	184	193	168	175
107.0	142	152	158	269	224	224	227	146	147	137	228	140	145	159	184	192	168	175
108.0	142	152	158	269	224	224	227	146	147	137	227	140	145	159	184	192	168	175
109.0	142	152	158	268	224	224	227	146	147	137	227	140	145	159	184	192	168	175
110.0	142	152	158	268	223	224	226	146	147	138	227	140	146	158	184	192	168	175
120.0	143	152	157	263	220	221	223	146	147	138	224	140	146	158	182	190	167	174
130.0	143	152	157	259	217	217	220	146	147	138	220	140	145	157	181	188	166	172
140.0	142	151	156	254	214	214	216	145	147	138	217	140	145	157	179	186	165	171
150.0	142	151	155	249	211	211	213	145	146	138	213	140	145	156	177	184	164	170
160.0	142	150	154	244	207	207	209	144	146	138	210	140	144	155	175	182	163	168
170.0	141	149	153	238	203	203	206	144	145	138	206	139	144	154	173	179	161	166
180.0	141	148	152	233	199	200	202	143	144	137	202	139	143	152	171	177	159	164
190.0	140	147	150	227	195	196	198	142	143	136	198	138	142	151	168	174	158	162
200.0	139	145	149	221	191	191	193	141	142	136	193	137	141	149	166	171	156	160
300.0	136	141	144	202	178	178	179	138	139	134	179	135	138	144	158	162	150	153
400.0	135	139	141	191	170	170	171	136	137	133	171	133	136	142	153	156	146	149
500.0	133	137	139	183	164	164	165	135	135	131	165	132	134	139	149	152	143	145
600.0	132	135	137	175	158	159	159	133	133	130	160	131	133	137	146	148	140	143
700.0	130	134	135	170	154	155	155	132	132	129	155	130	131	135	143	145	138	140
800.0	129	132	133	165	151	151	151	130	130	128	151	128	130	133	140	142	136	138
900.0	128	130	132	161	147	148	148	129	129	127	148	127	129	132	138	140	134	136
1000.0	127	129	130	157	145	145	145	128	128	126	145	126	127	130	136	138	133	134
1500.0	125	127	128	148	139	139	139	126	126	124	139	124	125	128	132	133	129	130
2000.0	117	119	119	134	127	127	127	118	118	117	127	117	118	119	122	123	121	121
2500.0	112	113	114	127	121	121	121	112	113	111	121	112	112	114	116	117	115	115
3000.0	107	109	109	121	115	115	115	108	108	107	115	107	108	109	111	112	110	111
3500.0	104	105	106	117	111	111	112	104	105	104	112	104	104	106	108	109	107	107
4000.0	101	102	103	113	108	108	108	102	102	101	108	101	101	103	105	105	104	104
4500.0	98	99	99	110	105	105	105	98	99	98	105	98	98	99	101	102	100	101
5000.0	95	96	96	106	101	101	101	95	96	95	101	95	95	96	98	99	97	98
5500.0	92	93	94	103	98	98	99	92	93	92	99	92	92	93	95	96	94	95
6000.0	90	91	91	100	96	96	96	90	90	89	96	89	90	91	93	93	92	92
6500.0	87	88	89	98	93	93	94	88	88	87	94	87	88	89	91	91	89	90
7000.0	85	86	87	96	91	91	91	86	86	85	91	85	86	87	88	89	87	88
7500.0	84	85	85	94	89	89	90	84	84	84	89	84	84	85	87	87	86	86
8000.0	82	83	83	92	87	87	87	82	83	82	87	82	82	83	85	85	84	84
8500.0	80	81	82	90	86	86	86	81	81	80	86	80	81	81	83	84	82	83
9000.0	79	80	80	88	84	84	84	79	80	79	84	79	79	80	81	82	81	81
9500.0	78	78	79	87	83	83	83	78	78	77	83	77	78	79	80	81	79	80
10000	76	77	77	85	81	81	81	76	77	76	81	76	76	77	79	79	78	78

Temperature Results for Backfill at 100 years

Temperatures at WP End (Axial Position: wpe) for 0.6 W/mK backfill

21 PWR Waste Package Emplaced OCID at 83 MTU/acre with 39.65 GWd/MTU burnup Average SNF (fy95cdaO-P), Sloped Backfill

Peak Internal temp. (E) based on Deg C/kW from WP-CDR MPC WPs and 10 year old, 48 GWd/MTU burnup Design Basis SNF

Time (years)	A	B	C	E	F	G	H	I	M	O	U	X	BC	BF	BG	BH	BI	BJ
100.0	142	143	143	147	146	146	146	139	138	135	145		19	19	19	19	19	144
100.1	130	135	137	187	183	184	185	133	130	132	185		132	138	158	145	145	146
100.2	134	140	144	205	201	201	203	136	135	132	203		137	146	171	155	155	157
100.3	137	143	147	210	206	206	208	138	138	133	208		139	149	175	158	158	161
100.4	138	144	148	212	207	208	210	139	140	133	210		140	150	176	160	160	163
100.5	138	145	149	213	209	209	212	140	140	134	212		141	151	177	161	161	164
100.6	139	145	150	214	209	210	212	140	141	134	212		141	151	178	161	161	165
100.7	139	146	150	215	210	211	213	141	141	134	213		142	152	178	162	162	165
100.8	139	146	151	215	210	211	213	141	142	134	213		142	152	178	162	162	165
100.9	139	146	151	215	210	211	213	141	142	135	213		142	152	178	162	162	166
101.0	140	146	151	215	210	211	213	141	142	135	213		142	152	179	162	162	166
102.0	140	147	152	216	211	212	214	142	143	136	214		143	153	179	163	163	167
103.0	140	147	152	216	211	212	214	142	143	136	214		143	153	179	163	163	167
104.0	141	147	152	216	211	212	214	143	143	136	214		143	153	179	163	163	167
105.0	141	147	152	215	210	211	214	143	143	136	213		143	153	179	163	163	167
106.0	141	147	152	215	210	211	213	143	143	136	213		143	153	179	163	163	167
107.0	141	147	152	215	210	211	213	143	144	136	213		144	153	179	163	163	167
108.0	141	147	152	215	210	211	213	143	144	137	213		144	153	179	163	163	167
109.0	141	147	152	214	210	211	213	143	144	137	213		144	153	179	163	163	167
110.0	141	147	152	214	209	210	212	143	144	137	212		144	153	179	163	163	167
120.0	141	147	152	212	207	208	210	143	144	137	210		144	153	178	163	163	166
130.0	141	147	152	209	204	205	207	143	144	137	207		144	153	176	162	162	165
140.0	141	147	151	206	202	202	204	143	144	137	204		144	152	175	161	161	164
150.0	141	146	151	203	199	200	201	143	143	137	201		143	152	173	160	160	163
160.0	141	146	150	200	196	197	198	142	143	137	198		143	151	171	159	159	161
170.0	140	145	149	196	193	193	195	142	142	137	195		142	150	169	157	157	160
180.0	140	144	148	193	189	190	192	141	142	136	191		142	149	167	156	156	158
190.0	139	143	147	189	186	187	188	140	141	136	188		141	147	165	154	154	157
200.0	138	142	145	185	182	183	184	139	140	135	184		140	146	162	152	152	155
300.0	135	139	141	173	171	171	172	137	137	133	172		137	142	155	147	147	149
400.0	134	137	139	166	164	164	165	135	135	132	165		135	139	150	144	144	145
500.0	133	135	137	160	159	159	160	134	134	131	160		134	137	147	141	141	142
600.0	131	134	135	155	154	154	155	132	132	130	155		132	135	144	139	139	140
700.0	130	132	133	152	150	151	151	131	131	129	151		131	134	141	137	137	138
800.0	129	131	132	148	147	147	148	129	130	128	148		129	132	139	135	135	136
900.0	128	129	130	145	144	144	145	128	128	127	145		128	131	137	133	133	134
1000.0	126	128	129	143	142	142	142	127	127	126	142		127	129	135	131	131	132
1500.0	125	126	127	137	136	137	137	125	125	124	137		125	127	131	129	129	129
2000.0	117	118	119	126	125	126	126	118	118	117	126		118	119	122	120	120	120
2500.0	112	113	113	120	119	119	120	112	112	111	120		112	113	116	114	114	115
3000.0	107	108	109	114	114	114	114	108	108	107	114		108	108	111	109	109	110
3500.0	104	105	105	111	110	110	110	104	104	104	110		104	105	107	106	106	106
4000.0	101	102	102	107	107	107	107	101	102	101	107		101	102	104	103	103	103
4500.0	98	98	99	104	104	104	104	98	98	98	104		98	99	101	100	100	100
5000.0	95	95	96	100	100	100	100	95	95	94	100		95	96	98	97	97	97
5500.0	92	93	93	98	97	97	98	92	93	92	98		92	93	95	94	94	94
6000.0	89	90	91	95	95	95	95	90	90	89	95		90	90	92	91	91	92
6500.0	87	88	88	93	92	92	93	88	88	87	93		88	88	90	89	89	89
7000.0	85	86	86	90	90	90	90	86	86	85	90		86	86	88	87	87	87
7500.0	84	84	85	89	88	88	89	84	84	83	89		84	84	86	85	85	86
8000.0	82	82	83	87	86	86	87	82	83	82	87		82	83	84	83	83	84
8500.0	80	81	81	85	85	85	85	81	81	80	85		80	81	83	82	82	82
9000.0	79	79	80	83	83	83	83	79	79	79	83		79	80	81	80	80	81
9500.0	77	78	78	82	82	82	82	78	78	77	82		78	78	80	79	79	79
10000	76	77	77	80	80	80	80	76	77	76	80		76	77	78	77	77	78

Temperature Results for Backfill at 100 years

Temperatures Between WPs (Axial Position: dfe) for 0.6 W/mK backfill

21 PWR Waste Package Emplaced OCID at 83 MTU/acre with 39.65 GWd/MTU burnup Average SNF (ly95cdaO-P), Sloped Backfill

Peak internal temp. (E) based on Deg C/kW from WP-CDR MPC WPs and 10 year old, 48 GWd/MTU burnup Design Basis SNF

Time (years)	A	B	C	E	F	G	H	I	M	O	U	X	BC	BF	BG	BH	BI	BJ
100.0	139	139	139	19				137	136	134		140	19					140
100.1	127	127	124	112				128	123	131		127	127					118
100.2	132	131	127	127				130	126	130		131	132					126
100.3	134	133	129	131				131	127	130		132	134					128
100.4	135	134	130	132				132	128	130		133	135					129
100.5	135	135	130	133				132	129	130		134	136					130
100.6	136	136	131	133				133	129	131		134	136					131
100.7	136	136	131	134				133	130	131		135	136					131
100.8	136	136	131	134				133	130	131		135	137					131
100.9	136	136	132	134				133	130	131		135	137					131
101.0	137	136	132	135				134	130	131		135	137					132
102.0	137	137	133	135				134	131	132		136	138					132
103.0	137	137	133	136				135	131	132		136	138					133
104.0	138	138	133	136				135	131	133		136	138					133
105.0	138	138	133	136				135	131	133		136	138					133
106.0	138	138	133	136				135	132	133		136	138					133
107.0	138	138	134	136				135	132	133		136	138					133
108.0	138	138	134	136				135	132	133		136	138					133
109.0	138	138	134	136				135	132	133		137	139					133
110.0	138	138	134	136				135	132	133		137	139					134
120.0	138	139	134	137				136	133	134		137	139					134
130.0	139	139	135	137				136	133	134		137	139					134
140.0	139	139	135	137				136	133	134		137	139					135
150.0	139	139	135	137				136	133	134		137	139					135
160.0	138	138	135	137				136	133	134		137	139					135
170.0	138	138	135	137				136	133	134		137	138					135
180.0	137	138	134	136				136	133	134		136	138					134
190.0	137	137	134	136				135	133	133		136	137					134
200.0	136	136	133	135				134	132	133		135	136					133
300.0	134	134	132	133				133	131	131		133	134					132
400.0	133	133	131	132				132	130	131		132	133					131
500.0	132	132	130	131				131	129	130		131	132					130
600.0	130	130	129	130				129	128	129		130	130					129
700.0	129	129	128	129				128	127	128		129	129					128
800.0	128	128	127	127				127	126	127		128	128					127
900.0	127	127	126	126				126	125	126		126	127					126
1000.0	126	126	125	125				125	125	125		125	126					125
1500.0	124	124	123	124				124	123	123		124	124					123
2000.0	117	117	116	117				117	116	116		117	117					116
2500.0	111	111	111	111				111	111	111		111	111					111
3000.0	107	107	107	107				107	107	107		107	107					107
3500.0	104	104	103	104				103	103	103		103	104					103
4000.0	101	101	101	101				101	101	100		101	101					101
4500.0	97	98	97	97				97	97	97		97	98					97
5000.0	94	94	94	94				94	94	94		94	94					94
5500.0	92	92	92	92				92	92	91		92	92					92
6000.0	89	89	89	89				89	89	89		89	89					89
6500.0	87	87	87	87				87	87	87		87	87					87
7000.0	85	85	85	85				85	85	85		85	85					85
7500.0	83	83	83	83				83	83	83		83	83					83
8000.0	82	82	82	82				82	82	82		82	82					82
8500.0	80	80	80	80				80	80	80		80	80					80
9000.0	79	79	79	79				79	79	78		79	79					79
9500.0	77	77	77	77				77	77	77		77	77					77
10000	76	76	76	76				76	76	76		76	76					76

INTENTIONALLY LEFT BLANK

APPENDIX B

Additional Details of Waste Package Degradation Simulation

Humid-Air and Aqueous Corrosion of Carbon Steel

Carbon steel, the candidate corrosion-allowance barrier material, undergoes active corrosion both in humid-air and aqueous environments. In the potential repository, it is expected that the waste container will be exposed to humid-air and aqueous conditions at elevated temperatures for extended periods of time. The term "humid-air corrosion" is used to refer to corrosion which takes place under a 'thin' film of water that forms on the container surface above a certain critical humidity threshold. Such a (thin) water film is capable of supporting electrochemical (corrosion) reactions under humid-air environment, but is not thick enough to behave as bulk water. As the near-field humidity increases, the water film becomes thicker by attracting more water molecules (from an increasing amount of water vapor in the humid-air). Above a certain humidity threshold, the water film will become thick enough to mimic (in terms of physical and chemical properties) bulk water. The term "aqueous corrosion" is used to refer to corrosion of metal in contact with bulk water.

Corrosion of metal consists of oxidation (or anodic) and reduction (or cathodic) reactions. Oxidation reaction is an electrochemical process in which metal dissolves and electron(s) are given off. For example, in the corrosion (or oxidation) of iron, the oxidation reaction can be written as

$$Fe(m) \rightleftharpoons Fe^{2+}(aq) \quad 2e^- \tag{1}$$

where (m) indicates metallic phase, (aq) aqueous phase, and e electron. In order for the iron corrosion to sustain, the electrons given off from the oxidation reaction (Equation (1)) must be consumed (or removed), and the electrochemical process is called reduction reaction. In natural water (or aqueous phase) with a neutral pH and insignificant concentrations of dissolved species, the electrons are consumed mostly by the reduction of dissolved oxygen and hydrogen such as

$$\frac{1}{2}O_2(aq) \quad 2H^+(aq) \quad 2e^- \rightleftharpoons H_2O(aq) \tag{2}$$

$$2H^+(aq) \quad 2e^- \rightleftharpoons H_2(g) \tag{3}$$

Although not shown in Equation (2), since oxygen is a much stronger oxidant, reduction of dissolved oxygen proceeds that of hydrogen ion. Thus, in natural water with a neutral pH and insignificant concentrations of dissolved species and at the atmospheric oxygen partial pressure (0.21 atm), corrosion rate is controlled by the availability of dissolved oxygen at the surface of corroding metal. The oxygen availability in aqueous phase is dependent on the solubility of (gas) oxygen and the mobility of dissolved oxygen (i.e., how fast dissolved oxygen is replenished at the corroding metal surface). This is also shown in that corrosion rate in a flowing water (at a flow rate that abrasion is insignificant) is higher than in a static water. An increase in temperature enhances the diffusivity of dissolved oxygen molecules and reaction rate, but at the same time decreases the solubility of oxygen gas. The net mass transport of oxygen increases with temperature until a maximum (at about 60 to 80°C) is reached where the net dissolved-oxygen at the corroding metal surface begins to decrease approaching the boiling point. This is shown in Figure 5.4-2 in TSPA-1995 (CRWMS M&O, 1995d). This temperature-dependency of corrosion (or oxygen solubility and mobility) would be

weaker in a carbonate-concentrated water (or aqueous phase) because carbonate species can also participate in reduction reaction. This is shown in Figure 5.4-5 of TSPA-1995.

In humid-air corrosion, a 'thin' water film supporting the corrosion electrochemical reactions on the corroding metal surface is very thin, and the effects of the decreased oxygen solubility and increased oxygen diffusivity with temperature (as in bulk water) are not directly applicable. Because of the very short distance dissolved-oxygen travels through the 'thin' film of water, its diffusivity is not a major factor to the corrosion rate. All the oxygen dissolved in the water film is immediately available to participate in the reduction reaction. Thus, a decreasing oxygen solubility with an increase in temperature would have much less effect in humid-air corrosion than in bulk water. In addition, the rates of the corrosion (anodic and cathodic) reactions (Equations (1) to (3)) are enhanced with an increasing temperature. This is shown in Figure 5.3-5 of TSPA-1995.

As discussed in the following section, the current waste package degradation model assumes that aqueous corrosion initiates at a threshold relative humidity (RH) between 85 and 95%. Thus, in an exposure condition of 90°C and 90% RH, aqueous corrosion is the dominant corrosion mode, and the aqueous corrosion model should be used instead of humid-air corrosion model which has a higher corrosion rate in the exposure condition. An extrapolation of the humid-air corrosion model into a higher humidity environment is not valid since the exposure condition dictates an aqueous corrosion condition. The conceptualization of the corrosion mode switch is more clear at lower temperature cases; that is, at 60°C, humid-air corrosion rate at RHs approaching 100% is close to the aqueous corrosion rate as shown in Figure 5.3-7b in TSPA-1995.

Major Assumptions in Waste Package Degradation Simulation

This section discusses the major assumptions made in the stochastic waste package degradation simulations. If not specifically indicated in each subsection, the assumptions are implicitly included.

1) Humid-air general and pitting corrosion of the carbon steel outer barrier initiate at a threshold RH which is uniformly distributed between 65 and 75 %. This threshold is independently chosen for each waste package. This assumption is based on numerous data found in the literature (see Haynie et al., 1978; Phipps and Rice, 1979; Vernon 1933).

2) Aqueous general and pitting corrosion of the carbon steel outer barrier initiate at a threshold RH which is uniformly distributed between 85 and 95 % RH. Visual observations indicating that steel coupon surfaces were covered with a thin film of water at about 85 % RH in a controlled environment chamber have been reported (Haynie et al., 1978).

3) For each waste package, complete and positive correlation of the humid-air corrosion initiation threshold and the transition threshold from humid-air corrosion to aqueous corrosion is assumed. That is, if humid-air corrosion initiates at 65 % RH, aqueous corrosion initiates at 85 % RH.

4) Corrosion-allowance outer barrier material (carbon steel) is subjected to general and pitting corrosion both in humid-air and aqueous conditions. The uncertainties in the humid-air and

aqueous general corrosion models (Equations (5.3-8) and (5.4-3)) were utilized to account for pit to pit variability and waste package to waste package variability. In the post-closure repository, about 10,000 waste packages will be spread over the repository area, and a local corrosion environment in one part of the repository may be different from that in another part. This variability of the local corrosion environment is referred to here as waste package to waste package variability. Also, since a waste container has a relatively large surface area (37.26 m^2), the general corrosion rate on one part of the waste package may be different from that on another part of the waste package. This variability in corrosion rate on a waste package is referred to here as pit to pit variability. Because information on the degree of the variability among waste packages and among pits is not available currently, the variabilities are accounted for in TSPA-1995 by equally splitting the uncertainties in the humid-air and aqueous general corrosion models into the variability among waste packages and the variability among pits.

5) Corrosion resistant inner barrier material (Alloy 825) is subjected to aqueous pitting corrosion only (not to general corrosion). The time-independent pit growth rate distributions discussed in Section 5.5 of TSPA-1995 (Equation (5.5-1)) were utilized to represent pit to pit variability and waste package to waste package variability. The same reasoning given in item (4) is applied also to account for the variability among waste packages and among pits.

6) When pits reach the inner barrier through the outer barrier, aqueous conditions are assumed there. This assumption is based on the observations that the capillary condensation of moisture by gel-like porous corrosion products of the outer barrier covering the inner barrier surface (Vernon 1933) and the hygroscopic nature of many corrosion products (Fyfe 1994; Haynie et al., 1978) would provide an aqueous corrosion condition at the surface of the inner barrier.

7) Pits form uniformly over the entire waste container surface. It is known that pits are most stable when growing in the direction of gravity because the dense, concentrated solution within a pit is necessary for its continuing activity (Fontana 1986, pp. 64-69). Elongation of pits growing in the direction of gravity has been observed (Ruijini et al., 1989). However, there is an uncertainty regarding crevice corrosion at the bottom of the waste container contacting the invert. Additionally, over the containment and isolation periods, rock may fall on the waste container, or backfill may be introduced. In these cases, there may be crevice corrosion occurring at the contact points between the rocks and waste container surface. Because of the uncertainty of the possibility of crevice corrosion at the side and bottom of waste containers, we assumed that pits form uniformly over the entire waste container surface.

8) All pits have a uniform area of 1 mm^2 which corresponds to a pit radius of 0.56 mm. This may be large for the pits forming in Alloy 825, which tend to be much narrower (Szklarska-Smialowska 1986, pp. 127-141).

9) The waste container surface has a pit density of 10 pits/cm^2 (Marsh and Taylor, 1988; Marsh et al., 1988; Strutt et al., 1985), and the same pit density is also assumed for the inner barrier.

10) Taking the pit density (10 pits/cm^2), the uniform pit area (1 mm^2) and the nominal surface area (37.26 m^2) of the waste container for a typical large waste package, the total number of pits that can form on the waste container is about 4 million. This corresponds to about 10 % of the total surface area.

11) All the pits on a waste package start to grow at the same time when the threshold humidity discussed in items (1) and (2) is reached. That is, pit initiation is not explicitly considered in TSPA-1995.

The following figures present humid air and aqueous corrosion rates predicted by the corrosion model at various RH values (65, 75, 85, and 90 %) and temperatures (0 to 100 deg C).

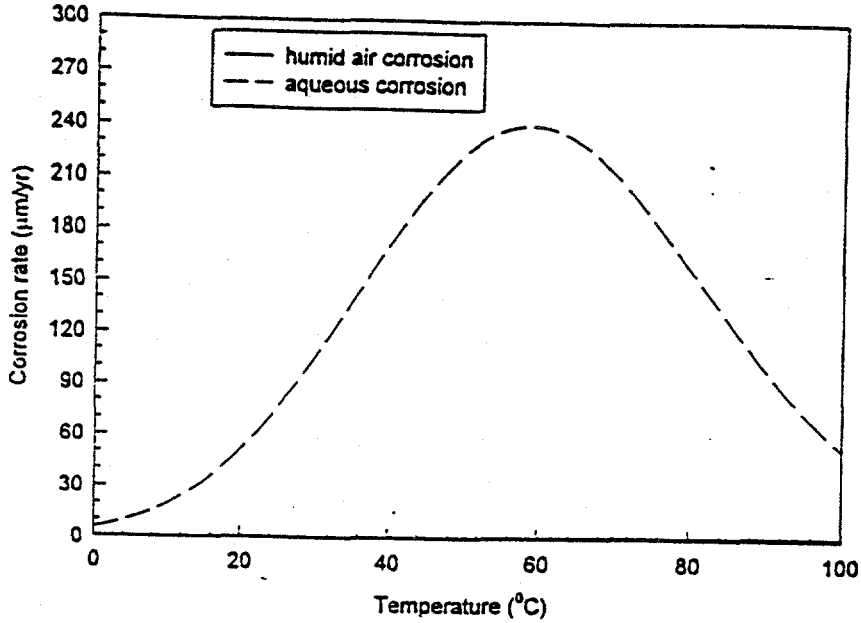

Figure B-1a Corrosion rates at 1 year for RH=65%

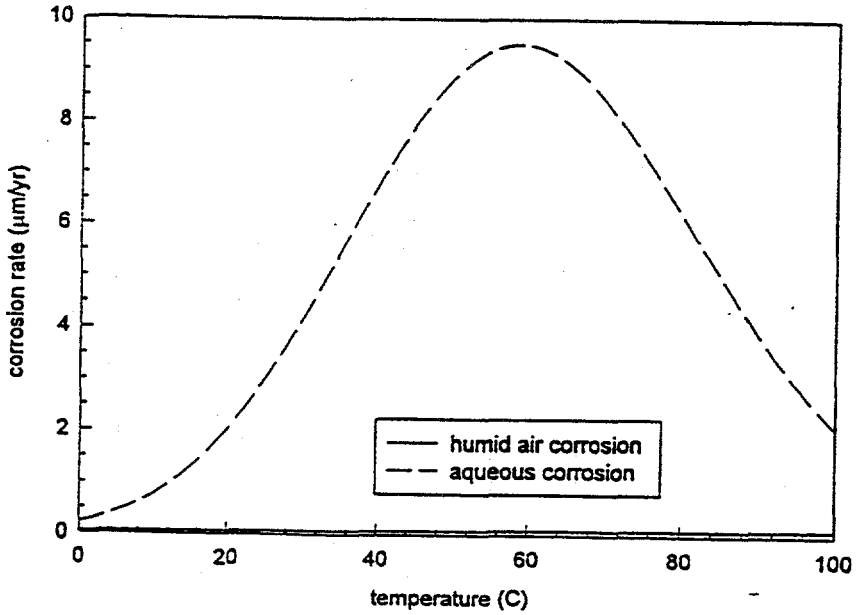

Figure B-1b Corrosion rate at 1000 years for RH=65%

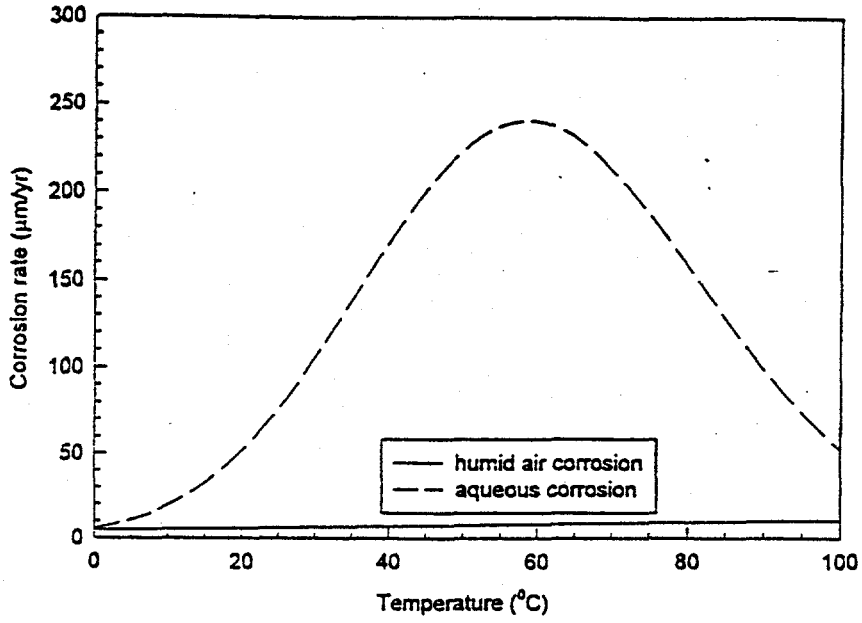

Figure B-1c Corrosion rates at 1 year for RH=75%

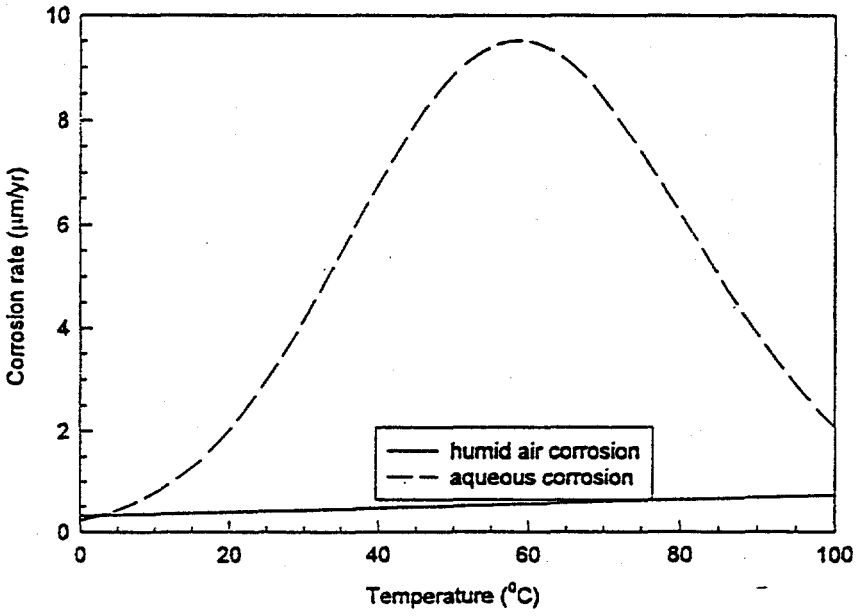

Figure B-1d Corrosion rates at 1000 years for RH=75%

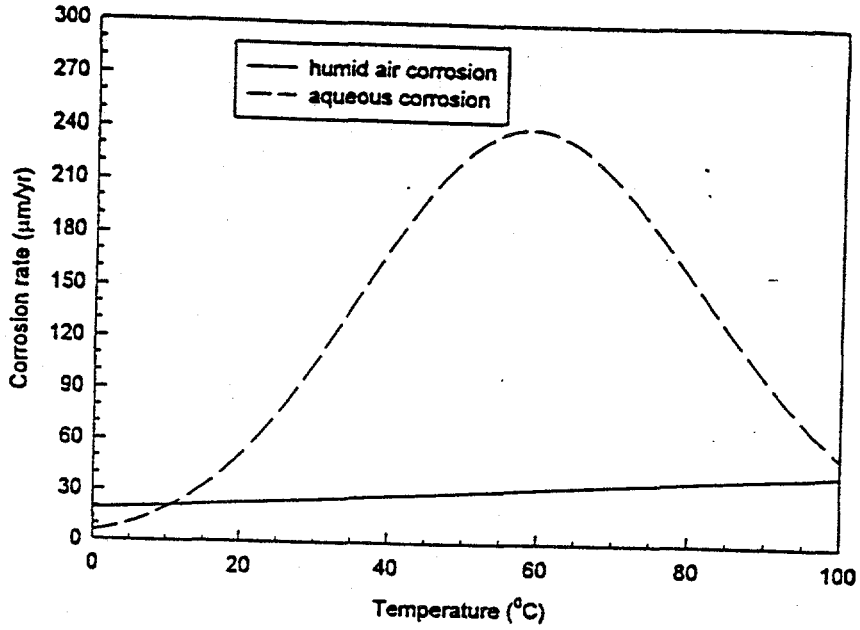

Figure B-1e Corrosion rates at 1 year for RH=85%

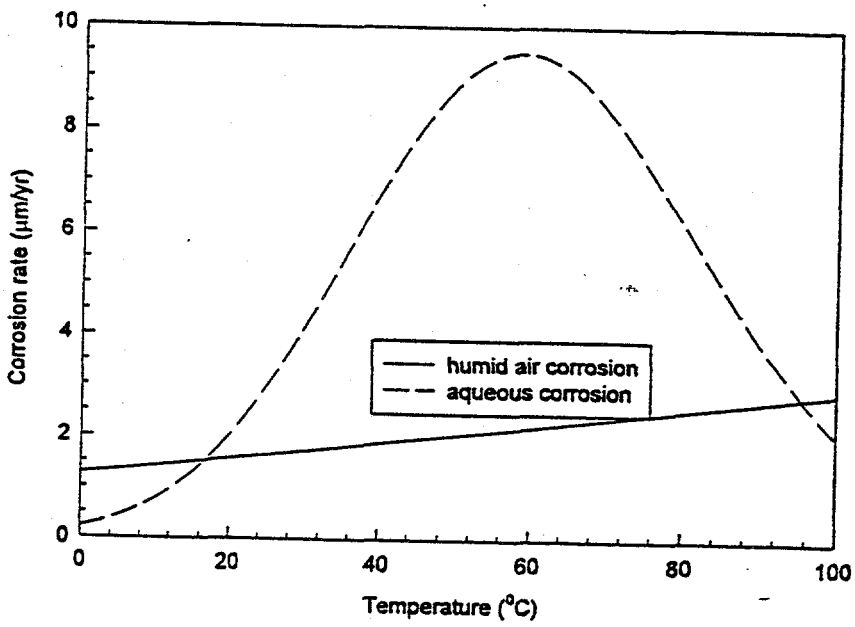

Figure B-1f Corrosion rates at 1000 years for RH=85%

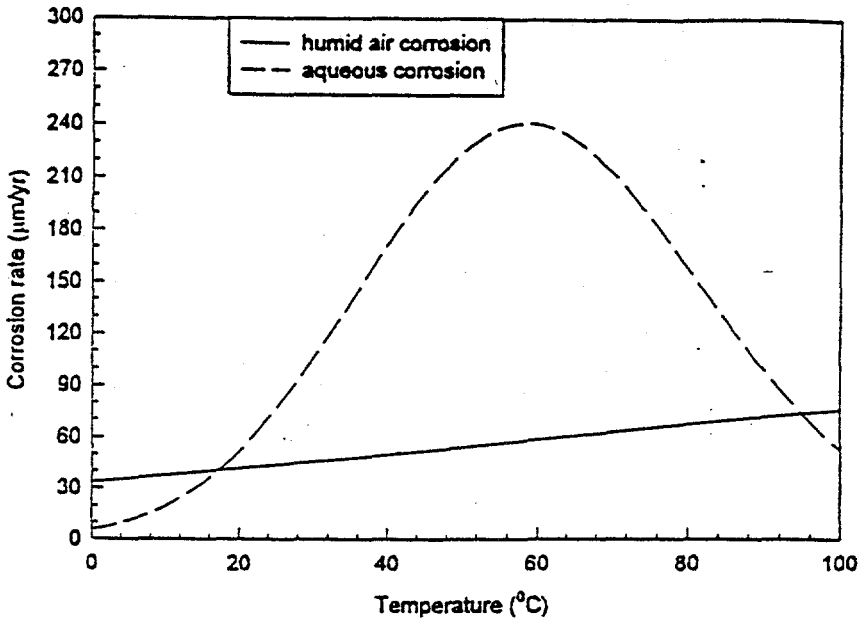

Figure B-1g Corrosion rates at 1 year for RH=90%

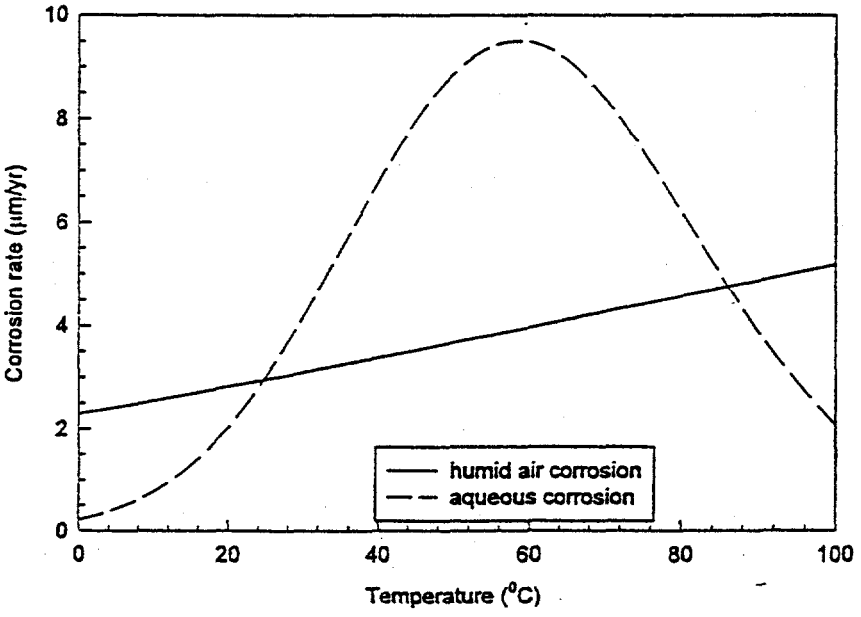

Figure B-1h Corrosion rates at 1000 years for RH=90%

INTENTIONALLY LEFT BLANK

APPENDIX C

Methodology and Diffusion Coefficients

Hydraulic Conductivity

The hydraulic conductivity was measured as a function of the water content using the Unsaturated Flow Apparatus (UFA), a technology developed by the scientists at NESTT together with the U. S. Department of Energy's Office of Technology Development. The UFA achieves hydraulic steady state in a few hours for most geologic materials, even those with very low water or fluid contents. There are specific advantages to using a centripetal acceleration as a fluid driving force. It is a whole-body force similar to gravity and, so, acts simultaneously over the entire system and independently of other driving forces, e.g., gravity or matric potential. The use of steady state centrifugation to measure steady state hydraulic conductivities has recently been demonstrated on various porous media (Nimmo et al., 1987; Conca and Wright, 1992).

The UFA instrument consists of an ultracentrifuge with a constant, ultralow flow pump (Figure A1) that provides fluid to the sample surface through a rotating seal assembly and microdispersal system. The ultracentrifuge can reach accelerations of up to 20,000 g (soils are generally run only up to 1,000 g), temperatures can be adjusted from -20° to 150°C, and constant flow rates can be reduced to 0.001 ml/h. Effluent from the sample is collected in a transparent, volumetrically-calibrated chamber at the bottom of the sample assembly. Using a strobe light, an observer can check the effluent collection chamber while the sample is being centrifuged. The UFA Method is effective because it allows the operator to set the variables in Darcy's Law. Darcy's Law states that the fluid flux equals the hydraulic conductivity times the fluid driving force. Under a centripetal acceleration in which water is driven by both the matric potential gradient, and the centrifugal force per unit volume, Darcy's Law is given by

$$q = -K(\psi)\,[d\psi/dr - \rho\omega^2 r] \qquad (1)$$

where q is the flux density into the sample, K is the hydraulic conductivity, ψ is the matric potential, $d\psi/dr$ is the matric gradient, $\rho\omega^2 r$ is the centrifugal force per unit volume, r is the radius from the axis of rotation, ρ is the fluid density, and ω is the rotation speed in radians per second (Nimmo et al., 1987).

Hydraulic conductivity is a function of either the matric potential or the volumetric water content. Above speeds of about 300 rpm, provided that sufficient flux density exists, the matric potential is much less than the acceleration, $d\psi/dr << \rho\omega^2 r$. Therefore, Darcy's Law is given by $q = -K(\psi)\,[-\rho\omega^2 r]$ under these conditions. Rearranging the equation and expressing hydraulic conductivity as a function of volumetric water content, θ, Darcy's Law becomes

$$K(\theta) = q/\rho\omega^2 r \qquad (2)$$

As an example, a silt from the Hanford formation accelerated to 2500 rpm with a flow rate of 0.01 ml/h achieved hydraulic steady state in 10 hours at a target volumetric water content of 16.4% and an unsaturated hydraulic conductivity of 4×10^{-10} cm/s. Appropriate values of rotation speed and flow rate into the sample are chosen to obtain desired values of flux density, water content, and hydraulic conductivity within the sample. Previous studies have verified the linear dependence of hydraulic conductivity on flux and the second order dependence on rotation speed. This method provides hydraulic conductivity to within ±8% at a volumetric water content known to within ±2% (Nimmo and Akstin, 1988). The high accuracy comes from the tight control on flow rate (±1% non-pulsating) and rotation speed (±5 rpm) and the ability to measure weight to ±0.001 g. The moisture distribution at steady-state in the UFA is very uniform, to within about 1% in homogeneous systems suggesting steady-state is achieved (Nimmo et al., 1987; Conca and Wright

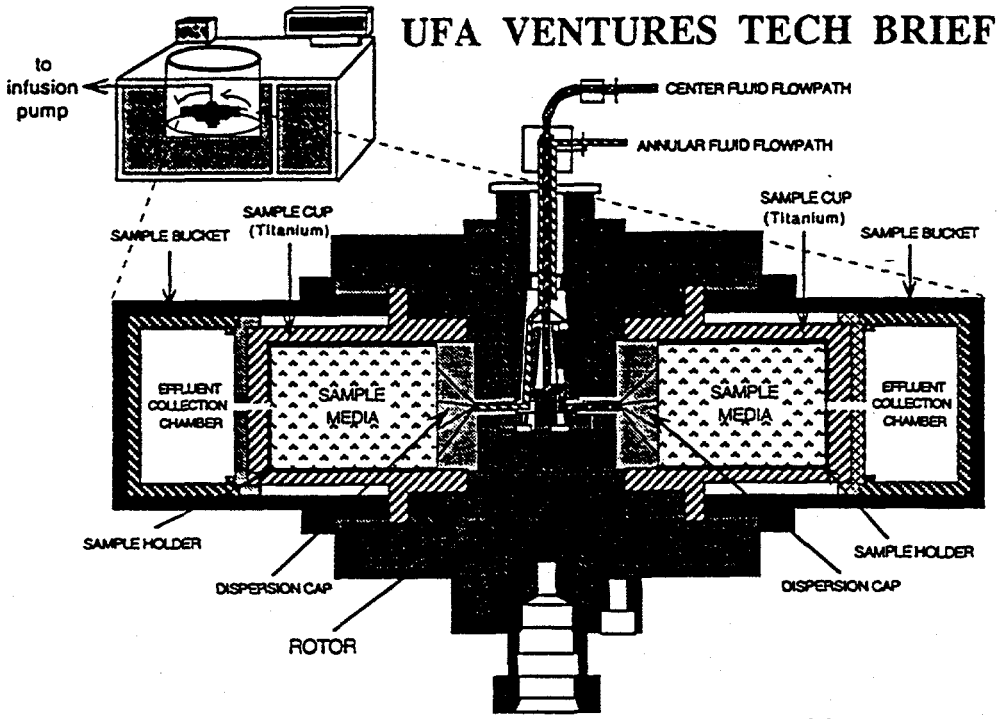

Figure A1. UFA Rotor and Seal Assembly

1992). In heterogeneous samples or multicomponent systems, each component reaches its own hydraulic conductivity and water content at steady state, as occurs under natural conditions in the field. However, the best verification of the UFA Method comes from investigations of the same soils using several techniques. Comparisons between the UFA Method and soil columns, van Genuchten/Mualem estimations and lysimeter measurements on the same soils have shown excellent agreement for sandy loams, silts and even rocks, in instances where the residual water content is reasonably well-known (Nimmo et al., 1987; Conca, 1993; Wright et al., 1994).

Hydraulic conductivity can be very sensitive to the solution chemistry, especially when samples contain expandable, or swelling, clay minerals. Actual groundwater or whatever fluid is of importance to the application should be used. In these experiments, a synthetic vadose zone water was used (Table A1) with an ionic strength of 0.0035 *M*.

TABLE A1. Vadose Zone Water Used In the UFA Experiments.

Species	Concentration (mol/l or M)
Na^+	0.00080
K^+	0.00010
Ca^{2+}	0.00043
Mg^{2+}	0.00031
HCO_3^-	0.00074
F^-	0.00004
Cl^-	0.00067
NO_3^-	0.00017
SO_4^{2-}	0.00039

Several issues involving flow in an acceleration field have been raised and addressed by previous and current research (Conca and Wright, 1992; Wright et al., 1994; Nimmo et al., 1987; Nimmo and Akstin, 1988; Nimmo and Mello, 1991; Nimmo et al., 1994). These have shown that compaction from acceleration is negligible for subsurface soils at or near their field densities. Bulk densities in these samples have remained constant because a whole-body acceleration does not produce high point pressures. The notable exception is surface soils and recently tilled soils, which can have unusually low bulk densities. Special arrangements must be made to preserve their densities. Whole rock, grout, ceramics or other solids are completely unaffected by these accelerations. Three dimensional deviations of the driving force with position in the sample are less than a factor of two (Nimmo et al., 1987). Theoretically, the situation under which unit gradient conditions are achieved in the UFA, in which the change in the matric potential with radial distance equals zero ($d\psi/dr = 0$), is best at higher fluxes, higher speeds, and/or coarser grain-size (Nimmo et al., 1994) and this is seen in potential gradient measurements in these ranges which all show $d\psi/dr = 0$. The worst case occurs at the lowest fluxes in the finer-grained materials, but even in the worst case, the hydraulic conductivity appears insensitive to variations in ψ (Wright et al., 1994).

Matric Potential Method

The matric potential can be determined using closed centrifugation where no fluid enters the sample during rotation (Hassler and Brunner, 1945; Hoffman, 1963). The sample begins saturated and the speed is stepwise increased from 300 rpm to 10,000 rpm. At each speed the sample drains until the overall matric potential is equal and opposite to the equivalent pressure of the acceleration. The sample weight is measured at each step and the run is continued at the next speed. The equivalent pressure at each speed can be determined by

$$P = \frac{\rho\omega^2}{2g}(r_1^2 - r_2^2) \qquad (3)$$

where

P is the equivalent pressure
g is the acceleration due to gravity
r_1 is the distance from the axis of rotation of sample top
r_2 is the distance from the axis of rotation of sample bottom
ω is the rotation speed
ρ is the fluid density

The pressure at each point is plotted against the water content to obtain the $\psi(\theta)$ relationship.

Falling Head Method

The procedure followed for falling head was developed at Pacific Northwest National Laboratory for the measurement of saturated hydraulic conductivity using the Falling Head Method and the Constant Head Method. The traditional falling-head method (Klute and Dirksen, 1986) is used to determine the saturated hydraulic conductivity, K, of samples before using the UFA to determine unsaturated hydraulic conductivity. Constant-head methods can also be performed on samples with high saturated conductivities, but could not be performed with these samples with our present set-up. The falling-head method employs a water-filled standpipe (a modified burette) connected to the sample holder bottom. The UFA sample holder was used for these experiments. After the

falling head measurement was made, the same sample was run in the UFA without disturbance. In falling-head experiments, while fluid drains out of the standpipe, the hydraulic pressure head changes across the sample in relation to the decreasing distance between the top of the water column and the water outflow point. The hydraulic conductivity is given by

$$K = (aL/At) \ln(H_1/H_2) \quad (4)$$

where

K is the hydraulic conductivity
a is the cross-sectional area of the standpipe
L is the length of the sample
A is the cross-sectional area of the sample
t is the time it takes for the top of the water column to fall from H_1 to H_2
H is the top of the water column at any particular time.

Vapor Diffusivity Method

Vapor diffusivity is determined by measuring the gas permeability of each sample after it reaches steady-state in the UFA at the target water content. The UFA gas permeameter set-up accepts the UFA sample holder directly as it comes out of the UFA (Figure A2). Air was used as the permeating gas. Air is input under pressure into a saturator that raises the relative humidity to near 100% so that the sample does not dry during the measurement. The inlet pressure, outlet pressure and air flow are measured and used in the following relationship:

$$k_a = \frac{qL\eta_a}{ghA\rho_f} \quad (5)$$

where

k_a is the coefficient of air permeability or intrinsic permeability of air (cm^2)
L is the sample length (cm)
A is the sample cross-sectional area (cm^2)
g is the acceleration due to gravity (981 dynes/g)
q is the flow rate (cm^3/sec)
h is the head difference across sample (cm H_2O)
ρ_f is the density of the manometer fluid (g/cm^3)
η_a is the viscosity of air (1.84×10^{-4} poise)

Gas conductivity or diffusivity is related to air permeability by the fluidity term, $\rho_g g/\eta_g$:

$$K_g = k_a \ \rho_g g/\eta_g \quad (6)$$

where

K_g is the gas conductivity (cm/sec)
ρ_g is the density of the gas (g/cm^3)
η_g is the viscosity of the gas (poise)

The limit of detection for a set-up with a low Δh that will not induce water redistribution is 10^{-11} cm^2 (gas conductivities of 10^{-7} cm/s).

UFA Gas Permeameter

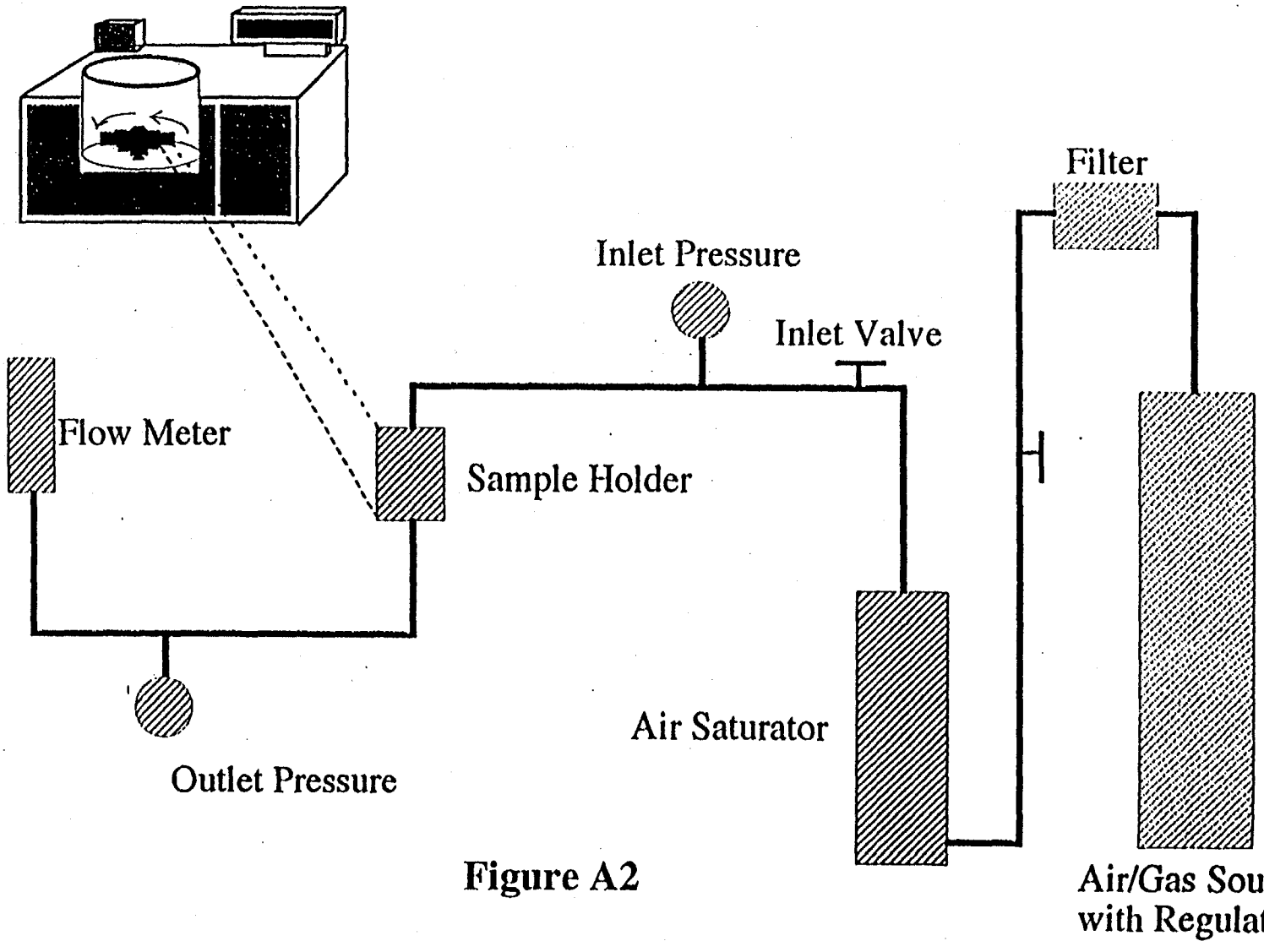

Figure A2

Diffusion Coefficient

The diffusion coefficient can be determined from the empirically-derived unsaturated aqueous diffusion curve for porous media (Conca et al., 1993) shown in Figure A3. All natural materials fit this relationship, including soils, gravels, rocks, grout, ceramic, and synroc. The volumetric water content in Figure A3 refers to the free volumetric water content (water not structurally bound) and care must be taken when choosing the free water content for materials having significant amounts of hydrous phases, e.g., clay minerals, gypsum and soluble salts. There are different representations of diffusion, describing various physicochemical properties of the media:

$$D_a(\varepsilon + \rho K_d) = D_e = D_s = \varepsilon D_v \phi = \varepsilon D_v \delta_D/\tau^2$$

where D_a is the apparent diffusion coefficient, D_e is the effective diffusion coefficient which is usually equal to the simple diffusion coefficient, D_s measured by electrical conductivity methods, D_p is the diffusion coefficient in the pore water, D_v is the diffusion coefficient in free water, ε is the porosity, ρ is the density, K_d is the distribution coefficient, ϕ is a geometric factor, δ_D is the constrictivity, and τ is the tortuosity. Figure A3 gives the effective or simple diffusion coefficient of the material. The distribution coefficient and the extent of retardation used in transport models need to be determined separately for each specific ionic species, media, and fluid composition. Retardation can significantly affect the migration of species in porous media, resulting in an

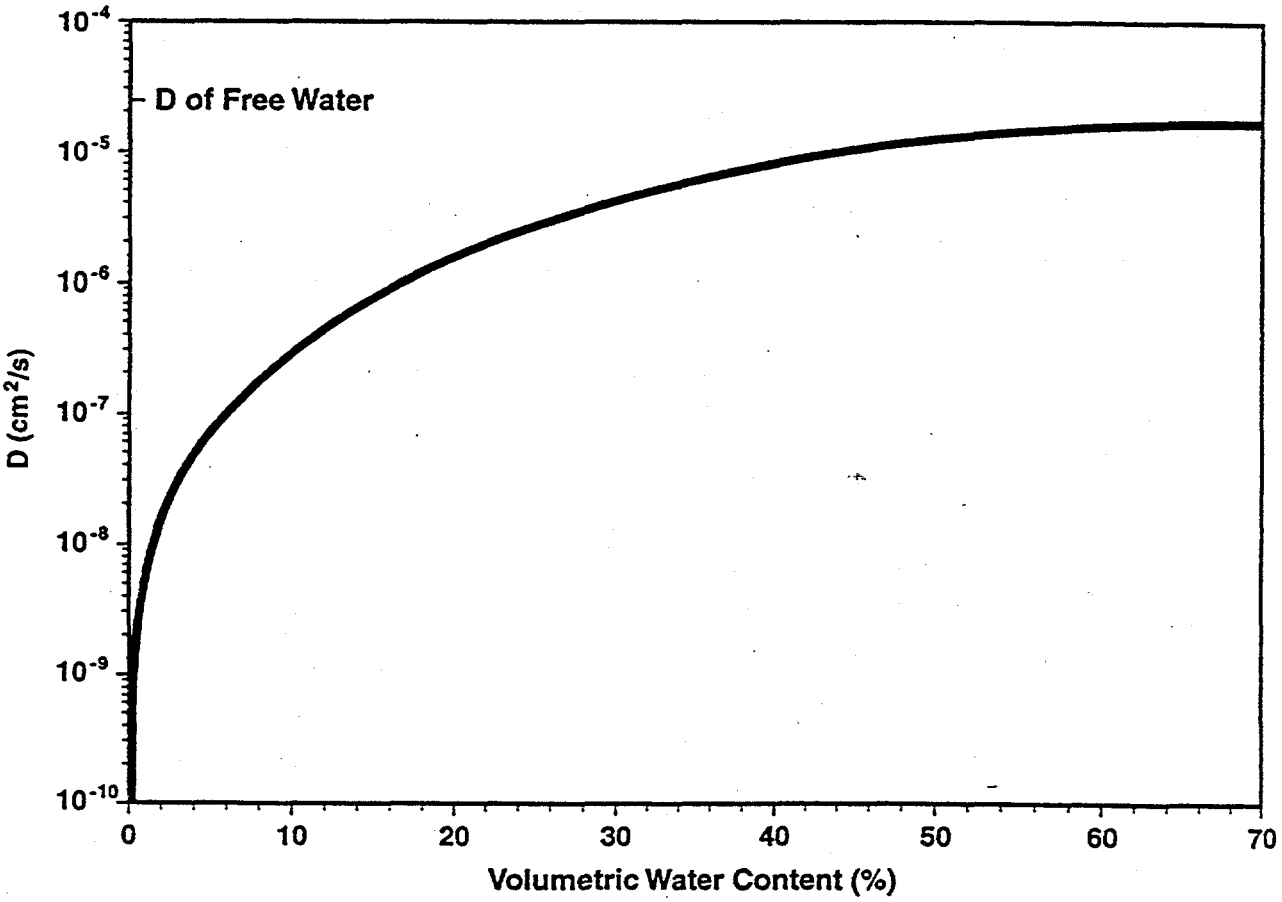

Figure A3. The Unsaturated Aqueous Diffusion Curve.

apparent diffusion coefficient that can be markedly different from the simple diffusion coefficient. However, this apparent diffusion coefficient is transient and will approach the simple diffusion coefficient as the sorption sites are filled or as the system otherwise tends toward chemical equilibrium. The diffusion coefficient for most aqueous species, including organics, are similar, differing by, at most, a factor of two from the self-diffusion coefficient of water which is 2.4 x 10^{-5} cm^2/s at 25°C. Diffusion coefficients in porous media that are less than 10^{-5} cm^2/s result from mechanisms or conditions other than the inherent mobility differences between the species themselves. These mechanisms include path length differences due to water content differences and retardation due to sorption and transient chemical effects. Figure A3 describes the change in diffusion coefficient as a result of path length differences from changes in the water content.

Estimation Methods Versus Direct Measurement

Hydraulic parameter estimation models such as van Genuchten/Mualem or Brooks-Cory methods assume an average pore-size with some variance about the mean pore size. Because of this assumption, the predicted $K(\theta)$ curves are smooth and show no kinks or other fine structure that reflect subtle pore-size distribution and sorting effects. However, pore connectivity changes as the water content decreases, and other property changes of real systems combine to distort the $K(\theta)$ curve. These effects can only be seen if $K(\theta)$ is directly measured. The $\psi(\theta)$ relationship is not as sensitive to the these properties as the $K(\theta)$ relationship, especially to the pore connectivity, and, thus, $\psi(\theta)$ remains a smooth curve. Hydraulic conductivity estimated from $\psi(\theta)$ will, therefore, always be smooth. Figure A4 shows two $K(\theta)$ curves for samples at 81 ft and 101 ft in borehole U3bh NW1 from the Nevada Test Site that show bimodal pore-size distributions, with a small variance about each. This type of behavior cannot presently be estimated but must be measured directly. Fortunately, the barrier materials investigated in this study are engineered for specific properties, and all are well-sorted and have unimodal pore-size distributions.

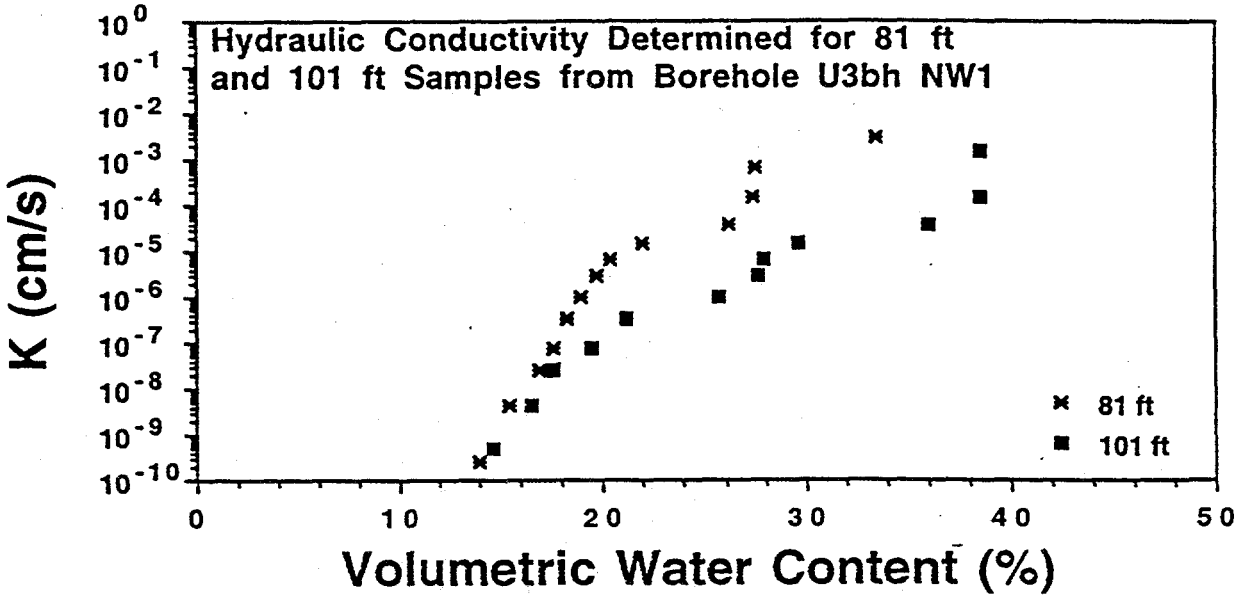

Figure A4. Unsaturated Hydraulic Conductivities for Two Samples from the Nevada Test Site Exhibiting Bimodal Pore-Size Distribution

UFA VENTURES/NESTT Sample Report

ent/PO#:	Los Alamos National Laboratory/Subcontract #215BA0016-3Y (TRW)
ID:	Tsp crushed gravel
n type:	Recomposited
bulk density (g/cm^3):	1.14

Hydraulic Conductivity Results			Moisture Potential Results		
moisture content%	K Value (cm/s)	Comments	Vol moisture content%	Matric Pressure (Bar)	Comments
56.04%	1.04E+01	column	0.5604	0	
7.38%	2.50E-05		8.07%	0.003	2 hr gravity drain
7.25%	9.00E-06		6.68%	0.04	
7.10%	4.00E-06		6.65%	0.17	
6.79%	1.80E-06		6.65%	0.30	
6.91%	6.75E-07		6.65%	0.47	
6.77%	2.25E-07		6.65%	0.68	
6.90%	4.50E-08		6.65%	1.06	
6.90%	1.70E-08		6.63%	1.53	
6.74%	2.88E-09		6.59%	2.08	
6.56%	2.28E-10		6.57%	2.95	
7.79%	1.00E-02	column	6.46%	4.25	
7.70%	1.00E-03	column	6.40%	5.63	
nments/Observations:			6.30%	7.56	
attached report for vapor diffusivity results.			6.17%	11.82	
			6.01%	17.02	
			5.84%	23.16	
			5.63%	30.25	
			5.41%	38.29	
			5.15%	47.27	

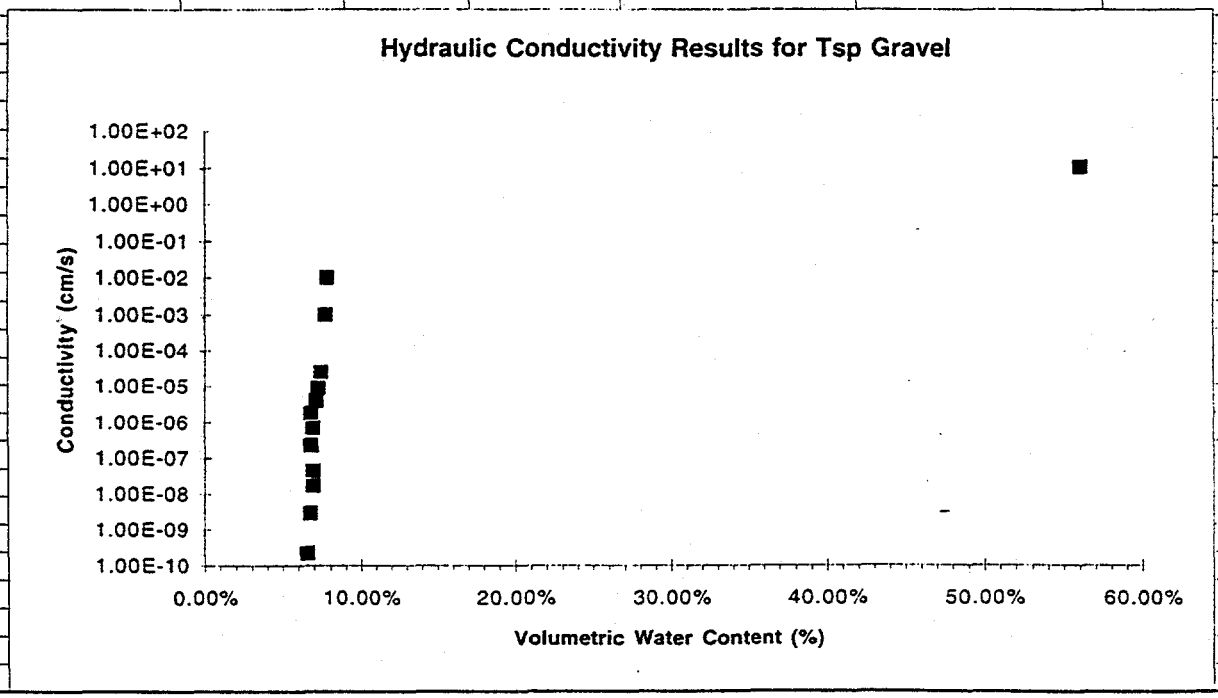

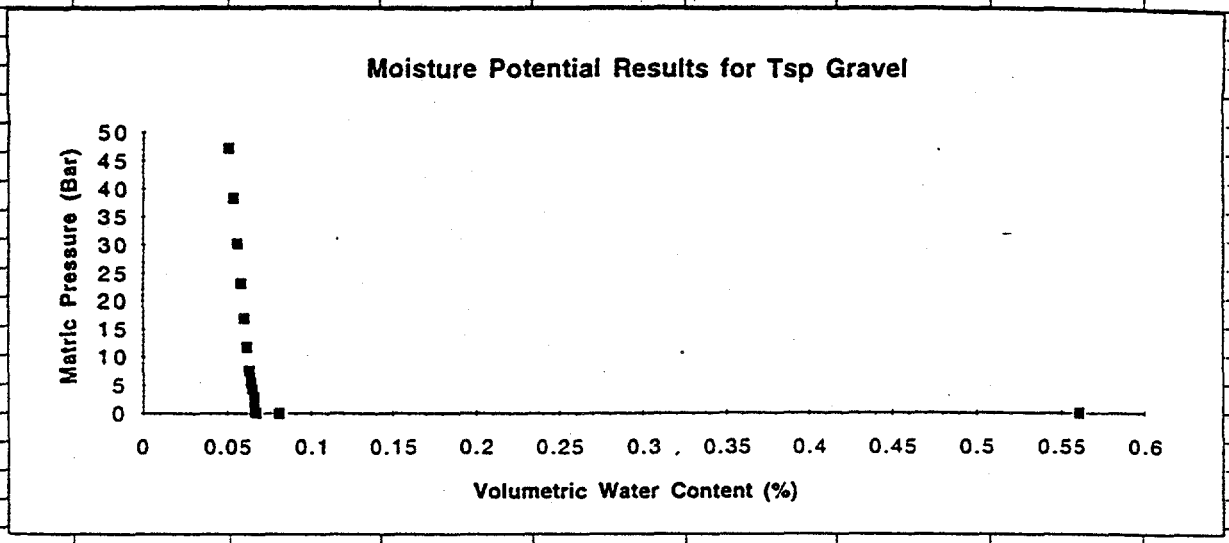
Moisture Potential Results for Tsp Gravel
Matric Pressure (Bar)
50
45
40
35
30
25
20
15
10
5
0
0
0.05
0.1
0.15
0.2
0.25
0.3
0.35
0.4
0.45
0.5
0.55
0.6
Volumetric Water Content (%)

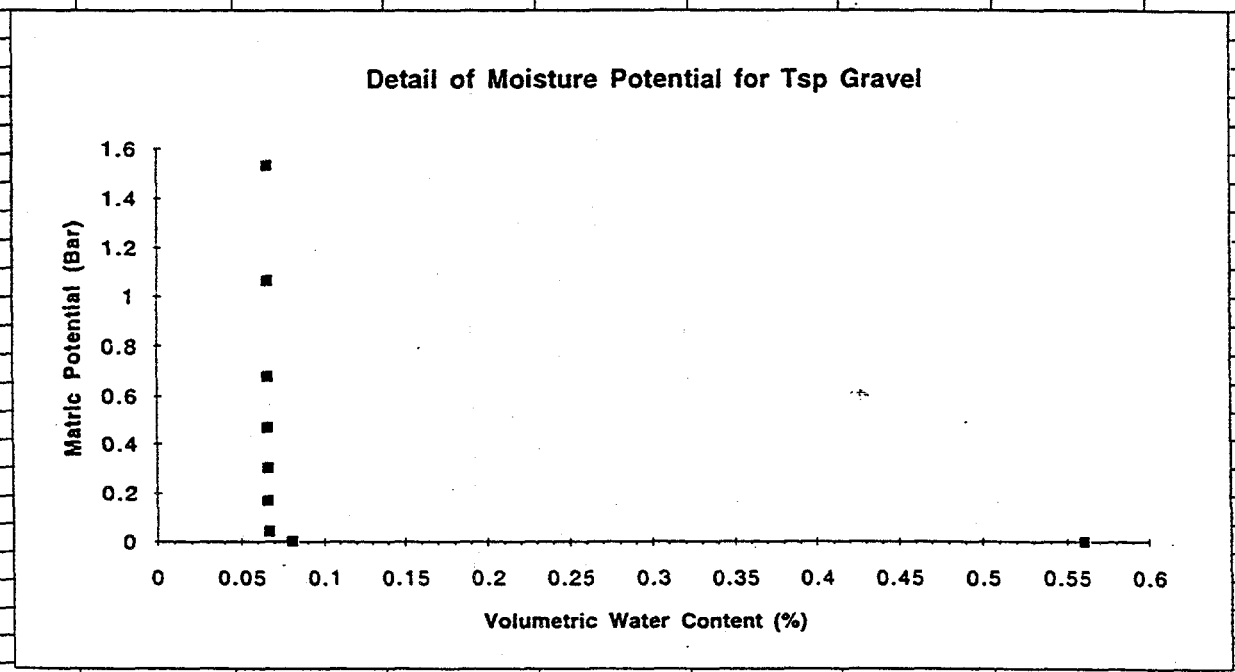
Detail of Moisture Potential for Tsp Gravel
Matric Potential (Bar)
1.6
1.4
1.2
1
0.8
0.6
0.4
0.2
0
0
0.05
0.1
0.15
0.2
0.25
0.3
0.35
0.4
0.45
0.5
0.55
0.6
Volumetric Water Content (%)

UFA VENTURES/NESTT Sample Report

nt/PO#:	Los Alamos National Laboratory/Subcontract #215BA0016-3Y (TRW)
ID:	Hanford River Cobble-Crushed Basalt
type:	Recomposited
bulk density (g/cm^3):	1.44

Hydraulic Conductivity Results

moisture content%	K Value (cm/s)	Comments
42.91%	9.20E+00	column
3.23%	2.50E-05	
2.76%	9.00E-06	
2.70%	4.00E-06	
2.71%	1.80E-06	
2.59%	6.75E-07	
2.59%	2.25E-07	
2.55%	4.50E-08	
2.56%	1.70E-08	
2.50%	2.88E-09	
2.35%	2.28E-10	

nments/Observations:
attached report for vapor diffusivity results.

Moisture Potential Results

Vol moisture content%	Matric Pressure (Bar)	Comments
0.4291	0	Gravity drain for 2 hrs
3.15%	0.002	
1.94%	0.04	
2.01%	0.17	
2.01%	0.30	
2.01%	0.47	
2.06%	0.68	
2.15%	1.06	
2.04%	1.53	
2.04%	2.08	
2.04%	2.95	
2.06%	4.25	
2.03%	5.63	
2.01%	7.56	
1.99%	11.82	
1.97%	17.02	
1.96%	23.16	
1.95%	30.25	
1.94%	38.29	
1.92%	47.27	

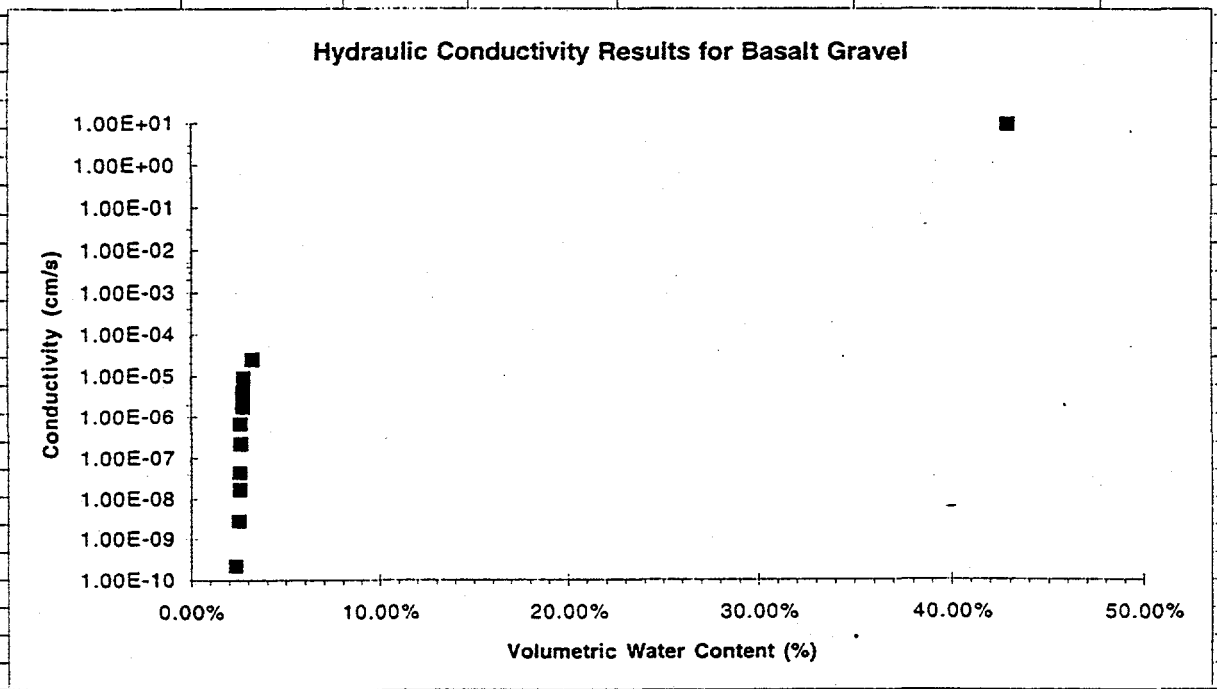

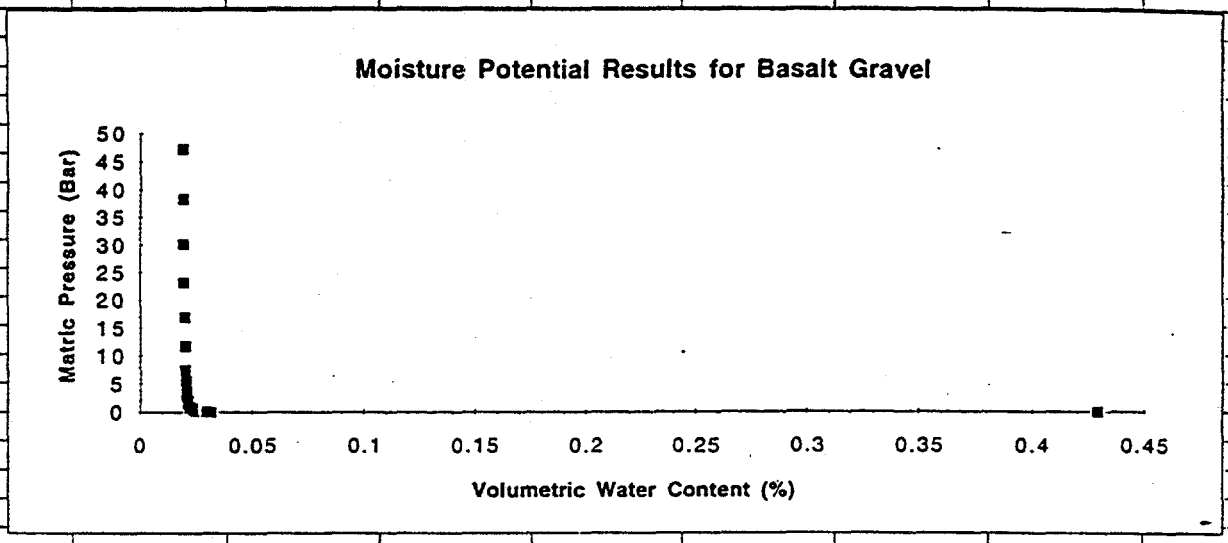
Moisture Potential Results for Basalt Gravel
Matric Pressure (Bar)
50
45
40
35
30
25
20
15
10
5
0
0
0.05
0.1
0.15
0.2
0.25
0.3
0.35
0.4
0.45
Volumetric Water Content (%)

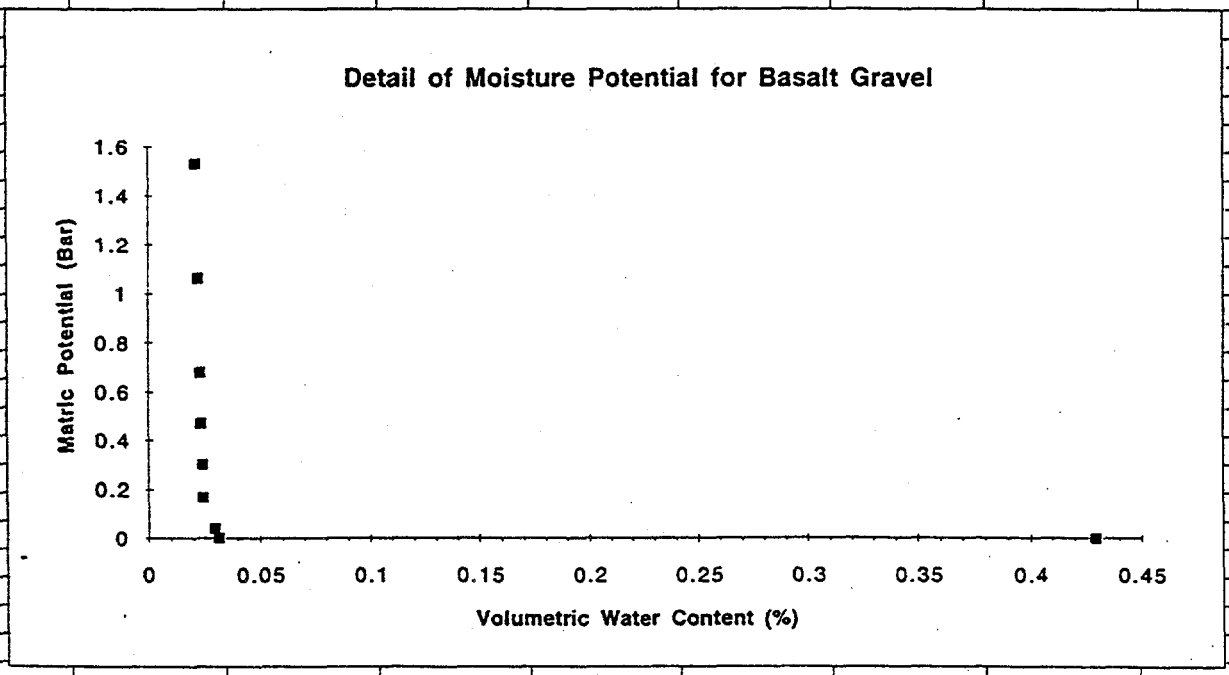
Detail of Moisture Potential for Basalt Gravel
Matric Potential (Bar)
1.6
1.4
1.2
1
0.8
0.6
0.4
0.2
0
0
0.05
0.1
0.15
0.2
0.25
0.3
0.35
0.4
0.45
Volumetric Water Content (%)

UFA VENTURES/NESTT Sample Report

nt/PO#:	Los Alamos National Laboratory/Subcontract #215BA0016-3Y (TRW)
ID:	Tsp tuff
type:	whole rock
bulk density (g/cm^3):	2.16

Hydraulic Conductivity Results

moisture content%	K Value (cm/s)	Comments
15.23%	8.79E-08	Falling Head Values
15.23%	5.39E-08	
14.90%	3.23E-08	
14.22%	5.47E-09	
14.19%	4.32E-10	
14.04%	3.28E-11	

Moisture Potential Results

Vol moisture content%	Matric Pressure (Bar)	Comments
15.08%	0.04	
15.05%	0.17	
14.84%	0.30	
14.78%	0.47	
14.78%	0.68	
14.75%	1.06	
14.63%	1.53	
14.55%	2.08	
14.34%	2.95	
14.01%	4.25	
13.72%	5.79	
13.39%	7.56	
12.77%	11.82	
12.06%	17.02	
11.23%	23.16	
10.46%	30.25	
9.81%	38.29	
9.21%	47.27	

ments/Observations:
attached report for vapor diffusivity results.

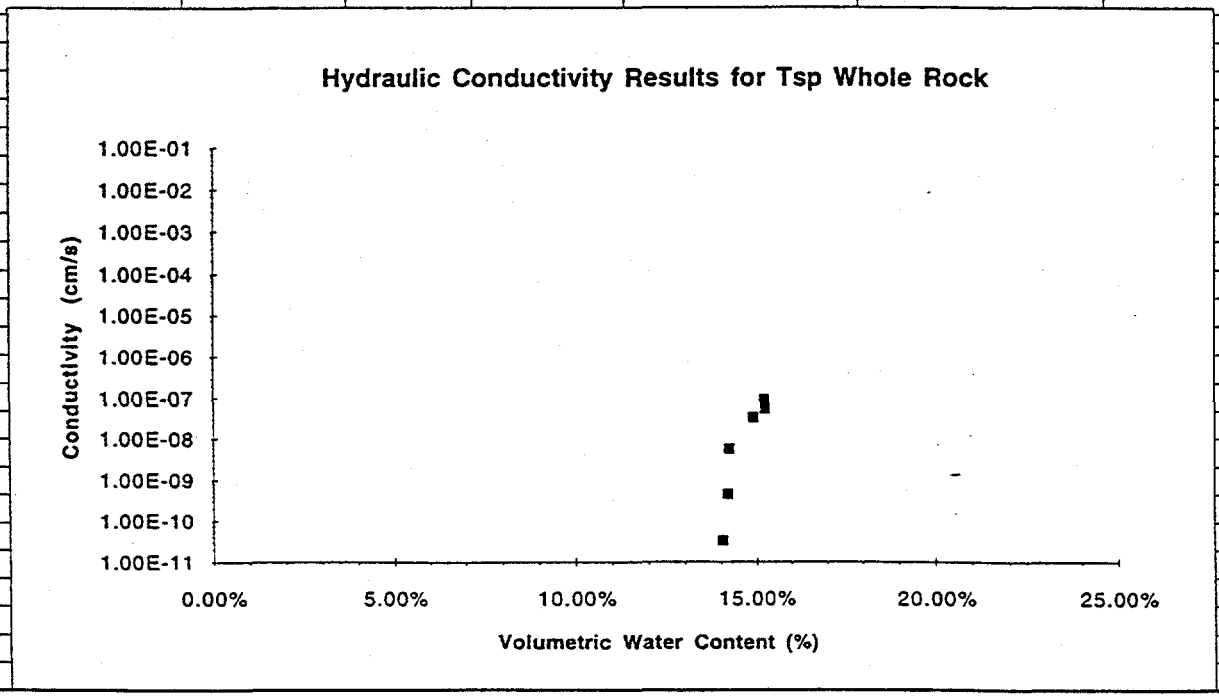

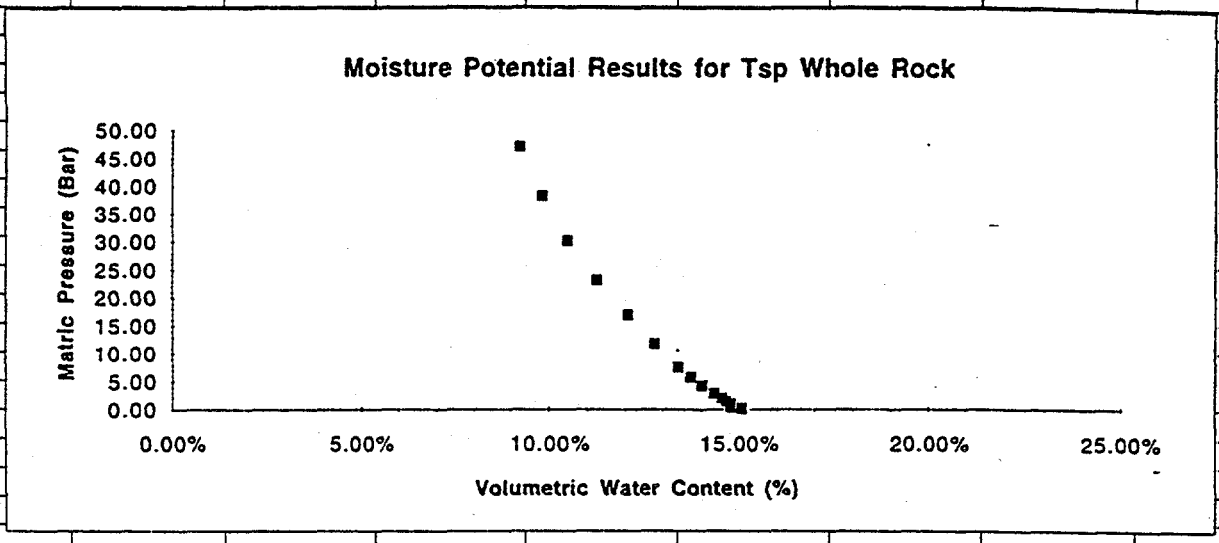
Moisture Potential Results for Tsp Whole Rock
Matric Pressure (Bar)
50.00
45.00
40.00
35.00
30.00
25.00
20.00
15.00
10.00
5.00
0.00
0.00%
5.00%
10.00%
15.00%
20.00%
25.00%
Volumetric Water Content (%)

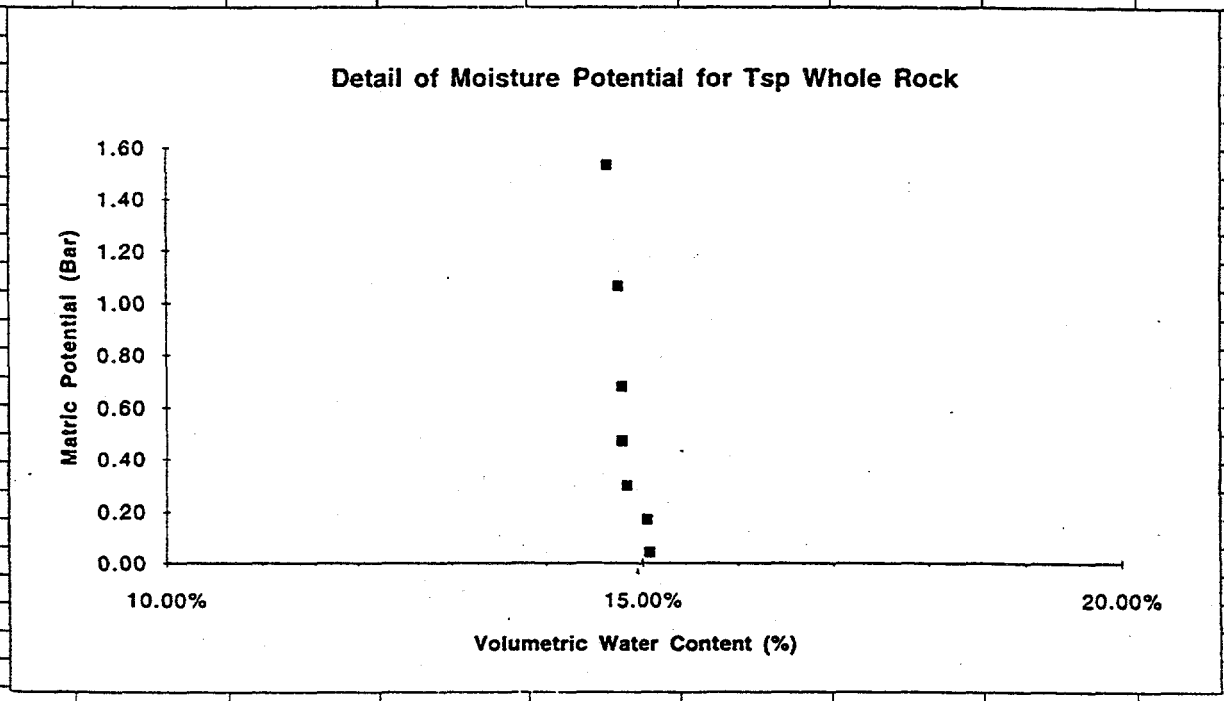
Detail of Moisture Potential for Tsp Whole Rock
Matric Potential (Bar)
1.60
1.40
1.20
1.00
0.80
0.60
0.40
0.20
0.00
10.00%
15.00%
20.00%
Volumetric Water Content (%)

UFA VENTURES/NESTT Sample Report

nt/PO#:	Los Alamos National Laboratory/Subcontract #215BA0016-3Y (TRW)
ID:	Apatite-North Carolina
type:	recomposite
bulk density (g/cm^3):	1.52

Hydraulic Conductivity Results

moisture content%	K Value (cm/s)	Comments
46.02	1.57E-02	Constant Head
45.29	1.58E-04	
43.43	3.96E-05	
22.07	1.43E-05	
17.98	6.33E-06	
16.64	2.85E-06	
15.90	1.07E-06	
15.14	3.56E-07	
13.81	2.69E-08	
13.81	1.08E-08	
13.24	4.56E-09	
13.00	3.60E-10	

ments/Observations:
attached report for vapor diffusivity results.

Moisture Potential Results

Vol moisture content%	Matric Pressure (Bar)	Comments
46.14%	0.04	
42.93%	0.17	
35.35%	0.30	
22.42%	0.47	
13.15%	0.68	
12.24%	1.06	
11.85%	1.53	
11.55%	2.08	
11.46%	2.95	
11.33%	4.25	
11.14%	5.79	
11.01%	7.56	
10.92%	11.82	
10.77%	17.02	
10.52%	23.16	
10.38%	30.25	
10.18%	38.29	
10.01%	47.27	

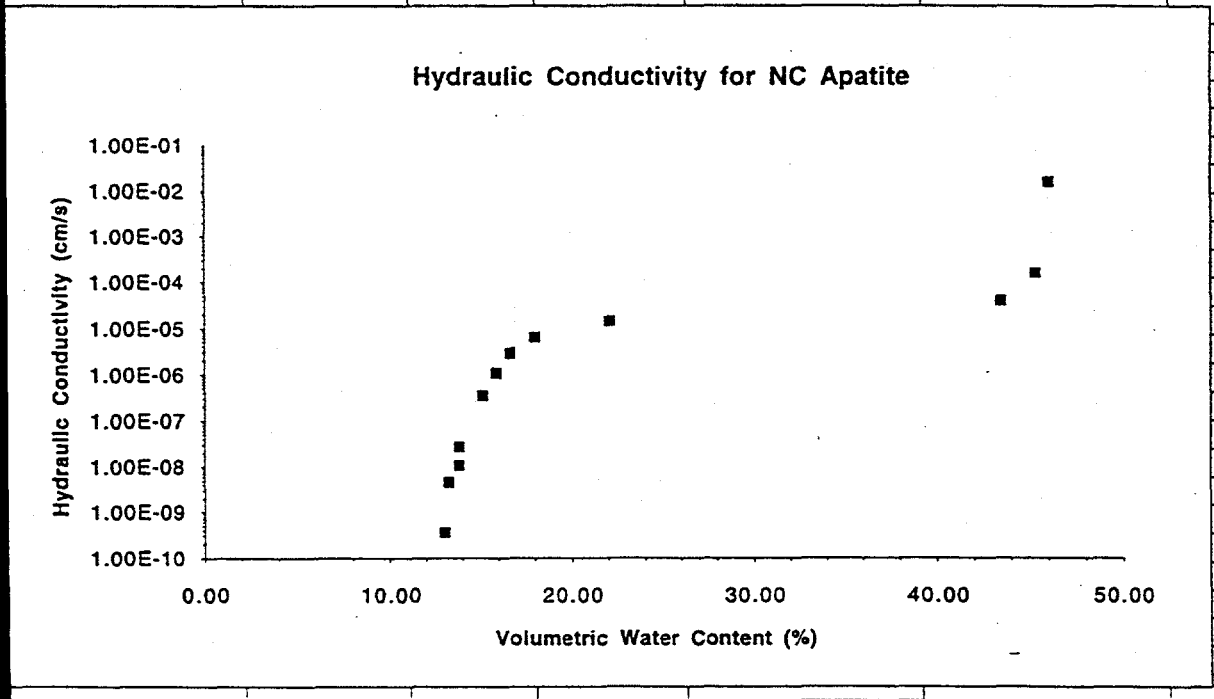

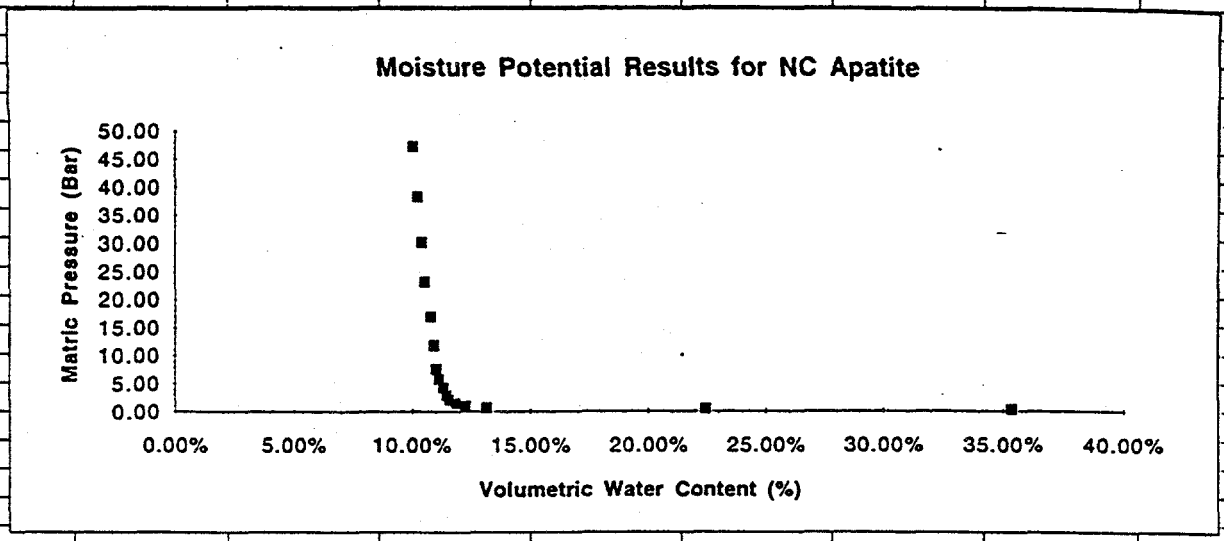
Moisture Potential Results for NC Apatite
Matric Pressure (Bar)
50.00
45.00
40.00
35.00
30.00
25.00
20.00
15.00
10.00
5.00
0.00
0.00%
5.00%
10.00%
15.00%
20.00%
25.00%
30.00%
35.00%
40.00%
Volumetric Water Content (%)

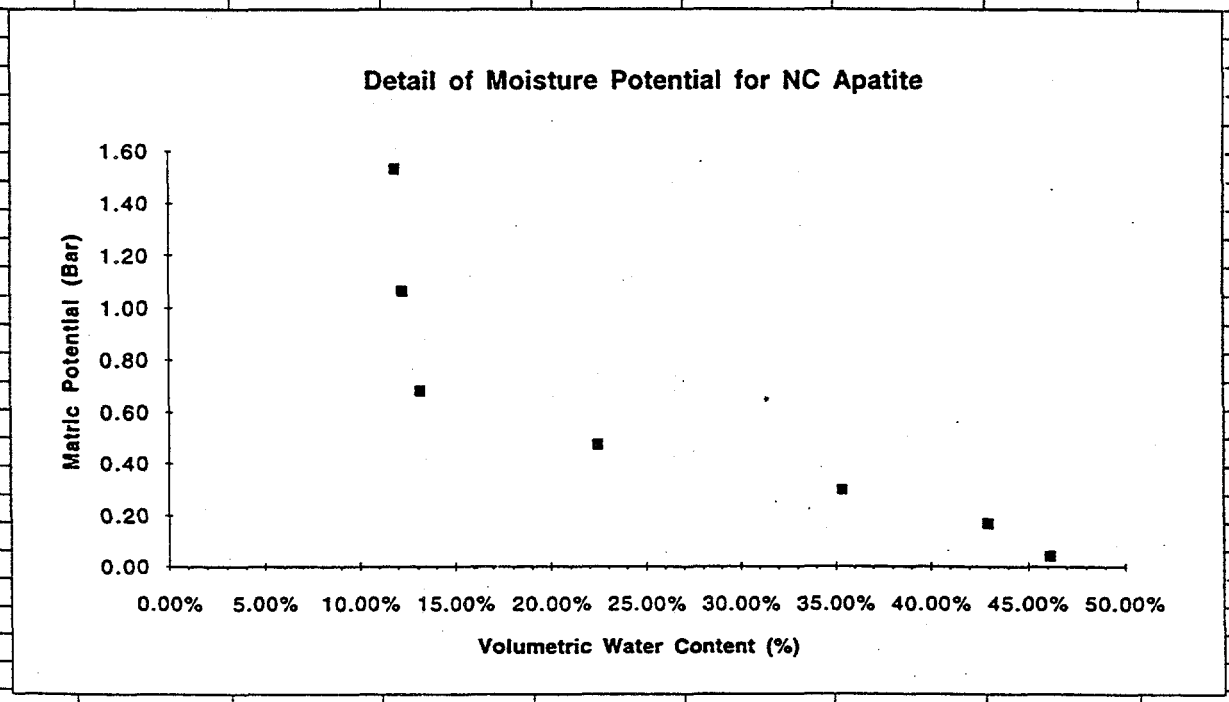
Detail of Moisture Potential for NC Apatite
Matric Potential (Bar)
1.60
1.40
1.20
1.00
0.80
0.60
0.40
0.20
0.00
0.00%
5.00%
10.00%
15.00%
20.00%
25.00%
30.00%
35.00%
40.00%
45.00%
50.00%
Volumetric Water Content (%)

UFA VENTURES/NESTT Sample Report

t/PO#:	Los Alamos National Laboratory/Subcontract #215BA0016-3Y (TRW)
D:	Japanese Sand
ype:	recomposited
ulk density (g/cm^3):	1.71

Hydraulic Conductivity Results			Moisture Potential Results		
oisture content%	K Value (cm/s)	Comments	Vol moisture content%	Matric Pressure (Bar)	Comments
33.00	1.02E-01	Constant Head	34.32%	0.04	
32.80	1.00E-02	column	29.13%	0.17	
31.30	1.00E-03	column	19.32%	0.30	
19.98	8.72E-04	Gravity Feed	6.47%	0.47	
14.19	3.64E-04		2.30%	0.68	
11.69	1.84E-04		2.06%	1.06	
9.36	4.60E-05		1.94%	1.53	
7.42	1.66E-05		1.83%	2.08	
5.95	7.36E-06		1.80%	2.95	
4.51	3.31E-06		1.68%	4.25	
3.69	1.24E-06		1.59%	5.79	
3.29	4.14E-07		1.49%	7.56	
2.90	8.28E-08		1.45%	11.82	
2.66	4.14E-08		1.35%	17.02	
2.41	6.54E-09		1.30%	23.16	
nents/Observations:			1.21%	30.25	
ttached report for vapor diffusivity results.			1.19%	38.29	
			1.16%	47.27	

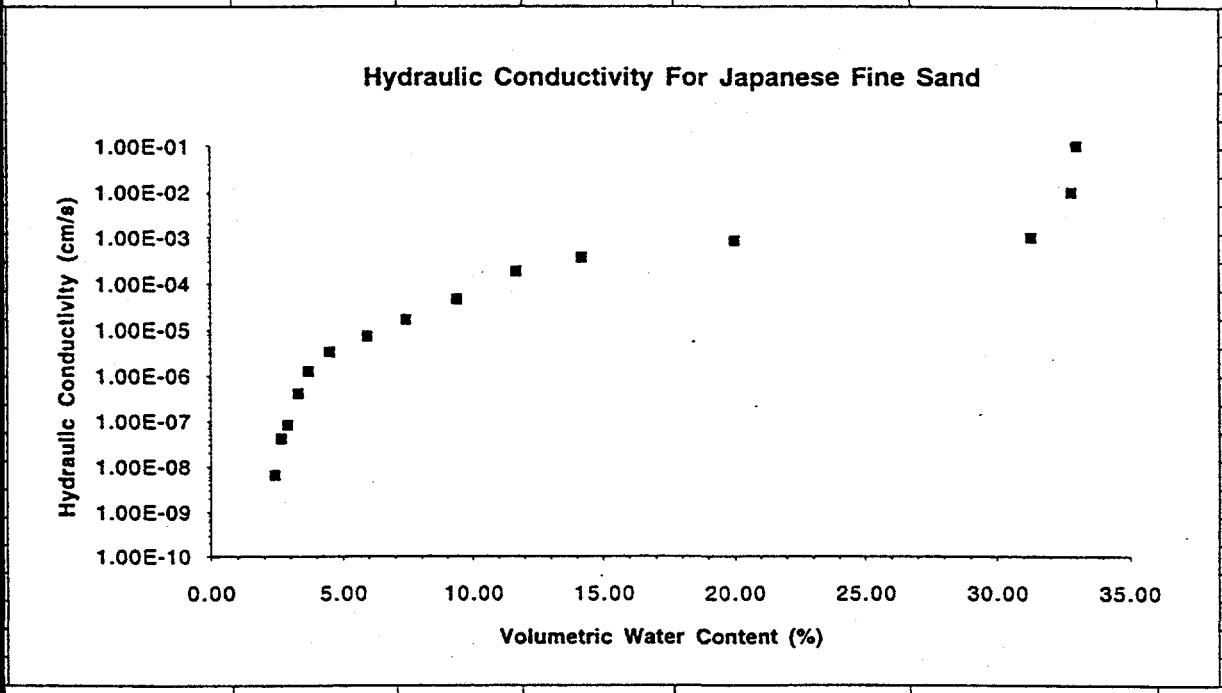

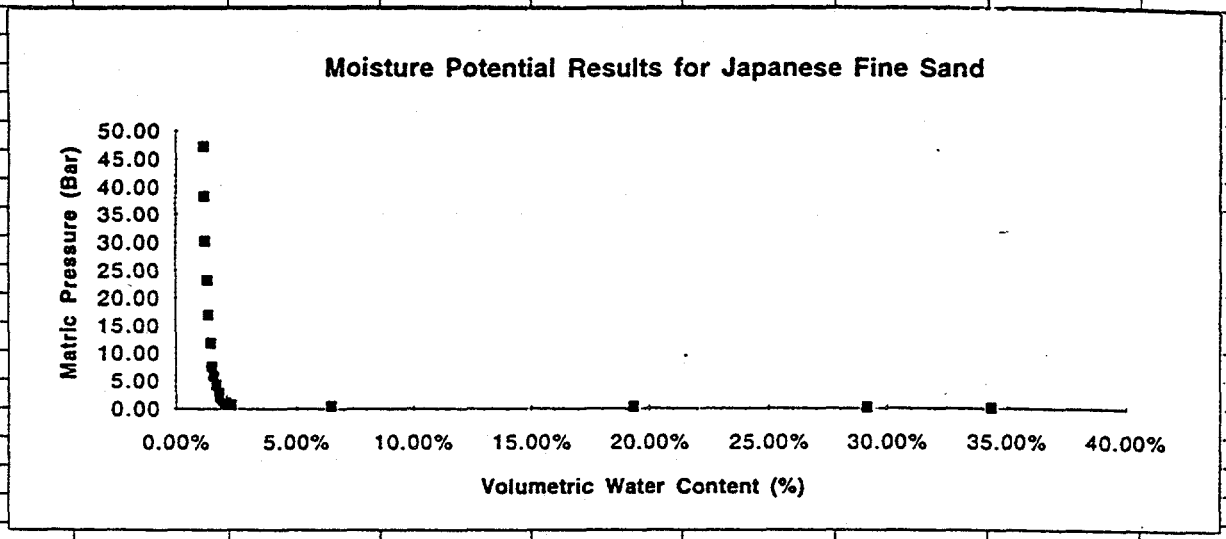
Moisture Potential Results for Japanese Fine Sand
Matric Pressure (Bar)
50.00
45.00
40.00
35.00
30.00
25.00
20.00
15.00
10.00
5.00
0.00
0.00%
5.00%
10.00%
15.00%
20.00%
25.00%
30.00%
35.00%
40.00%
Volumetric Water Content (%)

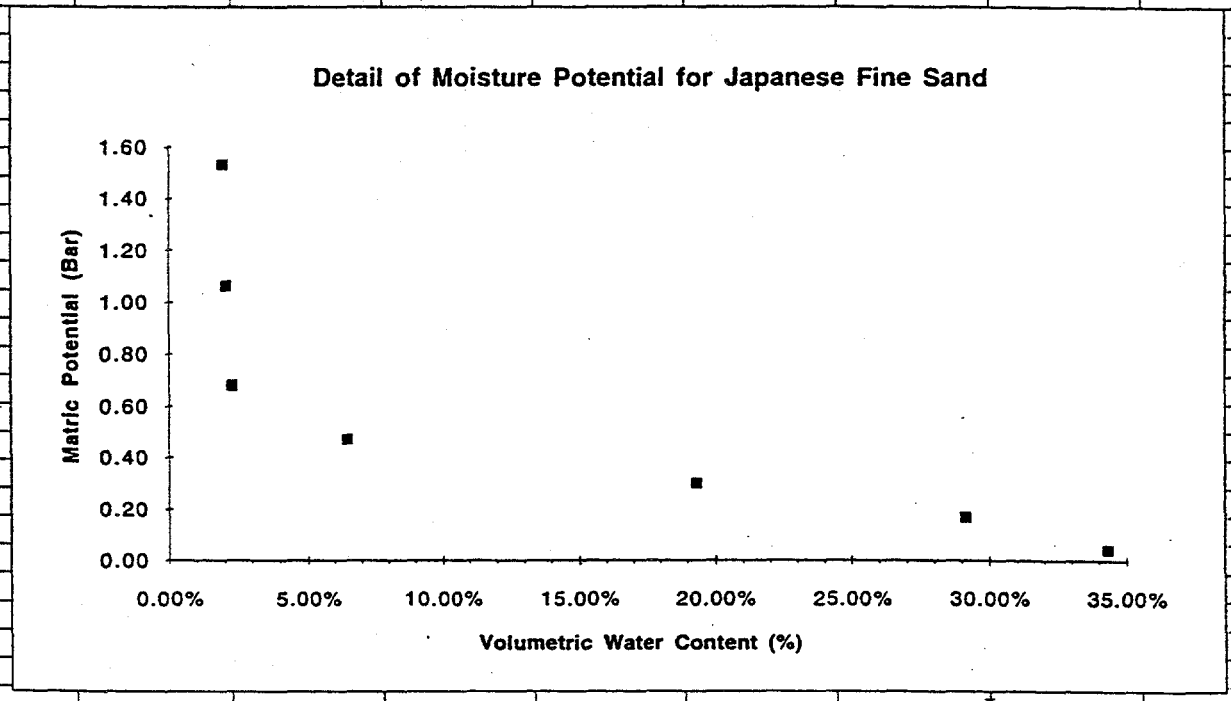
Detail of Moisture Potential for Japanese Fine Sand
Matric Potential (Bar)
1.60
1.40
1.20
1.00
0.80
0.60
0.40
0.20
0.00
0.00%
5.00%
10.00%
15.00%
20.00%
25.00%
30.00%
35.00%
Volumetric Water Content (%)

UFA VENTURES/NESTT Sample Report

nt/PO#:	Los Alamos National Laboratory/Subcontract #215BA0016-3Y (TRW)
ID:	Japanese Coarse Sand
type:	recomposited
bulk density (g/cm^3):	1.48

Hydraulic Conductivity Results			Moisture Potential Results		
moisture content%	K Value (cm/s)	Comments	Vol moisture content%	Matric Pressure (Bar)	Comments
42.00%	2.09E+00	Constant Head Values	19.49%	0.04	
34.90%	1.00E-02	column	19.27%	0.17	
27.50%	1.00E-03	column	5.64%	0.30	
7.06%	3.96E-05		4.67%	0.47	
4.95%	1.43E-05		4.61%	0.68	
3.89%	6.33E-06		4.48%	1.06	
3.34%	2.85E-06		4.41%	1.53	
2.94%	1.07E-06		4.33%	2.08	
2.70%	3.56E-07		4.26%	2.95	
2.42%	7.13E-08		4.16%	4.25	
2.04%	5.39E-09		4.09%	5.63	
			4.01%	7.56	
			3.91%	11.82	
			3.79%	17.02	
			3.69%	23.16	
ments/Observations:			3.58%	30.25	
attached report for vapor diffusivity results.			3.50%	38.29	
			3.43%	47.27	

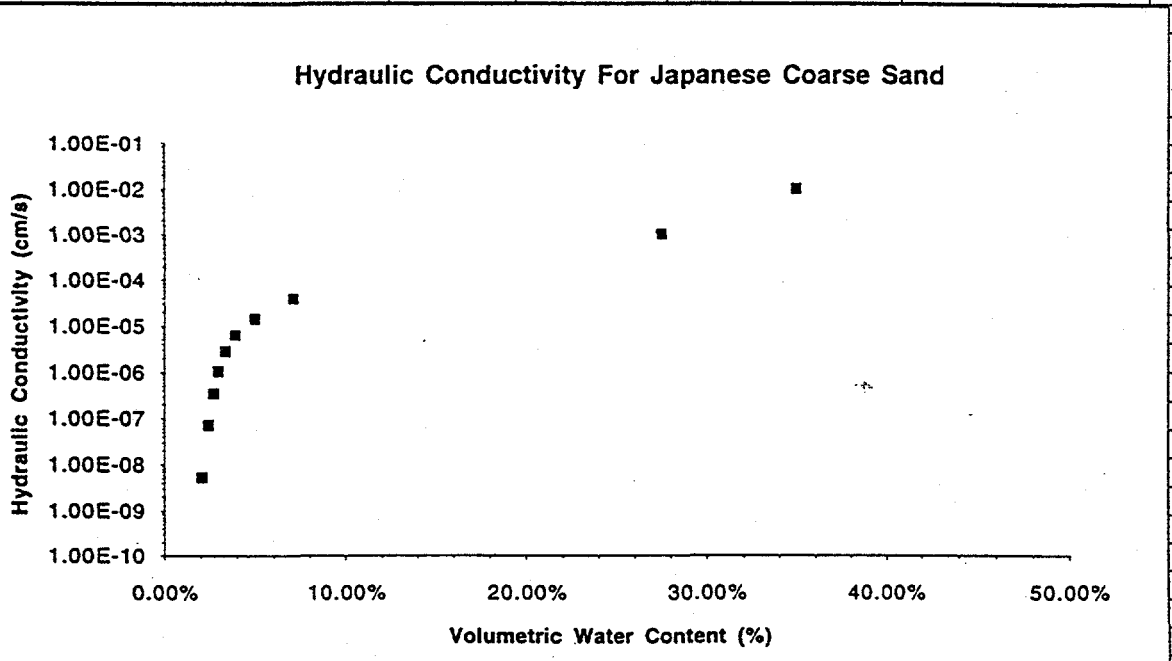

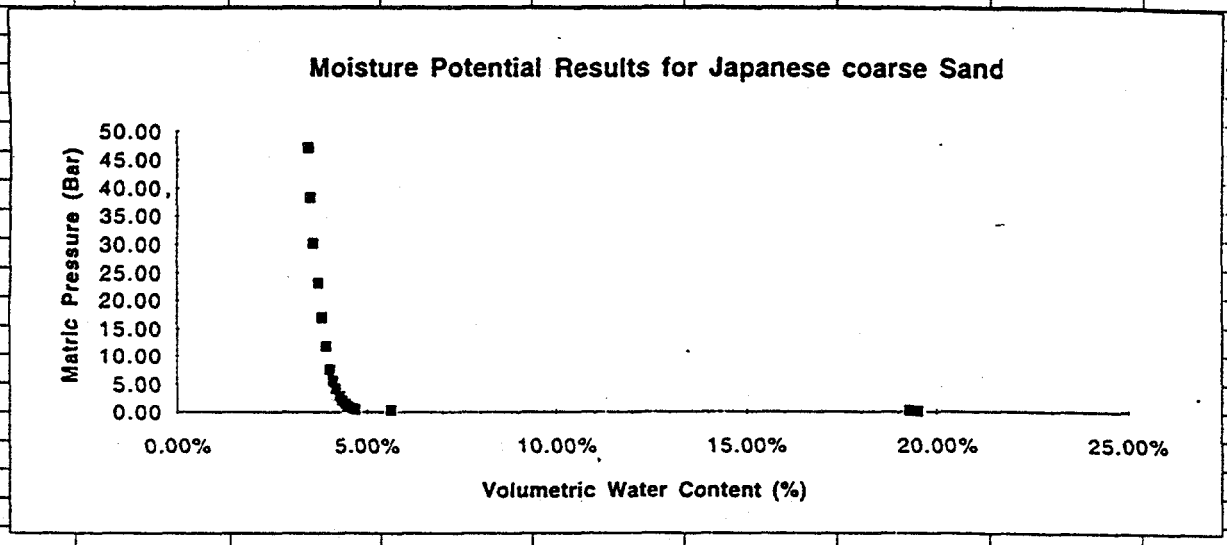
Moisture Potential Results for Japanese coarse Sand
Matric Pressure (Bar)
50.00
45.00
40.00
35.00
30.00
25.00
20.00
15.00
10.00
5.00
0.00
0.00%
5.00%
10.00%
15.00%
20.00%
25.00%
Volumetric Water Content (%)

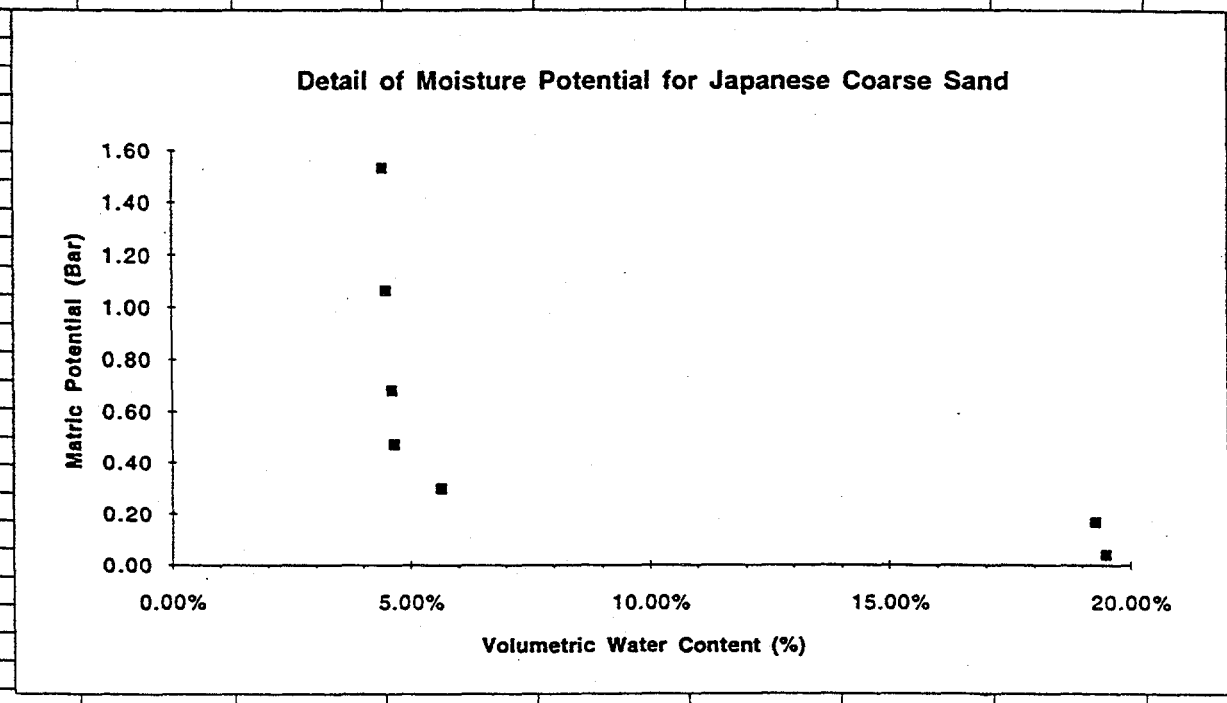
Detail of Moisture Potential for Japanese Coarse Sand
Matric Potential (Bar)
1.60
1.40
1.20
1.00
0.80
0.60
0.40
0.20
0.00
0.00%
5.00%
10.00%
15.00%
20.00%
Volumetric Water Content (%)

UFA VENTURES/NESTT Sample Report

nt/PO#:	Los Alamos National Laboratory/Subcontract #215BA0016-3Y (TRW)
ID:	Alluvium
type:	Recomposited
bulk density (g/cm^3):	1.890697075

Hydraulic Conductivity Results

moisture content%	K Value (cm/s)	Comments
26.32%	4.37E-07	Falling Head Values
26.25%	4.90E-07	Gravity Feed Values
25.53%	2.85E-07	
25.51%	2.85E-07	
23.71%	7.13E-08	
21.55%	2.69E-08	
20.11%	1.08E-08	
19.07%	4.56E-09	
18.14%	3.60E-10	

ments/Observations:
attached report for vapor diffusivity results.

Moisture Potential Results

Vol moisture content%	Matric Pressure (Bar)	Comments
28.48%	0.04	
27.42%	0.17	
25.93%	0.30	
24.84%	0.47	
24.42%	0.68	
23.63%	1.06	
22.68%	1.53	
21.52%	2.08	
19.93%	2.95	
18.24%	4.25	
17.05%	5.63	
15.94%	7.56	
14.40%	11.82	
13.27%	17.02	
12.28%	23.16	
11.50%	30.25	
10.92%	38.29	
10.37%	47.27	

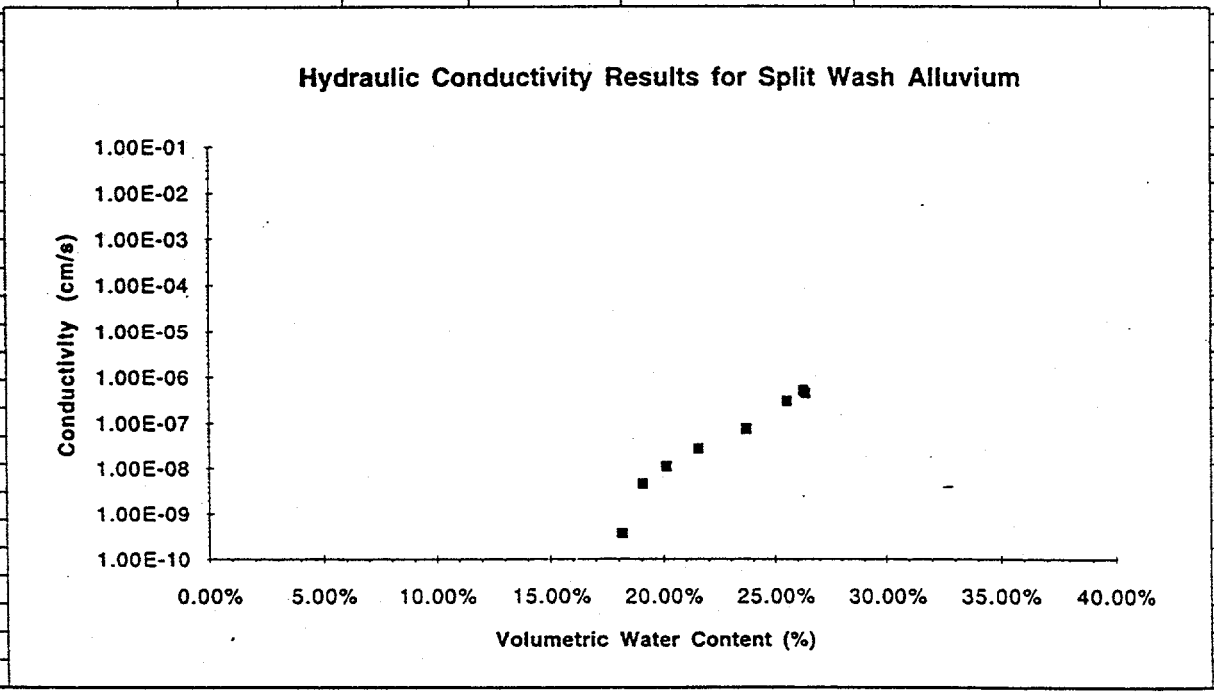

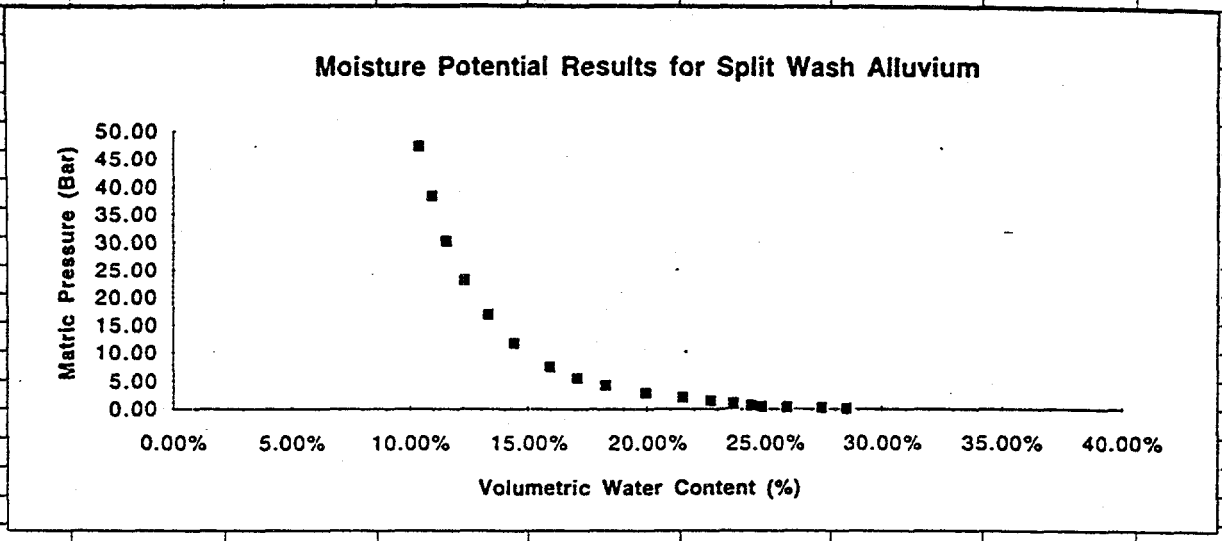
Moisture Potential Results for Split Wash Alluvium
Matric Pressure (Bar)
50.00
45.00
40.00
35.00
30.00
25.00
20.00
15.00
10.00
5.00
0.00
0.00%
5.00%
10.00%
15.00%
20.00%
25.00%
30.00%
35.00%
40.00%
Volumetric Water Content (%)

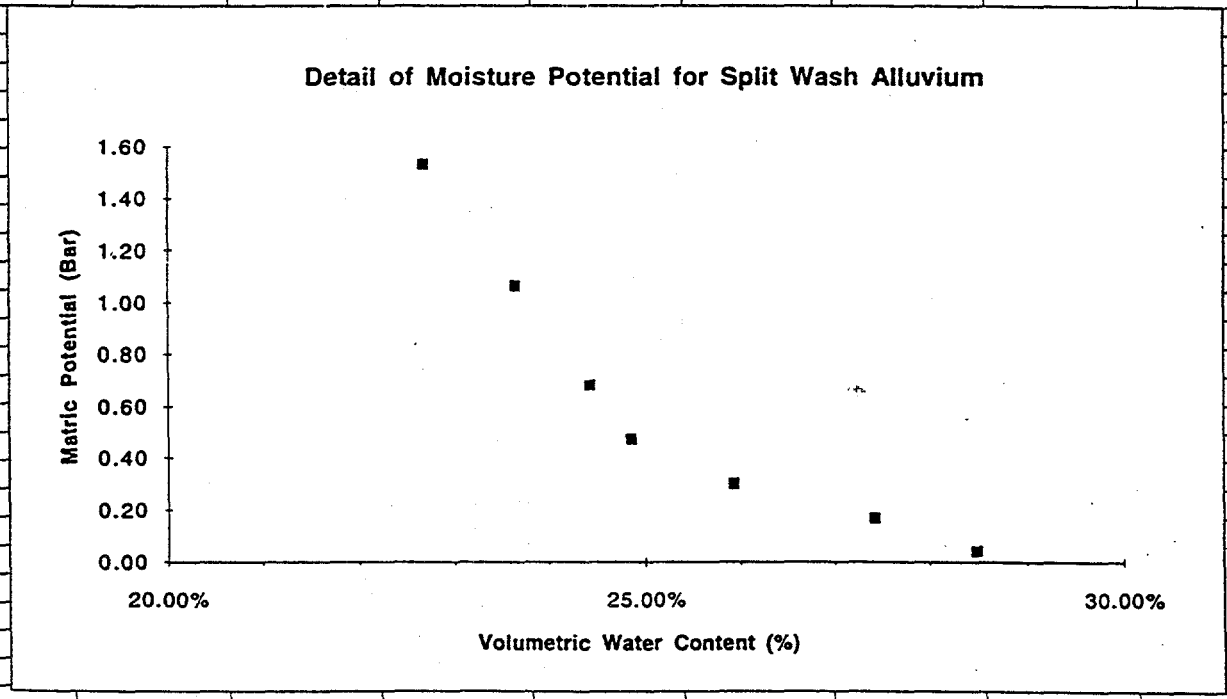
Detail of Moisture Potential for Split Wash Alluvium
Matric Potential (Bar)
1.60
1.40
1.20
1.00
0.80
0.60
0.40
0.20
0.00
20.00%
25.00%
30.00%
Volumetric Water Content (%)

	Volumetric Water Content (%)	Coeff. of Air Permeabil. (cm2)
Fine sand	33.00	5.00e-12
	10.99	2.33e-8
	9.59	1.54e-8
	7.90	4.81e-9
	6.48	4.79e-8
	5.53	4.21e-9
	4.11	5.89e-8
	3.16	1.53e-9
	2.21	2.16e-8
	2.21	2.45e-8
Coarse Sand	42.00	5.00e-12
	6.64	3.35e-8
	4.86	1.16e-8
	3.82	2.13e-8
	3.30	1.74e-8
	2.85	3.69e-8
	2.66	1.01e-8
	2.30	2.75e-8
	1.99	1.36e-7
Basalt Gravel	42.91	5.00e-12
	3.22	5.00e-12
	2.76	3.75e-6
	2.67	1.66e-6
	2.72	1.13e-6
	2.60	6.95e-6
	2.56	8.09e-7
	2.56	1.61e-6
	2.50	4.40e-6
	2.36	1.48e-6
Tsp Tuff Gravel	56.04	5.00e-12
	7.38	5.00e-12
	7.25	1.17e-6
	7.10	1.43e-6
	6.79	7.47e-7
	6.91	1.99e-6
	6.77	1.49e-6
	6.90	2.97e-6
	6.90	1.88e-6
	6.74	2.94e-6
	6.56	1.95e-6
Split Wash Alluvium	26.32	5.00e-12
	26.25	5.00e-12
	25.53	5.00e-12
	25.50	5.00e-12
	23.70	5.00e-12
	21.55	5.00e-12
	20.11	5.00e-12
	19.07	5.00e-12
	18.14	5.00e-12

		Volumetric Water Content (%)	Coeff. of Air Permeabil. (cm2)
57			
58	NC Apatite	46.02	5.00e-12
59		21.97	1.88e-8
60		20.31	1.68e-8
61		19.84	1.68e-8
62		16.75	3.04e-8
63		15.57	3.37e-8
64		13.91	6.45e-8
65		12.96	7.86e-8
66			
67	Tsp Whole Rock	15.23	5.00e-12
68		13.21	6.04e-9

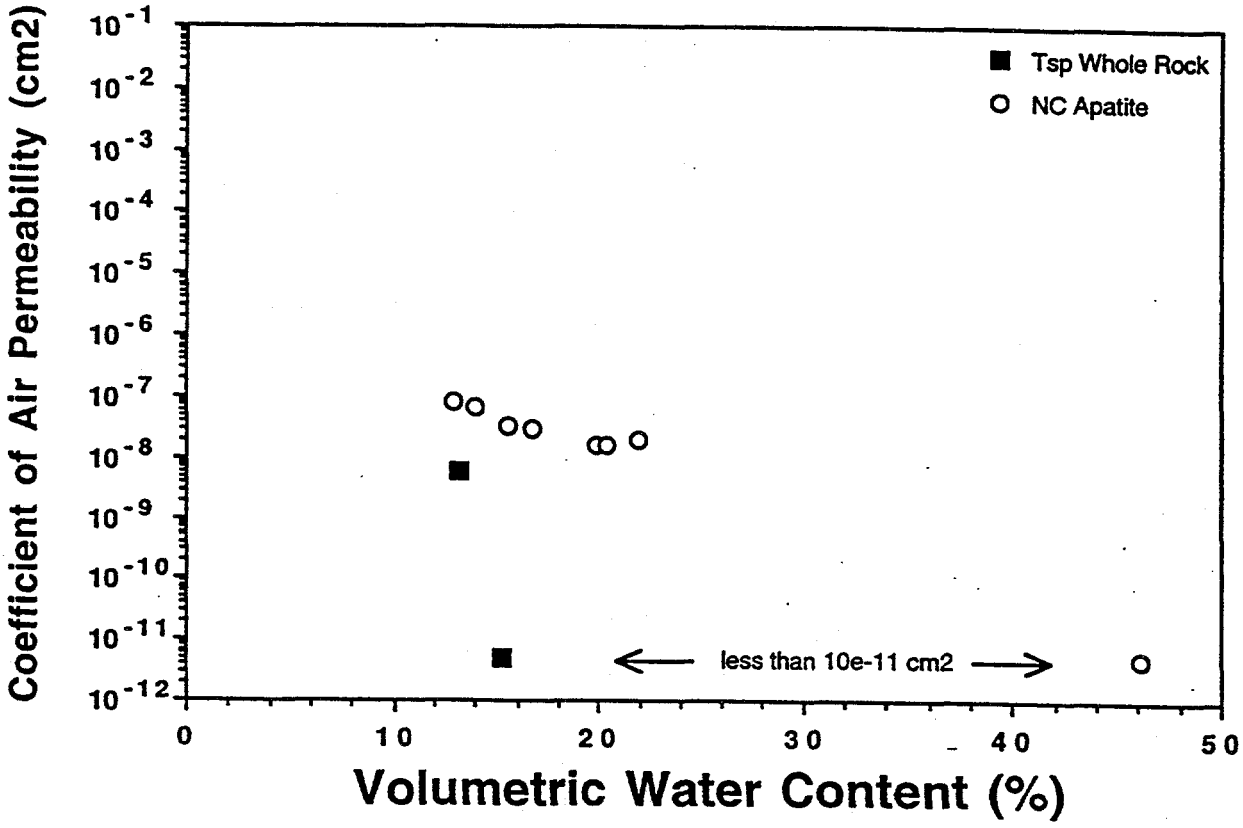

Air Permeability Curves for the Topopah Springs Tuff Whole Rock and NC Apatite

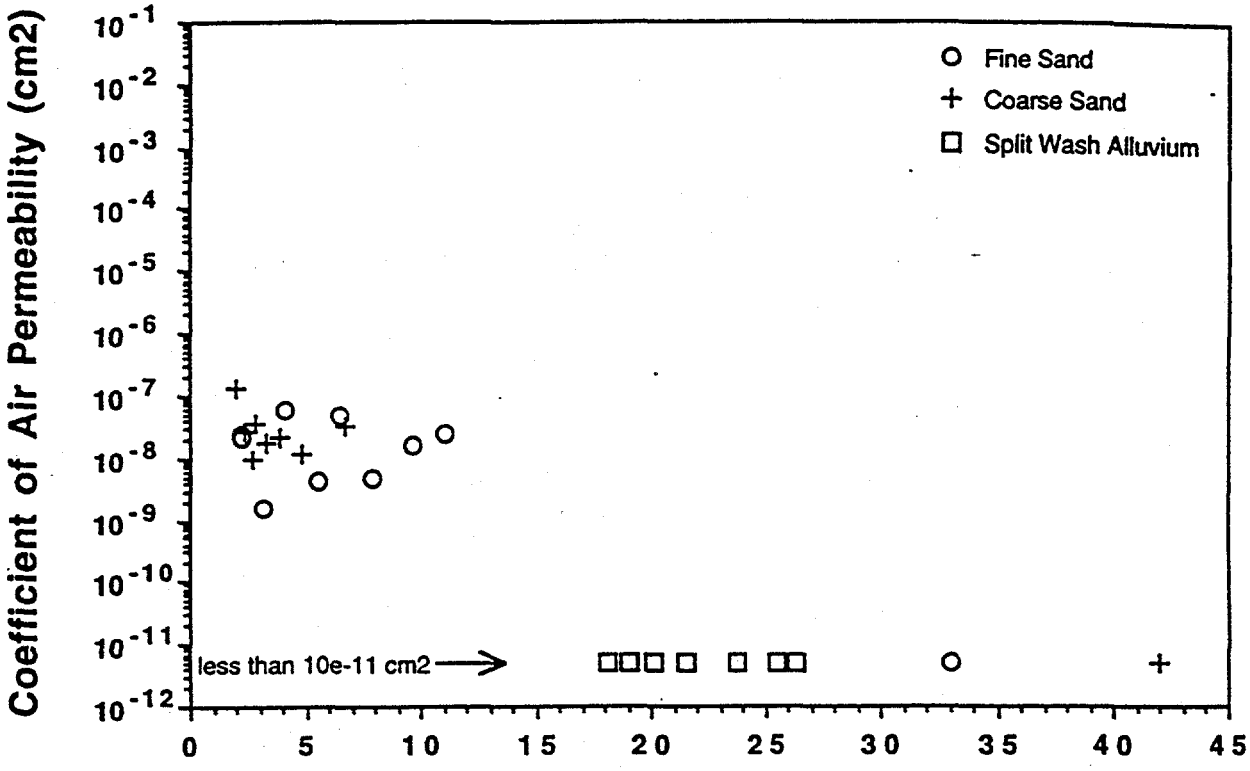

Air Permeability Curves for the Candidate Sands

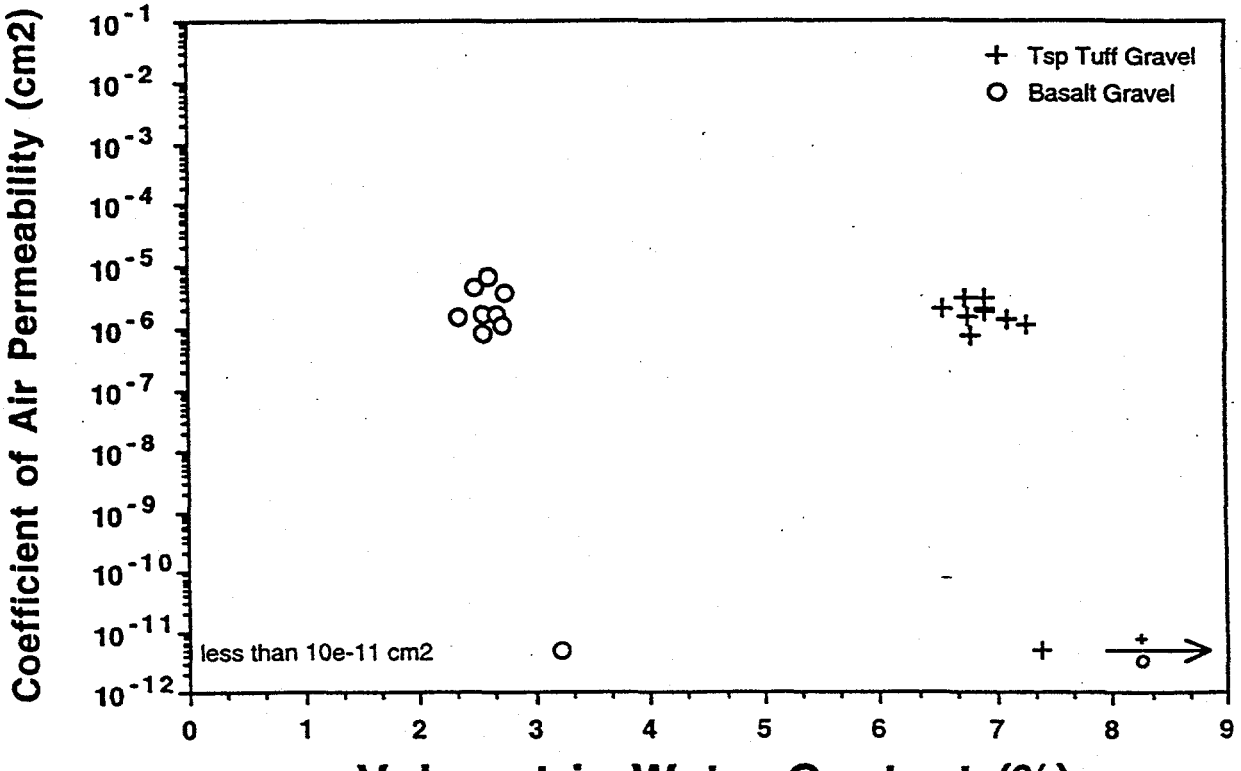

Air Permeability Curves for the Candidate Gravels

SIEVE ANALYSIS

WELL #	DEPTH	LAB# Japanese C.S.	HEIS #
TESTED BY PRH	CONTACT	PHONE	DATE 05/07/96

SAMPLE WT (g)	SIEVE SIZE IN.	CUMULATIVE WEIGHT	% WEIGHT RETAINED	% PASSING	Grain Size (mm)	COMMENTS
107.1	4"	0.00	0.00	100.00	101.60	
	2.5"	0.00	0.00	100.00	63.50	
	2"	0.00	0.00	100.00	50.80	
	1.5"	0.00	0.00	100.00	38.10	
	3/4"	0.00	0.00	100.00	19.00	
	#5	0.00	0.00	100.00	4.00	
WT.-#10	#10	0.00	0.00	100.00	2.00	
SAMP.(g)	#20	106.20	99.13	0.87	0.85	
107.1	#40	107.05	99.93	0.00	0.425	
	#60	107.07	99.94	0.00	0.250	
	#100	107.09	99.96	0.00	0.150	
	#200	107.09	99.96	0.00	0.075	

Sieve Analysis Data for Sample Japanese C.S.

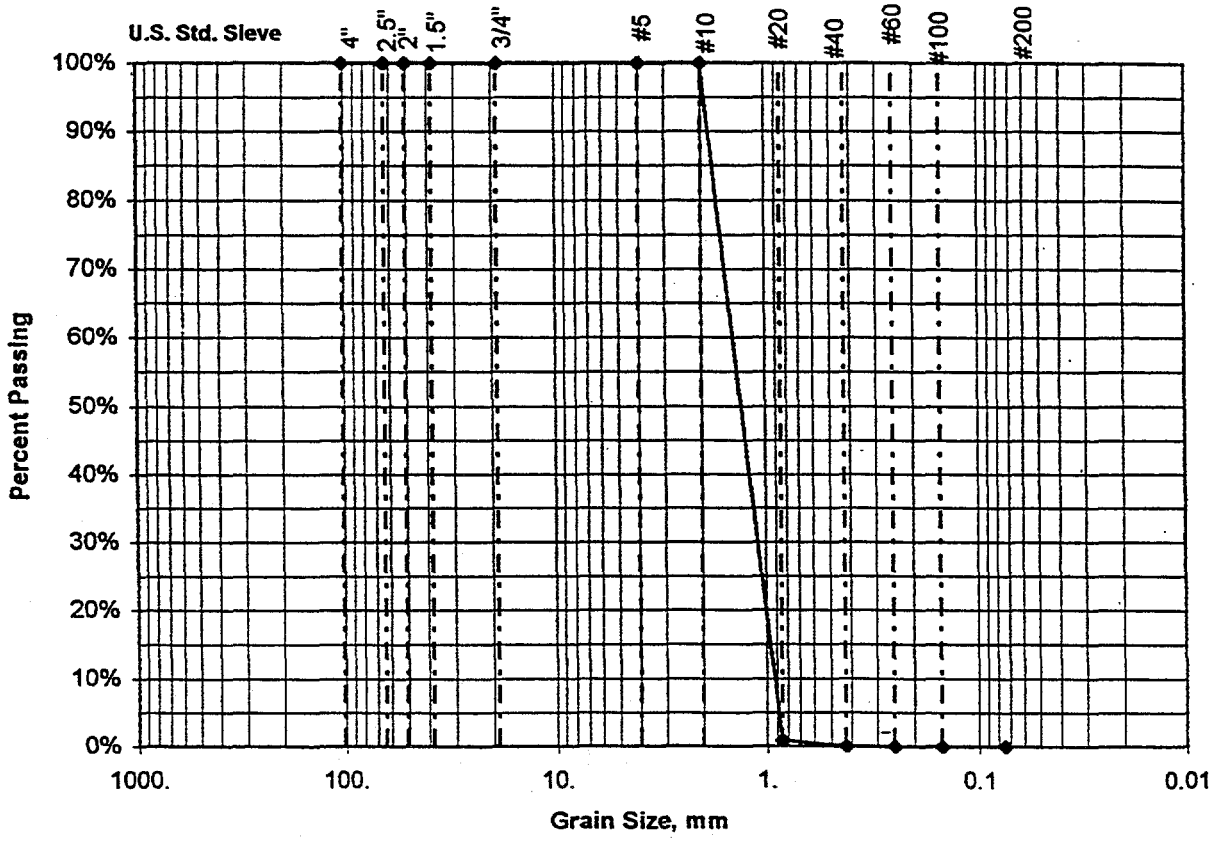

All data are accurately and completely recorded. The test operator was trained and used calibrated instruments.

Checked By: Date:

SIEVE ANALYSIS

WELL #	DEPTH	LAB# Japanese F.S.	HEIS #
TESTED BY PRH	CONTACT	PHONE	DATE 05/07/96

SAMPLE WT (g)	SIEVE SIZE IN.	CUMULATIVE WEIGHT	% WEIGHT RETAINED	% PASSING	Grain Size (mm)	COMMENTS
100.3	4"	0.00	0.00	100.00	101.60	
	2.5"	0.00	0.00	100.00	63.50	
	2"	0.00	0.00	100.00	50.80	
	1.5"	0.00	0.00	100.00	38.10	
	3/4"	0.00	0.00	100.00	19.00	
	#5	0.00	0.00	100.00	4.00	
WT.-#10	#10	0.00	0.00	100.00	2.00	
SAMP.(g)	#20	1.38	1.38	98.62	0.85	
100.3	#40	52.73	52.59	46.75	0.425	
	#60	88.50	88.27	11.57	0.250	
	#100	97.94	97.69	2.28	0.150	
	#200	99.90	99.64	0.35	0.075	

Sieve Analysis Data for Sample Japanese F.S.

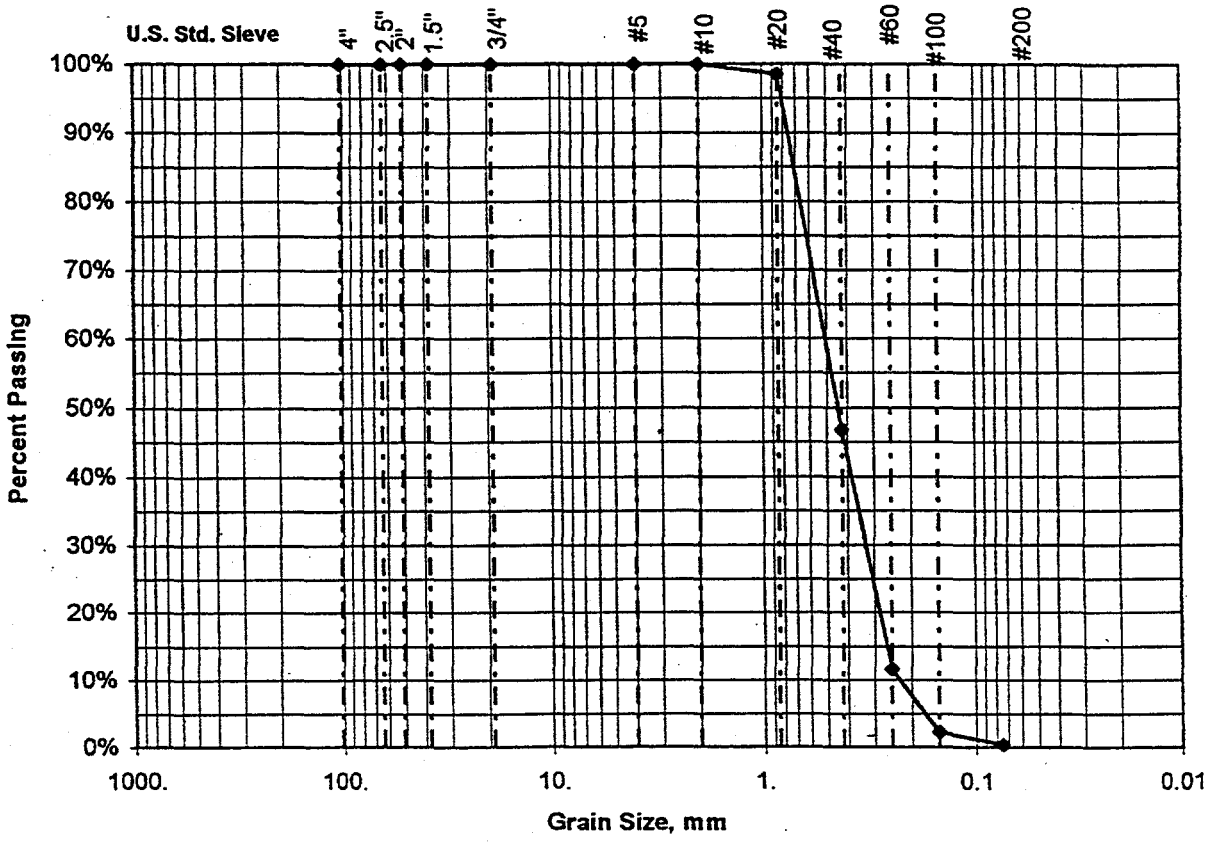

All data are accurately and completely recorded. The test operator was trained and used calibrated instruments.

Checked By: Date:

SIEVE ANALYSIS

WELL #	DEPTH	LAB# Split Wash Alluv	HEIS #
TESTED BY PRH	CONTACT	PHONE	DATE 05/07/96

SAMPLE WT (g)	SIEVE SIZE IN.	CUMULATIVE WEIGHT	% WEIGHT RETAINED	% PASSING	Grain Size (mm)	COMMENTS
87.78	4"	0.00	0.00	100.00	101.60	
	2.5"	0.00	0.00	100.00	63.50	
	2"	0.00	0.00	100.00	50.80	
	1.5"	0.00	0.00	100.00	38.10	
	3/4"	0.00	0.00	100.00	19.00	
	#5	3.31	3.77	96.23	4.00	
WT.-#10	#10	16.12	18.36	81.64	2.00	
SAMP.(g)	#20	24.29	27.67	72.33	0.85	
87.78	#40	28.59	32.57	48.77	0.425	
	#60	31.71	36.12	46.20	0.250	
	#100	40.37	45.99	39.06	0.150	
	#200	60.68	69.13	22.33	0.075	

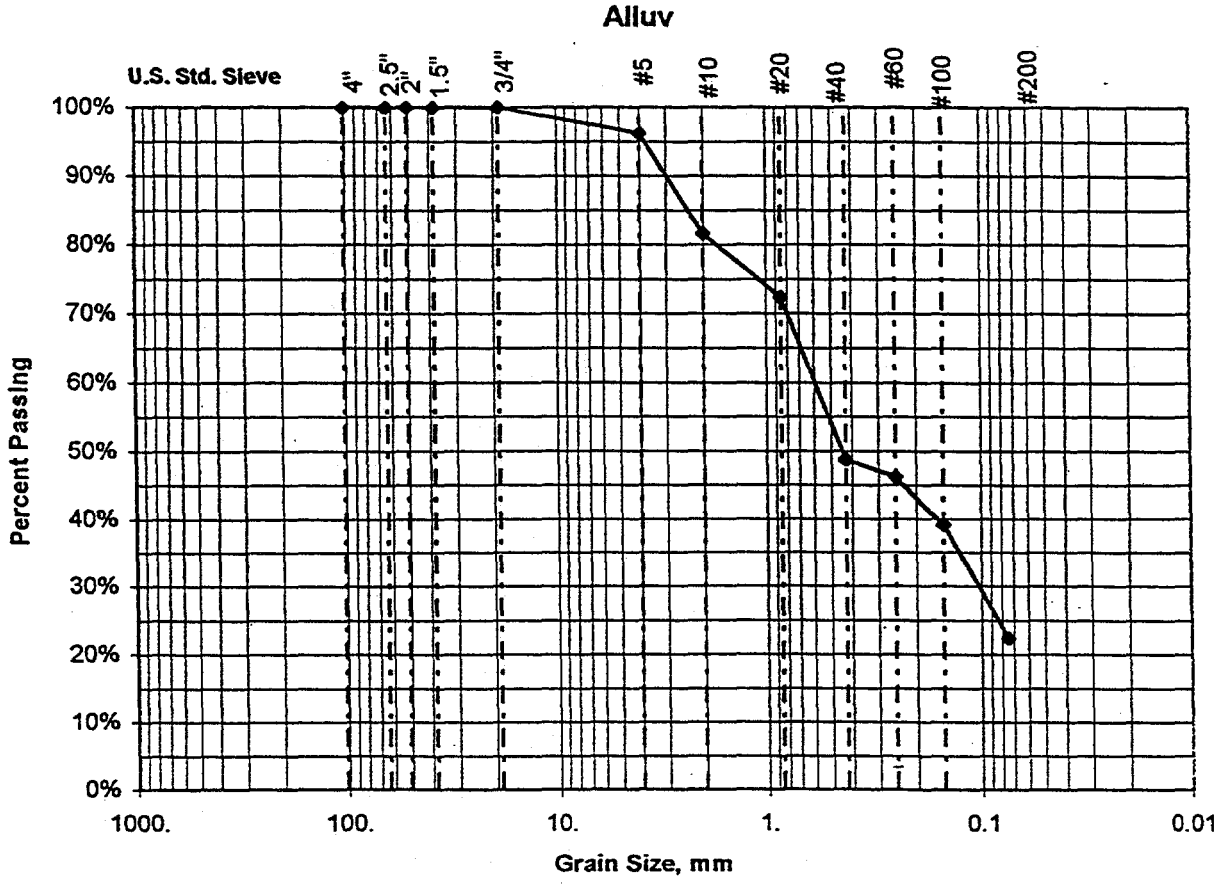

All data are accurately and completely recorded. The test operator was trained and used calibrated instruments.

Checked By: Date:

SIEVE ANALYSIS

WELL #	DEPTH	LAB# NC Apatite	HEIS #
TESTED BY PRH	CONTACT	PHONE	DATE 05/07/96

SAMPLE WT (g)	SIEVE SIZE IN.	CUMULATIVE WEIGHT	% WEIGHT RETAINED	% PASSING	Grain Size (mm)	COMMENTS
95.5	4"	0.00	0.00	100.00	101.60	
	2.5"	0.00	0.00	100.00	63.50	
	2"	0.00	0.00	100.00	50.80	
	1.5"	0.00	0.00	100.00	38.10	
	3/4"	0.00	0.00	100.00	19.00	
	#5	0.00	0.00	100.00	4.00	
WT.-#10	#10	0.00	0.00	100.00	2.00	
SAMP.(g)	#20	0.07	0.07	99.93	0.85	
95.5	#40	1.07	1.12	98.81	0.425	
	#60	17.27	18.08	81.86	0.250	
	#100	77.20	80.82	19.17	0.150	
	#200	94.99	99.45	0.55	0.075	

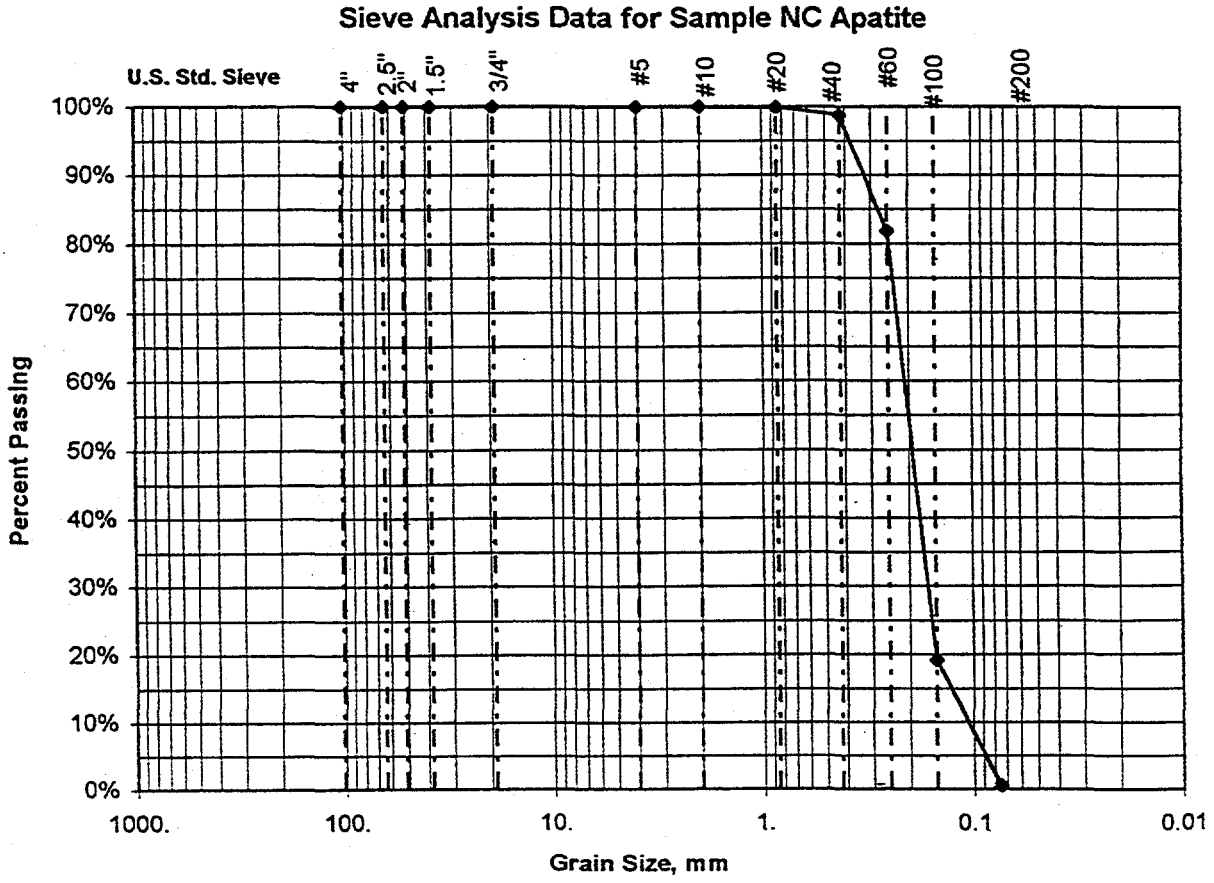

All data are accurately and completely recorded. The test operator was trained and used calibrated instruments.

Checked By: Date:

INTENTIONALLY LEFT BLANK